UNIVERSITY of PORTSMOUTH

Protection of the muscle stem cell state from premature differentiation

Federica Berti

Institute of Biomedical and Biomolecular Sciences

School of Pharmacy and Biomedical Sciences

University of Portsmouth

May 2016

The thesis is submitted in partial fulfilment of the requirements for the award of the degree of Doctor of Philosophy of the University of Portsmouth

Declaration

Whilst registered as a candidate for the above degree, I have not been registered for any other research award. The results and conclusions embodied in this thesis are the work of the named candidate and have not been submitted for any other academic award.

Federica Berti

May 2016

Word count: 69938

Acknowledgements

I would like to thank my supervisor Susanne for all her help and advice and for giving me the possibility to do a PhD project in her lab. I would like to thank my other supervisors Matthew Guille and Frank Schubert for all their help and useful tips for working in the lab. I need send a big thank you to all the people in my lab and my department for their support and coffee to keep me going. I need to thank all of my friends for their wonderful words as well as their offerings of chocolate in the hard times. And finally, but not least important, to my lovely Jack who helped me so much in these last years and whom at the end of this adventure will end up with the experience of two PhDs, one in Biochemistry and another unexpectedly in developmental Biology.

Dissemination of Research

Publications

Time course and side-by-side analysis of mesodermal, pre-myogenic, myogenic and differentiated cell markers in the chicken model for skeletal muscle formation

Federica Berti, Julia Meireles Nogueira, Svenja Wohrle, Debora Rodrigues Sobreira, Katarzyna Hawrot and Susanne Dietrich

Journal of Anatomy

Abstract :

The chicken is a well-established model for amniote (including human) skeletal muscle formation because the developmental anatomy of chicken skeletal muscle matches that of mammals. The accessibility of the chicken in the egg as well as the sequencing of its genome and novel molecular techniques have raised the profile of this model. Over the years, a number of regulatory and marker genes have been identified that are suited to monitor the progress of skeletal myogenesis both in wildtype and in experimental embryos. However, in the various studies, differing markers at different stages of development have been used. Moreover, contradictory results on the hierarchy of regulatory factors are now emerging, and clearly, factors need to be able to cooperate. Thus, a reference paper describing in detail and side-by-side the time course of marker gene expression during avian myogenesis is needed. We comparatively analysed onset and expression patterns of the key markers for the chicken immature paraxial mesoderm, for muscle-competent cells, for cells committed to myogenesis and for cells entering terminal differentiation. We performed this analysis from stages when the first paraxial mesoderm is being laid down to the stage when mesoderm formation comes to a conclusion. Our data show that, although the sequence of marker gene expression is the same at the various stages of development, the timing of the expression onset is quite different. Moreover, marker gene expression in myogenic cells being deployed from the dorsomedial and ventrolateral lips of the dermomyotome is different from those being deployed from the rostrocaudal lips, suggesting different molecular programs. Furthermore, expression of Myosin Heavy Chain genes is overlapping but different along the length of a myotube. Finally, Mef2c is the most likely partner of Mrf proteins, and, in contrast to the mouse and more alike frog and zebrafish fish, chicken Mrf4 is co-expressed with MyoG as cells enter terminal differentiation.

Oral presentations

'Protection of muscle stem cells'

Presented at the IBBS research day, University of Portsmouth in 2014

Poster presentations

'Balance of muscle stem cell maintenance vs. differentiation'

Presented at the IBBS research day, University of Portsmouth 2013; at the Anatomical Society meeting, Dublin 2013 and at the BSDB spring meeting, University of Warwick 2014

Abstract

The extraordinary capacity of regeneration exists in just certain species and tissue types. In vertebrates, the cells that regenerate tissues are called stem cells.

During adulthood, damaged muscle tissue regenerates through Satellite stem cells that re-enter the cell cycle from a quiescent state, giving rise to new muscle tissue. During development, newly forming organisms build tissues through proliferating stem cells that renew the stem cell pool whilst generating myogenic stem cells which will eventually differentiate into muscle cells. For many years the Myogenic Regulatory Factors (Mrf) genes have been considered to be the main genes driving this proliferation in adult and fetal stages.

Mrf genes have been shown to be capable of inducing non-myogenic cells to enter the myogenic lineage *in vitro*, but their role and capabilities *in vivo* have been less well characterised.

Here we show, using the developing chicken model, that Mrf genes and related genes are not capable of prematurely upregulating terminal muscle differentiation before HH20. MyoD and other combinations of gene misexpression were however shown to be capable of inducing Myosin upregulation between HH20 and HH24 indicating the existence of a time-frame dependent protection of premature development. These results indicate that the Mrf genes have a reduced proficiency for inducing differentiation in vivo compared with in vitro likely due to the presence of currently unidentified additional factors.

Our results demonstrate that the current understanding of the signals and cues of muscle stem cell differentiation are still insufficient to exploit the regenerative capabilities of muscle tissues towards regenerative therapies. The possible additional factors required for muscle stem cell differentiation are also discussed.

List of contents

List of Figures

List of Tables

Abbreviations

°C	Degrees Celsius
µ	Micro
µg	Micro gram(s)
µl	Micro litre(s)
µM	Micro molar
A	Adenine
AP	Alkaline phosphatase
ARLD	Alcohol Related Liver Disease
ATG	Start codon
ATP	Adenosine tri phosphate
ATPase	Adenosine tri phosphatase
b	Base(s)
BBR	Boehringer's blocking reagent
BCIP	5-Bromo-4-chloro-3-indolyl phosphate
bHLH	Basic helix-loop-helix structural motif
BLAST	Basic Local Alignment Search Tool
BLAT	BLAST-like alignment tool
BMD	Becker's Muscular Disorder
bp	Basepair(s)
C	Cytosine
C. elegans	*Caenorhabditis elegans*
C2C12	Mouse myoblast cell line
Ca^{2+}	Calcium ion
CACS	Cancer Anorexia Cachexia Syndrome
CAP	$m^7G(5')ppp(5')G$
CBP	CREB-binding protein
CDK	Cyclin-dependant kinase
ChIP on chip	Chromatin immunoprecipitation followed by microarray analysis
ChIP	Chromatin immunoprecipitation

ChIP-Seq	Chromatin immunoprecipitation followed by next generation sequencing analysis
cis-elements	region of non-coding DNA involved in regulation of a nearby gene
ClustalW	Command line interface multiple sequence alignment software
CMC	Chromatin-modifying complex
CMV	Cytomegalovirus
C-terminal	Carboxy terminus of a protein
CVD	Cardio Vascular Disease
Da	Dalton(s)
DAB	3,3'-Diaminobenzidine
ddH_2O	Double-distilled water
DEPC	Diethylpyrocarbonate
DGC	Dystrophin Glycoprotein Complex
DIG	Digoxigenin
DM	Dermomyotome
DMD	Duchenne Muscular Dystrophy
DML	Dermomyotomal lip
DNA	Deoxyribonucleic acid
E	Embryonic age
E box	Enhancer-box protein binding site on DNA
E. coli	*Escherichia coli*
EC culture	Early chick culture
EC	Embryonal Carcinoma cell
ECs	Endothelial Cells
ED domain	Eya domain
EDTA	ethylenediaminetetraacetic acid
EGFP	Enhanced green fluorescent protein
EGTA	Ethylene glycol tetraacetic acid
EMT	Epithelia-to-mesenchymal transition
ES	Embryonic Stem cell
ESC	Embryonic stem-like cells
F-Actin	Filamentous Actin
g	G-force
g	Gram(s)

G	Guanine
G0 phase	Period of the cell cycle in which cells exist in a quiescent state
G1 phase	The first stage in interphase and the cell cycle in which cells grow
G-Actin	Globular Actin
GEISHA	Gallus expression in situ hybridisation analysis
GFP	Green fluorescent protein
H_2O_2	Hydrogen peroxide
H3K4	Lysine four of Histone three
H3K4^{me3}	Trimethylation of Lysine four of Histone three
HAD	Haloacid dehalogenase
HAT	Histone acetyltrasnferase
HA-tag	Human influenza hemagglutinin epitope tag
HDAC	Histone deacetlyase
HH	Hamburger Hamilton stages of chicken development
HLH	Helix-loop-helix protein motif
hn	Henson's node
hr	Hour(s)
ht	Heart
Hz	Hertz
Ig	Immunoglobulin
IHC	Immunohistochemistry
iPSC	Induced Pluripotent Stem Cell
IRES	Internal ribosome entry site
ISH	*In situ* hybridisation
k	Kilo
kb	Kilobase(s)
kbp	**K**ilo basepair(s)
l	Litre(s)
LB	Luria-Bertani broth
M phase	Mitotic phase of the cell cycle including Mitosis and cytokinesis
m	Milli
M	Molar
MAB	Maleic acid buffer

MABT	Maleic acid buffer with Tween 20
MADS	**(**MCM1, agamous, deficiens, serum response factor) DNA binding motif
MBS	Modified Barth's saline
MCS	Multiple cloning site
MD	Muscular Dystrophy
MeOH	Methanol
mg	Milli gram(s)
Mg^{2+}	Magnesium ion
MI	Myocardial Infarction
min	Minute(s)
miRNA	Micro ribonucleic acid
ml	Milli litre(s)
mM	Milli molar
MOPS	3-(N-morpholino)propanesulfonic acid
mpc	Myogenic precursor cells
Mrf	Myogenic regulatory factor
mRNA	Messenger ribonucleic acid
mRNP	Messenger ribonucleoprotein
ms	milli second(s)
MSCs	Mesenchymal Stem Cells
MuSC	Muscle Stem cells
N	Any nucleotide
NBT	Nitroblue tetrazolium
not	Notochord
N-terminal	Amino terminus of a protein
NTP	Nucleoside triphosphate
OCT	Optimal cutting temperature compound
ORF	Open reading frame
PAGE	Polyacrylamide gel electrophoresis
PBS	Phosphate buffered saline
PBT	Phosphate buffered saline with Tween 20 detergent
pCab	Mammalian expression vector for the expression of a gene of interest in an operon with green fluorescent protein

PCP	Planar cell polarity
PCR	Polymerase chain reaction
PFA	Paraformaldehyde
poly (A)	Poly adenine tail
ps	Primitive streak
PSM	Presomitic Mesoderm
R	Any purine nucleotide
RCs	Reserve Cells
RE	Restriction enzyme
Red-Gal	Lactose analog that produces a red-pink coloured compound upon hydrolysis by β-Galactosidase
RFP	Red fluorescent protein
RNA	Ribonucleic acid
RNase	Ribonuclease
RNAseq	ribonucleic acid sequencing of complementary deoxyribonucleic acid (cDNA) by next generation sequencing
RSV	Respiratory syncitial virus
RT	Reverse transcription
RTK	Receptor tyrosine kinase
rv	Rib-vertebrae
S phase	Cell cycle stage in which the deoxyribonucleic acid genome is replicated
s	Somite
S200A	Serine position 200 mutated to an alanine
SC	Satellite Cells
SD-domain	Six domain
SDS	Sodium dodecyl sulphate
sec	Second(s)
SELEX	Systematic evolution of ligands by exponential enrichment
Ser200	Serine position 200
SMA	Spinal Muscular Atrophy
sp	Segmental plate
SP6	SP6 bacteriophage
SR	Sarcoplasmatic Reticulum

SSC	Saline, sodium citrate buffer
SV40	Simian vacuolating virus 40
SVZ	Subventricular Zone
T	Thymine
T3	T3 bacteriophage
T7	T7 bacteriophage
TAE	Tris, acetate, EDTA buffer
tRNA	Transfer ribonucleic acid
UCSC	University of California Santa Cruz genome browser
UTR	Untranslated region
V	Volts
VLL	Ventrolateral lip
WT	Wild type
X-Gal	Lactose analog that produces a blue colour compound upon hydrolysis by β-Galactosidase
α	Alpha
β	Beta

Chapter 1

1 Introduction

1.1 Regeneration of organs and body parts: the challenge for regenerative medicine

The regeneration of organs is one of the most important aspect of the medical research. The capability of the body to regenerate new cells and substitute damaged cells is due to the presence of stem cells. Every organism has its own way to regenerate damaged cells. Flat worms such as planaria can replace any missing body part and can regenerate the whole body from just a little piece of the previous organism (1,2). The superclass of *Tetrapoda* comprises the first four-limbed vertebrates and their descendants, including amphibians, birds and fish. Tetrapods are very well known for their capacity to regenerate a missing body part, among them, salamanders display by far the highest regenerative capacity that includes the eyes, heart, tails and entire limbs (3–5).

For more complex vertebrates, such as humans, the regeneration is much more complicated and requires a finely tuned system and communication between cells. A large network of signalling can drive the differentiation of cells and their behaviour (1). Sometimes the network doesn't work or it can be interrupted and the cells lose their capacity to communicate with other cells thereby interrupting regeneration. This massive failure brings about catastrophic consequences such as organ or tissue collapse (6). Bad lifestyle such as poor dietary intake of protein and fat coupled with inadequate physical exercise can increase the instance of cardiac disease, one of the leading causes of death in the world. Of course, diseases that impact the heart and the liver require immediate attention and in extreme cases, the transplantation of a new organ.

Genetic diseases represent another key factor that impact an organ's regeneration. Muscular Dystrophy (MD) is a group of genetic degenerative diseases that impact the structure of the muscle. In the last decade, a number of genes have been discovered to be part of Muscular Dystrophy diseases such as the gene Dystrophin (7,8). Duchenne Muscular Dystrophy (DMD) is caused by a mutation in the Dystrophin gene (*DMD*) found on the X chromosome (7). The *DMD* gene is one of the longest in the Human genome which encodes the 427 kDa protein dystrophin (9). In the case of DMD, the surgical correction solution cannot be approached. The disease is not localised in just one area of the body but extends throughout the whole muscular mass.

In each case, these diseases cause organ regeneration and the replacement of damaged tissues to fail. Regenerative medicine focuses on the of the natural behavior of stem cells, that represent the new frontier to fight incurable diseases (10). Stem cells in the adult body gradually resign their job of repair and maintenance with age, eventually causing tissue and organ failure. Based on the past decade of research, this occurs because stem cells become dormant in increasing numbers as

rising levels of age-related cellular damage change the mix of chemical signals propagating through tissues (11). The manipulation and the understanding of stem cells represents an important step towards the regeneration of tissue and organs and a new hope for numerous patients.

1.1.1 Regeneration in the animal kingdom

Salamanders, Xenopus frogs and zebrafish have all been used for many years to observe the behaviours of stem cell regeneration in vertebrates (1,12,13). These three vertebrates have different mechanisms and capabilities to regenerate a missing limb or part of a damaged tissue. Xenopus can regenerate a missing tail when in their larval stage as a tadpole, during which their cells are still in a pluripotent state (1)

Human tissues and organs have different ways to replace damaged cells (6). The skin for example is one of the more active tissues which replaces millions of cells every day (10). Organs like the liver can regenerate damaged hepatocytes or an entire damaged part of the organ (14). Muscle tissue is another part of the vertebrate body that can be regenerated after trauma. In this specific case the regeneration of the muscle is linked to a specific family of cells called Satellite cells, that after injuries are awaked from their dormant state and become active again (15).

Trying to understand the mechanism of regeneration could help us to comprehend the development of diseases like Muscular Dystrophy and create new techniques to cure or treat their degeneration. Currently, the majority of the experiments are performed *in vitro*, trying to recreate a representative and functional environment in which we can observe how cells divide and create new tissue (10,16). In essence, the gold standard is to use/develop autologous cells from a patient as they would be compatible with the patient's immune system. For organs that naturally have stem cells, these cells may be of direct use in therapy, provided they can be cultured and manipulated. Moreover, it may be possible to reprogram existing tissue-specific stem cells by making genes for alternative cell fates accessible. Likewise, with the discovery of protocols for the generation of induced pluripotent stem cells from adult, differentiated cells, possibilities have opened up to recapitulate developmental processes and derive desired precursor or stem cells *in vitro* prior to grafting them into a patient. Taken together, it appears that stem cell research may be the most promising route in regenerative medicine.

1.2 Stem cells

1.2.1 What is a stem cell?

Stem cells are undifferentiated, mitosis-competent cells that simultaneously generate cells for progressing towards differentiation whilst self-renewing (17). The cellular basis for this is asymmetrical cell division, in which one daughter cell will again be a stem cell and the other will become recruited into differentiation to build functional tissues and organs. The differentiating

cell may progress through one or several precursor cell stages in which the cell pool may expand by symmetric cell division (Figure 1.1). These cells are also referred to as transit amplifying cells. However, after the cells differentiate, they are no longer able to participate in the future renewal of organ tissue hence, a constant pool of stem cells is necessary to maintain the continued stability of the organism. (18).

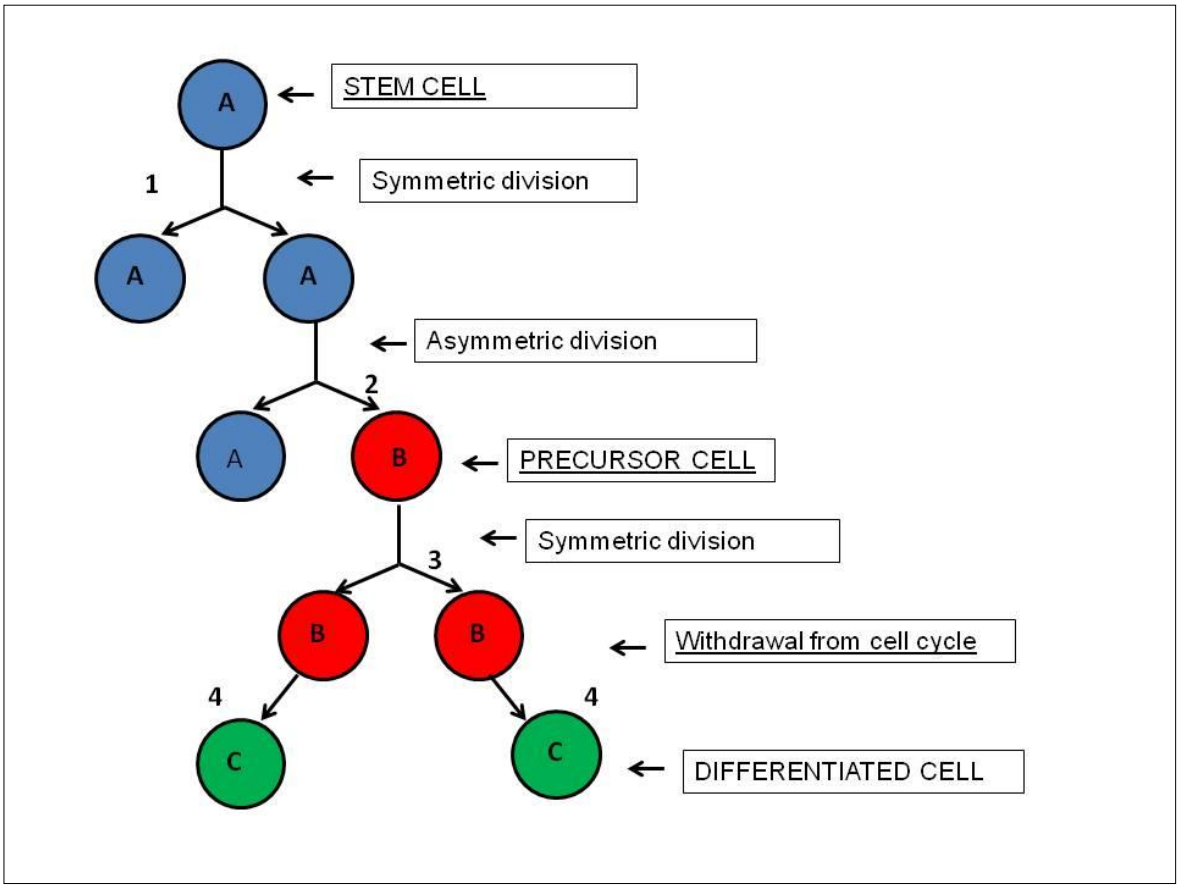

Figure 1. 1: Renewal and differentiation of stem cells.

Stem cells (A) and pre-differentiation progenitor cells (B) multiply by symmetrical cell division (1, 3). Asymmetrical division of a stem cell (3), provides cells the ability to build differentiated tissue, but at the same time provides a new stem cell to maintain the stem cell pool. The two cells obtain from the symmetric division of the cell (B), will now carry on differentiation (4) and they won't be able to divide again but they will carry on to form a final differentiated cells (C).

1.2.2 Stem cells can be distinguished by their potency

During embryo development, the potential of stem cells is gradually reduced. At the morula stage and early blastocyst, the stem cells are totipotent, meaning that they are able to give rise to any kind of tissue in the embryo (19).

The pluripotent stem cells are embryonic stem cells (ES) which are derived from the late blastula, just before the onset of gastrulation (20). In mammals, they constitute the inner cell mass, located inside the primordial embryo which eventually gives rise to the structure of the fetus (21). The pluripotency of ES means that they are able to differentiate into any of the three germ layers: endoderm (giving rise to: interior stomach lining, gastrointestinal tract and the lungs), mesoderm (giving rise to: muscle, bone, blood and the urogenital tissues), or ectoderm (giving rise to: epidermal tissues and the nervous system) (22).

The capability of the embryonic totipotent stem cells decreases during development reaching the unipotent adult stem cell stage in which proliferation occurs to maintain the tissue and replace the damaged cells (23). This means that adult stem cells can produce just the same cells found in that specific tissue. For example, the epidermis produces new cells to compensate for the high number of cells that are lost every day. There are many tissues in the Human body that have the same characteristics including: muscle stem cells, intestinal stem cells, and neural stem cells (24–26).

Embryonic stem cells are found just in the first stage of the generation of new tissue. At the final stages, these cells are replaced by satellite cells or adult stem cells. The embryonic stem cells express Mrf proteins in a specific order at specific stages of muscle development. The first marker expressed is Myf5 followed by MyoD, MyoG and Mrf4. Embryonic stem cells divide symmetrically then asymmetrically to produce two sister cells, one of which contributes to maintaining the stem cell pool whilst the other cell carries on differentiating. During this process a few of the cells will not express Mrf markers but they will keep expressing the pair box genes Pax3/Pax7 (27). These cells will form the adult satellite cells which will be in a dormant state until an eventual injury (28).

The proliferation capabilities of unipotent cells decreases with aging of the organism leading to aged individuals with difficulties in healing wounds and with slower recovery time following trauma.

1.2.3 Efforts to develop the use of stem cells for therapies

The discovery of the stem cell developed a new theory of the possibility to reprogram cells and re-create new tissues in the laboratory. The first engineered stem cells created in the laboratory were the induced pluripotent stem cells (iPSC). iPSCs are adult cells reprogrammed to be

pluripotent stem cells. These cells were developed for the first time in 2006 (Takahashi & Yamanaka, 2006). The first reprogramming was done in murine fibroblasts by viral overexpression of a specific set of pluripotency-associated genes; Oct4, Sox2, cMyc, Klf4.

The discovery that murine and human fibroblasts can be converted into stable and fully functional embryonic stem-like cells (ESCs), has encouraged scientists to look beyond ESCs for regenerative medicine, as well as to re-evaluate the terminology 'terminally differentiated state' and the notion of cellular plasticity (30). Since the discovery of iPSC, researchers have attempted to directly convert various adult cells to different cell types, by avoiding the pluripotent state, using a unique combination of cell type-specific key master regulators. Several medically relevant cell types have been generated, including hematopoietic cells, different neuronal cells and cardiomyocytes (31). However, despite remarkable progress in characterising the reprogramming process and the resulting iPSCs and directly converted cells, it remains to be seen if these converted cells are safe and of sufficiently high quality to facilitate their immediate use in the clinic (32). Theoretically, iPSCs and directly converted cells are ideal for regenerative medicine and for disease modelling. In contrast to ESCs, their use does not involve ethical issues and, because they can be derived from patients, they should not be rejected by the host. However, rigorous functional assays in the mouse system showed that, unlike ESCs, which are relatively uniform in their differentiation capacity, the quality of iPSCs varies widely between different colonies, creating cells that can over proliferate and lose the control. This could potentially create dangerous effect if transplanted into human bodies. The use of iPSC have to be tested to ensure the quality of the cells themselves before applying them to humans (22,32–36).

1.2.3.1 Tissue specific stem cells

Surgery to repair and heal devastating injuries are based of the implantation of new tissue that will help the regeneration of the damaged tissue (37). The tissue can be produced *in vitro* but the negative impact of this procedure is the body's potential reaction to the foreign engineered tissue causing what is defined as rejection. If the immune system of the patient rejects the newly transplanted cells it will treat them as an extraneous part and it will attempt to eject the tissue (38). Tissue specific stem cells may be a safer option for stem-cell based therapies, since they are committed to regenerate specific cells or organs. This technique could use cells taken from the body of the patient and in this way the body and the immune system will recognise the cells as 'self' with no rejection (38). An example of tissue specific stem cells are the bone marrow derived cells, used as a treatment for myocardial infarction (MI). Large improvements in myocardial function have been shown in the results of animal experiments and adult stem cell therapy clinical trials (39). Bone marrow-derived mesenchymal stem cells (MSCs) in particular present themselves as useful tools for cardiac repair following MI, due to their self-renewal and proliferation properties as well as their multiple lineages (40).

Another example of advances in stem cell therapy is the use of the olfactory epithelia cells as a treatment of spinal cord injuries. These specialised glial cells surrounding the olfactory sensory axons in the nose have been shown to have capabilities comparable to Schwann cells in supporting axon growth. Successful transplantation of olfactory ensheathing cells into mice with spinal cord injuries ranging from lesions to complete transection led to recovery of paw use and coordinated movements (41). However, no completely effective treatments have yet been developed for neurological repair following spinal cord injuries in humans.

1.1.1.1 *Muscle stem cells (MuSC) in the application of therapeutic treatment of muscular dystrophies and other types of muscle wasting diseases*

As explained in Section 1.1, Muscular Dystrophy is linked to the X chromosome and affects 1 in 3500 male births. In recent years little information has been collected to clarify the cause and possible solutions to cure this disease. The Dystrophin gene is considered the main cause for the progression of the disease (9). Dystrophin is an important cytoskeletal protein and a major component of the dystrophin glycoprotein complex (DGC) whilst also being responsible for the maintenance of cell integrity, mediation of cytoplasmic signalling and muscle cell function. Without dystrophin, muscle cells cannot form the DGC and degenerate as a result of mechanical stress during contraction (9,16).

A few murine models have been created to mimic the disruption caused by the absence of the Dystrophin protein (42). Attempts to cure the disease are separated into treatment via transplantation of autologous or allogenic cells. In the first case stem cells extracted from a patient afflicted with DMD were treated and genetically reprogrammed before replanting in the same patient. In the second case muscle stem cells taken from a healthy patient were transplanted into a DMD patient (9). One strategy used in gene therapy is for a healthy full-length dystrophin complementary DNA (cDNA) to be inserted into muscle precursor cells presenting muscular dystrophy. This can be achieved through the use of viral vectors, like the adeno associated virus (AAV) and lentiviral vectors. These vectors are used to insert a micro or mini-dystrophin gene, a necessary approach given by the fact that the dystrophin gene itself is one of the biggest genes in the Human genome and would be too large in its entirety (43,44). Another possible strategy is the exon skipping technique utilising the adeno virus. Experimentally, this involves introducing a small RNA or DNA molecule into cells which can then interfere with the normal splicing of a gene and consequently cause one of the exons to be removed. This process is used to skip the exons that contain nonsense mutations so as to restore an open reading frame. In the mdx mouse, it has been proven that skipping exons can allow the myofibres to produce dystrophin lacking only the region encoded by exon 23 (45,46).

The two techniques produced both positive and negative results. The first technique has the advantage that it does not cause any issues with rejection as the cells originate from the same

organism. The second technique allows the use of healthy cells without the need for reprogramming but carry the risk of being recognised as foreign by the patient's immune system and being rejected as the cells do not originate from the patient. Unfortunately, muscular dystrophy is not the only disease that can cause disruption, loss of muscle mass and function. Acquired immune deficiency syndrome (AIDS) is typically associated with 10 % loss of weight and muscle mass due to weakening of the body as well as changes in gene expression that bring about a loss of muscle control called disuse atrophy (47,48).

Patients with Cancer or other chronic illnesses often suffer from unintended weight loss and muscle wasting referred to as Cancer anorexia-cachexia syndrome (CACS). This syndrone is characterised initially as inadequate oral intake and metabolic changes and subsequently anorexia, weight loss and muscle wasting (49). Natural aging is associated with progressive loss of neuromuscular function, loss of skeletal muscle mass and strength commonly referred to as sarcopenia (50). The major contributor to the development of sarcopenia is loss of skeletal muscle fibres as a result of reduced motor neurons but other associated factors include decreased physical activity, change in hormone levels and decreased calorie and protein intake (51).

With a clear need for new and convincing strategies for transplanting muscle cells into patients, Cossu and colleagues described a variety of different techniques being trialled as well as the properties of satellite cells that lend themselves to be used for cell therapies (52). Satellite cells (SCs) are unipotent stem cells found under the basal lamina. They remain quiescent in adult individuals until they are activated following injury however, in patients with DMD this mechanism fails to work. Recent data demonstrated that SCs can be isolated pure and cultivated but unfortunately the cells lose their capacity to replicate if kept cultured for long periods (52).

Similarly, human hematopoietic stem cells and mesenchymal stem cells lose their capability to regenerate when transferred to cell culture (37,52–54). The loss of regenerative capacity of cultured stem cells is therefore an important barrier to overcome.

Evidence is accumulating that, in a healthy environment *in vivo*, the muscle stem cell state may be actively stabilised, therefore underlining the importance of *in vivo* format experiments (52,55,56).

1.3 Anatomy, function, homeostasis and regeneration of adult skeletal muscle

1.3.1 Muscle anatomy and function

Muscles are responsible for all the movements of our body, voluntary and involuntary. They are formed of myocytes which recruit more myocytes which fuse together, forming a muscle fibre (57).

The fibres are filled with contractile protein filaments, consisting of reiterated contractile units called sarcomeres (58). The muscle itself is surrounded by connective tissue and is anchored to the skeleton or skin via tendons.

Sarcomeres are basic contractile units of the muscle, and are arranged in series to form myofibrils which are aligned along their longitudinal axis and constitute the largest component of the muscle fibre. Satellite cells are situated between the basement membrane and the sarcolemma (Figure 1.2) and the myonuclei are located at the periphery of the myofibres just underneath the sarcolemma itself (15).

The sarcoplasmic reticulum is a network of flattened tubules around each myofibril and is responsible for the release and uptake of Ca^{2+} associated with muscle contraction. The function of the T-tubules is to transmit the action potential from the muscle fibre surface to its interior. Each mature myofibre is innervated by a single motor neuron that makes contact with the myofibre at the neuromuscular junction. Skeletal, cardiac and smooth cells all use the same molecular principle to generate force during the contraction (59,60). The energy for contraction is provided by ATP. The contraction mechanism involves the protein Myosin attaching to an Actin thin filament and pulling on it, causing Actin to slide past the Myosin thick filament (61). Myosin is a large protein of which the main body is composed of two heavy chains (62,63) and the head possesses ATPase activity and contains the Actin interaction site. The protein Actin forms a molecular rope that Myosin pulls on during contraction. Actin is synthesised as a globular protein (G-Actin) and then polymerised to form the (F-Actin) which contains two beadlike polymers braided in a helical confirmation (64,65). Actin expresses Myosin binding sites, but these must remain hidden until a signal to contract is received or else the muscle fibre may lock into a rigid state (rigor) (63). Access to the binding sites is controlled by Tropomyosin and Troponin, two regulatory proteins that lie in the grooves of the Actin helix near the binding site. Actin Tropomyosin and Troponin together constitute the thin filament (66).

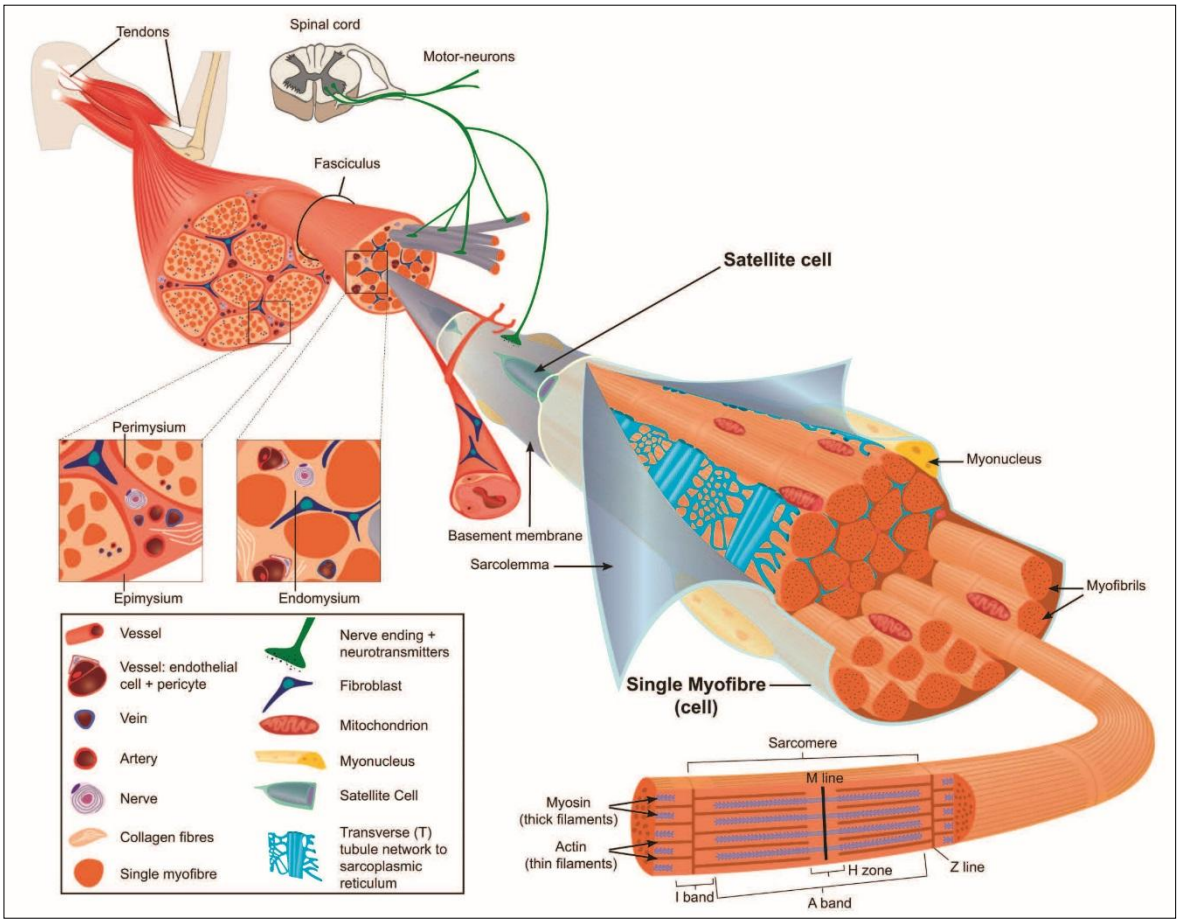

Figure 1. 2: Structure of the muscle.

Skeletal muscle is voluntary muscle controlled by motor neurons which innervate every single muscle myofibre. Muscles are composed of a series of layers and specific cells that contribute to making the tissue functional and responsive for every movement. A single fasciculum is made of numerous myofibres. The main components of the myofibre are satellite cells, myonuclei and myofibrils. Satellite cells are situated under the basal lamina and they are responsible for the maintenance of the tissue in the case of injuries. These cells can re-enter the cell cycle and give rise to new muscle stem cells. Myonuclei are positioned at the border of the myofibres, under the sarcolemma. The sarcoplasmic reticulum is responsible for the release and uptake of the Ca^{2+}. The single Myofibril represents the centre of the movement in a unit called the Sarcomere, made of Myosin and Actin filaments responsible for the muscle contraction and are Ca^{2+} dependent. Image adapted from (67).

1.3.2 The muscle satellite cell, muscle homeostasis and regeneration

Since their discovery, satellite cells (Mauro, 1961) have been the major candidate for the source of myogenic cells for muscle repair during injury-induced regeneration. (69,70). Transplantation of satellite cells into dystrophic muscle of a single muscle fibre generates plenty new myofibres and myofibre associated cells (17). Upon injury (or when muscle is explanted *in vitro*), satellite cells re-enter the cell cycle in G1. Moreover, they express some premyogenic genes such as *Pax7* in their quiescent state (Fig. 1.3), indicating that their cell cycle arrest is actively regulated (71–74).

Upon injury or growth stimulus, activated satellite cells, express myogenic factors Myf5 and/or MyoD and begin extensive proliferation to generate the progenitors for muscle regeneration. The myoblasts later downregulate Pax7 expression and upregulate MyoG and Mrf4 expression before exiting the cell cycle towards differentiation and the formation of fully formed, fused myofibers (52). Depletion of Pax7-expressing satellite cells results in lack of adult muscle regeneration thereby demonstrating that this process is responsible for the regenerative capabilities of skeletal muscles (75). Quite often the embryonic myoblast has been defined as a stem cell but in reality the myoblast cannot divide asymmetrically but just symmetrically, producing two sister cells which both will differentiate into myocytes (76).

As well as providing the progenitors for forming new myofibres, satellite cells also need to maintain the satellite cell pool through self-renewal (17,71). This balance between self-renewal and commitment is therefore important for the continued regenerative capability of skeletal muscle yet the dynamics of this process remain to be shown. A popular theory stipulates that the satellite cell pool is heterogeneously comprised of committed and non-committed cells that each have a predisposition for differentiation or self-renewal, respectively (77).

Some satellite cells generate large numbers of daughter cells that eventually differentiate, and do not produce cells that efficiently re-populate that SC niche (18,73,78)(18,78,79). These cells behave like myoblasts (mitotically active cells, committed to muscle formation) and qualify as transit amplifying cells rather than genuine stem cells (80,81). There are many intrinsic and extrinsic factors that control satellite cell function. Previous experiments have shown that the regulation of the cell cycle represents one of the crucial routes for satellite cell control (73,82).

The embryonic myogenic progenitors express the paired box proteins Pax3 and Pax7 after which their myogenic progression is controlled by a program of Mrf expression starting with Myf5 and/or MyoD activation followed by MyoG and Mrf4 (83,84). During late stages of mouse development at around E16.5-18.5 (E-embryonic day) a subpopulation, hypothesised to form the future satellite cell population, avoid Mrf expression and maintain Pax3/Pax7 expression (55).

Inactive adult satellite cells do not express MyoD however, Myf5 positive and negative cells can be distinguished in adult muscles. Moreover, approximately 10 % of satellite cells never express

Myf5 during development (85). This heterogeneity has been hypothesised to be the source of satellite cells with self-renewing capacity. Activated satellite cells expressing higher levels of Pax7 are less likely to commit to differentiation compared with the cells that express low levels of Pax7. The paired box family members Pax3 and Pax7 are discussed further in Section 1.3.3. Careful observation of Satellite cells in culture show that reserve cells, i.e. self-renewed satellite cells, are not immediately present. Their emergence is linked to a phase when MyoD-negative, mitotically silent and MyoD-positive, dividing cells appear (86). This phenomenon was followed by another study that shows satellite cells must divide at least once, and this division must be asymmetric, to generate a renewed satellite cell as well as a differentiating daughter cell (73). This indicates that in principle, quiescent satellite cells are genuine muscle stem cells. Precise control of the activation of satellite cells is essential to the maintenance and survival of muscle fibres. This firm control was revealed by microarray analysis which noted that more than 500 genes are highly upregulated in quiescent satellite cells compared with cycling myoblasts (87). The importance of the cell cycle is discussed in more detail in Chapter 10.

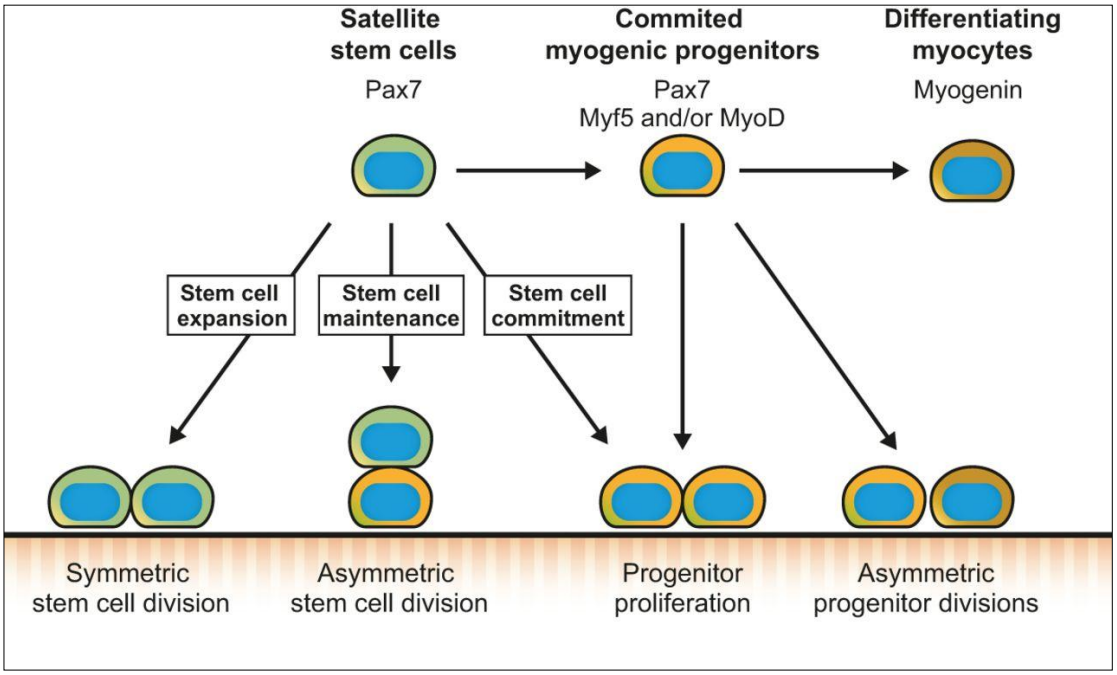

Figure 1. 3: Symmetrical and Asymmetrical division of satellite cells

Once activated, Pax7-expressing satellite cells may undergo symmetrical division to facilitate the expansion of the stem cell population. Similarly, they may undergo asymmetrical division to generate a new population of myogenic progenitors whilst maintaining the stem cell pool. Alternatively, the satellite cells can commit to become myogenic progenitor cells expressing Pax7, Myf5 and MyoD. Myogenic progenitors can proliferate to give rise to committed myogenic progenitors or they can differentiate into MyoG-expressing myocytes directly or via asymmetrical division. Image adapted from (87).

1.3.3 Pax7 is the universal marker for muscle stem cells

After the initial discovery of satellite cells, it took almost 30 years to identify the transcription factor, Pax7, as a key marker for these cells. This discovery allowed the behaviour of satellite cells to be studied in more detail. Data of genetically traced Pax7 expressed in injured muscle cells showed that Satellite cells have to regenerate muscle fibres and produce new satellite cells at the same time (75). Moreover, when *Pax7* expressing cells were ablated, muscle could not regenerate (88).

The Pax family of paired box domain transcription factors play key roles during tissue specification and organ development. In the context of myogenesis, Pax3 and Pax7 are important upstream regulators (89). Pax3 is expressed in all myogenic progenitor cells in the embryo whilst Pax7 is mainly present in the central domain of the dermomyotome, in the absence of Pax3 it is this domain that survives (90). These Pax3/Pax7 positive cells provide the self-renewing reserve cell population for muscle growth (91). After birth, Pax7 mouse mutants lose their satellite cells and Pax3 cannot compensate the role of the missing Pax7, perhaps because the protein is present at too low a level or because of divergent Pax3 and Pax7 functions by this stage (92). The role of Pax7 in adult satellite cells has been controversial. Studies showed that muscle regeneration is severely reduced when Pax7 is ablated in most satellite cells, preventing repopulation of the satellite cell pool (88,93). Consequently, in adults the satellite cell pool is not maintained, not due to cell death but probably because of premature differentiation at the expense of proliferation (93).

Artificial maintenance of Pax7 expression in myoblasts has been reported to delay differentiation (94,95). In this context, it has been proposed that Pax3 can promote satellite cell proliferation (96). As in the embryo, intervention by Pax7 gene is perhaps critical to maintaining the balance of self-renewal and differentiation.

Pax7 has been shown to directly activate Id3, which encodes a HLH inhibitor of myogenic factor activity, potentially partnering together with Id2 and preventing the onset of Myogenesis in quiescent satellite cells (97). New insight into potential Pax7 targets in satellite cells comes from genome wide ChIP-seq and transcriptome analysis carried out on primary myoblasts derived from cultured satellite cells, in which a tagged Pax7 protein is expressed (92). This data revealed that Pax7 targets many genes implicated in satellite cell function including genes involved in cell growth, cell adhesion and signalling pathways, whereas it represses genes involved in differentiation.

1.3.4 Muscle stem cells facilitate fetal and juvenile muscle growth in amniotes and continuous muscle growth in anamniotes.

The Pax7 gene is not only expressed in quiescent and activated adult muscle stem cells, but it is expressed in myogenic cells from embryonic stages (72). Ablation experiments in early stage mouse embryos show that in the absence of Pax7 positive cells, no fetal or juvenile muscle growth occurs and no adult muscle stem cells are ever organised (88). However, all studies agreed that the adult Pax7 expressing muscle stem cells (muscle satellite cells) are derived from the Pax7-expressing embryonic muscle stem cells. Moreover, they agreed that the initial role of the muscle stem cells is to create the bulk of the musculature (55).

In amniotes, after juvenile muscle masses have been laid down, adult muscle mass increases predominantly by filling muscle fibres with more contractile protein (muscle hypertrophy as opposed to muscle hyperplasia – increase in cell number) (98). However, in anamniotes such as the zebrafish, adult muscle still grows via hyperplasia similar to fetal and juvenile muscle in amniotes (12). This suggests that the basic role of muscle stem cells is to drive muscle growth. It also suggests that muscle stem cell quiescence is a special feature of amniotes.

1.4 Origin of muscle and muscle stem cells

1.4.1 All vertebrate skeletal muscle cells originate from the segmented paraxial mesoderm (the somites)

Skeletal muscles originate embryonically from the paraxial mesoderm which is a subdivision of the mesoderm, one of the three germ layers formed during the process of gastrulation early in embryogenesis (99).

Formation of mesodermal and endodermal organs takes place simultaneously with neural tube formation. The notochord forms between the base of the head and the tail with the neural tube above. Thick groups of mesodermal cells - referred to as the segmental plate in chickens and unsegmented plate in mammals - lie flanking the neural tube (66). Fate mapping experiments showed that the mesodermal cells which leave the primitive streak later on, settle anterior to the cells that leave the primitive streak earlier. As the primitive streak regresses its activity patterns the embryo in an anterior-to-posterior direction. After the complete regression of the primitive streak, new mesodermal cells are continuously added from the posterior by a mass of cells in the tail bud (100). Initially, the paraxial mesoderm is organised as mesenchymal tissue on either side of the axial midline. At this stage, the paraxial mesoderm is referred to as the segmental plate in chick and the presomitic mesoderm in mouse. Along the anterior-posterior axis, the paraxial mesoderm is later divided into segmented and nonsegmented mesoderm. The head paraxial mesoderm (which contributes to blood vessels, bones and muscles in the head) lies anterior to the otic vesicle and does not undergo segmentation. The paraxial mesoderm posterior to the otic

vesicle are segmented into reiterated units called somitomeres. These somitomeres compact and bind together encompassed by an epithelium which eventually separates from the segmental plate to form individual somites. A new pair of somites are formed every 30 minutes in the zebrafish, 90 minutes in the chick and 120 in the mouse (101). Despite being transient structures, somites are extremely important in organising the segmental pattern of vertebrate embryos. The somites eventually form the vertebrae and ribs, the dermis of the dorsal skin and the skeletal muscles of the back, body wall and limbs. Additionally, somites determine the migration paths of spinal nerve axons and neural crest cells (59). The important components of somitogenesis (somite formation) are periodicity, epithelialisation, specification, and differentiation. The first somite appears in the posterior portion of the trunk, and new somites emerge from the rostral end of the paraxial mesoderm at regular intervals (102).

1.4.2 Periodic Notch-Delta signalling, overlaid by an Fgf8 maturation gradient regulates the formation of segments

Somitogenesis has been shown to involve a molecular oscillator, the segmentation clock, which controls the periodicity of the expression of the genes involved in it. The genes are expressed rhythmically in the segmental plate. These genes belong to the Wnt and Notch pathway, in which the Wnt signalling lies upstream of Notch signalling. Axin2, an inhibitor of Wnts but directly activated by Wnt signalling, is a cyclic gene in the Wnt pathway (Fig. 1.4). The Notch related genes include members of the Hairy and Enhancer of split family of basic helix loop helix (bHLH) transcription factors that act downstream of Notch-Delta signalling, as well as the glycosyl transferase Notch signalling inhibitor, Lunatic fringe (101). Fibroblast growth factor 8 (Fgf8) signalling generates a moving front at which both segment boundary position and axial identity is established. *Fgf8* is downregulated and the cyclic genes stop oscillating around the time of somite formation when the basic-loop-helix (bHLH) transcription factor Pax3 (103) is expressed. After a defined number of expression cycles, cyclic gene expression discontinues and resolves into a stripe at the anterior or posterior border of a developing segment (101,104,105).

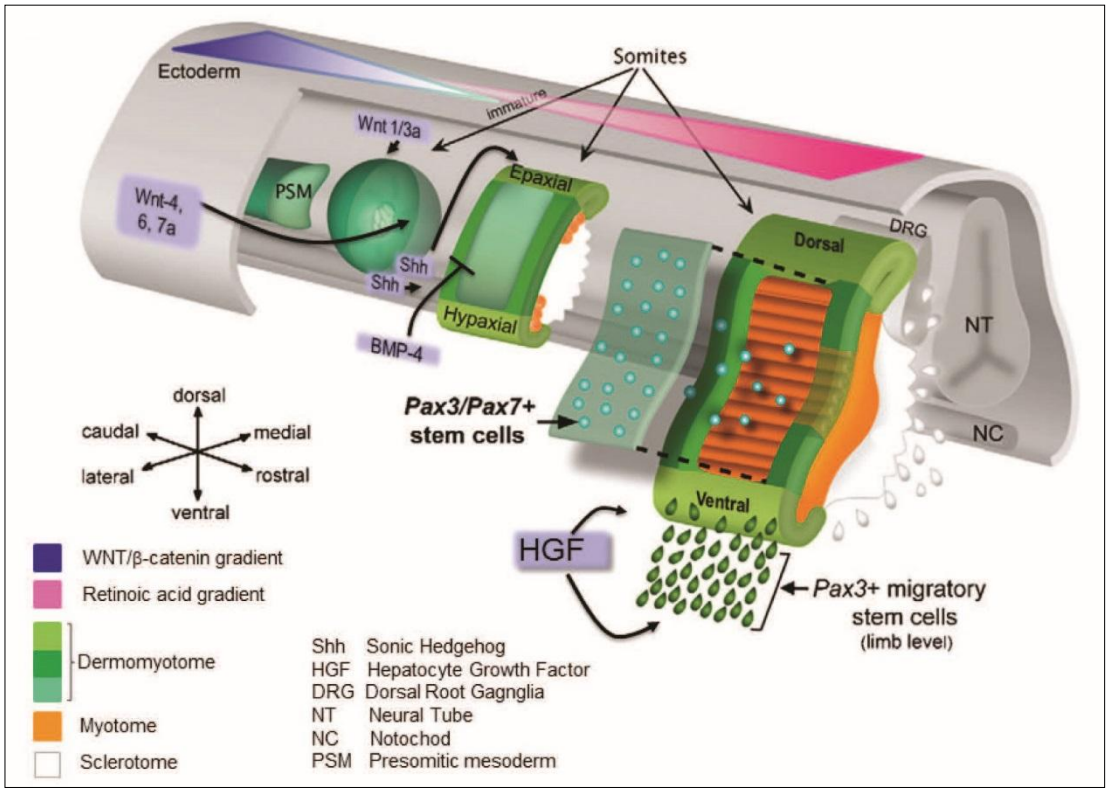

Figure 1. 4: The intricate network of genes and factors that are influencing the formation of the somite.
The positions of different factors create a map and an orientation for cell migration. The cells of the young somite developing from the presomitic mesoderm (PSM) start migrating and form an organised structure. Migration is initially influenced by the Wnt and Shh signalling factors that guide the first step forming a full somite. The presence of these two factors contributes to the elongation of the somitic structure, giving rise to the Epaxial and Hypaxial sides. The paired box proteins Pax7 and Pax3 are expressed in the dorsal part of the somites until the formation of the first muscle stem cell whereupon Pax genes are downregulated and the first Mrf gene (Myf5) is expressed. Cells of the somite start migrating from the dorsal part of the dermomyotome and colonise the layer below called the myotome, whereupon they differentiate into muscle cells. The position of the somite dictates the fate of the cells that develop from within it. At the limb level, the Pax3 cells will migrate towards the limb bud to give rise to the muscle cells that colonise the area. The presence of Hepatocyte Growth Factor (HGF) contributes to the migration of Pax3-expressing cells, guiding them to the limb. Image adapted from (106).

1.5 Gene regulatory networks controlling Myogenesis

1.5.1 Tbx6 regulates the specification of the paraxial mesoderm

T-box transcription factor (Tbx6) expression is essential for paraxial mesoderm development (107–109) whilst its paralog, Brachyury, is expressed in the axial mesoderm.

Tbx6 mutations show patterning defects in the somites which lead to malformations of the axial skeleton (110,111). These defects arise from possible misidentity of the anterior somite compartment and/or its reduction (112). Tbx6 has also been shown to affect the expression of the Notch ligand, Delta 1 (Dl) by experiments in chick and mouse showing lowered DL expression levels upon lowered or knocked out Tbx6 expression (107,110,112).

1.5.2 In amniotes, surface ectoderm derived signals upregulate Paraxis which controls somite epithelialisation

Paraxis is considered a pre-myogenic gene which facilitates the formation of the epithelial somites (104). Wnt6 is known to be expressed in the ectoderm overlying the anterior segmental plate and early somites of the chick embryo (113–116).

Wnt6 has been shown to promote the epithelial organisation of the segmental plate mesenchyme (117). Additionally, Wnt6 activity is thought to be mediated by a β-catenin-dependent pathway as blocking β-catenin or Lef1 activity in the dermomyotome depolarises somite cells and de-epithelialises the dermomyotome (118). The extended expression of Paraxis has also been demonstrated as sufficient to reverse de-epithelialisation. There, it is established that the epithelial organisation of the somites requires β-catenin activity, which in turn is mediated by Wnt6, Fz7 (Frizzled 7) and Paraxis (114) although the mechanism by which Paraxis controls dermomyotome construction remains to be clarified.

Interestingly, ectoderm Wnt genes regulate Paraxis and Pax3 in a similar manner indicating a close relationship between epithelialisation and cell differentiation processes.

Paraxis has however been shown to be expressed in non-epithelial cells such as the sclerotome (119), indicating that its epithelialising function may be context dependant and require additional factors (105,118,119).

1.5.3 Pax3 and Pax7, the master regulators of myogenesis in amniotes

Pax3 transcription is downregulated in fetal muscle, upon which Pax7 becomes the dominant factor in all myogenic progenitor cells (92). In the limb, Pax7 is initially co-expressed with Pax3 and genetic tracing experiments show that all later Pax7 positive cells in the fetal limb are derived from cells that had expressed Pax3 (76). Postnatal and adult satellite cells are marked by Pax7 expression, with continuing transcription of Pax3 in trunk muscles such as the diaphragm and some limb muscles (120). Pax7-negative satellite cells can initiate differentiation, probably due to

transcription of Myf5 in an increasing number of these cells from the perinatal period. Consistent with a role for Pax7 in the initiation of MyoD but not Myf5 transcription in most satellite cells in culture, introduction of dominant-negative Pax7 specifically abolishes MyoD but not Myf5 expression or satellite cell differentiation (72). Pax3 and Pax7 are normally downregulated prior to activation of Myogenin, cell cycle exit and differentiation and artificial maintenance of their expression in myoblasts has been reported to disrupt differentiation.

In this context, it has been proposed that Pax3 can promote satellite cell proliferation. Pax3 does not rescue the postnatal phenotypes of the Pax7 mutant mouse in muscles where both proteins are present in satellite cells. Functional differences between Pax3/Pax7 in postnatal versus prenatal Myogenesis may reflect post-translational modifications of the proteins and also association with different cofactors. During embryonic Myogenesis, Pax3 functions as a transcriptional activator (89); however, like other Pax proteins, it is a poor activator on its own, indicating the probable importance of co-activators. Pax7 has been shown to interact with the histone methyl transferase complex, which directs H3K4 histone modifications (121) in myoblasts from postnatal muscle. Pax7 mutant satellite cells show reduced heterochromatin condensation (93) pointing to a role in chromatin organisation, also recently suggested for Pax3 (122). Recent research begins to provide some insight, but mechanistically much remains to be understood about the function of Pax3 and Pax7 as transcription factors.

1.5.4 In amniotes, the somites are extensively patterned before muscle is made

The newly formed somites can be divided into two distinct parts, medial and lateral. The cells which are responsible for the formation of the two specific parts have different origins and they are fused together at the time of the gastrulation (123). The notochord and the floor plate of the neural tube produce and secrete the morphogen sonic hedgehog (Shh). The notochord also produces and secretes the bone morphogenetic protein (BMP) inhibitor, Noggin. Shh and Notch contribute to forming the ventral region of the medial somite as sclerotome, which is the origin of the ribs, vertebra, connective tissue and tendons. The sclerotomal progenitor located in the ventral region of the formed epithelial somite undergo SP ephitelia-to-mesenchymal transition (EMT) to form the new mesenchymal sclerotome (124,125). The dorsal part of the somites remained epithelia and the signalling from the Wnt and BMP from the dorsal neural tube and later, plate mesoderm, specified this region as epithelial dermomyotome (126). The dermomyotome later contributes to the formation of the trunk and limb muscles, dorsal dermis and the scapula (102). The influence from Wnt, BMP, *Paraxis and Pax3,* which were expressed in the segmental plate at the time of somite epithelialisation, become restricted to the newly formed dermomyotome (105,127). The neural tube and notochord together with the dorsal ectoderm overlying the somites influence the specification of the somitic cell fates.

1.5.5 The formation of the Dermomyotome in vertebrates

The newly formed dermomyotome matures, it extends dorsomedially and ventrolaterally as a single layer of cells resting on the basement membrane (Fig. 1.5A). In the early stage of the formation of the dermomyotome, the cells in the somites form a cavity in their centre called a lumen which is eventually filled with migrating cells to form the advanced structure of the somites (Fig. 1.5B). The cells located at the borders of the dermomyotome flex inwards ventrally, forming the dermomyotome lips, dorsomedial lip (DML), ventrolateral lip (VLL); rostral and anterior lips and caudal or posterior lips. The structure of the dermomyotome eventually disappears due to cells migrating ventrally to form the myotome and dorsally to form the dermatome (102,128). The dorsomedial part of the dermomyotome and myotome is specified by the signal of Shh and Wnt1/Wnt3a. These genes can trigger Myogenesis *in vitro* (129). The development of the later part of the dermomyotome/myotome is influenced by BMP with Wnt4/Wnt6/Wnt7 coming from the surface ectoderm (130,131). The formation of myotomal cells involves the complex translocation of the migrating dermomyotomal cells causing a phenomena called delamination (132).

1.5.6 The formation of the Myotome, the centre of muscle formation

The formation of the myotome occurs with a sequence of "**waves**" which contribute to the migration of cells and the formation of the final structure of the myotome itself (Fig. 1.5C) (133,134). The **first wave** of post-mitotic myoblasts (called pioneer myoblasts) located in the DML migrate to the rostral or caudal lip, then differentiate into myofibres to reach the caudal or rostral lip (i.e grow in a rostro-caudal direction) to form the primary myotome (Fig. 1.5D) (135). The dorsomedial-to-ventrolateral growth and expansion of the myotome occurs when a **second wave** of post-mitotic cells translocates directly into the myotome from the rostral and caudal dermomyotome lips (Fig. 1.5E). These cells intercalate between the pre-existing myofibres of the primary myotome, which acts as a scaffold. Even the DML and the VLL contribute to the formation of the myotome, but cells derived from these lips may first move to the sublip domain and then to the rostral and caudal dermomyotome lips before forming unilaterally extending myofibres (135–137). A study from Gros and colleagues showed that the cells derived from the DML or VLL do not migrate toward the rostral (or caudal) lip prior to differentiation, but they move to the myotome then elongate to reach the rostral and caudal lip (138). The second phase (or wave) combines the incremental growth at the DML and VLL and coherent growth at the rostro-caudal lips since the DML, VLL, rostral and caudal lips generate myoblasts to populate the myotome (138). In the **third wave** a population of mitotically active myoblasts enter the primary myotome from the rostral and caudal dermomyotomal lips (Fig. 1.5F) (139). At this point the myoblasts express the fibroblast growth factor receptor 4 *(Fgfr4*) (139). The dermomyotomal lips remain organised and continue to contribute to the myotome. The central dermomyotome will eventually de-

epithelialise as cells in this region undergo EMT (epithelial-to mesenchymal transition) at this point the cells will form the myotome and the dermatome (140). Recent studies show that when the central dermomyotyome de-epithelialises, the myotome experiences a massive flux of a final **fourth wave** of mitotically active, *Fgfr4*-expressing muscle precursors (141,142). In the adult muscle, the structure of the trunk is divided into two major groups: the epaxial and hypaxial muscle. The epaxial muscles are deep muscles of the back and these muscles have the important functions of maintaining posture as well as movement of the vertebral column and head. The hypaxial muscles form the limbs, the intercostal muscles and the body wall muscles that include the superficial back muscle and all lateral and ventral muscle. The hypaxial muscles are responsible for locomotion, breathing and movement of the abdomen (102,128).

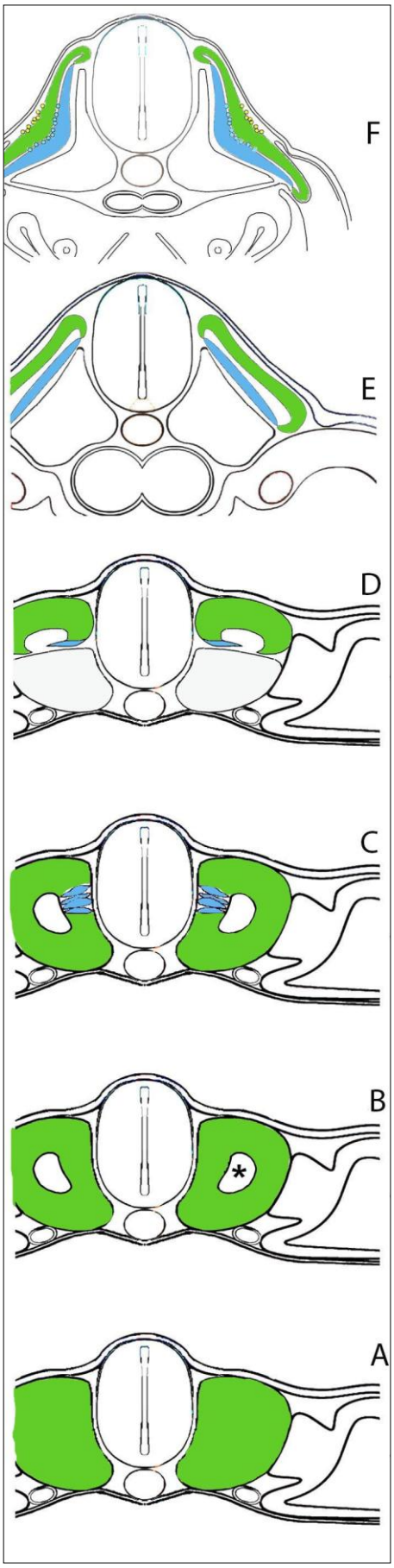
F
E
D
C
B
*
A

Figure 1. 5: Myotome formation and cell migration occurs in waves

The somites are formed through a series of cell migrations called 'waves'. Represented in the figure are the different stages of a developing chicken trunk, shown in transverse sections. The first two sections (A and B) show the early stages of development of the somites (green) whereupon the cells still express Pax7 and they are in a stem cell state. In B, the cells organise themselves for the formation of the dermomyotome upon which a cavity forms in the centre of the somites called a lumen (asterisk). The cells in the dermomyotome migrate to form a more organised structure whilst a selection of cells start to differentiate by expressing the first Mrfs, Myf5 and MyoD, giving rise to the first proliferating myoblasts (C, blue cells). The post-mitotic myoblasts migrate to the rostral or caudal lip and then differentiate into myofibres to reach the caudal or rostral lip to form the primary myotome (D, myotome in blue and dermomyotome in green). The expansion of the myotome occurs when post-mitotic cells migrate to the myotome from the rostral and caudal dermomyotome lips. These cells will form the scaffold of the myotome (E). The central dermomyotome (green) will start to de-epithelialise and will then undergo epithelial to mesenchymal transition (F). At this stage, the cells will form the myotome and dermatome.

1.5.7 Anamniotes and the quick formation of muscle during the larva stage

The formation of the muscle in anamniotes presents a few differences when compared with the formation of the muscle in amniotes. In xenopus, the first differentiated fibres in the vicinity of the notochord arise from the medial Myogenesis, whereas dorsomedial and ventrolateral groups that appear to continue growing at the tail bud stage arise from the lateral Myogenesis. The most lateral cells of the marginal zone were shown by cell tracing of the circumblastoporal gastrula cells to give rise to muscle fibres in the dorsal and ventral regions of somites (143). These experiments also showed that the most medial (dorsal) cells contribute to the association between the notochord in the head and trunk.

After stage 26, a second wave of Myogenesis is generated from the dermomyotome (144,145). Comparison of embryonic Myogenesis of mice and xenopus reveals that the first median and lateral Myogenesis shown in the frog was lost in the mammal as all trunk and limb muscles arise from dermomyotome. Despite this, similarities between the second wave of xenopus Myogenesis and mammalian Myogenesis still remain. These include: the generation of epaxial and hypaxial myogenic cells from dermomyotome; initiation with Myf5 and strong MyoG expression (146), as well as concomitant expression of Mef2c expression in the intersomitic space (146,147).

Similarly, the third wave of Myogenesis in xenopus is suggested to originate in the Pax3/Pax7 expressing progenitors of the somites (142,148). This is corroborated by the observation of Pax7-expressing muscle stem cells in the stage 46 xenopus myotome (149). It is thought that Myf5 expressing cells could participate in plurinucleated cell formation in the third wave which takes place from stage 45 onwards (150).

1.5.8 The Myogenic regulatory factor (Mrf) family of bHLH transcription factors control myogenic commitment and differentiation in amniotes

Myogenic commitment and differentiation of muscle cells is driven by the expression of Myf5, MyoD, MyoG and Mrf4, a family of bHLH transcription factors known as myogenic regulatory factor (Mrfs). They bind to E-boxes (concensus sequence = CANNTG, N - any nucleotide) as heterodimers with the E2 protein. The Mrfs can activate the transcription of muscle-specific genes, even in non-muscle cell types (151). Myf5 and MyoD are the first of the Mrfs to be expressed in muscle precursor cells (myoblasts) in the DML and VLL, and the newly formed post-mitotic myotome. However, they are not initially expressed in the same myoblasts during early Myogenesis (151,152). The epaxial myoblasts are the first to be generated in the DML and the dorsomedial wall of the dermomyotome (128). Myf5 is the first to be expressed in the epaxial myoblast where it activates the transcription of MyoD in these cells later in the post-mitotic primary myotome. The hypaxial myoblasts are generated in the VLL and express MyoD first followed by Myf5. As more cells are deployed from the DML and VLL, the myoblasts of both

lineages eventually meet and the expression of the Myf5 and MyoD becomes continuous in the primary myotome (151,152).

In *Myf5* knockout mice, the development of the myotome and subsequent expression of *MyoD, MyoG,* and *MRF4* is delayed but there is no loss of muscle phenotype (153). Similarly, muscle also develops normally in *MyoD* mice, although elevated levels of *Myf5* still persist into postnatal stages (154). However, homozygous *Myf5* and *MyoD* double knockout mice die soon after birth due to a lack of any skeletal muscles (154).

These results demonstrate that *Myf5* and *MyoD* are required for specification of myoblasts, and they can compensate for each other (Fig. 1.6). However, unlike *Myf5, MyoD* also has a function in differentiation just like *MyoG* and *Mrf4,* which direct the terminal differentiation of myoblasts into myocytes, fusion of myocytes into myotubes and eventually the alignment of myotubes into bundles or myofibres. Consistent with this, they are expressed later, in differentiated muscles (151,152). *Myf5* and *MyoD* activate the transcription of *MyoG* and *Mrf4* in epaxial and hypaxial myoblasts (155). The Mrf genes do not act alone in the stimulation of proliferation and muscle differentiation but they cooperate with other genes, like Mefs and Six that are defined as co-factors (Fig. 1.6). These genes cooperate with the Mrf genes during the various steps of the muscle formation.

1.5.8.1 Mrf proteins structure and function

The Mrf proteins are classified as transcription factors and they have a basic Helix Loop Helix (bHLH) domain structure.

The bHLH domain is ~60 amino acids long and it has a DNA-binding basic region, followed by two α-helices separated by an adjustable loop region (156,157). This domain is the site of dimerisation, allowing the formation of homodimeric or heterodimeric complexes between different family members. In this case, the Mrf proteins can dimerise with E proteins to form an important complex for myogenic activation. The two basic domains brought together through dimerisation bind specific hexameric DNA sequences referred to as “E Boxes” which have the consensus sequence (CANNTG).

The bHLH proteins have been divided into four different groups: A, B, C and D. The most important group regarding this project are group A which includes tissue specific proteins such as the Mrf members (158).

1.5.8.2 MyoD acts as a heterodimer with E12/E47

There are three different genes of E-protein in the group A of the vertebrates species: TCF3/E2A, TCF4/E2-2 and TFC12/HEB. All of these proteins can heterodimerise with MyoD and other myogenic bHLH proteins to give rise to a functional transcription factor complex (159,160). The

single knockout of individual E-proteins in the skeletal muscle has been shown not to produce any specific muscle phenotype, indicating that expression of these proteins is redundant.

The E2A gene produces alternatively spliced transcripts encoding E12 and E47, which differ by just the bHLH region (160). The E2A proteins are post-transcriptionally regulated, the most important example of which is in the case of E47, which is controlled by Notch signalling and MAP kinase activity (160). Notch signalling and the MAP kinase play an important role in skeletal muscle development which will be described in more detail later in section 1.6.2.1.

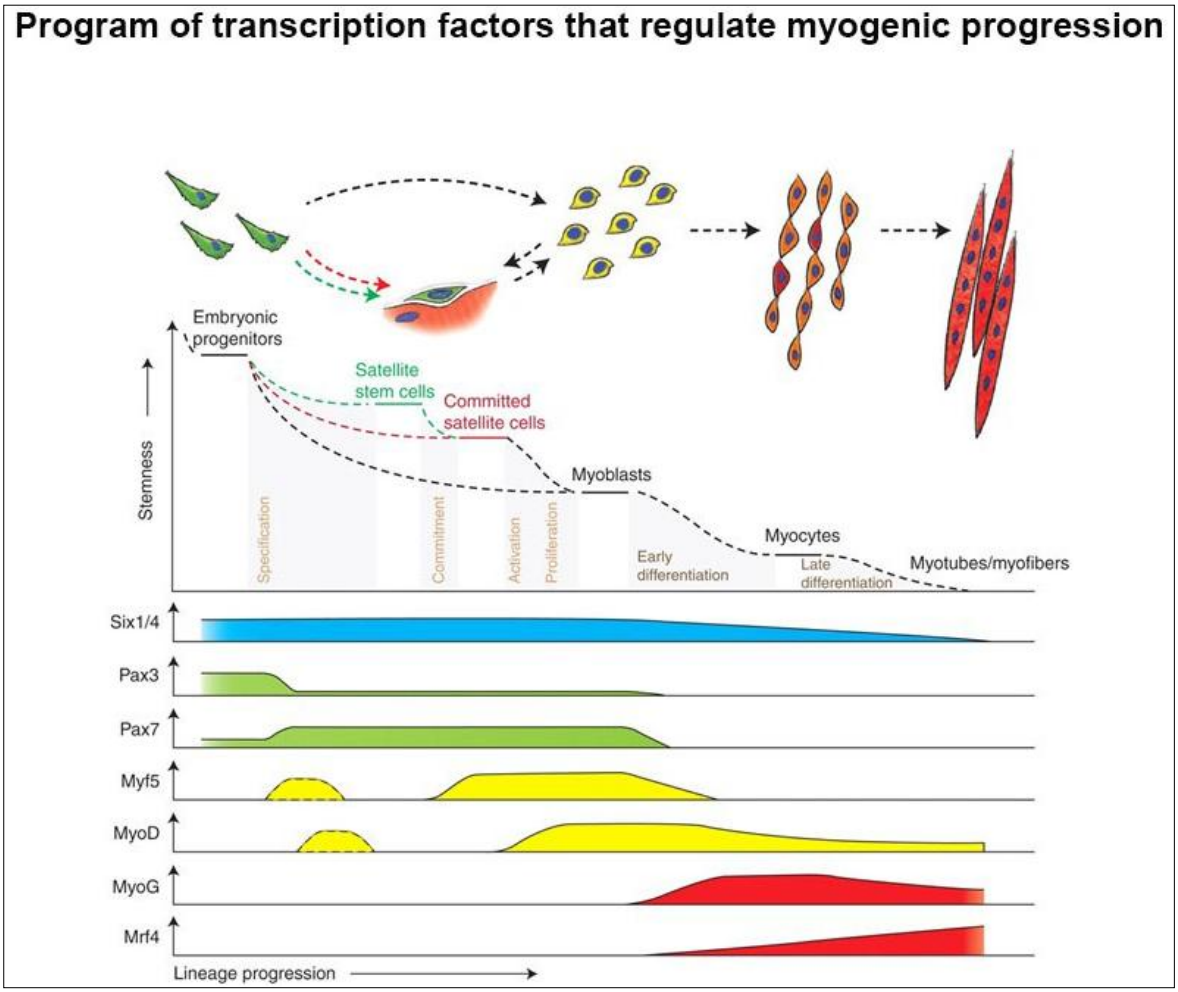

Figure 1. 6: Program of transcription factors that regulate myogenic progression

The expression of transcription factors is regulated during the differentiation of the cells through the myogenic lineage. The embryonic progenitors leave the cell cycle and differentiate into myoblasts, while a small number of satellite cells return to the quiescent state. The expression of Six1/Six4 and Pax3/Pax7 represents the master regulators of the early lineage specification, while Myf5 and MyoD commit cells to differentiate. The expression of MyoG and Mrf4 represent the last step of differentiation bringing the cell to form myocytes which will eventually fuse to form myotubes. Image adapted from (57).

1.5.9 Sine oculis and Six4 type members of the Six family of homeoproteins, activated by Eya phosphatases, aid the onset and progression of myogenesis

Six genes encode transcription factors belonging to the Orthodenticle subfamily of paired-type homeodomain proteins (reviewed in (161,162). In the vertebrate genome we can find 7 different Six genes, *Six4-Six1-Six6*, *Six2-Six3* and *Six5-Six*. RNAseq data deposited in the Ensembl data base (S. Dietrich, unpublished observations) and expression data obtained from mouse, chicken and zebrafish expression (156,163–168) showed that, with the exception of *Six9*, the *so* and *Six4*-type genes are expressed in skeletal muscle whereas the *optix* genes are predominantly expressed in the developing nervous system (169).

Six proteins carry two conserved domains. The first is the homeodomain that facilitates DNA binding of specific target sites. The second is the more N-terminally located Six domain (SD), which aids DNA binding and interacts with Groucho, Dach and Eya proteins. This interaction determines whether Six proteins act as transcriptional repressors or activators.

Groucho/Grg/TLE proteins are transcriptional co-repressors. Vertebrates have 5 Groucho genes, all of which are expressed in the young somites albeit at different levels. Dach proteins are recruited to additional sites in the chromatin by other transcription factors such as Six proteins, but also Jun or Smad 4, in this context typically acting as transcriptional repressor. Vertebrates have 2 *Dach* paralogs (teleosts: 4), and both are expressed in the dermomyotome/somite (see RNAseq data in the Ensembl database and (165).

Eya proteins carry a C-terminal 271 amino acid long Eya domain or ED that facilitates interaction with other proteins, most notably Six and Dach proteins. They also carry the two consensus sequences typical for the haloacid dehalogenase (HAD) family of phosphohydrolases. Thus, Eya proteins dephosphorylate tyrosines on target proteins in an Mg^{2+}-dependent fashion. Eya-mediated phosphorylation of Six or Six-Dach complexes allow the recruitment of the CBP co-activator as well as RNA polymerase II for the activation of target genes. Thus, the presence of Eya proteins renders Six or Six-Dach complexes transcriptional activators (170,171); reviewed in (172).

Vertebrates have 4 *Eya* genes, all of which are expressed in the somite and/or skeletal muscle (173,174) and S. Dietrich, unpublished observations). In mice, the expression of the closely related *Eya1* and *2* genes and the more distantly related *Eya4* first occurs in the dermomyotome and its dorsomedial and ventrolateral lips and later in the myotome. *Eya3* is weakly expressed in the somites yet has been shown to cooperate with Ski and Six1 in the differentiation of C2C12 myoblasts (174–177). Given that Eya proteins facilitate the activation of *Six* targets, it is not surprising that Six and Eya proteins synergise (165). *Six1* mutant mice show correct initiation of Myogenesis with muscle fibres being diminished at E13.5 of development whilst *Six4* mutants have no developmental defects (178). However, in *Six1-Six4* double mutants, expression of *MyoD*

is reduced, that of *MyoG* and *Mrf4* is abolished at E10.5, and most skeletal muscle is missing at E13.5 (164). Likewise, strong muscle phenotypes occur in an allelic series of *Eya* knockout mice only when *Eya1* and *Eya2* genes are inactivated together (174). However, the precise role of *Six* and *Eya* genes during skeletal muscle formation is complicated and controversial.

Sine oculis and the *Six4* type genes can bind to the promoters of *MyoD* and *MyoG* as well as the limb-specific enhancer of *Myf5* and drive gene expression from them (179–181) . Therefore, *Six* and *Eya* genes, like *Pax3/7* and *Paraxis*, have also been referred to as pre-myogenic genes. In the ventrolateral lips of the mouse dermomyotome, *Pax3* expression is lost when *Six* and *Eya* genes are mutated, while in *Pax3* mutant *Splotch*, ventrolateral *Six* and *Eya* expression is maintained (164,174). Thus, in this case, *Six* and *Eya* genes act upstream even of the *Pax* genes. Furthermore, Six binding to the *MyoD* promoter occurs in the context of *Myf5* deficiency, which is also an artificial situation. *Six* and *Eya* genes regulate the expression of enzymes and structural genes required for the establishment of the fast-twich, glycolytic muscle fibre type (182). Thus, *Six-Eya* genes display a key role far downstream in Myogenesis and their description as "pre-myogenic" genes may be somewhat misleading. Indeed, although *Six1* is expressed in quiescent and activated satellite cells, it is not required for satellite cell maintenance or activation, nor for *Myf5* expression. However, it plays a role in *MyoD* and *MyoG* regulation as well as satellite cell differentiation and, via the upregulation of the Erk1/2 inhibitor Dusp6 (Pyst/ Mpk3), a role in the return of the remaining satellite cells to quiescence (183).

Muscle differentiation requires cell cycle exit and the return of satellite cells to quiescence requires cell cycle pausing. It is curious that Six proteins are involved in this, given that in many cancer cell lines, Six-Eya proteins enhance transcription of Cyclin D1 during the G1 phase of cell cycle and of Cyclin A during late S phase, thereby promoting cell cycle. The role of Six-Eya proteins is highly context dependent and the link between muscle regulatory genes and cell cycle control will be explored in more detail in Chapter 10.

1.5.10 The Mef2 family of MADS box transcription factors act as Mrf cofactors

Mrf activity has been shown to be assisted by the myocyte enhancer factor 2 (Mef2) family of transcription factors in regulating the expression of muscle-specific genes (184). Mef2 proteins belong to the MADS (MCM1, agamous, deficiens, serum response factor) box-containing transcription factor family. The Mef2 family contains four members, Mef2a, b, c and d, all encoded by separate genes. In contrast to the Mrfs, Mef2 genes show widespread expression during development. Mef2 proteins specifically recognise A/T-rich DNA sequences common to the promoters of multiple muscle-specific genes (185). Mef2c transcripts are upregulated during Myogenesis in tissue culture and are induced in 10T1/2 fibroblasts by MyoG, suggesting that the Mef2c gene is a target for myogenic bHLH proteins. Mef2c transcripts appear for the first time in

myocytes, in the myotome of the somites between developmental days 8.5 and 9 with Mef2a and Mef2d expressed soon thereafter. Mef2c expression in the myotome initiates about one day later than the initial appearance of Myf5 transcripts and several hours later than the appearance of MyoG transcripts (186).

In vitro, Mef2 expression in cell lines does not result in the reproduction of the myogenic cascade. Additionally, *in vitro* evidence shows Mef2 and MyoD directly interact to activate E box/Mef2 binding site-driven reporters (representative of a muscle-specific cis-element (187)) suggesting that Mef2s may serve to support the Mrfs (188–190).

Inactivation of the murine *Mef2c* gene resulted in lethal cardiac morphogenic defects however, the lack of defects observed in the skeletal muscle was attributed to the redundancy of the Mef2 genes (191). The expression of the Mef2 family members in skeletal muscle is altered in response to the expression of MyoD and this reinforces the idea of a strong link between these proteins during muscle progenitor differentiation (192).

1.5.11 MyoD, Mef2 and Six proteins interact with each other and with histone modifying enzymes to activate muscle structural genes

As mentioned previously, the *Mrf* genes do not act alone in their activation and maintenance of skeletal muscle differentiation, but act in collaboration with other cofactors. Six1 and Mef2 proteins present themselves as the most important for this essential collaboration as they are directly induced by *MyoD* and cooperate to activate muscle genes ((181) Fig. 1.7A). Interestingly, recruitment of a demethylase to the MyoG locus (193,194) along with Six1 upregulates Pax3, Myf5, MyoD and MyoG (164,181) as well as fast-twitch muscle-function genes (195). Six1 and Six4 are essential for final muscle differentiation (164,196) and this function is in cooperation with the muscle regulatory factors (*Mrfs) MyoD* and *MyoG* in the activation of target gene transcription (196). Data revealed a strong correlation between Six binding and target gene activation during differentiation (196). *MyoD* targets chromatin remodelling complexes to the *MyoG* promoter which form a stable DNA-bound complex (197). The presence of *MyoD* facilitates the acetylation of histones at the *MyoG* promoter followed by the recruitment of *Swi/Sn*f which bind MyoD and Mef2 factors. MyoD is consequently secured to the *MyoG* promoter with the help of HATa p300 (Histone acetyltransferase) and PCAF. Subsequent rearrangement of the *MyoG l*ocus-containing chromatin exposes the E-boxes and binding sites of other factors such as *Mef2* and *Six*, creating a multi-protein regulatory complex (Fig. 1.7B (198)).

A

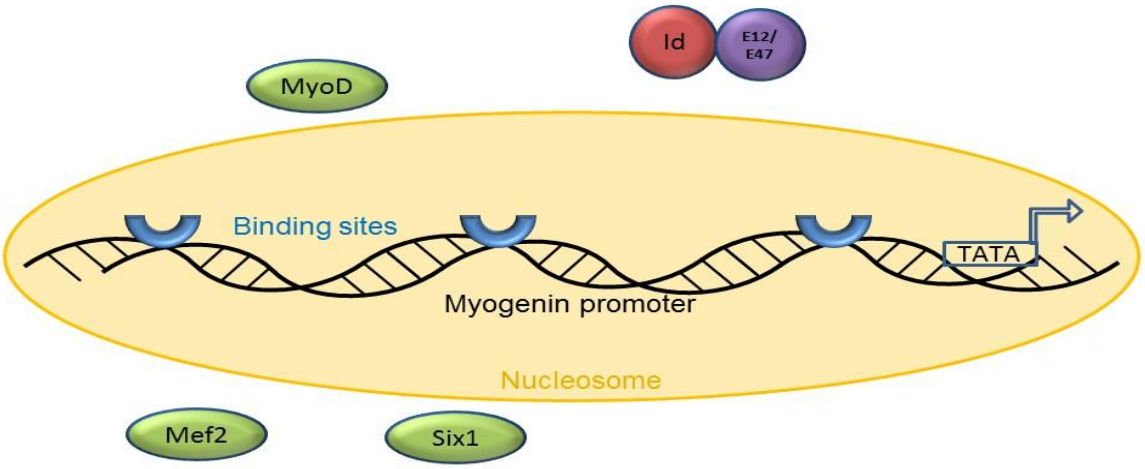
Id
E12/
E47
MyoD
Binding sites
TATA
Myogenin promoter
Nucleosome
Mef2
Six1

B

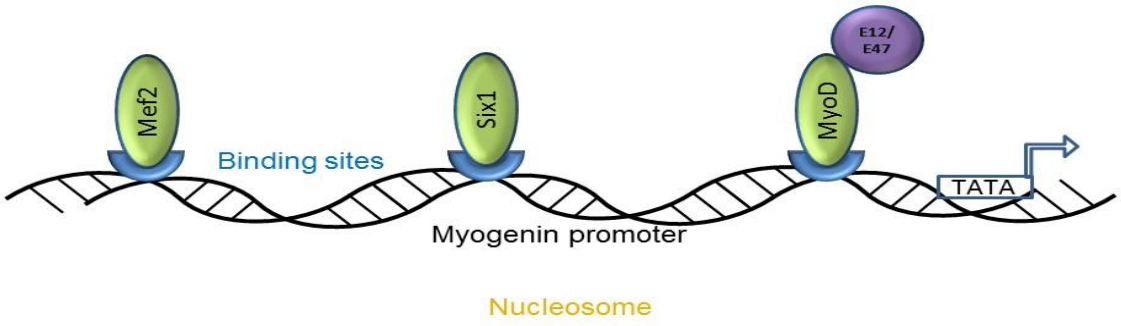
E12/
E47
Mef2
Six1
MyoD
Binding sites
TATA
Myogenin promoter
Nucleosome

Figure 1. 7: MyoG promoter activation by MyoD-targeted chromatin-remodelling.
A) In the undifferentiated myoblast, a nucleosome (yellow) is expected to obscure the relevant binding sites of Mef2 and Six factors. Id proteins sequester E-proteins, preventing the formation of MyoD/E12/E47-protein heterodimers. Mef2 and Six proteins are present but not bound to the MyoG promoter. At this stage, the chromatin is acetylated through a mechanism not yet fully understood.
B) Decreasing Id levels facilitate MyoD/E-protein heterodimerisation that interact at the MyoG promoter to recruit HATs and the Swi/Snf complex which acetylate the histones and remodel the chromatin, respectively. Remodelling of the chromatin liberates the DNA for proteins to recognise their cognate sites. Adapted from (395).

1.5.12 In parallel to the activation of muscle genes, differentiating cells must withdraw from the cell cycle

The final stage of muscle fibre formation and differentiation requires the withdrawal from the cell cycle to allow differentiation into myocytes. Recent studies have shown that *MyoD*, *Myf5* and *MyoG* have opposite roles in the control of the cell cycle. In fact both *MyoD* and *Myf5* promote the expansion of the muscle progenitor population (81,199), while *MyoG* possesses an intrinsic activity that requires the exit from the cell cycle that consequently leads myoblasts to differentiate into myocytes (200).

The Mrf proteins show different levels of expression during the cell cycle (201). *Myf5* for example shows a spike in G0, decreasing again at the end of G1 where it remains stable through mitosis, meanwhile, *MyoD* has a low spike in the G1/S transition (202). Studies that observe the behaviour of satellite cells during injuries, have discovered that satellite cells can be in a G Alert state (Fig. 1.8). This different group of Satellite cells have the capability to re-enter and conclude the first cell cycle faster than normal satellite cells. This allows the body to respond promptly to injury (203). The level of MyoD protein oscillates from a high spike in G1 and reduces in G1/S, increasing again between S and M phase of mitosis (201).

The regulation of MyoD and Myf5 protein levels is regulated by post-translational modifications which target them for degradation. Specifically, Myf5 protein levels are modulated by its phosphoregulated degradation at mitosis (204,205). At late G1, MyoD is processed through the ubiquitin degradation pathway triggered by cyclin E/CDK2-dependent phosphorylation of MyoD at Ser200 (206,207). Cyclins are a group of proteins essential for the control of the cell cycle and they can control the transcriptional activity of the Mrf genes through phosphorylation. MyoD, for example can be phosphorylated by cyclin B/Cdc2 specifically at residues Ser5 and Ser200. Phoshorylation of these amino acids reduces the DNA binding activity and the capability to activate transcription (208).

It is therefore evident that Myf5 and MyoD are closely linked to the cell cycle through regulation of their stability and activity. This is further corroborated by data demonstrating that MyoD and even Myf5 efficiently bind regulatory regions of cell cycle genes, establishing their own modulation of the cell cycle (209–211)(81).

Additionally, mouse myoblasts lacking MyoD fail to exit the cell cycle (200) demonstrating the importance of MyoD for cell cycle function. The exit from the cell cycle induced by the expression of MyoG causes the activation of CDKN1 (p21cip) (94,212) and the upregulation of specific microRNAs. It has been shown that microRNAs can directly target the mRNA of the E2F proteins and inhibit their translation (213,214). Therefore MyoG can indirectly downregulate E2F family

protein levels (215). The expression of MyoG represents a ‘point of no return’ upon which the Mrf genes initiate commitment to the program that leads the myoblasts to withdraw from the cell cycle (216). From this data, we can conclude that MyoD and Myf5 facilitate cell cycle progression whereas MyoG and Mrf4 induce exit from the cell cycle. The cell cycle and cyclins are discussed in greater depth in Chapter 10.

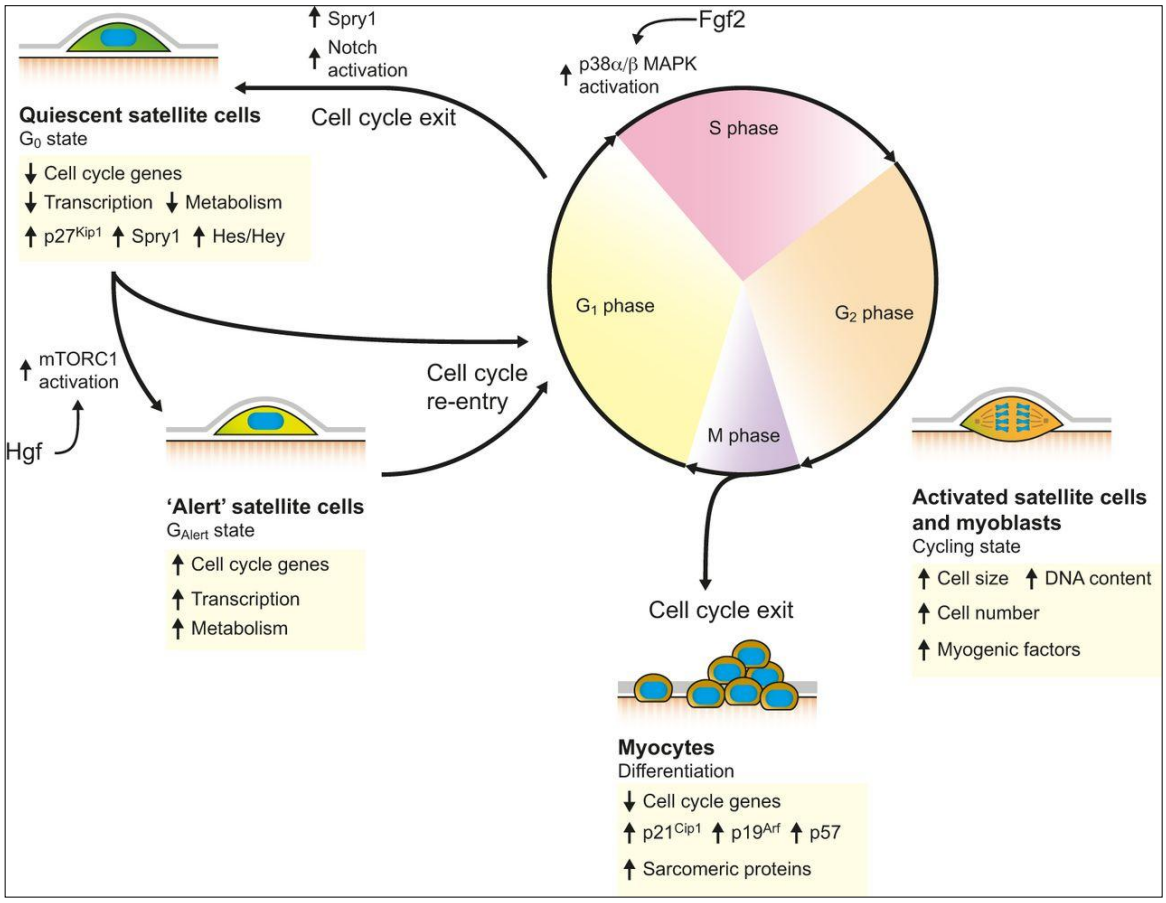

Figure 1. 8: Intrinsic and extrinsic factors regulate the cell cycle of satellite cells

The effect of intrinsic signals regulate the dormant state of satellite cells in a reversible G0 state. In case on injury, the Satellite cells re-enter the cell cycle or via the intermediate state "G-alert". The satellite cells can return to quiescent state through the expression of Spry1 or Notch. Exit from cell cycle will force the satellite cells to differentiate into myoblasts and then myocytes, consequently upregulating the expression of the cell cycle inhibitors such as p21, p19 and p57 whilst downregulating the cell cycle genes. Image adapted from (87)

1.5.13 Differentiating muscle cells switch off the precursor/stem cell genes – a role for miRNAs

The human genome contains thousands of non-coding RNAs of which the most studied are microRNAs (miRNAs). This group of RNAs regulate gene expression at the post-transcriptional level by suppressing the translation of mRNAs through the recognition of complementary 'seed' regions of one or more mRNAs, usually in the 3'UTR (217). Recognition of an mRNA target by a miRNA results in downregulation of the target through either blocking translation and/or the degradation of the target in a process called RNA interference (218). Many miRNAs are expressed in skeletal and cardiac muscle suggesting their specific role in the control of Myogenesis (219). The more common muscle-specific miRNAs are: miR-1, miR-133, miR-206 and miR-208, which appear to be under the control of MyoD and the bHLH transcription factor Twist which cooperate with Mef2 (220,221). Data extracted from chromatin immunoprecipitation followed by microarray (ChIP on chip) showed that MyoD and MyoG bind sequences upstream of miR-1 and mir-133 (222).

Analysis of mice deficient in Myf5 and MyoD revealed a specific requirement of Myf5 for miR-1 and miR-206 (223). At early developmental stages, the expression of both miR-1 and miR-206 was almost entirely absent in the somites of Myf5-mutant embryos, whereas mouse embryos lacking MyoD showed an apparently normal expression of both miRNAs (224). Whilst miR-133 and miR-206 are expressed from independent loci, miR-208 is derived from the intron of the α-myosin heavy chain (αMHC) mRNA (225). Some experiments suggest that miRNAs are strictly involved in myogenic differentiation as indicated by the absence of miR-1 and miR-133 in undifferentiated myoblasts which are conversely upregulated upon differentiation (226).

The regulatory roles of miR-206, miR-486, and miR-27 for example are not just linked to the Mrf family genes but are involved with a wider number of genes such as Pax3 and Pax7 (227). miR-1 and miR-206 have been shown to downregulate Pax3 during muscle differentiation (227,228). Similarly, Pax7 was described to be under the control of miR-1 and miR-206 (229,230). Consequently the feedback loop that amplifies MyoD-induced terminal muscle differentiation involves the transcriptional switch towards late factors such as Mef2c but also the epigenetic downregulation of muscle stem cell factors such as Pax3 and Pax7 (229). Given the roles that they play, it can be concluded that miRNAs are a key determinant in myogenic gene control therefore, efforts made to expand the understanding of these mechanisms would provide valuable information. However, current understanding of miRNAs functions remains contradictory due to issues with experimental strategies. Overexpression experiments in which the miRNAs are expressed at high levels may not be representative of the miRNAs expressed at endogenous levels. The presence of non-physiological levels of miRNAs might cause off target effects and therefore wrong conclusions about function as it has been shown for small interfering RNAs (231).

1.6 Intrinsic and extrinsic factors which could influence the possible protection of the muscle stem cell state *in vivo*

The generation of muscle cells occurs by numerous steps that start from gastrulation and the formation of the germ layers before progressing to the formation of the primitive streak and the cell migrations to construct the immature paraxial mesoderm in chick. Later the tissue will then advance and generate the dermomyotome and then establish the myotome through epithelialisation, whereupon the cells that migrated from the dermomyotome will colonise the myotome and differentiate in the final stage of muscle cell formation. During this process, muscle stem cells are exposed to many different cell and tissue types which can affect the progression of differentiation through extrinsic factors. The intricate network of genes which drive myogenic progenitor differentiation coupled with extrinsic signals which are considered most important in muscle stem cell differentiation are therefore important to consider (87,232).

1.6.1 Systemic factors involved in the control of muscle stem cells

1.6.1.1 Oxytocin

Muscle aging is characterised by a lower capacity to regenerate after injuries as well as muscle atrophy which together compromise the function of the muscle and is called sarcopenia (233). The satellite cells localised in the aged muscle can repair the damaged tissue but they are reversibly inhibited by the aged niche (234). Recent experiments identified the presence of numerous factors that influence the aging of cells such as TGF-β, Wnt and CCL11 chemokine which reduce neurogenesis, influencing cognition and memory (235–237). An important factor linked to satellite cell maintenance is Oxytocin, a nanopeptide produced by the hypothalamus (238). Oxytocin acts through its receptor which upon activation binds protein kinase C and induces intracellular calcium release which in turn acts as a second messenger to induce a cascade of intracellular changes (239). Oxytocin is required for muscle tissue regeneration and homeostasis, but during aging its levels in plasma decline, reducing its effects on the muscular tissue. Data shows that inhibition of oxytocin in young mice reduces muscle regeneration whilst genetic deletions of oxytocin cause no developmental defects in muscle but instead lead to premature sarcopenia (240).

1.6.1.2 Diabetes and enhanced Tgf beta signalling

The production of pancreatic β-cells is essential for the control of glucose homeostasis. Autoimmune and non-autoimmune diabetes cause depletion of pancreatic β-cells which result in mild and severe metabolic disorders along with increased blood glucose levels (241,242). Förster and colleagues showed that the depletion of the β-cells caused by the injection of streptozotocin *in vivo* (a compound used to induce toxicity in β-cells) caused drastic changes in the regenerative response of muscle stem cells, measured by the ability to give rise to proliferating myoblasts. Regeneration competency quickly deteriorated *in vivo* and muscles fail to repair after injuries

(243). It was shown however, that the injection of insulin into diabetic mice restores muscle tissue regeneration (244). Streptozotocin inhibits satellite cell responses by inducing Myostatin/pSmad3 signalling, and follistatin (a small molecule inhibitor of TGF-β receptor) which recover satellite cell response and improves muscle repair in the diabetic patients. Myostatin is discussed in more detail in Section 1.6.2.2.

1.6.2 Local control by cell-cell communication

1.6.2.1 Lateral inhibition involving Notch-Delta signalling

Notch signalling mediates cell-cell communication by the interaction with the two ligands Delta and/or Serrate, thereby activating a signalling cascade (245). The role of Notch has been attributed to the regulation of embryonic and post-natal skeletal muscle (246) and it has been shown that the forced activation of Notch in cultured myoblasts inhibits their differentiation (247). Later, this was shown to be true *in vivo* as well (132). Notch signalling is also involved in muscle stem cell proliferation and differentiation (248) and can influence somitogenesis (249). For this, Notch guides the formation of the somite structure by imposing somite borders as well as establishing anterior and posterior polarity (102,250). Delta null mice present prominent defects in skeletal muscle and dramatic hypotrophy of the muscle tissue. This defect seems to be caused by the premature differentiation of the muscle stem cells, followed by the loss of the Pax3/Pax7-expressing myogenic progenitor cell pool (251). Myogenesis in Delta null mice is present in the early embryo but is prematurely terminated disallowing formation of normal musculature. This data confirm the role of Notch in the prevention of precocious differentiation and thereby the maintenance of progenitor pool expansion (252).

1.6.2.2 Suppression of Tgf beta signal transduction

Myostatin, a secreted factor of the TGF-β superfamily, is another important regulator of muscle growth. Deletion of Myostatin in animals creates a dramatic increase in muscle mass (253,254) whilst its overexpression in skeletal muscle induces a decrease in muscle mass (255). In recent years, Myostatin levels were revealed to correlate with muscular dystrophy as dowregulation of Myostatin improved the muscular mass in the context of various myopathies (256,257). Cultured myogenic cell lines of primary myoblasts used to investigate Myostatin function *in vitro* demonstrated inhibition of myoblast proliferation and cell cycle withdrawal through activation of the CDK inhibitor p21 (258,259), as well as simultaneously inhibiting myogenic differentiation (259). Myostatin is used to maintain the undifferentiated state of the satellite cells (260) however, this hypothesis has not yet been tested *in vivo*.

The introduction of Myostatin protein-coated microbeads into developing chick limb buds altered proliferation of Pax7-expressing cells as well as downregulating the genes: Myf5, MyoD and Pax3 (253,261). This specific effect of Myostatin is reversible upon removal of the beads (262). In adult

satellite cells, myostatin signalling reverses quiescence and causes muscle progenitors to withdraw from differentiation (260). Additionally, overexpression of Myostatin in somites changes the balance between differentiated muscle cells and muscle progenitors in the favour of differentiated cells (262)

1.6.2.3 Suppression of Fgf signal transduction

Reversible quiescence is widely accepted to be a defining property of adult stem cells. This alternation between quiescence and activation is essential for the maintenance of tissue stem cells and the tissue as a whole (263). The mechanism by which satellite cells revert back to quiescence to renew the stem cell pool is only partially understood. A key component of regeneration processes and myogenic fate decision is Receptor Tyrosine Kinase (RTK) signalling (264,265). The ligands involved in RTK signalling such as FGF and HGF, are known to be proficient in activating satellite cells (266). Elevated levels of FGF, sourced principally from aged satellite cells results in loss of quiescence and depletion of the local stem cell pool which therefore reduce regenerative capacity (267). The consequences of aged stem cells is therefore their incapability to retain stem cells in a quiescent state (267).

1.6.2.4 Ang1 signalling from nearby non-muscle cells return satellite cells to quiescence

Several markers have been associated with murine quiescent satellite cells, such as M-cadherin (268,269), syndecan 3 and 4, CD34, calcitonin receptor (270), and Myf5. However, satellite cells have been shown to have greater proficiency in self-renewing when not expressing Myf5 (18). Many genes are involved in the regulation of myogenic cell proliferation and differentiation, but direct regulators of quiescence and self-renewal are scarcely known; p130 from the Rb family impedes cell cycle progression and differentiation in human cultures, thereby regulating the stem cell pool (271). Satellite cells in normal adult skeletal muscle are located close to capillaries (272). Ang1 and Tie2, expressed highly in quiescent and undifferentiated stem cells, bind each other to cause reversion to stem cell status. This was confirmed *in vivo* by loss- and gain of function experiments in skeletal muscle satellite cells (273).

1.6.2.5 Wnt7a and the expansion of the stem cell pool by promoting symmetrical cell division

Wnt signalling is very important in the paraxial mesoderm for embryonic myogenic induction (274,275), as well as in the control of differentiation during muscle fibre development. The Wnt planar cell polarity (PCP) pathway drives the orientation of myocyte growth in the developing myotome (276). Wnt signalling is required for activation of adult stem cells for the repair of damaged muscle tissue (277).

Canonical Wnt/β-catenin signalling activates and recruits reserve myoblasts (278) as well as controlling myogenic lineage progression by limiting Notch signalling and thus promoting differentiation in satellite cells within adult muscle (279).

Wnt receptor Fzd7 has been shown to be markedly upregulated in quiescent satellite stem cells indicating involvement of non-canonical Wnt signalling. Wnt7a was later revealed to be expressed during muscle regeneration and enhances muscle regeneration through the induction of symmetric satellite stem cell division by acting via the Fzd7 and Vangl2 components of the planar cell polarity (PCP) pathway. The PCP pathway is thereby indicated to regulate the renewal of the stem cell pool during adult skeletal muscle regeneration (280).

Elevated quantities of fibronectin (FN) in the microenvironment of committed satellite cells were discovered at the initial response to injury. Ligation of FN to the Fzd7/Sdc4 receptor complex is essential for the early stage expansion of the stem cell pool by Wnt7a as was shown by knock down of FN, consequently causing reduction of the satellite cell pool and the subsequent capacity of the muscle to regenerate (281).

This auto-regulation of the FN content in satellite cells was shown to be an essential ability for correct maintenance of satellite cell pools.

The FN content of satellite stem cells was demonstrated to be lower than in satellite myogenic cells (281) indicating that committed daughter cells of an asymmetrical division are capable of instructing the satellite cell to enhance its sensitivity to Wnt7a/Fzd7 signalling. This feedback between satellite myogenic and satellite stem cells is proposed to provide a means by which the size of the satellite cell pool and the ratio of its committed/non-committed components is controlled.

Wnt7a–Fzd7 activation of the planar cell polarity pathway is completely independent of IGF-receptor activation resulting in enhanced skeletal muscle repair. Wnt7a–Fzd7 therefore activates specific pathways at defined developmental stages during the progression of Myogenesis through a non-canonical anabolic signalling pathway in skeletal muscle (282).

1.6.2.6 JAK-STAT signalling stimulates symmetrical division of satellite cells

The regenerative capacity of skeletal muscle diminishes with age which is characterised in mice as a reduction of satellite cell contribution to regeneration and self-renewal. Analysis of gene expression in relatively older mice identified increased JAK-STAT signalling (283). Investigation with JAK2/STAT3 knockdown in cultured myofibres significantly stimulated satellite stem cell division. Moreover, genetic knockdown of JAK2 or STAT3 in satellite cells transplanted into regenerating tibialis anterior muscle greatly enhanced repopulation capacity. Investigation into pharmacological inhibition of JAK2 and STAT3 produced similar expansion and engraftment results. Subsequent use of these drugs by intramuscular injection enhanced muscle repair and force generation following cardiotoxin injury. This shows promising prospects for future development of a therapy for tackling muscle wasting disease (284,285).

1.7 Aims of this study

Previous reports showed that the Mrfs are sufficient to drive non-myogenic cells to become muscle cells *in vitro*. Currently, limited evidence exists to support that this is the case *in vivo*, whilst preliminary data indicates the contrary. Broadly, the aim of this project was to investigate this gap in knowledge. The use of embryonic muscle stem cells importantly allows us to characterise the behaviour of cells during muscle formation. This approach could help understand the pathologies associated with muscle degeneration and how muscle diseases could be detected in early development. As explained in section 1.3.2, satellite cells (adult muscle stem cells) are considered a heterogeneous group of muscle stem cells with different markers expressed compared to the embryonic myoblasts. It is therefore thought that future therapies utilising reprogrammed stem cells would be more easily developed by starting with embryonic myoblasts. The aims of this work will link together basic investigations to understand wild type myogenic differentiation with more applied investigations into how the genes involved in muscle development can be used to manipulate muscle generation.

This study will specifically involve:

1. Characterising the expression of known myogenic genes at a range of developmental stages to enable the compilation of a time course to inform future experiments.
2. Misexpressing Mrfs and/or known cofactors in various early stage stem cell tissues and analysing the effects on gene expression by various molecular techniques such as *in situ* hybridisation and immunohistochemistry.
3. Searching for gene misexpression conditions under which early stage stem cell tissues can be forced to differentiate into muscle cells.

Chapter 2

2 Materials and Methods

2.1 Stock solutions

Unless otherwise stated, solutions used in RNAse sensitive protocols were treated with 0.05 % (v/v) DEPC and autoclaved. Water double distilled/deionised (ddH_2O) in a water purification unit was sterilised by subsequent autoclaving. All the other stock solutions were sterilised by autoclaving.

2.1.1 *In Situ* Hybridisation (ISH) and Immunohistochemistry (IHC) stock solutions

10 % BBR — Boehringer 's blocking reagent (Roche) dissolved in MAB by autoclaving and stored in 10 ml aliquots at -20°C.

Bleaching solution — 5 % Formamide (Sigma) 0.5 × SSC pH 4.5
10 % H_2O_2 (Sigma)

2 % Cysteine — 4 g cysteine (Sigma) 150 ml 0.1 M MBS
10 pellets of concentrated NaOH
5 M NaOH was added to bring the solution to pH 8.0

Detergent mix — 1 % Igepal (Sigma), 1 % SDS, 0.5 % Sodium Deoxycholate (Sigma), 50 mM Tris-HCl pH 8.2, 1 mM EDTA and 150 mM NaCl (Fisher) in DEPC-ddH_2O.

Glycerol — Glycerol (Fisher) diluted in DEPC-PBS to 20 %, 50 % and 80 %.

Goat Serum — Goat serum (Sigma), heat inactivated at 56 °C for 30 min and stored in aliquots of 10 ml at -20 °C.

Hybridisation mix — 50 % Formamide (Sigma), 5 x SSC pH 4.5, 2 % SOS, 2 % BBR, 250 µg/ml tRNA (Roche), 100 µg/ml heparin (Sigma) in DEPC-ddH_2O.

1M Levamisole — Levamisole (Sigma) dissolved in ddH_2O and stored in aliquots of 1 ml at -20 °C.

MAB pH 7.5 — 100 mM Maleic acid (Sigma), 150 mM NaCl in ddH_2O, ddH_2O treated and autoclaved.

MABT — MAB with 0.1 % Tween-20 (Sigma)

MBS — (Modify Barth's Saline) 88 mM NaCl, 1 mM KCl, 2.4 mM $NaHCO_3$, 15 mM HEPES-NaOH pH 7.6, 0.3 mM $Ca(NO_3)_2$, 0.41 mM $CaCl_2$, 0.82 mM $MgSO_4$, 50 mg/ml Gentamycin.

MEMFA

0.1 M MOPS pH 7.5	2 ml	0.5 M
2 mM EGTA pH 8	40 µl	0.5 M
1 mM Mg_2SO_4	20 µl	0.5 M
3.7 % Formaldehyde	1 ml	37 %

NTMT with azide	100 mM NaCl, 100 mM Tris-HCl pH 9.5, 50 mM $MgCl_2$, 1% Tween-20, 2mM Levamisole, 0.02 % Sodium azide (Sigma) in ddH_2O.
NBT	Stock 100 mg/ml in demethylformamide (Boehringer)
BCIP	Stock 50 mg/ml in demethylformamide (Boehringer)
1 x PBS	Phosphate buffered saline tablets (Sigma) dissolved in ddH_2O according to manufacturer's instructions, DEPC treated and autoclaved.
PBT	PBS with 0.1 % Tween-20.
4 % (w/v) PFA	Paraformaldehyde (Sigma) dissolved in PBS with stirring and, heating at 60 °C. 10 ml aliquots were stored at -20°C.
20 % SDS	Sodium dodecyl sulphate (Sigma) dissolved in DEPC-ddH_2O.
20 x SSC pH 4.5	3 M NaCl, 0.3 M sodium citrate (Sigma) dissolved in DEPC-ddH_2O. pH adjusted to 4.5 with 1 M citric acid.
Solution X	50 % Formamide, 2 x SSC pH 4.5 and 1 % SDS in ddH_2O.
Solution 1	50 % de-ionised formamide, 5 × SSC pH 4.5, 1 % SDS in ddH_2O
Solution 2	5 M NaCl, 1 M Tris pH 7.5, Tween 20 in ddH_2O
Solution 3	50 % formamide, 2 × SSC pH 4.5
Tris-HCl pH7.5, 8.2, 9.5	Trizma base (Sigma) dissolved in DEPC-ddH_2O, pH adjusted with concentrated hydrochloric acid (HCl).
Triton X-100	4-(1,1,3,3-Tetramethylbutyl) phenyl-polyethylene glycol (Sigma).
Tween-20	Polyoxyethilene sorbitan monolaurate (Sigma)

2.1.2 Molecular Biology solutions

1.5 % LB Agar	Agar (Sigma) mixed in LB medium.
LB medium	1 litre Luria-Bertani medium: 10 g tryptone (Sigma), 5 g yeast extract, 10 g NaCl in ddH_2O. pH adjusted to 7.5 with sodium hydroxide and autoclaved.
50 x TAE	242 g Tris base (Sigma), 57.1 ml glacial acetic acid, 100 ml 0.5 M EDTA (pH 8), in ddH_2O to 500 ml.

2.1.3 Albumin Petri dishes culture solutions

35 mm Petri dishes (Fisher).
50 ml Falcon tubes (Fisher).
10 ml pipettes
120 ml of thin albumen, collected from 2 dozen incubated eggs.
120 ml of simple saline, autoclaved (7.19g NaCl/ 1 l distilled water).
0.72 g Bacto-Agar (Sigma).
Penicillin/Streptomycin (Sigma)

2.1.4 β-galactosidase

50 mM $K_4Fe(CN)_6$
50 mM $K_3Fe(CN)_6$
1 M $MgCl_2$
10 % NP40
40 mg/ml X-Gal (Euromedex) in formamide
40 mg/ml Red-Gal (Sigma) in formamide
PBS/$MgCl_2$:1 × PBS containing 2 mM $MgCl_2$

2.2 Molecular Biology

Unless otherwise stated, a benchtop centrifuge (Heraeus instruments PICO 21) at 13000 rpm (17900 x g) was used for all centrifugation steps.

2.2.1 Plasmid Vector and bacterial strain

The general cloning vector was pCAB-GFP conferring ampicillin resistance. This was used for cloning all the genes used in chicken models. The vector is 5770 bp and it has a cytomegalovirus (CMV) enhancer and chicken beta actin promoter. More details are described in Chapter 4 (Fig. 4.5). The vector pCS2+ was used to clone Mrf and mouse MyoD constructs genes for producing mRNA used in Xenopus injections. Contains a strong enhancer/promoter (simian CMV IE94) followed by a polylinker and the SV40 late polyadenlyation site. An SP6 promoter is present in the 5' untranslated region of the mRNA from the sCMV promoter, allowing *in vitro* RNA synthesis of sequences cloned into the polylinker. A T7 promoter in reverse orientation between the polylinker and the SV40 polyA site allows probe synthesis, as well as a second polylinker after the SV40 polyA site to provide several possible sites to linearise the vector for SP6 RNA transcription. The vector backbone is from pBluescript II KS+ and includes the ampicillin resistance gene. α-select Chemically Competent cells (Silver Efficiency) (Bioline) were used for the transformation step.

2.2.2 Transformation of competent cells

Frozen 10 µl aliquots of competent α-cells were thawed on ice, mixed in a 1.5 ml micro-centrifuge tube with 0.5 µg of plasmid DNA, and kept on ice for 5 minutes. The DNA was forced into the cells by heat shocking the bacteria at 42 °C for 45 seconds, then placed on ice for a further 2 minutes. Following this, 900 µl of pre-warmed SOC medium was added to the tube. The cells were then plated onto pre-warmed LB agar plates containing 100 µg/ml ampicillin to select for transformed cells. The plates were incubated overnight at 37 °C.

2.2.3 Bacterial Stock

Bacterial stocks were prepared by re-suspending 200 µl of homogenised bacteria, cultured overnight at 37 °C, in 800 µl glycerol. The mixture was quickly frozen in liquid nitrogen and then stored at -80 °C.

2.2.4 Ligation

DNA fragment/insert of interest was isolated by gel eletrophoresis and purified by gel extraction kit (section 2.2.10). Both the insert and the desired vector were digested with the same restriction enzymes, again isolated and purified by the same methods. T4 DNA ligase in the DNA rapid ligation kit (Roche) was used to ligate the insert and vector at room temperature for 5 minutes. Once complete, the ligated product was directly transformed into bacteria.

2.2.5 Screening for transformants and PCR

Successfully ligated transformants were screened by PCR with the following conditions: 95°C tor 1 minute, then denatured, annealed and extended at (95°C tor 15 seconds, 65°C *tor* 15 seconds, 72°C *tor* 2 minutes) for 5 cycles; (95°C *tor* 15 seconds, 50°C *tor* 15 seconds, 72°C tor 2 minutes) for 25 cycles, and then at 72°C for 6 minutes. Individual colonies from the original LB plate with transformants were dipped into a free grid cell on a replica LB plate and then dipped into the corresponding PCR tube/well. The replica plate was incubated at 37°C overnight. The transformants containing the insert of interest was cultured in LB medium overnight tor mini-preparation, and confirmed by restriction enzyme digest and DNA sequencing.

2.2.6 Mini-preparation of plasmid DNA

A single colony of transformed *E.coli* cells was inoculated into 5ml of LB medium with 1OOµg/ml ampicillin and cultured overnight at 37°C shaking at 250 rpm in an IKA KS 4000 I control orbital incubator. The cells were homogenised by brief vortexing and pelleted by centrifugation for 5 minutes. The Qiagen miniprep kit was used to extract DNA according to the manufacturers' instructions. Briefly, the pelleted cells were resuspended in Buffer P1 to which RNaseA had been added to a final concentration of 1OOµg/ml. The cells were lysed by adding Buffer P2 to the suspension and mixed by inverting the tube. The lysis reaction was neutralised with Buffer N3, which precipitates genomic DNA and proteins. The solution was mixed thoroughly by inverting the tube, and then centrifuged tor 1O minutes. The supernatant containing the plasmid DNA was applied to the QIAprep spin column and centrifuged for 1 minute. The DNA bound to the column was washed with Buffer PE and eluted with 50 µl ddH_2O by centrifugation, again tor 1 minute. The miniprep DNA was stored at-20°C.

2.2.7 Maxi preparation of plasmid DNA

Ali centrifugations in this process were performed in a Heppendorf 5804R at 4°C. A single colony of transformed *E.coli* cells was inoculated into 250ml LB medium with 25Oµg/ml ampicillin, cultured overnight at 37°C with shaking at 250 rpm. The overnight culture was divided into 50ml polypropylene centrifuge tubes and centrifuged. The cell pellets were combined into a single 50ml polypropylene centrifuge tube before proceeding with the Qiagen Maxi Kit protocol.

2.2.8 Agarose gel electrophoresis

DNA and RNA were routinely analysed by gel electrophoresis with 1 % (w/v) agarose gels in 1 × TAE buffer. Typically 1 g of agarose (Sigma) was dissolved in 100 ml TAE buffer by heating in a microwave. The molten gel was cooled and ethidium bromide (Sigma) was added to a final concentration of 0.5 µg/ml before pouring. The gel was run at 70 V in an electrophoresis tank (Bio-Rad) using TAE as the running buffer. DNA was visualised under ultraviolet illumination. A 1 kb or a 100 bp DNA ladder (Promega) was run alongside the samples as a marker to determine the size of the DNA fragments.

2.2.9 Restriction analysis

Plasmid DNA was digested using restriction enzymes and buffers provided by New England Biolabs (NEB), Promega or Roche. A typical reaction mixture consisted of up to 2µg of plasmid DNA, 1 µl of the appropriate restriction enzyme (final activity, 0.2-0.5 units/µl), 5 µl of the corresponding buffer and sterile ddH_2O added to a total volume of 50 µl. The digest was incubated for 3-12 hours at 37 °C. Specific DNA fragments and linearised plasmid DNA were purified using gel extraction techniques.

2.2.10 Gel extraction and purification

Following a double restriction digest or a polymerase chain reaction (PCR), a specific DNA fragment was purified using the Machenery-Nagel (NucleoSpin Gel and PCR Clean-up) gel extraction kit. The DNA was first separated on an agarose gel using eletrophoresis. The fragment was excised under UV illumination and weighed. Three volumes of Buffer NTI were added to 1 volume of gel (assuming that 10 µl-100 mg) and the gel was melted at 50 °C for 10 minutes. One gel volume of isopropanol was added to the sample, mixed, then applied to a spin column and centrifuged tor 1 minute. Buffer NT3 containing ethanol was used to wash the bound DNA in the column by centrifugation. The column was then transferred to a fresh 1.5 ml microcentrifuge tube and the DNA was eluted with 50 µl of ddH_2O, again by centrifugation.

2.2.11 NTP/CAP

The PCR template the mMESSAGE mMACHINE Kit is designed to function best with templates that code for RNA transcripts in the 0.3 to 5 kb range. The kit can be used to produce shorter, or longer

RNA. 4 µl of water was mixed with 10 µl NTP/CAP, 10 µl 10 x reaction buffer, 1-2 µl DNA (1 µg) and 2 µl of Enzyme mix. The mixture was incubated for 2 hrs at 37 °C. 1 µl Turbo DNAse was then added to the mixture and incubated for a further 15 mins at 37 °C.

2.2.12 NanoDrop

All nucleic acids produced for the experiments were analysed at the NanoDrop 2000c (UV-Vis spectrophotometer) to verify the absorbance and the initial analysis for the purity.

2.2.13 DNA sequencing

DNA sequencing was conducted offsite by DNA sequencing service provided by Source Biosciences, Cambridge. DNA and primers were diluted in ddH_2O to a final concentration specified by the provider. Inserts cloned into pCAB-GFP vector were sequenced with the universal M13 forward (5' - CCAGGGTTTTCCAGTC ACG - 3') and the M13 reverse (5' - TCACACAGGAAACAGCTATG - 3') primers or with pCAB-F forward (5'- CTACAGCTCCTGGGCAACGTGC - 3') and pCAB-R reverse (5' – GCTGAACTIGTGGCCGTTIAC - 3') primers. Different primers were used to sequences the constructs cloned in pCS2+. Sp6pCS2+ (5'-ATTTAGGTGACACTATAGAAGAGAAGC-3') and T3pCS2+ (5'-AATTAACCCTCACTAAAGGGAGAAAAAG-3').

2.3 Subcloning Mrf constructs into pCS2+ vector for preparing mRNA

The chicken Mrfs (Myf5, MyoD, MyoG and Mrf4) and three different mouse MyoD were cloned in pSC2+ vector. The constructs were digested with Cla1 and EcoR1 to cut the ORF with the restriction digestion analysis. The fragments were ligate in the pSC2 (see 2.3.4) and transform in competent cells. Colonies were verified and test with PCR and run in agarose gel. Colonies were chose and used for the mini prep and incubate overnight. The mini prep were digested and run in the gel to verify the exact size of the fragment. One verified the mini prep were linearised with Not1. The DNA of the constructs was treated with transcription reaction using (Fisher mMessage mMachine KiT) using a NTP/CAP. This transcription mixture allows the single step production of 5'-prime capped mRNA. The RNA was nanodrop for measuring the concentration and to verify the initial assessment of the purity. Few problems came out with the MyoG constructs and we could to not cloned it pSC2 via subcloning therefore another an alternative strategy was used. The ORF was PCR-amplified using a Forward primer (ATTTAGGTGACACTATAGAAGAGAAGC) incorporating an upstream SP6 promoter and the Reverse primer (AATTAACCCTCACTAAAGGGAGAAAAAG).

2.4 Manipulation of embryos

2.4.1 Chicken embryos

Fertilised chicken eggs were obtained from Henry Stewart and Co (Peterborough, UK). They were incubated at 38 °C for the required stage (4.5 hours per stage). The embryo was harvested by cracking the egg open into a glass dish. The embryo was removed from the yolk by cutting into the yolk sac and putting the embryo into PBS using a spatula to wash. The vitelline membrane was removed and for embryos HH14 onwards the amnion was removed over the top of the rostral region. Embryos were thenput into fixative.

For embryos HH9 to around HH14, the embryos were staged by counting somites. However not all somites are the same within a given HH embryos, since the earlier formed anterior somites are developmentally more mature than later formed posterior somites. Thus, the developmental age or flank/trunk somites (S) was determinate according to Christ and Ordahl 1995 (128), modified by Pourquie' in 1999 (286) , which takes into consideration both the maturation of the somites and HH of the embryos. For older stages embryos HH20/23/24 staged according to the morphological features described by Hamburger and Hamilton (287).

2.4.1.1 Fixing embryos

Chicken embryos fixed in 4 % PFA/PBS were left overnight and then stored long term in PBS. Xenopus embryos were fixed in MEMFA for 30-40 minutes, followed by two 30 minute methanol washes and then stored long term in methanol. All embryos were stored at 4 °C.

2.4.1.2 Filter rings culture (ES)

Heat a water bath to 49 °C. Add the saline to a sterile 500 ml flask and bring it to boiling, using a hot plate/stirrer. Add the agar and stir until it is dissolved. While the agar is dissolving, collect the thin albumen in a sterile Falcon tube (50 ml) or similar container. Place the tubes into the water bath at 49 °C. Once the agar is dissolved, put the flask into the water bath. Allow the liquid to equilibrate at 49 °C. On a flat surface, lay the sterile Petri dishes with their lids removed. Add the albumen to the flask containing the dissolved agar, and mix by swirling for 30–60 sec. Also add the penicillin/streptomycin to this mixture, 5 U/ml. Using a sterile 10 ml pipette or similar device, aliquot 2.5 ml of the mixture per Petri dish. Once the aliquoting is complete, replace the lids of the Petri dishes and leave the dishes for several hours or overnight at room temperature to dry. Store them at 4 °C. After the 21 hr of incubation to reach HH4 according to Hamburger and Hamilton (287) eggs were spray with ethanol 70 % and let cold down on the bench for 30 minutes. Eggs were opened in a glass petri dish and the thin albumin was removed using pieces of tissue paper. A piece of filter paper with a central aperture was placed gently onto the vitelline

membranes, such that the embryo is framed in the centre. Using scissors, cut through the vitelline membranes around the filter paper, taking care to cut completely around its perimeter. With forceps, gently pull the filter paper away from the yolk in an oblique direction. Place the embryo in the petri dish with the albumin and place the plate under the microscope and remove the excess of the yolk with saline using a pastette. Keep the embryos in box keeping the moist with wet paper.

2.4.1.3 Dil labelling

Fluorescent vital dyes Dil (Invitrogen) was diluted in ethanol to 0.5 % Dii. The dye was injected into the primitive streak of the HH4, 5 and 6 embryos as showed in the chapter 5 (Fig. 5.1). The labelling was performed under a Zeiss Stemi SV11 fluorescent stereomicroscope. And analysed under the Zeiss Axioskop 2 plus after the amount of time necessary to allow the embryos to reach the desired HH10.

2.4.2 Xenopus embryos manipulation

Xenopus laevis embryos were de-jellied in 2 % cysteine to separate the embryos, and were carefully washed in 1 × MBS to remove the cysteine. The embryos were then transferred into 0.1 × MBS and no more than 50 embryos were placed into a large Petri dish. The embryos were incubated at 14, 18 or 23 °C for the required stage (288). Once the embryos reached the required stage they were then into fixative. Embryos were staged according to Nieuwkoop and Faber (289).

2.5 Electroporation

2.5.1 In *ovo* electroporation

Fertilised chicken eggs were incubated until HH16. The eggs were sprayed with ethanol to prevent contamination and sellotape was placed over the top of eggs. Using a sterile needle (Fisher), a hole was placed at one end of the egg and 2-2.5 ml of albumin was removed. Another hole was placed, slightly off centre at the top of the egg, through the sellotape. A window was cut into the shell using curved scissors to expose the live embryo. 2- 3 drops of PBS + ampicillin were added to prevent the embryos drying out. 1 µl of fast green (Sigma) was added to 5 µl of expression construct in a 1.5 ml reaction tube and a small quantity was transferred to a fine glass needle and placed into a micromanipulator.

The vitelline membrane was removed from above the embryo with fine forceps. The injection needle was placed inside the caudal somites and the construct was injected into the lumen of the somites. The platinum cathode (set up on micromanipulator) was placed into the neural tube and the tungsten cathode (hand-held) was used to give pulsed to the somites (Fig.2.1). The fine microsurgical electrode was used to pierce the somites and allow the construct to migrate towards the positive electrode. 3 pulses of 15 V with 50 ms width, 50 ms delay and 50 Hz frequency was applied and the electrodes were then removed. A further 1-2 drops of PBS were applied to the embryo; the lid of the egg was replaced and sealed with sellotape. The embryos were then reincubated until the required stage.

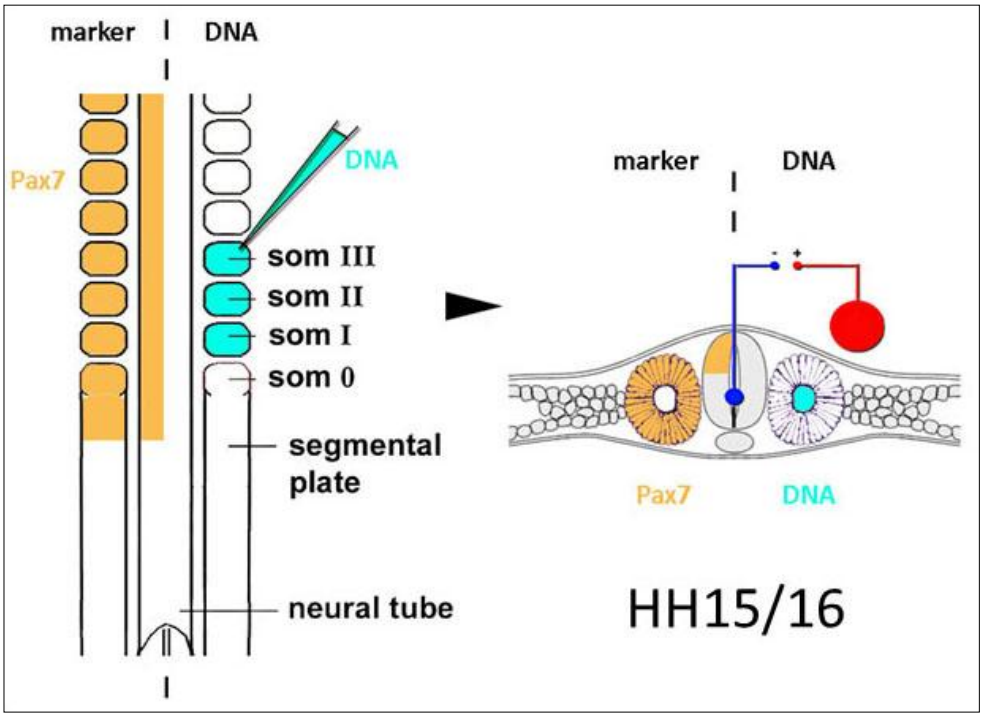

Figure 2. 1: Electroporation in somites

Schematic view of the electroporation *in ovo*. The somites were electroporated injecting the lumen of the somites with a microsurgical needles. The negative electrode was place in the centre of the neural tube and the positive electrode was moved close to the electroporated somites, giving one pulse or two per somites.

2.5.2 Electroporation in EC

Electroporation was performed in EC culture with the embryo facing ventral side up, HH4. The embryos was place in a custom made chamber in an electrode build in the center of it. A small volume of saline was put on the top of the embedded electrode to avoid the embryos to stick to the bottom of the chamber and increase the conductibility. The embryos were transferred from the petri dish to the chamber and saline was add on top to the embryos to avoid fiscal contact between the electrode and the tissue. DNA at 1 mg/ml was mixed with fast green to allow visualization of the injection and injected into the primitive streak using an Eppendorf Fem-microinjector capillary needles (Fig. 2.2). Electrodes were made from 1 mm diameter platinum wires flame sharped. These were placed above the area to be electroporated and five pulsed of 50 V, 50 ms width, 50 ms delay and 50 Hz were delivered using an Intra-cell TSS20 Dual Pulse isolated stimulator. Embryos were then incubated at 38 °C for 12 hours which the embryos to reach HH10.

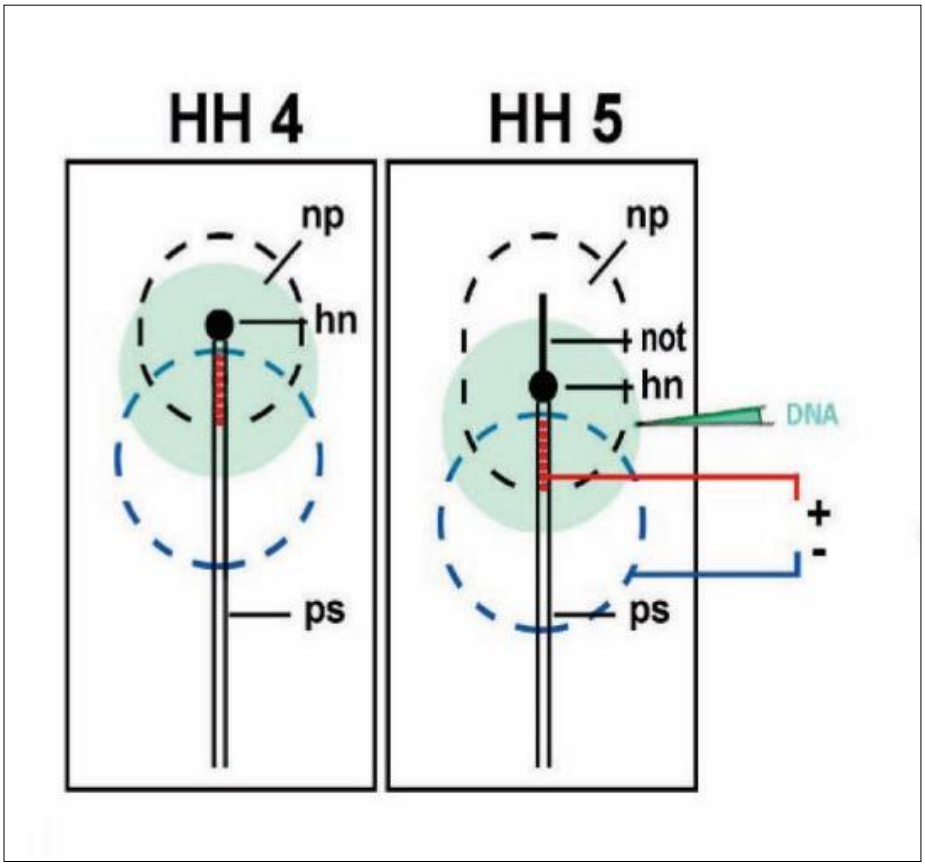

Figure 2. 2: Electroporation of HH4-5 embryos in EC culture

The embryos were electroporated ventral side up. The HH4 embryos were placed on custom made chamber and the embryos was placed on the top of the electrode imbedded in the chamber and moved to reach the desire position with the Hansen's node and the neural plate on the electrode (dashed black circle). The embryos was electroporated on the primitive streak (Dashed blue circle). The HH5 embryos showed the first appearance of the notochord. In this case the primitive streak appear shorter and the neural plate appeared bigger (dashed back circle). The embryos was electroporated in the primitive streak (dashed blue circle) and pulses were applied to pull the DNA towards the positive electrode.

2.5.3 Fixation after electroporation

Embryos electroporated at HH4 were harvested after 12 hrs of incubation. The embryos were taken out of the albumin plates and put in trays and covered with PBS. Using sharp scissors, the filter ring around the embryos was removed as well as the excessive tissue around the embryos. The head was freed from vitelline membrane and the forebrain was subsequently pierced to improve the quality of the IHC and ISH staining. Using a spatula, the embryos were placed carefully in a petri dish and covered with 4 % PFA.

Embryos harvested at HH20/24 were taken out from the egg with a spatula and put in a petri dish with PBS. The embryos were dissected using sharp forceps and scissors and the amnion and allantois were removed. Once the embryos were freed from all membranes, punctures were made in the telencephalon and the mesencephalon. This important step was included to facilitate the unhindered movement of the IHC and ISH solutions thus allowing the reduction of background signal.

2.6 Immunohistodetection of proteins in whole mount

Embryos fixed in 4 % PFA/PBS were already stored in PBS so were ready to use. As embryos fixed in MEMFA and were stored in methanol, they needed to be rehydrated from 75 % MeOH to 25 % MeOH and then placed in PBS. Chick embryos were prepared by opening up the hindbrain roof plate and making a cut between the telencephalon vesicles, to improve penetration of the antibody into the tissue.

2.6.1 Use of the primary antibody

Embryos were placed into individual wells in a 24-well dish, in which all washes were performed at 4 °C on a shaking platform. The pigmentation of the *Xenopus* embryos was removed in an additional bleaching step. Bleaching solution was added to the embryos and placed on a light box for approximately 20 minutes until the embryos were white. The bleaching solution was removed by washing three times with PBS. Three 1 hour washes with PBS removed any excess fixative or bleaching solution, followed by PBS/5 % serum/1 % Triton X-100/0.1 % H_2O_2 that was left overnight at 4 °C. Goat serum (Sigma) was used to block non-specific protein binding. Triton X-100 was used as it is a non-ionic detergent and allows cell permeabilisation and PBS (Phosphate Buffered Saline) was used as it ensures the pH of the solutions remain constant.

The H_2O_2 solution was washed off with three 1 hour washes of PBS/5 % serum/1 % Triton X-100. The primary antibody was then added at the relevant concentration (Table 2.1) to the following solution: PBS/10 % serum/1 % Triton X-100/0.02 % Na-azide. This solution was left on the embryos for 3-4 nights at 4 °C to allow the antibody to diffuse throughout the embryo and bind to

its appropriate antigen. The addition of Na-azide allows the primary antibody solution to be preserved and used again.

2.6.2 Use of the secondary antibody

Any unbound primary antibody was washed off with three 1 hour washes of PBS/1 % serum/1 % Triton X-100, followed by the addition of the secondary antibody at the relevant concentration (Table 2.2) with the following solution: PBS/5 % serum/1 % Triton X-100. The secondary antibody solution was left on overnight at 4 °C. If a fluorescent antibody was used the embryos were kept in the dark. Any unbound secondary antibody was then washed off with three 1 hour washes of PBS/1 % serum/1 % Triton X-100.

2.6.3 DAB (3,3'-Diaminobenzidine) labelling with HRP (horseradish peroxidase) conjugated antibody

HRP conjugated antibodies were washed twice with 100 mM Tris-HCl pH 7.5 for 30 minutes and incubated with inactive DAB solution (filtered) for 3 hours. Active DAB stain (3 µl H_2O_2 per 1 ml DAB) was added to the embryos for up to 15 minutes (no longer than 1 hour) until the somites and the heart were clearly labelled. To stop the reaction the embryos were rinsed with ddH_2O three times, followed by three 30 minute PBS washes. The embryos were fixed with 4 % PFA/PBS overnight and then put into 80 % glycerol for long term storage.

2.6.4 Fluorescence immunostaining

For fluorescently labelled antibodies, the embryos were washed with PBS for 30 minutes followed by fixing with 4 % PFA/PBS for 1 hour. The embryos were then put into long term storage with 80 % glycerol.

2.6.4.1 Double-labelling immunohistochemistry

The basic protocol (Sections 2.7.1 and 2.7.2) was followed but two different primary antibodies that were raised in different species (rabbit and mouse) were used. Both the primary and secondary antibodies were added to the solutions at the same time. The secondary antibodies used were conjugated to different colour fluorescent dyes so they could be individually detected and distinguished by exciting at different wavelengths.

2.7 Immunohistofluorescence detection of proteins in OCT treated sections

2.7.1 Cryostat sections and antigen retrieval

Chicken embryos were used for immunohistochemistry on cryosection slices. The embryos store in 4 % PFA in PSB were rise 5 times in PBS. The whole embryos was dissected to extract the central part of the truck that contained the electroporated somites and washed in 10 % sucrose in PBS overnight. Then wash in 20 % sucrose in PBS 6 hrs. Embedding standard wells (VWR) were

used to embed the embryos in OCT. A volume of OCT was placed in the well to fill the bottom then a pastette was used to transfer the embryos in to the well. The embryos were moved to be in a correct vertically straight position. The block was left in dry ice for a few minutes to make sure that the OCT and the embryos were thoroughly frozen and then transferred to be stored at -80 °C.

The block was then mounted onto the cryo-block using OCT in the cryostat machine (HM525 NX). The block was trimmed using a razor blade and left in the machine to reach the stable temperature of -22 °C. The sections that were cut were between 10-15 µm. The sections were positioned on adhesion microscope slides (MARIENFELD) ready to use and store in a box overnight at 4 °C and then moved to -80 °C.

2.7.2 Use of the primary antibody

The slices were positioned in a tray were we could manipulate them without any problems. The slices were first fix in 4 % PFA in PBS using 400 µl per slide, spreading over the sections and using a blue tips held at a shallow angle. We decided to don't use the bucket to avoid the loss of the slices. The slices were wash 3 times for 3 min with PBS and then left one hr in 5 % serum in PBS.

The primary antibody was added in 5 % serum in PBS and left over night at 4 °C. To keep the antibody to don't dry out we placed a small cover slips made from clear parafilm. The slide was positioned carefully with forceps and removed the day after. Antibodies used in the immunos are all collected in Table 2.1.

2.7.3 Use of the secondary antibody

After the overnight incubation slices were wash 5 times with PBS for 3 min each. The secondary antibody was added in 5 % serum in PBS and left incubate for 2 hr room temperature. After the incubation the slices were washed 3 time in PBS and fixed for 5 minutes in 4 % PFA in PBS. The PFA was rinsed away in two PBS washes.

2.7.4 Dapi staining

10 µl Dapi/Hoechst in 12 ml PBS was incubated on the slides for 5 min. The Dapi was washed away with PBS and then rinsed with H_2O. The slices were left to dry and then covered with 125 µl of Fluoromount-G (Fisher) and subsequently with a cover slip.

Table 2. 1: Primary and secondary antibodies used in this work

Primary antibodies (red heading) are listed by the name, supplier, antigen determinant, type, antigen retrieval and dilution. The same order is used for the secondary antibodies (yellow heading).

Primary antibodies	Supplier	Antigenic determinant	Type	Antigen retrieval	Dilution
anti-Desmin	Dako	human Desmin purified from skeletal muscle, known to recognise the avian protein	mouse monoclonal (IgG1)	HIER pH 9	1:50-1:100
MF20	Developmental Studies Hybridoma Bank	light Meromyosin from chicken pectoralis muscle, detects all sarcomeric Myosins	mouse monoclonal (IgG2b)	-	1:200
anti-Myh7	Sigma	partial human Myh7 peptide, 87 % identity with corresponding chicken sequence	rabbit polyclonal	HIER pH 6	1:100
anti-Myh15	Sigma	partial human Myh15 peptide, 58 % identity with corresponding chicken sequence	rabbit polyclonal	HIER pH 6	1:50
anti-TroponinI (skeletal, slow)	Sigma	partial human Tnni1 peptide, 79 % identity with corresponding chicken sequence	rabbit polyclonal	HIER pH 6	1:50
Anti-GFP	Abcam		mouse monoclonal IgG1		1:500
Anti-GFP	Life Techonoly		rabbit polyclonal		1:500
Anti-Pax7	Hybridoma Bank		mouse monoclonal IgG1		1:10
Anti-Histone H3	Millipore		Rabbit polyclonal		1:500
Secondary antibodies	**Supplier**	**Antigenic determinant**	**Type**	**Antigen retrieval**	**Dilution**
anti-mouse IgG+IgM (H+L) horse radish peroxidase	Jackson Immuno	mouse IgG and IgM and light chains of other mouse Ig	goat	-	1:200
anti-mouse IgG (H+L)- Alexa fluor 594	Jackson Immuno	whole mouse IgG	goat	-	1:200

anti-rabbit IgG (H+L)-Alexa Fluor 488	Invitrogen/ Jackson	whole rabbit IgG	donkey	-	1:200
anti-mouse IgG1 Alexa fluo 488	Jackson immuno		goat	-	1:200
anti-mouse IgG1-DyLight 594	Jackson immuno		goat	-	1:200

2.8 Whole mount *in situ* hybridisation

2.8.1 DNA template synthesis

The DNA template for the probes required for analysis by *in situ* hybridisation was amplified using PCR (Section 2.2.5).

The following reagents were mixed in a 0.2 ml PCR tube: 21.5 µl dH_2O, 25 µl 2 × BioMix Red (Bioline), 2 µl DMSO, 0.5 µl M13 (100 µm) F-primer, 0.5 µl M13 (100 µm) R-primer, 0.5 µl Plasmid.

The programme used was: 1 minute at 95 °C, 5 × (95 °C for 15 seconds, 65 °C for 15 seconds, 72 °C for 2 minutes), 25 × (95 °C for 15 seconds, 50 °C for 15 seconds, 72 °C for 4 minutes) and a final step of 72 °C for 8 minutes.

2.8.2 RNA probe synthesis

A reaction mixture containing 37.5 µl dH_2O, 5 µl 10 × transcription buffer (Roche), 2 µl RNA labelling mix (DIG or Fluorescein, Roche), 0.5 µl RNase inhibitor (Roche), 3 µl PCR template (Section 2.3.2) and 2 µl RNA polymerase (T3, T7 or SP6, depending on the template, Roche) was put into a 1.5 ml reaction tube. The reaction was incubated for 2 hours at 37 °C and 2 µl of the reaction was run on a gel to check the probe had been synthesised correctly. 2 µl RNase-free DNaseI (Roche) was added to the reaction and incubated for 15 minutes at 37 °C. This was then purified with post reaction clean up columns (Sigma) and the probe was stored at -20 °C. All the probes used are displayed in Table 2.2.

2.8.3 Preparation of the embryos

Chicken embryos fixed in 4 % PFA/PBS were prepared by cutting between the telencephalic vesicles and opening the hindbrain roof. The embryos were dehydrated then stored in methanol at -20 °C overnight or longer. This allows the membranes to become permeable and enhance staining.

2.8.4 Hybridisation of the embryos

Embryos were placed into individual wells in a 24-well dish, rehydrated and bleached with 6 % H_2O_2/MeOH, followed by two 5 minute PBT washes to remove any remaining methanol. The embryos were washed three times in detergent mix for 20 minutes, for 20 minutes and again followed by PBT washes. The detergent mix washes were different between the stages. We realised that the use of the 3 washes in detergent mix were making the HH4, 8 and 10 embryos very permeable and fragile, so we decided to reduce the number of washes to just 3 for 5 minutes. The standard washes were kept for the HH13 to 24. The embryos were then put into 4 % PFA/PBT for 20 minutes and then washed 3 times for 5 mins in PBS. The pre-hybridisation mix was pre-warmed to 70 °C and pre-incubated with the embryos for 1 hour. The hybridisation mix,

which contains 5 µl of probe per 1 ml pre-hybridisation mix was added to the embryos and incubated overnight at 70 °C.

2.8.5 Detection of the probe using alkaline phosphatase (AP)-conjugated antibodies

Solution X was pre-warmed to 70 °C and used to wash the embryos four times for 30 minutes each, removing the hybridisation mix and any unbound probe. MABT was then used to remove the Solution X with two 30 minute washes at room temperature. MABT/2 % BBR/20 % serum bleaching solution was added to the embryos for 1 hour. AP-conjugated anti-digoxigenin antibody (1:2000, Roche) was added to the MABT/2 % BBR/20 % serum solution and incubated with the embryos for 3 nights at 4 °C. The antibody was then washed off with seven 1 hour MABT washes and then one overnight wash at 4 °C.

To avoid a back ground embryos were sometime treated with RNAse. After the one night incubation with probes embryos were washed with the pre-warmed Solution 1 3 time for 30 minutes at 70 °C. Than 1/10 Solution 1/Solution 2 for 10 min at 70 °C and washed 3 times for 5 minutes with the Solution 2. 100 µg/ml RNAse A was add at the Solution 2 and incubated for 30 minute at 37 °C for two washed. The embryos were washed twice with the pre-warmed Solution 2 at 70 °C and we carry on with the same protocol with MABT washes.

2.8.6 Staining reaction

To stain the embryos they were first washed with NTMT (pH 9.5) for 10 minutes. The substrate solution was made with 10-20 µl of NBT/BCIP (Roche) per 10 ml NTMT. The substrate solution was removed from the embryos and washed with NTMT for 5 minutes and replaced with fresh substrate solution every time that the substrate changed to a pink colour. The substrate solution was left on the embryos for hours or days to allow staining. Once staining was finished, the embryos were washed in NTMT and then PBT for 10 minutes each. The embryos were finally fixed in 4 % PFA/PBS overnight and then put either into 80 % glycerol for long-term storage or PBS for double-labelling with immunohistochemistry.

2.9 β-galactosidase staining

β-galactosidase mRNA was injected into the blastomeres with a total amount of 250 pg in a volume of 9.2 nl. Embryos were fixed for 20 minutes in MEMFA, followed by 5 washes for 5 minutes in PBS/$MgCl_2$. Subsequently, embryos were stained for 2 h at 37 °C by using fresh Fe/Na-phosphate solution containing 0.1 % Triton X-100 and 0.027 % X-gal (5-bromo-4-chloro-3-indolyl-β-d-galactopyranoside), refixed for 1 h in MEMFA (0.1 M MOPS, 2 mM EGTA, 1 mM MgSO4, 3.7 % formaldehyde, pH 7.4) and stored in 100 % methanol. The *in situ* hybridisation protocol was then carried out.

Table 2. 2 Antisense probes for *in situ* hybridisation:

Probes used for whole mount *in situ* hybridisation (ISH). Cloning of inserts into the vectors pMK-RQ and pMA-T was carried out by Life Technologies, Germany. Unless stated otherwise, sequences are from *Gallus gallus*.

Gene	Source	Fragment size (base pairs)
Genes expressed in the gastrulating and immature trunk paraxial mesoderm		
Tbx6	RT- PCR fragment obtained from HH13-17 cDNA using the primers F: 5'- CCTGCTGGTGAGCAGGGAG-3' RT7: 5'-TAATACGACTCACTATAGGGAGA-CTGCATGATCCACAGCCGCG-3' The fragment was verified by sequencing.	597
Trunk premyogenic genes		
Paraxis	gift from E. Olson(Šošic et al., 1997)	717
Pax3	gift from P. Gruss (Goulding et al., 1993)	660
Pax7	gift from P. Gruss (Goulding et al., 1993)	582
Six1	gift from C. Tabin (Heanue et al., 1999)	700
Eya1	gift from A. Streit (Christophorou et al., 2009)	1000
Myogenic regulatory factor genes		
Myf5	open reading frame, synthesised and cloned into pMK-RQ	785
MyoD	open reading frame, synthesised and cloned into pMK-RQ	909
MyoG	open reading frame, synthesised and cloned into pMK-RQ	694
Mrf4	open reading frame, synthesised and cloned into pMK-RQ	738
Mef2 genes		
Mef2a-probe 1	EST clone WTSIp6101M23667Q	730
Mef2a-probe 2	open reading frame, synthesised and cloned into pMK-RQ	1647
Mef2c probe 1	gift from T. Schultheiss (Alsan and Schultheiss, 2002)	500
Mef2c probe 2	open reading frame, synthesised and cloned into pMK-RQ	1431
Mef2d	RT- PCR fragment obtained from HH13-17 cDNA using the primers F: 5'-CGTGACCAACCAGAACACAC-3' RT7: 5'-TAATACGACTCACTATAGGGAGA-GAGTGAGTCGCTTGGGAGAC-3' The fragment was verified by sequencing.	450
Mef2b	RT- PCR fragment obtained from HH13-17 cDNA using the primers F: 5'-AATGAGGGCATGGATCTGAC-3' R: 5'-TAATACGACTCACTATAGGGAGA-GAAACCAGTGAAGGCTGTGG -3' The fragment was verified by sequencing.	414
Genes labelling myogenic cells generated from the rostro-caudal edges of the dermomyotome		
Follistatin	gift from A. Graham (Graham and Lumsden, 1996)	800
Pitx3	gift from T. Ogura (unpublished PCR fragment, 3' half	1000

	of open reading frame)	
Genes encoding proteins facilitating cell adhesion and muscle contraction		
Cdh4 = Cadherin 4 = R-Cadherin	gift from C. Redies (unpublished PCR fragment)	900
Des = Desmin	3' half of the open reading frame, synthesised and cloned into pMK-RQ	747
Troponin I 1 (Tnni 1)	RT- PCR fragment obtained from HH13-17 cDNA using the primers F: 5'-AGCAGCTCCCAGGAGATCAG-3'; RT7: 5'-TAATACGACTCACTATAGGGAGA-CATGCAGCTGCATGGGCAC-3' The fragment was verified by sequencing.	921
Myh15	position 1168-2388 of the open reading frame, synthesised and cloned into pMA-T	1224
Myh7	position 2173-3138 of the open reading frame, synthesised and cloned into pMA-T	966
Genes involved in cell cycle control		
	Cyclins	
CcnA1	open reading frame, synthesized and cloned into pMA-T	507
CcnA2	open reading frame, synthesized and cloned into pMK-RQ	492
Ccn B2	gift of F. Pituello	1310
CcnB3	open reading frame, synthesized and cloned into pMK-RQ	1309
Ccn D1	gift of F. Pituello	878
Ccn D2	gift of F. Pituello	877
Ccn D3	gift of F. Pituello	879
Ccn E	gift of F. Pituello	1226
Ccn E2	gift of F. Pituello	509
CcnO	open reading frame, synthesized and cloned into pMK-RQ	924
Cyclin dependent kinases		
Cdk1	gift of F. Pituello	689
Cdk2	open reading frame, synthesized and cloned into pMA-T	403
Pseudopodoces humilis Cdk4	open reading frame, synthesized and cloned into pMK-RQ	737
Alligator mississipiensis Cdk4	open reading frame, synthesized and cloned into pMK	738
Cdk6	gift of F. Pituello	721
Cdk activators		
Cdc25a	gift of F. Pituello	723
Cdc25b	gift of F. Pituello	1029
	Cyclin dependent kinase inhibitors	
Cdkn1a	open reading frame, synthesized and cloned into pMK-RQ	465
Cdkn1b	open reading frame, synthesized and cloned into pMK	606

Cdkn1d (need to confirm identity)	open reading frame, synthesized and cloned into pMK-T	579
Taeniopygia guttata Cdkn2a	open reading frame, synthesized and cloned into pMK-RQ	435
Gg Cdkn2a-ARF	open reading frame, synthesized and cloned into	192
Cdkn2b = Ink4b=p15, probe 1	gift of F. Pituello	1749
Gg Cdkn2b, probe 2	open reading frame, synthesized and cloned into pMK-RQ	429
Gg Cdkn2c	open reading frame, synthesized and cloned into pMK-RQ	513
Gg Cdkn3	open reading frame, synthesized and cloned into pMK-RQ	633

2.10 Sectioning

2.10.1 Gelatine embedding

The embryos stored in 4 % PFA/PBS were washed 3 times for 1 hr in PBS. The embryos were sectioned and just the trunk with the electroporated somites was left in the well. The PBS was replaced with 1 ml of 20 % gelatine/PBS pre-warmed to 50 °C. The gelatine-suspended embryos were returned to the water bath at 50 °C to allow the gelatine to settle. The gelatine-suspended embryos were then transferred to the embedding moulds. The embryos were orientated in the desired position and a second layer of gelatine overlaid and allowed to settle. The embryos were then moved to the fridge at 4 °C to allow the gelatine to set. Once the gelatine was set the block was removed from the mould using the blunt end of a scalpel blade and neatly trimmed whilst the block was still cold. The block was then fixed in approximately 10-fold volume of 4 % PFA/PBS for several days at 4 °C.

2.10.2 Vibratome sectioning

The fixed block of gelatine in 4 % PFA/PBS was dried on a piece of blue towel and transferred onto a vibratome mounting stand. The block was fixed in place with super glue in the centre of the vibratome mounting stand, in the correct orientation. The vibratome mounting stand was placed in the centre of the tank submerged in PBS. The vibratome (Leica VT1000S) was set to cut 50 µm slices. The slices were collected with a fine brush and transferred to adhesion microscope slides (MARIENFELD). The slides were carefully dried and covered with 120 µl of glycerol/DABCO.

2.11 Microscopy

2.11.1 Stereomicroscopy

Whole embryos at HH10 were mounted on a slide dorsal up and stage HH16 up to HH24 with the right side facing up. To improve the visibility of somitic expression patterns for older specimens, embryos were split midsagitally, and the neural tube and underlying mesenchymal tissue were removed using flame-sharpened tungsten needles. The embryos were examined under a Zeiss Axioskop2 microscope using Nomarski optics or fluorescence; digital images were captured using a Zeiss AxioCam digital camera (Imaging Associates).

The same conditions were used to photograph sections. Images were assembled and edited using Adobe Photoshop 9.

2.11.2 Compound microscopy using fluorescence and Nomarski optics

The electroporated embryos were mounted on a slide dorsal side up or right side facing up for older stages. The embryos were analysed with the Zeiss AxioCAm digital camera fluorescence

microscope. The Normaski and the fluorescence images were mounted and analysed with Adobe Photoshop 9.

2.11.3 Confocal microscopy

Whole embryos and sections treated with immunohistochemistry with fluorescently-labelled antibodies were analysed with a Zeiss LSM 710 confocal microscope. The confocal was set for the use of multiple lasers to detect different dyes; 488 nm (Green), 561 nm (Red), 405 nm (blue) excitation wavelengths were used. The confocal microscope was focussed for optimal signal and Z-Stack pictures were taken. The confocal was set manually for the desired starting point and end point of the picture with the best focus. 35 pictures were taken starting from the distal point to the proximal point building up a 3D picture to allow the best images of the trunk of the embryos or the sections. The stacks were set at 0.50 µm intervals.

The pictures were analysed and mounted with Adobe Photoshop 9.

Chapter 3

3 Introduction

3.1 Markers to monitor myogenic progression in the avian model

In this study, we planned to explore whether and how the immature, pre-somitic paraxial mesoderm and the embryonic muscle stem cells developing in the dermomyotome of the somite could be forced out of their precursor or stem cell state, respectively, and into myogenic differentiation. Owing to its versatility and size, we planned on using the chicken as model; for more details on the choice of the approach and model, see chapter 4. The interpretation of phenotypes would rely on changes in marker gene expression. We therefore had to consider, which markers would be informative.

In the introduction to this thesis, the key players in the gene regulatory network controlling myogenesis have been discussed. These players are candidate marker genes. However, it has been highlighted already that for example the sequence of somatic Mrf expression differs between zebrafish, Xenopus and mouse, and specifically the onset of Mrf4 expression is not known for the chicken (145,290,291). It also has been outlined that in all model organisms, the programs controlling myogenesis during the embryonic phases of somitic myogenesis, in the fetus/ juvenile and in the adult show slight variations (102,292). Additional variations on the theme of myogenesis are used by migratory muscle precursors or precursors of craniofacial muscles (293). To perform the planned work, we required certainty as to when marker gene would be expressed in chicken somites.

A growing number of gene expression patterns are being deposited in the GEISHA (Gallus Expression *in situ* Hybridization Analysis) database (http://geisha.arizona.edu). Yet, astonishingly, myogenic gene expression has not been systematically analysed. For example, where premyogenic and myogenic gene expression may overlap, and which of the four *Mef2* genes might be the most prominent partner of *Mrfs* in the chicken myotome is not known. In functional studies, *Myf5*, *MyoD* and sarcomeric Myosin expression have all been used as indicators for myogenic differentiation, even though *Myf5* and *MyoD* expression is associated with proliferating myoblasts and the expression of sarcomeric Myosins with contractile myotubes or myofibres (294,295). This makes the comparison of the various experimental data difficult. To avoid this problem for our work, we decided to establish in detail the status of marker gene expression at the stages we planned to use for our experiments.

To target the immature paraxial mesoderm, we planned to electroporate expression constructs into the primitive streak of young embryos; it has been suggested that construct expression is

detectable after 6 hours (296), and we planned to analyse the embryos after an overnight incubation, i.e. 18 hours after electroporation. Thus, we needed to establish marker gene expression at stages HH4-5, HH8, HH10. To target the embryonic muscle stem cells in the dermomyotome, we planned to electroporate the flank somites of embryos at HH15-16, the construct would be expressed at HH16-17, and after an overnight incubation, the embryos would have reached stages HH19-20 (287) Given the rapid progression of development between HH10 and 15/16, we decided that we should include stage HH13/14 in our analysis. Thus, our analysis would cover the stages when the prospective somitic mesoderm is being laid down, when the first somites emerge, when the primary and secondary myotome form, to the stage when almost all of the 50 chicken somites have been generated and when embryonic muscle stem cells get ready to populate the myotome in the third wave of myogenesis.

Our comparative expression analysis encompassed markers suggested to be instrumental for formation of the immature paraxial mesoderm (*Tbx6*;(108)), for muscle-competent cells (premyogenic genes including the stem cell marker *Pax7*, (297)), for cells committed to myogenesis and for cells entering terminal differentiation (*Mrf* genes, *Mef2* genes, *Cadherin4* and muscle structural genes; (298–300)). Gene expression was monitored by *in situ* hybridisation; to detect sarcomeric proteins, in addition antibody stainings were performed. The onset of gene expression is shown side-by-side for HH4/5 (Fig. 3.1), HH8 (Fig. 3.2), HH10 (Fig. 3.3), HH14 (Fig. 3.4), HH16 (Fig. 3.5). Expression in mature flank somites of HH19-20 embryos is shown side-by-side in Fig. 3.6; additional, detailed marker comparisons at HH19-20 are displayed in Fig. 3.7-3.9. The developmental age of somites was determined as in (McGrew and Pourquie, 1998), counting the condensing somite as somite 0, the first fully formed somite as somite 1, the next as somite 2 etc. Results are summarised in Table 3.1. The work was carried out in collaboration with Júlia Meireles Nogueira, Svenja Wöhrle, Débora Rodrigues Sobreira and Katarzyna Hawrot.

Myogenic regulatory network

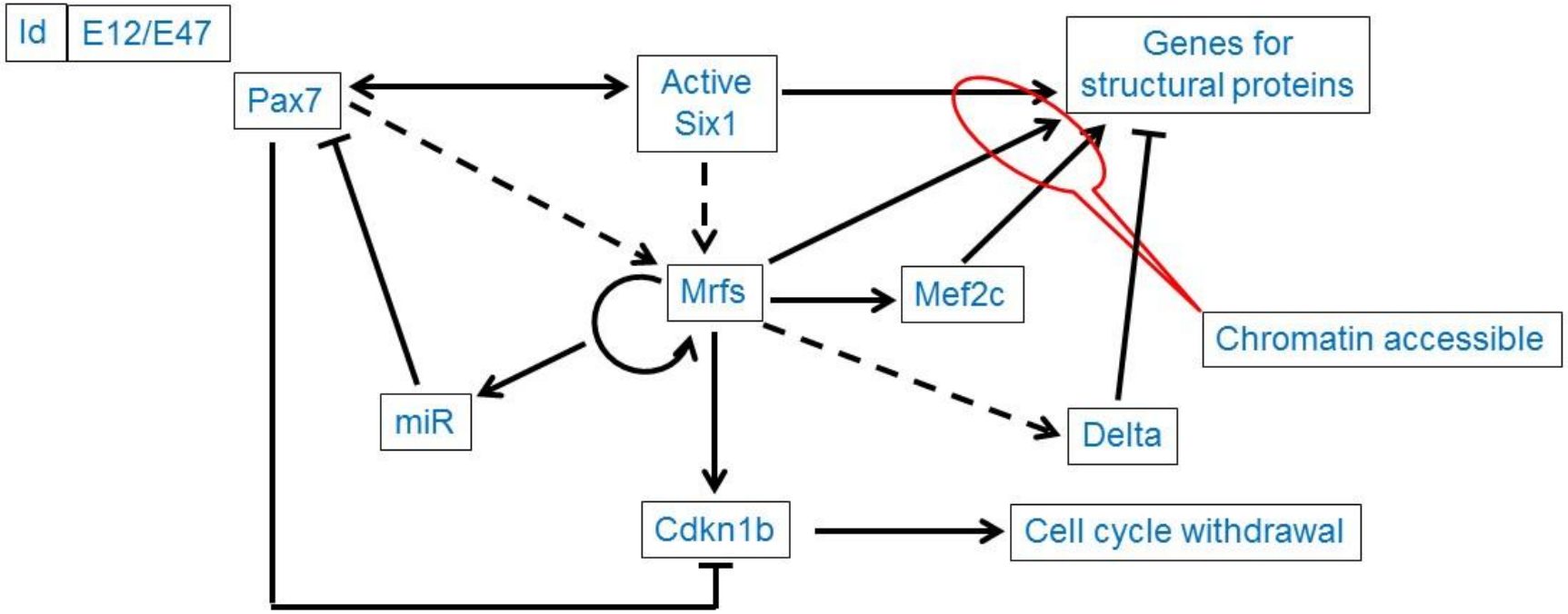

Figure 3. 1: Myogenic regulatory network

The main genes involved in muscle differentiation and their roles are summarised. Initially, Id sequesters the E12/E47 proteins to avoid them binding to MyoD and stimulating differentiation prematurely (top left). Pax7 (top left) is important for the maintenance of the muscle stem cell state and collaborates with Six1, which is considered to be involved in the early stages of development but is essential for the activation of MyoD for muscle differentiation as well. Pax7 indirectly activates the Mrf genes and keeps Cdk1b inactivated. At the same time, Pax7 is controlled by miRs which are important in keeping the Mrf genes repressed in order to not prematurely activate differentiation. Mrfs (centre), especially MyoD are redundant and self-activating as indicated by the cyclical arrow. The activation of the Mrfs will upregulate miR which in turn, downregulate Pax7. Activated Six1 along with Mef2c will contribute to the progression of differentiation (top right). Mrf activation of Cdk1b (bottom) forces the cells to withdraw from the cell cycle. Delta signal along with Notch keeps the cell undifferentiated and when these signals are downregulated the cells are finally permitted to differentiate into myoblasts. At this point the genes for structural proteins can be activated (top right).

Table 3. 1: Maturation age of the paraxial mesoderm expressing a gene at selected stages of development

stage	HH4/5	HH8	HH10	HH14	HH16	HH19/20	comments
key feature	fully extended primitive streak - streak beginning to retract, head process visible	4 somites	10 somites	22 somites	26-28 somites	37-43 somites	
gene							
Tbx6; expression encompasses:	n=2; ps/ emerging mesoderm	n=3; ps, sp, s0	n=5; ps, sp, s0-s2/3	n=5; tb, sp, s0	n=5; tb, sp, s0-s1	n=3; tb-s1/2	
onset:							
Paraxis	n=3; condensing somite	n=2; rostral sp, s0	n=10; rostral sp, s0	n=3; rostral sp, s0	n=4; rostral sp, s0	n=10; sp-s0	
Pax3	n=4; ps, epiblast	n=4; s0	n=2; s0	n=5; s0	n=5; rostral sp, s0	n=10; sp-s0	prominent expression in the neural tube and in neural crest cells
Pax7	n=4; ps, neural plate border	n=4; s0	n=5; s0	n=4; s0	n=4; rostral sp, s0	n=9; sp-s0	prominent expression in the neural tube and in neural crest cells
Six1	n=2; head mesoderm	n=2; s0	n=7; s0	n=2; s0	n=5; rostral sp, s0	n=10; rostral sp, s0	expression in the HH5-10 head mesoderm
Eya1	n=2; ps	n=1; s0	n=3; s0	n=2; s0	n=1; rostral sp, s0	n=6; sp, s0	
Myf5	n=3; -	n=4; -	n=7; s0-s1	n=7; s0-s1	n=8; s0-s1	n=11; s0-1	
MyoD	n=3; -	n=3; -	n=4; -	n=8; s4/5	n=6; s1/2	n=7; s1/2	
MyoG	n=1; -	n=1; -	n=1; -	n=4; s9/10	n=4; s6/7	n=4; s5	
Mrf4	n=2; -	n=3; -	n=2; -	n=9; s9/10	n=7; s8/9	n=7; s6-8	low overall expression levels
Mef2a	n=5; ps	n=2; -	n=1; -	n=7; s1	n=8; s1; myotome s10	n=1; s1	low overall expression levels; HH7-16: widespread expression, strongest: cardiac precursors; HH16 onwards: upregulated in the mature myotome
Mef2c	n=1; -	n=8; weak signal in somites	n=8; weak signal in s1-3	n=5; s5-7	n=4; s3/4	n=3; s3	HH7-14: strongest signal in cardiac precursors
Mef2d	n=1; -	n=1; -	n=1; -	n=2; s6-8	n=2; s7-9	n=2; s4/5	low overall expression levels, strongest: cardiac precursors
Mef2b	n=1; -	n=1; s1	n=1; s1	n=3; s1	n=1; s1	n=1; s1	HH7-14: widespread expression, strongest in ps and somites
Cdh4	n=1; -	n=2; -	n=5; -	n=6; s7-9	n=2; s0,s1; then from s7/8 onwards	n=10; s3/4	HH7-10: notochord; from HH13/14 onwards: intermediate mesoderm; low overall expression levels
Desmin	n=1; -	n=1; -	n=1; -	n=2; s10-12	n=2; S11-13	n=6; s7/8	weak signal; HH13/14 onwards: prominent

							expression in heart; low overall expression levels
Tnni1	n=1; -	n=2; -	n=1; -	n=1; s9/10	n=2; s5/6	n=6; s4/5	HH7-10 onwards: cardiac precursors; heart
Myh15	n=1; -	n=2; -	n=3; -	n=3; s20/21	n=3; s14/15	n=2; s11/12	HH7-10 onwards: cardiac precursors; heart
Myh7	n=1; -	n=2; -	n=3; -	n=3; -	n=3; s19/20	n=2; s11-13	low overall expression levels; HH7-10: precursors of cardiac inflow tract; HH13/14 onwards: heart
sarcomeric Myosins	n=3; -	n=1; -	n=3; -	n=2; s16/17	n=4; s14-16	n=4; s8-9	HH9/10 onwards: heart

Our data reveal a set sequence of gene expression, yet the timing of expression onset was quite different at different stages of development (summarised in Fig. 3.10). Moreover, marker gene expression in myogenic cells being deployed from the dorsomedial and ventrolateral lips of the dermomyotome was different from those being deployed from the rostrocaudal lips, suggesting different molecular programs. Furthermore, expression of Myosin Heavy Chain genes was overlapping but different along the length of a myotube. Finally, our work revealed that *Mef2c* is the most likely partner of Mrfs, and, in contrast to the mouse and more akin to the frog and zebrafish fish models, chicken *Mrf4* did not show an expression phase prior to that of *MyoD*, and instead, was co-expressed with *MyoG* as cells enter terminal differentiation. Our data are consistent with those of (301) which was published back-to-back with ours.

3.2 Results

3.2.1 Expression of Tbx6

Initial expression of *Tbx6* was first detected in the primitive streak in cells destined to become paraxial mesoderm (Fig. 3.1A). At HH8 (Fig. 3.2A), expression was localised to the rostral primitive streak. Cells that leave the streak to settle as paraxial mesoderm continue expressing *Tbx6*, these cells constitute the tissue known as segmental plate or pre-somitic mesoderm. Notably, while *Tbx6* is thought to label pre-somitic tissues only (302), expression could still be detected in the condensing somite (Fig.3.2A). At HH10 (Fig. 3.3A), a similar expression pattern was seen; in strongly stained specimen, *Tbx6* expression was detectable up to the somite 2/3, labelling the medial-rostral edge of the somite most intensely. At HH14 (Fig.3.4A) and HH16 (Fig.3.5A), *Tbx6* labelled the paraxial mesodermal cells emerging from the tail bud. As before, expression continued in the segmental plate and the youngest somites. At HH19-20, mesoderm formation is almost complete. As increasingly fewer cells are being contributed by the tailbud, the process of somite formation consumes the segmental plate; hence the youngest somites are located close to the tail bud. At this point, intense *Tbx6* expression was observed in the tailbud with lower expression levels in the youngest two somites (Fig. 3.6A and 3.7A).

3.2.2 Expression of Paraxis

Paraxis expression was observed in the prospective somitic mesoderm as early as HH4 (Fig. 3.1B). At HH8 (Fig. 3.2B), expression was located in the rostral segmental plate, continuing in somites as they segregated from the segmental plate. The same pattern was observed at HH10 (Fig. 3.3B), HH14 (Fig. 3.4B), HH16 (Fig. 3.5B) and HH19-20 (not shown). As somites matured, *Paraxis* expression became confined to the somitic dermomyotome and sclerotome. The strongest expression was found in the dorsomedial (epaxial) portion of the dermomyotome (Fig. 3.6B and Bi). Thus, *Paraxis* expression partially overlapped with that of *Tbx6*, but continued to be expressed at high levels in myogenic precursor cells.

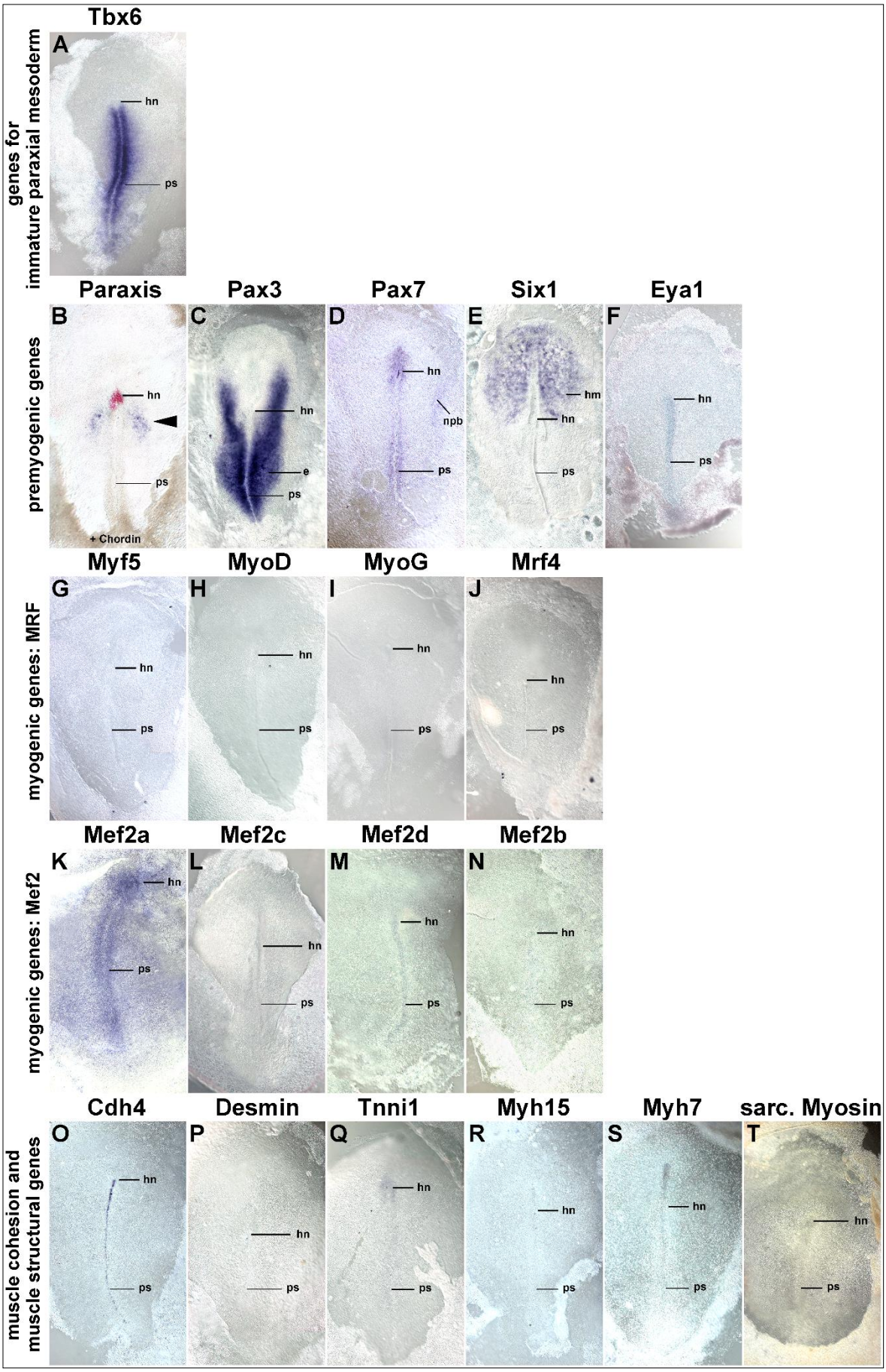
genes for immature paraxial mesoderm
Tbx6
A
hn
ps
premyogenic genes
Paraxis
Pax3
Pax7
Six1
Eya1
B
C
D
E
F
hn
ps
+ Chordin
e
npb
hm
myogenic genes: MRF
Myf5
MyoD
MyoG
Mrf4
G
H
I
J
myogenic genes: Mef2
Mef2a
Mef2c
Mef2d
Mef2b
K
L
M
N
muscle cohesion and muscle structural genes
Cdh4
Desmin
Tnni1
Myh15
Myh7
sarc. Myosin
O
P
Q
R
S
T

Figure 3. 2: Marker gene expression at HH4-5.

Dorsal views of primitive streak stage chicken embryos at stages HH4 (extended primitive streak) or HH5 (head process visible), rostral to the top. Markers are shown on top of each individual image; in (B) the node is additionally stained for Chordin expression in red. Tbx6 and, more weakly, Mef2a and Pax7 label prospective paraxial mesoderm cells in the primitive streak; Paraxis labels the cells preparing to form somites (arrowhead). Other genes are not expressed, or are expressed in tissues not contributing to somite development with Six1 labelling non-somitic head mesoderm, Pax3 the embryonic epiblast, Pax7 the neural plate border.

Abbreviations: e, epiblast; hn, Hensen's node; npb, neural plate border; ps, primitive streak.

3.2.3 Expression of Pax3 and Pax7

3.2.3.1 Pax3

Pax3 showed a complex expression pattern, and at HH4-5 was expressed in the epiblast and along the primitive streak (Fig. 3.1C). This expression continued at HH8 (Fig. 3.2C), but additional expression could be seen in the lateral aspect of the condensing somites and the overlying edge of the neural plate (the neural folds). At HH10 (Fig. 3.3C), *Pax3* expression was similarly present in the remaining epiblast flanking the remnant of the primitive streak whilst again being found in the neural folds/dorsal neural tube and the condensing as well as well-formed somites. At HH14 (Fig. 3.4C), HH16 (Fig. 3.5C) and HH19-20 (Fig. 3.6C and Ci), *Pax3* was expressed in the tail bud, the dorsal neural tube, the lateral aspect of the condensing paraxial mesoderm and the somites. As somites matured, expression became confined to the dermomyotome, with relatively low levels in the dermomyotomal centre and comparatively strong expression in the dorsomedial and ventrolateral lips (Fig. 3.6C and Ci). Thus, *Pax3* expression tightly overlapped with that of *Paraxis*, but distinct areas of elevated expression levels were observed.

3.2.3.2 Pax7

Overall, the expression pattern of *Pax7* was very similar to its paralog *Pax3* (Fig. 3.2-3.6 D and Di). At gastrulation stages, however, *Pax7* did not show prominent expression in the epiblast or tail bud and instead showed weak expression in the primitive streak, Hensen's node and the emerging notochord cells. Moreover, the developing neural plate border from which neural crest cells will develop showed staining (Fig. 3.1D). From HH8 onwards, *Pax7* strongly labelled the migrating cranial neural crest cells (Fig. 3.2D and 3.3D, ncc). Expression in the paraxial mesoderm began in the rostral segmental plate as seen for *Pax3*. The HH19-20 mature somite showed strongest expression in the dermomyotomal centre, occupying a dorsoventrally wider region than *Paraxis* (Fig. 3.6 D and Di).

3.2.4 Expression of Six1

Six genes evolved from an ancestral *Six1/2/9/sine oculis* gene, a *Six4/5* gene and a *Six3/6/7optix* gene, with *Six4/5* and *optix*-related genes possibly having arisen from an earlier, common ancestor (161). Mammals and birds only have *Six1/2*, *Six4/5* and *Six3/6*, of which *Six1/Six2* and *Six4*/5 are co-expressed in the newly formed somite, the developing dermomyotome, eventually becoming confined to the dermomyotomal lips and the myotome; other *Six* genes do not show prominent expression in the somite (163–168). Single *Six1*, but not *Six4* or *Six5* mutations cause somitic phenotypes, indicating *Six1* to have a more prominent role in myogenesis (164). We therefore focused on *Six1* in this study. At HH4-5, *Six1* was expressed in the non-somitic head mesoderm and the pre-placodal ectoderm (Fig. 3.1E). At HH8 (Fig. 3.2E) and HH10 (Fig. 3.3E), expression was also seen in the pre-chordal plate and the developing somites. At HH14 (Fig. 3.4E)

and HH16 (Fig. 3.5E) expression in the rostral segmental plate and somites was also evident. Differentiating somites maintained strong *Six1* expression in the dermomyotome, thus overlapping with the expression of *Paraxis*, *Pax3* and *Pax7* (not shown). In contrast, in mature somites such as the flank somites at HH19-20, strongest *Six1* expression was found in the dorsomedial and ventrolateral lips of the dermomyotome and the underlying myotome (Fig. 3.6E and Ei). Thus, developing embryonic muscle stem cells do not express *Six1*, cells contributing to the myotome do.

3.2.5 Expression of Eya1

Eya family proteins are protein tyrosine phosphatases which have multiple roles including the conversion of Six proteins into strong transcriptional activators (Li et al., 2003; Tootle et al., 2003); reviewed in (172) . Vertebrates have four *Eya* genes. In the mouse, the closely related *Eya1* and *Eya2* genes and the more distantly related *Eya4* are all co-expressed initially in the dermomyotome and its dorsomedial and ventrolateral lips and later in the myotome. These *Eya* genes have functionally overlapping roles. *Eya3* is weakly expressed in the somites only and is known to cooperate with Ski and Six1 in the differentiation of C2C12 myoblasts (174,176,177,303). Expression of chicken *Eya2* has been described (165) and matches that of the mouse, hence we focused on *Eya1*. No expression was observed for *Eya1* at HH4-5 (Fig. 3.1F), but later stages of development showed very similar expression to that of *Six1* at stages HH8, HH10, HH14 and HH16 (Fig. 3.2F, 3.3F, 3.4F and 3.5F, respectively). The strongest expression observed in HH19-20 mature somites was found in the dorsomedial and ventrolateral lips of the dermomyotome and in the myotome (Fig. 3.6F and Fi). This suggests that throughout somite development, Eya1 is available to convert Six1 into a transactivator that can activate myogenic genes, and both genes are in the position to continuously drive myogenic differentiation in the myotome.

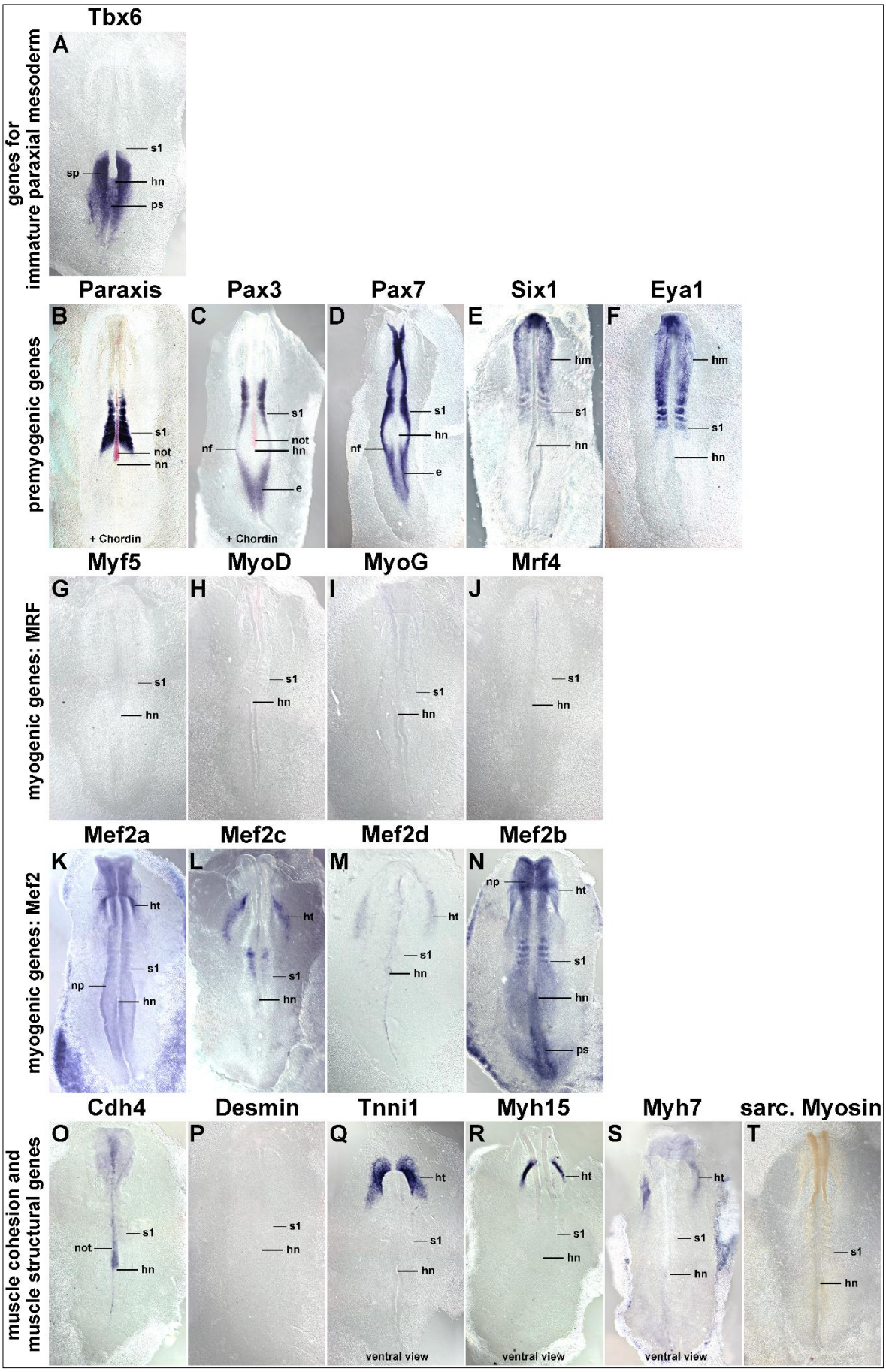
genes for immature paraxial mesoderm
Tbx6
A
s1
sp
hn
ps
premyogenic genes
Paraxis
Pax3
Pax7
Six1
Eya1
B
C
D
E
F
s1
not
hn
+ Chordin
nf
e
hm
myogenic genes: MRF
Myf5
MyoD
MyoG
Mrf4
G
H
I
J
myogenic genes: Mef2
Mef2a
Mef2c
Mef2d
Mef2b
K
L
M
N
ht
np
ps
muscle cohesion and muscle structural genes
Cdh4
Desmin
Tnni1
Myh15
Myh7
sarc. Myosin
O
P
Q
R
S
T
ventral view

Figure 3. 3: Marker gene expression at HH8.

Dorsal views (Q-S: ventral views) of chicken embryos with 3-5 somites, rostral to the top. Markers are shown on top of each individual image; in (B,C) the notochord is additionally stained for Chordin expression in red. Note the overlapping expression of Tbx6 and the pre-myogenic genes in the rostral segmental plate and most recently formed somite (s1). Mrf genes are not yet expressed. Mef2c and 2d display some somitic expression. However, the main expression of Mef2 genes, and of Tnni1, Myh15, Myh7 is in heart precursors (ht).

Abbreviations as in Fig.1 and: hm, head mesoderm; ht, cardiac precursors; nf, neural folds; not, notochord; np, neural plate; s, somite; sp, segmental plate; the position of the youngest somite (s1) is indicated.

3.2.6 Expression of Mrf genes

3.2.6.1 Myf5

Myf5 has been described as the earliest *Mrf* gene to be expressed. Even though embryos at HH7-8 have 1-4 somites, *Myf5* expression was not detectable (Fig. 3.2G). We initially found a somewhat diffuse signal in condensing and newly formed somites at HH10, with somite 4/5 to somite 10 showing expression in their medial wall (Fig. 3.3G). This is the region from which the cells building the primary myotome arise (135). At HH14 (Fig. 3.4G) and HH16 (Fig. 3.5G), a similar pattern was observed. From somite 9 onwards, *Myf5* expression began to spread laterally, coinciding with the establishment of the myotomal scaffold. In mature somites at HH19-20 (Fig. 3.6G and Gi; Fig. 3.9A and Ai), *Myf5* expression was detected in the sub-lip domain of both the dorsomedial as well as the ventrolateral lip, overlapping with myogenic cell production from both lips (304–306). Moreover, robust expression was seen throughout the myotome. However, the immediate sub-lip domains of the rostral and caudal lips that also contribute to the myotome (Kahane et al., 1998a), did not express *Myf5* (Fig. 3.9A and Aii). Nevertheless, at a relatively short distance from these lips, individual *Myf5*-postive cells were observed (Fig. 3.9A, arrows), suggesting that after the entry into the myotome, cells derived from the rostrocaudal lips quickly activated *Myf5*.

3.2.6.2 MyoD

MyoD expression was not detected at stages HH4-10 of development (Fig. 3.1H, 3.2H and 3.3H). At HH14, expression was observed in the dorsomedial region of somites 4/5 and older, as seen for *Myf5* (Fig. 3.4H); at HH16, this expression was already seen in somites 1/2 (Fig. 3.5H). Expression then expanded laterally as seen for *Myf5*, but this expansion lagged behind by 1-2 somites. At HH19-20, *MyoD* expression in mature somites was nearly indistinguishable from that of *Myf5* (Fig. 3.6H and Hi). However, the immediate dorsomedial and ventrolateral sub-lip domains showed no staining, and expression appeared more intersperse than that of *Myf5*, suggesting that not all cells expressed *MyoD*.

3.2.6.3 MyoG

MyoG expression was first detected at HH13-14, i.e. in animals with a total of 19-22 somites, commencing in somite 9/10 (Fig. 3.4I). As was the case for *Myf5* and *MyoD*, expression spread laterally in older somites. Notably, at HH16, expression was already visible from somite 6/7 onwards (Fig. 3.5I), and at HH19-20, expression was already present in the 5th youngest somite (Fig. 3.7B), suggesting that the progress of somite maturation speeds up as development progresses. At HH19-20, *MyoG* expression in mature somites appeared throughout the myotome as for *MyoD* (Fig. 3.6I and Ii); also similarly to *MyoD*, not all cells appeared *MyoG*-positive.

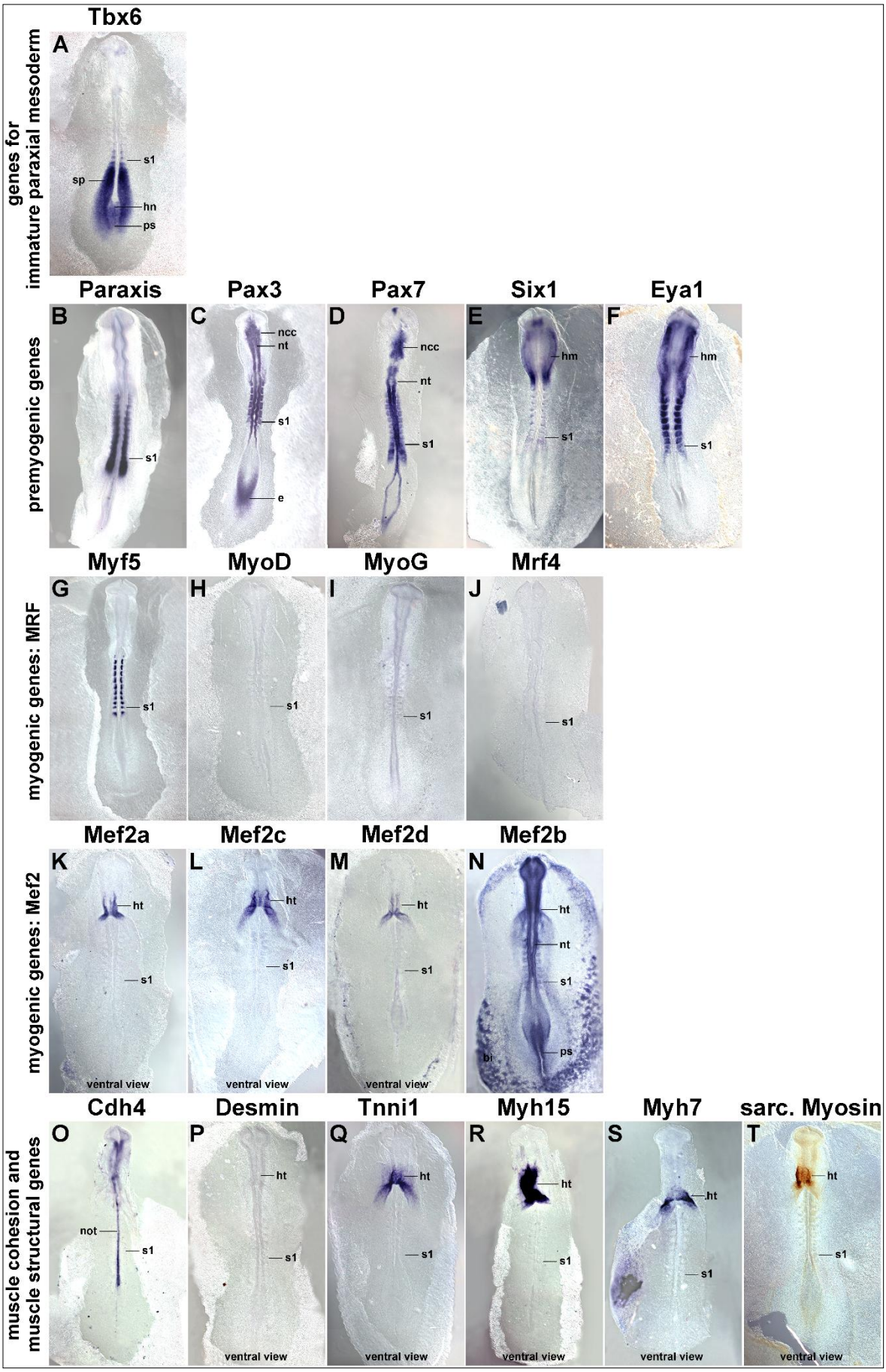
genes for immature paraxial mesoderm
Tbx6
A
s1
sp
hn
ps
premyogenic genes
Paraxis
Pax3
Pax7
Six1
Eya1
B
C
D
E
F
s1
ncc
nt
e
hm
myogenic genes: MRF
Myf5
MyoD
MyoG
Mrf4
G
H
I
J
myogenic genes: Mef2
Mef2a
Mef2c
Mef2d
Mef2b
K
L
M
N
ht
bi
ventral view
muscle cohesion and muscle structural genes
Cdh4
Desmin
Tnni1
Myh15
Myh7
sarc. Myosin
O
P
Q
R
S
T
not

Figure 3. 4: Marker gene expression at HH10.
Dorsal views (P-T: ventral views), rostral to the top. Markers are indicated on top of each individual image as before. Tbx6 and the pre-myogenic genes show overlapping expression in the rostral segmental plate and most recently formed somite. The pre-myogenic genes label the condensing as well as fully formed, epithelial somites. Of the Mrf genes, Myf5 is expressed weakly in the condensing somite, and more robustly in the medial wall of the epithelial somites. Similar to HH8, Mef2c and 2d display some weak somitic expression, but the main expression of the Mef2 genes, of Tnni1 and the Myosins remains in heart (ht).

Abbreviations as in Fig.1,2 and: bi, blood islands; ncc, neural crest cells; nt, neural tube; the position of the youngest somite is indicated (s1).

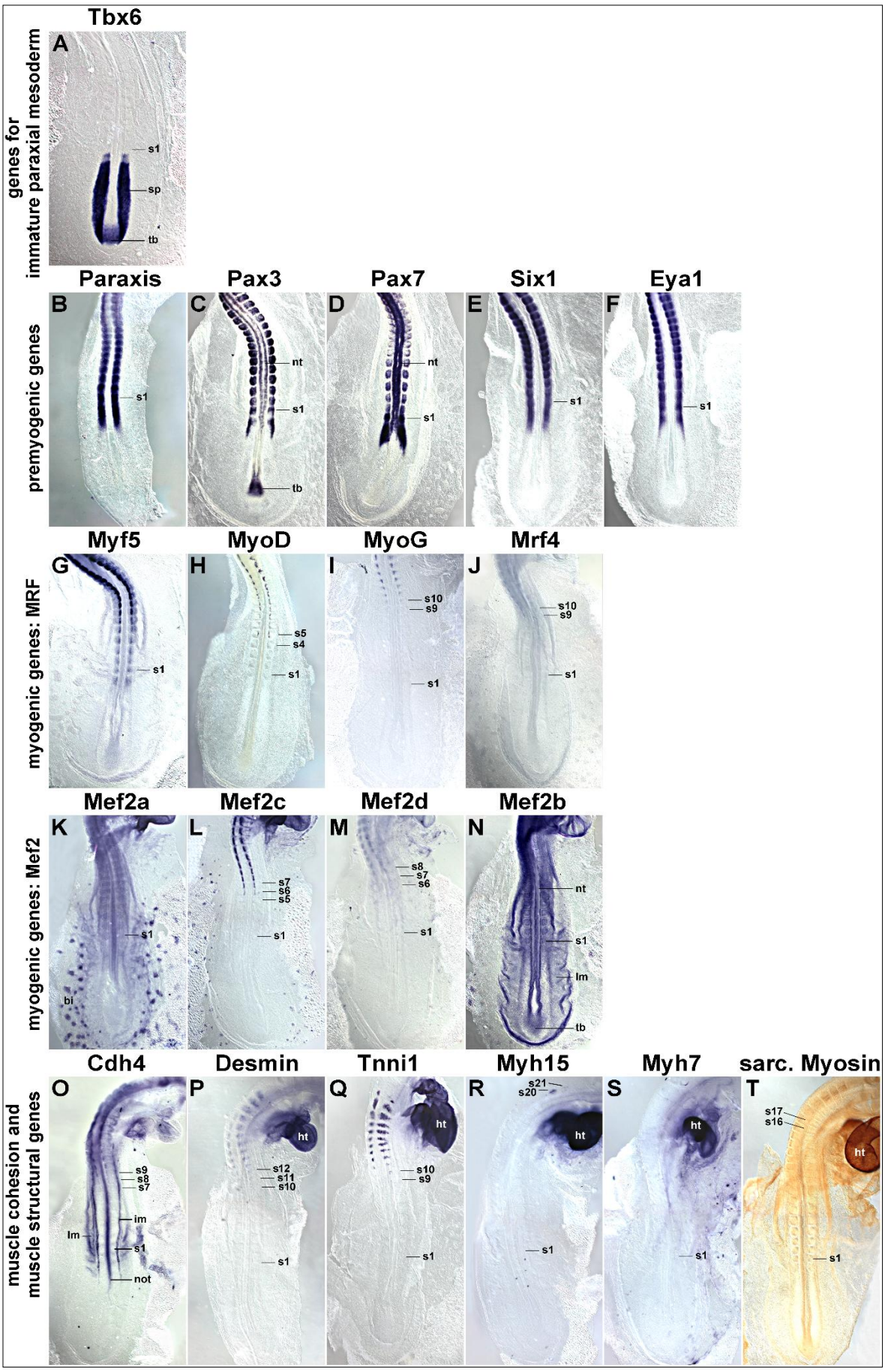
genes for immature paraxial mesoderm
premyogenic genes
myogenic genes: MRF
myogenic genes: Mef2
muscle cohesion and muscle structural genes
Tbx6
A
s1
sp
tb
Paraxis
Pax3
Pax7
Six1
Eya1
B
C
D
E
F
nt
Myf5
MyoD
MyoG
Mrf4
G
H
I
J
s10
s9
s5
s4
Mef2a
Mef2c
Mef2d
Mef2b
K
L
M
N
s8
s7
s6
bl
lm
Cdh4
Desmin
Tnni1
Myh15
Myh7
sarc. Myosin
O
P
Q
R
S
T
ht
s21
s20
s17
s16
im
not

Figure 3. 5: Marker gene expression at HH14.

Dorsal views of the caudal region of HH14 chicken embryos, rostral to the top. Similar to earlier stages, Tbx6 expression and the expression of pre-myogenic genes and of Myf5 overlaps in the rostral segmental plate and youngest somite. More mature somites sequentially express MyoD, Mef2c, Mef2d, Cdh4, MyoG, Mrf4, Tnni1, Desmin and the Myosins (exception: Myh7; not yet expressed).

Abbreviations as in Fig.2,3 and: im, intermediate mesoderm; lm, lateral mesoderm; tb, tail bud; the position of the youngest somite is indicated (s1)

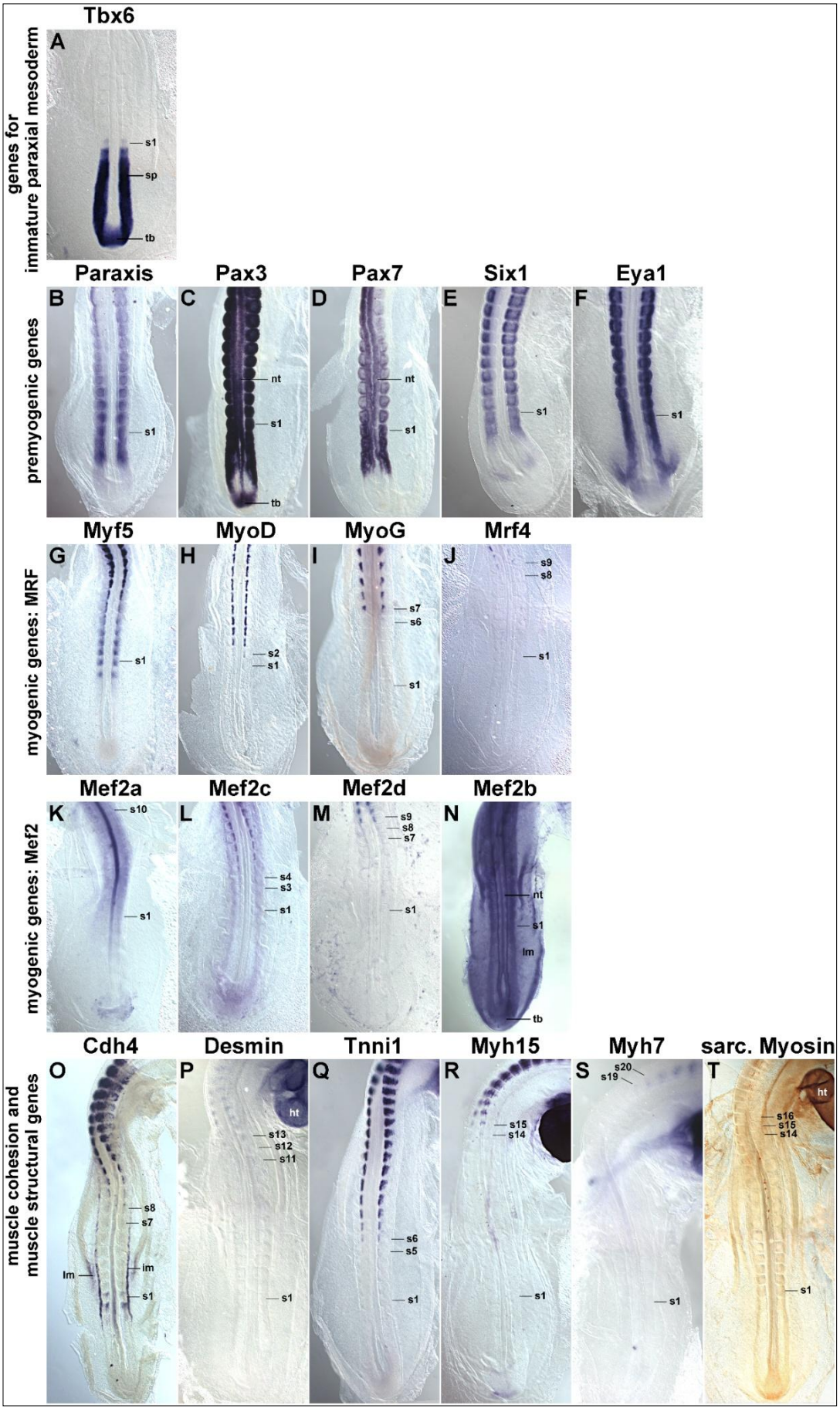
genes for immature paraxial mesoderm
Tbx6
A
s1
sp
tb
premyogenic genes
Paraxis
Pax3
Pax7
Six1
Eya1
B
C
D
E
F
nt
s1
tb
myogenic genes: MRF
Myf5
MyoD
MyoG
Mrf4
G
H
I
J
s2
s7
s6
s9
s8
myogenic genes: Mef2
Mef2a
Mef2c
Mef2d
Mef2b
K
L
M
N
s10
s4
s3
lm
muscle cohesion and muscle structural genes
Cdh4
Desmin
Tnni1
Myh15
Myh7
sarc. Myosin
O
P
Q
R
S
T
ht
s13
s12
s11
s15
s14
s20
s19
s16
im

Figure 3. 6: Marker gene expression at HH16.
Dorsal views of the caudal region of HH16 chicken embryos, rostral to the top. Expression patterns are similar to those at HH14; however, expression of MyoD, MyoG, Mrf4, Mef2c, Mef2d and the muscle structural genes begins earlier. Myh7 is now also expressed; elevated expression in the myotome of somite 10 is visible for Mef2a. Abbreviations and annotations as in Fig.1-4.

3.2.6.4 *Mrf4*

Mrf4 expression commenced in somites 9/10 at HH13-14, roughly following the expression of *MyoG* (Fig. 3.4J). At HH16, somites 8/9 were the earliest in which staining was visible (Fig. 3.5J), whereas at HH19-20, the earliest somites that were stained were 6-7 (not shown). Compared to the other *Mrf* genes, *Mrf4* expression levels were low. Expression of *Mrf4* in mature somites was detected in the myotome but no staining was detected in the sub-lip domains of the dermomytome (Fig. 3.6J and Ji). Expression was concentrated in the centre of the myotome, with stronger staining in the epaxial domain and weaker staining in the hypaxial domain. Expression appeared even more intersperse than that of *MyoD* or *MyoG*, indicating that only a fraction of cells in the myotome expressed the gene.

3.2.7 Expression of Mef2 genes

Vertebrates have retained the four *Mef2* genes that were generated during their two rounds of genome duplication (307). Of these, *Mef2a* and *Mef2c* are thought to have arisen from one of the ancestral genes generated in the first duplication event, and the genes have since remained relatively unchanged. *Mef2b* and *Mef2d* are thought to have stemmed from the other ancestral gene; yet, *Mef2b* appears to have diverged more extensively. The genes are displayed according to their similarity to *Mef2a*.

3.2.7.1 *Mef2a*

Mef2a was already weakly expressed in the primitive streak at HH4-5 (Fig. 3.1K). From stages HH7-8 and onwards, low-level widespread staining was observed, with the strongest expression seen in the precursors of the primitive heart (Fig. 3.2K and 3.3K; ht). The early heart, blood island and the notochord showed prominent expression at HH14 (Fig. 3.4K), and from this stage onwards, the somites also showed *Mef2a* expression (Fig. 3.4K and 3.5K). At HH16 (Fig. 3.5K) and HH19-20 (Fig. 3.6K and Ki), mature somites showed elevated expression in the myotome in a pattern similar to that of *MyoG* and *Mrf4*.

3.2.7.2 *Mef2c*

Mef2c expression coincided with *Mef2a* expression in the cardiac precursors of HH7-8 embryos and the primitive heart of HH10 embryos (Fig. 3.2L and 3.3L; ht). At these stages, weak, diffuse staining could also be seen in the somites. At HH14, prominent somitic expression was seen in somites 5/6 onwards, labelling the dorsomedial region as seen for *MyoD* (Fig. 3.4L). At HH16, somites 3/4 were already *Mef2c*-positive (Fig. 3.5L), with expression spreading laterally as observed for the Mrf genes. At HH19-20, mature somites showed robust expression in the

myotome, with elevated expression in the myotomal centre (Fig. 3.6L and Li). Notably, *Mef2c* expression at that stage also showed strong staining in the region beneath the rostral and caudal lips of the dermomytome (Fig. 3.9B and Bii, arrowheads).

3.2.7.3 Mef2d

Overall, *Mef2d* showed low expression levels with weak staining scarcely detectable in cardiac precursors at HH7-8 and the primitive heart at HH10 (Fig. 3.2M and 3.3M). At HH14, expression in the medial aspect of the somites was detectable from somite 6-8 onwards. A similar range was displayed at HH16 (Fig. 3.4M and 3.5M) whereas at HH19-20, staining was seen in somites 3/4 onwards. *Mef2d* expression in the mature somites of the flank was confined to the myotome.

3.2.7.4 Mef2b

Mef2b showed widespread expression in all germ layers, with strongest staining in the primitive streak, neural plate, cardiac precursors and the somites at HH7-8 (Fig. 3.2N). Similar expression was seen at HH10; however, the staining appeared weaker in the somites when compared with the staining for the neural tube and primitive streak (Fig. 3.3N). Widespread expression was also seen at stages HH14, HH16 and HH19-20 (Fig. 3.4N, 3.5N and 3.6N). Cross sections revealed that the expression was located to the myotome as was the case with the other *Mef2s*, but the sclerotome was also stained (Fig. 3.6Ni).

3.2.8 Expression of Cadherin 4 (R-Cadherin, Cdh4)

Cdh4 has been shown to be expressed in the developing myotome, and its ability to support cell adhesion in epithelia suggests it has a role in myogenic cell alignment and cohesion (308,309) We observed initial *Cdh4* expression in the developing notochord at HH7-8 and 9-10 (Fig. 3.2O and 3.3O). At HH14 (Fig. 3.4O), a complex expression pattern encompassing the notochord and the intermediate mesoderm-derived nephric duct was observed. Weak expression was seen in the condensing somite as well as the first 1-3 newly formed somites. However, more robust expression was found in the medial region of somites 7-9. In further rostral somites, the expression was spread more laterally, concomitant with the developing myotome as observed for the *Mrf* genes. Notably, 9-10 somites rostral to the somite expressing the gene first, a new expression domain emerged in the lateral lip and sub-lip domain of the dermomyotome. At HH16 (Fig. 3.5O) and HH19-20 (Fig. 3.6O), a similar expression pattern was seen. Cross sections of HH19-20 flank somites confirmed that *Cdh4* was expressedf in the myotome and throughout the ventrolateral dermomyotomal lip (Fig. 3.6Oi).

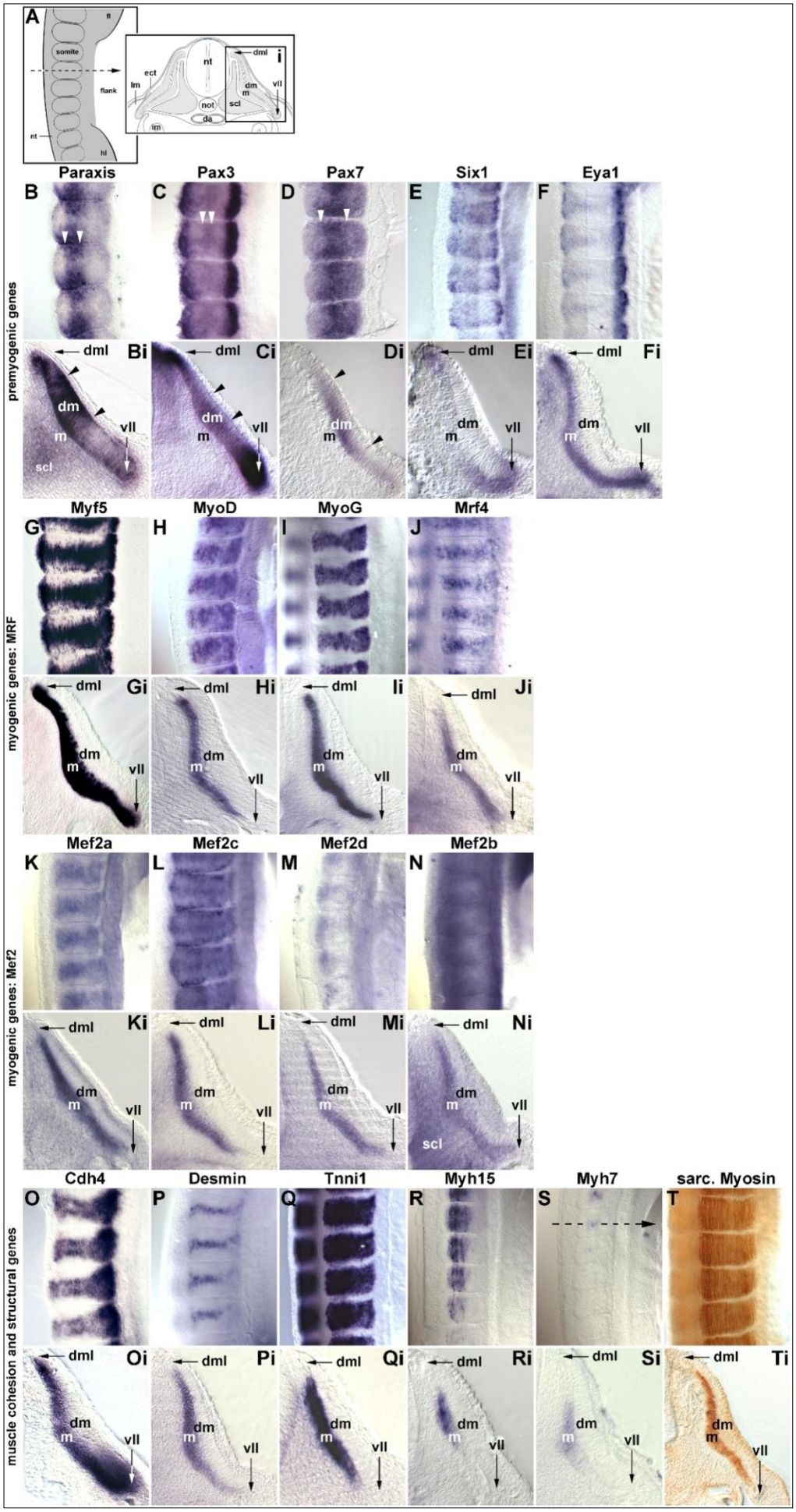
A
fl
somite
flank
nt
hl
nt
ect
lm
dml
i
dm
m
vll
not
scl
da
im
premyogenic genes
Paraxis
Pax3
Pax7
Six1
Eya1
B
C
D
E
F
Bi
Ci
Di
Ei
Fi
dml
dm
m
vll
scl
myogenic genes: MRF
Myf5
MyoD
MyoG
Mrf4
G
H
I
J
Gi
Hi
Ii
Ji
myogenic genes: Mef2
Mef2a
Mef2c
Mef2d
Mef2b
K
L
M
N
Ki
Li
Mi
Ni
muscle cohesion and structural genes
Cdh4
Desmin
Tnni1
Myh15
Myh7
sarc. Myosin
O
P
Q
R
S
T
Oi
Pi
Qi
Ri
Si
Ti

Figure 3. 7: Marker gene expression in the flank of embryos at HH19-20.

(A)Schematic representation of the images displayed in B-T (lateral view of flank somites on the right of the embryo, rostral to the top, lateral to the right) and Bi-Ti (cross section to flank somites, dorsal to the top, lateral to the right; section (Si) is from the forelimb- flank boundary as indicated in S). Markers are indicated as before.

Paraxis, Pax3 and Pax7 show distinct areas of elevated expression in the dermomyotome (B,Bi-D,Di; arrowheads). Their expression overlaps in dorsomedial and ventrolateral lips with that of Six1, Eya1 and Myf5; in the ventrolateral lip, expression overlaps also with that of Cdh4. The Mrf genes, the Mef2 genes and the genes encoding cell adhesion and muscle structural proteins show overlapping expression in the myotome, with the late commencing markers still being confined to the more medial territories.

Abbreviations as in Fig.1-4 and: da, dorsal aorta; dm, dermomyotome; dml, dorsomedial lip of dermomyotome; ect, surface ectoderm; fl, fore limb; hl, hind limb; m, myotome; scl, sclerotome; vll, ventrolateral lip of dermomyotome.

3.2.9 Expression of muscle structural genes

Desmin, Tnni1 (Troponin I 1), Myh15 (Myosin Heavy Chain 15 or ventricular Myosin Heavy Chain) and Myh7 (Myosin Heavy Chain, slow/cardiac or atrial Myosin Heavy Chain) are components of the functional sarcomere and have been reported to be expressed early on in the developing embryo (http://geisha.arizona.edu). We therefore included these muscle structural genes in our analysis. To monitor the availability of Myosins independent of individual contributing genes, we used the MF20 antibody to detect pan-sarcomeric Myosin. To evaluate the levels of protein production, whole mount antibody staining of HH21 embryos were performed with antibodies known (Desmin) or predicted (Tnni1, Myh17, Myh7) to recognise the avian proteins.

3.2.9.1 Desmin

Desmin mRNA was first detected at HH13-14, with somites 10-12 and older showing staining (Fig. 3.4P). Similar expression was seen at HH16, (Fig. 3.5P) but at HH19-20, expression was already detected from somites 7/8 onwards (not shown). Expression was found in the centre of the myotome which contains the myonuclei (Fig. 3.6P and Pi). Overall, somitic *Desmin* transcription was low, whereas the staining was more prominent in the heart. Notably, Desmin protein was more readily detectable (Fig. 3.8H), suggesting that rate of production and/or half-life is greater for the protein than for the mRNA. In contrast to the mRNA, the protein was found throughout the myotube, suggesting an active distribution mechanism.

3.2.9.2 Tnni1

At HH4-5, weak expression of *Tnni1* mRNA was found in the rostral primitive streak and the lateral mesoderm which contributes to the heart (Fig. 3.1Q). At HH7-8, this expression strengthened, and throughout the developmental stages analysed here, the cardiac precursors and the heart showed the most prominent *Tnni1* expression (see Fig. 3.2Q and 3.3Q; ht). At HH14, somites 9/10 showed *Tnni1* expression (Fig. 3.4Q), whilst at HH16 and HH19-20, expression started already in somites 5/6 (Fig. 3.5Q) and 4/5 (Fig. 3.7C), respectively. *Tnni1* mRNA was readily detectable, as was the Tnni1 protein (Fig. 3.8I), and was found to label the myotome throughout (Fig. 3.6Q and Qi).

3.2.9.3 Myh15

Myh15 expression was detected from HH7-8 onwards in the cardiac precursors and subsequently the heart (Fig. 3.2R and 3.3R; ht; (Bisaha and Bader, 1991)). Myogenic expression was first found in somites 20/21 at HH14, i.e. the two oldest somites (Fig. 3.4R). At HH16, earlier expression was seen in somites 14/15, labelling the myotomal centre (Fig. 3.5R and 3.8A). At HH19/20, expression appeared already in somites 11/12. Expression was confined to the developing myotubes, but the strongest expression was located in their rostral and caudal extremities (Fig. 3.6R and Ri; Fig. 3.8B-D, arrows). Protein detection was comparatively less robust than mRNA detection; however, at

HH21, Myh15 protein was enriched along the rostral and caudal edges of the myotome, similar to the *Myh15* mRNA (Fig. 3.8J).

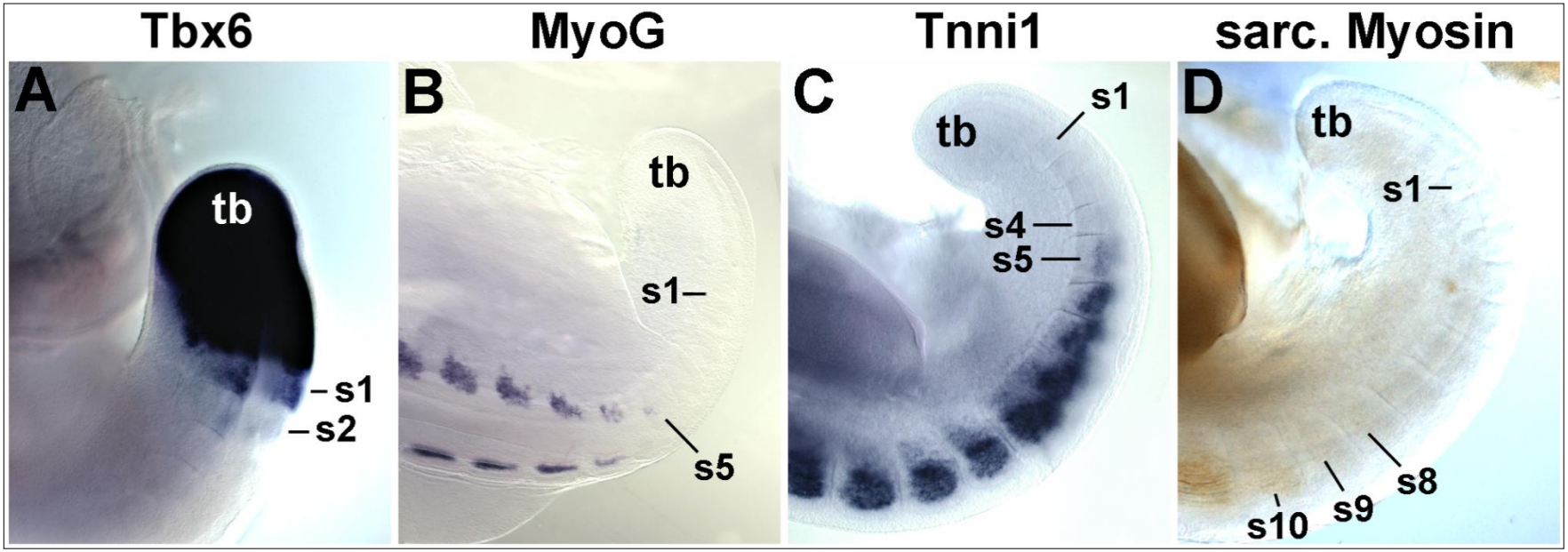
Tbx6
MyoG
Tnni1
sarc. Myosin
A
tb
s1
s2
B
tb
s1
s5
C
tb
s1
s4
s5
D
tb
s1
s8
s9
s10

Figure 3. 8: Expression of selected markers at the caudal end of HH19-20 embryos.
Dorsolateral views of the caudal end of HH19-20 embryos, the position of the tail bud (tb) is indicated. Marker genes are indicated above the individual images as before. Similar to earlier stages, Tbx6 expression still continues in the recently formed somites. However, the onset of MyoG, Tnni1 and sarcomeric Myosins expression occurs significantly earlier, i.e. closer to the tail bud. Annotations as before.

3.2.9.4 *Myh7*

Myh7 expression levels were low, lower than those of *Myh15*, which is consistent with reports from Oana (310). At HH7-8 *Myh7* was expressed in cardiac precursors, and from HH9/10 onwards, expression was found in the atrium of the heart (Fig. 3.2-3.5S; ht). At HH16, somites 19/20 showed expression (Fig. 3.5S) whilst at HH19-20, expression was visible from somites 11-13 onwards (Fig. 3.6S). Expression was confined to the developing myotubes, with the strongest expression found in their centre (Fig. 3.8E-G, arrow). Myh7 protein was not easy to detect, but also showed enrichment in the myotomal centre (Fig. 3.8K).

3.2.9.5 *Pan-sarcomeric Myosin detection*

The MF20 antibody recognises the rod-like tail of all sarcomeric Myosins and therefore generally detects terminally differentiated cardiac and skeletal muscle independent of the individual contributing *Myosin* gene (311). Initially, the antibody detected only the developing heart (Fig. 3.3T, ht). At HH14, the antibody also stained somites 16/17 and older (Fig. 3.4T). At HH16, somites 14-16 and older were stained (Fig. 3.5T), and at HH19/20, somites 8-9 showed staining (Fig. 3.7D). The expression was found to be confined to myotubes (Fig. 3.6T and Ti; Fig. 3.8L).

3.2.10 Comparative analysis of Myf5, Mef2c, Follistatin and Pitx3 along the four dermomyotomal lips

Myf5 and pre-myogenic genes shown here presented overlapping expression, occurring first in the dorsomedial and then in the ventrolateral lip of the dermomytome. Expression of *MyoD*, *MyoG*, *Mef2* genes and *Cdh4* overlapped with that of *Myf5* in the dorsomedial and ventrolateral sublip regions. In contrast, *Mef2c* expression was also found along the rostrocaudal dermomyotomal lips (compare Fig. 3.9A, Ai, Aii and B, Bi, Bii). We screened our embryo collection for additional markers present in this region. We found that the gene encoding the TGFβ (transforming growth factor beta) inhibitor *Follistatin* was expressed from HH6 onwards in condensing and newly formed somites (Bothe et al., 2011). Expression continued in the dermomyotome, where upregulated expression was seen along all four dermomyotomal lips (not shown). At HH19/20, mature somites of the flank showed expression in these lips as well as in the myotome (Fig. 3.9C, Ci and Cii). *Pitx3* expression was initially found in the lens of the eye. At HH16 (not shown) and 19/20 (Fig. 3.9D, Di and Dii), expression was seen in the mature somitic myotomes. Notably, the strongest expression was seen along the rostrocaudal edges of the myotome, with the most prominent expression found in the lateral aspect of the caudal sublip domain.

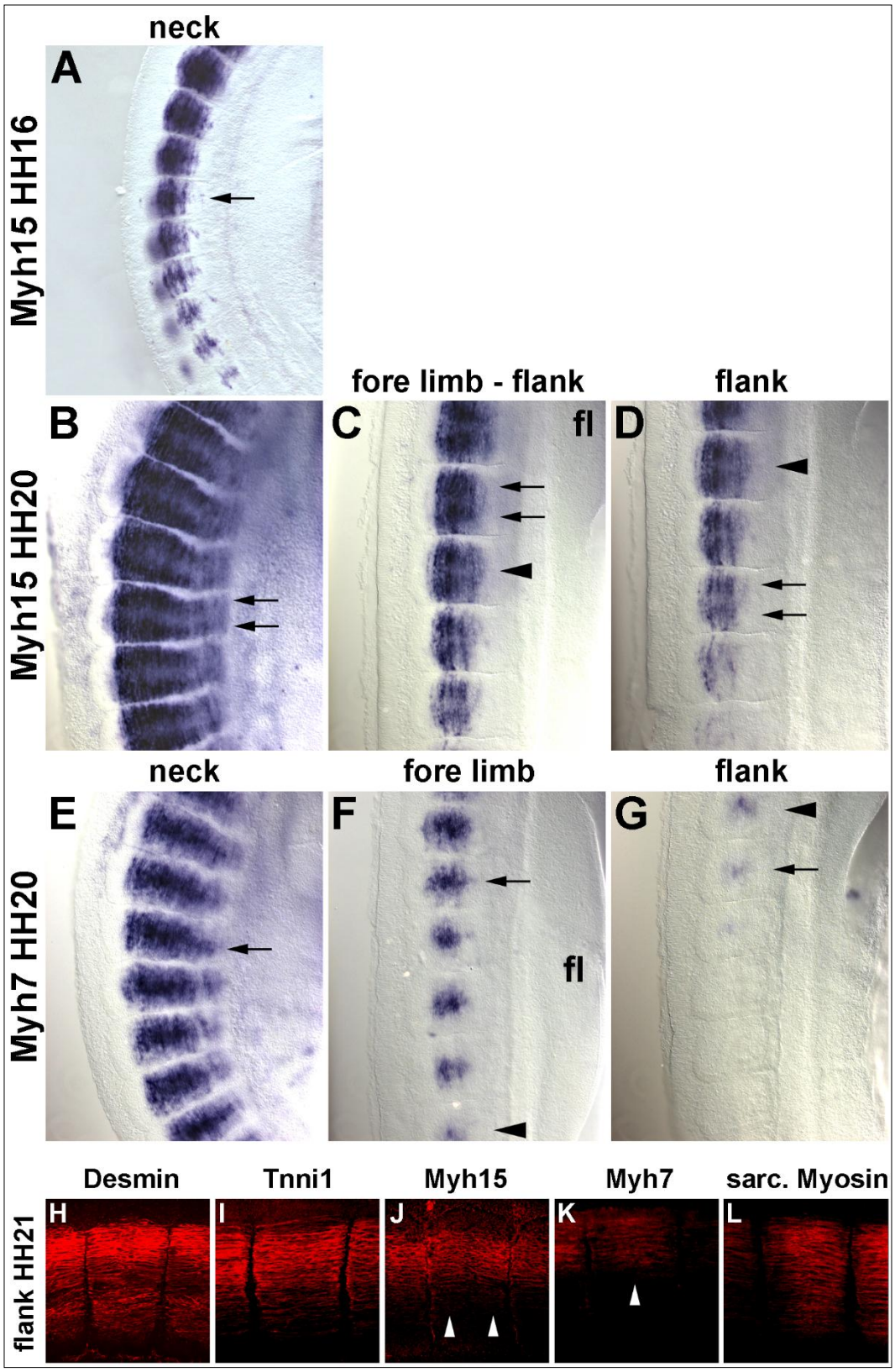
neck
A
Myh15 HH16
fore limb - flank
flank
B
C
fl
D
Myh15 HH20
neck
fore limb
flank
E
F
G
fl
Myh7 HH20
Desmin
Tnni1
Myh15
Myh7
sarc. Myosin
H
I
J
K
L
flank HH21

Figure 3. 9: Comparison of Myh15 and Myh7 expression at HH16, 20 and 21.
(A-D) Myh15 mRNA expression in the somites of the HH16 neck (A) and the HH20 neck (B), fore limb-flank border (C) and the flank (D). (E-G) Myh7 mRNA expression in the HH20 neck (E), at fore limb levels (F) and in the flank (G). Anterior is to the top in all, dorsal to the left. Arrowheads mark the same somites in (C,D) and (F,G),respectively. Note that at HH16, Myh15 expression is strongest in the centre of the developing myotubes; at HH20 expression is strongest at the rostro-caudal ends (arrows) while Myh7 labels the centres of the myotubes (arrows).

(H-L) Flattened confocal z-stacks of HH21 flank somites, stained with antibodies detecting the proteins indicated on the top of the panel. Lateral views, dorsal to the top, anterior to the right. Note that Myh15 protein accumulated more strongly along the rostro-caudal edges of the myotome, while Myh7 protein is more concentrated in the centre (arrowheads).

Annotations as before.

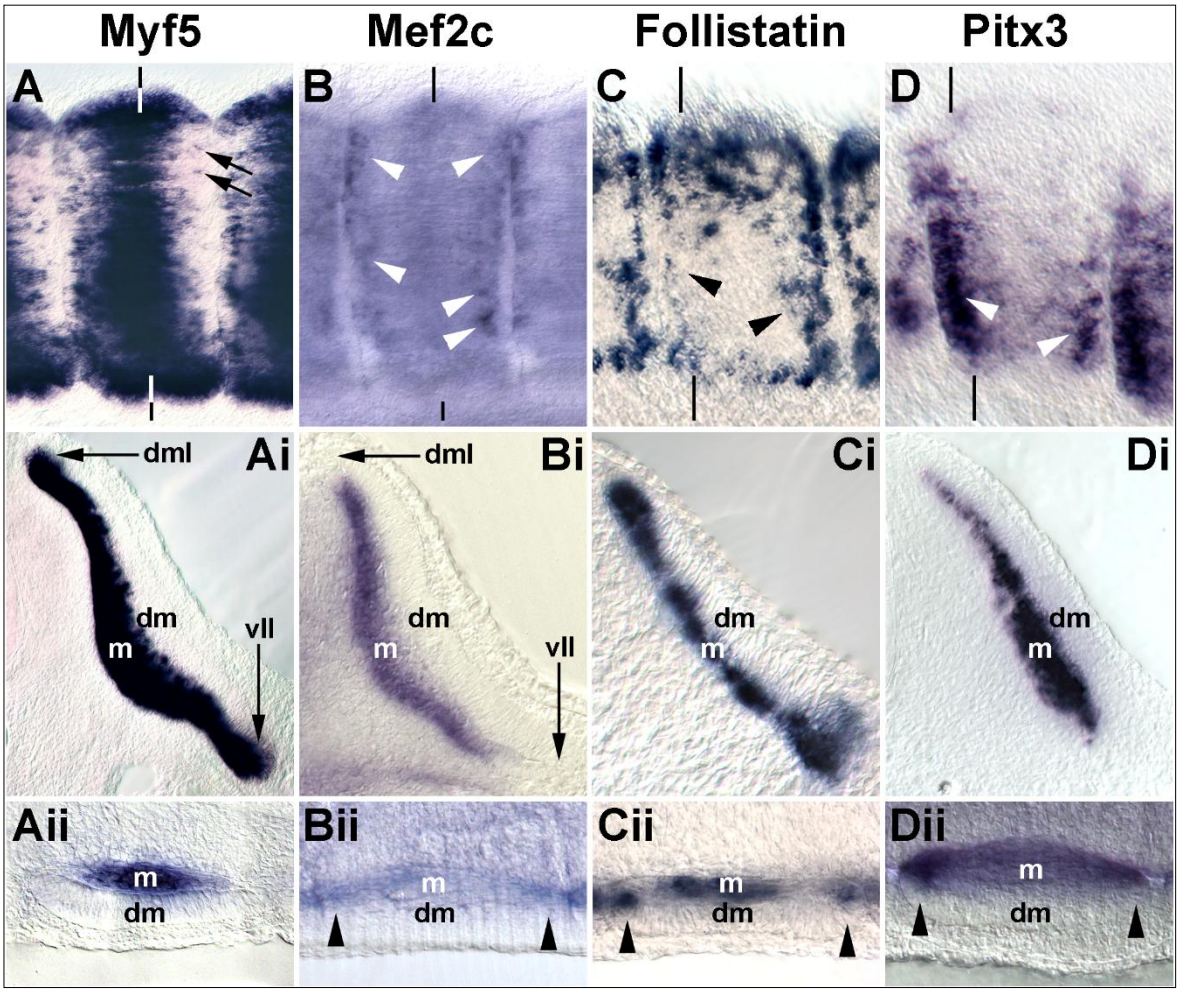

Figure 3. 10: Comparison of markers labelling myogenic cells from the dorsomedial-ventrolateral and rostrocaudal lips of the dermomyotome.

(A-D) Lateral views of flank somites on the right of the embryo, rostral to the right, dorsal to the top. (Ai-Di) Cross sections of these somites, with (Ai, Bi) leading through the centre and (Ci, Di) sectioned along the caudal edge of the somite as indicated by the vertical lines. (Aii-Dii) Frontal sections, medial to the top, rostral to the right. Individual cells along the rostrocaudal sublip domain of the myotome express *Myf5* (A, arrows). In contrast, robust and widespread expression in this domain is found for *Mef2c*, *Follistatin* and *Pitx3* (B-D, Bii-Dii; arrowheads).

3.3 Discussion

Aim of this part of the study was to perform in the chicken embryo a side-by-side analysis of the key markers associated with the progression from an immature state of the paraxial mesoderm to myogenic commitment and, eventually, to myogenic differentiation. This was needed to ensure that data obtained from our functional studies would be interpreted correctly. Yet our study also provided novel insight into the process of skeletal muscle formation. Our key findings are summarised in Fig.3.10.

3.3.1 Myf5 is the first gene to indicate myogenic commitment.

Mrf genes are thought be the drivers of myogenesis, with *Myf5* and *MyoD* playing similar roles in the still mitosis-competent myoblast (reviewed in (Aziz et al., 2010; Fong and Tapscott, 2013). We found, however, that *Myf5* was always the first *Mrf* being expressed, with initial diffuse expression in the epithelialising somite, followed by robust expression in the medial wall of a newly formed somite, the dorsomedial lip of the dermomyotome and the expanding myotome. Later on, additional mirroring expression in the ventrolateral aspect of the somite was seen. Following *Myf5*, *MyoD* expression was activated in the dorsomedial and ventrolateral sublip domains of the dermomyotome, not the dermomyotomal lips themselves. This suggests that *Myf5* is a marker for myogenic commitment, whereas *MyoD* marks cells that are ready to enter differentiation. Significantly, no myogenic differentiation was observed at the start of *Myf5* expression. Thus, *in vivo*, *Myf5* may not be as proficient in driving myogenesis as *in vitro*. However, the continued expression of genes associated with an immature state such as *Tbx6* may present a suitable explanation for this. Furthermore, it was shown that in quiescent satellite cells, the *Myf5* mRNA is sequestered in mRNP granules together with miR31, preventing *Myf5* translation (Crist et al., 2012), and this mechanism may also operate in the embryo. Interestingly, an expression profile similar to that of *Myf5* has recently been shown for avian *Rgm* genes, of which the functional relationship is yet to be shown (312) .

3.3.2 In contrast to the mouse, Mrf4 (Myf6) is the last Mrf to be expressed.

During all of the stages investigated, *Myf5* expression was always followed by expression of *MyoD*, and subsequently followed by the expression of *MyoG* and *Mrf4*; an early onset of *Mrf4* expression as shown in the mouse (Summerbell et al., 2002) was not observed. It is not clear whether the murine expression pattern is representative of all mammals; yet the avian sequence of *Mrf* gene expression is comparable to that shown for Xenopus and zebrafish, suggesting that this is the general configuration for jawed vertebrates. *MyoG* is known to promote exit from the cell cycle and terminal differentiation (reviewed in (193,313) , yet *MyoD*, *MyoG* and *Mrf4* were eventually all co-expressed in the dorsomedial and ventrolateral sublip regions of the myotome.

This indicates that cells entering the myotome via these lips may withdraw from the cell cycle in the sublip domain and begin differentiation within this compartment before being displaced to a position away from the lips by the next cells entering from the dermomyotome.

3.3.3 Mef2c is the likely partner for Mrf proteins in somitic myogenesis.

Mrf genes are important regulators of myogenic commitment and differentiation, yet their proficiency in target gene activation relies upon their interaction with Six/Eya and Mef2 proteins (reviewed in (193,313) . Our analysis suggests that Six and Eya proteins are constantly available to Mrf proteins since their expression was seen in epithelialising somites, the early dermomyotome, and then the dorsomedial and ventrolateral dermomyotomal lips as well as the myotome. Of the *Mef2* genes, only *Mef2c* showed strong expression in the developing somites, highlighting *Mef2c* as a likely partner of Mrf proteins. *Mef2c* expression followed that of *MyoD* and therefore may explain the fact that terminal differentiation does not occur prior to the onset of *MyoD* expression.

3.3.4 All cells in the amniote somite have a history of pre-myogenic gene expression.

Our study showed that the immature chicken paraxial mesoderm invariably expresses *Tbx6*. When the tissue condenses and epithelial somites form, *Tbx6* expression is gradually replaced with the expression of the pre-myogenic genes (*Paraxis, Pax3, Pax7, Six1, Eya1*). The pre-myogenic genes are all expressed throughout the developing somite before becoming confined to the dermomyotome (*Paraxis, Pax3, Pax7*) or the dorsomedial and ventrolateral dermomyotomal lips and the myotome (*Six1, Eya1*). The same sequence of gene expression has been reported for the mouse (104,314). This suggests that in amniotes, the trunk paraxial mesoderm adopts a specific pre-myogenic state before cells are being released into differentiation. Interestingly, in Xenopus and zebrafish, expression of *Mrf* genes begins concomitant or prior to somite formation; differentiation of functional skeletal muscle occurs shortly thereafter (145,300). Expression of *Pax7* appears later and is associated with the formation of muscle stem cells and the emergence of the dermomyotome (90,315). Moreover, in Xenopus, the area delivering the *Pax7* expressing cells initially expressed *MyoD*. Thus, in anamniotes, functional muscle that allows the larvae to swim is made quickly whereas cells with muscle stem cell features arrive later.

This furthermore suggests that the anamniote embryo is geared up towards myogenesis, while in amniotes, myogenesis is held back.

3.3.5 The pre-myogenic genes may have distinct roles in the myogenic programme.

Our study showed that the pre-myogenic genes are initially expressed throughout the young somite and later, their expression overlaps with that of the *Mrf* genes in the dorsomedial and ventrolateral dermomyotomal lips of the dermomyotome. All the pre-myogenic genes have previously been demonstrated to be activators of *MyoD*, at least in the context of a *Myf5* knock-out (121). This therefore suggests that they all act upstream of the *Mrf* cascade for similar effect. However, the postmitotic cells of both the primary and secondary myotome show no expression of *Paraxis*, *Pax3* and *Pax7;* in the mature somite; *Pax7* expression appears in the myotome only when the mitotically active embryonic muscle precursor come in at E3.5, thereby forming the tertiary myotome (316). This suggests that in the context of a naturally developing amniote somite, the *Paraxis/Pax3/Pax7* gene set may control the expansion of the precursor/stem cell pool and establish the myogenic fate. However, the genes do not immediately initiate myogenic differentiation. This idea is corroborated by studies in which wildtype and dominant negative forms of *Pax3* and *Pax7* were misexpressed in vitro. These studies showed that *Pax3* and *Pax7* keep the myogenic cells mitotically active while impeding immediate differentiation (317,318). Moreover, *Pax7*, while co-expressed with *Myf5* or *MyoD* at the time when the cells commit to myogenesis, is shut down by MyoG when the cells enter terminal differentiation (319).

In contrast to *Paraxis* and Pax3/7, we found that *Six1* and *Eya1* expression eventually declined in the dermomyotome but continued in the differentiating cells of the myotome. Notably, Six and Eya proteins have been shown to accumulate in the nuclei of human myotomal cells at the time that *MyoG* is expressed, not before, indicating a role in the activation of genes required for muscle differentiation (173) . *Six1* has also been shown to be an activator of *MyoG* and of genes encoding proteins required for muscle contraction, particularly proteins for glycolytic, fast-twitch contraction (181). *Six1* is therefore a myogenic gene more than a pre-myogenic gene. This theory is corroborated by *Pax3/7* double knock-out mice which were seen to struggle with forming a myotome whereas *Six1/4* mice form a myotome which fails to develop further (164,297)

In the early somite, *Six* and *Eya* genes are expressed along with *Dach* and *Groucho/TLE* co-repressor genes, whereas in the myotome, some *Groucho* gene expression remains but *Dach* gene expression is shut down (165,245). The relative levels of Six, Dach, Groucho and Eya proteins may determine whether Six-Groucho and Six-Dach complexes repress their respective target genes, or whether Six-Eya or Six-Eya-Dach complexes act as transcriptional activators. It has yet to be confirmed that Six and Eya proteins can be localised to the nucleus in young somites (173); however, the presence of some protein at the promoters of target genes cannot be excluded. Thus, it is feasible that Six proteins play a role in the early somite, but likely as a temporary repressor of the myogenic program. Studies on Six4, MyoD and Mef2d binding to DNA revealed that these proteins create a poised promoter that is loaded with the transcriptional machinery

but require further input before transcription is fully activated (reviewed by (193). Thus, it is plausible that the distinct pre-myogenic role of Six proteins is to prepare promoters of muscle genes for activation.

3.3.6 Expression of the first muscle structural genes is concomitant with that of MyoG.

Our study revealed that at a given stage in development, the exact beginning of gene expression varied somewhat, most likely because the embryos were in a different phase of segmentation and epithelial somite formation. Furthermore, the extended time needed for the staining reaction when analysing weakly expressed genes (up to two weeks) led to somewhat divergent results. However, we found that the order of marker gene expression was in agreement at all stages investigated, with *Myf5* showing expression before *MyoD*, followed by the onset of *Mef2c*. This was subsequently followed by the expression of *MyoG* and the first muscle structural gene, *Tnni1*, and ultimately the expression of sarcomeric *Myosin* genes (Fig. 3.10). The approximately coinciding expression of *MyoG* and *Tnni1*, followed by the expression of other structural genes is in line with suggestions that *MyoG* is involved in the initiation of terminal differentiation and the activation of late muscle genes (210). However, at HH15 and HH19/20 *Tnni1* expression appeared to occur prior to that of *MyoG*. This may be within the assay margin of error but a double *in situ* hybridisation assay would be required to clarify this point. MyoD and MyoG recognise similar DNA sequence elements but also have unique protein-protein interaction domains which allow MyoD and MyoG each to target a subset of distinct promoters independent of their protein-DNA interaction sites. MyoD recognises alone a few structural genes such as *Tnni1*, *Myosin* heavy chain, *Myosin* light chain and *Desmin* (320). Using ChIP essays Bergstrom showed that in *vivo* MyoD is recruited in the early stages of myogenesis. However late MyoD targets such as Desmin was not detected until 24 hr after the induction of MyoD. This is shows that MyoD action is delayed until the proper key time of activation and the binding of MyoD was prevented entirely at E boxes in genes not expressed in the skeletal muscle. Bergstrom demonstrated that the promoter-specific regulation of MyoD binding is a critical mechanism for patterning gene expression (320). MyoD starts the histone modifications and alone is enough for the expression of early genes but requires to be combined with MyoG at late stages. In culture MyoG does not substantially activate muscle gene expression in the absence of MyoD. This could be explain by the fact that MyoG needs MyoD to permit the histone modifications, critical to form a stable DNA binding complex (210).

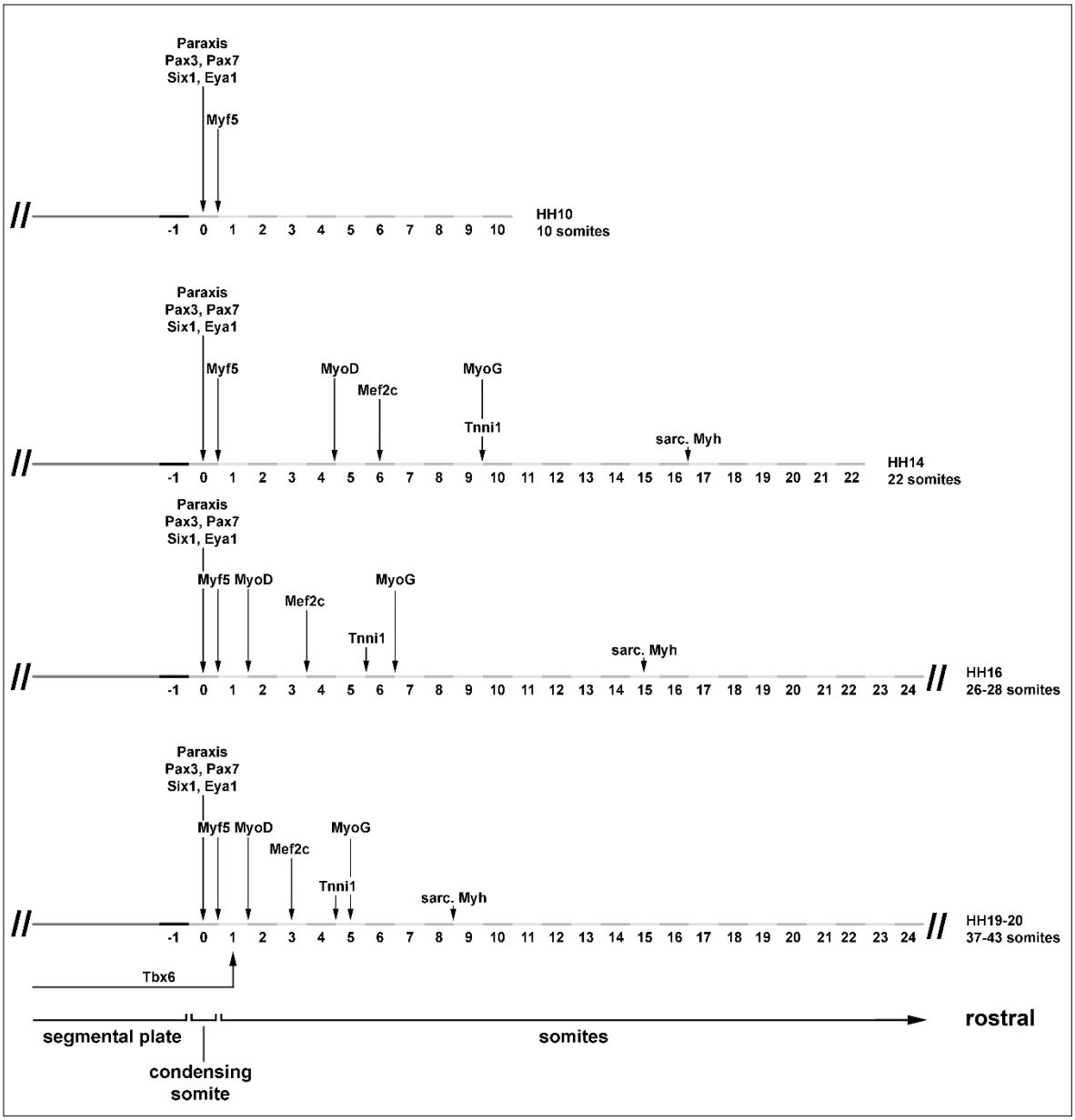

Figure 3. 11: Summary

Progression of marker gene expression from HH10-HH19/20, focusing on the onset of the most strongly expressed genes as their onset can be determined most precisely. At all times, the expression of *Tbx6*, of pre-myogenic genes and of *Myf5* overlaps. As development proceeds, the onset of markers associated with myogenic progression and terminal differentiation occurs earlier, indicating that the process accelerates in comparison to the progress of somite formation.

3.3.7 Differentiation catches up with somitogenesis.

At the early stages of development, the markers for differentiation initiation were not yet expressed (HH10) or were expressed at a distance away from the segmental plate (HH14). As development progressed, this distance decreased (HH16, HH19/20), suggesting that the process of differentiation catches up with the process of somitogenesis, and may ultimately contribute to the consumption of immature cells in the tail bud of the embryo. The decline of Wnt and Fgf signalling in the tail bud, combined with increased retinoic acid levels as a result of Raldh2 expression, has been attributed to controlling the cessation of somite formation and body elongation (321,322). However, these changes occur after the time period considered here, suggesting that additional contributing factors are involved in the acceleration of somite differentiation.

3.3.8 Distinct combinations of gene expression distinguish cells from the dorsomedial, ventrolateral and rostrocaudal dermomyotomal lips.

Myf5 expression was tightly associated with cells in the dorsomedial and ventrolateral lips of the dermomyotome and the linked sublip regions, which accounts for the incremental growth of the myotome (304–306,323). The rostrocaudal lips themselves are a further source of myogenic cells and are considered the driver of the myotomal centre expansion (Kahane et al., 1998a). Yet, while *Mef2c* and *Follistatin* expression is shown in cells emerging from all dermomyotomal lips, this was not the case for *Mrf*. Moreover, the rostrocaudal lips but not the dorsomedial or ventrolateral lips expressed *Pitx3*, suggesting that distinct myogenic cascades exist in the four lips. However, *Myf5* was expressed in cells nearby the rostrocaudal lips, indicating that ultimately, all cells express *Mrf* and the cascades converge.

3.3.9 Gene products are differentially distributed along the rostrocaudal length of the myotube.

Skeletal muscle (myofibrils) is constructed out of distinct repetitive arrangements of contractile protein complexes called sarcomeres (324). It is therefore interesting to note that *Myh15* and *Myh7* gene expression, although initially being present in the myotomal centre, became differentially distributed in the mature myotome, with *Myh15* mRNA and protein being enriched at the rostrocaudal extremes and *Myh7* gene products in the centre. Given that *Myh7* expression is staggered after that of *Myh15*, it is feasible that *Myh7* expression may become similarly redistributed as for *Myh15*. However, it is also possible that the contractile specifications vary along the length of a myotube. Many Fgf signalling molecules have been reported to be specifically expressed in the myotomal centre where they control the release of the embryonic muscle stem cells from the overlying dermomyotome (325,326). Future exploration into these processes and the details of the proposed link may provide an interesting insight.

Chapter 4

4 Design and validation of Mrf expression constructs

4.1 Introduction

In the previous chapter, we described, how the basis of the study was laid, analysing a palette of genes that could serve as marker genes to monitor myogenic progression. In this chapter, it will be described, how the experimental approach to test muscle stem cell protection was developed, and which steps were undertaken to ascertain that this approach would work.

4.1.1 The working hypothesis of this project: suppression of premature differentiation ensures the in vivo maintenance of the muscle stem cell state.

Muscle stem cells cultured *in vitro* quickly lose their stem cell characteristics and their ability to efficiently differentiate into muscle (15). In a healthy organism *in vivo*, however, a pool of muscle stem cells persists throughout life; in fact, muscle stem cells can even be collected from a recently deceased (327). This suggests that in a healthy individual, mechanisms exit that protect the muscle stem cell state.

In the introduction to this thesis, possible factors that contribute to the stem cell niche and the maintenance of the stem cell pool were discussed, and efforts are being made to recapitulate these conditions when culturing muscle stem cells *in vitro*. However, eventually, extrinsic cues have to be molecularly integrated inside the cell, and hence, intrinsic mechanism must exist, too. This idea is reinforced by the observation that muscle stem cells can be recovered from a cadaver where the environment of the muscle stem cells ceased to support the stem cell. Yet the intrinsic mechanism of stem cell protection is not known.

The previous expression analysis showed that in amniotes, the naïve paraxial mesoderm sequentially expresses a series of marker genes until markers associated with a muscle stem cell state - the pre-myogenic genes - are established in the somite. Cells then have the choice to retain stem cells features or to enter the differentiation program for muscle. The may also contribute to the dorsal dermis or the axial skeleton and connective tissue (328). However, the somite evolved as a structure to provide muscle for locomotion before the ability to generate cartilage and bone was acquired (135). Moreover, in anamniote vertebrates that develop via free-feeding juvenile stages, the paraxial mesoderm rapidly lays down skeletal muscle (329). We thus hypothesised that the main protection muscle stem cells require is a protection from premature differentiation since this guarantees a balance between muscle formation and maintenance of the stem cell pool. This idea is supported by the fact that pre-myogenic genes – though possibly at different steps -

are involved in the acquisition of myogenic competence and the activation of myogenic genes. Yet differentiation does not immediately occur when the pre-myogenic genes are expressed; in fact, prolonged expression of specifically *Pax3* and *Pax7* delays differentiation, and these genes are shut off during the differentiation process (318).

4.1.2 The experimental approach: in *vivo* misexpression of *Mrf* genes

Entry into myogenesis is marked by the sequential expression of *Six/Eya*, *Mrf* and *Mef2* genes, followed by the activation of muscle structural genes ((330)) and this study). Phylogenetic studies established that members of the gnathostome *Six*, *Eya*, *Mrf* and *Mef2* gene families arose during the whole genome duplications that occurred early during the evolution of this group of vertebrates (161,307,331). Therefore, it was not surprising that paralogous genes had some functional redundancy, and in loss-of-function experiments, several had to be inactivated simultaneously to show that these genes are required for myogenesis. However, gain-of-function experiments showed that of the *Six/Eya*, *Mrf* and *Mef2* genes, only the *Mrf* genes are sufficient to drive myogenesis: when misexpressed *in vitro*, they can force myogenic as well as non-myogenic cell lines into myogenic differentiation (186,332,333). Moreover, when prematurely expressed in blastula-stage Xenopus embryos, *Mrf* can force non-myogenic cells into muscle differentiation (334–336). Furthermore, when misexpressed in the chicken neural tube/neural crest cells, *Mrf* can trigger expression of sarcomeric Myosins (albeit with very low efficiency; (337). Therefore, it was concluded that the *Mrf* genes are master regulators of myogenesis. Consequently, we chose as our first experimental series an *Mrf* misexpression approach in live muscle stem cells in vivo.

4.1.3 The experimental model for *in vivo* misexpression: the chicken embryo

Biomedical research aims at developing muscle stem cells for therapy in a patient. Hence, research will have to deliver the knowledge and understanding to manipulate adult muscle stem cells. The majority of these cells, at least in amniotes, are held in a quiescent state (77). Therefore, return to quiescence is typically interpreted as a sign that a muscle stem cell retained stem cell features and self-renewed. As explored in the introduction, muscle stem cell quiescence represents a specialised form of stem cell behaviour. Moreover, suspension in the G0 phase of the cell cycle is not per se a sign of stem cell properties. Yet it is difficult to experimentally separate the maintenance of generic muscle stem cell features (being muscle-competent, but undifferentiated and self-renewing) from a return to quiescence. Thus, we turned to a model where muscle stem cells quiescence is not an issue, namely embryonic muscle stem cells.

Embryonic muscle stem cells are held in the somitic dermomyotome until released to populate the myotome (139). Thus, muscle stem cells can be selectively targeted. The chicken embryo is the ideal model to do so since it is accessible in the egg, the largest of all vertebrate models, and protocols to introduce molecular constructs into the dermomyotome are well established (338–

340). The mouse embryo develops in utero and hence, is not accessible for transient assays. Instead, costly transgenic mouse lines that allow gene misexpression selectively in the dermomyotome would have to be created. Xenopus and zebrafish embryos are accessible but small. Constructs are typically delivered at the 1- or 2-cell stage, and hence early phenotypes arise before the desired stage of development is reached. The generation of transgenic fish and frog lines are options, but this would render the work as costly as for the mouse. Moreover, as will be discussed below, we suspected that in the anamniote models, rapid myogenesis is promoted, not suppressed. Hence, the chicken, being an amniote like mammals, remained the preferred choice of model. Consequently, we had to optimise the misexpression approach for the chicken.

4.1.4 Criteria to generate appropriate Mrf constructs

Structure and function of Mrf proteins has been investigated in numerous studies. However, these studies differed in the choice of expression vector, details of the molecular construct, use of autologous or heterologous *Mrf* genes and the use of proteins tags. We will below consider these differences and explain the criteria we used to create the, we hoped, most potent chicken *Mrf* expression constructs.

4.1.4.1 Selection of a strong promoter/ enhancer

To fully explore the potency of *Mrf* in enforcing myogenic differentiation of muscle precursor and stem cells *in vivo*, it was important to generate constructs with optimal molecular properties. *In vivo*, gene transcription is controlled by chromatin remodelling proteins, transcription factors and the protein complex facilitating RNA synthesis (trans-regulatory elements) which act on gene specific enhancer and promoter sequences (cis-regulatory elements; (341)). The interplay between trans- and cis-acting factors is a product of genome evolution, and the level of transcription of an endogenous gene may not be high (342,343). Yet misexpression studies *in vitro* showed that *MyoD*-driven myogenic conversion was more efficient when construct expression was driven from a strong promoter such as the human cytomegalovirus (CMV) or Rous sarcoma virus (RSV) promoter, and less efficient when driven from the in comparison weaker Simian vacuolating virus 40 (SV40) promoter (332,344). Thus, the expression vector of choice should also contain this promoter/ enhancer.

4.1.4.2 Inclusion of a Kozak sequence for strong translation

The Kozak sequence was identified as a consensus sequence for the initiation of translation from vertebrate mRNAs (345). It is recognised by the ribosome and facilitates the use of the ATG included in this sequences as translation initiation site. The most conserved position in this motif is the purine (R) in position -3 (three nucleotides upstream from the ATG codon) which occurs in 97% of vertebrates mRNA (346). Mrf coding sequences do not necessarily have a full Kozak consensus at the translation initiation site, and hence, translation levels may vary. All the

constructs designed for use in this study were appended with the Kozak sequence and therefore, all construct mRNAs will have translation initiated at equally high rates. This allows us to standardise experimental conditions.

4.1.4.2.1 Factors that affect translational control

mRNA translation is affected by the RNA processing steps. It has been shown that correct removal of introns by splicing as well as processing of poly A signals can stabilise a primary mRNA and ensure that it is not prematurely degraded (347). During translation, the progress of the ribosome is affected by RNA secondary structure and codon usage. Areas of strong RNA structure or including rare codons with low abundance cognate tRNAs, cause the ribosome to progress at a slower rate and thus affect the overall equilibrium of protein concentrations within the proteome (348).

4.1.4.3 Use of autologous versus heterologous Mrf proteins

Mrf expression constructs have been used extensively, and misexpression studies have been performed in cells of many different species *in vitro* but also *in vivo*. In some studies, heterologous *Mrf* genes were misexpressed since this allows to discriminate transgene and endogenous gene expression. An example is the study by Delfini and Duprez (2004), in which mouse Myf5 and MyoD were misexpressed in the chicken neural tube and neural crest cells (224,337). In other studies, the autologous genes were used as these genes should be evolutionarily optimised for the chosen experimental model. An example is the study by Sweetman et al. (2008), in which tagged versions of chicken Mrf were expressed in the chicken neural tube and neural crest cells (224,337); for an evaluation of tags, see below). Unfortunately, the efficiency of heterologous Mrf driven from otherwise identical constructs has not systematically been explored. We therefore undertook a detailed comparison of vertebrate Mrf protein sequences to establish, how much proteins may differ between species and whether it would be advisable to use chicken Mrf. This comparison will be shown in the results section below.

4.1.4.4 Avoidance of tags that might interfere with Mrf protein function

Epitope fusion tags are a widely employed strategy for detecting protein expression due to their simple application. The tag is a short peptide sequence that is recognised by a commercially available monoclonal antibody. When fused to a protein of interest, the proteins can be detected even if no antibody for this specific protein currently exists. Yet some recent reports have shown that epitope tags can influence the function of the proteins they are fused to. Positioning a tag N- or C-terminally can influence the protein's affinity with its binding partner if positioned close to a binding site, and if positioned internally could affect the folding of the protein itself (349). Z. Shevtsova et al. compared the function of tagged and untagged Enhanced Green Fluorescent Protein (EGFP) and found that the migration pattern of EGFP on SDS-PAGE gels differed,

depending on whether an HA-tag was fused to either the amino or the carboxy terminus of the protein. Intriguingly, all HA-tagged EGFP proteins also showed considerably reduced fluorescence when compared to EGFP alone or to EGFP fused to other epitope tags (350).

Previous studies on the sequence and structure of Mrf proteins revealed that these transcription factors have a highly conserved basic domain linked to a helix-loop-helix domain, required for nuclear localisation, DNA binding and interaction with their E-protein partners. These domains are located in the N-terminal half of the proteins. The proteins also carry a conserved, Myc-like C-terminal domain involved in gene transactivation, this domain is longer in Myf5 and MyoD where it is referred to as a Myf5-domain. Work by Tapscott et al. (1988) and Bergstrom et al. (2001) showed that in Myf5 and MyoD, the ultimate C-terminus is also conserved and functionally relevant (157,351). We investigated more closely the conservation of Mrf protein termini, to decide whether or not the use of tags would be advisable (see below). We found no site that would allow to safely place an epitope tag without the risk of compromising protein function, and for this reason we decided to not add any epitope tags to the proteins sequences.

4.1.5 Test systems to validate the constructs

Our hypothesis is that the Mrf constructs are not sufficient to enforce premature myogenesis in amniote muscle stem cells. If this were to be correct, then misexpression of Mrf in the chicken embryo would not lead to the premature and ectopic expression of sarcomeric Myosins in the dermomyotome. A result like this however would be indistinguishable from results obtained by non-functional constructs. We therefore needed a positive control to confirm the activity of the constructs before inferring biological relevance from negative results.

As will be shown below, our comparative bioinformatics analysis of Mrf proteins suggested that the use of untagged, chicken-specific Mrf proteins would be advisable to generate constructs best suited for misexpression in the chicken embryo. Detection of translation of the misexpression constructs would therefore rely on antibodies specific to the individual protein. However, these do not currently exist and it was considered too time consuming and costly to generate these antibodies for this project. Therefore, we planned a series of experiments to validate the activity of our constructs.

To confirm the generation of biologically active Mrf proteins, we decided to replicate the experiments of Ludolph in 1994 (334), where they injected Xenopus embryos at the 1 or 2-cell stage or the early blastula stage with Xenopus *MyoD* or *Myf5* mRNAs. They showed that on the injected side, non-myogenic cells were recruited into myogenesis. When injected at the 2 cell stage, cells underwent myogenic differentiation even before gastrulating, such that almost the entire half of the embryos expressed sarcomeric Myosin. We expected that our own constructs would lead to similar phenotypes when fully functional.

As will be shown below, we largely obtained the expected results. We therefore, as the last of our preparatory experiments, established in the chicken, when exactly after electroporation cells would be exposed to the products of our misexpression constructs, i.e. from which time point onwards phenotypes might emerge.

4.2 Results

4.2.1 Determination of the desired sequences

4.2.1.1 Phylogenetic tree of Mrf proteins

The data collected from Dr. Dietrich synteny analysis allowed us to allocate Mrf sequences to the four *Mrf* paralog groups. To further corroborate this allocation, a phylogenetic analysis of Mrf protein sequences was carried out. *Mrf* genes have been found in not only in jawed vertebrates, but also in agnathans and in invertebrates. In Drosophila melanogaster, an insect and hence belonging to the ecdysozoan branch of protostome animals, the *mrf* gene is known as *nautilus* (352). To carry out a meaningful phylogenetic analysis, we strived to identify Mrf protein sequences across bilateria, performing protein and cDNA database searches using the BLAT/BLAST algorithm as before. The complete list of animals searched and their phylogenetic relationship is provided in Annex Table 3.A. The protein sequences were aligned in Bioedit using ClustalW. The alignments were manually adjusted where ClustalW failed to align similar sequence stretches owing to different sequence length. The alignments were trimmed and phylogenetic unrooted and rooted trees were constructed by F. Schubert, using MPhyl3. Trees were then constructed using iTol (Fig.4.1) (353). The first trees (Fig.4.1 A, B) contained the Drosophila and red flour beetle nautilus sequences, and these were used as outgroups to root the tree. However, as the protostome sequences were very divergent, the relationship of the deuterostome sequences was not resolved well. We therefore generated a second set of trees with the protostome sequences excluded. To root this deuterostome Mrf tree, the echinoderm sequences were used as outgroups (Fig.4.1 C, D).

In the tree analyses, gnathostome Myf5, MyoD, MyoG and Mrf4 protein sequences formed distinct subgroups. Moreover, the teleost proteins belonging to the conserved MyoD locus and to the more divergent MyoD locus were grouped separately, the latter with a bootstrap value of 100. This indicates that our previous allocation of Mrf proteins to paralog groups was correct. The grouping of proteins within a paralog group largely followed the known animal phylogeny, with sarcopterygian sequences being grouped away from actinopterygian and condrichthyan sequences. Exceptions were Latimeria Mrf4 that was equidistant from sarcopterygian and actinopterygian Mrf4 proteins, elephant shark MyoG that grouped with the sarcopterygian sequences, and Human, Xenopus and elephant shark MyoD that grouped with the actinopterygian

MyoDs (see Fig.4.1 D). However, bootstrap values for these allocations were low, indicating that the grouping is not robust. Additional analyses using additional phylogenetic algorithms will solve this problem (354).

Interestingly, in all trees, Myf5 and MyoD formed one metagroup, and MyoG and Mrf4 formed a second. Moreover, the invertebrate sequences fell between the Myf5/MyoD and the MyoG/Mrf4 subgroups, respectively. This suggests also in the lineage leading to vertebrates, once an ancestral Mrf gene existed that combined properties of the current gnathostome Mrfs. It also suggests that after the first genome duplication, Myf5-MyoD arose from one ancestral gene, and MyoG-Mrf4 from another ancestral gene, in line with (355). Unexpectedly, the hagfish Mrf sequence which we had expected to also lie between the Myf5-MyoD and MyoG-Mrf4 group, instead grouped with the Myf5-MyoD set. However, agnathan sequence information was limited and the sequence used here may not have been representative.

Moreover, the first round of vertebrate genome duplication may have occurred before the agnathan-gnasthostome split (356–358), and hence the existence of a further agnathan Mrf gene/ protein, possibly more closely related to MyoG-Mrf4, cannot be excluded.

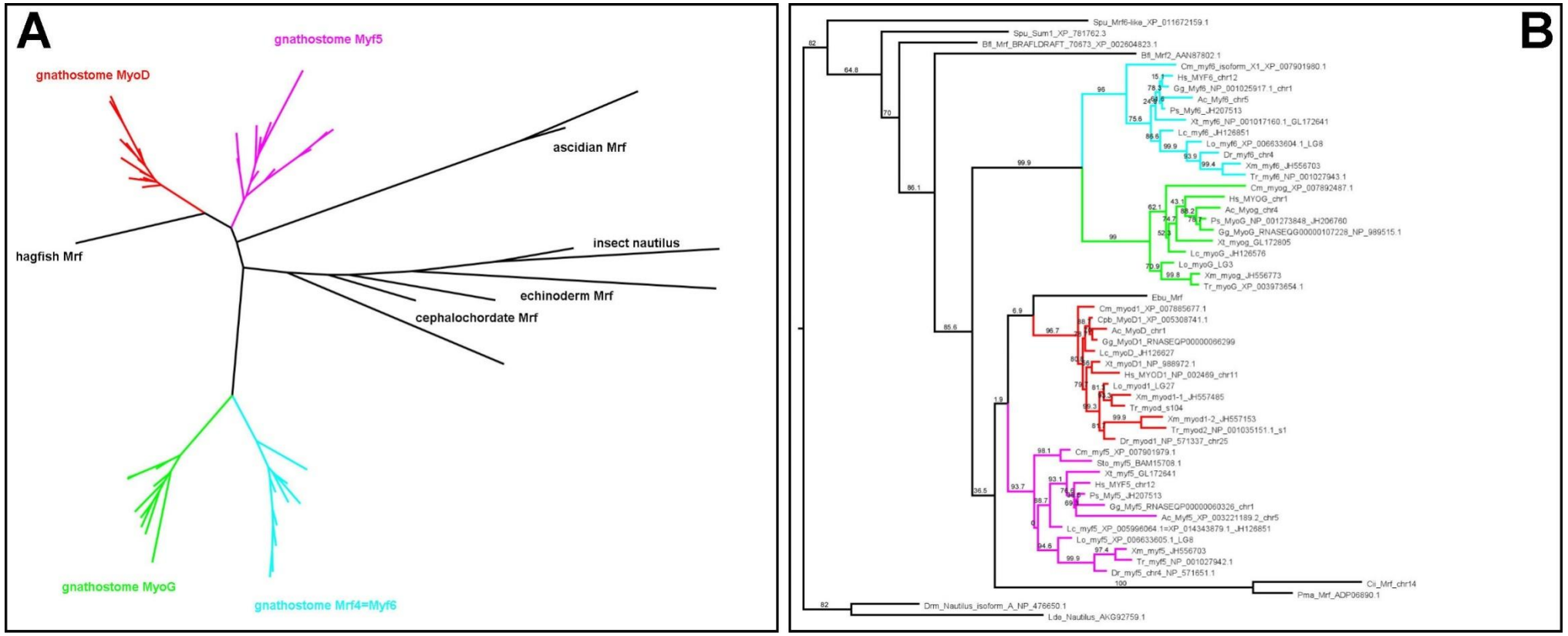
A
gnathostome Myf5
gnathostome MyoD
ascidian Mrf
hagfish Mrf
insect nautilus
echinoderm Mrf
cephalochordate Mrf
gnathostome MyoG
gnathostome Mrf4=Myf6
B
Spu_Mrf6-like_XP_011672159.1
Spu_Sum1_XP_781762.3
Bfl_Mrf_BRAFLDRAFT_70673_XP_002604823.1
Bfl_Mrf2_AAN87802.1
Cm_myf6_isoform_X1_XP_007901980.1
Hs_MYF6_chr12
Gg_Myf6_NP_001025917.1_chr1
Ac_Myf6_chr5
Ps_Myf6_JH207513
Xt_myf6_NP_001017160.1_GL172641
Lc_myf6_JH126851
Lo_myf6_XP_006633604.1_LG8
Dr_myf6_chr4
Xm_myf6_JH556703
Tr_myf6_NP_001027943.1
Cm_myog_XP_007892487.1
Hs_MYOG_chr1
Ac_Myog_chr4
Ps_MyoG_NP_001273848_JH206760
Gg_MyoG_RNASEGG00000107228_NP_989515.1
Xt_myog_GL172805
Lc_myoG_JH126576
Lo_myoG_LG3
Xm_myog_JH556773
Tr_myoG_XP_003973654.1
Ebu_Mrf
Cm_myod1_XP_007885677.1
Cpb_MyoD1_XP_005308741.1
Ac_MyoD_chr1
Gg_MyoD1_RNASEQP00000066299
Lc_myoD_JH126627
Xt_myoD1_NP_988972.1
Hs_MYOD1_NP_002469_chr11
Lo_myod1_LG27
Xm_myod1-1_JH557485
Tr_myod_s104
Xm_myod1-2_JH557153
Tr_myod2_NP_001035151.1_s1
Dr_myod1_NP_571337_chr25
Cm_myf5_XP_007901979.1
Sto_myf5_BAM15708.1
Xt_myf5_GL172641
Hs_MYF5_chr12
Ps_Myf5_JH207513
Gg_Myf5_RNASEQP00000060326_chr1
Ac_Myf5_XP_003221189.2_chr5
Lc_myf5_XP_005996064.1=XP_014343879.1_JH126851
Lo_myf5_XP_006633605.1_LG8
Xm_myf5_JH556703
Tr_myf5_NP_001027942.1
Dr_myf5_chr4_NP_571651.1
Cii_Mrf_chr14
Pma_Mrf_ADP06890.1
Drm_Nautilus_isoform_A_NP_476650.1
Lde_Nautilus_AKG92759.1

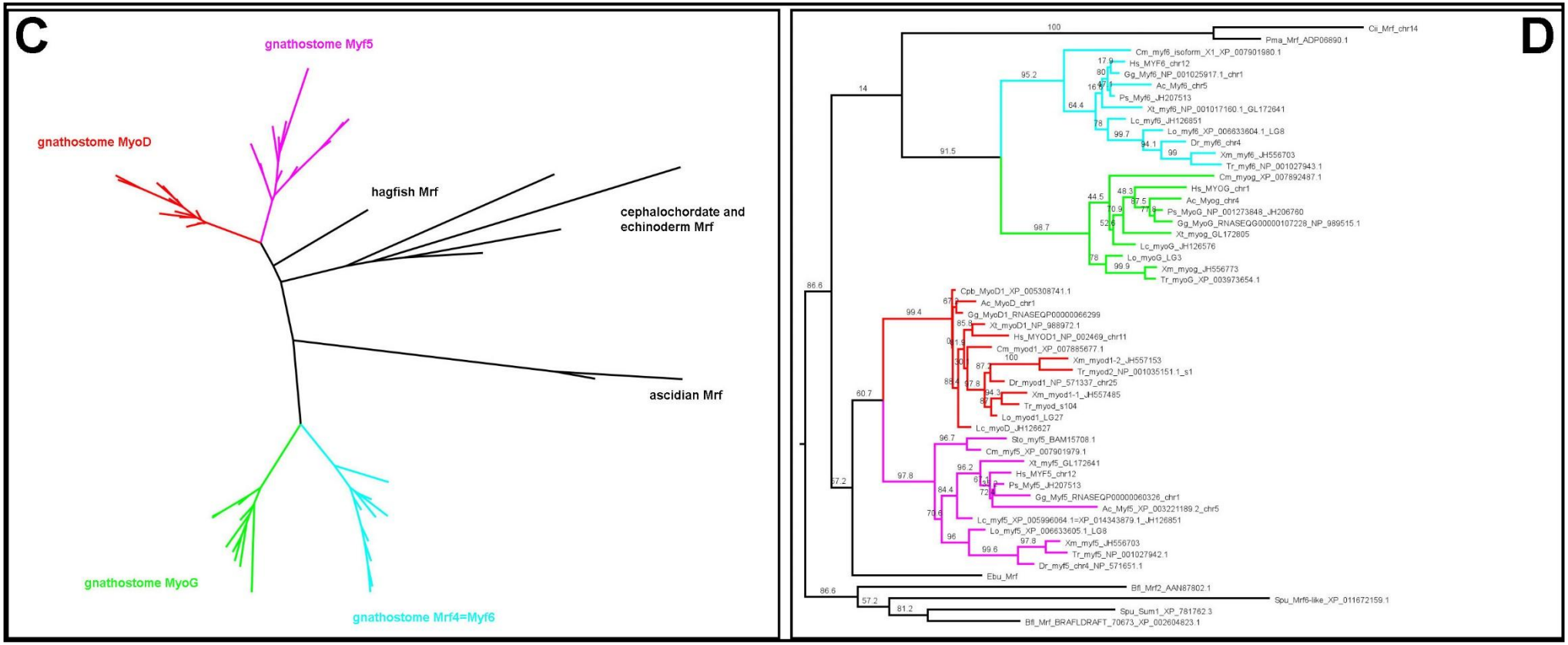
C
gnathostome Myf5
gnathostome MyoD
hagfish Mrf
cephalochordate and
echinoderm Mrf
ascidian Mrf
gnathostome MyoG
gnathostome Mrf4=Myf6
D
Cii_Mrf_chr14
Pma_Mrf_ADP06890.1
Cm_myf6_isoform_X1_XP_007901980.1
Hs_MYF6_chr12
Gg_Myf6_NP_001025917.1_chr1
Ac_Myf6_chr5
Ps_Myf6_JH207513
Xt_myf6_NP_001017160.1_GL172641
Lc_myf6_JH126851
Lo_myf6_XP_006633604.1_LG8
Dr_myf6_chr4
Xm_myf6_JH556703
Tr_myf6_NP_001027943.1
Cm_myog_XP_007892487.1
Hs_MYOG_chr1
Ac_Myog_chr4
Ps_MyoG_NP_001273848_JH206780
Gg_MyoG_RNASEQG00000107228_NP_989515.1
Xt_myog_GL172805
Lc_myoG_JH126576
Lo_myoG_LG3
Xm_myog_JH556773
Tr_myoG_XP_003973654.1
Cpb_MyoD1_XP_005308741.1
Ac_MyoD_chr1
Gg_MyoD1_RNASEQP00000066299
Xt_myoD1_NP_988972.1
Hs_MYOD1_NP_002469_chr11
Cm_myod1_XP_007885677.1
Xm_myod1-2_JH557153
Tr_myod2_NP_001035151.1_s1
Dr_myod1_NP_571337_chr25
Xm_myod1-1_JH557485
Tr_myod_s104
Lo_myod1_LG27
Lc_myoD_JH126627
Sto_myf5_BAM15708.1
Cm_myf5_XP_007901979.1
Xt_myf5_GL172641
Hs_MYF5_chr12
Ps_Myf5_JH207513
Gg_Myf5_RNASEQP00000060326_chr1
Ac_Myf5_XP_003221189.2_chr5
Lc_myf5_XP_005996064.1=XP_014343879.1_JH126851
Lo_myf5_XP_006633605.1_LG8
Xm_myf5_JH556703
Tr_myf5_NP_001027942.1
Dr_myf5_chr4_NP_571651.1
Ebu_Mrf
Bfl_Mrf2_AAN87802.1
Spu_Mrf6-like_XP_011672159.1
Spu_Sum1_XP_781762.3
Bfl_Mrf_BRAFLDRAFT_70673_XP_002604823.1

4.1: Phylogenetic trees of vertebrate Mrf proteins

(A) Unrooted and (B) rooted phylogentic trees for deuterostome Mrf proteins as well as Drosophila and Trilobium castaneum nautilus proteins. In (B), the tree was rooted with the insect sequences. (C) Unrooted and (D) rooted phylogentic trees for deuterostome Mrf proteins; in (D), the tree was rooted with the echinoderm Mrf sequences. In (B, D), the abbreviations of proteins names were used as delineated in Table 1 and Appendix Fig.1. In (B,D), Bootstrap values are also indicated. Note that gnathostome Myf5, MyoD, MyoG and Mrf4(=Myf6) proteins form clearly distinguished groups. Also note that Myf5-MyoD and MyoG-Mrf4 form meta-groups, supported by high bootstrap values. This suggests that Myf5 and MyoD genes arose from one, MyoG and Mrf4 genes from the other ancestral gene that evolved after the first vertebrate genome duplication.

4.2.1.2 Protein motif analysis

Having established the allocation to the four gnathostome Mrf groups, we now separately aligned the individual Mrf paralogs to compare similarities and differences. For the chicken, the various version available for a particular protein were also included. The alignments are shown in Appedix 1; conserved features as well as differences between the chicken proteins are annotated. The features of Mrf proteins are summarised in Table 4.1.

Table 4. 1: Typical features of Mrf proteins

Amino acids are displayed in 1-letter-code, colour code as in Appendix 1.

Note the similarity between the Myf5/MyoD and MyoG/Mrf4 protein termini and the presence of a complete Myf5 domain in Myf5/MyoD only, supporting the idea that Myf5/MyoD and MyoG/Mrf4 are phylogenetically and functionally related.

	Gnathostome Myf5	Gnathostome MyoD	Gnathostome MyoG	Gnathostome Mrf4	
Feature					**Shown in**
N-terminus	Consensus: M-E/D-V-M-D	Consensus: M-E/D-L/M-L/S/T. This motif is duplicated in non-mammalian tetrapods	Consensus: M-E-L-F-E-T-N/S	Consensus: M-M-D-L-F-E-T	Appendix 1, brackets
Basic domain	conserved	conserved, contains a H-rich domain (exception: mammals)	conserved	conserved	Appendix 1, blue shading
HLH domain	conserved	conserved	conserved	conserved	Appendix 1, green shading
Myf5 domain	present and conserved	present and conserved	incomplete, but sequences conserved	incomplete, but sequences conserved	Appendix 1, pink shading
C-terminus	Consensus: T-Y-Q-A-L in birds, I/V-Y-H-V-L in all other gnathostomes (no information available for crocodylians)	Consensus: I-Y-Q-V-L (not conserved for the teleost 2nd MyoD)	Conserved in diapsis; consensus: E-E-R-V-Q-N	Conserved in amniotes, consensus: E-E-V/A/L-V/A-E-K	Appendix 1, arrows

4.2.1.2.1 Myf5

The alignment of the Myf5 sequences revealed a high degree of conservation for the basic (Appendix 1A, blue shading), helix-loop-helix (green shading) and the Myf5 domain (pink shading). Notably, in all animals except teleosts and lepidosaurs (Anole lizard and python), the first 5 amino acids are highly conserved; the consensus sequence in 1-letter-code is M-E/D-V-M-D (Appendix Fig.1A, black bracket). Likewise, the C-terminus typically shows the presence of T-Y-Q-A-L in birds (T-C-L-A-I in the zebra finch), I/V-Y-H-V-L in all other gnathostomes (Appendix Fig 1.A, arrows). Exception for the latter are the sequences for the budgerigar (premature stop codon), and the sequences for the peregrine falcon, the rock dove and crocodylians. Here the sequence downstream to the 2nd splice site (2nd black triangle) are highly divergent. Yet these sequences are currently predicted sequences only, suggesting that the 3rd exon may not yet have been properly identified. However, the conservation of the internal protein domains and the sequences at the protein termini suggested they are all functionally important and therefore, to avoid interfering with the activity of these domains, we decided not to tag the proteins.

Interestingly, avian Myf5 sequences showed a few special features. This included a stretch enriched in prolines and charged amino acids in the centre of the basic domain (position 35-45 in the gapped alignment) and a stretch enriched in prolines towards the C-terminus (position 293-295). Given that prolines can change the 3-D structure of proteins, in particular break helices, this features might be relevant (359). Thus, the use of chicken-derived sequences might be the safest option when using the chicken model. Importantly, for chicken *Myf5* the RNAseq-derived sequences and the sequences predicted on the basis of the sequenced genome are identical, but differ from the curated (NP) protein sequence at 2 positions inside the *Myf5* domain (Appendix Fig.1A, black boxes). Yet the RNAseq-derived and genomic sequences closely match the sequences of other amniotes. Thus, the curated sequence was deemed unreliable, and the RNAseq-derived/ genomic sequences were used for our construct design.

4.2.1.2.2 MyoD

The alignment of MyoD sequences indicated that a number of sequences were incomplete at the N-terminus (fly catcher, ostrich, Latimeria). Moreover, a number of sequences lacked exon 2-encoded sequences (atlantic cod, Medaka MyoD-2) or exon 3-encoded sequences (MyoD of the Chinese softshell turtle, MyoD encoded by cod scaffold gs298, Medaka MyoD from scaffold 3975). However, we had sufficient information from all animal taxa to characterise the features of their MyoD proteins.

The tetrapod MyoD N-terminus (Appendix Fig. 1B, bracket) typically encompassed the sequence M-E/D-L-L, which in most diapsids was followed by G-P/H. Also in tetrapods, a variation of the N-terminal theme occurred a second time, and in non-mammalian species, this matched closely the

N-terminus of the actinopterygian and chondrichthyan sequences (M-E-M/V/I-T versus M-E-L-S/P or M-E-I-T; Appendix 1B, 2nd black bracket), suggesting an internal sequence duplication. In the middle of the basic domain, we found for all species an extended histidine-rich stretch with the exception of mammalian MyoDs. Notably, this H-rich stretch was not present in the curated chicken MyoD sequence. Histidine stretches are enriched in developmentally important transcription factors and involved in locating proteins to nuclear speckles (360). Hence, this difference may be significant. Further downstream, all proteins continued with the highly conserved basic, helix-loop-helix and Myf5 domains (Appendix 1B, blue, green, pink shading). In most MyoD proteins, C-terminus ended in the sequence I-Y-Q-V-L (arrows), the exception being the less well conserved the C-termini in the more divergent, 2nd teleost MyoD proteins. The conservation of the MyoD termini suggests that also in this case, an untagged version of the protein should be used.

Notably, diapsid MyoD proteins, in addition to the extended stretch of conserved amino acids at the N-terminus, contained an expansive serine-rich stretch just before the C-terminus (position 351-356 in the gapped aligment). Serines are prime targets for phosphorylation, and MyoD activity is known to be controlled by phosphorylation (206,361). Therefore, we decided to use chicken MyoD as this would be most adapted to the chicken system. Yet in the chicken, the curated MyoD not only lacked the H-stretch, but differed at 3 further positions (black boxes) from the RNAseq-derived sequence. The latter however matched the sequences found specifically in other birds. Therefore, as with Myf5, the RNAseq-derived sequence was deemed most likely to be the correct sequence and was consequently used in the construct design.

4.2.1.2.3 MyoG

The alignment of MyoG sequences revealed a highly conserved sequence at the N-terminus that constituted the start of the basic domain of the protein (Appendix 1C, bracket, blue shading). This sequences consisted of M-E-L-F/Y-E-T-N/S-A/P, the exception being quail MyoG (contained M-S-D-F-I-L-K) and Xenopus MyoD (started with an extra M). The proteins continued with the highly conserved basic and helix-loop-helix domain (Appendix 1C, blue and green shading). MyoG proteins were shorter than Myf5/MyoD proteins and lacked the full Myf5 domain. Nonetheless, the C-termini (from position 269 in the gapped alignment shown in Appendix 1C) were highly conserved, in diapsids invariably ending with E-E-R-V/G/S-Q/H-N (arrows), again, suggesting that an epitope tag should not be used. Overall, sarcopterygian MyoG sequences were very similar. However, to be consistent, we decided to continue using the chicken sequences. The various sequences deposited in the database for chicken MyoG did not differ and were deemed reliable.

4.2.1.2.4 Mrf4

Mrf4 proteins resembled MyoG proteins in that they carried a conserved N-terminus (M-M-D/E-L/M-F-E-T/S, Appendix 1D, bracket; in half the sequences preceded by a further M) at the start of the conserved basic domain (blue shading), which was followed by the equally conserved helix-loop-helix domain (Appendix 1D, green shading) and a truncated version of the Myf5 domain. In amniotes, the proteins ended with two acidic amino acids, followed by V/A/L-V/L/A-E-K, suggesting that also in this case, no epitope tags should be added. As for MyoG, sarcopterygian sequences were very similar, but we decided to continue using the chicken proteins. The chicken Mrf4 sequences were identical and matched the sequences of other birds, and hence, were also deemed reliable.

4.2.1.3 Selection of the expression vector

Having established which sequences to use to express chicken Mrf genes, we now considered possible expression vectors. Several expression vectors have a long standing use in the avian system, including pCab-GFP which contains a separate open reading frame (orf) for EGFP and vectors such as pCAGGS in which the EGFP orf is used as a tag, being fused to the orf of the gene of interest. Importantly, these vectors are typically driven by the cytomegalovirus (CMV) enhancer and the chicken beta Actin promoter, which fulfils our requirements for strong cis-regulatory transcriptional elements. However, as we did not wish to tag our constructs, the second type of vectors was dismissed, and pCab-GFP was used to clone the constructs for misexpression in chicken embryos. The features of this vector are shown in Fig. 4.2.

Figure 4.2 (A), shows the circular map of the pCab expression vector generated by the Gene Snap program. On the right (Fig.4.2 B) the functional elements that facilitate expression of the gene of interest and the tracing of targeted cells are represented graphically; map drawn to scale. In brief, ubiquitous eukaryotic expression is driven by the cytomegalovirus (CMV) enhancer and the chicken beta Actin promoter. If a gene of interest is cloned into the multiple cloning site (MCS), transcription generates a bi-cistronic transcript that contains the sequences of the desired gene, followed by the CMV derived internal ribosomal entry site (IRES) and the coding sequence for enhanced green fluorescent protein (EGFP). Thus, presence of EGFP-dependent fluorescence indicates that the construct was transcribed in full and that translation is occurring. The inclusion of the chicken beta Actin-rabbit beta Globin intron downstream of the transcriptional start site results in a single splicing event known to stabilise the mature transcript. The rabbit beta Globin poly (A) signal downstream of the EGFP ORF ensures transcript polyadenylation and consequently stabilisation. Translation occurs simultaneously via cap-dependant initiation of the gene of interest and via cap-independent initiation (through the IRES) of the EGFP.

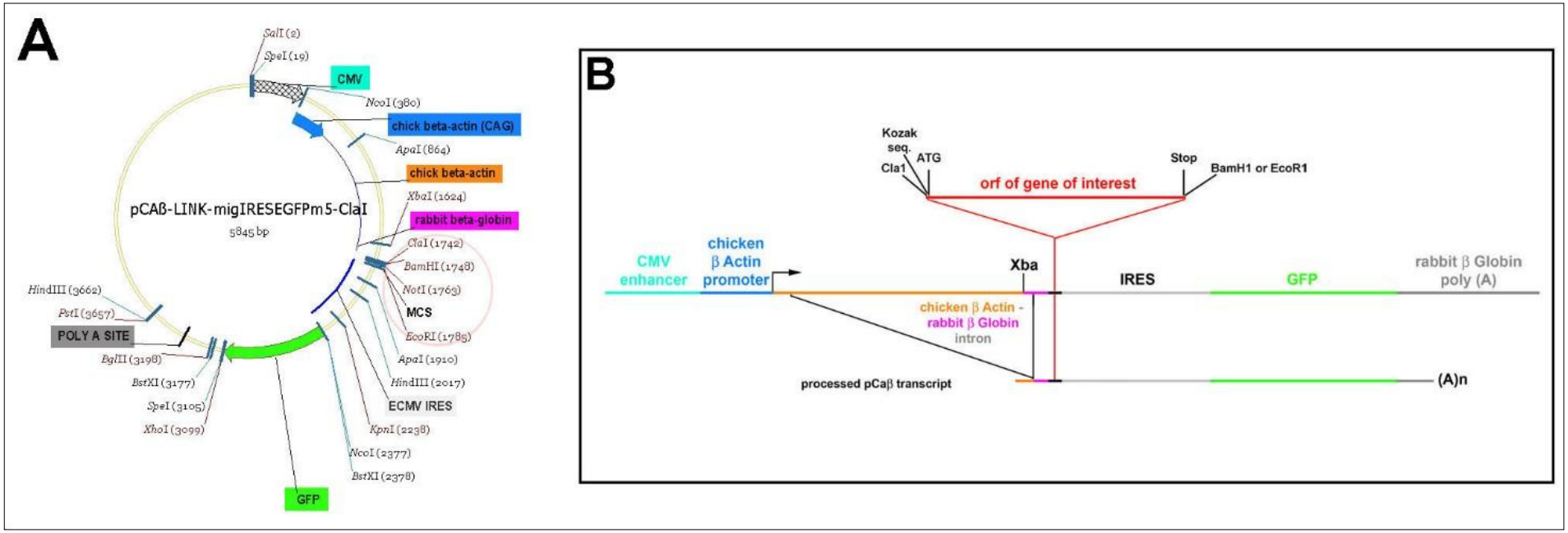
A
SalI (2)
SpeI (19)
CMV
NcoI (380)
chick beta-actin (CAG)
ApaI (864)
chick beta-actin
XbaI (1624)
pCAß-LINK-migIRESEGFPm5-ClaI
5845 bp
rabbit beta-globin
ClaI (1742)
BamHI (1748)
NotI (1763)
MCS
EcoRI (1785)
ApaI (1910)
HindIII (2017)
ECMV IRES
KpnI (2238)
NcoI (2377)
BstXI (2378)
GFP
HindIII (3662)
PstI (3657)
POLY A SITE
BglII (3198)
BstXI (3177)
SpeI (3105)
XhoI (3099)
B
Kozak seq.
Cla1
ATG
orf of gene of interest
Stop
BamH1 or EcoR1
CMV enhancer
chicken β Actin promoter
Xba
IRES
GFP
rabbit β Globin poly (A)
chicken β Actin - rabbit β Globin intron
processed pCaβ transcript
(A)n

Figure 4. 1: Properties of the pCab expression vector

(A) Circular map of the pCab expression vector generated by the SnapGene Viewer program. (B) Graphic representation of the functional elements that facilitate expression of the gene of interest and the tracing of targeted cells. Ubiquitous eukaryotic expression is driven by the cytomegalovirus (CMV) enhancer and the chicken beta Actin promoter. If a gene of interest is cloned into the multiple cloning site (MCS), transcription generates a bi-cistronic transcript that contains the sequences of the desired gene, followed by the CMV derived internal ribosomal entry site (IRES) and the coding sequences for enhanced green fluorescent protein (GFP). Owing to the fused chicken beta Actin-rabbit beta Globin intron downstream of the transcriptional start site, the transcript is spliced once. The rabbit beta Globin poly (A) sequences downstream of the GFP sequences ensure transcript polyadenylation and hence stabilisation. Simultaneous translation then occurs from the sequences upstream of the gene of interest and from the IRES.
If cells or tissues targeted with the pCab construct are being analysed by in situ hybridisation, care has to be taken to avoid unwanted hybridisation of the probe with the pCab-derived transcript. pCab / pCab transcripts do not contain M13-derived sequences typically included in plasmids ISH probes are generated from (B, bottom; lines markers by asterisks). Hence standard ISH probes pose no risk. ISH probes generated from construct intermediates cloned into pMK/pMA contain 124 nucleotides that match the chicken beta Actin - rabbit beta Globin sequences of the unspliced and 86 nucleotides of the spliced pCab-derived transcript, respectively (orange-pink line). Stringent hybridisation conditions however will suppress cross-hybridisation.

4.2.2 Attempts to obtain the chicken *Mrf* open reading frames by RT-PCR

We had been kindly provided with expression constructs for mouse Myf5 and MyoD by D. Duprez (337) and with constructs expressing tagged chicken Mrf by A. Münsterberg (224). In initial sets of experiments we electroporated these constructs into chicken somites, but did not obtain any phenotypes (not shown). To optimise the constructs as discussed above, we decided to generate constructs for untagged versions of chicken Mrf. Our expression analysis had established that chicken Mrf are all robustly expressed in somitic myotomes at E3. Therefore, bodies of E3 (HH20) were collected, total RNA was isolated and reverse transcribed to generate cDNA. To obtain the Mrf sequences, a nested primer approach was used. A set of primers upstream of the ATG codon and downstream of the stop codon were used in the first PCR, followed by a second PCR with primers located at the ATG and the stop codon. This second set of primers was designed such that restriction enzyme (RE) sites for cloning into pCab and the Kozak sequence at the translational start site would also be introduced. The sequences and location of these primers are shown in Appendix 2A-D. Our established PCR conditions (Biomix Red system employing a non-proof-reading DNA polymerase, annealing temperature 5 degrees below the primers' melting temperature) did not produce any fragments of the expected sizes, possibly owing to the high GC (Guanine-Cytosine) content of the chicken sequences. Therefore proof-reading enzymes, PCR kits optimised for GC-rich sequences and various conditions for primer annealing were used. Some PCRs produced fragments of the expected size, and these fragments were cloned into pCab and sequenced. However, none of the clones contained the correct Mrf orf; all contained small deletions or frame-shift mutations (not shown). Therefore, gene synthesis was outsourced and the desired sequences were chemically synthesised and cloned by Life Technologies (GeneArt).

4.2.3 Gene synthesis

Life Technologies were provided with the desired chicken *Mrf* cDNA sequences and the sequences of the pCab vector. Out of convenience, the company did not use the Cla1 restriction site that would link the 5' end of the fragment to the pCab polylinker, but synthesized the Mrf orf and pCab upstream sequences up to the Xba1 site of the vector. The synthesized sequences were linked to Sfi1 restriction sites and subcloned into the company's own vectors, pMA or pMK. These are simple cloning vectors with a T7 promoter upstream of the inserts and M13-derived sequences suitable to prime PCR and sequencing reactions from either side of the insert. Subsequently, the inserts were excised for pMA/pMK using Xba1-EcoR1/BamH1 as required, and directionally cloned into pCab, using the matching restriction sites, producing the constructs as desired.

4.2.4 Validation of synthesised constructs

4.2.4.1 Confirmation of correct sequences by dideoxy (Sanger) sequence analysis

To confirm that the Life technologies products indeed yielded the correct sequences, both strands of each construct were re-sequenced; sequences were assembled and aligned and compared with the desired sequences using the Bioedit software. This information is included in (Appendix Fig. 2A-2D), and shows, that for all four *Mrf* constructs, the correct sequences were obtained.

4.2.4.2 Evaluating construct activity in the heterologous frog system

The African clawed frog (*Xenopus laevis*) is a well-established vertebrate model for the *in vivo* analysis of gene function. Specifically, has been used for the evaluation of the *Mrf* function. Co-culture experiments showed that the early gastrula ectoderm (corresponds to the epiblast in amniotes) inhibits the differentiation of muscle precursors (362). However, when Xenopus *Myf5* or *MyoD* mRNA was injected into single blastomeres at the 1 or 2-cells stage or early morula stages of development, the descendants of these cells were recruited into myogenesis and expressed sarcomeric Myosins (334); mouse *MyoD* has a similar effect (A. Philpott, personal communication). We therefore expected that chicken *Mrf* construct would also be active in the Xenopus model. To misexpress the genes in this system, they had to be cloned into a vector from which *in vitro* translation and mRNA preparation would be possible. Thus, in collaboration with Professor Matthew Guille (University of Portsmouth) the open reading frames of the synthesised *Mrfs* were excised by restriction digest and cloned into the pCS2 (cuts with Cla1 and EcoR1) vector and sequenced (Fig. 4.3) . The genes were transcribed using the SP6 RNA polymerase, making use of the SP6 promoter located upstream of the insert; as control, βGal mRNA was used (see materials and methods).

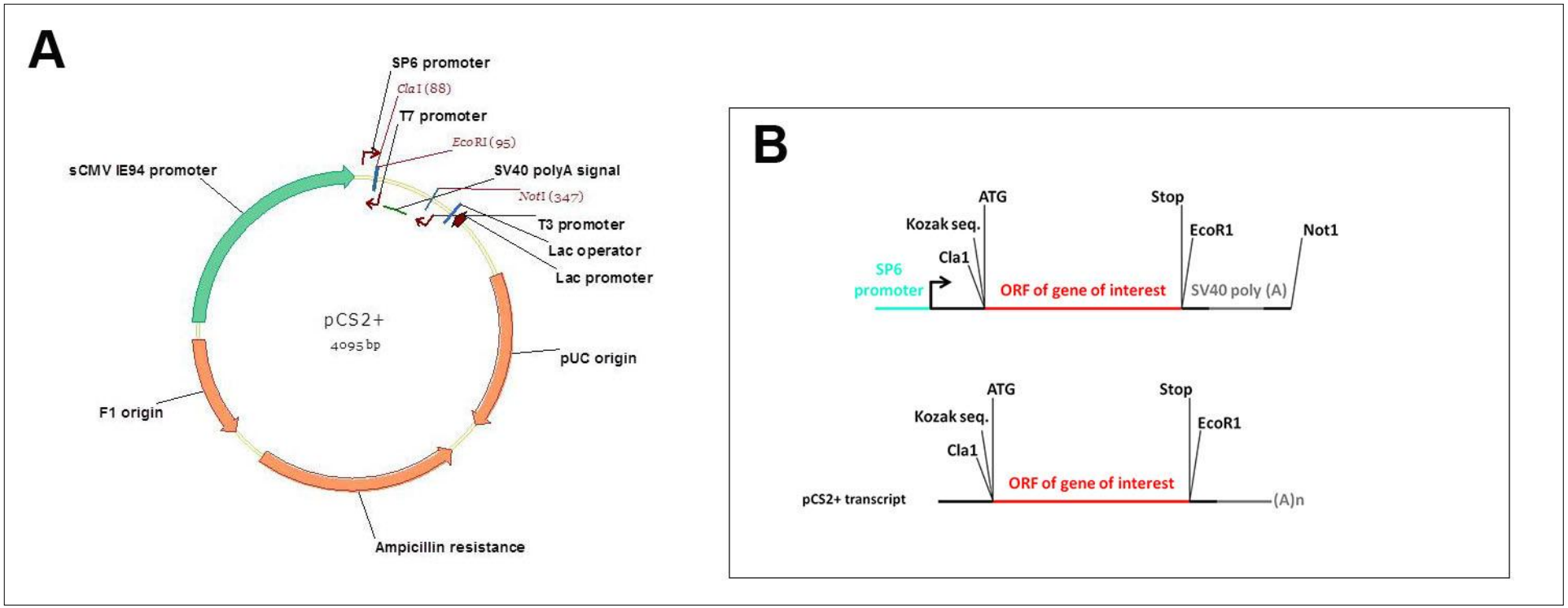
A
SP6 promoter
ClaI (88)
T7 promoter
EcoRI (95)
sCMV IE94 promoter
SV40 polyA signal
NotI (347)
T3 promoter
Lac operator
Lac promoter
pCS2+
4095 bp
pUC origin
F1 origin
Ampicillin resistance
B
ATG
Stop
Kozak seq.
EcoR1
Not1
Cla1
SP6
promoter
ORF of gene of interest
SV40 poly (A)
ATG
Stop
Kozak seq.
EcoR1
Cla1
ORF of gene of interest
pCS2+ transcript
(A)n

Figure 4. 2: Properties of the pCS2+ expression vector

(A) Circular map of the pCS2+ expression vector generated by the SnapGene Viewer program. The vectors pCS2+ contains a strong enhancer/promoter (CMV) followed by a polylinker and the SV40 late polyadenlyation site. An SP6 promoter is present in the 5' untranslated region of the mRNA from the sCMV promoter, allowing in vitro RNA synthesis of sequences cloned into the polylinker. A T7 promoter in reverse orientation between the polylinker and the SV40 polyA site for probe synthesis, as well as a second polylinker after the SV40 polyA site to provide several possible sites to linearize the vector for SP6 RNA transcription. The vector backbone is from pBluescript II KS+ and includes the amp resistance gene.

(B) The vector pCS2+ does not have GFP on its sequence so all the constructs that have been cloned in this vector need to be co-electroporated with pCAB to be visualised at the fluorescence microscope. The constructs that were cloned in pCS2+ vector are identical to the constructs cloned in pCAB. The ORF were restriction digested using Cla1 and EcoR1 and cloned back in pCS2+.

The RNA was *in vitro* translated and capped, quantified, 1ng of Mrf mRNA was injected into one cell of 2-cell stage Xenopus embryos; 250pg of a mRNA encoding β-Gal was used as lineage tracer. As the first cell cleavage of Xenopus zygote separates the left and right half of the animal, one side of the embryo will be the experimental side and one side will be the control side as used by (334). In total, 30 embryos were injected per Mrf construct, 30 were injected with the lineage tracer alone, and 30 were left uninjected. Embryos were incubated at 18°C until they reached stage 26 and analysed using the MF20 antibody to detect Myosin Heavy Chains. Representative embryos are shown in Fig. 4.4, the data are summarised in Table 4.2. This experiment revealed that MyoG and Mrf4 only recruited non-myogenic cells into myogenesis. Myf5 and MyoD did not give us any upregulation of the Myosin staining, the phenotype was comparable with the wild type, and the phenotype of the injected side were comparable with the control side.

Of the 30 uninjected embryos, all survived. 11 were analysed for sarcomeric Myosin expression and showed the wildtype expression pattern (Fig.4.4 A,B). Of the embryos injected with the β-Gal mRNA, 18 survived, indicating that the injection somewhat compromised development. However, all embryos showed the same, wildtype Myosin expression as the uninjected embryos (Fig.4.4 C,D). Of the embryos injected with chicken *Myf5* or *MyoD* mRNA, 14 and 10, respectively, survived. They appeared largely normal; in a few cases, we observed a slight reduction in head size or enlarged occipital somites (Figure 4.4 F, arrowhead). Of the embryos injected with *MyoG* or *Mrf4* mRNA, only 6 or 5, respectively, survived. Of those, half (*MyoG*) or 4/5 (*Mrf4*) were malformed. These embryos showed widespread ectopic expression of sarcomeric Myosin on the injected side (Fig.4.4 J, L, asterisks). They also had failed to complete gastrulation and to close the blastopore (Fig.4.4 J,L, arrows). Owing to the defective gastrulation, also the uninjected side was truncated and head structures were reduced (Fig.4.4 I,K). However, somites showing correctly aligned, Myosin expressing myotubes were present. The phenotype caused by the misexpression of chicken *MyoG* and *Mrf4* resembled the phenotypes obtained from misexpresison of Xenopus *Myf5* and *MyoD* (334). Thus, the experiment shows that the design of our *Mrf* expression cassette (Kozak sequence followed by the *Mrf* open reading frame) permits high level translation in a heterologous system, and in the case of MyoG and Mrf4, produced biologically active protein. Since all Mrf constructs were designed the same way, we can infer that all can be translated. The reasons why chicken *MyoG* and *Mrf4* but not chicken *Myf5* and *MyoD* reproduced previously published results will be evaluated in the discussion section.

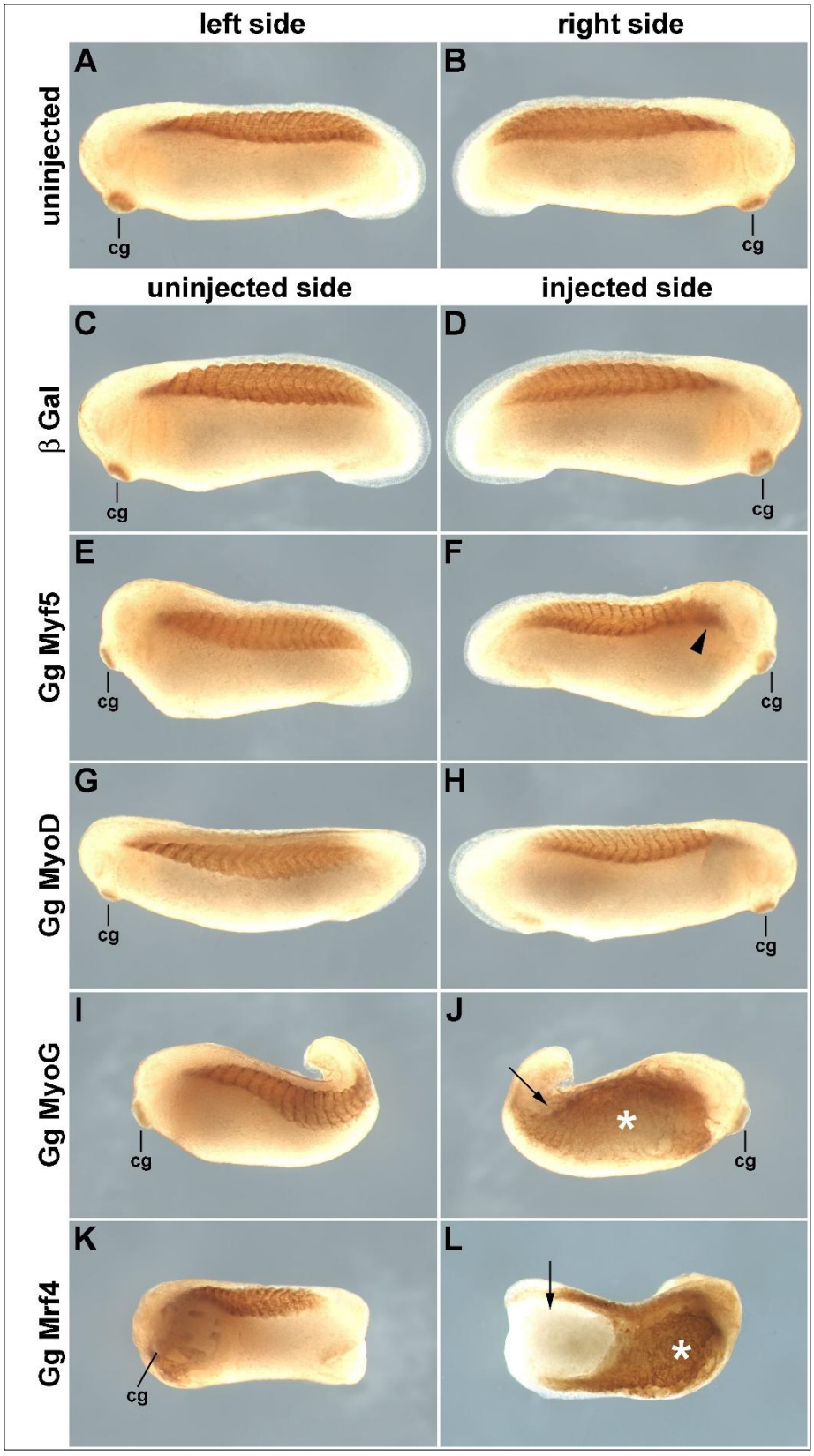
left side
right side
uninjected
A
B
cg
cg
uninjected side
injected side
β Gal
C
D
cg
cg
Gg Myf5
E
F
cg
cg
Gg MyoD
G
H
cg
cg
Gg MyoG
I
J
cg
*
cg
Gg Mrf4
K
L
cg
*

Figure 4. 3: Chicken Mrf misexpression in frogs

A batch of Xenopus leavis embryos was subdivided into 9 groups of 30 embryos. One set was left to develop (A,B); of the others, one cell each was injected with βGal mRNA (C,D), or with βGal mRNA plus the *Mrf* RNA indicated on the left of the panel (E-R). Embryos were collected when the control embryos had reached st26 and stained for sarcomeric Myosin expression (brown staining). Representative embryos were photographed, showing the untreated (C,E,G,I,K,M,O; rostral to the left) and treated sides (D,F,H,J.L,N,P; rostral to the right) in lateral views. Note that embryos injected with chicken *Myf5* and *MyoD* appeared largely normal, sometimes displaying slightly reduced head sizes or enlarged occipital somites (F, arrowhead). Embryos injected with chicken *MyoG* or *Mrf4* showed extensive ectopic expression of sarcomeric Myosin (asterisk). Owing to the recruitment of cells into myogenesis earlier on, embryos had failed to complete gastrulation and to close the blastopore (arrows). The experiment indicates that of the four *chicken* Mrfs, those associated with late phases of myogenesis and terminal differentiation can force Xenopus cells into myogenesis, those associated with myogenic commitment cannot.
Abbreviations: cg, cement gland.

Table 4. 2: Xenopus experiments

In each experiment, 30 2-cell stage Xenopus laevis embryos were used. They either were left to develop (control 1), injected with 250pg β-Gal mRNA (control 2) or injected with a mix of 250pg β-Gal mRNA and 1ng of Mrf RNA. RNAs were delivered in a total of 5nl water. Note that RNA injection reduced the survival rate by 40%. Injection of chicken *Myf5* or *MyoD* RNA reduced survival rates further, but surviving embryos appeared largely normal, sometimes displaying somewhat smaller heads (*MyoD*) or enlarged occipital somites (*Myf5*). When injected with chicken *MyoG* or *Mrf4*, survival rates were poor, and in half (*MyoG*) or most embryos (*Mrf4*), the injected side showed widespread ectopic muscle formation at the expense of correct gastrulation.

Construct	No of experimental embryos	No of survivors at stage 26	WT	Malformed
-	30	30	11 analysed, all wt	0
β-Gal	30	18	18	0
Gg *Myf5*+β-Gal	30	14	14	0
Gg *MyoD*+β-Gal	30	10	10	0
Gg *MyoG*+β-Gal	30	6	3	3
Gg *Mrf4*+β-Gal	30	5	1	4

4.2.4.3 Evaluating construct activity in the autologous chicken system

The misexpression of chicken *Mrf* constructs in Xenopous embryos revealed that *MyoG* and *Mrf4* are sufficient for enforcing premature myogenesis in this system. Importantly, the experiments also confirmed that our constructs design allows to the production of functional protein. Eventually, however, we wished to use the chicken *Mrf* constructs in chicken embryos. Therefore, it was important to establish the expression from these constructs directly in the chicken system.

The aim of the study was to challenge immature paraxial mesoderm and developing muscle stem cells in the somitic dermomyotome with Mrf expression constructs. Hence we turned to the somite. Three tests were carried out: (1) Flank somites at HH15/16 were electroporated with the *Mrf* constructs or with the parental pCab-GFP vector, and, after overnight re-incubation that allowed the embryos to reach HH20, messenger RNA made from all the constructs was monitored by in situ hybridisation. (2) An electroporation time course was carried out, and the presence of EGFP-fluorescence was used to monitor onset and duration of transgene expression.

The first set of experiments revealed that GFP expression was readily detectable for the pCab vector as well as the vectors containing Mrf orf as inserts (Fig 4.5 A,C,E,G,I). Assaying the electroporated embryos for the presence of the GFP orf (Fig, 4.5 B) or the Mrf orf (Fig.4.5 D,F,H,J) in the mRNA from the construct, we found that this was the case: strong signals were obtained in a pattern that matched the GFP signal (arrows). Notably, the intensity of the GFP-derived fluorescence and the staining obtained from the in situ hybridisation corresponded, inferring that high levels of fluorescence can be interpreted as high levels of transgene expression.

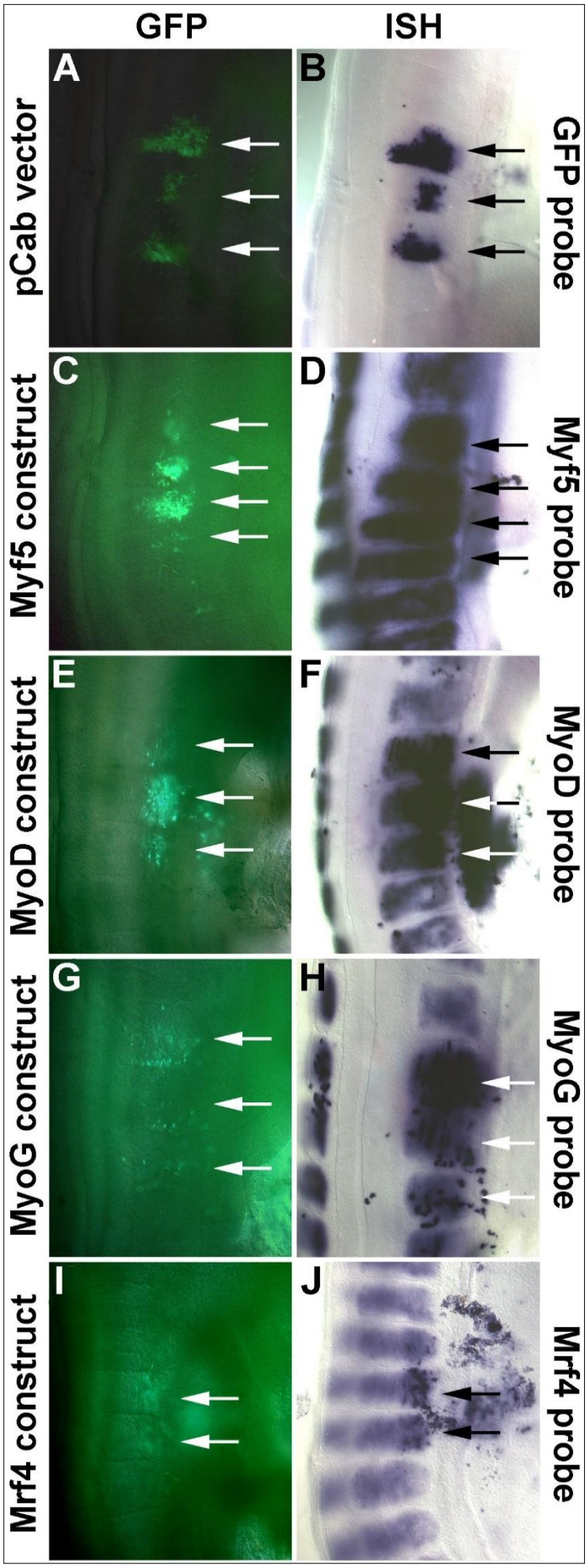
GFP
ISH
pCab vector
GFP probe
Myf5 construct
Myf5 probe
MyoD construct
MyoD probe
MyoG construct
MyoG probe
Mrf4 construct
Mrf4 probe
A
B
C
D
E
F
G
H
I
J

Figure 4. 4: Confirmation of *Mrf* construct expression in chicken somites

Lateral views of the electroporated somites in the right side of the chicken embryo 18 hours after electroporation; rostral is up, the dorsal midline is to the left. (A,C,E,G,I) GFP expression recorded immediately after fixation. (B,D,F,H,J) Same embryos as in (A,C,E,G,I), showing the signals obtained by in situ hybridisation with a GFP probe that recognises the pCab-derived transcript (B) or with *Mrf* probes that recognise both the transcript and the endogenous gene (D,F,H,J); constructs and probes are indicated on the sides of the panel, the corresponding somites are indicated by arrows. Note that the constructs produce readily detectable mRNA well above the expression levels of the endogenous genes

In the second experiment, embryos were harvested immediately after the electroporation, 6 hours, 18 hours and 42 hours after electroporation (Fig. 4.6). At time zero, no fluorescence was observed, as expected (Fig. 4.6 A). After just 6 hours from electroporation, robust fluorescence could be detected in the electroporated somites (Fig. 4.6 B). After 18 hours even more intense fluorescence was detected (Fig. 4.6 C), indicating accumulation of construct-derived gene products. When the centre of the somite was targeted, cells in the dermomyotome fluoresced as evidenced by the rounded shape of cells when photographed in a dorsolateral view. After 42 hours (Fig .4.6 D), fluorescence was still readily detectable. Notably, now round cells atop elongated cells beneath were labelled, indicating that some cells had had stayed in the dermomyotome while others had contributed to the myotome and formed myotubes, in tune with the normal progress of myotome development. The time course is fully in line with a time course that was carried out for the occipital somites (363).

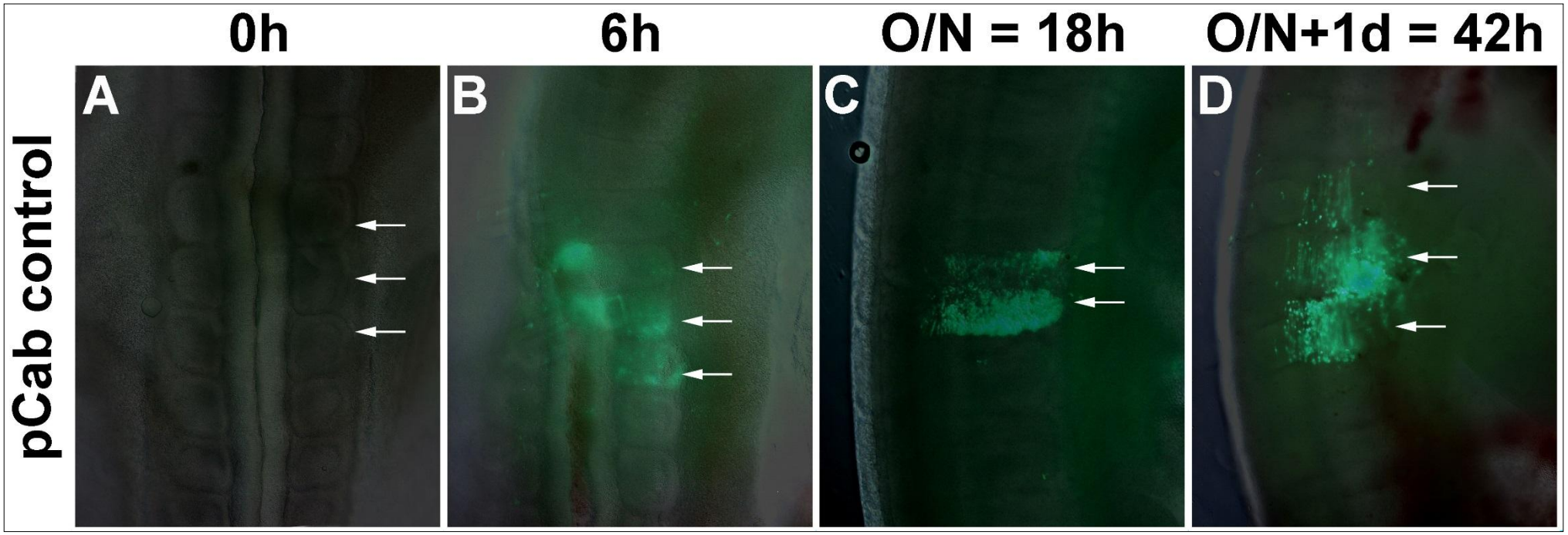
0h
6h
O/N = 18h
O/N+1d = 42h
pCab control
A
B
C
D

Figure 4. 5: Time course for the expression from pCab vectors in chicken somites

Epithelial somites in the right side of HH15/16 chicken embryos were electroporated with the pCab vector and analysed for GFP expression immediately thereafter (A), 6 hours later (B), after an overnight incubation (O/N, i.e. 18 hours later; C), or after an additional day of incubation (42 hours; D). The targeted somites are shown in dorsal (A), dorsolateral (B) and lateral views (C,D). Note that the construct is well expressed 6 hours after electroporation, and expression levels continue to be high during the duration of the experimental time period

4.2.4.4 Analysis of Mrf gene expression

In recent years, reports of misexpression experiments of *Mrf* in the chicken embryo in vivo have been published. Sweetman in 2008 and Delfini in 2004 showed that the electroporation of one of the *Mrfs* can lead to upregulation of other *Mrf* family members (224,337). In both studies, the *Mrfs* were misexpressed in the neural tube and the effects were analysed with *in situ* hybridisation using *Mrf* probes. Both the studies used constructs based on the pCab vector. Delfini misexpressed the native protein of mouse Myf5 and MyoD, while Sweetman used a HA-tagged version of the chicken Mrfs. Expression of endogenous *Mrf* was analysed by in situ hybridisation after overnight re-incubation of the treated embryos. To validate our results and our experimental methods we sought to replicate the results from Sweetman 2008 and Delfini 2004, except in our case we misexpressed the constructs in the somites. Our constructs contained untagged orfs for chicken *Mrf*, cloned into the pCab vector. All the embryos were analysed with ISH after 18 hours of re-incubation at approximately HH19/20. Since our ISH probes contained the *Mrf* orf, we were not in the position to monitor the endogenous expression of the *Mrf* we introduced as a transgene.

Embryos electroporated with the pCab vector only displayed wildtype expression for all four *Mrfs* (Fig. 4.7 Ai, Bi, Ci, Di). When *Myf5* was misexpressed, *MyoD*, *MyoG* and *Mrf4* were upregulated in the targeted somites (Fig. 4.7 Fi, Gi, Hi, arrows). The *MyoD* construct upregulated *Myf5*, *MyoG* and *Mrf4* (Fig. 4.7 Ii, Ki, Li arrows). The *MyoG* construct upregulated *Myf5*, *MyoD* and *Mrf4* (Fig. 4.7 Mi, Ni, Pi arrows). The *Mrf4* construct upregulated *Myf5* and *MyoD* (Fig. 4.7 Qi, Ri arrows) in areas corrispondng to the fluorescent somites (Fig. 4.7 Q,R arrows). We however didn't detect any upregulation of *MyoG* (Fig. 4.7 S-Si).

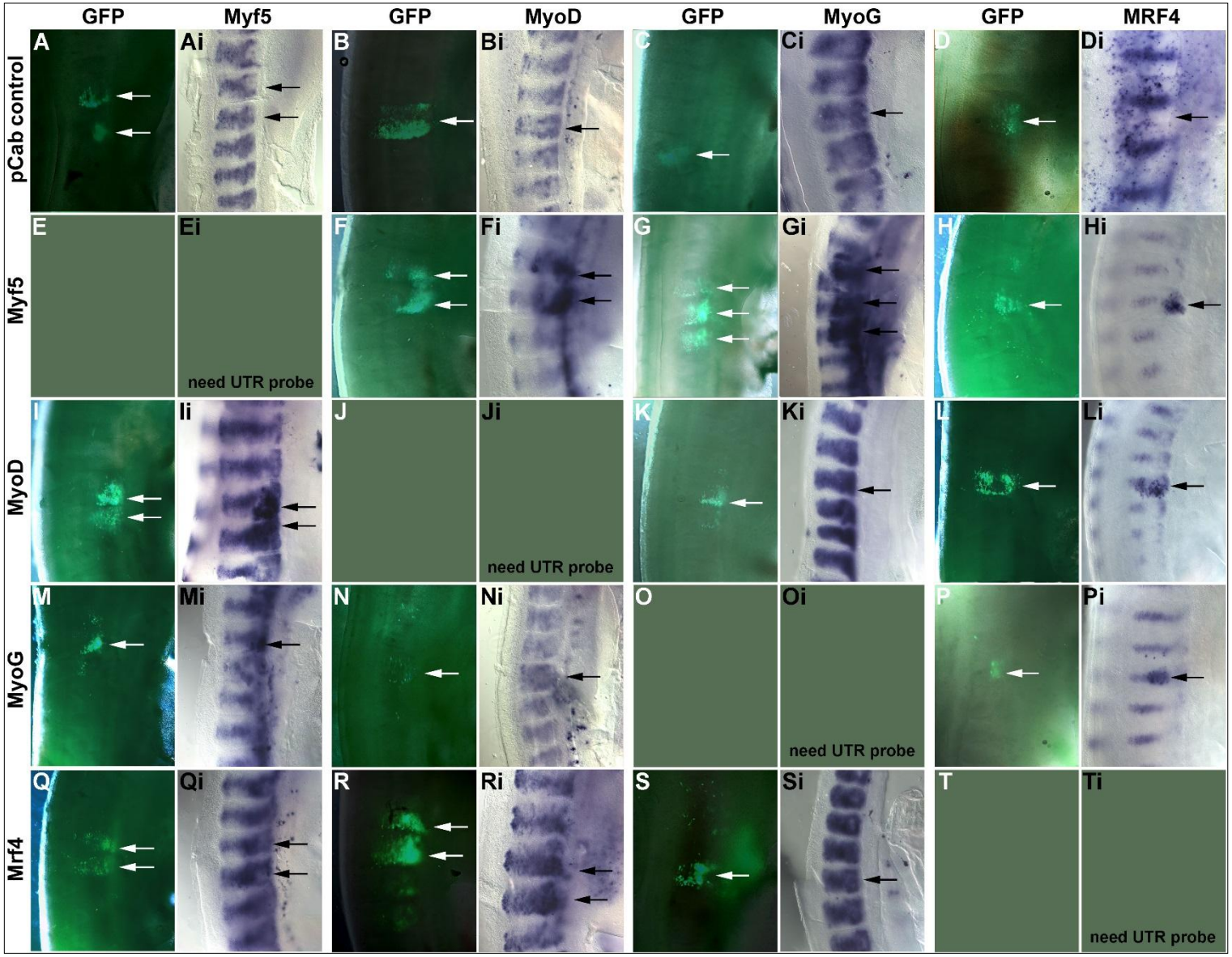
GFP
Myf5
GFP
MyoD
GFP
MyoG
GFP
MRF4
pCab control
Myf5
MyoD
MyoG
Mrf4
A
Ai
B
Bi
C
Ci
D
Di
E
Ei
need UTR probe
F
Fi
G
Gi
H
Hi
I
Ii
J
Ji
need UTR probe
K
Ki
L
Li
M
Mi
N
Ni
O
Oi
need UTR probe
P
Pi
Q
Qi
R
Ri
S
Si
T
Ti
need UTR probe

4.2: Misexpression of Mrf genes between HH16-20 upregulates transcription of other Mrf genes.

Flank somites were electroporated at HH15/16 and embryos harvested at HH19/20 as before. GFP fluorescence was recorded and Mrf mRNA expression detected by in situ hybridisation. Mrf self-regulation could not be tested due to lack of probes detecting the untranslated regions (UTRs) of the mRNAs. Note that Myf5 upregulated the expression of MyoD (Fi), MyoG (Gi) and Mrf4 (Hi). MyoD upregulated Myf5 (Ii), MyoG (Ki) and Mrf4 (Li). MyoG upregulated Myf5 (Mi), MyoD (Ni) and Mrf4 (Pi). Mrf4 upregulated Myf5 (Qi) and MyoD (Ri), but did not elevate MyoG expression beyond its endogenous expression in the myotome (Si).

4.3 Discussion

In this section, we carried out preparatory experiments that would set the stage for the subsequent attempts to coax muscle precursors out of their stem cell state. This included the design of the most appropriate *Mrf* constructs for the chicken system, tests that these constructs would deliver functional proteins, and tests for the time frame in which the constructs would be expressed after electroporation into chicken somites. This has been achieved.

4.3.1 Chicken *Mrf* are most appropriate for expression studies in the chicken system

After initial obstacles regarding the allocation of Mrf proteins to the correct paralog group (which led to the discovery of a second *MyoD* gene in teleost fish other than the zebrafish), we were able clearly assign gnathostome Mrf sequences to their cognate groups. Sequence comparison confirmed a high degree of conservation for the known functional groups, the basic, the helix-loop-helix and the Myf5/ transactivating domain. Interestingly, the comparison also revealed a number of short sequence stretches in specifically diapsid Mrf proteins that distinguished these proteins from other members of their respective paralog group, including stretches enriched in prolines in Myf5 and a histidine-rich stretch in MyoD. Unfortunately, detailed information regarding the function of these regions, in terms of linear sequence, protein folding and targets for posttranslational modification are not available, work on motif and protein structure have manly be carried out using the mammalian proteins (364). In the context of proteins other than Mrf, the sequence variations have been shown to be relevant (364).Given the conservation of these sequences throughout diapsids, it is likely that they have been selected for during diapsid evolution and hence, may be relevant in the chicken system. This finding suggested the use of chicken Mrf rather than heterologous Mrf for misexpression in the chicken embryo.

For all Mrf, various sequences have been contributed to the various sequence databases, the most recent being RNAseq data for whole embryos and somites published in Ensembl. The sequences for MyoG and Mrf4 proteins were identical however, significant differences were found between the curated Myf5 and MyoD sequences and the sequences derived from the mRNA information obtained by RNAseq. The most obvious was the presence of a histidine-rich stretch in the basic domain of MyoD in all non-mammalian proteins, but not in the curated version of chicken MyoD. Sequences for muscle genes have been found to differ between layer and broiler stains of chicken (365). In laboratory research, chicken tissue is frequently obtained from birds bred as mixed flocks, hence sequence variations may indeed occur. However, given the high level of conservation of sequences, and in the absence of studies that investigated the effect of these sequence variations, the sequence that matched the conserved pattern were used. As the information collected from RNAseq data shows the presence of the histidine-rich stretch in all

Mrf sequences, this can be taken as good evidence that this specific sequence is correctly carried through from the genome to the transcripts.

4.3.2 Conserved Mrf protein termini suggest the use of untagged constructs

When we scrutinised Mrf sequences for conserved proteins domains, we found in line with previous studies (156,355,366) that the basic domain, the helix-loop-helix domain, the Myf5 domain (Myf5 and MyoD), and the shortened version of this domain in MyoG and Mrf4 were all highly conserved. Moreover, both the N-termini and the C-termini were conserved, with an extended degree of conservation found in diapsids. Previous studies showed that both the N- and C-terminus have a strong influence on the activity of the protein (156,367,368). This suggested that the use of epitope tags, both at the termini and in the centre of the protein, would likely interfere with protein function as shown for other proteins (350). Hence, we decided to use untagged proteins only.

4.3.3 Chicken *Mrf* proteins are functional in the Xenopus system

The evolution of the somites in chordates is essential to facilitate the movement of the body axis, and locomotion in the water. Jawless and anamniote jawed vertebrates develop via free-feeding larvae, this means that development of the muscle must occur very fast to allow the larvae to swim. If myogenic genes are expressed in the early blastula, then the transgene expression could upregulate the system while it is likely geared up towards myogenesis. This could explain why the Xenopus early blastula cells can easily be reprogrammed to enter myogenesis.

The misexpression experiments in the chicken showed that our constructs readily produce mRNA and can be translated from the 2nd cistron in all cases. Why, then, can Xenopus Myf5/MyoD (334), and chicken MyoG/Mrf4 but not chicken Myf5/MyoD (in this study) drive Xenopus blastula cells into myogenesis. The data that we obtained confirmed that during the two rounds of gnathostome genome evolution, the Myf5/MyoD pair and MyoG/Mrf4 pair evolved. This is in line with earlier studies (355). The sequence of gene expression (334) and in this study, together with the body loss of function experiments (316,369) established that Myf5/MyoD are involved in the commitment to myogenesis whereas MyoG/Mrf4 are involved in the initiation of terminal differentiation. Mrf4 in mammals has acquired an earlier role, possibly by tapping into some of the cis-regulatory elements for Myf5 expression (as they are linked in the genome; (370)), MyoD is the gene reaching over to the differentiation genes via the feed-forward mechanism with MyoG (210,371). Yet depending on how much the individual Myf5/MyoD genes may diverge from the original, they may have lost the ability to fully activate differentiation genes. If this were to be the case, then chichen/bird/diapsid genes may not be able to force cells into terminal differentiation, while MyoG/Mrf4, being optimised for the role, can.

To fully explore this, one would need to co-express Myf5- or MyoD reporters with the expression constructs and monitor to which extent, both in Xenopus and in the chicken, the transgenes can activate the reporters. It also would be interesting to test the function of chimeric, part chicken-part Xenopus. For this study, we rely on the fact that all constructs were designed in the same way, all are expressed, biological activity was confirmed for MyoG/Mrf4 in Xenopus, and by inference, and this should be the same for Myf5 an MyoD. Another possible experiment could be to express the Mrf constructs via transfection in cell culture, utilising fibroblasts as a positive control. The results for this experiment obtained by Weintraub and colleagues in 1989 (332) were that MyoD expressing transfected fibroblasts became muscle cells. This experiment was not performed as all constructs were tested in chicken as shown in Figure 4.7. After electroporation of the constructs, the levels of Mrf mRNAs were shown by *in situ* hibridisation to be upregulated, confirming biological activity of the constructs.

4.3.4 Chicken *Mrf* constructs are expressed within 6 hours of electroporation in the chicken somite

The test electroporations revealed that the constructs are robustly expressed 6h after electroporation; expression persists for the next two days, in line with (363). Therefore, if the embryos are left to develop overnight, they will have been exposed to the proteins derived from the constructs for a minimum of 12 hours. If the embryos are left to develop for another day, they will have been exposed for a minimum of 36 hours. Somite electroporation experiments conducted by various groups including ours (276,372) showed that phenotypes in terms of changed cell behaviour and marker gene expression can be readily obtained, exposing the cells to the products of expression constructs overnight. Therefore, we can be confident that muscle stem cells will show measurable changes in their behaviour if the Mrf constructs were able to force them out of their stem cell state.

4.3.5 Mrf misexpression in the somatic dermomyotome upregulates the transcription of other Mrf genes

The use of the Mrf constructs in the somitic dermomyotome showed that they stimulate the premature transcription of the other Mrf genes, confirming that the designed constructs are active. The unexpected upregulation of Myf5 in response to the other constructs can be explained by the use of the different constructs including conserved sequences that cannot be compared with the constructs used in the laboratories of Delfini and Sweetman (224,337).

Chapter 5

5 Misexpression of chicken Mrf in the immature chicken paraxial mesoderm

5.1 Introduction

Mrf misexpression experiments using 2-cell stage Xenopus embryos showed that chicken *MyoG* and *Mrf4* can enforce terminal muscle differentiation in early stage embryos, thereby blocking the completion of gastrulation on the treated side (Section 4.2.4.2). In contrast, misexpression of chicken *Myf5* and *MyoD* had little effect. Given that (i) all *Mrf* constructs were made the same way, (ii) all were confirmed by sequencing, (iii) all were actively transcribed from the pCab vector when electroporated into chicken somites, and (iv) GFP protein was readily produced from the Internal Ribosome Entry Site (IRES) of the bi-cistronic mRNA transcribed from pCab vectors, we inferred that in principle, all constructs deliver protein and are biologically active. We thus reasoned that chicken *Myf5* and *MyoD*, while controlling myogenic commitment, may have lost the ability to support terminal differentiation. Alternatively, the bird-specific variations in the Myf5 and MyoD protein sequence may have rendered these proteins non-functional in the frog. However, in the autologous chicken system, the proteins should be functional. To explore these possibilities we now turned to the avian system, aiming to misexpress the *Mrf* constructs in tissues ideally as immature as the frog cells.

When chickens lay their eggs, the embryos are already at a late blastula stage and ready to enter gastrulation, i.e. the early cell divisions of the fertilised egg take place inside the hen (287). Therefore, it is not possible to fully recapitulate the frog experiments. However, earlier studies in our laboratory suggested that expression constructs similar to pCab-based constructs can be electroporated directly into the primitive streak (i.e. the epiblast region undertaking gastrulation) of the early gastrula stage embryo without disturbing the progression of development (D. Sobreira and S. Dietrich, unpublished observations). Moreover, this work showed that, when the rostral primitive streak was electroporated, cells contributing to the paraxial mesoderm were able to take up the construct. This was in line with past studies that had mapped the fate of gastrulating cells in the primitive streak (99,296,373).

Importantly, the primitive streak is of a different length at different stages of development: it extends between HH2-3 in the direction of the future rostral end, has maximal length at HH4, and shortens in a rostral to caudal direction from HH4+ to HH10/11, when the remnant of the primitive streak becomes the tail bud (374). At the earliest stages of gastrulation, the primitive

streak delivers the definitive (gut) endoderm, at HH3-4 it delivers the head mesoderm, and from HH4 onwards it delivers prospective trunk mesoderm (375). When the primitive streak delivers mesoderm, different areas of the streak contribute different types of mesoderm, with the rostral tip of the streak (Hensen's node) generating the axial mesoderm (notochord), the caudally adjacent area provides the paraxial mesoderm, and the further caudal areas produce the intermediate, lateral and extraembryonic mesoderm, respectively. The precise territory contributing a particular type of mesoderm changes as the streak retracts (376).

To define the stages and regions of the primitive streak most suitable for *Mrf* misexpression, and to ensure that the electroporated cells encompass the paraxial mesoderm as this will later provide the myogenic cells, we first performed a series of cell labelling experiments. For this purpose DiI (3H-Indolium,2-[3-(1,3-dihydro-3,3-dimethyl-1-octadecyl-2H-indol-2-ylidene)-1-propenyl]-3,3-dimethyl-1-octadecyl-, perchlorate 41085-99-8) was injected into the primitive streak at early stages of development (5.2.1.1). Thereafter, we performed control-electroporations with the pCab vector (expressing GFP only) to confirm that the electroporation experiments match the DiI labelling experiments (5.2.1.2.1). This was followed by test electroporations to determine the onset of pCab expression in this experimental setting (5.2.1.2.2). Finally, we electroporated the constructs for chick *Mrf*, using two different immunohistochemical methods to assay for muscle differentiation (5.2.2). These experiments revealed that in the chicken, none of the chicken *Mrf* can drive immature paraxial mesodermal cells into terminal muscle differentiation.

5.2 Results

5.2.1 Establishing the experimental approach

Preliminary data utilising DiI labelling collected by Dr Dietrich and Mr Cardon, showed that HH4 is the most appropriate early chicken development stage to use for these experiments. At this stage the embryos are at the beginning of development showing just the primitive streak. The embryos labelled with DiI and incubated overnight showed a wide range of cells labelled in the lateral mesoderm which will give rise to the future somites. The same results were obtained when repeated using GFP expressing control constructs; the majority of the fluorescent cells are in the lateral mesoderm. Looking at this data we decided to electroporate our Mrf constructs at HH4 and let them develop overnight to reach HH10 before analysing them with MF20 antibody staining. At HH10 the only myosin expressed is in the heart. The cells forming the somites are too young to express Mrf or any structural genes and the only relevant protein expressed at this moment is Pax7.

5.2.2 Electroporation of *Mrf* constructs into the HH4 rostral primitive streak

Having established the protocol for the electroporation of the immature paraxial mesoderm, we now proceeded to misexpress the *Mrf* constructs. Given that the first myogenic cells do not appear before stage HH10 (the first stage that *Myf5* is expressed), and given that we did not know which level of myogenic competence cells had earlier, we decided to let the embryos develop to HH10. Thus, embryos were re-incubated for 18 hours after electroporation to reach this stage. The experimental approach is summarised in Fig. 5.4.

In the first series of experiments, the Mrf constructs, or as a control, the empty pCab vector, were electroporated. Embryos with readily detectable GFP-derived fluorescence and overall normal morphology were photographed and the subjected to a 3,3'-Diaminobenzidine (DAB) antibody staining, using the MF20 antibody to detect sarcomeric Myosins (293). This work was carried out in collaboration with T. Stone in the lab (5.2.2.1). In a second series, GFP was detected by an anti-GFP antibody and sarcomeric Myosins with MF20, subsequently detecting the primary antibodies with fluorochrome-coupled secondary antibodies (5.2.2.2). Since at HH10, embryos already have a functional primary heart, the MF20 staining of the heart served as internal control for the quality of the staining. We expected that embryos misexpressing the chicken *Mrf* constructs would show premature sarcomeric Myosin expression within the targeted cells, if the experimental system were to resemble the frog system. The results are summarised in Table 1.

5.2.2.1 Analysis of electroporated embryos for the expression of sarcomeric Myosin, MF20-DAB staining

In the first collection of embryos, all showed robust expression of sarcomeric Myosins in the heart, as evidence by the brown staining (included in Fig. 5.5 G,H; ht). Notably, despite the high level of construct expression as evidence by bright GFP fluorescence (Fig.5.5, A-E), none of the *Mrf* expressing cells showed any premature expression of sarcomeric Myosins (Fig.5.5, G-J).

A. Time scale of electroporation experiment conducted at HH4/5

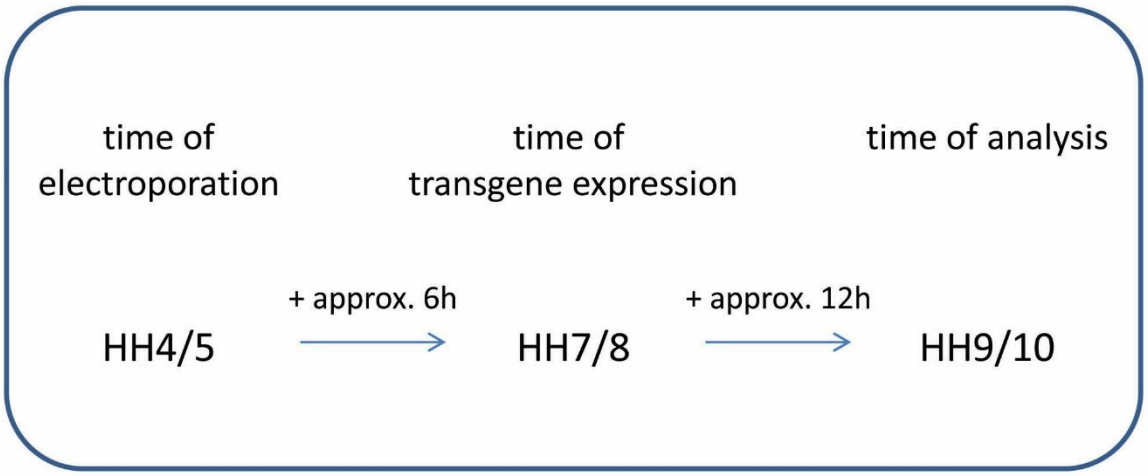

B. Schematic representation of the electroporation experiment at HH4/5

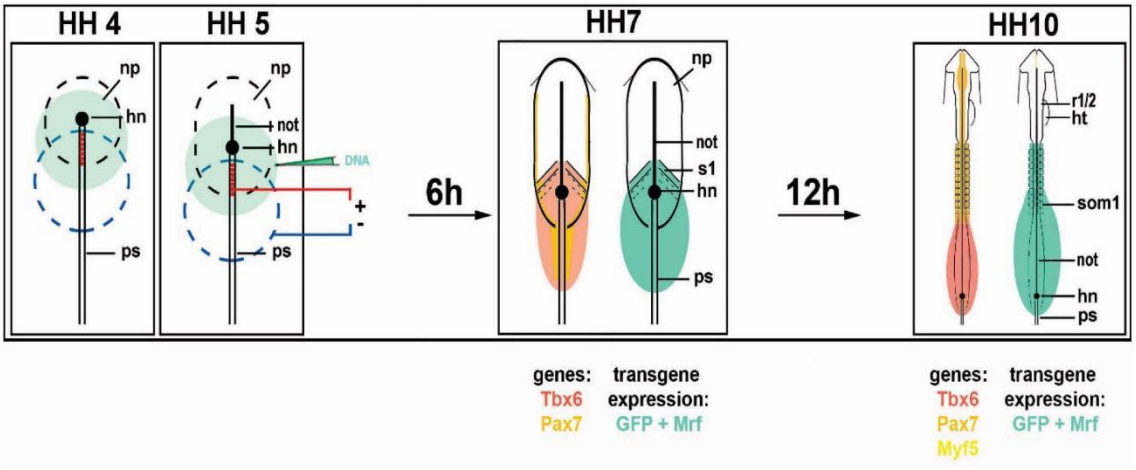

Figure 5. 1: Time scale and schematic representation of the electroporation experiments suited to target the immature paraxial mesoderm and young somites

(A) When the rostral primitive streak is electroporated with a pCab construct at stage HH4/5, this construct will be reliably expressed after 6 hours when the embryos have reached HH7. When analysing the embryos at HH9/10, the embryos will have been exposed to the construct for 12 hours.

(B, left) To electroporate stage HH4/5 embryos, they were mounted on filter rings and placed in a custom-made electroporation chamber, ventral side up, such that the rostral primitive streak, but not Hensen's node, were on top of the negative electrode (blue dotted line). DNA was injected between the epiblast and the vitelline membrane (green circle). The positive electrode was placed over the rostral-most primitive streak and a rectangular pulse was given. This was repeated several times, each time moving the positive electrode to a more caudal position, until the area marked in red had been covered. (B, middle) *Tbx6* expression (red), *Pax7* expression (orange) and transgene expression (green) 6 hours after electroporation. (B, right) *Tbx6* expression (red), *Pax7* expression (orange), *Myf5* expression (yellow) and transgene expression (green) at the time of harvesting, 18 hours after electroporation. Transgene expression overlaps with that of the molecular markers.

Images courtesy of Dr. Dietrich

5.2.2.2 *Analysis of electroporated embryos for the expression of sarcomeric Myosin using MF20 and anti-GFP primary and fluorescent secondary antibodies*

For a more optimal approach and to confirm the results shown in Section 5.2.2.1, we decided to repeat the experiments with a double-labelled immunofluorescence approach, by utilising two primary antibodies and two distinct fluorescently-labelled secondary antibodies. This time, as well as the MF20 antibody, a GFP antibody was used to mark the cells that expressed the pCab-GFP constructs during the electroporation. This approach enabled detection of both signals at the same time, reducing the errors that occurred when overlapping the fluorescence and the Normaski micrographs. The embryos were processed as described in the previous paragraph (Section 5.2.2.1). Again, while sarcomeric Myosins were readily detectable in the heart, none of the embryos showed upregulation of the sarcomeric Myosins in the area of the fluorescence, and all Mrf misexpressing embryos resembled the control embryos only carrying the pCab vector. This indicated that, chicken Mrf, while able to prematurely trigger myogenesis in the frog, are unable to do so in the immature mesoderm of a gastrulating chicken.

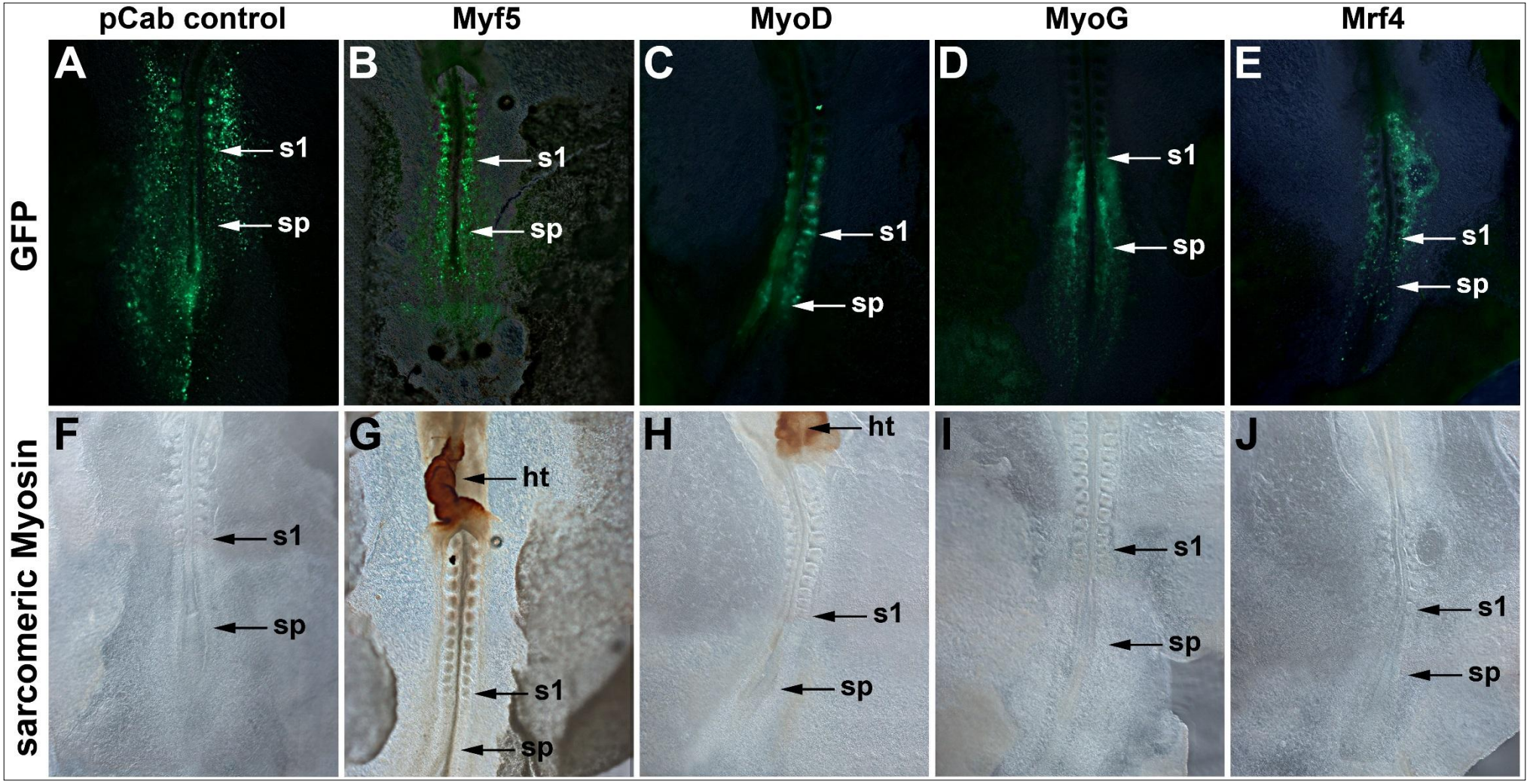
pCab control
Myf5
MyoD
MyoG
Mrf4
GFP
sarcomeric Myosin
A
B
C
D
E
F
G
H
I
J
s1
sp
ht

Figure 5. 2: Mrf misexpression in the naïve paraxial mesoderm and young somites does not trigger premature muscle differentiation (I)
The rostral primitive streak of HH4/5 embryos was electroporated with the constructs indicated on top of the panel. 18 hours later, the GFP expression was recorded (A-E). Embryos were analysed for Sarcomeric Myosin expression, using the MF20 antibody and DAB staining (F-J). MF20 recognised the Sarcomeric Myosins of the developing heart (see G, H, ht). However, the construct expressing cells did not show any sign of Sarcomeric Myosin expression. Abbreviations: ht, heart; s1, youngest somite; sp, segmental plate.
Images (A, C-E, F, H-J) are courtesy of T. Stone.

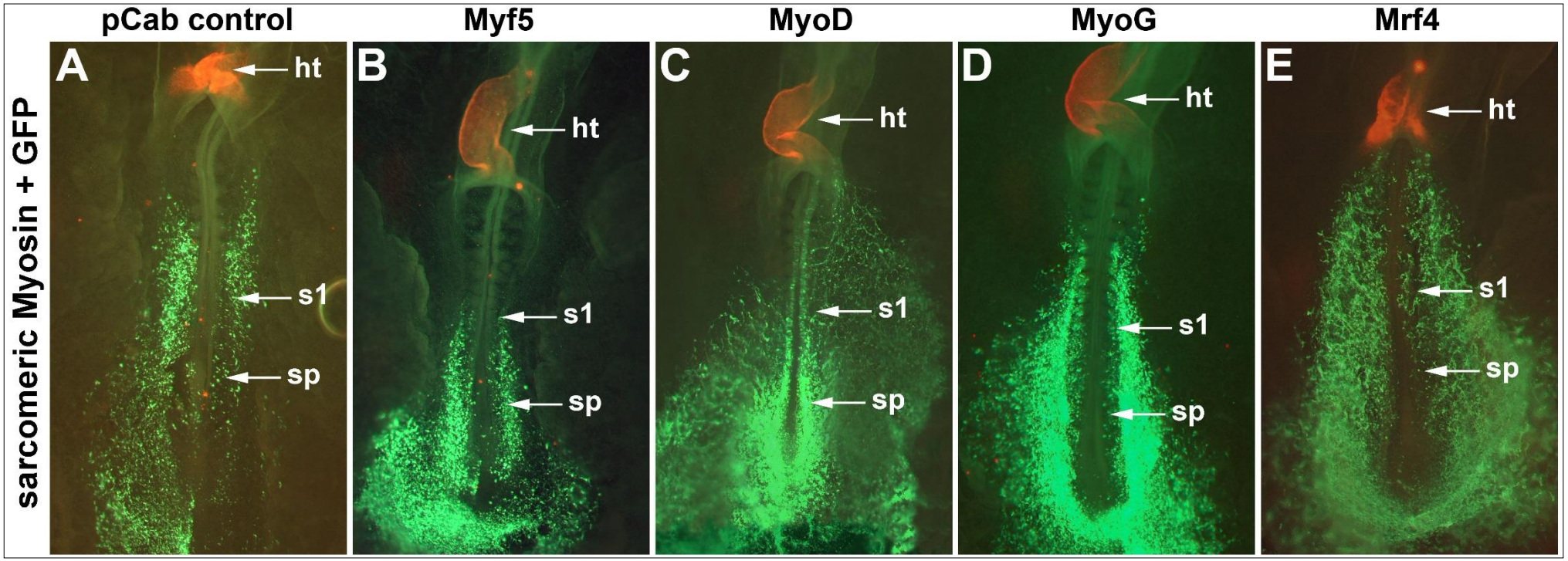
pCab control
Myf5
MyoD
MyoG
Mrf4
sarcomeric Myosin + GFP
A
B
C
D
E
ht
s1
sp

Figure 5. 3: *Mrf* misexpression in the naïve paraxial mesoderm and young somites does not trigger premature muscle differentiation (II).
The rostral primitive streak of HH4/5 embryos was electroporated with the constructs indicated on top of the panel. 18 hours later, GFP was detected with an anti-GFP antibody (green fluorescence) and Sarcomeric Myosin expression was detected with the MF20 antibody (red fluorescence). Note that both in the control and in the Mrf misexpressing embryos, the MF20 antibody recognised Sarcomeric Myosins in the heart. However, neither the control nor the Mrf expressing embryos showed Sarcomeric Myosin expression in the targeted.
Abbreviations: ht, heart; s1, youngest somite; sp, segmental plate.

Table 5. 1: Summary electroporation experiments shown in chapter 5

Numbers displayed as: Total: wildtype/upregulated/downregulated

In this table we can observe the number of the electroporated embryos that were analysed during the experiments. We can observe the number of the embryos analysed with the immunohistochemistry for MF20 antibody detecting Sarcomeric Myosin light chain. All embryos showed no upregulation of Myosin expression.

EP targeting the immature paraxial mesoderm in the segmental plate and young somites		
Specimen analysed for	**Sarcomeric Myosin (MF20)**	
	DAB staining	**Fluorescent 2nd antibody**
Construct		
pCab	4:4/0/0	3:3/0/0
Gg Myf5	5:5/0/0	4:4/0/0
Gg MyoD	5:5/0/0	3:3/0/0
Gg MyoG	4:4/0/0	4:4/0/0
Gg Mrf4	3:3/0/0	4:4/0/0

5.3 Discussion

5.3.1 Electroporation into the rostral primitive streak allowed targeting of the immature paraxial mesoderm and newly formed somites

We previously showed that chicken *MyoG* and *Mrf4,* when misexpressed in 2-cell-stage Xenopus embryos, can enforce muscle differentiation (this study), as can Xenopus *Myf5* and *MyoD* (334) but not chicken *Myf5* and *MyoD*. We thus had to test whether any of the chicken *Mrf* can evoke myogenesis in the autologous chicken system when mimicking the experimental conditions used in the frog. Given that it is not possible to fully recapitulate the Xenopus experiment in the chicken, we tried to recreate this approach at the youngest stage we could manipulate, which is a gastrula stage embryo. We thus established the electroporation conditions to target the gastrulating cells in the primitive streak, ensuring that the prospective paraxial mesoderm (i.e. muscle-competent cells) were included. Our experiments show that when electroporating the rostral primitive streak at HH4/5, the gastrulating mesoderm including the prospective paraxial mesoderm can be targeted. Cell targeting matched our DiI cell labelling experiments and were in line with earlier fate mapping studies (296). However, in our electroporation experiments more cells were targeted than when injecting DiI; in fact besides cells still resident in the streak, GFP expression was found in cells contributing to the paraxial, intermediate and lateral mesoderm as well as in cells contributing to the neural plate (the latter are derived from the epiblast lateral to the rostral streak; (302)). This is likely a result of using a custom-made electroporation chamber which had a 1mm-wide negative electrode embedded in the bottom of the chamber. Thus, even with a flame-sharpened 0.1mm tungsten needle as positive electrode, many cells were exposed to the electrical field. The constructs are driven from the ubiquitously active CMV enhancer/ chicken beta actin promoter, and DNA was injected such that the space between epiblast and the vitelline membrane was filled. Therefore, many cells were in the position to take up and express the constructs. However, given that this electroporation approach did not prevent normal development, and given that a more widespread misexpression gave more cell types the chance to respond to *Mrf*, we deemed this approach very suitable indeed.

5.3.2 The constructs were active 6 hours after electroporation

Previous studies had indicated that the efficiency of myogenic conversion depended on the level of *Mrf* expression, which in turn accounts for the speed by which Mrf protein may accumulate (344). It was important to know when the transgene was first expressed following the electroporation. Understanding the timing of expression allowed us to identify how long the target tissue was exposed to the transgene encoded protein. To do this, we misexpressed pCab-GFP in HH4 embryos and analysed them for GFP-derived fluorescence after 6, 8 and 10 hours after electroporation. We found that GFP was readily detectable 6 hours after electroporation, akin to the somite system (Chapter 4 and Lours-Calet et al., 2014). Thus, when embryos are left to

develop for 18 hours to HH10, the stage when the first *Myf5* expressing cells appear, cells will have been exposed to the transgene for at least 12 hours. Previously, we and others have observed responses to misexpression constructs in this time window (337). Therefore, this experimental set-up allow us to determine cellular responses to *Mrf* misexpression.

5.3.3 Chicken *Mrfs* are unable to drive the chicken immature paraxial mesoderm into terminal muscle differentiation

The aim of this section was to test whether in the autologous system, chicken *Mrf* can drive immature cells into myogenic differentiation. The limitation of the experimental set-up was that cells as immature (in fact pluripotent; (377)) as early Xenopus blastomeres could not be tested. On the other hand, when electroporating into the HH4/5 rostral primitive streak and allowing the embryos to develop for 18 hours to HH10, cells still resident in the streak, cells contributing to the mesoderm, cells incorporated into the paraxial mesoderm, cells that already have become part of a somite, cells in the somite that have begun to express *Myf5* alongside cells in the epiblast that will contribute to neural tissue all will have the chance to respond to *Mrf*. Yet, while sarcomeric Myosins were readily detected in the cardiac muscle of the heart of the embryos which at HH10 is already beating, we found no sarcomeric Myosins in the electroporated cells, neither when using DAB immunostaining nor when using fluorescing secondary antibodies. Even *MyoG* and *Mrf4*, which were able to force Xenopus cells into muscle differentiation, did not upregulate sarcomeric Myosin expression in the chicken. This suggests that *Mrf* did not trigger prmature skeletal myogenesis in immature chicken cells.

A simple explanation for this difference may be that the chicken experiment did not recapitulate the experiment conducted in the frog: in the chicken, gastrulating cells were targeted whereas in the frog, blastomeres were exposed to *Mrf*. These cells have different properties, with gastrulating cells becoming committed to a particular germ layer while early blastomeres are still pluripotent. However, (334) also reported a recruitment of later stage blastomeres in to myogenesis which suggests that the ability to readily engage in myogenesis may be a generic property of early embryonic frog cells. As discussed in chapter 4, anamnia such as Xenopus embryos have to undergo myogenesis at an early stage to allow the tadpole to swim (145,378). In amniotes including birds, there is no necessity to develop skeletal muscle at such an early stage. A fully formed chick will hatch at 21 days of incubation, whereas a Xenopus tadpole has to be able to swim at stage 31 (between two to three days, depending on the temperature of incubation), but they are able to respond to stimulus even earlier and they can move at stage 24 (289). Therefore, it is possible that in Xenopus, chromatin at muscle gene loci is already in an accessible (poised) state, whereas corresponding chromatin in the chicken may be tightly closed. If this were to be the case, we would expect that close to the onset of skeletal muscle formation, i.e. when muscle stem cells develop from the somites, the cells will be able to respond to *Mrf*. If however

the muscle stem cell state itself is protected, the cells will not engage in premature myogenesis. With this in mind, we now turned to the developing muscle stem cells in the dermomyotome of somites. Another explanation could be the time of incubation, it could be that the constructs need more time to complete the process and activate muscle structural genes. In a future experiment we could let the embryos develop for 48 hours until HH16. The embryos could be analysed with MF20 antibody with immunohistochemistry and with Mrf probes with an *in situ* hybridisation to see if the constructs can upregulate the transcription of the other family members.

Chapter 6

6 Misexpression of Mrf genes in the somitic dermomyotome and developing muscle precursor cells

6.1 Introduction

Our previous analyses revealed that misexpression of chicken *Mrfs*, when introduced into gastrulating cells at HH4 to target the newly formed paraxial mesoderm and somites, was insufficient to drive these cells to terminal muscle differentiation (see Chapter 5). These results differed from *Mrf* misexpression experiments frog embryos in which at least the late *Mrfs*, namely chicken *MyoG* and *Mrf4,* were able to convert immature cells in the early blastula and gastrula into terminally differentiated muscle cells (see Chapter 4). In the frog, the paraxial mesoderm engages in muscle formation before the somites are properly formed (145,378). Moreover, muscle has to be made quickly to allow the tadpole to swim (289,379,380). In contrast, amniotes develop directly, i.e. not via distinct larval intermediates, and they do not rely on functional skeletal muscle for a prolonged period of time from fertilisation. It thus is conceivable that in amniotes, the immature paraxial mesoderm is not yet muscle-competent, and hence *Mrfs* may be unable to enforce terminal muscle differentiation. Once the amniote somite is formed, however, it readily begins to engage in muscle formation. First, cells from the epithelial wall of the somite form the primary myotomal scaffold (134). Thereafter, cells from cells from the edges of the dermomyotome are recruited to participate in an extensive second wave of myogenesis. Finally, the dermomyotome de-epithelialises and releases a third wave of myogenic cells into the myotome, the embryonic muscle precursor cells. These are crucial both for fetal and juvenile muscle growth and for the deployment of adult muscle stem cells (55,57). Thus the dermomyotome has to be considered a muscle-competent tissue. Consequently, the next aim was to directly target the developing embryonic muscle precursor cells in the dermomyotome to test the effect of *Mrf* misexpression.

6.1.1 The experimental paradigm

Our test electroporations had revealed that pCab-based constructs are expressed 6 hrs after electroporation, both when electroporating the HH4/5 primitive streak and stage HH15-16 flank somites (Chapters 4, 5 and (363)). Moreover, we readily detected construct activity for 2 days despite the fact that the constructs, being plasmid-based and thus not replicated along with the host cell's genome, must eventually become dilute as cells divide (Chapter 4 and (363)). We therefore had a wide window of opportunity to target the dermomyotome. Our expression analysis had shown that during development, somite differentiation speeds up whereas somite

formation proceeds at constant pace (Berti et al., 2015, see Chapter 3). This suggests that the later we electroporated, the closer to differentiation the targeted cells would be. The dermomyotome begins to release muscle precursor cells into the underlying myotome at E3-E3.5 (135,142). Thus the electroporation cannot be so late in the development of the chicken otherwise we will not be able to target the muscle precursor cell, this is why we decided to use an earlier stage. At this point in time, a transgene electroporated in the dermomyotome would no longer reach the muscle precursor cells. Therefore, we had to electroporate early enough to target these cells and allow them to be exposed to the construct for a sufficient amount of time. In previous studies, we had observed changes in marker gene expression when flank somites of HH15/16 embryos were left to develop for 18 hours (i.e. exposure to the construct was at least 12 hours), thereby reaching stage E3/HH19-20. Since this type of electroporation would meet our requirements, we initially followed this experimental paradigm. As the initial experiments in which *Mrfs* were misexpressed in dermomyotomal cells did not yield ectopic muscle differentiation, a second series of experiments was performed, in which we extended the re-incubation time to 42 hours.

The experimental strategy is summarised in Fig. 6.1. In brief, we microinjected the expression construct directly into the lumen of the HH15/16 flank somites, which are epithelially organised at this stage. The positive electrode was be placed on the dorsolateral side of the somite that we are targeting and the negative electrode will fed through the neural tube and placed underneath the somites (Fig. 6.1 B). We applied 1-2 rectangular pulses at 17 Volts. Embryos were be re-incubated for 18 or 42 hours, respectively. Thereafter, embryos with wildtype overall morphology and readily detectable fluorescence were analysed for the changes in marker gene expression, the unelectroporated side served as internal control side; embryos electroporated with the pCab vector served as control embryos.

A. Time scale of electroporation experiment conducted at HH15/16

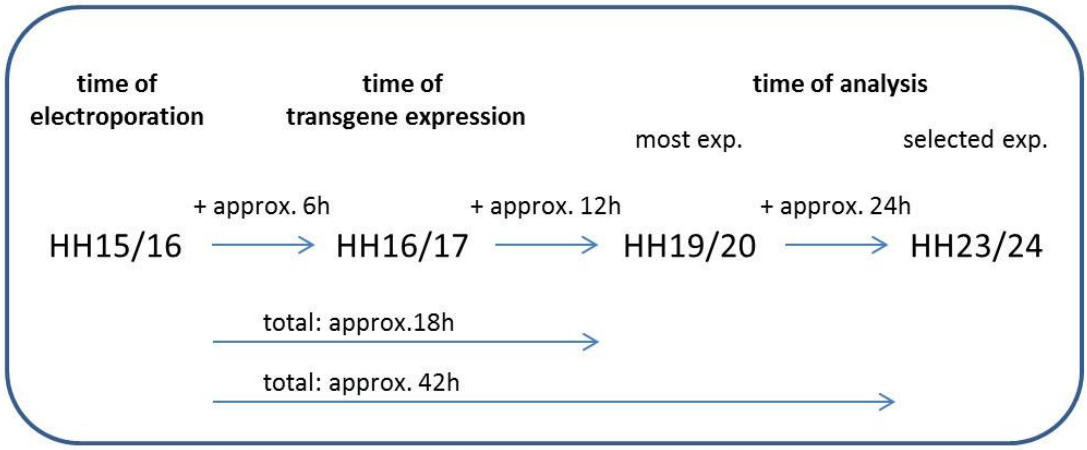

B. Schematic representation of the electroporation experiment at HH15/16

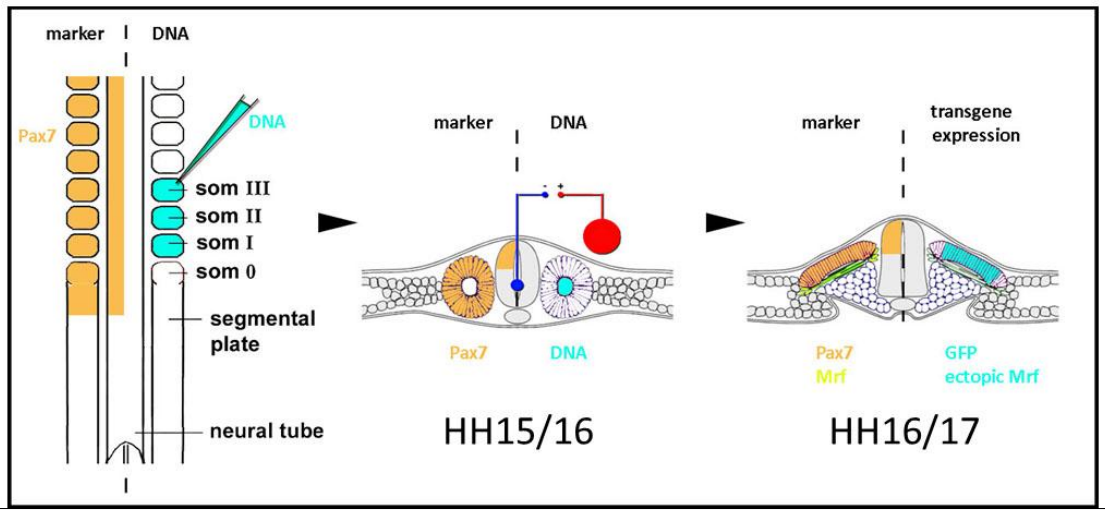

Figure 6. 1: Time scale and schematic of electroporation experiments using HH15-16 flank somites.
Embryos were injected with DiI in one of the three positions indicated in the schemes on the left. Embryos were re-incubated overnight (ON) for 12 hours, reaching stages HH10-11. Images on the right show microphotographs obtained by Nomarski optics, overlaid with images obtained by fluorescence microscopy, of embryos at these stages; ventral views of the trunk, anterior to the top. The numbers on the images reflect the injection site. Abbreviations: hn, Hensen's node, lm, lateral mesoderm, np, neural plate, not, notochord, ps primitive streak, s, somite.
Note that, as the primitive streak lays down the body sequentially from rostral to caudal, later injections lead to the labelling of more caudal areas in the body. This will be important for the planned electroporation experiments, the area of the primitive streak that contributed to the paraxial mesoderm becomes smaller as development proceeds.
Images courtesy of Dr. Dietrich.

6.1.2 Markers to monitor Mrf effects

The function of muscle fibres requires the presence and correct interaction of sarcomeric proteins (295). The MF20 antibody readily detects sarcomeric Myosins (382) and during our expression analysis (Chapter 3), the antibody proved to be reliable. Therefore MF20 antibody staining continued to be the main tool to investigate the response of electroporated somites to *Mrf* misexpression. Since we did not observe any response when the electroporated embryos were re-incubated for 18 hours, we systematically analysed whether any of the earlier expressed genes would be ectopically expressed. Therefore, we analysed the experimental embryos for the expression of: the premyogenic/myogenic genes *Six1* and *Eya1*, for the expression of endogenous *Mrf* genes; for the expression of *Mef2c*, the most likely partner of Mrfs in the somite; and for *Tnni1*, the first structural gene to be expressed. This analysis was done by *in situ* hybridisation, following the same procedures that were employed in Chapter 3. Our analysis showed that in the first 18 hours after electroporation, Mrf proteins can activate some genes in the early myogenic cascade but were insufficient to drive full muscle differentiation.

6.2 Results

6.2.1 Mrf misexpression, assaying for the premature expression of sarcomeric Myosins

6.2.1.1 Analysis after 18 hours of re-incubation HH20

When analysed 18 hours after electroporation, more than 90 % of the embryos were alive with the heart beating and overall good morphology. The embryos were analysed by MF20 antibody staining using DAB as described in the previous chapter; numbers of experimental specimen and results of the experiment are shown in Table 6.3. As shown in Figure 6.2, both sides of the experimental embryos were photographed and compared with both sides of the pCAb control embryos (Fig. 6.2 B, C). Notably, all the embryos presented the same phenotype in that the electroporated side didn't present any upregulation of sarcomeric Myosin (Fig. 6.2 F, I, L, O) compared with the control side (Fig 6.2 E, H, K, N). The striped appearance of the stained somites suggested that only the myotubes expressed sarcomeric Myosin. To confirm this, embryos shown in Fig.6.2 were vibratome-cross sectioned. Comparison of the control sides (Bi, Ei, Hi, Ki, Ni) and the electroporated sides (Ci, Fi, Ii, Li, Oi) showed that indeed, in all specimen sarcomeric Myosin expression was confined to the myotome; there was no ectopic expression in the electroporated dermomyotome.

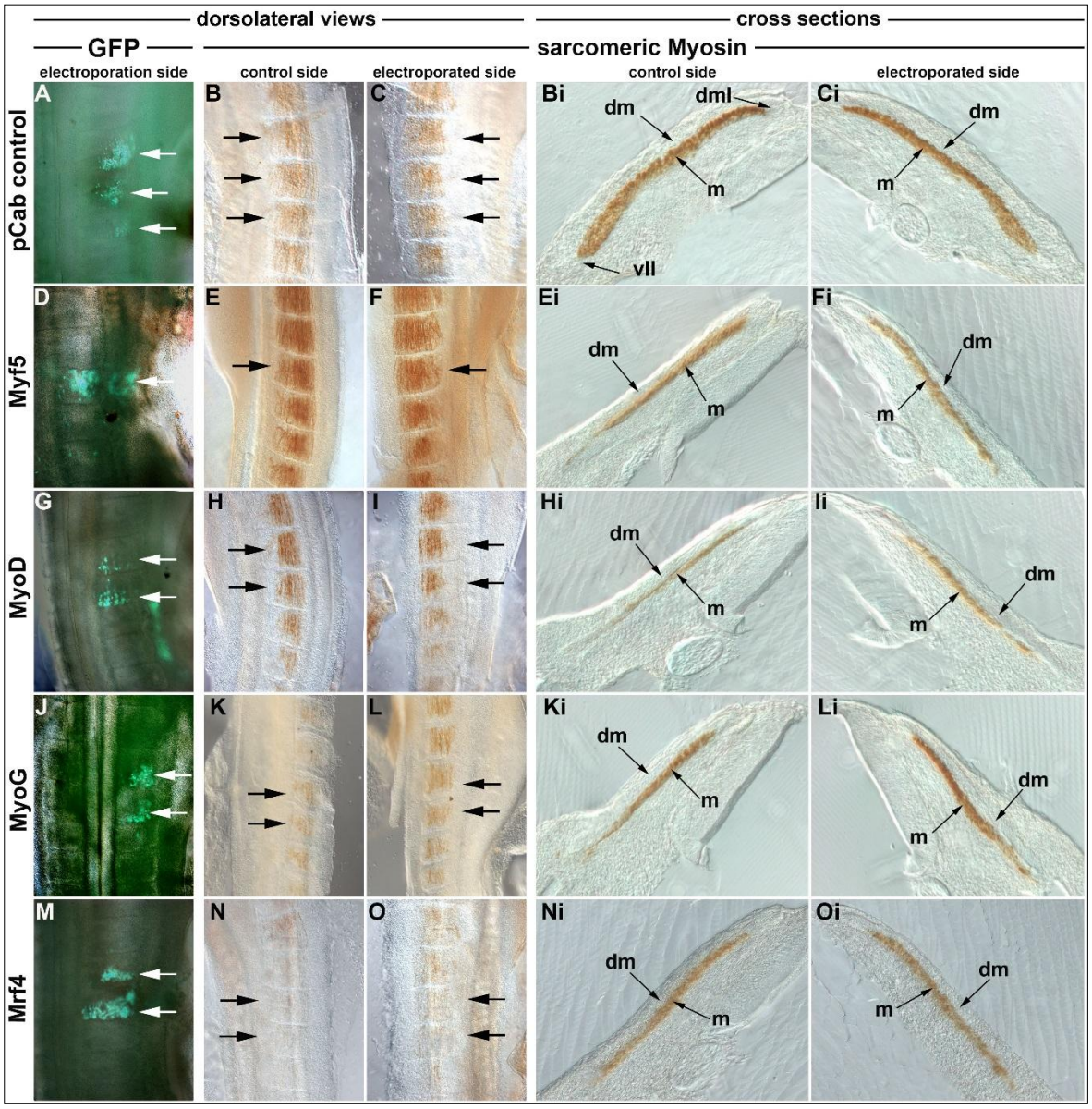
dorsolateral views
cross sections
GFP
sarcomeric Myosin
electroporation side
control side
electroporated side
control side
electroporated side
pCab control
Myf5
MyoD
MyoG
Mrf4
A
B
C
Bi
Ci
D
E
F
Ei
Fi
G
H
I
Hi
Ii
J
K
L
Ki
Li
M
N
O
Ni
Oi
dm
dml
m
vll

Figure 6. 2: Misexpression of Mrfs between HH16-20 is insufficient to induce Sarcomeric Myosin expression in the chicken dermomyotome.

Flank somites were electroporated at HH15/16 with GFP (control) or GFP and Mrf expressing constructs as indicated on the left of the panel. Embryos were harvested 18 hours later at HH19/20, i.e. they were exposed to Mrf and/or GFP proteins for at least 12 hours. (A,D,G,J,M) Overlays of the Nomarski and fluorescence photomicrographs of the electroporated flanks, dorsolateral views, rostral to the top. GFP expression indicates that 1-3 somites were targeted (green fluorescence, arrows). (B,E,H,K,N) Nomarski images of the un-electroporated control sides, and (C,F,I,L,O) of the electroporated sides of the embryos shown in (A,D,G,J,M), assayed with MF20-DAB staining to reveal Sarcomeric Myosin expression (brown staining), views as in (A,D,G,J,M). The targeted somites and their un-electroporated counterparts are indicated by arrows. Note, the levels of Sarcomeric Myosin expression are the same on either side. (Bi,Ei,Hi,Ki,Ni) and (Ci,Fi,Ii,Li,Oi) Nomarski images of cross sections of the flanks shown in (B,E,H,K,N) and (C,F,I,L,O), respectively. Note the absence of Sarcomeric Myosin expression in the electroporated dermomyotomes. Abbreviations: dm, dermomytome; dml, dorsomedial lips of the dermomyotome; m, myotome.

6.2.1.2 Analysis after 42 hours of re-incubation HH24

The previous experiment indicated that that 18 hours after electroporation, i.e. a minimum of 12 hours exposure to the transgene, none of the *Mrf* was able to drive developing muscle precursor cells into premature differentiation. This suggested that the myoblast state may be protected in these cells. To explore whether after prolonged exposure, *Mrf* would overcome this myoblast state, we electroporated embryos at HH15/16 as before, this time re-incubating the embryos for 42 hrs. This gave the embryos time to reach approximately HH23/24 after which they were analysed for GFP-derived fluorescence and sarcomeric Myosin expression as before (Fig. 6.3). The numbers of specimen and the results are also included in Table 6.3.

At the stage of harvesting, muscle precursor cells are in the process of populating the myotome with some cells producing differentiating daughter cells. Thus, as expected, some of the electroporated cells were still in the dermomyotome (round GFP-filled cells), others were in the myotome and had produced elongated myotubes (elongated fluorescing cells). Owing to the progress in development, the somites were much larger in size than a day earlier (Fig.6.3). Figure 6.3 B and C shows both sides of a pCab-electroporated control embryo, which, as expected, didn't show any upregulation of sacromeric Myosin. Electroporations using the *Myf5, MyoG* and *Mrf4* expression constructs similarly showed wild type MF20 staining on both sides (Fig. 6.3 E-F, K-L, N-O). In contrast, MyoD induced strong upregulation of sarcomeric Myosin expression within the fluorescing cells (Fig.6.3 I). Comparison of the cross sections confirmed the upregulation of sarcomeric Myosin in the dermomyotome of the *MyoD*-misexpressing somites (Fig. 3.6 Ii). This phenotype was obtained in two of six embryos (see Table 6.3). This suggests that after the after 36 hours of exposure to MyoD, the protection of the myoblast state can now be overcome.

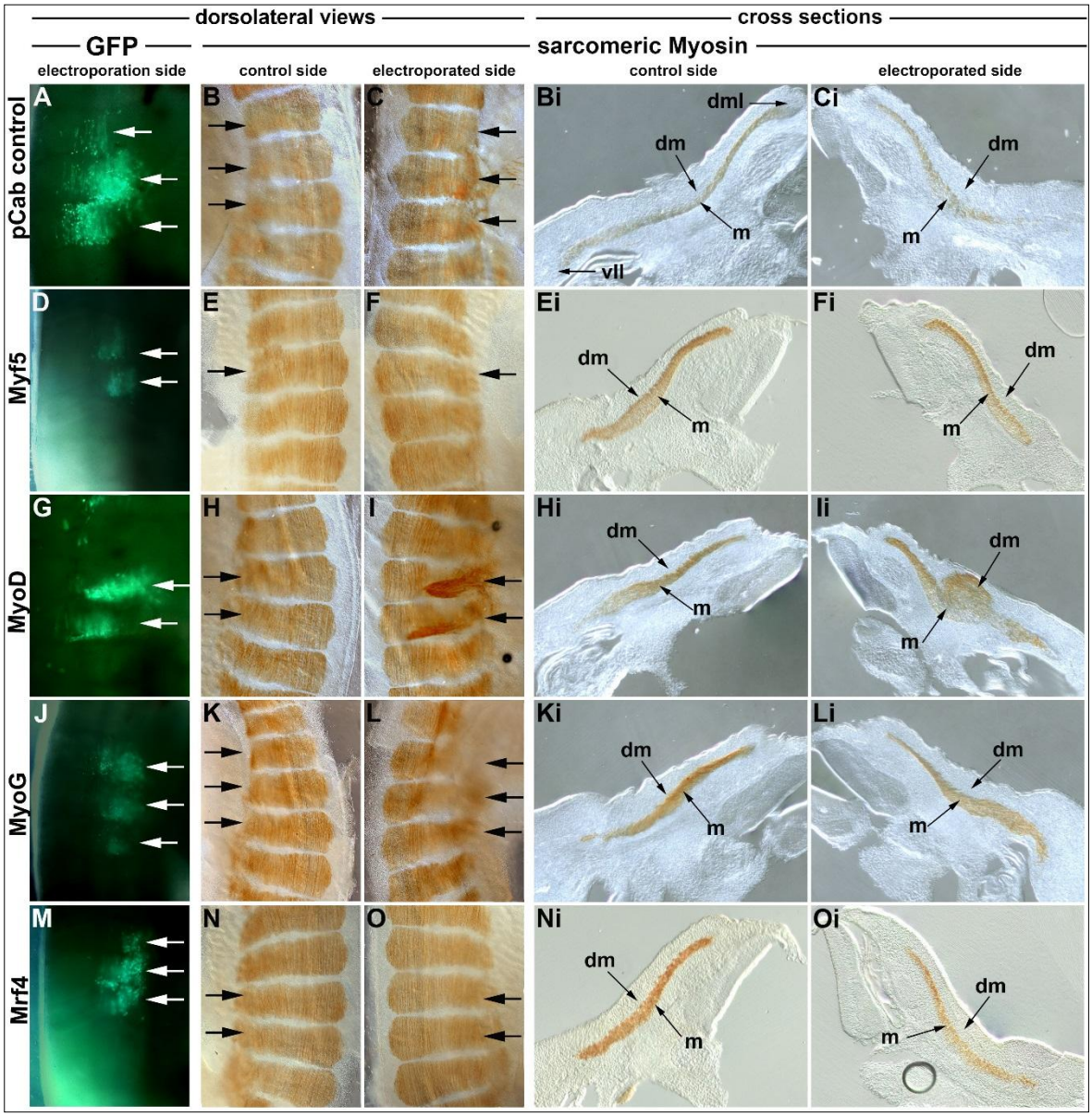
dorsolateral views
cross sections
GFP
sarcomeric Myosin
electroporation side
control side
electroporated side
control side
electroporated side
pCab control
Myf5
MyoD
MyoG
Mrf4
A
B
C
Bi
Ci
D
E
F
Ei
Fi
G
H
I
Hi
Ii
J
K
L
Ki
Li
M
N
O
Ni
Oi
dml
dm
m
vll

Figure 6. 3: Misexpression of *MyoD* but not other *Mrfs*, induces Sarcomeric Myosin expression in the chicken dermomyotome between HH16-24.

Flank somites were electroporated at HH15/16 with *GFP* (control) or *GFP* and *Mrf* expressing constructs as in Fig. 6.2 but embryos were harvested 42 hours later at HH23/24, i.e. cells were exposed to the proteins expressed from constructs for at least 36 hours. The location of the construct expressing cells was visualised by means of GFP expression and Sarcomeric Myosin expression was detected with the MF20 antibody as before. In the embryo electroporated with the *MyoD* expression construct, the area expressing the construct (G, arrows) shows strongly elevated Myosin expression (I, arrows). The corresponding cross section (Ii) shows that this elevated Myosin expression is confined to the dermomyotome of the electroporated somite, indicating that after prolonged exposure, *MyoD* is able to drive muscle stem cells into myogenic differentiation. The ectopic muscle is disorganised, probably because it developed without the scaffold of the post-mitotic myotome. The data suggest that between HH16 and HH20, the developing muscle stem cells are protected from premature differentiation. Abbreviations: dm, dermomytome; dml, dorsomedial lips of the dermomyotome; m, myotome.

6.2.2 Assaying for markers of myogenic progression after 18 hours of Mrf misexpression

Expression of sarcomeric Myosin demarcates the terminal differentiation of muscle cells, which did not occur when embryos were reincubated for 18 hours and thus exposed to Mrf proteins for 12 hours. We were wondering whether nonetheless, cells would undertake some steps towards myogenesis. We therefore repeated the initial 18 hour- electroporation experiments, this time monitoring the expression of genes which, according to our expression analysis, demarcate earlier steps in myogenesis. To assay for gene expression, we performed *in situ* hybridisation with the antisense RNA probes used in chapter 3. In order to minimise any binding of probe to the sequences derived from the pCab vector, embryos were treated with RNAse A after hybridisation. The results are also included in Table 6.3.

6.2.2.1 Analysis of Six1 and Eya1 expression

The first set of electroporated embryos was analysed for the expression of the premyogenic genes *Six1* and *Eya1*. In Chapter 3, we showed that at the time of electroporation at HH15/16, both genes are expressed in the epithelial somites, but proteins may not act as transcriptional activators yet. At the time of harvesting, *Six1* and *Eya1* are normally expressed in the dorsomedial and ventrolateral dermomyotomal lips and in the myotome, together with the *Mrf* genes (see Chapter 3). Thus, if *Mrf* were to prematurely initiate steps towards myogenesis including *Six1* and *Eya1* activation, we would expect to see upregulated expression of these genes in the dermomyotome.

In all embryos, GFP-derived fluorescence was recorded and the electroporated and neighbouring somites were photographed after completion of the *in situ* hybridisation as shown in Fig. 6.4. When analysing the expression of *Six1*, we found that all somites showed wildtype expression only (Fig.6.4 B,F,J,N,R). When analysing the expression of *Eya1* expression, we found that the overall staining was unexpectedly weak and hence, results have to be interpreted with caution. However, an upregulation of *Eya1* was also not observed (Fig.6.4 D,H,L,P,T). In contrast with the experiments in tissue culture, Mrf in vivo were unable to upregulate the Six1 and Eya genes (383).

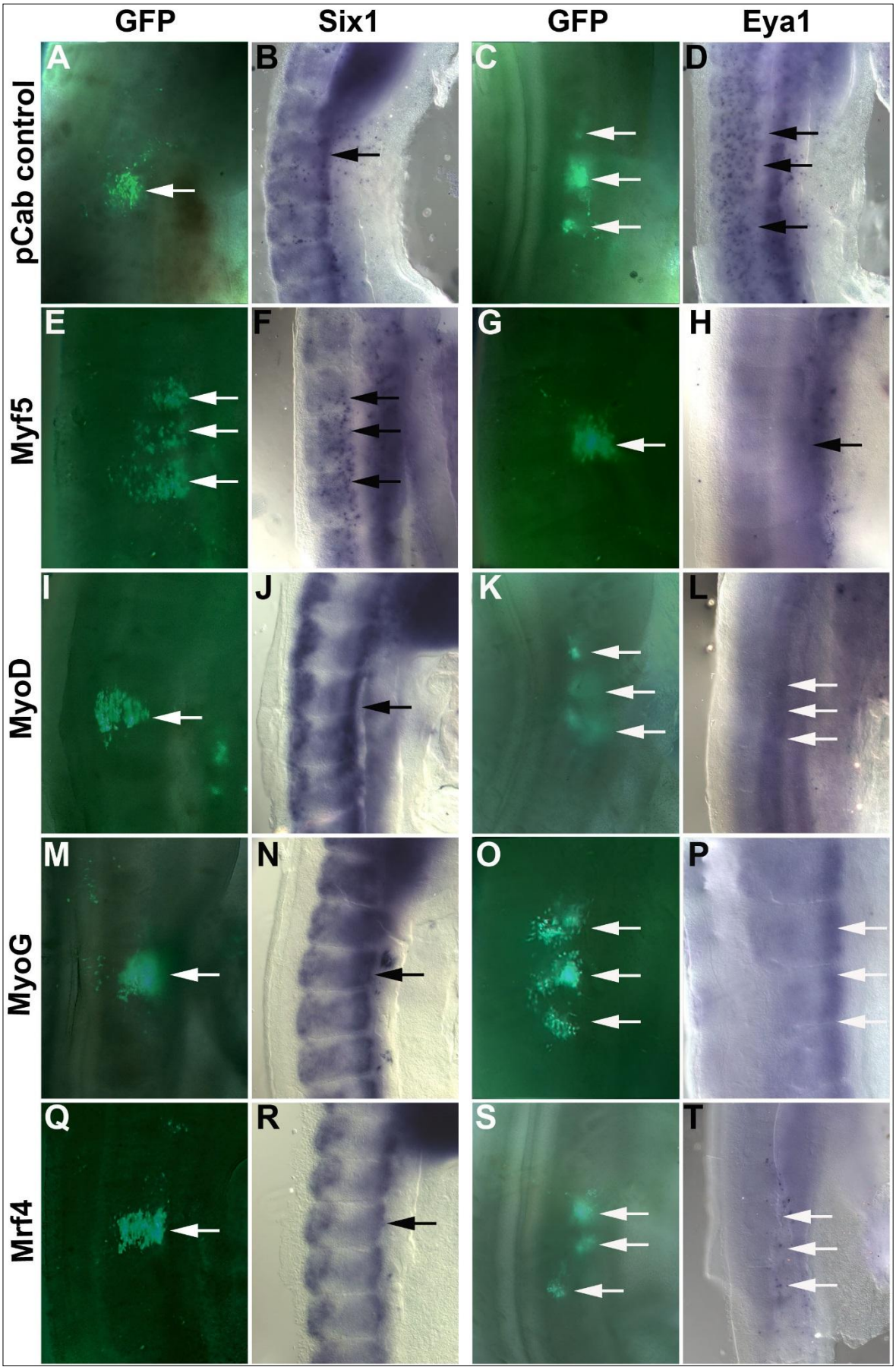
GFP
Six1
GFP
Eya1
pCab control
Myf5
MyoD
MyoG
Mrf4
A
B
C
D
E
F
G
H
I
J
K
L
M
N
O
P
Q
R
S
T

Figure 6. 4: Misexpression of Mrf genes between HH16-20 is insufficient to upregulate Six1 or Eya1 transcription.

Flank somites were electroporated at HH15/16 and embryos harvested at HH19/20 as shown in Fig. 6.2. Thus, the embryos were exposed to the constructs for a least 12 hours. GFP expression was recorded, and then the embryos were analysed for the expression of *Six1* and *Eya1* mRNA expression by *in situ* hybridisation as indicated on top of the panel. Normal expression of these genes was observed in the somitic myotomes and the dorsomedial and ventrolateral dermomyotomal lips, mirroring the expression on the control side (not shown). Ectopic expression in the targeted cells in the dermomyotome was not observed.

6.2.2.2 Analysis of Mef2c expression

The four members of Mef2 family of transcription factors are important Mrf co-factors (189,384,385). However, we previously showed that in the context of the chicken somite, Mef2c is the most likely partner of the Mrf proteins, overlapping with the expression of the Mrf in the dorsomedial and ventrolateral dermomyotomal lips and the myotome (381). We hence investigated whether *Mrf* may upregulate the expression of *Mef2c*. Unfortunately, in this set of experiments, high levels of background staining were obtained (Fig.6.6). Yet elevated levels of *Mef2c* expression were clearly detectable in somites electroporated with the *Myf5*, *MyoD* or *MyoG* constructs (Fig. 6.6 D, F, H).

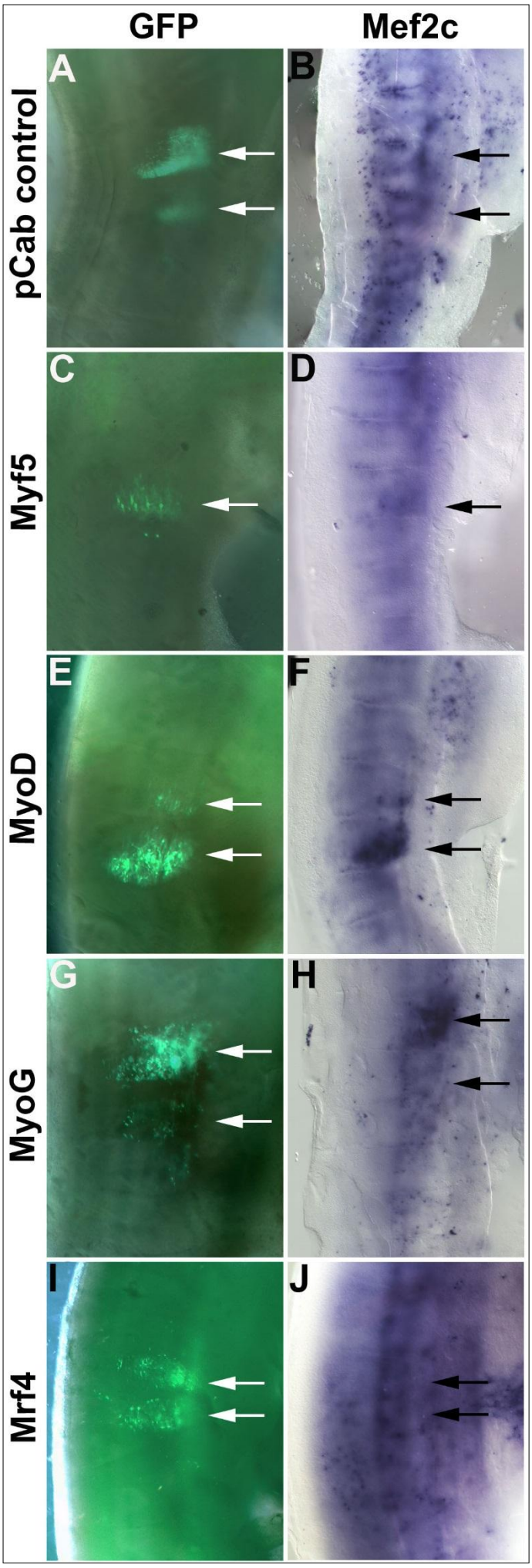
GFP
Mef2c
pCab control
Myf5
MyoD
MyoG
Mrf4
A
B
C
D
E
F
G
H
I
J

Figure 6. 5: Misexpression of Myf5, MyoD and MyoG but not Mrf4, between HH16-20 upregulated Mef2C transcription.

Flank somites were electroporated at HH15/16 and embryos harvested at HH19/20 as before. GFP fluorescence was recorded and *Mef2C* mRNA expression detected by *in situ* hybridisation. *Myf5* weakly induced whereas *MyoD* and *MyoG* induced stronger ectopic *Mef2C* expression (D,F,H, respectively).

6.2.2.3 Analysis of Tnni1 expression

We showed in chapter 3 that the *Troponin I 1* gene which encodes for a component of the sarcomeric multiprotein complex is the first muscle structural gene to be expressed, labelling the myotome at the stage that also *MyoG* is expressed (chapter 3, (381). Yet we found that neither the pCab control nor the *Mrf* expression constructs caused any upregulation of *Tnni1* expression (Fig. 6.7).

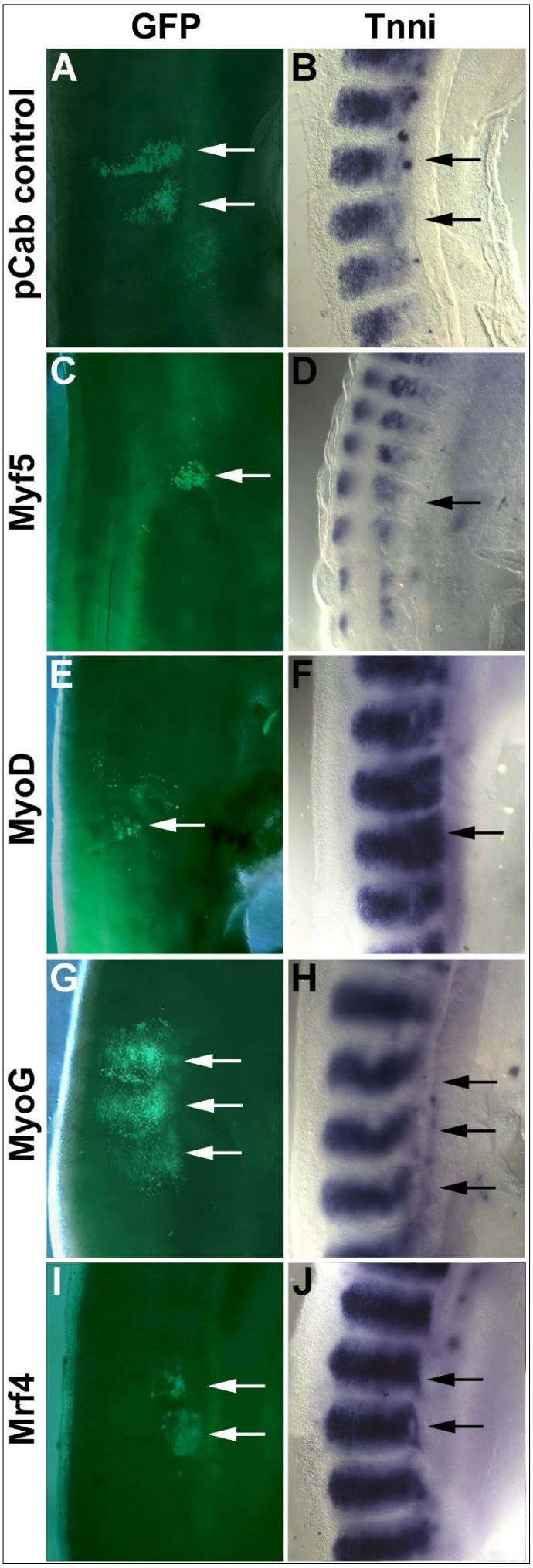
GFP
Tnni
pCab control
Myf5
MyoD
MyoG
Mrf4
A
B
C
D
E
F
G
H
I
J

Figure 6. 6: Misexpression of Mrf genes between HH16-20 is insufficient to upregulate Tnni1 transcription.

Flank somites were electroporated at HH15/16 and embryos harvested at HH19/20 as before. GFP fluorescence was recorded and *Tnni1* mRNA expression detected by *in situ* hybridisation. Note that neither the pCab control plasmid nor the *Mrf* expression constructs were able to induce ectopic *Tnni1* expression.

6.3 Discussion

Previous sections showed that while chicken *MyoG* and *Mrf4* can trigger premature myogenesis in early Xenopus blastomeres, none of the chicken *Mrf* was able to drive the chicken gastrulating mesoderm and early paraxial mesoderm into forming skeletal muscle. Aim of this section was to explore whether developing muscle stem cells could be driven into myogenesis as these cells are only one step away from myogenic differentiation. Therefore, the chicken *Mrf* expression constructs were electroporated into the developing muscle stem cells in chicken flank somites. Embryos were analysed to the premature expression of markers indicating myogenic progression and terminal differentiation. These experiments revealed that *Mrf* activated some of the early muscle regulatory genes including other *Mrf* family members. However, in an 18 hours time window, *Mrf* were unable to enforce terminal muscle differentiation.

6.3.1 Mrf misexpression in the somitic dermomyotome leads to the premature activation of some myogenic genes

When electroporated into the somite, chicken Mrf can activate the expression of other Mrf family members and of Mef2c within 18 hours, with Myf5, MyoD and MyoG being the most potent activators. These findings indicate that our constructs are biologically active. They are in in line with the initial in vitro studies that once established that all Mrf can evoke skeletal muscle differentiation, and the in vitro studies that showed that MyoD can activate MyoG and Mef2 family members (386). This is also similar to misexpression experiments conducted in the chicken neural tube in vivo which showed that mouse Myf5 and MyoD can activate chicken MyoD and MyoG (Mrf4 not tested), and that a tagged version of chicken Myf5 can activate MyoD, MyoG, Mrf4, tagged MyoD can activate MyoG and Mrf4, tagged MyoG can activate MyoD and Mrf4 and Mrf4 can activate MyoG (224,337). The differences that were observed in the chicken experiments may be due to a somewhat different type of expression construct used, as well as the fact the in the neural tube, the range of genes accessible to Mrf proteins may be different to the range available in the somite (summarised in Table 6.1). Nevertheless, the experiments all indicated Mrf can upregulate the expression of transcription factors needed for the subsequent expression of myogenic genes.

Remarkably, Tnni1, a muscle structural gene normally expressed simultaneous with MyoG and before Mrf4, was not activated by any Mrf, suggesting that in contrast to experiments in vitro and experiments in the frog, chicken Mrf were unable to force cells into terminal differentiation. This was corroborated by the absence of any premature expression of sarcomeric Myosins in the electroporated cells. This suggests that Mrf activate genes associated with readying the cells for myogenesis but in the contexts of the developing muscle stem cells, do not force premature differentiation (summarised in Fig. 6.8).

Table 6. 1: Comparison of results obtained in this study (Berti) with those obtained in previous studies (Delfini or Sweetman)

Mrf electroporations analysed by *in situ* hybridisation or by immunohistochemistry from this study are summarised and evaluated alongside those of two other important published papers (224,337). Data is colour-coded by study (Delefini-Blue, Sweetman-Red and Berti-Green). The observed upregulation of a gene is represented by a tick in the corresponding colour. The results of all three works are mostly in agreement but differ in some experiments.

	Marker																	
	Myf5	**MyoD**	**MyoG**	**Mrf4**	**Pax3**	**Pax7**	**FgfR4**	**Id1**	**miR1**	**miR206**	**Six1**	**Eya1**	**Mef2c**	**Tnni1**	**Mox2**	**Notch1**	**Serrate1**	**Sarcomeric Myosin (MF20 staining)**
Construct																		
pCab control	-	-	-	-							-	-	-	-				
Myf5	(construct*) -	✓✓✓	✓✓ ✓	✓✓					✓	✓	-	-	-✓	-				✓ after 4d
MyoD	- -✓	(construct*) ✓	✓✓✓	✓✓	maybe slightly down		✓	✓		✓	-	-	✓✓	-	-	✓ in cell next to diff. cells	✓ in diff. cells	✓ after 4d ✓ after 2d
MyoG	-✓	✓✓	(construct*)	✓✓					✓	✓	-	-	✓	-				
Mrf4	-✓	- ✓	✓-	(construct*)						✓	-	-	nd	-				

Abbreviations: diff., differentiated; EP, electroporation. (✓= expression, - = no expression, nd = not defined)

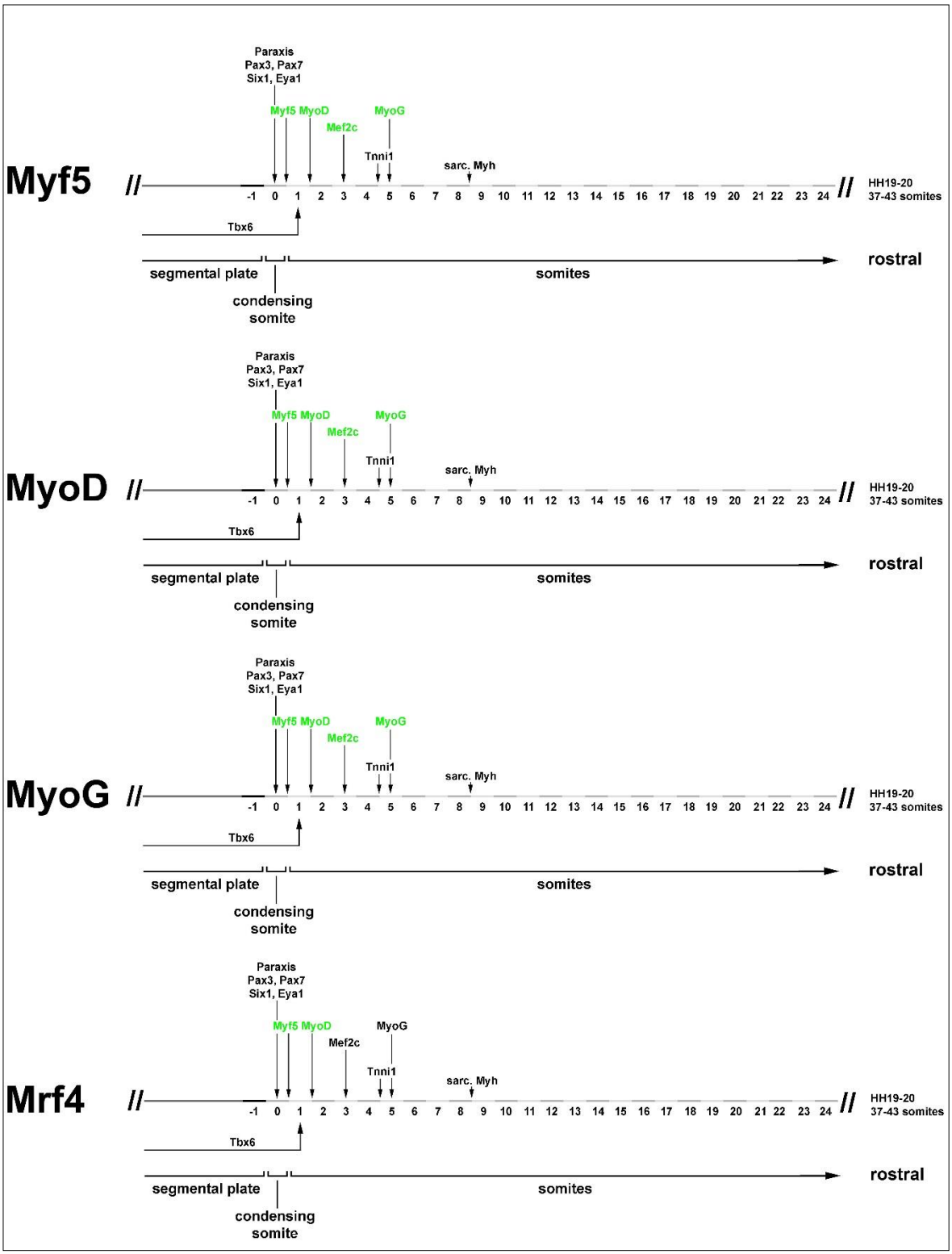
Myf5
Paraxis
Pax3, Pax7
Six1, Eya1
Myf5 MyoD
Mef2c
MyoG
Tnni1
sarc. Myh
-1 0 1 2 3 4 5 6 7 8 9 10 11 12 13 14 15 16 17 18 19 20 21 22 23 24
HH19-20
37-43 somites
Tbx6
rostral
segmental plate
somites
condensing
somite
MyoD
Paraxis
Pax3, Pax7
Six1, Eya1
Myf5 MyoD
Mef2c
MyoG
Tnni1
sarc. Myh
-1 0 1 2 3 4 5 6 7 8 9 10 11 12 13 14 15 16 17 18 19 20 21 22 23 24
HH19-20
37-43 somites
Tbx6
rostral
segmental plate
somites
condensing
somite
MyoG
Paraxis
Pax3, Pax7
Six1, Eya1
Myf5 MyoD
Mef2c
MyoG
Tnni1
sarc. Myh
-1 0 1 2 3 4 5 6 7 8 9 10 11 12 13 14 15 16 17 18 19 20 21 22 23 24
HH19-20
37-43 somites
Tbx6
rostral
segmental plate
somites
condensing
somite
Mrf4
Paraxis
Pax3, Pax7
Six1, Eya1
Myf5 MyoD
Mef2c
MyoG
Tnni1
sarc. Myh
-1 0 1 2 3 4 5 6 7 8 9 10 11 12 13 14 15 16 17 18 19 20 21 22 23 24
HH19-20
37-43 somites
Tbx6
rostral
segmental plate
somites
condensing
somite

Figure 6. 7: Summary of changes in marker gene expression induced by Mrfs in the flank dermomyotome in 18 hour timeframe between HH16-20.

Schematic representation of the onset of marker gene expression in chicken somites at HH20 as revealed by the expression analysis in Chapter 3. The immature paraxial mesoderm is shown on the left, the oldest somites are shown on the right; somites are numbered consecutively from youngest to oldest. The *Mrf* that was misexpressed is indicated on the left. Genes that are normally expressed in the myotome and that become upregulated in the dermomyotome upon 12 hour exposure to the *Mrfs* are shown in green. Note that *Mrfs* upregulate some myogenic genes, but fail to activate muscle structural genes.

6.3.2 The precursor/ stem cell state of cells in the somitic dermomyotome is likely protected

Our experiments showed that when electroporated embryos were re-incubated overnight such that developing muscle stem cells were exposed to Mrf for a minimum of 12 hours, Mrf did not trigger premature expression of muscle structural proteins. However, when embryos were left to develop for additional 24 hours, then a third of the embryos electroporated with a MyoD expression construct showed ectopic sarcomeric Myosin expression in the dermomyotome. This indicates that after prolonged exposure specifically to MyoD, muscle stem cells can undertake complete muscle differentiation. This finding is in line with the experiments conducted in the chicken neural tube, where it took 3-4 days of exposure until some limited myogenic conversion of cells was obtained (337). Cells in the neural tube are not normally geared up to engage in myogenesis, thus, the reluctance of neural cells to express muscle genes is perhaps not surprising. Developing muscle stem cells however are set up for myogenesis. Moreover, Mrf are able to activate a number of co-factors essential for the efficient activation of muscle genes. Therefore, the delay in muscle differentiation of Mrf misexpressing embryonic muscle stem cells is, at first sight, surprising. We hypothesised at the outset of this study that the muscle stem cells state might be protected from premature differentiation. We summarise in Table 6.2 the expected results if the muscle stem cell state were to be protected. Our results are compatible with the idea that the muscle stem cells state is protected from premature differentiation. Moreover, our result suggest a time frame for the protection of the stem cell state between HH15/16 and HH23/24, when the first terminally differentiated cells appear in the targeted dermomytomes.

Table 6. 2: Expected and obtained outcomes of in vivo misexpression in chicken *Mrf*

The experiments conducted in early Xenopus embryos suggested different roles for Myf5/MyoD and MyoG/Mrf4 genes. They are however also compatible with (i) a possible difference in the myogenic competence of immature cells in amniotes and anamnia or (i) with species-specific differences between chicken and frog Mrf. The experiments conducted in the chicken suggest that the immature paraxial mesoderm and the developing muscle stem cells are protected from precocious differentiation.

	Results obtained in this study when misexpressing chicken *Mrf*				
Scenario	**Expected result following *Mrf* misexpression in muscle precursor or muscle stem cells in vivo**	**In 2-cell stage Xenopus embryos, targeting pluripotent cells (chapter 4)**	**In gastrula stage chicken embryos, targeting the immature paraxial mesoderm and young somites (chapter 5)**	**In chicken somites, targeting the developing muscle stem cells; 18h incubation (chapter 6)**	**In chicken somites, targeting the developing muscle stem cells; 42h incubation (chapter 6)**
All *Mrf* are sufficient to drive myogenesis	all will drive muscle precursor/ muscle stem cells into differentiation				
Mrf have different roles, with *Myf5* controlling myogenic commitment, *MyoD* prepares for the entry into differentiation, and the late expressed *MyoG* and *Mrf4* control terminal differentiation	only *MyoG* and *Mrf4* will drive cells into terminal differentiation	✓			
MyoD triggers myogenesis via a feed forward mechanism	*MyoD*, alone or together with *MyoG* will drive terminal differentiation				✓
The precursor/ muscle stem cell state is protected	*Mrf* will not be able to enforce myogenic differentiation		✓	✓	

6.3.3 Possible explanations for the protection of the precursor/ stem cell state

6.3.3.1 Insufficient levels of MyoD and MyoG to activate late-phase myogenic genes

After close analysis of the previous results we decided to dedicate more time to investigate why the cells are in such a protected state and how we could achieve differentiation of the muscle stem cells. We therefore agreed that the first step towards this analysis was to try a co-electroporation of MyoD and MyoG. MyoD has always been considered one of the main guides of myogenesis and thought to push the muscle stem cells to leave the cell cycle and start differentiating. Alternatively MyoG is considered responsible for the final differentiation and the formation of the myofibers. We hypothesised that the presence of both the constructs in the same electroporation at HH16 will likely be the key to obtaining the final differentiation of the muscle stem cells (see Chapter 7).

6.3.3.2 Insufficient levels of Mef2 cofactors

As described in Section 6.2.1, Mef2C was chosen as the most likely co-factor involved in myogenesis in chickens. During myogenesis, Mrf have been found to interact with Mef2 proteins, and neighbouring binding sites for these factors have been found in the promoters of muscle genes (387). Mef2 misexpression per se has been shown to be insufficient to initiate myogenesis, but the presence of Mef2 proteins accelerates this process, absence of Mef2 prevents it (388). We showed that in the chicken somite, Mef2c is the first Mef2 gene to be transcribed in the somite, followed be Mef2a (381). Misexpression of Myf5, MyoD and MyoG led to upregulated Mef2c mRNA expression. However, we had no means to establish whether sufficient Mef2c protein was made to accompany the Mrf proteins, and it is possible that Mef2c (or Mef2a) proteins levels were too low to support efficient myogenesis. Therefore, we tested in chapter 8, whether elevation of both, Mrf and Mef2c levels would overcome the protection of the muscle stem cell state.

6.3.3.3 Absence of Six1

Six1 was chosen because it was believed to be the most closely related of the Six family genes to muscle formation in chickens. We decided to analyse the expression of *Six1* mRNA after the misexpression of the Mrfs. The results of the *in situ* hybridisation showed that there was no detectable changes in the mRNA levels. The role that Six1 plays is somewhat controversial as previous research has shown that it is also active further downstream in myogenesis hence, their description as “pre-myogenic” genes may be somewhat misleading (182). We theorised that it would be important to test the misexpression of Six1 itself and as a co-electroporation with MyoD. It could be possible that high levels of a premyogenic gene could activate the molecular cascade of myogenesis causing myogenic differentiation (see Chapter 9).

6.3.3.4 Persistence of muscle differentiation inhibitors

In the intricate network of myogenesis, we don't find just genes that trigger the muscle cell division or differentiation but there are a lot of molecules that contribute to maintaining the important balance between proliferation and stem cell state. Pax7 is one of the most important markers involved in the control of the stem cell state. Additionally the micro RNA miR206 has been defined as an important factor in somite development since loss of miR206 is correlated with loss of expression of MyoD (389). We will therefore analyse the expression of both of these genes following electroporation of the Mrf constructs. We formulated the hypothesis that 18 hrs after electroporation, the expression of Pax7 could be downregulated whilst in contrast, the expression of miR206 will be upregulated (Chapter 10).

6.3.3.5 Failure to withdraw from the cell cycle

A possible explanation for the failure of the upregulation of Myosin could be related to lack of cell cycle withdrawal. Cells that need to differentiate have to leave the cell cycle to reach the final stage of development into a muscle fibre. We reasoned that an important step would be to investigate which Cyclin-dependant kinase (Cdk), activators and inhibitors play an important role in myogenesis. We will analyse the mRNA levels in the somites and then we will focus our attention on choosing the best candidate for misexpression/co-misexpression experiments using electroporation. MF20 antibody staining with DAB will be performed to test the level of the Sarcomeric Myosin expression in the electroporated somites (Chapter 11).

6.3.3.6 Inhibiting phosphorylation of MyoD

The heterodimerisation of MyoD and E proteins is an essential step in binding to the chromatin during myogenesis. The process of heterodimerisation is facilitated in part by E protein phosphorylation through P38 MAPK. This kinase has been demonstrated as an essential component in myogenesis and the regulation of MyoD/E47 heterodimerisation (390). Conversely, phosphorylation of MyoD by cyclin dependant kinases (CDKs) has been demonstrated to target it for rapid degradation by the ubiquitin pathway (206). A phosphorylation-site mutant construct of the mouse MyoD gene will be used to further investigate whether phosphorylation of the transgene encoded MyoD could be inhibiting its activity in the chicken (Chapter 12).

Table 6. 3: Summary electroporation experiments shown in chapter 6

Numbers displayed as: Total: wildtype/upregulated/downregulated

Summary of the number of electroporated embryos that were analysed with ISH using antisense probes, or with immunohistochemistry using MF20 antibody, together with the number of altered phenotypes observed. Blue boxes highlight when upregulation was observed in mRNA or Myosin levels. The asterisk in the final column highlights that the upregulation results were observed in multiple sets of electroporation experiments.

EP targeting the embryonic muscle stem cells in the somitic dermomyotome										
specimen analysed for	**Six1 mRNA**	**Eya1 mRNA**	**Myf5 mRNA**	**MyoD mRNA**	**MyoG mRNA**	**Mrf4 mRNA**	**Mef2c mRNA**	**Tnni1 mRNA**	**Sarcomeric Myosin (MF20)**	
	18h									**42h**
pCab	3:3/0/0	2:2/0/0	3:1/0/0	2:1/0/0	2:1/0/0	2:1/0/0	3:2/0/0	2:1/0/0	4:4/0/0	4:2/0/0
Gg Myf5	3:3/0/0	2:2/0/0		2:0/2/0	3:0/3/0	4:1/3/0	3:1/2/0	2:2/0/0	5:5/0/0	5:5/0/0
Gg MyoD	3:3/0/0	2:2/0/0	3:0/3/0		2:1/1/0	2:0/2/0	2:0/2/0	1:1/0/0	3:3/0/0	6:4/2*1/0
Gg MyoG	2:2/0/0	2:2/0/0	2:1/1/0	2:0/2/0		2:0/2/0	2:0/2/0	2:2/0/0	3:3/0/0	3:3/0/0
Gg Mrf4	1:1/0/0	2:2/0/0	2:0/2/0	2:0/2/0	2:2/0/0		2:2/0/0	1:1/0/0	5:5/0/0	2:2/0/0

*1 from two separate EP sessions

Chapter 7

7 Combined misexpression of MyoD and MyoG

7.1 Introduction

The tissue culture experiments conducted in the nineteen eighties established that all Mrf have the capacity to drive myogenic and some non-myogenic cell types into muscle differentiation (332,391). Our experiments conducted in the chicken embryo in vivo however showed within a time window of 18 hours, Mrf genes were unable to enforce skeletal muscle differentiation, not even from developing muscle precursors. Only when left to develop for another day, and only when treated with MyoD, then 1/3 of embryos showed signs of ectopic muscle deployment.

Expression analyses including the analysis conducted here showed that in vivo, Mrf are expressed sequentially in the order Myf5-MyoD-MyoG-Mrf4 (exception mouse, where Mrf4 is expressed earlier; (370,392)). Phylogenetic analyses including the one conducted here revealed that during the two rounds of gnathostome genome duplication, Myf5 and MyoD pair arose from one, MyoG and Mrf4 from the other gene generated during the first duplication round. Since then, both the bHLH and the Myf5/transactivation domains diversified (393) such that to date Mrf proteins have overlapping but also distinct target genes they bind to (394). Significantly, Myf5 and MyoD are not only expressed early, they also preferentially bind to genes activated at the onset of myogenesis (395). MyoG on the other hand, in addition to being expressed late, it specifically activates muscle structural genes and genes that promote cell cycle exit (200). In line with this observation, removal of Myf5 and MyoD function blocks myogenesis early since it prevents the formation of myoblasts; this phenotype cannot be rescued by an earlier activation of MyoG. Removal of MyoG however prevents the formation of myocytes and terminal differentiation (57), underlining that for myogenesis to be completed, MyoG is essential.

In vitro studies showed that once MyoD is activated, it enhances its own expression and activates MyoG. Both genes together then activate the subsequent set of muscle genes. This constitutes a feed-forward mechanism, and suggests that once a cell has invested into the onset of myogenesis, it will eventually complete the differentiation process (57,395). Our experiments showed that misexpression of MyoD led to the upregulation of endogenous MyoG, and misexpression of MyoG led to the upregulation of endogenous MyoD, suggesting a similar, self-perpetuating mechanism in vivo. However, terminal differentiation of developing muscle precursor was only achieved after prolonged exposure to MyoD.

In vitro misexpression studies for MyoD indicated that the myogenic conversion rate of tissue culture cells correlates with the levels of MyoD expression, and hence, the accumulation of MyoD protein (57,396). We thus wondered whether the same may hold true for MyoG, and whether simultaneous, high level misexpression MyoD and MyoG would be required to obtain fully differentiated muscle from developing moblasts. We therefore planned a series of co-electroporation experiments. However, it was not known whether simultaneously electroporated constructs would enter the same cell. We therefore first performed a set of test-electroporations using pCab-GFP and pCab-RFP (Red Fluorescing Protein). These electroporation experiments were conducted by S. Dietrich and confirmed dual construct uptake. Thereafter, we co-electroporated the *MyoD* and *MyoG* expression constructs. We found, however, that combined MyoD-MyoG expression did not accelerate myogenesis from muscle precursor.

7.2 Results

7.2.1 Co-electroporations to test for dual construct uptake

As explained previously we hypothesised that the simultaneous delivery of MyoD and MyoG expression constructs may overcome the stem cell state of developing muscle precursor and drive these cells into immediate muscle differentiation. As the constructs act cell-autonomously, they would have to be taken up by the same cell. We therefore tested whether this is the case. In the first experiment, two pCab vectors were used, containing different fluorescent proteins: GFP (green fluorescent protein) and RFP (red fluorescent protein). The two vectors were electroporated into two adjacent flank somites. Embryos were harvested after 18 hrs of re-incubation at approximately HH19/20 and analysed with Normarski, fluorescence and confocal microscopy. This experiment showed that GFP- and RFP-dependent fluorescence can clearly be distinguished (Fig. 7.1 D, E, F). In the second part of the experiment the two constructs were co-electroporated into the same somite. The concentrations of the two constructs were adjusted to be equal. In this case, RFP and GFP expression occurred in the same cells (Fig. 7.1, compare H-I and K- L) creating a yellow appearance upon overlay of the individual images (G-J). This confirmed that two constructs co-electroporated into somites can enter the same cell and this cell will be exposed to the products of both constructs.

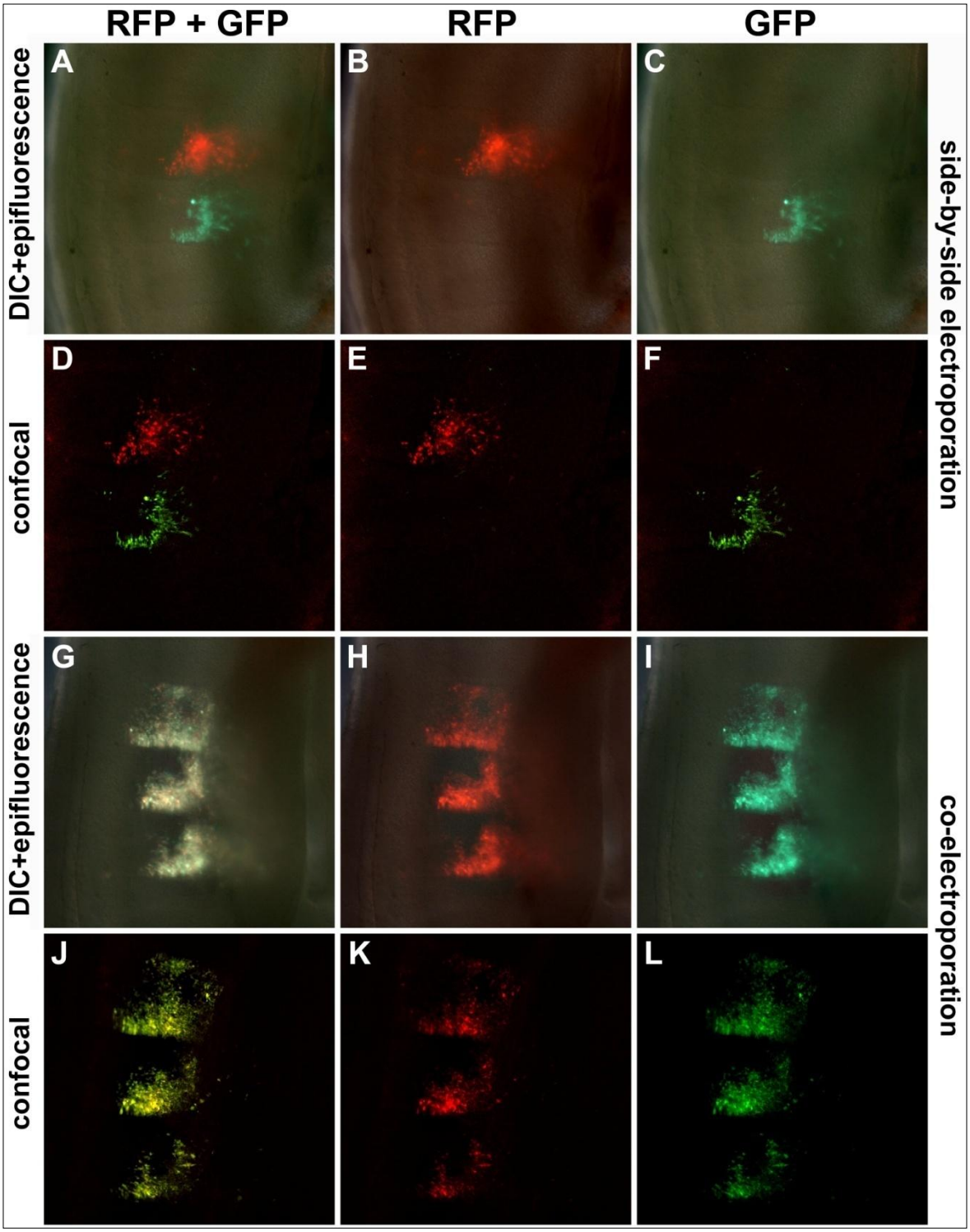
RFP + GFP
RFP
GFP
DIC+epifluorescence
confocal
DIC+epifluorescence
confocal
side-by-side electroporation
co-electroporation
A
B
C
D
E
F
G
H
I
J
K
L

Figure 7. 1: Constructs co-electroporated into somites enter the same cell.
(A-F) To test whether GFP and RFP generated by two distinct pCab vectors can be distinguished, these constructs were electroporated individually into neighbouring somites at HH15. Embryos were harvested at HH19 and subjected to Normarski and fluorescent microscopy (A-C) and confocal microscopy (D-E). Both microscopical methods detected red fluorescence only in the RFP expressing somite and green fluorescence in the GFP expressing somites, indicating that the contribution from each vector can be distinguished.
(G-L) Both the GFP and the RFP encoding vectors were electroporated simultaneously at HH15. At HH19, embryos were analysed by Normarski and fluorescent microscopy (G-H) and confocal microscopy (J-L) as before. This analysis showed that RFP and GFP were co-expressed in the same cells (compare H,I and K,L), hence the combined signal appears yellow (G,J). Thus, when constructs are co-electroporated into somites, they enter the same cell, and this cell will be exposed to the products of both constructs.
Images courtesy of S. Dietrich.

7.2.2 Co-electroporation of MyoD and MyoG expression constructs

Previous data confirmed that two constructs can be co-electroporated into the same somites and they will be taken up by the same cells. We now co-electroporated HH15/16 embryos with equal concentrations of the expression constructs for *MyoD* and *MyoG* (2µg/µl each); embryos were re-incubated for 18 hours to reach HH19/20 or for 42 hours to reach HH23/24. Immunohistochemistry using MF20 antibody/DAB staining and vibratome sectioning was performed as before. A comparison of specimen obtained here with specimen electroporated individually with *MyoD* and *MyoG* constructs (at 4µg/µl) is shown in Fig.7.2; results are summarised in Table 7.1. We found that 18 hours after co-electroporation of both, the *MyoD* and *MyoG* expression constructs, the morphology of the electroporated somites was normal. Notably, as with the earlier *MyoD* and *MyoG* misexpression experiments, no upregulation of sarcomeric Myosin was observed (Fig. 7.2 B-C, E-F, H-I). When left to develop for 42 hours, in 2 out of 2 embryos, ectopic sarcomeric Myosin expression was found. In one embryo, the GFP expressing cells were found in a small confined domain, resembling the phenotype found in the *MyoD* expressing embryo at that stage (Fig.7.2 J-Li and not shown). In the second, more cells had taken up the construct, and hence, misexpression was more widespread (Fig.7.2 P-Ri). Sarcomeric Myosin expression was found throughout the targeted cells, and extensive ectopic muscle had formed. The ectopic muscle appeared disorganised, probably because the differentiation of cells occurred outside the scaffold of the myotome. Taken together, *MyoD* and *MyoG* expression constructs electroporated together can promote myogenesis in muscle precursor as can the *MyoD* construct alone. However, *MyoD-MyoG* co-electroporation did not bring muscle formation forward in time.

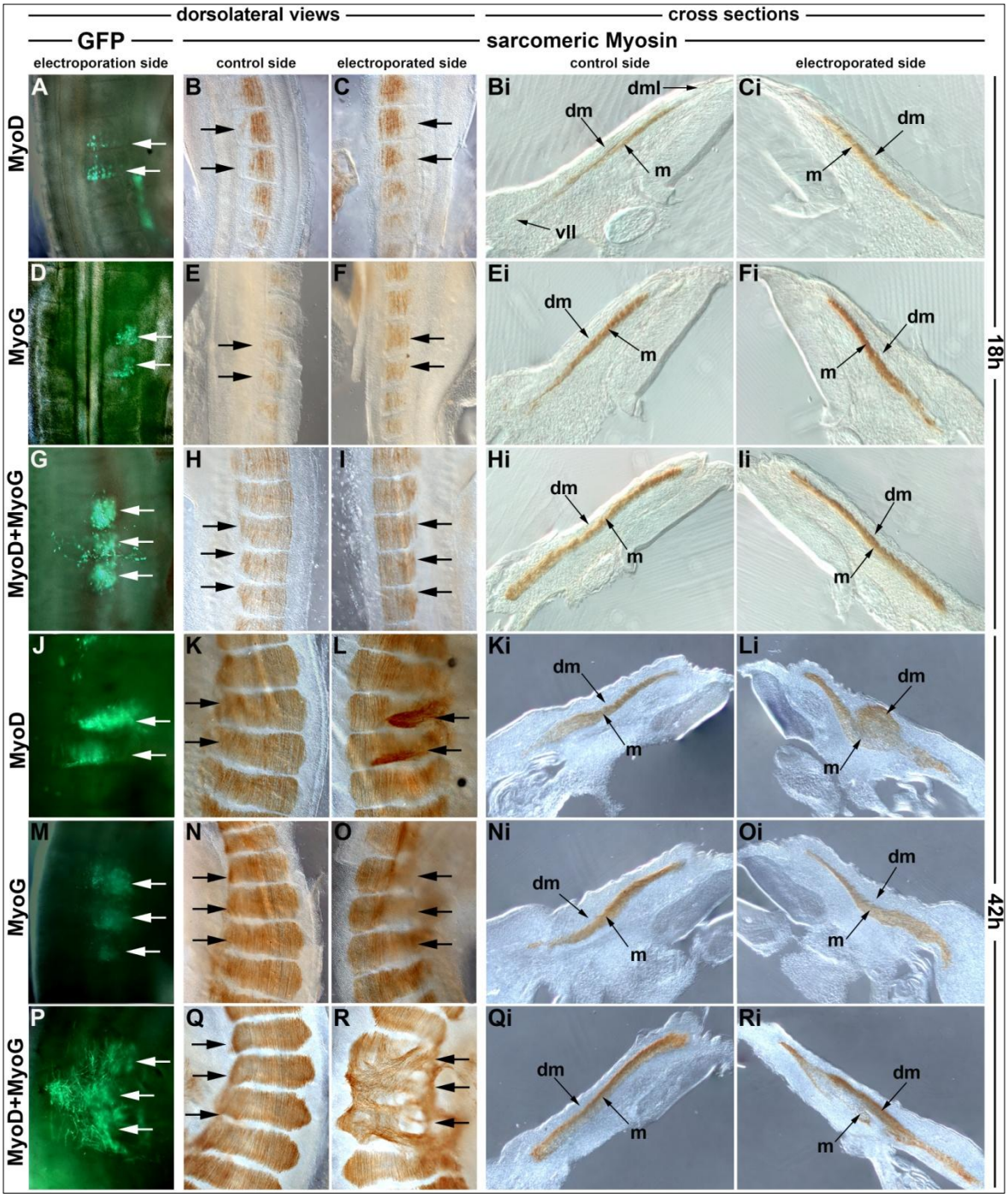
dorsolateral views
cross sections
GFP
sarcomeric Myosin
electroporation side
control side
electroporated side
control side
electroporated side
MyoD
MyoG
MyoD+MyoG
MyoD
MyoG
MyoD+MyoG
18h
42h
A
B
C
Bi
Ci
D
E
F
Ei
Fi
G
H
I
Hi
Ii
J
K
L
Ki
Li
M
N
O
Ni
Oi
P
Q
R
Qi
Ri
dml
dm
m
vll

Figure 7. 2: MyoD and *MyoD-MyoG* co-electroporation did upregulate Myosin light chain in the electroporated somites

Flank somites were electroporated at HH15/16 with pCAB-GFP (control) or GFP and Mrf expressing constructs as indicated on the left of the panel. Embryos were harvested 18 hours later at HH19/20, or 42hrs at HH23/24 i.e. They were exposed to Mrf and/or GFP proteins for at least 12 hours or 36 respectively (A,D,G,J,M,P). Overlays of the Nomarski and fluorescence photomicrographs of the electroporated flanks, dorsolateral views, rostral to the top. GFP expression indicates that 1-3 somites were targeted (green staining, arrows). (B,E,H,K,N,Q) Nomarski images of the un-electroporated control sides, and (C,F,I,L,O,R) of the electroporated sides of the embryos shown in (A,D,G,J,M,P), assayed with MF20-DAB staining to reveal sarcomeric Myosin expression (brown staining), views as in (A,D,G,J,M,P). The targeted somites and their un-electroporated counterparts are indicated by arrows. Note, the levels of sarcomeric Myosin expression are the same on either side in the pictures for (B-C, E-F, H-I,N-O). The 42 hrs developed embryos electroporated with MyoD (K-L) and co-electroporated MyoD-MyoG (Q-R) showed upregulation of Myosin staining in the area of the fluorescence. (Bi,Ei,Hi,Ni) and (Ci,Fi,Ii,Oi) Nomarski images of cross sections of the flanks shown in (B,E,H,N) and (C,F,I,O), respectively. Note the absence of sarcomeric Myosin expression in the electroporated dermomyotomes. The cross sections (Ki-Li and Qi-Ri), of the flanks somites (K-L and Q-R), respectively. Note the upregulation of the Myosin expression in the electroporated dermomyotome.

Abbreviations: dm, dermomytome; dml, dorsomedial lips of the dermomyotome; m, myotome.

7.3 Discussion

7.3.1 These electroporation conditions allowed the simultaneous uptake of several molecular constructs into one cell

In this chapter we aimed to misexpress two individual transgenes together in the same cells in order to test their combined effect separate to their individual effect. This strategy has been employed previously and therefore should be appropriate to our specific application (315,397). This strategy was initially tested with two constructs that express RFP and GFP, respectively. Electroporation of the individual constructs in adjacent somites and analysed by fluorescence microscopy showed that the fluorescence from each construct could be visualised and clearly distinguished. Subsequently, both constructs were co-electroporated into the same somite and analysed by fluorescence microscopy as before which showed overlapping of green and red fluorescence, appearing yellow, indicating cells were expressing both fluorescent proteins. We therefore used identical experimental parameters in future experiments to ensure simultaneous uptake of multiple constructs in order to specifically observe their additive effect.

7.3.2 *Co-expression of MyoD and MyoG does not overcome the protection of the muscle stem cell state in the time window between HH15/16 and HH19/20*

The co-electroporation of MyoD and MyoG was important to test whether the simultaneous expression of MyoD and MyoG allows not only the activation of genes that prepare cells for myogenesis, but also activates muscle structural genes, thereby driving developing myoblast into terminal muscle differentiation. We obtained a phenotype similar to the misexpression of MyoD alone. The embryos analysed showed premature differentiation of muscle precursor located in the dermomyotome, but specimen numbers are too low to establish whether the rate of myogenic conversion obtained with combined MyoD-MyoG misexpression is significantly different to the rate of conversion obtained after misexpression of MyoD alone. The important finding however was that even in the presence of both MyoD and MyoG, developing muscle precursor did not engage in muscle differentiation any earlier than when exposed to MyoD alone, supporting the idea that in the 18h time window between HH15/16 and HH19/20, embryonic muscle precursor are safeguarded against premature differentiation.

7.3.3 Muscle ectopically developing in the dermomyotome is disorganised

Amniote muscle development begins when cells from the medial wall of the somite form the primary myotome. This provides a scaffold into which the second wave of muscle cells intercalate when they detach from the four dermomyotomal lips (141,398). This secondary myotome serves as a scaffold for the muscle precursor that enter when the dermomyotome centre de-epithelialises (66,399). The process is aided by Wnt11 in the dorsomedial dermomyotomal lip which controls the directed elongation of differentiating myotubes (276). Myf5 in the early myotome is required for maintaining alpha6-beta1 integrin expression on myogenic precursor

cells. alpha6-beta1 integrin is necessary for myotomal laminin matrix assembly and cell guidance into the myotome. Engagement of laminin by alpha6-beta1 integrin also plays a role in maintaining the undifferentiated state of cells in the dermomyotome prior to their entry into the myotome. Conversely, cells away from the alpha6-beta1 laminin matrix express MyoG and continue differentiation (Bajanca et al., 2006). During 2nd and 3rd myotome formation, N-cadherin-mediated adhesion maintains the epithelial configuration of the dermomyotome domains and also promotes the onset of MyoD transcription and the translocation of cells into the myotome (Cinnamon et al., 2006). The receptor Robo and its ligand Slit drive directional migration of pioneer myoblasts (Halperin-Barlev and Kalcheim, 2011). Wnt11 function in the dorsomedial lip of the dermomyotome, via the PVP pathway, controls the organisation and elongation of myocytes/myotubes and the failure of Wnt11 expression leads to disorganisation of myotomes (Gros et al., 2009).

After the primary myotomal scaffold formed, cells use this scaffold to contribute to the myotome and elongate in the same direction as the cells deployed earlier. The requirement of this scaffold is particularly obvious in the hypaxial domain where the absence of the primary myotome prevents the formation of an organised hypaxial myotome. When in our experimental set up muscle precursor eventually differentiate, they do this within the dermomyotome and in the absence of a primary myotomal scaffold, and this may be the reason why muscle is disorganised. However, cells in the dermomyotome normally express genes associated with the formation of somitic boundaries. Yet in one of our embryos obtained after MyoD-MyoG misexpression, we did observe myotubes that spanned more than one somite. Since the embryo was not seen at an earlier stage, it cannot be decided whether or not the somite had been injured during electroporation, leading to a disturbance of somite boundaries. Since the focus of this study is to discover conditions for premature initiation of the muscle formation from muscle precursor, we did not investigate this phenomenon any further.

Table 7. 1: Summary of N.numbers for electroporation experiments of chapter 7

Key - total:wild type/upregulated/downregulated

Summary of the number of electroporated embryos that were analysed for Myosin levels using immunohistochemistry with MF20 antibody detection and DAB staining, together with the number of altered phenotypes observed. The misexpression of MyoD and the combination of MyoD and MyoG caused upregulation of the Myosin level in the electroporated somites after 42hr of incubation (blue shade). The asterisk highlights that the upregulation results were observed in multiple sets of electroporation experiments

EP targeting the embryonic muscle precursor in the somitic dermomyotome		
Specimen analysed for	**Sarcomeric Myosin (MF20)**	
	18h	42h
Gg MyoD	3:3/0/0	6:4/2*1/0
Gg MyoG	3:3/0/0	3:3/0/0
Gg MyoD+MyoG	3:3/0/0	2:0/2/0

*1 from two separate EP sessions

Chapter 8

8 Combined misexpression of MyoD or MyoG with Mef2 genes

8.1 Introduction

As described in Section 1.5.10, there are four *Mef2* genes in vertebrate species: *Mef2a, b, c,* and *d*. Mrf proteins are expressed exclusively in skeletal muscle and have not been detected in the heart, despite the fact that many of the genes that they regulate are expressed in both skeletal and cardiac muscle (146,384).

Mef2 DNA-binding activity is upregulated during differentiation of established muscle cell lines and can be induced in non-muscle cells by *MyoG* and *MyoD* (400,401), consistent with the notion that *Mef2* lies in a regulatory pathway downstream of these myogenic factors. However, there is also evidence that *Mef2* participates in the regulation of the *Mrf* genes. A *Mef2* site in the promoter of the *MyoG* gene, for example, is essential for *MyoG* transcription in cultured skeletal muscle cells (402); mutation of this site also alters the expression of reporter genes linked to the *MyoG* promoter in the somites and in the limb buds of transgenic mouse embryos (191,291). Mef2 has little ability to trigger myogenesis alone, but the absence of Mef2 genes caused defects in muscle development and regeneration (403). This is due to the fact they bind to target sequences found in close proximity to Mrf binding sites, thereby enhancing the efficiency of Mrf to drive muscle formation (404,405). Our expression analysis (Chapter 3) showed that chicken Mef2c was the first Mef2 family member to be transcribed in the chicken somite, followed by Mef2a. This was in line with observations in the mouse (146,406). We also found that Mef2c, while being expressed along the rostral and caudal dermomyotomal lips before cells leaving these lips express Mrf, expression in the dorsomedial and ventrolateral lips and in the myotome commenced just after that of MyoD. We therefore reasoned that Mef2c may be the main Mrf partner during the somitic myogenesis, possibly followed by Mef2a.

Binding studies have established that MyoD and MyoG proteins upregulate Mef2 genes, with Mef2 proteins operating a positive feedback mechanism, enhancing the expression of Mrf. In line with this observation, when misexpressing Mrf in the chicken somite, we found that Mef2c was transcribed in the targeted cells. However, within a time window of 18 hours, muscle structural genes were not activated and cells did not reach a fully differentiated state. This suggests that possibly, Mef2c (or 2a) protein levels are still not high enough to support myogenesis initiated by the Mrfs. To test this possibility, Mef2c and Mef2a expression constructs were electroporated into chicken flank somites as before, either alone or in combination with MyoD or MyoG

expression constructs. However, these experiments revealed that, again, within the 18 hour time interval after electroporation, no premature myogenesis occurred.

8.2 Results

To misexpress *Mef2c* and *Mef2a* genes, expression constructs were made using the same approach as for the *Mrf* constructs. The Kozak sequences and the open reading frames of chicken *Mef2c* and *Mef2a* were synthesised and cloned into the pCab vector as before. The constructs were then verified by sequencing. They were electroporated into chicken flank somites at HH15/16 as before, either alone (at 4µg/µl) or in combination with MyoD or MyoG expression constructs (at 2µg/µl each). 18 hours later, embryos with readily detectable GFP-derived fluorescence were analysed for the differentiation of the targeted cells into contractile skeletal muscle, assaying for the presence of sarcomeric Myosin using the MF20 antibody and DAB staining. Embryos were bisected along the midline of the neural tube, to allow the comparison of the control side and the electroporated side. Results are summarised in Table 8.1.

8.2.1 Misexpression of *Mef2c* alone or in combination with *MyoD* or *MyoG* in chicken somites

When *Mef2c* was misexpressed alone, analysis of the fluorescence micrographs revealed that the anatomy of the electroporated somites were comparable to the non-electroporated somites, confirming that the structure of the tissue wasn't compromised by the electroporation (Figure 8.1 A, arrowed somites). The MF20 antibody staining revealed that in the treated somites, no upregulation or ectopic expression of sarcomeric Myosins had occurred (Figure 8.1 B,C). When *Mef2c* was misexpressed together with *MyoD* (Fig. 1.8 D-F) or *MyoG* (Fig. 1.8 G-I), the anatomy of the electroporated somites appeared again unaffected by the experiment and comparable with the rostrocaudally adjacent non-electroporated somites or the somites in the control side. Importantly, the electroporated somites did not show any upregulation of sarcomeric Myosin expression.

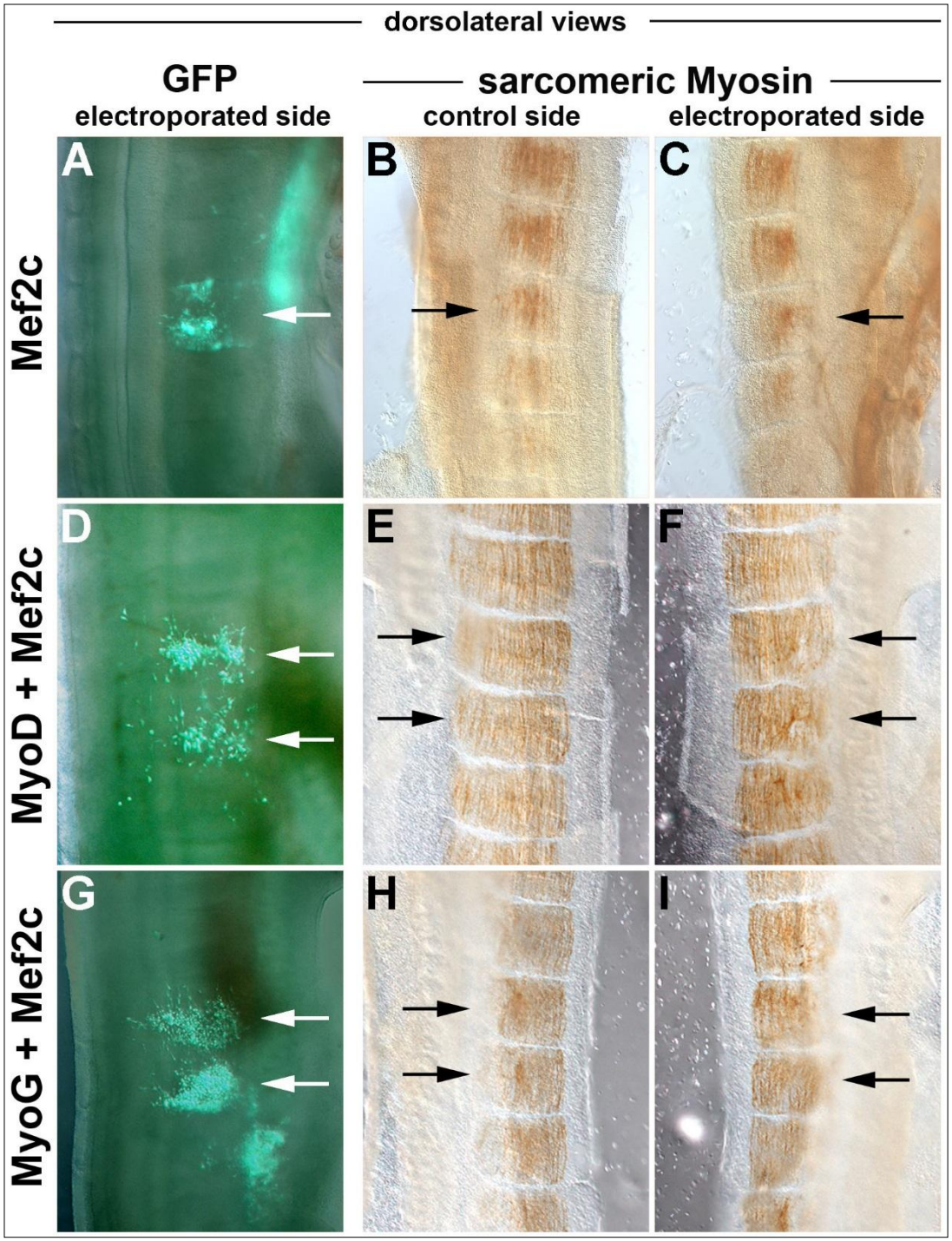
dorsolateral views
GFP
electroporated side
sarcomeric Myosin
control side
electroporated side
Mef2c
MyoD + Mef2c
MyoG + Mef2c
A
B
C
D
E
F
G
H
I

Figure 8. 1: Mef2c does not enhance the ability of MyoD or MyoG to induce premature differentiation of muscle precursor between HH16 and HH20

HH16 embryos were electroporated (as shown in Chapter 6) with Mef2c individually (A-C), co-electroporated with MyoD (D-F) or co-electroporated with MyoG (G-I). Embryos were re-incubated to develop for a further 18 hours until HH19/20. GFP fluorescence was imaged to locate the successfully electroporated somites (arrows), followed by antibody staining for sarcomeric Myosins with the MF20 antibody (brown staining). Comparison of control vs. electroporated somites revealed no change in staining for Mef2c (compare B with C), Mef2c with MyoD (compare E with F) or Mef2c with MyoG (compare H with I).

8.2.2 Misexpression of *Mef2a* alone or in combination with *MyoD* or *MyoG* in chicken somites

After the first set of experiments we focused our attention on the *Mef2a* gene. The *Mef2a* expression construct was electroporated individually and with *MyoD* or *MyoG* expression constructs; successfully electroporated somites were located by fluorescence microscopy (Fig. 8.2 A, D and G). Subsequent MF20 antibody staining revealed that the individual misexpression of *Mef2a* did not lead to premature sarcomeric Myosin expression (Fig. 8.2 B and C). Similar results were obtained from co-electroporation experiments using *Mef2a* together with *MyoD* constructs (Fig. 8.2 E and F) and *Mef2a* with *MyoG* constructs (Fig. 8.2 H and I).

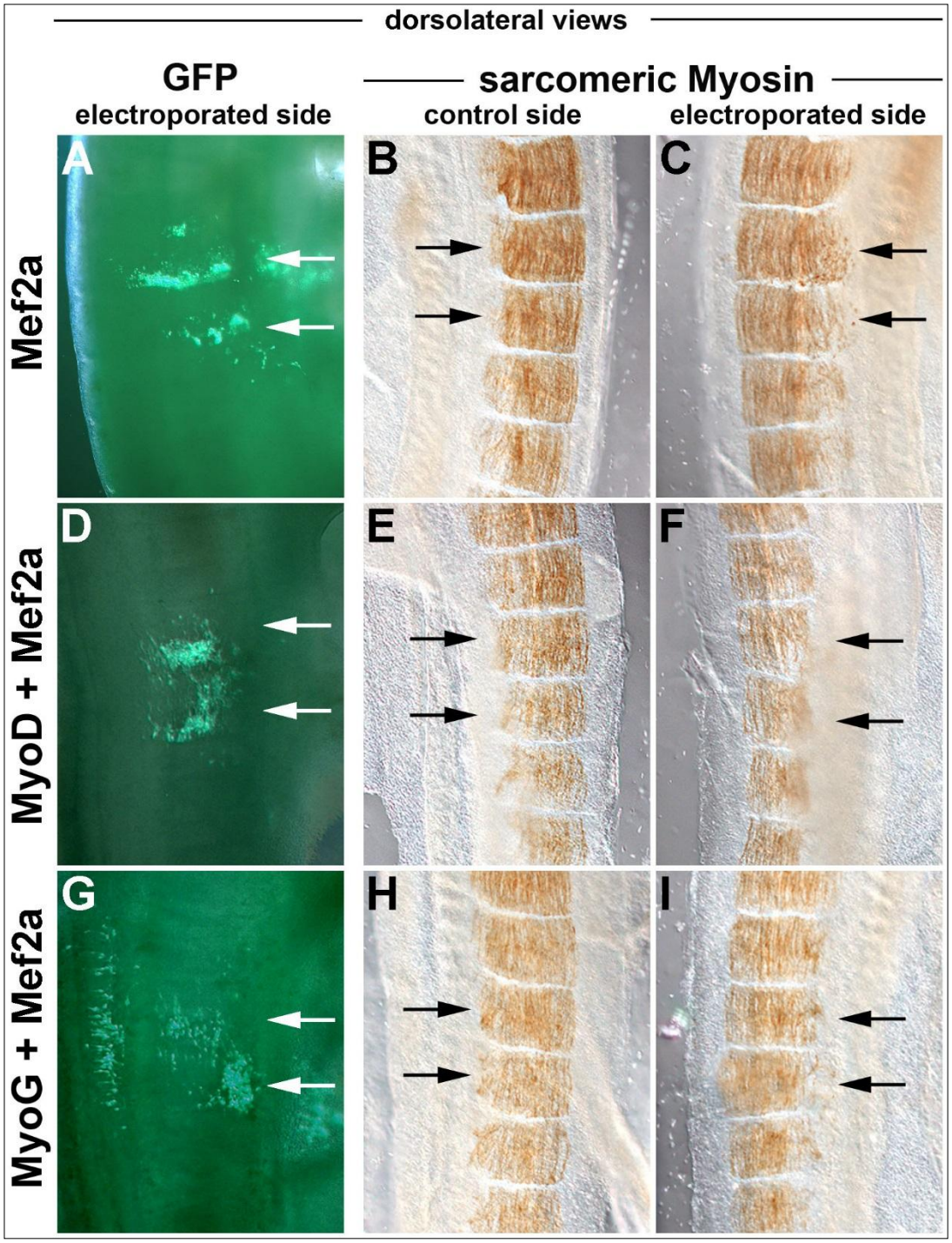
dorsolateral views
GFP
electroporated side
sarcomeric Myosin
control side
electroporated side
Mef2a
MyoD + Mef2a
MyoG + Mef2a
A
B
C
D
E
F
G
H
I

Figure 8. 2: Mef2a does not enhance the ability of MyoD or MyoG to induce premature differentiation of muscle stem cells between HH16 and HH20

HH16 embryos were electroporated (as shown in Chapter 6) with Mef2a individually (A-C), co-electroporated with MyoD (D-F) or co-electroporated with MyoG (G-I). Embryos were re-incubated to develop for a further 18 hours until HH19/20. GFP fluorescence was imaged to locate the successfully electroporated somites (arrows), followed by antibody staining for sarcomeric Myosins with the MF20 antibody (brown staining). Comparison of control vs. electroporated somites revealed no change in staining for Mef2a (compare B with C), Mef2a with MyoD (compare E with F) or Mef2a with MyoG (compare H with I).

8.3 Discussion

8.3.1 Co-expression of *Mrf* and *Mef2* genes did not overcome the protection of the muscle stem cell state in the time window between HH15/16 and HH19/20

Given the tight relationship specifically of *Mef2c* and *Mef2a* and *MyoD* and *MyoG* (307,384,404), we hypothesised that the simultaneous misexpression of these *Mef2* genes with one of the two *Mrfs* would be sufficient to drive muscle precursor out of their stem cell state and into terminal muscle differentiation, visible as upregulated, ectopic expression of sacromeric Myosins in the electroporated dermomyotomes. On the other hand, given that *Mef2* genes have little myogenic function by themselves (58,188,388), we expected that the *Mef2* genes alone would not be sufficient to drive myogenesis from muscle precursor. Indeed, the results showed that individual electroporation of either *Mef2c* or *2a* constructs into chicken somites was not sufficient to cause premature sarcomeric Myosin expression. However, the co-expression of *Mef2* genes with either *MyoD* or *MyoG* also proved insufficient to upregulate sarcomeric Myosin expression, thus indicating that, again in contrast to experiments performed in tissue culture (188), the muscle precursor or muscle stem cell state cannot easily be overcome *in vivo*.

Binding studies showed that Mrf and Mef2 proteins are present at the promoters of muscle genes before chromatin is opened and transcription of these genes starts (407,408). Chromatin opening is facilitated by Six proteins. However, when *Mrf* were misexpressed, *Mef2c* expression was upregulated as seen with *in situ* hybridisation while *Six1* and its activator *Eya1* did not show any upregulation (see Chapter 6). We therefore decided to investigate a possible requirement for Six1 for the completion of muscle differentiation in muscle precursor (explored in Chapter 9).

Table 8. 1: Summary electroporation experiments shown in chapter 8

Numbers displayed as: Total: wildtype/upregulated/downregulated

Summary of the number of electroporated embryos that were analysed for Myosin levels using immunohistochemistry with MF20 antibody detection with DAB staining at 18h of incubation.

EP targeting the embryonic muscle precursor in the somitic dermomyotome	
Specimen analysed for	**Sarcomeric Myosin (MF20)**
	18h
Gg Mef2c	6:6/0/0
Gg Mef2c + MyoD	4:4/0/0
Gg Mef2c + MyoG	4:4:0/0
Gg Mef2a	7:7/0/0
Gg Mef2a + MyoD	3:3/0/0
Gg Mef2a + MyoG	5:5/0/0

Chapter 9

9 Combined misexpression of Six1, MyoD and Mef2c genes

9.1 Introduction

Our study has revealed that MyoD, alone or in combination with MyoG, may overcome the stem cell state of developing muscle precursor *in vivo*, provided cells were exposed to the transgenes for 36 hours. In the time frame of 18 hours after construct electroporation (a minimum of 12 hours exposure), Mrfs were able to activate a few other genes that set the cell up for myogenesis. However, in this time window, neither Mrfs alone, nor MyoD in combination with MyoG, nor Mrfs in combination with Mef2 proteins were able to drive muscle precursor into terminal differentiation. Mrf and Mef2 proteins have been shown to occupy their binding sites in the promoters of muscle genes long before these genes are being transcribed (384,408). Thus, we reasoned that further cofactors might be required to drive muscle precursor into terminal muscle differentiation.

In Chapter 1, we introduced Six proteins and their Eya cofactors as multifunctional regulators of myogenesis. During amniote development, *Six* (exception optix homologs) and *Eya* genes are expressed in the paraxial mesoderm as early as the pre-myogenic genes *Pax3/7* and *Paraxis* ((169,297,314,328); this study). Six proteins, when turned into transcriptional activators with the aid of Eya phosphatases (Li et al., 2003), have been shown to upregulate *Pax3* and *Myf5* in mouse limb muscle precursors (164,179). In the somite, at least in mouse mutants devoid of *Myf5*, Six1/4/2 contribute to the activation of *MyoD* (180). Together, this has suggested that *Six* genes are pre-myogenic genes.

Our expression analysis has shown that when muscle forms, the expression of *Six* and *Eya* genes is downregulated in the somitic dermomyotome but persists in the dorsomedial and ventrolateral dermomyotomal lips and the myotome (83). (Fougerousse et al., 2002) showed that in the human somite, Six proteins are only detectable in the nuclei of cells and hence able to act as transcription factors, when the cells begin to express sarcomeric Myosins. Binding studies in tissue culture cells showed that Six1 contributes to the activation of *MyoG*, binding to a target sequence next to the binding sites of MyoD and Mef2 proteins (181). Similarly, in activated satellite cells, Six proteins do not regulate *Myf5* but *MyoG* (183). Six proteins also bind to the promoters of muscle structural genes and genes encoding enzymes essential for the establishment of a fast-twitch muscle phenotype, in fact Six proteins can enforce a muscle fibre-type switch from slow to fast (409). This suggests a myogenic rather than pre-myogenic function of Six-Eya protein complexes.

When Six proteins or complexes of Six and its co-repressor Dach are phosphorylated by Eya proteins, they are able to open chromatin and to recruit the CBP co-activator and RNA polymerase II, which then starts the transcription of target genes (Li et al., 2003). We found that when *Mrfs* were misexpressed in the somite, endogenous *MyoG* expression was initiated but expression of *Six1* and *Eya1* was not, indicating that in the context of muscle precursor, the regulation of *MyoG* was not Six-Eya dependent. However, we reasoned that, in order to promote the completion of myogenesis in developing myoblasts, Six function may be required in addition to the function of Mrf and Mef2 proteins to activate muscle structural genes. We thus set out to misexpress *Six1* alone, or in combination with *MyoD* and *Mef2c*.

9.2 Results

9.2.1 Six1 expression constructs

Owing to time constraints, we were unable to generate chicken-specific *Six1* expression constructs. However, constructs to misexpress various wildtype and mutant versions of mouse *Six1* were kindly provided by Dr. Pascal Maire (Institut Cochin, University Descartes, Paris). Of these constructs, we chose to use a construct encoding a Six1-GFP fusion protein and a construct encoding a fusion protein between the Six1 protein and the VP16 transactivation domain (182,410). VP16 is formed of 490 amino acids and two important functional domains: a core domain in the central region and the carboxy-terminal transactivation domain. The core domain is important for indirect DNA binding (411,412). By comparison GFP, a commonly used fusion protein within this study, is 238 amino acids long (413).

We expected the Six1-GFP protein to act like wildtype Six1. Thus, in the central dermomyotome, where Groucho and Dach co-repressors are present and the Eya co-activators are absent (165,245,414), the protein should not be able to activate Six targets. The Six1-VP16 protein however should be independent from activating phosphorylation by Eya proteins and hence be a constitutive transcriptional activator all the time. Constructs were based on the pCR3 vector, which, similar to pCab, uses the CMV (cytomegalovirus) promoter and enhancer to drive strong transgene expression (415). Therefore, the constructs should be expressed at levels comparable to pCab. The pCR3 vector however does not encode for a cell lineage tracer. Therefore, when testing Six1-VP16 function alone, we electroporated the construct together with pCab. The Six-GFP protein fluoresces on its own account, and we exploited this to determine whether the proteins would translocate to the nucleus – a prerequisite to act as transcription factor. We found that indeed, the Six1-GFP protein was present in the nucleus. Unexpectedly, however, the Six1-GFP protein was able to drive premature expression of sarcomeric Myosins in developing myoblasts. In contrast, Six1-VP16, neither alone nor in combination with MyoD and Mef2c, was unable to achieve this.

9.2.2 Six1-GFP triggers an unexpected upregulation of sarcomeric Myosin expression

The aim of these experiments was to explore whether Mrf proteins, when accompanied by Mef2 and Six cofactors, might be able to force developing myoblasts into premature differentiation. To test this, we used two mouse *Six1* constructs. In one, the *Six1* open reading frame was linked with the coding sequences for the VP16 transactivation domain. Thus, Six1-VP16 should be independent from activating phosphorylation by Eya1 and act as a constitutive transcriptional activator.

Recent data showed that the use of a transactivation domain can have the opposite effect to the activation, causing negative feedback and repressing transcription. The use of VP16 can have negative effects on cells in which they have been injected (416). Ryu and colleagues developed a system Gal4-VP16, transactivator component assembled through the fusion of the DNA binding domain of Gal4 with the VP16transactivation domain. When the Gal4-VP16 transactivator was expressed at high levels it was shown to inhibit transcription by binding and titrating out transcription factors. This could explain why we could not see any upregulation of Myosin expression with the use of the Six1-VP16 and the co-electroporation. The presence of the VP16 transcriptional activator could have a feedback mechanism which influences the role of transcription factors, forcing them to be inactivated.

The other electroporation construct used was the fusion of Six1 protein with the lineage tracer GFP. This protein was expected to require activating phosphorylation by Eya proteins. In the somite, the Six co-repressors Dach and Groucho are expressed in the dermomyotome, while Six and Eya proteins become confined to the dorsomedial and ventrolateral lips of the dermomyotome and the myotome (169,417). We therefore expected that Six1-VP16 was more likely than Six-GFP to change gene expression when misexpressed in the myoblast that develop from the dermomyotomal centre (169). To our surprise, however, Six1-GFP but not Six1-VP16 triggered upregulation of sarcomeric Myosin expression in the targeted cells. Six1-GFP fluorescence was also found in patterns that indicated nuclear localisation whereas when Six1-VP16 electroporated together with pCab-GFP, only showed disperse fluorescence consistent with cytoplasmatic localisation of the independently translated GFP. Therefore, a biological/biochemical explanation was more likely (Fig. 9.1). In Figure 9.1, a comparison of the fluorescence between Six1-GFP and pCAB-GFP is shown. Fluorescence micrographs of both embryos are shown at 10 × and 20 × magnification. The morphology of the fluorescence visible in the Six1-GFP expressing embryo (Fig. 9.1A, B) appeared concentrated to small areas, presumably localised to the nucleus of the cells (Fig. 9.1B white rectangle). In comparison, the fluorescence visible in the pCAB-GFP expressing embryo (Fig. 9.1Ai, Bi) appeared more disperse, presumably localised in the cytoplasm of the cells (Fig. 9.1 Bi white rectangle).

Addition of proteins tags, especially large tags such as the GFP protein, have been shown to alter protein function (350). Given that Six proteins interact with a number of co-factors (173,409), it is possible that the presence of GFP severely disrupted normal protein-protein interactions and may even have facilitated new, artificial interactions. This in turn may have changed both the recognition of target promoter sequences as well as the ability to transrepress or transactivate targets. Six1-GFP may also more strongly interact with some partners, thereby sequestering them. As a result, Six1-GFP protein may not function identically to the native protein inside the cell. Further experiments such as RNAseq could reveal how cells misexpressing Six1-GFP are affected when compared to normal cells undergoing myogenesis.

While the phenotype obtained by Six1-GFP misexpression is likely an artefact, it is nonetheless interesting. Following the electroporation of the *Six1-GFP* construct, the cells showing elevated sarcomeric Myosin expression were located in the myotome and were oriented in the same direction as normal myotubes. This was distinct from the cells that differentiated into a disorganised array of myotubes in the dermomyotome when exposed to MyoD or MyoG for a prolonged period of time. This suggests that Six1-GFP protein accelerated recruitment of cells into the earlier myotomal scaffold. Moreover, the Six1-GFP misexpressing cells showed a larger diameter than normal myotubes, suggesting that overall sarcomeric protein production was enhanced. Quantitative assays such as Western blotting would be useful to further elucidate this phenotype. Finally, it has to be considered that Six proteins activate genes required for the establishment of fast-twitch, anaerobic muscle fibre and override slow-twitch, aerobic muscle fibre (409). In the early embryo, myotomal muscle has a slow-twitch fibre type (418). Use of antibodies that discriminate between fast and slow Myosin Heavy Chain proteins would reveal whether Six1-GFP may have triggered a cascade that bypassed normal myotomal differentiation and instead, enforced a fast-twitch muscle fibre type.

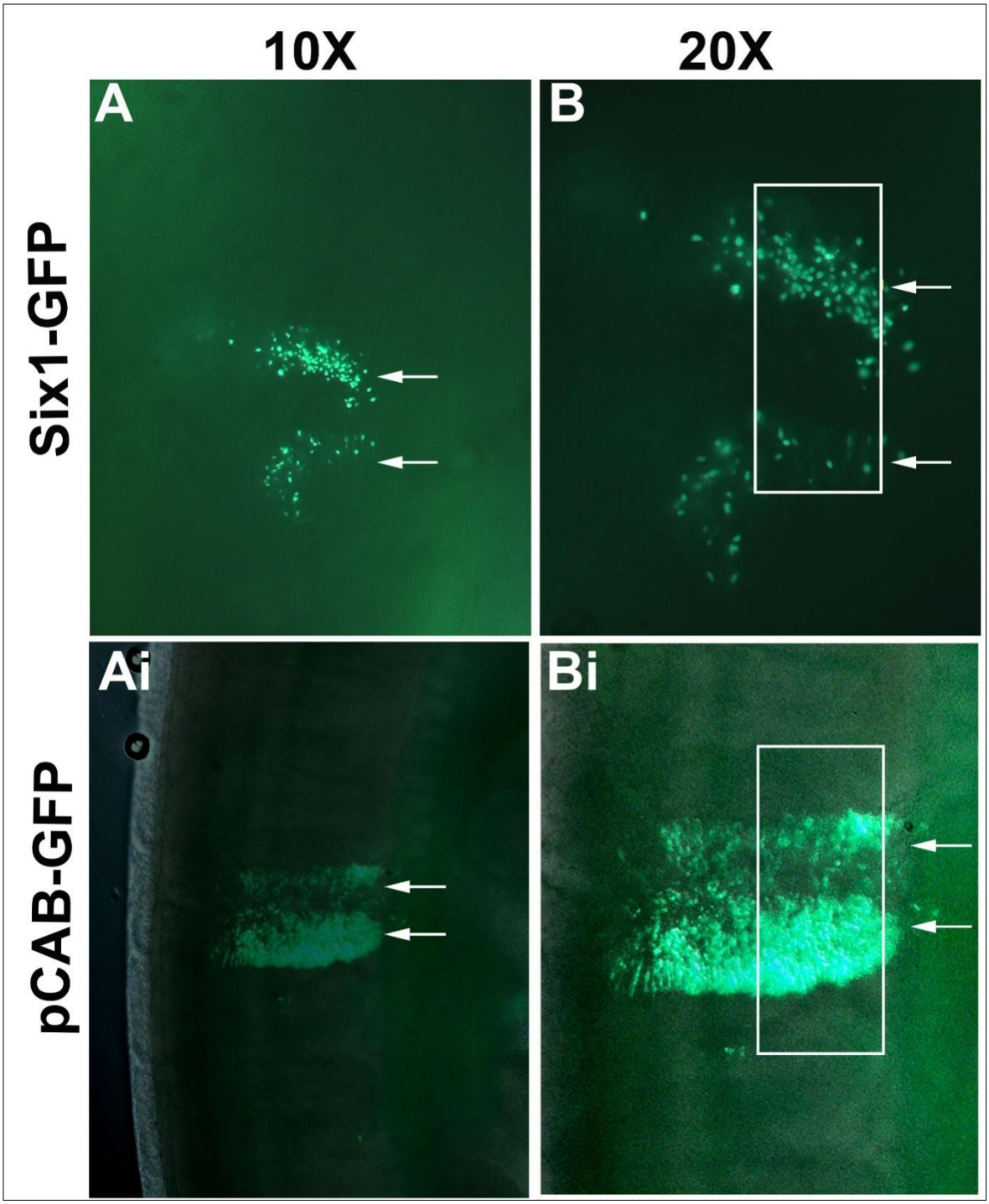
10X
20X
A
B
Six1-GFP
Ai
Bi
pCAB-GFP

Figure 9. 1: Six1-GFP fluorescence compared with control pCAB-GFP fluorescence reveals specific localisation of the fusion protein

Six1-GFP fluorescence (A and B) is compared with pCAB-GFP fluorescence (Ai and Bi). Photographs are shown at 10 × magnification as standard (A and Ai). At 20 × magnification (B and Bi), pCAB-GFP fluorescence appears disperse presumably localised in the cytoplasm (Bi, white box). Comparably, Six1-GFP fluorescence appears localised to specific areas, presumably localised within the nuclei of the cells (B, white box).

9.2.3 MyoD in combination with Mef2c and Six1-VP16 is still unable to drive muscle precursor into terminal muscle differentiation

Binding studies have shown that muscle gene promoters are loaded with MyoD and Mef2 proteins, but may require activated Six proteins for the chromatin to open, the transcriptional machinery to be recruited and gene transcription to start (reviewed in (193)). We therefore reasoned that our earlier attempts to force embryonic muscle precursor into terminal differentiation failed because activated Six1 was lacking. However, when misexpressing MyoD, Mef2c and the constitutively active Six1-VP16, we did not observe sarcomeric Myosin expression any earlier than when misexpressing MyoD alone. Cumulative evidence suggest that our constructs are active given the data showed in Chapters 6 and 4. Having established that mouse Six1 protein can translocate to the nucleus of the targeted chicken cells, we now systematically explored whether Six1, alone or in combination with MyoD, Mef2c, or both MyoD and Mef2c, could accelerate terminal muscle differentiation in developing muscle precursor in HH15/16 flank somites. To test this, we electroporated a DNA mixture made of combinations of multiple constructs together. The contribution of each construct becomes smaller, as more constructs are added. However, we previously observed that when the MyoD expression construct was "diluted" with the MyoG expression construct, the ability of MyoD to enforce muscle stem cell differentiation after 42 hours of embryo re-incubation was not diminished; it may even have been enhanced (Chapter 7). Moreover, all constructs are driven by strong promoters/enhancers. Therefore, it is likely that protein levels are sufficient to in principle activate target promoters. This could be tested, co-electroporating a reporter construct that contains a MyoD-Mef2-Six-dependent promoter such as the MyoG promoter (181). Yet our results suggest that it is not the mere absence of Mrf, Mef2 and Six-Eya proteins that prevents premature differentiation of muscle precursor.

Embryos were harvested 18 hours after electroporation and assayed for sarcomeric Myosin expression using MF20-DAB staining as before. Results are summarised in Table 9.1. When the Six1-GFP construct was used (Fig. 9.2 A-C), the electroporated somites showed stronger MF20-DAB staining than the neighbouring somites or the somites on the contralateral control side. The strong staining was in elongated cells located in the myotome and orientated rostrocaudally as myotubes would be at this stage. Moreover the strongly stained cells appeared thicker in diameter than the myotubes in neighbouring somites. This suggests that either Six1-GFP recruited additional dermomyotomal cells to contribute to the myotome or Six1-GFP expressing myotubes expressed higher level of sarcomeric proteins than usual, or both. When the Six1-VP16 construct was electroporated, no upregulated expression of sarcomeric Myosins was found (Fig. 9.2.D-F). Likewise, no change in the levels of sarcomeric Myosin production or the size of myotubes was observed when misexpressing Six1-VP16 together with MyoD (Fig. 9.2 G-I), with Mef2c (Fig. 9.2.J-

L) or with both, MyoD and Mef2c together (Fig. 9.2.M-O). Moreover, no ectopic sarcomeric Myosin expression was found in the dermomyotome, indicating that the three factors were unable to advance myogenesis in muscle precursor.

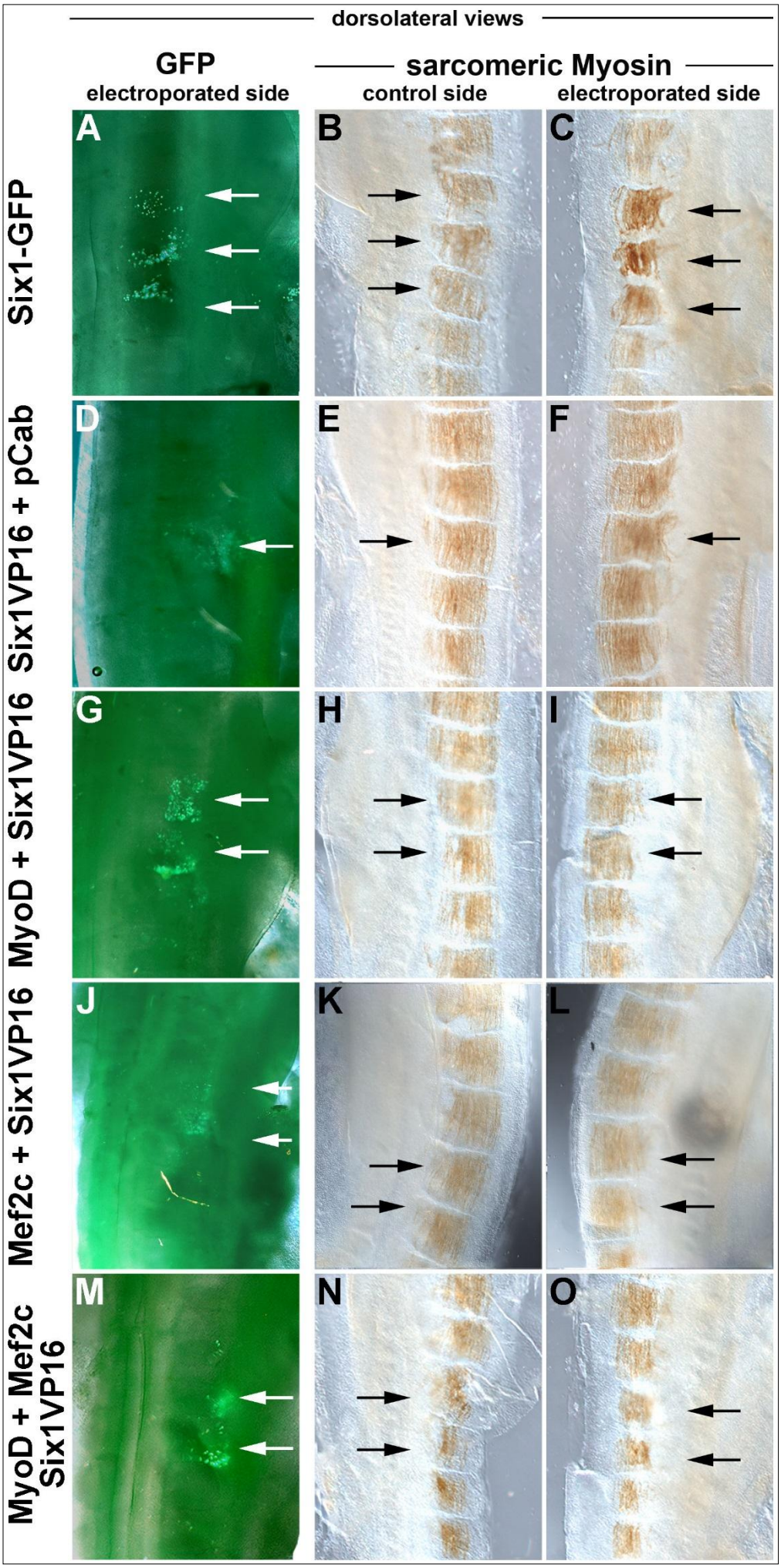
dorsolateral views
GFP
electroporated side
sarcomeric Myosin
control side
electroporated side
Six1-GFP
Six1VP16 + pCab
MyoD + Six1VP16
Mef2c + Six1VP16
MyoD + Mef2c
Six1VP16
A
B
C
D
E
F
G
H
I
J
K
L
M
N
O

Figure 9. 2: Misexpression of Six1VP16 alone and in combination with MyoD and Mef2c as well as Six1-GFP alone

Embryos were electroporated with Six1-GFP (A-C), or co-electroporated with Six1VP16+GFP (D-F), MyoD+Six1VP16 (G-I), Mef2c+Six1VP16 (J-L), MyoD+Mef2c+Six1VP16 (M-O). Embryos were left to develop for 18 hours as before. GFP expression was recorded (electroporated somites indicated by the white arrows), followed by antibody staining for sarcomeric Myosins with the MF20 antibody (brown staining). (C) Six1-GFP alone induces premature Sarcomeric Myosin expression in the 18 hour time window between HH15/16 and HH19/20 (The black arrows are indicating the correspondent electroporated somites). The strong staining of the Myosin reflected the area of the fluorescence. The Six1VP16 construct combined with pCAB, MyoD, Mef2c and MyoD and Mef2c together did not induce any premature sarcomeric Myosin expression in the 18 hour time window between HH15/16 and HH19/20.

9.3 Discussion

9.3.1 The muscle stem cell state may be actively maintained

Even providing MyoD, Mef2c and Six1 with our electroporations and co-electroporations, muscle precursor situated in the dermomyotome would not undergo terminal muscle differentiation.

The Six1-GFP misexpression experiment suggests that the protein enters the nucleus. The experiments conducted in the chicken somite indicate that the Mrf constructs readily lead to upregulation of genes involved in setting the cell up for myogenesis. The experiments in the frog and the experiments in the chicken where the muscle precursor were exposed to Mrf for a longer time indicated that the Mrf constructs are able to drive myogenesis. Therefore, biologically active proteins are being made. Yet in the 18 hour time window between HH15/16-HH19/20, Mrf, even in combination with Mef2c and Six1-VP16 were unable to drive the muscle precursor into terminal differentiation. This indicates it is not the mere absence of myogenic regulators that prevents premature differentiation of muscle precursor. Rather, there are factors that actively preserve the stem cell state.

In the myogenic cascade, the premyogenic *Pax* genes have been shown to ready the cells for myogenesis, to activate Myf5, and when Myf5 is absent, to contribute to the activation of MyoD (419,420). However, the Pax genes keep cells in a proliferative state (unless additional factors enforce adoption of a quiescent state) and they prevent muscle differentiation (297). When cells commit to myogenesis, they express microRNAs such as miR-206 which target the Pax mRNAs, thereby clearing the cell of inhibitors of muscle differentiation (229,230). We therefore reasoned that Mrf may not be able to drive muscle precursor into immediate differentiation because Pax gene expression has not been stopped. This will be explored in the next Chapter.

Table 9. 1: Summary electroporation experiments shown in Chapter 9

Numbers displayed as: Total: wildtype/upregulated/downregulated

Summary of the number of electroporated embryos that were analysed for Myosin levels using immunohistochemistry with MF20 antibody detection and DAB staining, together with the number of altered phenotypes observed. We observed upregulation of Myosin levels with the use of Six1-GFP construct only (Blue shade).

EP targeting the embryonic muscle precursor in the somitic dermomyotome		
Specimen analysed for	**Sarcomeric Myosin (MF20)**	
	18h	**42h**
Mm Six1-GFP	4:2/2/0	
Mm Six1-Vp16 + pCab	3:3/0/0	
Mm Six1-Vp16 + Gg MyoD	3:3/0/0	
Mm Six1-Vp16 + Gg Mef2c	2:2/0/0	
Mm Six1-VP16 + Gg MyoD + Gg Mef2c	2:2/0/0	

Chapter 10

10 Prolonged expression of Pax7 may contribute to the *in vivo* protection of the muscle stem cell state

10.1 Introduction

Misexpression experiments suggested that the muscle stem cell state of developing muscle precursor *in vivo* is actively protected. Hence, factors have to be considered that are associated with myogenic competence but at the same time, prevent differentiation. Such a factor is *Pax7* and its paralog *Pax3*.

The two *Pax* genes arose from a common ancestor during vertebrate evolution (72). Gene function diversified somewhat, with *Pax3* but not *Pax7* being crucial for the development of migratory limb muscle precursors (421). However, both vertebrate P*ax* genes have redundant roles in the early embryo and without them, no myogenic cells form (89).

In adult muscle precursor (satellite cells) and C2C12 myoblasts *in vitro*, misexpression of a dominant-negative form of Pax7 or Pax3 prevented muscle differentiation and led to cell death by apoptosis. Constitutive expression of Pax7 or Pax3 resulted in increased proliferation and decreased cell size as well as significant delay of differentiation. This occurred despite the *Pax* genes upregulating expression of *Mrf* genes such as *Myf5* and *MyoD* (318,422), indicating that the *Pax* genes provide myogenic competence but support the undifferentiated stem cell state.

When muscle precursor differentiate, both *in vivo* or *in vitro*, they downregulate Pax7 (317,423). This is facilitated by regulatory miRNA molecules: differentiating cells have been shown to express microRNAs including miR1, miR206 and miR486 (424,425). Specifically, miR206 and miR486 target sequences in the 3' untranslated region (UTR) of the *Pax7* mRNA, promoting its degradation (229,230). Notably, loss of this regulation by microRNA inhibition causes differentiation to be delayed, whilst a microRNA-resistant form of Pax7 inhibits differentiation (230). Thus, microRNAs are a key mechanism to clear differentiating cells of Pax7 (and Pax3) gene products, thereby ensuring that differentiation can proceed.

Notably, in mice mutant for *Myf5* (but not *MyoD*), expression of miR1 and miR206 is lost (224). In myoblasts *in vitro*, *MyoD* upregulated the expression of miR206 and miR486 (230). When (tagged versions) of chicken Mrf proteins were misexpressed in the chicken neural tube, they were able to trigger miR1 (Myf5 and MyoD) and miR206 expression in this tissue (all Mrfs, (224). This points to a molecular mechanism by which *Mrf*, by means of miRNA expression, remove the differentiation-inhibiting muscle stem cell factors.

When misexpressing (untagged) chicken *Mrf* in developing muscle precursor *in vivo*, we found that only a selection of early myogenic genes were upregulated, and cells were unable to differentiate for another day. We thus wondered whether the *Mrf* were unable to activate miRNAs and to remove *Pax7* gene products. Thus, we misexpressed *Mrf* once again, this time assaying for the expression of Pax7 protein, *Pax7* mRNA and miR206 (the miRNA that can be activated by all Mrf,(224). The *in situ* hybridisation assaying for miR206 expression required special reagents and was therefore carried out in collaboration with D. Sweetman (University of Nottingham, UK). Results are summarised in Table 10.1.

10.2 Results

10.2.1 Analysis of Pax7 protein expression after misexpression of Mrf genes

Chicken embryos were electroporated with the Mrf constructs and pCAB vector as a negative control, then, stained for Pax7 protein as seen in computationally combined images of dorsolateral views. The embryos electroporated with pCAB construct appeared somewhat subdued in the electroporated region (Fig. 10.1, Bi-iii). However, closer inspection revealed that the subdued staining occurred in the targeted as well as the surrounding cells (Fig.10.1, Bii, Biii; 3rd somite from the top). Analysing the entire z-stack of images obtained for this specimen, we realised that Pax7 protein was readily detectable throughout the dermomytome (not shown). The cross sections confirmed that in the targeted cells in the dermomyotome, Pax7 protein was at the same level as in the surrounding, un-electroporated cells (Fig. 10.1, Ci-iii). This suggested the computational combination of images obtained from the z-stack may lead to wrong conclusions. It also indicated that individual images obtained in the z-stack and cross sections would have to be carefully analysed. This was done for all specimens, but for space constraints, only the combined dorsolateral views and a single cross-sectional view are shown.

When analysing specimens electroporated with Mrf expression constructs, we found that in dorsolateral views, Pax7 protein was detectable in the targeted cells at the same level as in the surrounding cells, even though in the combined image, at times expression levels appeared lower (Fig.1.10, E,H,K,N i-iii). Inspection of cross sections confirmed that Pax7 protein was present in the electroporated cells in the dermomyotome (Fig. 10.1.C,F,I,L,O i-iii). At first sight, the specimen electroporated with the *Myf5* construct seemed to be an exception: here, Pax7 expression appeared reduced on the electroporated side compared to the contralateral control side (Fig. 10.1.Fi-iii). However, this section unfortunately is oblique, and hence, different somitic areas are represented on both sides. When closely analysing the targeted, GFP-expressing cells (green fluorescence) and the neighbouring GFP-negative cells, they display the same red fluorescence obtained from the Pax7 antibody.

Taken together, our results suggest that Pax7 protein was present when muscle precursor in the somitic dermomyotome were exposed to Mrf for a minimum of 12 hours (18 hours of re-incubation after electroporation).

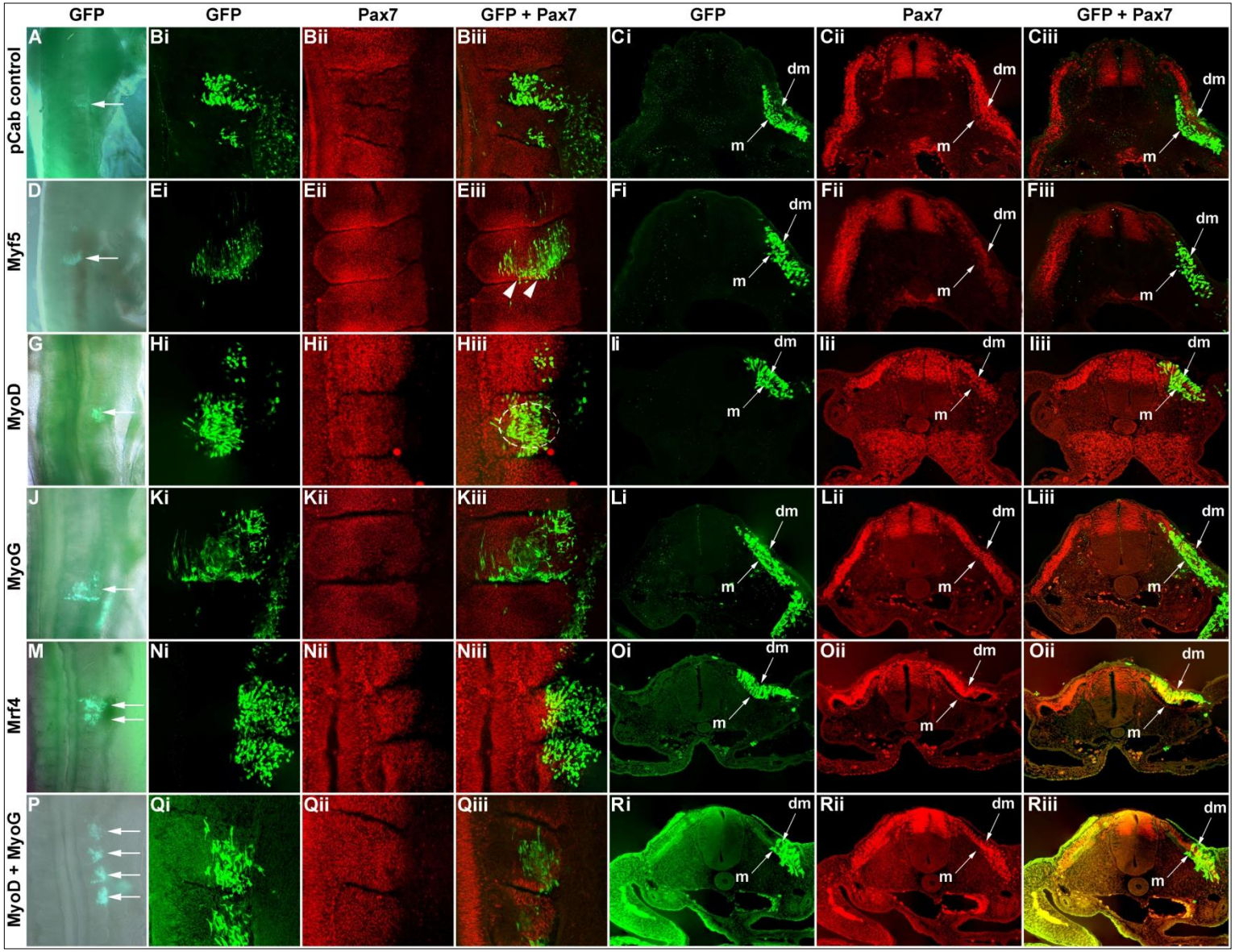
GFP
GFP
Pax7
GFP + Pax7
GFP
Pax7
GFP + Pax7
pCab control
Myf5
MyoD
MyoG
Mrf4
MyoD + MyoG
A
Bi
Bii
Biii
Ci
Cii
Ciii
D
Ei
Eii
Eiii
Fi
Fii
Fiii
G
Hi
Hii
Hiii
Ii
Iii
Iiii
J
Ki
Kii
Kiii
Li
Lii
Liii
M
Ni
Nii
Niii
Oi
Oii
Oii
P
Qi
Qii
Qiii
Ri
Rii
Riii
dm
m

Figure 10. 1: In the 12 hour time window between HH16-20, just MyoD and Myf5 proteins may partially downregulate Pax7 protein expression.

Flanking somites were electroporated at HH15/16 with the pCab control construct or with Mrf expressing pCab constructs as indicated on the left. Embryos were harvested at HH19/20 and GFP expression was recorded (A,D,G,J,M,P). Embryos were then subjected to fluorescent immunohistochemistry, using an anti-GFP antibody (green fluorescence) and an anti-Pax7 antibody (red fluorescence). The position of the fluorescent signals was analysed using confocal microscopy; flattened z-stacks of dorsolateral views are shown in (B,E,H,K,N,Q i-iii). Thereafter, somites were cross-sectioned on a vibratome and analysed by confocal microscopy (C,F,I,L,O,R i-iii). Note that targeted cells contributed to the myotome and formed myotubes when the electroporated side encompassed the rostral or caudal dermomyotomal lips. This contribution was irrespective of the construct that was used (see Eiii, arrowheads). Relevant electroporations were those where the centre of the dermomyotome was targeted (see Hiii) since this is where the muscle stem cells developed. Here, electroporated cells remained in the dermomyotome. Weaker Pax7 staining in the treated compared to the untreated dermomyotome was observed after electroporation with Myf5 and MyoD and MyoG (F, I, L i-iii) but we hypothesised in this case analysis of the sections was influenced by the Z-Stack technique of the confocal, see main text.

10.2.1. Analysis of *Pax7* mRNA and miR206 expression after *Mrf* misexpression

So far we have focused our attention on Pax7 protein, because this is the functionally relevant *Pax7* gene product. However, Pax7 protein turnover may be low. Moreover, in differentiating myoblasts, the main mechanism of Pax7 removal is the degradation of *Pax7* mRNA involving Mrf-induced *miRNAs* (230). Therefore, we electroporated embryos with *Mrf* constructs as before, this time analysing for the expression of *Pax7* mRNA and miR206, using *in situ* hybridisation.

Embryos were electroporated at HH16 and reincubated for 18 hrs to reach HH20. We misexpressed the Mrf members and used the pCAB as a negative control. Successfully electroporated cells were located by fluorescence microscopy (Fig. 10.2 A-Q) and all embryos, control and electroporated somites alike, displayed normal *Pax7* mRNA expression in the somitic dermomyotome, including the typical upregulated expression in the dermomyotomal centre (Fig. 10.2 B-R and Bi-Ri). A second group of embryos was electroporated with Mrfs constructs and analysed for miR206. Successfully electroporated cells were located by fluorescence microscopy (Fig. 10.2 C-S). The embryos showed probe staining in the somitic myotome as shown by (224) and no ectopic expression of miR206 was observed in the electroporated somites (Fig.10.2 D-T and Di-Ti).

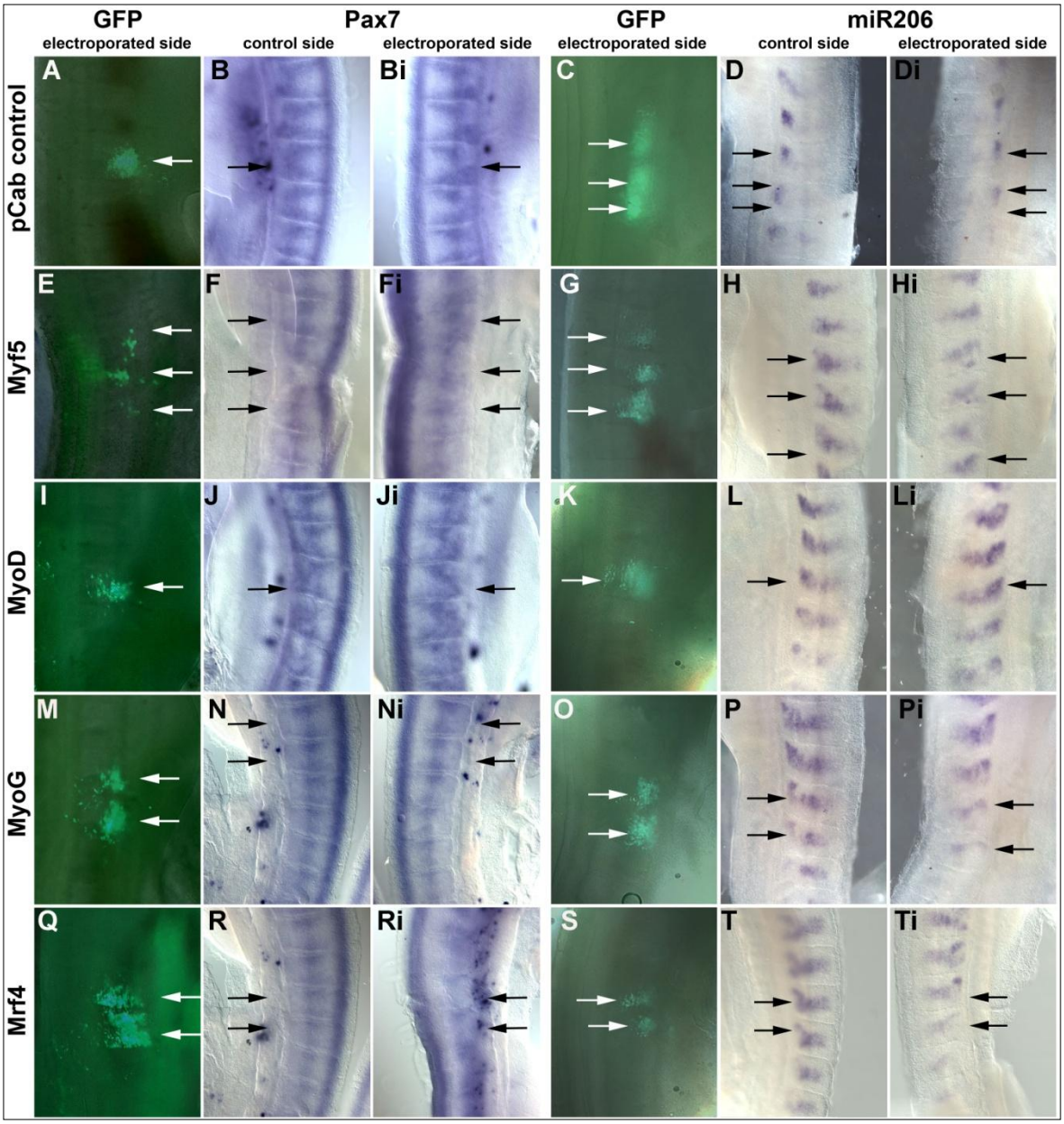
GFP
electroporated side
Pax7
control side
electroporated side
GFP
electroporated side
miR206
control side
electroporated side
pCab control
Myf5
MyoD
MyoG
Mrf4
A
B
Bi
C
D
Di
E
F
Fi
G
H
Hi
I
J
Ji
K
L
Li
M
N
Ni
O
P
Pi
Q
R
Ri
S
T
Ti

Figure 10. 2: In the 12 hour time window between HH16-20, Mrf misexpression did not change levels of Pax7 mRNA or miR206 expression.

Flanking somites were electroporated at HH15/16 with the pCab negative control or with *Mrf* expressing pCab constructs. Embryos were harvested at HH19/20 and GFP expression was recorded as before (A,E,I,M,Q and C,G,K,O,S). The expression of *Pax7* and miR206 was analysed by *in situ* hybridisation (blue staining). No differences in expression levels were observed when comparing the electroporated somites and the corresponding somites on the untreated control side (arrows). Both sets of embryos analysed for *Pax7* and miR206 showed no changes in RNA expression levels after electroporation.

10.3 Discussion

10.3.1. mRNA levels of *Pax7* and miR206 are unaffected after *Mrf* misexpression

The misexpression of the Mrfs constructs did not influence the expression levels of Pax7 protein in the dermomyotome in the electroporated somites. This would explain the reason why we did not see any upregulation of Myosin expression after the electroporation of Mrfs as shown in Chapter 6. The level of Pax7 protein is still stable after 12 hrs of incubation from the electroporation, this means that the cells in the dermomyotome are still undifferentiated and these data are in line with other studies that describe Pax7 as essential for the maintenance of the muscle stem cell state (89,229,230). Recent studies have underlined the importance of microRNAs during muscle proliferation and differentiation, controlling an elevated number of transcription factors and signalling molecules (424,149). miR-206 is activated during the myoblast differentiation and stimulates muscle differentiation by directly targeting and downregulating Pax7 protein and mRNA (230). Expression of microRNAs in myoblasts accelerates differentiation, whereas inhibition of these microRNA causes persistence of Pax7 protein and inhibits differentiation (230). Our experiments showed that the levels of miR-206 were not influenced by the electroporation of the Mrf constructs. These data support the results of Pax7 protein expression. The presence of undifferentiated cells which do not enter into myogenic differentiation even after transgene electroporation are unchanged and consequently still show high levels of Pax7 protein. A future experiment could be the analysis of Pax3 gene expression. As Pax3 is also regulated by muscle specific mircoRNAs in somites and it would be interesting to see if the expression level of this gene decreases with the misexpression of Mrf constructs and if mir206 levels increase after the electroporation. This experiment could also be carried out in cell culture.

Experiments conducted *in vitro* by Dey and colleagues in 2011, showed that *Pax7* expression levels in C2C12 cells was comparable with that of mouse primary myoblasts when analysed by qRT-PCR. After the withdrawal of serum, Pax7 protein levels decreased followed by the increase of Myosin expression, indicating that the cells were differentiating. The decrease in Pax7 protein started from day 1 with levels going below detection by day 4 (230). The experiments conducted *in vivo* by Sweetman and colleagues in 2008 which showed upregulation of miR-1 and miR-206 in the neural tube as a result of Mrf construct electroporations could potentially be explained by lesser protection of myogenic fate control in the cells of the neural tube due to the alternative fates of those cells. This hypothesis could explain the results observed in this Chapter.

Alternatively, the time frame used in our experiments between the electroporation and the analysis of the Pax7 may have been insufficient to observe the eventual decrease in protein levels as compared with that used in the study of Dey and colleagues. It would be interesting to further

investigate the expression levels of Pax7 protein after Mrf construct electroporation, but with an experimental time frame extended up to 4 days.

If our hypothesises proves correct we would expect to see a decrease in Pax7 expression in the electroporated somites coupled with the upregulation of miR-206 levels.

Table 10. 1: Summary electroporation experiments shown in chapter 10

Numbers displayed as: Total: wildtype/upregulated/downregulated

Summary of the number of electroporated embryos that were analysed for protein levels of Pax7 and RNA levels of *Pax7* and miR-206 after 18h of incubation.

EP targeting the embryonic muscle precursor in the somitic dermomyotome			
specimen analysed for	**Pax7 mRNA**	**Pax7 protein**	**miR-206**
			18h
pCab	3:3/0/0	5:5/0/0	3:3/0/0
Gg Myf5	3:3/0/0	3:3/0/0	4:4/0/0
Gg MyoD	3:3/0/0	4:4/0/0	3:3/0/0
Gg MyoG	4:4/0/0	3:3/0/0	3:3/0/0
Gg Mrf4	4:4/0/0	3:3/0/0	2:2/0/0
Gg MyoD+MyoG		5:5/0/0	

Chapter 11

11 Requirement of cell cycle withdrawal for the terminal differentiation of muscle precursor

11.1 Introduction

In the previous chapters, we showed that in a time window between HH15/16 and HH19/20, the stem cell state of developing myoblasts was protected from premature differentiation. Moreover, we showed that in this time window the pre-myogenic and muscle stem cell factor Pax7 persisted when *Mrf* genes were ectopically expressed. Pax7 provides myogenic competence but delays differentiation. Moreover, when misexpressed in adult muscle stem cells or in C2C12 myoblasts, PAx7 supported cell proliferation. When myoblasts enter terminal differentiation and become myocytes, however, they withdraw from cell cycle (230). This is concomitant with (i) the downregulation of cell cycle promoting Cyclins (426), (ii) upregulation of members of the p21/p27/p57-Cdkn1 family and the p16-Ink4-Cdkn2 family of Cyclin dependent kinase inhibitors which block cell cycle in G1 (reviewed in (Sherr and Roberts, 1995), and (iii) the hypo-phosphorylation of the retinoblastoma protein pRb which both inhibits DNA synthesis and promotes the activation of muscle genes (427,428) . Misexpression of Cyclin D1 (Ccn D1) or of CcnA/E together with the Cyclin dependent kinase Cdk2 inhibited myogenesis (426,429), while misexpression of p16/Cdkn2a and p21/Cdkn1a in myoblasts supported some muscle-specific gene expression even in growth medium (430) . On the other hand, when in amniote muscle fibres pRb or p53 together with Cdkn2a/ARF was removed, cells re-entered cell cycle, expressed Pax7 and dedifferentiated (431,432), mimicking muscle dedifferentiation that occurs in the context of salamander limb regeneration(433). Therefore, cell cycle control is a key step in the terminal differentiation of myogenic cells.

Given that the misexpression of Mrf in chicken muscle precursor did not lead to a downregulation of Pax7, we wondered whether the cells were still in a mitotically active state, preventing their differentiation. We therefore decided to investigate expression levels of *Cdkn* genes. We also decided to misexpress *Cdkn* genes alone or in combination with *MyoD* or *MyoG*. Yet the number and expression of cell cycle regulators in the chicken was not fully characterised. Specifically, it is controversial whether birds have the *Cdkn2a* member of the p16/Ink4/Cdkn2 family, whether they have an alternative upstream *Cdkn2a* exon that is translated in an alternative reading frame (hence this Cdkn2a isoform is also referred to as ARF) (434) . In a combined effort of S. Wöhrle and S. Dietrich in the lab and F. Pituello at Université P. Sabatier, Toulouse, France, we used bioinformatics to determine the members of the *Cdkn* gene families in the chicken, and we

analysed their expression in comparison to that of *Cdk* and *Cnn* genes by in situ hybridisation. This analysis revealed chicken *Cdkn1b* as the most likely regulator of cell cycle withdrawal during early chicken myogenesis. The subsequent functional analyses suggested however that *Cdkn1b* was unable to promote terminal differentiation in developing myoblasts.

11.2 Results

11.2.1. Identification of avian *Cdkn* genes

In mammals, the *Cdkn1*, *Cdkn2* and the small *Cdkn3* family of cell cycle suppressors are well characterised (87,435). Information on *Cdkns* in other vertebrate species is fragmentary. In order to establish which *Cdkn* would be a likely regulator of cell cycle exit during early chicken myogenesis, we searched the NCBI, Xenbase and Ensembl databases for *Cdkn* sequences, using the same approach as for the *Mrf* genes (see chapter 4). This work was carried out by S. Wöhrle and S. Dietrich, the data are summarised in (Table 11.1). In placental mammals, the *Cdkn1* gene family encompasses the *Cdkn1a*, *Cdkn1b* and *Cdkn1c* genes. However, in the marsupial opossum, in all bird species analysed and in lepidosaurs (lizards and snakes), *Cdkn1c* was not found. Given that *Cdkn1c* was present in alligators and turtles which are more closely related to birds than lizards and snakes, our data suggest that during evolution, *Cdkn1c* was lost independently in some amniote lineages. In teleost on the other hand, duplicates of *Cdkn1c* and, in zebrafish, duplicates of *Cdkn1b*, were found, in line with the three rounds of genome duplication that occurred during teleost evolution (436,437). Interestingly, in actinopterygians (exception: spotted gar) as well as in birds, alligators, turtles, lizards/snakes, and Latimeria, a fourth *Cdkn1* family member, called *cdkn1d* in teleost and *Cdkn1a* or *d* in birds, was found. Comparison of protein sequences suggested that the so far unknown sarcopterygian Cdkn1 family member was similar to teleost cdkn1d. These data suggest that in most vertebrates, cell cycle control may involve a further Cdkn1 member, which has been lost in mammals. The synteny analysis revealed that, where the new *Cdkn1* gene was present, it was linked to *Cdkn1b*. This analysis also revealed that extensive rearrangements between *Cdkn1* gene loci had occurred. Therefore a full phylogenetic analysis will have to be carried out to establish the relationship of the new *Cdkn1* gene with the known *Cdkn1* paralogs. However, the fact that different vertebrate species have different complements of *Cdkn* genes is quite important: Studies in mammals showed that *Cdkn1b* is required for adult muscle stem cell (satellite cell) self-renewal including the suppression of differentiation and the return to quiescence, whereas *Cdkn1a* is required for cell cycle arrest when myoblasts enter terminal differentiation (438). In zebrafish however, it is *cdkn1c* that assists *myod* during myogenesis in the cells to differentiate first, the adaxial cells (435). This suggests that after the generation of *Cdkn1* genes during the two (teleosts: three) rounds of gnathostome genome duplication, distinct sub-functionalisation has occurred. Consequently, *Cdkn* gene function has to be established for each species separately.

The search for *Cdkn2* family members revealed that placental mammals have four paralogs, *Cdkn2a,b,c,d*. Moreover, they have an alternative first exon for *Cdkn2a* which, when spliced to the 2nd exon of *Cdkn2a*, creates an alternative reading frame and hence produces a distinct protein, Cdkn2a-ARF (439). Homologs of mammalian *Cdkn2b* and *c* we found in all osteichthyan ("bony") vertebrates analysed. In contrast, *Cdkn2d* was absent in birds and possibly also in turtles. *Cdkn2a* as well as *Cdkn2a-ARF* was missing in marsupial and monotreme mammals, Xenopus, Latimeria and in all actinopterygians. The information we were able to obtain for diapsids is incomplete because the loci where, according to our synteny analysis, we expected *Cdkn2a/ARF* to be situated, are not fully sequenced. Nevertheless, we detected evidence for *Cdkn2a-ARF* in galliform (chicken, turkey), anseriform (duck) and passeriform (zebrafinch, flycatcher) birds, but not in turtles or lizards/snakes. When performing a BLAST-search using mouse sequences, we obtained a hit for ARF, followed by a 2nd hit for ARF and a hit for the 2nd exon of *Cdkn2a* at a location on chromosome Z where genes typically linked to Cdkn2a/ARF were found. We furthermore found evidence for *Cdkn2a* in passeriform birds and the budgerigar, as well as for turtles and the Burmese python, suggestion that *Cdkn2a* is present in diapsid animals.

To complete the analysis, we searched for *Cdkn3* genes and we found that all vertebrates with the exception of Xenopus had a single *Cdkn3* gene, located in a conserved environment, suggesting immediately after the two round of genome duplication, all duplicates with the exception of the extant *Cdkn3* were lost.

Table 11. 1: Presence of Cdkn genes in osteichtyans

Table showing cross reference of Cdkn genes with species investigated.

Cdkn1a, b, c, d and Cdkn2a ARF, a, b, c, d and 3 have been summarised. Columns 1 to 4 dictate the classification of the species investigated. Remaining columns dictate the genes being investigated. The colour code indicated the data base sources (dark green Ensemble, light green NCBI) and light beige see annotation at the bottom row. N/A indicates non availability of the data. The yellow boxes underline where we are have fragments of the sequences.

Some of the sequences have gaps and we have just fragmented information. Few of the sequences have the corresponding Cdkn sequence but just in one exon. And in a couple of cases we found the sequences in chicken but not in turkey.

			species investigated	Cdkn1a	Cdkn1b	Cdkn1c	Cdkn1d	Cdkn2a-ARF	Cdkn2a	Cdkn2b	Cdkn2c	Cdkn2d	Cdkn3
Sarcopterygians													
	Mammals	Placentals	Human, mouse	✓	✓	✓	-	✓	✓	✓	✓	✓	✓
		Marsupials	Opossum	✓	✓	-	-	-	✓	✓	✓	✓	✓
		Monotremes	Platypus	N/A	N/A	N/A	N/A	-	N/A	N/A	N/A	N/A	N/A
	Birds	Galliformes	Chicken, turkey	✓	✓	-	✓	Gg ✓ for ex1	Gg ?	Gg ✓	✓	-	✓
		Anseriformes (waterfowl)	Duck	✓	(blast hit)	-	✓	-	-		✓	-	✓
		Passeriformes	Zebrafinch, flycatcher (Tibetian ground tit, white throated sparrow)	✓	✓	-	-	Blast hits for ex1	✓	✓	✓	-	✓
		Parrots	Budgerigar	✓	✓	-	-		✓	✓	N/A	N/A	N/A
	Alligators, crocodiles		Chinese and American alligator	✓	✓	(✓)	✓	N/A	N/A	N/A	N/A	N/A	N/A
	Turtles		Chinese softshell turtle (painted turtle, green sea turtle)	(gaps)	✓	✓	✓	-	(blast hit)	✓	✓	?	✓
	Lizards and snakes		Anole lizard (Burmese python)	✓	✓	-	✓	-	✓	✓	✓	✓	✓
	Amphibians		Xenopus tropicalis, Xenopus laevis	✓	✓	✓	-	-	-	✓	✓	✓	-
	Coelocanths		Latimeria	✓	✓	✓	✓	-	-	✓	✓	✓	✓
Actinopterygians													
	Holosts		Gar	✓	✓	✓	-	-	-	✓✓	✓	✓✓	✓
	Teleosts	Cypriniformes	Zebrafish	✓	✓ ✓	✓✓	✓	-	-	✓	✓	✓	✓
		Gadiformes	Atlantic cod	✓	✓	✓✓	-	-	-	✓	✓	✓	✓
		Beloniformes	Medaka	✓	-	✓✓	✓	-	-	(gaps)	✓	✓	✓
		Tetraodontiformes	Fugu, green spotted pufferfish	(blast hit)	✓	✓✓	✓	-	-	✓	✓	✓	✓
		Gasterosteiformes	Stickleback	✓	✓	(blast hits)	✓	-	-	✓	✓	✓	✓
							Bird & lizard gene upstream of Cdkn1b. Gene is similar to teleost **cdkn1d**; but could also be a duplicated Cdkn1a	where present, Cdkn2a/ARF is downstream of Cdkn2b					

11.2.2. Expression analysis for chicken cell cycle regulators

Having identified the *Cdkn* family members present in the chicken genome, we next examined which of them are expressed during somitic myogenesis. Moreover, we analysed the expression of *Cyclin* (Ccn) genes, *Cdk* genes and *Cdc25* genes that promote cell cycle and hence, might be expressed in developing myoblasts. The analysis was performed by *in situ* hybridisation of HH13/14 embryos. Fabienne Pituello kindly provided us with her collection of *in situ* probes (see Materials and Methods), all other probes were synthesised according to the sequences we extracted from the databases. Since we were unable to find the sequences for *Cdk4* in the chicken, we instead used the sequences we found for *Pseudopodoces humilis* (Tibetian ground tit) and the American alligator. Since the *Cdkn2* sequences we found in the chicken were very short, we used the sequences for zebrafinch *Cdkn2a* instead. This zebrafinch probe was also tested on stage-matched zebrafinch embryos. Moreover, we used a *CcnB2* sense probe as negative control. The results are shown in Fig.11.1 and 11.2, with images sorted according to the phase of the cell cycle in which the proteins are active.

Amongst the Cyclins, we found that *Ccn D1*, *B2* and *B3* were strongly expressed in the somites and in the neural tube, *Ccn D2*, *E* and *E2* had similar expression patterns but at lower expression levels. *Ccn A1* and *A2* were expressed throughout the embryo and in blood islands, the latter also showed expression of *Ccn D3* (which interestingly can act as positive regulator of differentiation; (440)); for *Ccn O*, no expression was detected. For *Cdk4* we were unable to detect any specific expression, which may be due to the fact that we only had heterologous probes. *Cdk6* was strongly expressed in the neural tube and lateral mesoderm, but not in the somites. In contrast, widespread expression that also encompassed the somites was found for *Cdk2* and *Cdk1*, with expression levels of *Cdk1* being higher than those of *Cdk2*. Both *Cdc 25* genes were expressed in the neural tube, somites and lateral mesoderm. Amongst the *Cdkn* genes, widespread expression encompassing the somites was found for *Cdkn1a*, *Cdkn2c* and *Cdkn3*. Widespread expression not including somites was found for *Cdkn2b*, no signal was detected for *Cdkn1d*, *Cdkn2a*, *ARF*. However, a specific signal in the somites that began in the medial-most area and then spread laterally was observed for *Cdkn1b*. This expression pattern was similar to that of myogenic genes, suggesting that specifically *Cdkn1b* might be involved in cell cycle exit during somitic myogenesis. Finally, the *Ccn B2* sense probe did not produce any staining as expected, indicating that any staining we obtained was trustworthy. In summary, somites expressed *Ccn D1, D2, E, E2, A1, A2, B2, B3, Cdk2, Cdk1, Cdc 25a, Cdc25b*, low levels of *Cdkn1a, 2c, 3*. Moreover they expressed *Cdkn1b* is a pattern reminiscent of that for myogenic genes.

Since the *Cdkn1b* staining resembled that we obtained with myogenic genes analysed in chapter3, we in more detail investigated the dynamics of *Cdkn1b* expression in comparison with that of *Myf5* and *MyoD* (Fig. 11.3). At HH4-5, the expression of *Cdkn1b* was visible along the primitive streak (Fig. 11.3 A). At HH8 *Cdkn1b* staining was observed in the early rostral neural plate in the developing cardiac cells and the youngest two somites (Fig.11.3 B). At both stages, the two *Mrf* genes were not expressed (Fig.11.3 G,H,M,N). At HH10, *Cdkn1b* and *Myf5* were transcribed throughout the 10 somites present, but Cdkn1b was also expressed in the neural tube, the cardiac mesoderm and the primitive streak (Fig. 11.3 C,I). *MyoD* was not expressed yet (Fig.11.3, O). At HH13/14 *Cdkn1b* was expressed in the dorsomedial edge of the somites, spreading laterally as somites matured (Fig.11.3 D). A similar expression pattern was observed for *Myf5*. However, *Myf5* was consistently expressed in the condensing somite whereas *Cdkn1b* was not (Fig. 11.3 J). *MyoD* expression commenced in somewhat more mature somites, somites 4-5 (Fig.11.3.P). A similar patterns was observed at HH15/16, with MyoD expression beginning already in somites1/2 (Fig.11.3 E,K,Q). At HH20, the overall blue staining of the embryo hybridised with the Cdkn1b probe suggested more widespread expression. In the somites, however, *Cdkn1b*, *Myf5* and *MyoD* were expressed in similar pattern (Fig.11.3 F,L,R). To verify the similarity of *Cdkn1b* and *Mrf* expression, the flank regions of HH20 embryos stained for the expression of *Myf5*, *MyoD*, *MyoG*, *Mrf4* and *Cdkn1b* were vibratome-cross-sectioned (Fig. 11.4). This analysis showed that *Myf5* was expressed in the dorsomedial and ventrolateral lips of the dermomyotome, whereas the other *Mrfs* and *Cdkn1b* were expressed in the myotome. Taken together, our data suggest a close link between *Cdkn1b* and myogenesis. In terms of timing of expression, *Cdkn1b* appeared after that of *Myf5* and before that of *MyoD*, which is earlier than the withdrawal of myogenic cells from cell cycle. However, we do not currently have information on the emergence of Cdkn1b protein. In addition, no other *Cdkn* gene showed an expression pattern that would link it to myogenesis. Thus, chicken *Cdkn1b* remained the cell cycle suppressor most strongly linked to muscle differentiation.

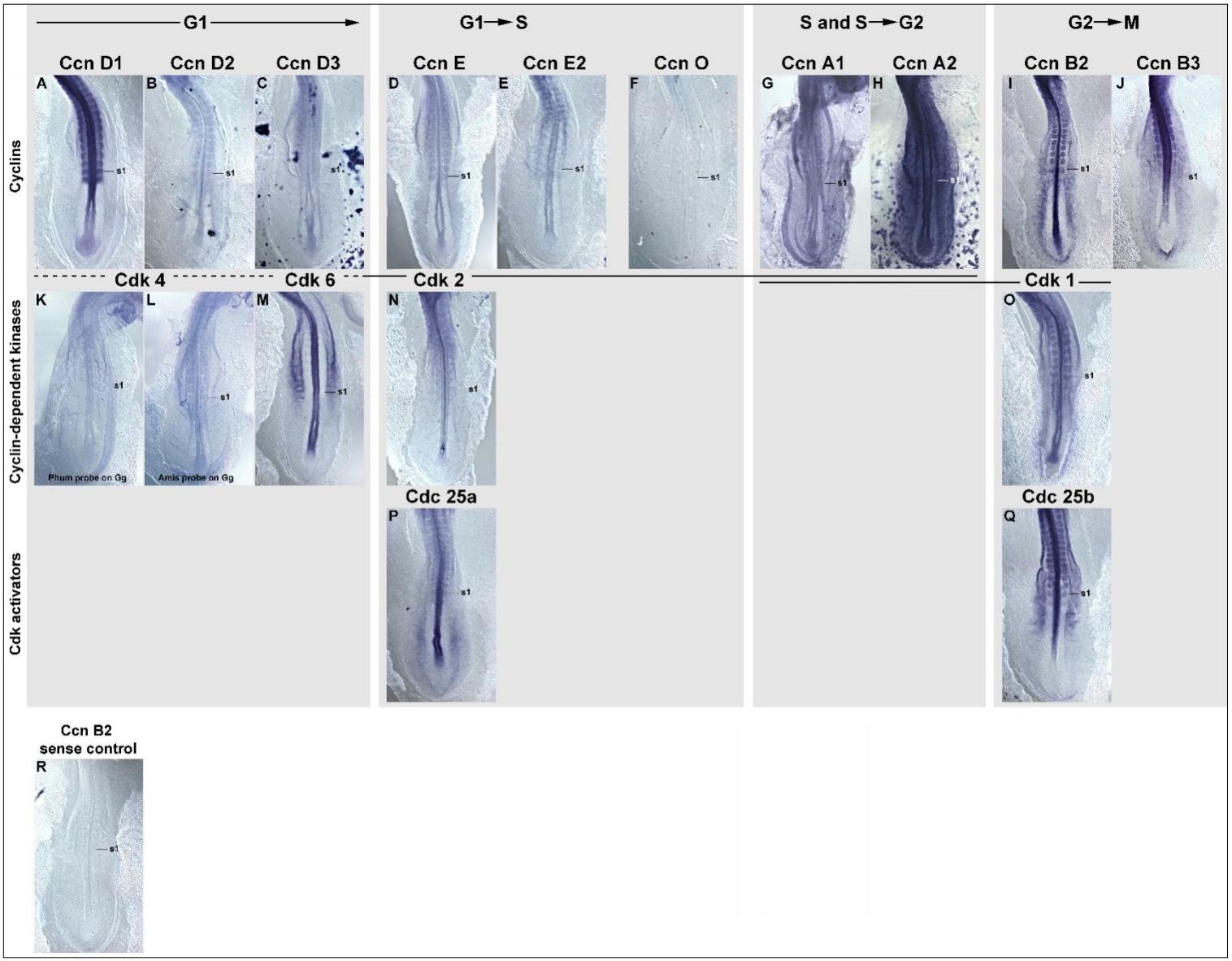
G1
G1→S
S and S→G2
G2→M
Ccn D1
Ccn D2
Ccn D3
Ccn E
Ccn E2
Ccn O
Ccn A1
Ccn A2
Ccn B2
Ccn B3
A
B
C
D
E
F
G
H
I
J
Cyclins
Cdk 4
Cdk 6
Cdk 2
Cdk 1
K
L
M
N
O
Phum probe on Gg
Amis probe on Gg
Cyclin-dependent kinases
Cdc 25a
Cdc 25b
P
Q
Cdk activators
Ccn B2
sense control
R
s1

Figure 11. 1: Expressions of positive cell cycle regulators at HH14:

Analysis of the expression of cell cycle promoters in different phases of the Mitosis. Embryos analysed at HH13-14 (19-22 somites). In this experiment, it was observed which cell cycle promoter have more possibility to be involved in the Myogenesis. From A to J, the cyclins have been analysed with in situ hybridisation (see Material and Methods). Ccn D1, CCn A2, Ccn B2, Ccn B3 (images A, H. I, J) are the cyclins that showed the best mRNA signal in somites. From figure K to O, Cyclin-dependent kinase have been analysed, finding that Cdk1 showed the best expression in the somite. Finally P and Q represent the Cdk activators where just Cdc 25b showed strong staining in the somites. Figure R, sense probe.

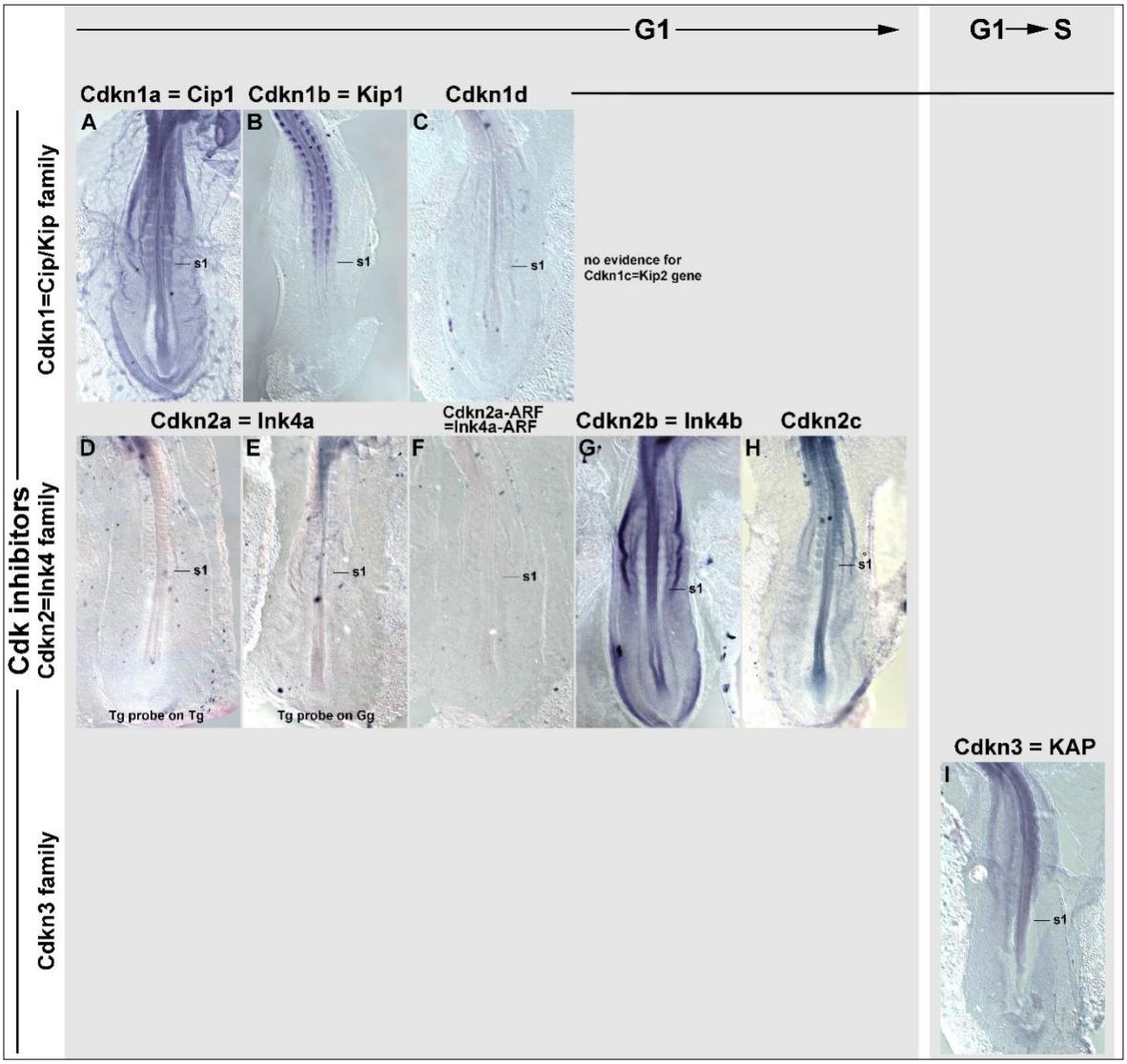
Cdk inhibitors
Cdkn1=Cip/Kip family
Cdkn2=Ink4 family
Cdkn3 family
G1
G1→S
Cdkn1a = Cip1
Cdkn1b = Kip1
Cdkn1d
A
B
C
s1
no evidence for
Cdkn1c=Kip2 gene
Cdkn2a = Ink4a
Cdkn2a-ARF
=Ink4a-ARF
Cdkn2b = Ink4b
Cdkn2c
D
E
F
G
H
Tg probe on Tg
Tg probe on Gg
Cdkn3 = KAP
I

Figure 11. 2: Expression of negative cell cycle regulators

Cdk inhibitors have been analysed. From figure A to C show; Cdkn1=Cip/Kip family analysed with in situ hybridisation. Cdkn1b (B) showed strong expression in the somites. On the Cdkn2=Ink4 family, Cdkn2C (H), showed a low level of mRNA expression in the somites. While in the Cdkn3 family, no signal was identified.

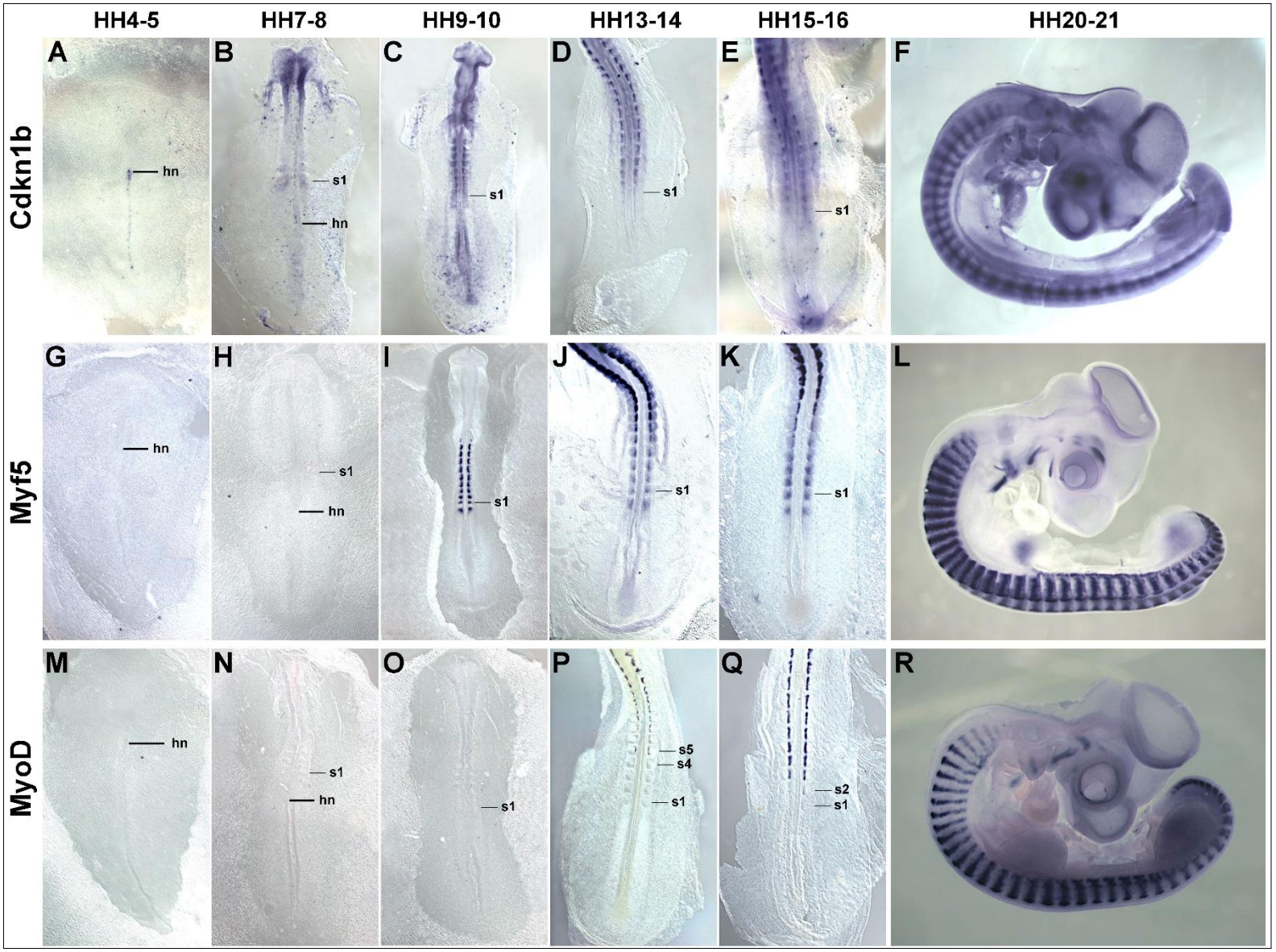
HH4-5
HH7-8
HH9-10
HH13-14
HH15-16
HH20-21
Cdkn1b
Myf5
MyoD
A
B
C
D
E
F
G
H
I
J
K
L
M
N
O
P
Q
R
hn
s1
s5
s4
s2

Figure 11. 3: Comparison of Cdkn1b, Myf5, MyoD expression, time course

The strong staining of the mRNA after ISH treatment gave strong information of the similar staining of the Cdkn1b compare to Myf5 and MyoD. In this template stages HH4-5 to 20-21 have been compared to see the affinity and the resemblance of the 3 pattern. A to F, Cdkn1b looks appear earlier of the other two genes. This gene was express in HH4 and 8, there was not any record for Myf5 and MyoD for this early expression. At the HH10, Cdkn1b has still a strong where it is detect for the first time the appearance of Myf5 (figure C and I), Myod is not appearing at this early stage. Myf5 has a strong expression in the somites from HH10 to 20-21, where MyoD appears at HH-13-14 in the oldest somites until somites 5 (s5) from the primitive streak. All three the genes had a strong expression in mRNA levels the HH15 -16 until HH20. The staining appeared to have a different distribution in the somites that could be observed in the figure 10.5 with the analysis of the sections

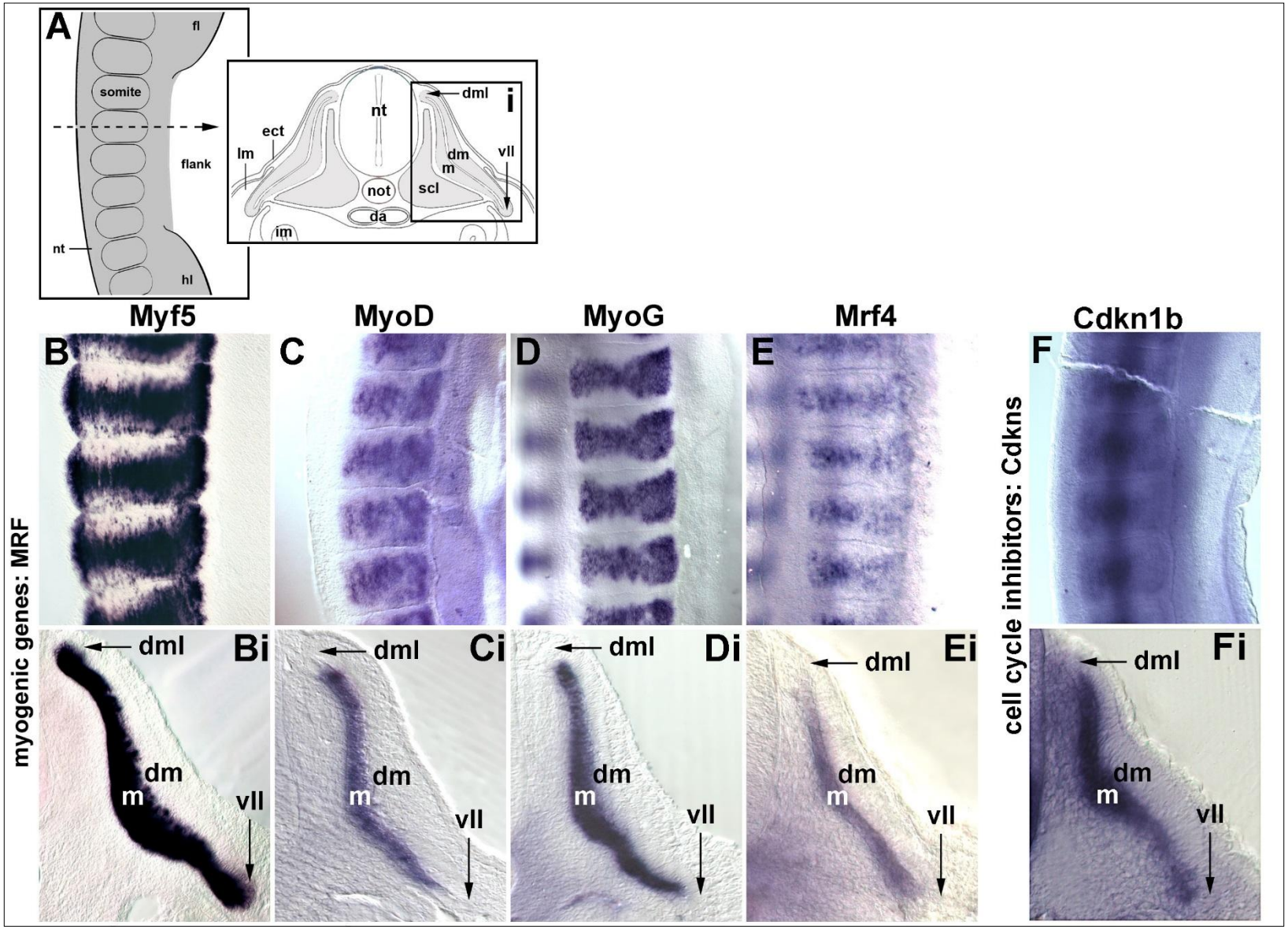
A
fl
somite
flank
nt
hl
ect
lm
nt
dml
i
dm
m
vll
not
scl
da
im
Myf5
MyoD
MyoG
Mrf4
Cdkn1b
B
C
D
E
F
myogenic genes: MRF
cell cycle inhibitors: Cdkns
dml
Bi
dm
m
vll
dml
Ci
dm
m
vll
dml
Di
dm
m
vll
dml
Ei
dm
m
vll
dml
Fi
dm
m
vll

Figure 11. 4: Analysis somite-expressed Mrf in comparison with Cdk1b

(A) Schematic representation of the images displayed in B-F (lateral view of flank somites on the right of the embryo, rostral to the top, lateral to the right) and Bi-Fi (cross section to flank somites, dorsal to the top, lateral to the right; section (Si) is from the forelimb- flank boundary as indicated in S). Markers are indicated as before. The *Mrf* genes and Cdk1b show overlapping expression in the myotome, with the late commencing markers still being confined to the more medial territories.

11.2.3. Analysis of *Cdkn1b* expression after *Mrf* misexpression

The analysis of *Cdkn1b* expression suggested that a close link with of this gene with the process of myogenesis. Yet expression emerged after that of *Myf5*, suggesting the possibility that *Cdkn1b* could be regulated by Myf5 and, if generic E-Box sequences were to be located in the *Cdkn1b* promoter, by other Mrf proteins. To test this, HH15/16 embryos were electroporated with the pCab control vector, with the various *Mrf* expression constructs or with both *MyoD-MyoG* constructs. The embryos were re-incubated for 18 hours to reach HH19/20 and analysed by *in situ* hybridisation for the expression of *Cdkn1b* (Fig.11.5). The results are summarised in Table. 11.2.

The experiment revealed that electroporation of the pCab vector did not change the expression of *Cdkn1b* (Fig. 11.5 A,B). In contrast, any of the *Mrf* and *MyoD* and *MyoG* together caused a significant upregulation of *Cdkn1b* in the electroporated cells (Fig. 11.5 C-N), the weakest effect having been obtained with Mrf4 Fig.11.5, I,L). These results indicate that *Mrf* are sufficient to ready the cells for myogenesis and cell cycle exit but not yet for terminal differentiation.

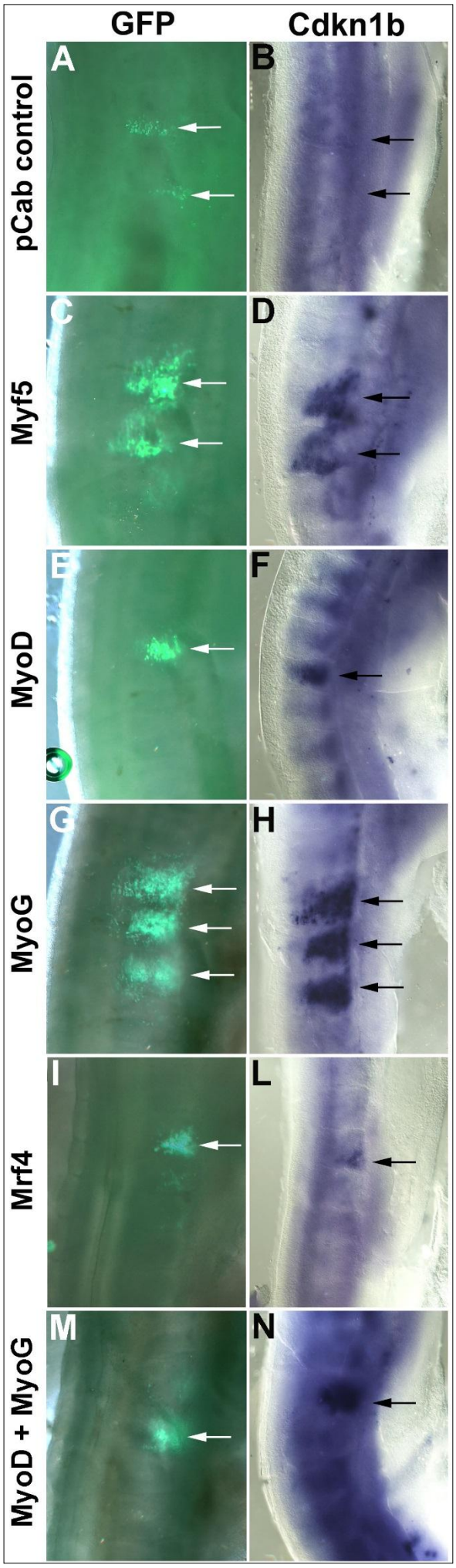
GFP
Cdkn1b
pCab control
Myf5
MyoD
MyoG
Mrf4
MyoD + MyoG
A
B
C
D
E
F
G
H
I
L
M
N

Figure 11. 5: Mrf Misexpression of Mrf genes, analysis of Cdk1b expression

Embryos were electroporated with plasmids encoding the factor shown and GFP and grown to HH20. Fluoresce was visualized at the microscope (figure from A to M). Embryos were analised with ISH to detect mRNA for Cdk1b. The misexpression of the Mrf upregulate Cdk1b, localized in the area of the fluorescence (arrowed figure D, F, H, L, N).

11.2.4. Misexpression of *Cdkn1b* in chicken somites

11.2.1.1 Effect on cell cycle

To investigate whether *Cdkbn1b* or any of the *Mrf* indeed facilitate cell cycle exit of myogenic cells, a *Cdkn1b* expression constructs was generated. Chicken embryos at HH15/16 were electroporated with *Cdkn1b* or *Mrf* expression constructs, harvested after 18 hours, cross-sectioned on a cryostat and analysed for the presence of Histone H3 phosphorylated at Serine 10, using immunohistochemistry. The anti-pH3 antibody detects cells with compacted chromatin ready for or undertaking mitosis (361). Simultaneously, sections were stained with an anti-GFP antibody to trace the targeted cells and with DAPI (4',6-diamidino-2-phenylindole, dilactate) to reveal cellular nuclei (Fig.11.6,7). Overall, the number of cells that could be stained with the pH3 antibody was low, possibly owing to the fact that cell-cycle is not fast. We therefore were unable to determine whether and how fast *Cdkn1b* or *Mrf* misexpression led to a withdrawal from cell cycle.

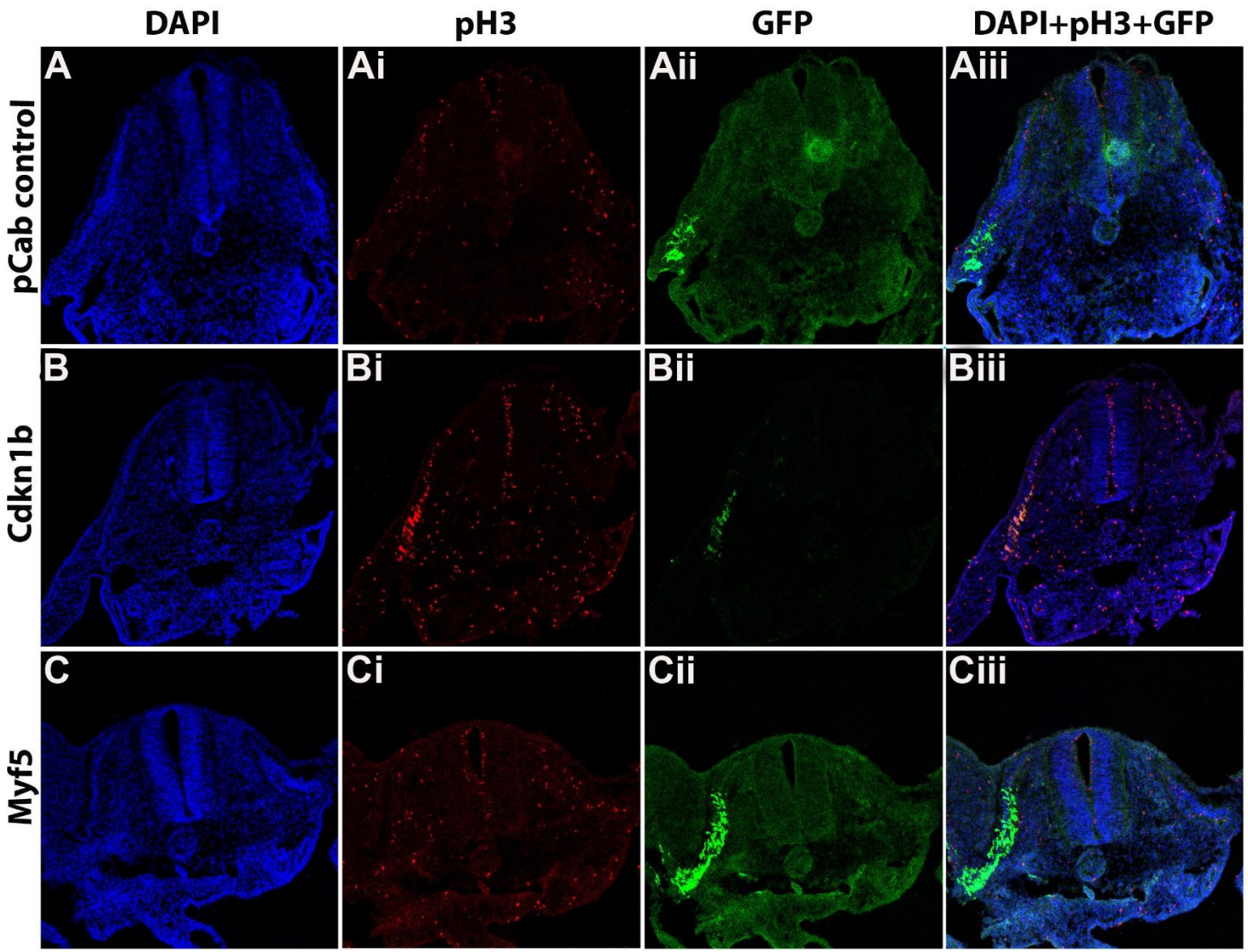
DAPI
pH3
GFP
DAPI+pH3+GFP
pCab control
Cdkn1b
Myf5
A
Ai
Aii
Aiii
B
Bi
Bii
Biii
C
Ci
Cii
Ciii

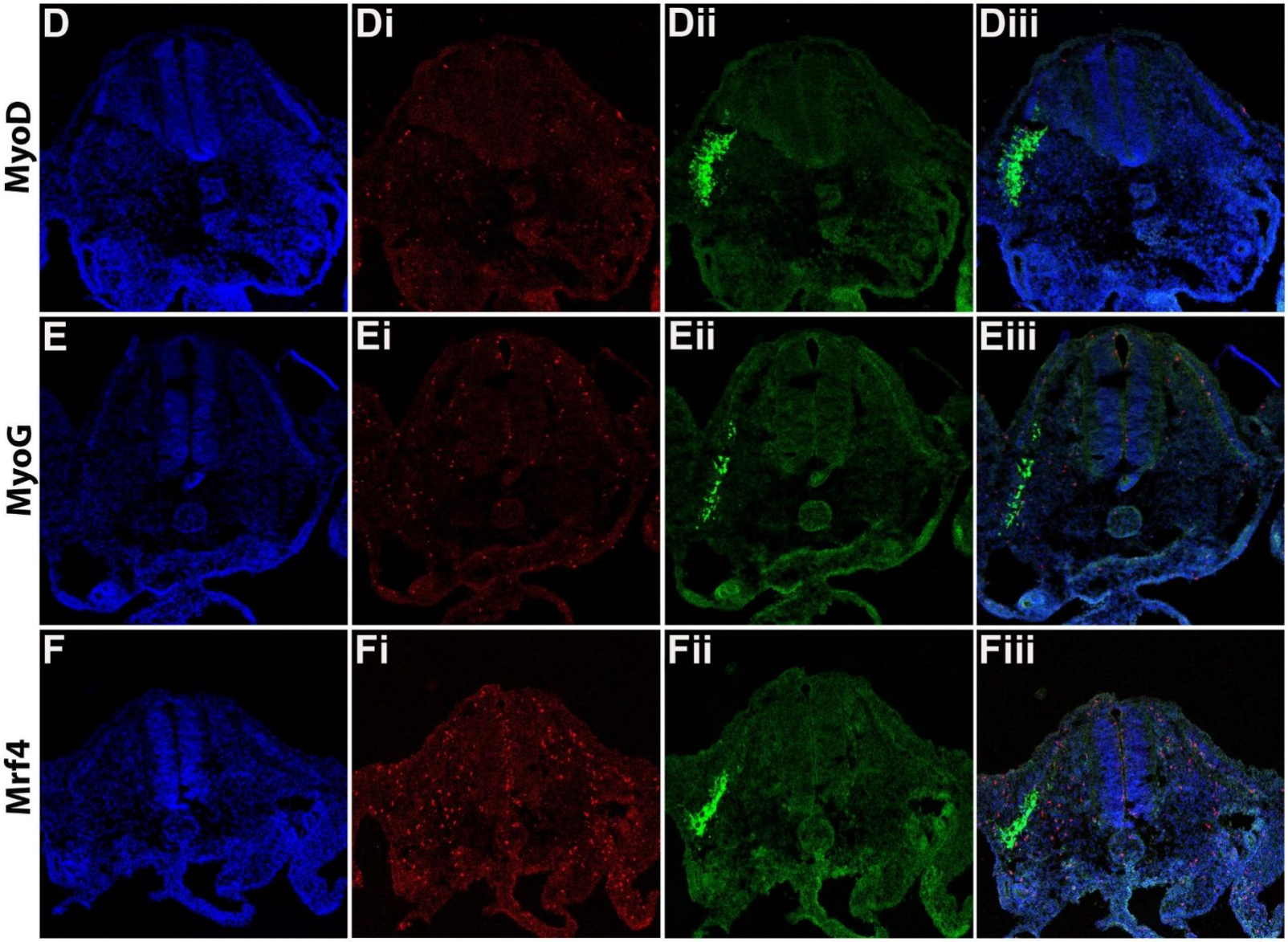
D
Di
Dii
Diii
MyoD
E
Ei
Eii
Eiii
MyoG
F
Fi
Fii
Fiii
Mrf4

Figure 11. 6 Misexpression Mrf and Cdk1b genes; analysis for cell cycle withdrawal (pH3 staining).
Embryos were electroporated with plasmids encoding the factor shown and GFP and grown to HH20. Fluorescence was visualised at the microscope. Embryos were treated in OCT (see material and methods) and section at the cryostat at 15 µm. The sections were treated with fluoresce immunohistochemistry for pH3 (anti-phospho-Histone H3) anti GFP and DAPI. Analysis of the EP embryos doesn't show any significant change in the staining.

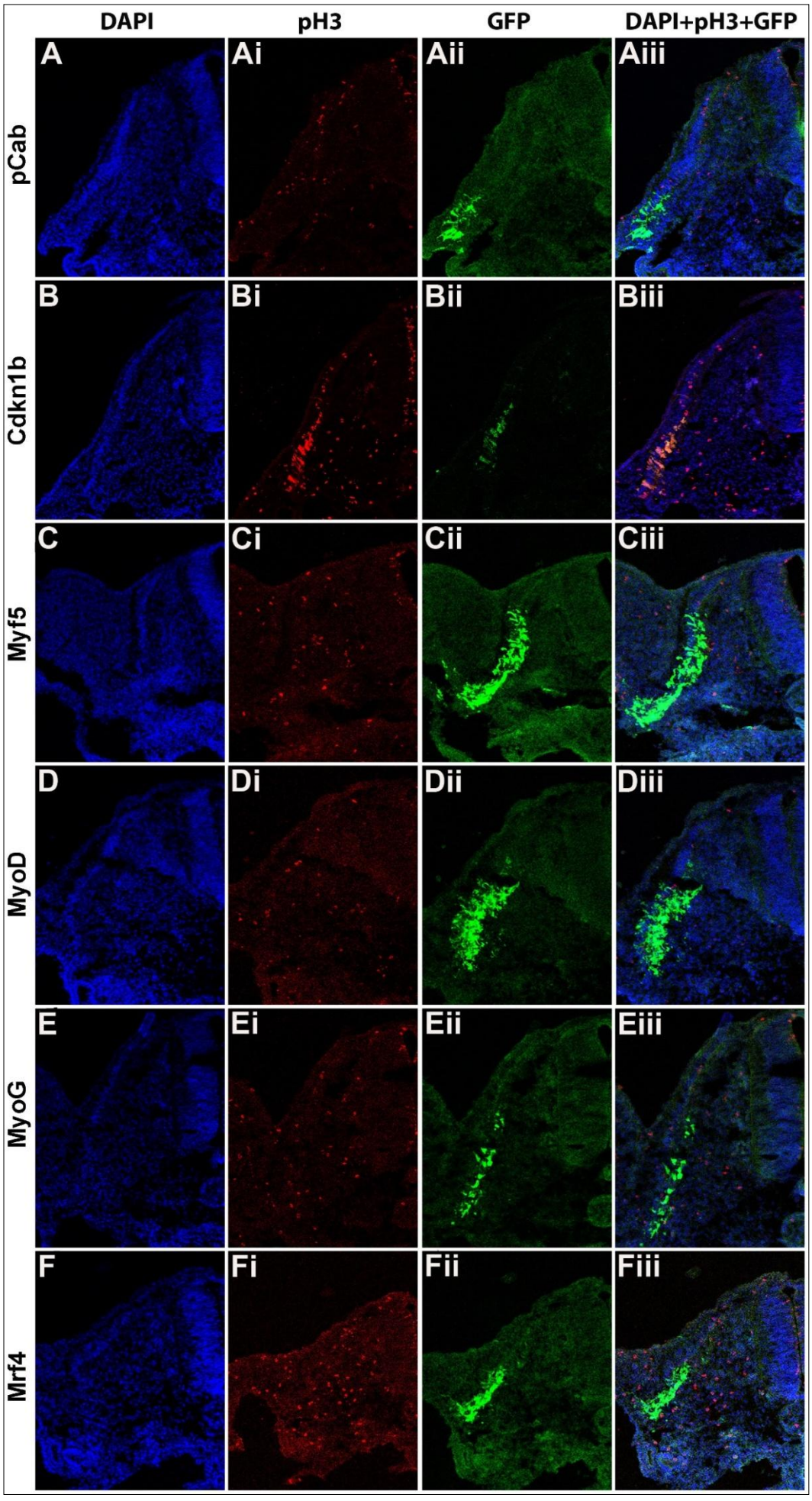
DAPI
pH3
GFP
DAPI+pH3+GFP
pCab
Cdkn1b
Myf5
MyoD
MyoG
Mrf4
A
Ai
Aii
Aiii
B
Bi
Bii
Biii
C
Ci
Cii
Ciii
D
Di
Dii
Diii
E
Ei
Eii
Eiii
F
Fi
Fii
Fiii

Figure 11. 7:Misexpression Mrf and Cdk1b gens; analysis for cell cycle withdrawal (pH3 staining) (detail lip of the somite)

Embryos were electroporated with plasmids encoding the factor shown and GFP and grown to HH20. Fluoresce was visualised and the microscope. Embryos were treated in OCT (see material and methods) and section at the cryostat at 15 um. The sections were treated with fluoresce immunohistochemistry for pH3 (Anti-phospho-Histone H3) anti GFP and DAPI. DAPI (A-F), pH3 (Ai-Fi), GFP (Aii-Fii) and overlapped images (Aiii-Fiii). Pictures were taken a higher magnification for the lip of the somites to have more detailed images of the staining. The analysis of the immune staining doesn't show any significant change

11.2.1.2 Effect on myogenesis

To test whether *Cdkn1b*, alone or in combination with *Mrf* might be able to accelerate myogenesis in developing muscle precursor, we misexpressed *Cdkn1b* alone and in combination with *MyoD* and *MyoG*, re-incubated the embryos for 18 hours and performed a MF20-DAB antibody staining (Fig.11.8; results are summarised in Table 11.2). , no upregulation or changes were observed (Fig. 11.8 B,C). Yet, none of the embryos displayed ectopic expression of sarcomere Myosin and the electroporated side was comparable with the control one.

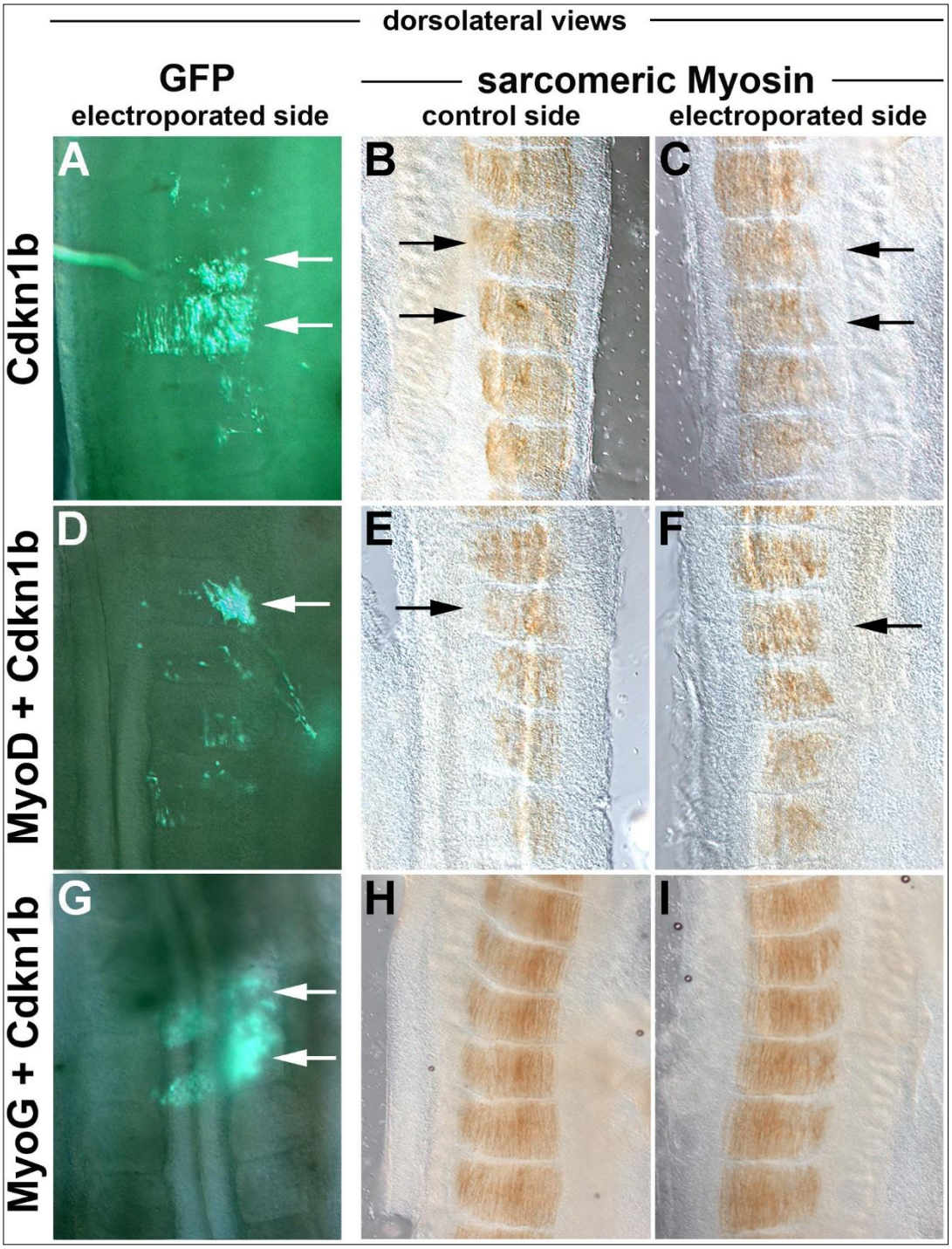
dorsolateral views
GFP
electroporated side
sarcomeric Myosin
control side
electroporated side
Cdkn1b
MyoD + Cdkn1b
MyoG + Cdkn1b
A
B
C
D
E
F
G
H
I

Figure 11. 8: Misexpression of Cdk1b alone or with Mrf; analysis for sarcomeric Myosin expression
Embryos were electroporated with plasmids encoding the factor shown and GFP and grown to HH20. GFP was visualised (arrowed in A, D, G) and sarcomeric myosin expression detected by antibody staining with DAB. No changes in sarcomeric myosin levels were detected when the control and electroplated sides were compared together.

11.3. Discussion

11.3.1. *Cdkn1b* is a likely regulator of cell cycle exit during early chicken myogenesis

The differentiation of the muscle stem cell is strictly related to the cell cycle control (333,426,441). Muscle precursor have to leave the cell cycle to differentiate and develop from myoblast to myocytes giving rise to muscle fibres. We hypothesised that this was the key step for cells to move forward into the differentiation. We decided to focus our attention on the expression of the Cyclin Dependent kinase, cyclin activators and inhibitors in chick embryos and see which one could be considered the best candidate to carry on our studies and find the best one that could be expressed in the somites push the cell to leave the cell cycle.

We realised that Cdkn1b showed an impressive resemblance during the *in situ* hybridisation comparable to Myf5 and MyoD. We therefore decided to focus our attention on this particular Cyclin inhibitor. We electroporated Mrfs constructs and analysed hybridising the antisense probe for Cdkn1b. All Mrfs constructs caused an upregulation of Cdkn1b mRNA levels. The analysis of the embryos electroporated with Mrfs constructs with the antibody against the Phosho Histone H3 Serine 10, show that we could not detect a satisfying quantity of data from the cryostat sections and we could not see any difference between the electroporated and the non electroporated sides. Due to time constraints an insufficient number of repeat experiments were performed to make a conclusive analysis. Also, proper quantification by cell counting was not possible to provide a robust quantification. Given more time, these experiments would be repeated to provide more conclusive analysis. In Figure 10.6-7 Bi-iii, antibody staining can be seen in the electroporated area. Again, as the number of repeats was too low, the significance of this observation and its validity cannot be commented on with complete certainty.

Future experiments would require comparison with a positive control for Ph3, the most common one is the immunostaining in mouse or human carcinoma cells. These cells have a high rate of division so the antibody would detect mitotic phosphorylation of H3 Thr3 in prophase and its dephosphorylation during anaphase (442).

Cell counting could be performed using the program CellProfiler (cellprofiler.org) or ImageJ (imagej.net). These programs efficiently create boundaries between the cells visible in the image to ensure that cells in close proximity aren't excluded. The programs can be set for specific fluorescence wavelengths and will repeat the counting process several times giving an average number of the cells. These programs can be used both for cultured cells and in sectioned tissues.

11.3.2. *Cdkn1* gene misexpression does not advance myogenesis from developing muscle precursor

When we compare the staining of the Mrfs mRNA levels with Cdkn1b, we realised that from the sections we could confirm that the staining of this cyclin inhibitor is very similar to Myf5 and MyoD and MyoG. The staining is along the line of the myotome and it is reaching the dorsomedial and the ventrolateral lip. We decided to misexpress Cdk1nb in the somites and to use the co-electroporation technique to expresses the cyclin inhibitor with MyoD and MyoG. If we were able to force the cell to leave the cell cycle, may be Cdkn1b alone would be enough to give an upregulation in the Myosin staining, and the co-electroporation with MyoD and MyoG would have caused the cell to leave the cycle and in the same time to push the cell to differentiate. In all three cases we did not see any changes in the Myosin staining, all the somites, are showing the same pattering comparable with the control. The N.number (Table 10.2) of the experiments are confirming the results obtained and the reproducibility of the experiment itself. We hypothesised that even in this case there is a time frame in which the muscle precursor are highly protected and the use of cyclin inhibitors does not influence the exit from the cell cycle. In a forming embryo, the cells must replicate to ensure a high number of cells to create a new tissue, but at the same time they have to ensure to renew the stem cell pool. This is an important step in embryogenesis. The stem cell pool is essential for renewing or substituting damaged tissue in adulthood, and consequently its control and maintenance is important. Therefore in the embryos the myoblasts cannot leave the cell cycle too early because they have to make sure to renew the stem cell pool. We hypothesised that there could be another mechanism of control which contributes to the protection of the stem cell state. Looking at the literature we found that MyoD protein could be inactivated by phosphorylation of specific residues (207,443). MyoD contains several consensus cyclin-dependent kinase (CDK) phosphorylation sites which if mutated can protect the MyoD protein from phospho-regulated degradation (444). In line with these findings, we decided to use murine phospho-incompetent MyoD constructs for studying its misexpression in HH16 chicken somites. The mutated mouse MyoD should be constitutively activated because it is protected from phosphorylation and therefore is hypothesised to cause upregulation of Myosin expression levels.

Table 11. 2: Summary N. number of the experiments in Chapter 11.

Numbers displayed as: total: wildtype/upregulated/downregulated

The table summarises the N.number of the experiments shown in Chapter 11: immunohistochemistry, *in situ* hybridisation and electroporation. We saw upregulation of mRNA levels with the electroporation of Mrf constructs (Myf5, MyoD, MyoG and Mrf4) analysed with the antisense probe for *Cdkn1b* after 18hr of incubation. (Blue shade).

EP targeting the embryonic muscle precursor in the somitic dermomyotome			
specimen analysed for	**sarcomeric Myosin (MF20)**	**Cdkn1b mRNA**	**pHistone3**
	18h		
pCab	4:4/0/0	2:2/0/0	3:3/0/0
Gg Myf5		3:1/2/0	2:2/0/0
Gg MyoD		3:0/3/0	2:2/0/0
Gg MyoG		2:0/2/0	2:2/0/0
Gg Mrf4		3:1/2/0	1:1/0/0
Gg MyoD+MyoG		3:1/2/0	
Gg Cdkn1b	3:3/0/0		3:3/0/0
Gg Cdkn1b + MyoD	4:4/0/0		
Gg Cdkn1b + MyoG	3:3/0/0		

Chapter 12

12 Inactivation of MyoD by phosphorylation

12.1 Introduction

In chapters 5-9, we systematically explored whether chicken *Mrf* genes, either alone, or in combination with other *Mrf*, with *Mef2c* and with *Six1*, could drive premature paraxial mesoderm (chapter 5) or developing muscle promoter (chapters 6-9) out of their stem cell state and into myogenesis. Our data indicated that *Mrf* were able to activate a small collection of early myogenic genes, but were not able to enforce terminal differentiation. This suggested that it is not the absence of myogenic factors but rather a more active mechanism that protects the muscle stem cell state. In Chapters 10 we investigated whether the continued presence of the premyogenic and muscle stem cell factor Pax7 might contribute to the protection of the muscle stem cell state, and found that indeed was the case. Since Pax7 promotes proliferation, we in Chapter 11 explored whether the continued ability of cells to undertake mitosis might prevent terminal differentiation. However, this was not the case. We were therefore left with: (i) Mrf can initiate the transcription of a few myogenic genes and (ii) Mrf are unable to activate the full complement of myogenic genes that ensures expression of muscle structural genes and removal of premyogenic/ stem cell factors. This suggested that possibly, the efficacy of *Mrf* as transcription factors mighty be limited.

A number of molecular studies have established that MyoD protein activity can be negatively regulated. MyoD can be inactivated through sequestration by the basic-helix-loop-helix protein association with proteins Id or when interacting with the histone deacetylases HDAC4 and HDAC5 (385,387). MyoD may also be subjected to inactivating phosphorylation executed by Cyclin Dependent Kinase (Cdk) activity, specifically Cdkn1 and 2 (443,445). In proliferating C2C12 mouse myoblasts in vitro, high levels of phosphorylated MyoD are found which gradually decrease during muscle differentiation. Moreover, mouse MyoD contains a Cdk consensus site comprising of a serine at position 200 which is phosphorylated *in vivo* in myoblasts and *in vitro* by Cdk1 and Cdk2. Phosphorylation of MyoD by Cdks has been shown to target the protein for rapid degradation by the ubiquitin pathway (206). When serine 200 was changed to a non-phoshorylateable alanine (S200A mutation), the mutant protein showed great ability to convert 10T1/2 fibroblast to muscle cells (206,443,445). Our expression analysis for cell cycle regulators revealed that Cdk1 and 2 are expressed in somites (see chapter 9). Moreover, experiments conducted in Xenopus 2-cell stage embryos suggested that the S200A mutation of mouse MyoD has a stronger myogenic effect that wildtype mouse MyoD, and this effect was enhanced when additional amino acids were rendered non-phosphorylateable (A. Philpott and L. Harwick, personal communication). We thus wondered

whether also in chicken muscle promoter, MyoD phosphorylation might prevent MyoD from activating genes required for terminal differentiation.

To explore this possibility, Professor Anna Philpott and Dr. Laura Harwick kindly provided us with 3 constructs, expressing a variant of wildtype mouse MyoD, mouse MyoD with the S200A substitution, and a penta-mutant construct with 5 substitutions S(200, 262, 277, and 298)A; T296A, which protects against MyoD hyperphosphorylation (personal communication with S. Dietrich). These constructs were cloned in the pCS2+ vector, allowing transcription of mRNA from a sp6 promoter and misexpression in amniote cells from the CMV promoter (see chapter 4). We injected the *in vitro* transcribed mRNAs in Xenopus 2-cell stage embryos to confirm their biological activity. We then electroporated the constructs into chicken HH15/16 flank somites and once more, analysed for the premature expression of sarcomeric Myosins after 18 hours of re-incubation. We found that in contrast to the frog blastomeres, developing chicken myoblasts could not be forced into differentiation.

12.2 Results

12.2.1 Misexpression of mouse *MyoD* mutant constructs in Xenopus embryos

To test the biological effect of the constructs we decided to use the mouse *MyoD* constructs in the Xenopus system, following the strategy initially used when validating the chicken constructs in Xenopus embryos (Chapter 4). The three mouse *MyoD* constructs were transcribed *in vitro* to obtain mRNA for injection into 30 2-cell stage Xenopus embryos, utilising βGal as a lineage tracer. Embryos were harvested at stage 26 and analysed using the MF20 antibody to detect sarcomeric Myosin. Embryos were compared to those obtained by injection of βGal mRNA or RNA for βGal and chicken *MyoD*. The results are summarised in Table 12.1.

When mRNA encoding the lineage tracer (Fig. 12.1 A-B) alone or with an mRNA for chicken *MyoD* was injected (Fig. 12.1 C-D), no ectopic expression of sarcomeric Myosins was observed on the injected side. When mRNA for mouse *MyoD* was injected, survival rates of embryos was lower that survival rates of embryos injected with chicken *MyoG* or Mrf4 *mRNA*. Of the 3 surviving embryos, 2 showed ectopic expression of Myosin expression and gastrulation defects akin to those obtained with chicken *MyoG* and *Mrf4* (Fig. 12.1 E-F, compare with Fig. 4.7 I-L). When the S200A mutant of mouse MyoD was used, 13 of 30 embryos survived, with 12 showing ectopic MF20 staining and gastrulation defects (Fig. 12.1 G-H). Upon injection of the penta-mutant mRNA, 2 embryos with normal Myosin expression survived. The remaining 28 embryos were too malformed to reach stage 26. Thus, when arranging the constructs with respect to the severity of phenotypes they cause, the order from weaker to stronger is: mouse S200A MyoD, chicken MyoG/Mrf4, mouse MyoD, mouse penta-mutant of MyoD.

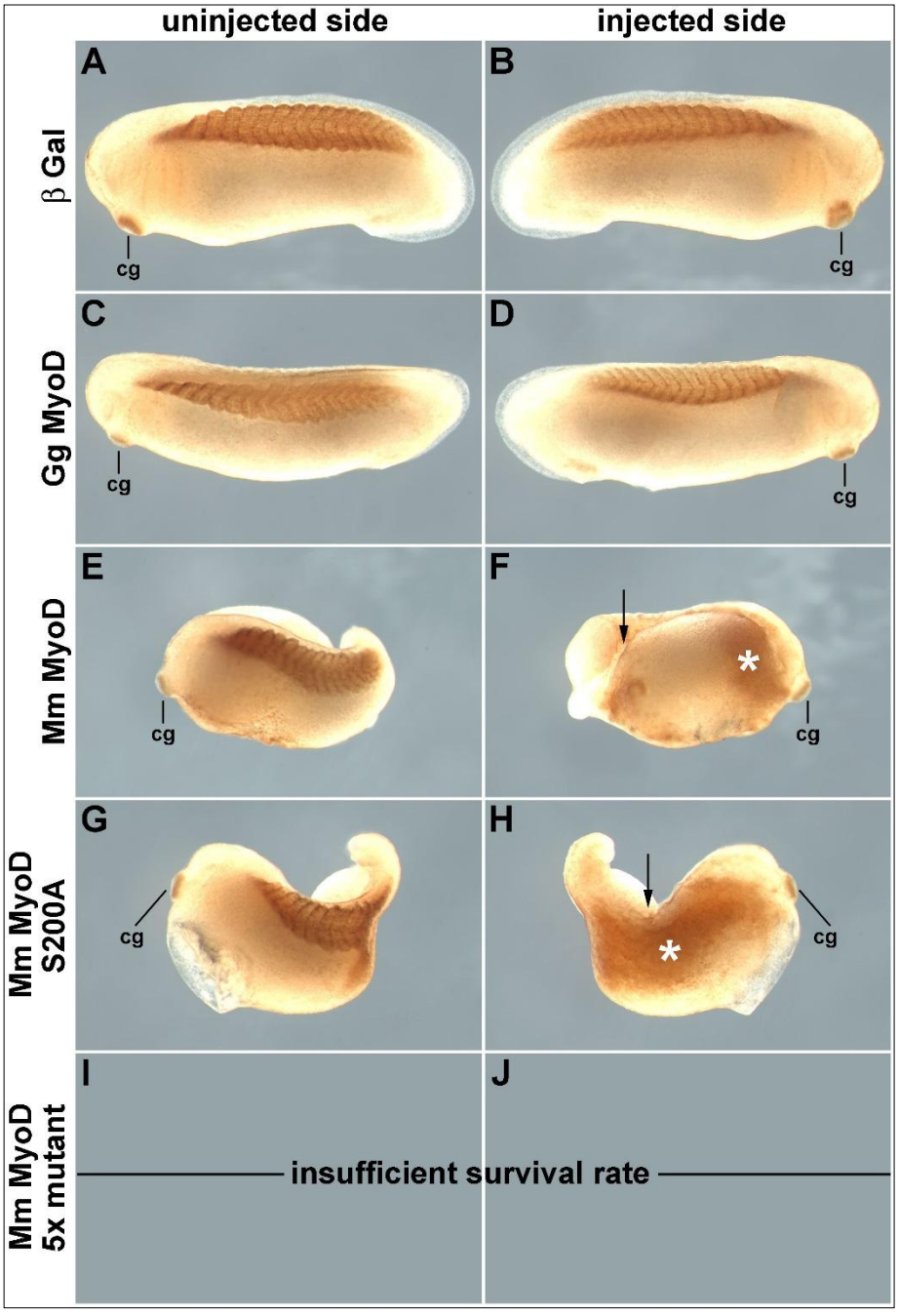
uninjected side
injected side
β Gal
Gg MyoD
Mm MyoD
Mm MyoD S200A
Mm MyoD 5x mutant
A
B
C
D
E
F
G
H
I
J
cg
insufficient survival rate

Figure 12. 1: Misexpression of WT and phosphorylation-incompetent mutant mouse MyoD proteins in xenopus embryos causes upregulation of Myosin expression between two-cell and stage 26

A batch of *Xenopus leavis* embryos were subdivided into 9 groups of 30 embryos. One set of embryos was left to develop as normal (A,B); of the other embryos, one cell each was injected with βGal mRNA (C,D), or with βGal mRNA plus the *Mrf* RNA (E,F,G,H). Embryos were collected when the control embryos reached stage 26. Representative embryos were photographed, showing the untreated (C,E,G; rostral to the left) and treated sides (D,F,H; rostral to the right) in lateral views. Embryos injected with mouse MyoD appeared largely normal (E,F). Embryos injected with the S200A mutant of mouse *MyoD* showed similar survival rates (G,H), but most embryos had ectopic MF20 staining (asterix F,H) and truncated bodies, the latter suggesting a gastrulation defect (arrowed F,H). Upon injection of the RNA encoding the S(200, 262, 277, 298)A; T296A mutant of mouse *MyoD*, only two, healthy-looking embryos survived, suggesting that most embryos became too malformed to develop beyond gastrulation. Abbreviations: cg, cement gland.

12.2.2 Misexpression of mouse *MyoD* and *MyoD* mutants in chicken somites

Given that we were able to confirm the biological activity of the mouse constructs, we next electroporated them in the chicken system. Since the pCS2+ vector containing the mouse sequences does not encode the GFP lineage tracer, these constructs were co-electroporated with pCAB-GFP vector. The pCS2+ vector not carrying any insert was co-electroporated with pCAB-GFP vector as a negative control. Electroporation of HH15/16 embryos was performed in a consistent manner with previous experiments; embryos were harvested after 18 hours of re-incubation as before (see Chapter 2 for Methods). Electroporated cells expressing p-Cab-derived GFP fluorescence were located with fluorescence microscopy; embryos were analysed with immunohistochemistry using the MF20 antibody to detect sarcomeric Myosins and re-photographed as before (Fig.12.2). The results are summarised in Table 12.2. This analysis revealed that in control and experimental somites, sarcomeric Myosins were expressed in the myotomes, as expected. However, no upregulated or ectopic expression ever occurred. Thus, different to the frog system, phosphorylation-resistant mouse MyoD was unable to advance myogenesis in developing myoblasts.

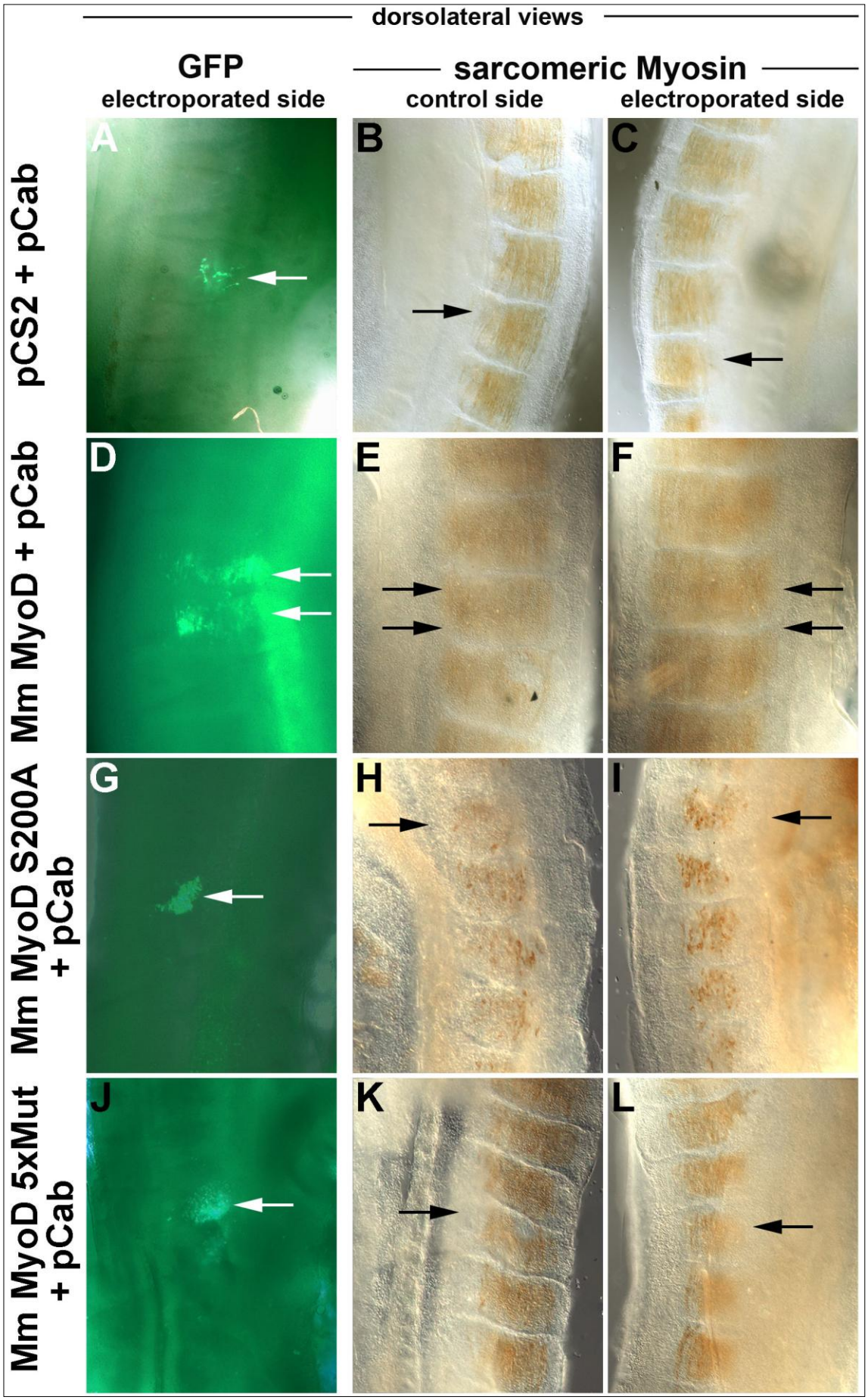
dorsolateral views
GFP
electroporated side
sarcomeric Myosin
control side
electroporated side
pCS2 + pCab
Mm MyoD + pCab
Mm MyoD S200A + pCab
Mm MyoD 5xMut + pCab
A
B
C
D
E
F
G
H
I
J
K
L

Figure 12. 2: Misexpression of WT and phosphorylation-incompetent mutant mouse MyoD proteins in the chick somites is insufficient to upregulate Myosin expression between HH16 and HH20

Embryos were electroporated with plasmids encoding the factor pCS2, MyoD+pCAB, MyoD S200A+pCAB, MyoD, 5 Mut+ pCAB. After electroporation, the embryos were reincubated until HH20. GFP was visualised (arrows in A,D,G,J) and sarcomeric Myosin expression detected by antibody staining by immunohistochemistry. The embryos were dissected following the line of the neural tube from the caudal to the rostral part of the embryos, this allowed the comparison between the two sides of the neural tube, the control and electroporated (B-C, E-F, H-I, K-L). No changes in sarcomeric Myosin levels were detected when the control and electroplated sides were compared.

12.2.3 Comparative analysis of putative phosphorylation sites in gnathostome MyoD protein sequences

The misexpression of the phosphorylation-resistant mouse *MyoD* constructs in chicken somites did not lead to premature entry of muscle precursor into differentiation. However, during our initial analysis of Mrf sequences, we had noticed differences between gnathostome Mrf proteins (see Chapter 4). We therefore wondered whether the amino acids mutated in mouse MyoD might not be conserved, and hence, avian MyoD function might not be controlled in the same fashion as that of mouse MyoD. To extend this analysis, we comparatively analysed which and how many amino acids in could be subjected to phosphorylation in mouse (curated and variant version), diapsid (chicken, python), Xenopus, zebrafish, and elephant shark MyoD, using the Netphos 2.0 server to computationally predict phosphorylation sites. Fig. 12.3 shows an alignment of chicken and zebrafinch MyoD sequences, the mouse MyoD sequence obtain from the Ensemble and NCBI data bases, the variant version of MyoD that was used as control in A. Philpott's and L. Harwick's constructs, and the two mutant MyoD proteins derived from that. This alignment shows that S200 of mouse MyoD is located at the N-terminus of the Myf5 domain, and this region is strongly conserved also in the avian MyoD proteins. However, of the remaining four amino acids mutated in the S(200, 262, 277, and 298)A; T296A of mouse CAA3836.1 MyoD, only two are conserved in the avian MyoDs and hence may not be relevant for MyoD activity in birds. Interestingly, in birds, the C-terminus of MyoD contains many more serines, including a serine also conserved in the mouse protein. This suggests that inactivating phosphorylation of the misexpressed MyoD proteins may well be possible. Indeed, when analysing gnathostome MyoD proteins for potential phosphorylation sites, these serines were predicted as phosphorylation targets with high statistical significance (Fig. 12.4). Counting potential phosphorylation sites (Table 12.3), we found little difference in the number of potential threonine and tyrosine phosphorylation sites but a significant difference with respect to possible serine phosphorylation sites, with the mouse having 14, elephant shark 16, zebrafish 17, but Xenopus 21, chicken 22 and python 26. This suggests that non-mammalian MyoD may be under much tighter control than non-mammalian MyoD.

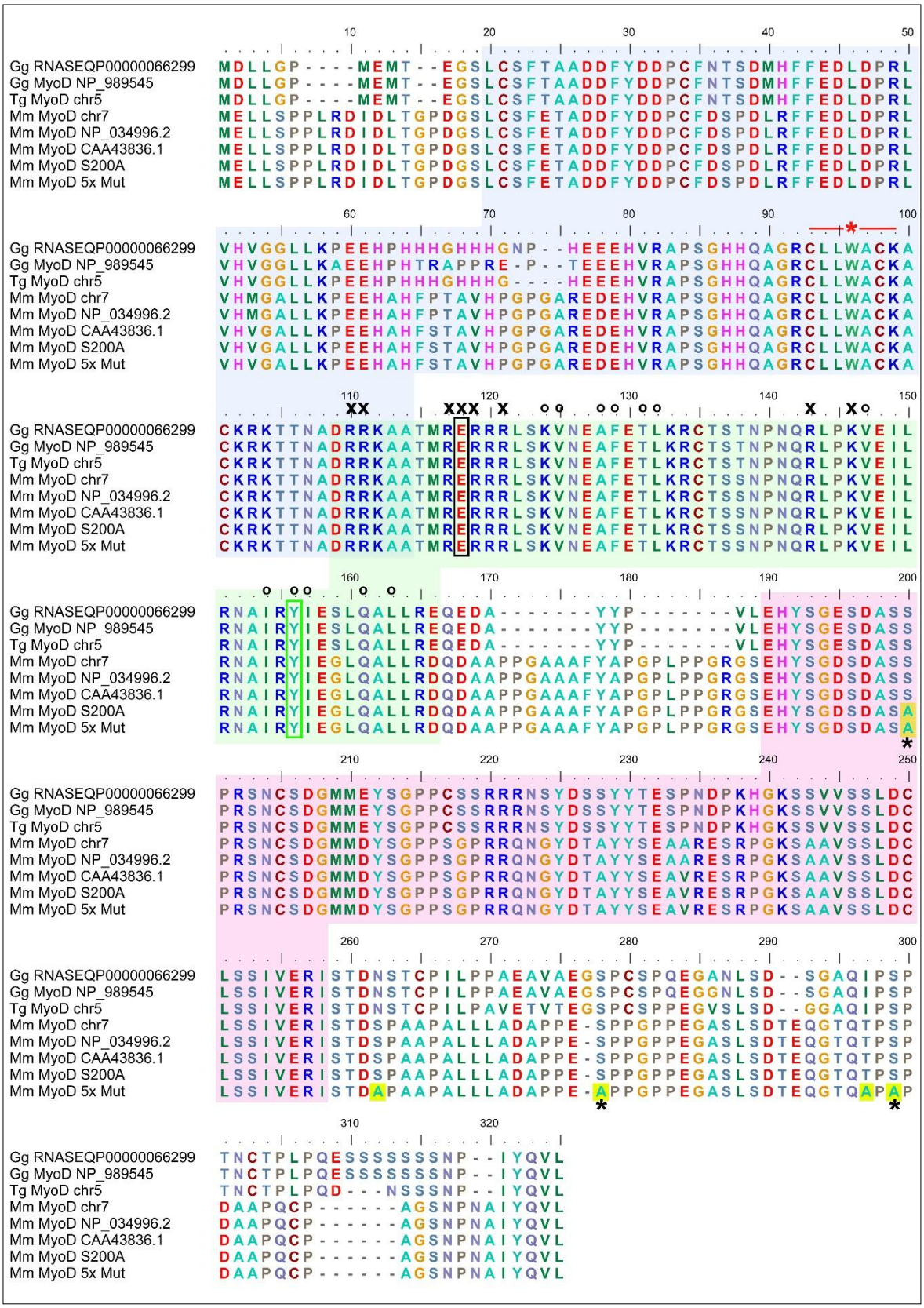
Gg RNASEQP00000066299
Gg MyoD NP_989545
Tg MyoD chr5
Mm MyoD chr7
Mm MyoD NP_034996.2
Mm MyoD CAA43836.1
Mm MyoD S200A
Mm MyoD 5x Mut

Figure 12. 3: Alignment of chicken (Gg), zebrafinch (Tg) and mouse (Mm) wild type MyoD protein sequences with mouse (Mm) phosphorylation-incompetent mutant MyoD sequences

Protein sequences shown in one-letter code. Blue shading: the alpha-helical basic domain involved in DNA binding; the Pbx/Meis binding motif N-terminal of the core basic domain indicated by a red line, the conserved tryptophan indicated by an asterisk. Green shading: the helix-loop-helix domain; amino acids required for protein dimerisation were marked with "o", amino acids required for DNA binding with "X", and the amino acid determining binding specificity to the CANNTG-E-box was marked with a black frame. Pink shading: the Myf5 domain involved in gene activation/ transactivation; core amino acids 246-258. The tyrosine at position 157 that, when phosphorylated, stabilises MyoD indicated by a green box. The serine at position 200 targeted by Cdk1 and Cdk2 and converted to an alanine in the S200A mutant was highlighted in yellow. Also highlighted in yellow: the four serines and the threonine converted to alanines in the S(200, 262, 277, 298)A; T296A mutant. Note: the mouse sequences used to generate the MyoD mutants shows slight variations in amino acid sequence to the previously annotated sequences at positions 53, 66 and 234. Also note: with the exception of the serine in position 262 and the threonine in position 296, the targeted serines were conserved in amniotes (black asterisks; see also Chapter 4 Appendix Fig.1B). Yet the high serine content in the chicken and zebrafinch MyoD C-termini (and in other diapsid and anapsid proteins) suggested that in avians, an even higher degree of MyoD phosphorylation may occur compared with mammals.

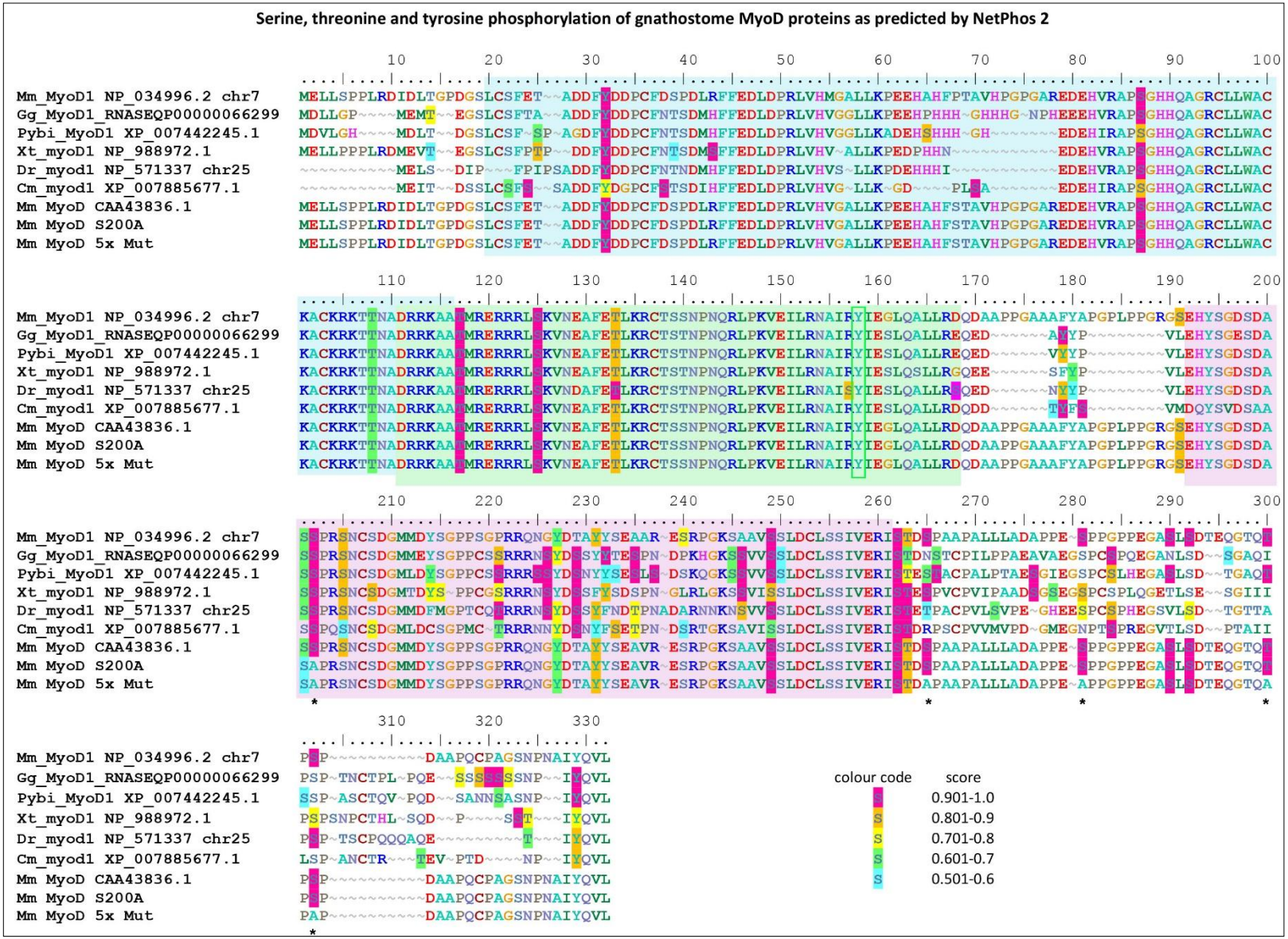
Serine, threonine and tyrosine phosphorylation of gnathostome MyoD proteins as predicted by NetPhos 2
Mm_MyoD1 NP_034996.2 chr7
Gg_MyoD1_RNASEQP00000066299
Pybi_MyoD1 XP_007442245.1
Xt_myoD1 NP_988972.1
Dr_myod1 NP_571337 chr25
Cm_myod1 XP_007885677.1
Mm MyoD CAA43836.1
Mm MyoD S200A
Mm MyoD 5x Mut
colour code
score
0.901-1.0
0.801-0.9
0.701-0.8
0.601-0.7
0.501-0.6

Figure 12. 4: Alignment and prediction of phosphorylation sites in gnathostome MyoD proteins

Serine (S), threonine (T) and tyrosine (Y) phosphorylation sites predicted by the NetPhos 2.0 Server (http://www.cbs.dtu.dk/services/NetPhos/) as above the threshold score of 0.5 were shown for a collection of gnathostome MyoD proteins, the value of the phosphorylation is indicated by the colour code, from magenta with the higher score and more likely to be phosphorylated to blue shade with a low value.

We also showed the mouse protein prediction of the constructs kindly provided by A.Philpot. The prediction of the phosphorylated serine is significantly higher in chicken, python and *Xenopus tropicalis* whereas the mouse proteins have the lowest number of phosphorylation sites.

This suggested that the mouse MyoD might be less prone to inactivating phosphorylation than the MyoD proteins of other species.

12.3 Discussion

12.3.1 Mouse MyoD and phosphorylation-independent versions of mouse MyoD promote myogenesis from Xenopus early blastomeres

The injected of the mouse MyoD constructs showed a strong phenotype in Xenopus embryos at stage 26. The use of the mouse wild type showed upregulation of the Myosin at ectopic level, while the mouse construct with the single mutation of serine 200 to alanine, caused change a drastic change in the morphology of the embryos influencing even the control side. Mouse MyoD has fewer sites that might be subject to inactivating phosphorylation, providing an explanation as to why mouse MyoD but not chicken MyoD could force myogenic differentiation of blastomeres. The position of the serine in the MyoD sequence of these three species could be the key to understand why we could not see any changes in the Myosin expression after the MyoD chicken injection. We hypothesise that the chicken MyoD could have been recognised and phosphorylated before it could have any effect in the xenopus system. While on the other hand, the presence of fewer phosphorylation sites in the mouse MyoD may be insufficient to allow post-translational silencing and consequently allowed ectopic expression of Myosin in xenopus. In this case the MyoD has not been recognised by the host system and it is permitted to affect myogenic development. The 5x mutations but not the S200A mutation aggravated this phenotype. The 4 additional mutations were all located at the C-terminus, underlining our suspicion that the C-terminus is an important functional domain (see chapter 4).

It would be interesting to carry on further the experiments and misexpress elephant shark MyoD or zebrafish or combining chicken with frog MyoD with the mouse C-terminus, to test whether the lower number of phosphorylation sites renders the protein biologically active.

12.3.2 Mouse MyoD and phosphorylation-independent versions of mouse MyoD do not drive terminal muscle differentiation from developing chicken muscle precursor

The larvae of a frog develop via free-feeding and the time of development is a lot faster if compared to another vertebrate like a chick. A tadpole of a frog is able to swim or anyway move and respond to stimulus at a young stage of formation, around st26 (378). This means that the tadpole has already a muscle structure to allow the larvae to move and of course the formation of the first myogenic cells begin very early in development. This could be link at the results that we obtained after the electroporation of the mouse constructs. It could be that in frog there may be less protection against premature myogenesis. Another possibility is that in blastomeres, since they normally do not encounter MyoD, they are may be little protection against the activity of specific differentiation genes, whereas in myoblasts, since there only one step away from differentiation, this has to be tightly controlled. The experiments that mimic the misexpression of

MyoD in blastomeres cannot be done in chicken. However, once the Pax7 promoter is available from the frog, it should be possible to misexpress Mrf specifically in frog myoblasts. It would be interesting to see whether to not they enter myogenesis as easily as blastomeres.

12.3.3 Promoters of MyoD target genes may be closed.

In undifferentiated myoblasts, the unscheduled activation of the differentiation program is precluded by recruitment of histone deacetylases (HDACs) on the chromatin of muscle genes (446). Class I HDACs preferentially associate with MyoD (and possibly other muscle bHLH proteins), while class II HDACs are dedicated repressors of MEF2-dependent transcription. These interactions prevent the local hyperacetylation on the regulatory elements of muscle genes. During muscle differentiation, HDACs are displaced from muscle bHLH and MEF2 proteins by distinct mechanisms, thereby allowing productive interactions with acetyltransferases p300 and PCAF. Histone methyltransferases belonging to the SET-domain containing families are other critical mediators of muscle gene repression in myoblasts. For instance, Suv39 h1-mediated methylation of H3 lysine 9 and Polycomb-mediated trimethylation of H3 lysine 27 are essential epigenetic modifications that restrict the temporal expression of muscle genes in myoblasts. The enzymatic component of the Polycomb complex (PcG), the H3-K27 methyltransferase Ezh2, is recruited to the chromatin of muscle regulatory regions via interaction with YY1 binding site and its interaction with HDAC1 forms a repressive complex (193,447).

Data showed that in primary myoblasts, Snail-HDAC1/2 repressive complex binds and activate excludes MyoD from its targets. Snail binds E-box motif that are G/C rich in their central diucleotides and such sites are almost exclusively associated with genes expressed during differentiation (448). But in contrast Snail does not bind the A/T-rich E-boxes associated with MyoD targets in myoblasts. The complex Snail1-HDAC1/2 prevents MyoD occupancy on differentiation-specific regulatory elements and the change from Snail to MyoD binding often results in enhancer switching during differentiation. All these results underlined a regulatory paradigm that directs distinct gene expression programs in progenitors versus terminally differentiated cells (449).

Table 12. 1: Injected Xenopus with mouse MyoD showed upregulation of ectopic Myosin and malformation during development

In each experiment, 30 2-cell stage *Xenopus laevis* embryos were used. These embryos were either left to develop (control 1), injected with 250 pg β-Gal mRNA (control 2) or injected with a mix of 250 pg β-Gal mRNA and 1 ng of Mrf RNA. RNA was delivered in a total of 5 nl of water. Note that the RNA injection reduced the survival rate by 40%. Injection of chick *Myf5* or *MyoD* RNA reduced the survival rates further, but surviving embryos appeared largely normal, sometimes displaying smaller heads (*MyoD*) or enlarged occipital somites (*Myf5*). Embryos injected with the S200A mutant of mouse *MyoD* showed similar survival rates, but most embryos had ectopic MF20 staining and truncated bodies, the latter suggested a gastrulation defect. When injected with chicken *MyoG*, chicken *Mrf4* or variant mouse *MyoD* RNAs, survival rates were poor, and most embryos were malformed. Upon injection of the RNA encoding the S(200, 262, 277, 298)A T296A mutant of mouse *MyoD*, only two, healthy-looking embryos survived, suggesting that most embryos became too malformed to develop beyond gastrulation.

Construct	No of experimental embryos	No of survivors at stage 26	WT	Malformed
-	30	30	11 analysed, all wild type	0
β-Gal	30	18	18	0
Gg Myf5+β-Gal	30	14	14	0
Gg MyoD+β-Gal	30	10	10	0
Gg MyoG+β-Gal	30	6	3	3
Gg Mrf4+β-Gal	30	5	1	4
Mm MyoD+β-Gal	30	3	1	2
Mm MyoD S200A mutant+β-Gal	30	13	1	12
Mm MyoD S(200, 262, 277, 298)A; T296A mutant+β-Gal	30	2	2	0

Table 12. 2: Number of electroporation in chicken embryos of the chapter 12

Numbers displayed as: total: wildtype/upregulated/downregulated

All the data collected from the electroporated mutant mouse constructs were summarised in this table. None of the electroporations showed upregulation of the Myosin.

EP targeting the embryonic muscle precursor in the somitic dermomyotome	
Specimen analysed for	**Sarcomeric Myosin (MF20)**
	18h
pCS2+ pCab*	5:5/0/0
Mm MyoD + pCab*	4:4/0/0
Mm MyoD S200A + pCab*	6:6/0/0
Mm MyoD 5xMut + pCab*	5:5/0/0

Table 12. 3: Number of predicted phosphorylation sites in gnathostome MyoD proteins

The number of serine (S), threonine (T) and tyrosine (Y) phosphorylation sites predicted by the NetPhos 2.0 Server (http://www.cbs.dtu.dk/services/NetPhos/) as above the threshold score of 0.5 are shown for a collection of gnathostome MyoD proteins. The number of sites in the mouse proteins expressed from the constructs kindly provided by A. Philpott are also shown. Note that the number in particular of predicted serine phosphorylation sites significantly higher in chicken, phyton and Xenopus tropicalis whereas the mouse proteins have the lowest number of phosphorylation sites. This suggests that mouse MyoD might be less prone to inactivating phosphorylation than the MyoD proteins of other species.

Animal species	Abbreviation	S	T	Y
Mouse	**Mm**	14	5	3
Chicken	**Gg**	22	5	5
Phyton	**Pybi**	26	6	6
Xenopus tropicalis	**Xt**	21	8	5
Zebrafish	**Dr**	17	8	6
Elephant shark	**Cm**	16	8	5
Mouse	**Mm CAA4336**	14	5	3
Mouse	**Mm S200A**	12	5	3
Mouse	**Mm 5x mutant**	9	4	3

Chapter 13

13 Conclusions

13.1 The stem cell state of developing muscle stem cells is temporally protected in vivo and the expression of Mrfs is insufficient to overcome this protected state

A critical step in muscle development is the transition from the fate-committed but proliferating muscle stem cell to the non-proliferating myocyte (125,126,135,145). The Mrf genes have long been established as regulators of this process due to their ability to drive muscle differentiation in non-myogenic cells in culture (450). Yet, it is not clear if Mrf expression is sufficient to start muscle differentiation in muscle precursor, or whether *in vivo* the muscle stem cell state is protected. The first aim of this study was to provide, in the avian model for somitic myogenesis, a side-by-side analysis of the key markers associated with the progression from an immature state of the paraxial mesoderm to myogenic commitment and, eventually, to myogenic differentiation. Our study also provided novel insight into the process of skeletal muscle formation (Chapter 3).

We misexpressed Mrfs and/or known cofactors in different avian embryonic stages and analysed the effects of genes expression by various molecular techniques such as *in situ* hybridisation and immunohistochemistry. The lack of Myosin upregulation following the misexpression of the Mrf constructs in HH4 embryos indicated that terminal muscle differentiation does not occur, therefore the protection of the stem cell state in the paraxial mesoderm is not overcome (Chapter 5). Co-misexpression of the Mrfs with cofactors in HH16 embryos did not overcome the muscle stem cell state protection but did show upregulation of Mef2c and Mrf family member transcription in the first 18hr of incubation after the electroporation. The misexpression of MyoD and the combination of MyoD and MyoG showed upregulation of Myosin protein levels after 42hrs of incubation, but these were the only combinations shown to be sufficient to change the phenotype of the targeted cells (Chapter 7). The reason for the observed lack of muscle differentiation was hypothesised to be due to the absence of myogenic co-factors. This hypothesis was tested with the misexpression of Mef2a and c and the use of Six1-GFP and Six1-VP16 fusion constructs. Upregulation of Myosin levels were only seen following Six1-GFP individual misexpression however, this unexpected result could be qualified as an artefact due to altered function of the fusion protein. Previous reports have highlighted the role of Pax7 in the maintenance of muscle precursor (91,451). Normally, Pax3/7-positive skeletal muscle progenitor cells, which are derived from the central dermomyotome region of the somites (141,142), are either activated to differentiate into skeletal muscle fibres through the myogenic regulatory

genes, or remain as a proliferating reserve cell population within the muscle mass (142,297,451). The lack of induced differentiation could therefore be explained by immunohistochemistry results that show Pax7 protein levels persist after the electroporation of the Mrf constructs. If the cells are under tight control to the premature differentiation, the level of Pax7 protein must remain high until the correct moment, whereupon the cells would be able to differentiate. Additionally, miR-206 microRNA, which represses Pax7 translation levels at the point of muscle stem cell differentiation (230,452), was shown by *in situ* hybridisation not to be upregulated after the misexpression of the Mrfs. Together, this data confirming that high Pax7 protein levels persist after the electroporations could be explained by the active protection of precursor against immature differentiation.

To evaluate the possible strategies for overcoming the protection of the muscle stem cell state we analysed the literature and found extensive data describing how the expression levels of cyclin inhibitors increase during differentiation of muscle precursor (438,427). Cyclin inhibitors force muscle precursor to withdraw from the cell cycle and differentiate into muscle cells (453). The analysis of Cdkn1b transcript levels in wild type HH14 embryos showed surprisingly strong levels of expression in the somites comparable with that of Myf5 and MyoD. We later discovered that misexpression of the Mrf constructs upregulated Cdkn1b mRNA levels. Consequently, we electroporated Cdkn1b individually and in collaboration with MyoD or MyoG but no combinations showed upregulation of Myosin expression levels.

13.2 Mrfs may be negatively phosphoregulated to inhibit differentiation and/or require additional signals to promote differentiation

The results so far reinforce the theory that muscle precursor present strong protection of their stem cell state that is difficult to overcome. Consideration of the literature for possible mechanisms of protection highlighted the importance of MyoD activation in growing Myoblasts through stabilisation by cyclin inhibitors (454). Conversely, phosphorylation by CDKs has been shown to inactivate MyoD (443,455). Kitzmann and colleagues showed that MyoD phosphorylation was higher in proliferative C2 Myoblasts but decreases during muscle differentiation. MyoD was subsequently shown to be phosphorylated at Serine 200 *in vitro* by Myoblast-derived Cdk1 and Cdk2 (443,456). Following this, a phospho-incompetent MyoD mutant (S200A) demonstrated great ability to convert 10T1/2 fibroblasts into muscle cells (443).

The data in the literature therefore suggested that use of the phospho-incompetent murine constructs would upregulate muscle differentiation due to the constitutively active MyoD protein. Our results however, did not corroborate this hypothesis *in vivo*. This result could be explained by

the fact that our experiments were performed *in vivo* in contrast to the *in vitro* studies shown in the literature. Alternatively, the use of a heterologous host in our experiments (mouse proteins in chicken host) could mean that there is incompatibility between the murine and chicken phospho-regulation of MyoD. Misexpression of the mutated murine MyoD construct was insufficient to enforce differentiation in chicken muscle precursor, but same experiment performed in xenopus showed ectopic expression of Myosin in the injected side. This could be explained by the fact that anamniote embryos require differentiated muscle cells early in development to allow the larvae to swim. This characteristic could allow the mouse constructs to easily upregulate the level of Myosin protein.

The inability of the Mrfs to force myogenic differentiation *in vivo* may be due to the added complexity given by extrinsic signalling from neighbouring tissues not present in cell culture experiments. The Mrfs do not act alone but in collaboration with numerous genes and signalling cascades in which many include protein kinases, phosphorylating enzymes. Little is known about kinase activity in Myogenesis and the signalling pathways that regulate satellite cell quiescence and activation as well as myocyte fusion but it is likely that numerous kinases could be involved in regulation of the Mrfs.

Kinase activity in Myogenesis is known to play a part in the formation of the myotube from a population of embryonic precursor cells or satellite cells (457,458). It has been shown that the presence of specific Wnt genes (Wnt1, Wnt7) can induce the activity of Protein Kinase A (PKA) thereby committing myogenic precursors to form a pool of dividing myoblasts (459). The presence of growth factors and other extrinsic components activate ERK1/2, Akt1 and cyclin D/CDK2, 4 and 6 to promote proliferation which act together with PKA to block differentiation (459). Intrinsic cell cycle signals regulate the level of cycles A, B and E which together with the respective CDKs promote cell cycle progression, inhibiting differentiation. While myoblasts expand, their cell-cell contacts can switch off ERK which will silence cyclin D/CDK2,4 which inhibits additional proliferation (460). At this point, cell-cell contacts can activate p38 promoting differentiation. The activity of p38 is relocalised to the cytoplasm where it promotes differentiation (73,390,461).

As MyoD is known to be phosphoregulated, detailed phosphorylation site mapping will need to be performed in order to fully understand the stoichiometry of the phosphoregulation and to reliably identify novel phosphosites. Such an approach would involve tandem mass spectrometry analysis of transgenic protein extracts (462). Verification of novel sites can then be performed by site-directed mutagenesis on Mrf constructs to introduce phospho-incompetent or phosphomimetic mutations followed by misexpression and phenotype analysis.

13.3 Myogenesis of muscle stem cells *in vivo* may be under stronger epigenetic control than previously appreciated

MyoD has been defined as a strong transcription factor able to bind the chromatin and induce transcription in the cell (332,337). This may be true *in vitro* but the data described in the previous chapters suggests that the same theory may not apply *in vivo*. Transcription activation requires remodelling of the strictly controlled chromatin structure which can only happen when a specific remodelling complex is formed ready to allow access to otherwise masked cis- acting elements (341,463).

Kinases can directly regulate the chromatin-modifying complex (CMCs), by phosphorylating the individual components. p38 activity can be triggered in active satellite cells and has an important role in regeneration (80,464). p38 directly mediates the phosphorylation of E47 and the heterodimerisation between E47 and muscle proteins (390,465). Heterodimerisation of muscle proteins is required to facilitate binding to the E-Box sequence in the regulatory region of muscle genes. Phosphorylation of the Mef2 proteins causes the activation and recruitment of the protein Trithorax (TrxG) to the chromatin of the muscle genes thus promoting trimethylation of histone 3 lysine-4 ($H3K4^{me3}$) and subsequent transcription (466–468). The proteins Trithorax (TrxG) and Polycomb (PcG) have been shown to play an essential role in the control of chromatin remodelling and histone modification. Trithorax promotes the transcription of Pax7 in stem cell asymmetric division by the methylation of lysine 4 on histone 3 ($H3K4^{me3}$), whilst Polycomb represses the Mrfs by methylation of lysine 27 on histone 3 ($H3K27^{me3}$). During muscle formation, Polycomb and Thrithorax proteins help silence or activate various genes (467,468).

Chromatin remodelling may be a limiting step in the progression of cell differentiation as the Mrfs cannot overcome the protection of the chromatin structure due to the unavailability of p38 at the early stage of muscle precursor differentiation (469).

One of the most important chromatin remodelling complexes in muscle differentiation is the SWI/SNF complex (470,471). During differentiation, phosphorylated MyoD/E protein heterodimers together with the phosphorylated Mef2 will activate muscle-specific promoters. The SWI/SNF complex will recruit HATs and Trithorax which help the demethylation of the DNA and the chromatin is acetylated and consequently 'opened'. We hypothesise that this complex is not present in muscle precursor. Experimentally, this could be tested utilising Chromatin Immuno-Precipitation (ChIP). An antibody against one of the subunits of the SWI/SNF complex, BAF60c could be used to isolate the DNA associated with these modification events (472,473). Unfortunately there is not an antibody available that we could use in chicken.

Investigation into the state of the chromatin by using (ChIP) would help reveal the state of the chromatin associated with the muscle genes and other genes of interest by utilising antibodies specific to modifications known to be associated with active/repressed genes. This protocol could be applied to differentially evaluate the chromatin state as a result of construct misexpression. Additionally, a similar strategy of co-immunoprecipitating misexpressed proteins could be used to ascertain which if any of their target promoters they are binding to. During the electroporations at HH16, we know that Pax7 protein is expressed in the somite but none of the Mrf genes are present at this stage. Analysis of the chromatin state associated with muscle-specific genes could be performed in order to understand which genes are likely expressed at this stage of development. Experimentally, this would involve dissecting somites and performing ChIP experiments using antibodies against histone modifications associated with open or closed chromatin states. We could use a antibody raised against $H3K4^{me3}$ this will indicate the open state of the chromatin while the closed state will be analyse with an antibody detecting $H3K27^{me3}$. We hypothesise that the myosin and troponin1 structural genes are likely to be associated with closed chromatin given that misexpressed Mrf proteins were shown to be unsuccessful in upregulating these genes.

We hypothesise that the individual misexpression of Polycomb and Trithorax constructs in HH16 somites, or with MyoD or other cofactors like Six1 of Mef2C could induce a change in the structure of the chromatin. Unfortunately, the use of these affinity orientated protocols requires an antibody or similar affinity molecule to allow enrichment of the target protein from cell extracts. As discussed before, there are currently no available antibodies for chicken Mrfs. We also decided to avoid the use of epitope tags for affinity recognition to avoid any inadvertent modulation of activity, especially as we have predicted a potential C-terminal protein domain for phosphoregulation present in MyoD (Chapter 12). Therefore, before employing these protocols antibodies would have to be raised by injecting purified protein/peptide into mammals and extracting the antiserum. Alternative approaches include the use of phage display for generating synthetic antibody fragments (474) or the use of SELEX (systematic evolution of ligands by exponential enrichment) for generating high affinity aptamers, also shown to be useful in protein detection in tissues (aptahistochemistry,(475)).

13.4 Negative feedback mechanisms: premature presence of Mrfs may upregulate the Notch-Delta system of lateral inhibition

The stem cell state protection may not be confined to just the somites themselves but may be regulated by a universal signal that controls and maintains stem cells. As described in Chapter 1, Notch and Delta signalling control the premature differentiation of myoblasts. In mouse C2C12 myoblast cell lines, constitutively activated Notch delays the expression of the myogenic

differentiation markers MyoD and MyoG (476). The forced activation of Notch *in vivo* using chicken caused the overexpression of Delta that delayed muscle stem cell differentiation (119). Other experiments have shown that the activation of Notch can cause the downregulation of MyoD, detected in cells which are withdrawing from the cell cycle, but not Pax7 or Myf5, expressed in proliferating myogenic precursor cells (96). The presence and activity of Notch-Delta could influence the misexpression of the Mrf genes in the somites. We hypothesised that the electroporation of the myogenic factors in young somites could cause a feedback mechanism activating the Notch Delta signalling that detect premature expression of the myogenic genes, and subsequently repressing them. This could provide further explanation of why we didn't observe any change in Myosin expression during the time frame between development stages HH16 to HH20 *in vivo*. To test if this is indeed the case, Mrf misexpression coupled with loss of function experiments by the application of morpholino antisense oligonucleotides to knock down the Notch-Delta system may recover the Mrf activity (477)

13.5 Summary

In our study we found that muscle precursor are actively protected from prematurely entering differentiation. The misexpression of Mrfs *in vivo* individually or with other co-factors does not influence the expression levels of Myosin in the first 18hrs of incubation after electroporation. Surprisingly the expression of MyoD and the co-electroporation of MyoD and MyoG were shown to have an effect on Myosin expression after 42hrs of incubation. The time frame of protection that we observed appeared to diminish as we were able to change the Myosin expression levels in the later stages of development only.

A possible explanation for this observed time frame is that there is insufficient time for the Mrf transgenes to induce early MF20 expression. This could be evidenced by the absence of MF20 expression after 18 hrs whilst there is expression after 42 hrs. However, this is not likely to be the case as the Sx1-GFP experiment demonstrated that it is possible to induce early MF20 expression in the 18hr time frame. We therefore hypothesise that the likely reason that Mrf transgenes do not induce early MF20 expression after 18hrs is that the cells are protected from premature differentiation by Mrfs.

It is possible that at the more mature stages of somite development, Trithorax and Polycomb proteins allow the transcription factor MyoD to bind the chromatin and induce transcription, causing upregulation of Myosin in the area of transgene expression.

We hypothesise that the main genes that keep the cells in an undifferentiated state are those involved in chromatin remodeling such as SWI/SNF, Polycomb and p300. All of these complexes have been shown to be regulated by the retinoblastoma protein pRb, which is not present at this

stage of muscle development. pRb is therefore also a potential candidate for inhibiting cells from progressing in differentiation.

Future work is needed to investigate this time frame hypothesis further and to verify other aspects of our hypotheses including the state of the chromatin and the extrinsic factors contributing to the protection of the stem cell state.

References

1. Tanaka EM, Reddien PW. The cellular basis for animal regeneration. Dev Cell [Internet]. 2011 Jul 19 [cited 2015 May 21];21(1):172–85. Available from: http://www.sciencedirect.com/science/article/pii/S1534580711002504

2. Pellettieri J, Fitzgerald P, Watanabe S, Mancuso J, Green DR, Sánchez Alvarado A. Cell death and tissue remodeling in planarian regeneration. Dev Biol [Internet]. 2010 Feb 1 [cited 2015 Sep 23];338(1):76–85. Available from: http://www.sciencedirect.com/science/article/pii/S0012160609011932

3. Yvernogeau L, Auda-Boucher G, Fontaine-Perus J. Limb bud colonization by somite-derived angioblasts is a crucial step for myoblast emigration. Development [Internet]. 2012 Jan 15 [cited 2015 Jan 7];139(2):277–87. Available from: http://dev.biologists.org/content/139/2/277.figures-only

4. Fröbisch NB, Bickelmann C, Olori JC, Witzmann F. Deep-time evolution of regeneration and preaxial polarity in tetrapod limb development. Nature [Internet]. Nature Publishing Group, a division of Macmillan Publishers Limited. All Rights Reserved.; 2015 Oct 26 [cited 2015 Oct 27];527(7577):231–4. Available from: http://dx.doi.org/10.1038/nature15397

5. Fröbisch NB, Bickelmann C, Witzmann F. Early evolution of limb regeneration in tetrapods: evidence from a 300-million-year-old amphibian. Proc Biol Sci [Internet]. 2014 Nov 7 [cited 2015 Nov 26];281(1794):20141550. Available from: http://rspb.royalsocietypublishing.org/content/281/1794/20141550

6. Liu Y, Yang R, He Z, Gao W-Q. Generation of functional organs from stem cells. Cell Regen (London, England) [Internet]. 2013;2(1):1. Available from: http://www.pubmedcentral.nih.gov/articlerender.fcgi?artid=4230490&tool=pmcentrez&rendertype=abstract

7. Rahimov F, Kunkel LM. The cell biology of disease: cellular and molecular mechanisms underlying muscular dystrophy. J Cell Biol [Internet]. 2013 May 13 [cited 2015 Jul 16];201(4):499–510. Available from: http://www.pubmedcentral.nih.gov/articlerender.fcgi?artid=3653356&tool=pmcentrez&rendertype=abstract

8. Bertini E, D'Amico A, Gualandi F, Petrini S. Congenital muscular dystrophies: a brief review. Semin Pediatr Neurol [Internet]. 2011 Dec [cited 2015 Nov 26];18(4):277–88. Available from: http://www.pubmedcentral.nih.gov/articlerender.fcgi?artid=3332154&tool=pmcentrez&rendertype=abstract

9. Hoffman EP, Brown RH, Kunkel LM. Dystrophin: The protein product of the duchenne muscular dystrophy locus. Cell [Internet]. 1987 Dec [cited 2015 Aug 23];51(6):919–28. Available from: http://www.sciencedirect.com/science/article/pii/0092867487905794

10. Metcalfe AD, Ferguson MWJ. Tissue engineering of replacement skin: the crossroads of biomaterials, wound healing, embryonic development, stem cells and regeneration. J R Soc Interface [Internet]. 2007 Jun 22;4(14):413–37. Available from: http://rsif.royalsocietypublishing.org/content/4/14/413.abstract

11. Oh J, Lee YD, Wagers AJ. Stem cell aging: mechanisms, regulators and therapeutic opportunities. Nat Med [Internet]. 2014 Aug [cited 2015 Sep 16];20(8):870–80. Available from: http://www.pubmedcentral.nih.gov/articlerender.fcgi?artid=4160113&tool=pmcentrez&rendertype=abstract

12. Siegel AL, Gurevich DB, Currie PD. A myogenic precursor cell that could contribute to regeneration in zebrafish and its similarity to the satellite cell. FEBS J [Internet]. 2013 Sep [cited 2016 Feb 22];280(17):4074–88. Available from: http://www.ncbi.nlm.nih.gov/pubmed/23607511

13. Morrison JI, Lööf S, He P, Simon A. Salamander limb regeneration involves the activation of a multipotent skeletal muscle satellite cell population. J Cell Biol [Internet]. 2006 Jan 30 [cited 2016 Mar 21];172(3):433–40. Available from: http://jcb.rupress.org/content/172/3/433.short

14. Fausto N. Liver regeneration and repair: hepatocytes, progenitor cells, and stem cells. Hepatology [Internet]. 2004 Jun [cited 2015 Oct 22];39(6):1477–87. Available from: http://www.ncbi.nlm.nih.gov/pubmed/15185286

15. Yin H, Price F, Rudnicki MA. Satellite cells and the muscle stem cell niche. Physiol Rev [Internet]. 2013 Jan 1 [cited 2015 Jan 22];93(1):23–67. Available from: http://physrev.physiology.org/content/93/1/23.long

16. Nelson SF, Crosbie RH, Miceli MC, Spencer MJ. Emerging genetic therapies to treat Duchenne muscular dystrophy. Curr Opin Neurol [Internet]. 2009 Oct [cited 2015 Nov 26];22(5):532–8. Available from: http://www.pubmedcentral.nih.gov/articlerender.fcgi?artid=2856442&tool=pmcentrez&rendertype=abstract

17. Collins CA, Olsen I, Zammit PS, Heslop L, Petrie A, Partridge TA, et al. Stem cell function, self-renewal, and behavioral heterogeneity of cells from the adult muscle satellite cell niche. Cell [Internet]. 2005 Jul 29 [cited 2015 Jul 27];122(2):289–301. Available from: http://www.ncbi.nlm.nih.gov/pubmed/16051152

18. Kuang S, Kuroda K, Le Grand F, Rudnicki MA. Asymmetric self-renewal and commitment of satellite stem cells in muscle. Cell [Internet]. 2007 Jun 1 [cited 2016 Jan 18];129(5):999–1010. Available from: http://www.sciencedirect.com/science/article/pii/S0092867407005132

19. Wada MR, Inagawa-Ogashiwa M, Shimizu S, Yasumoto S, Hashimoto N. Generation of different fates from multipotent muscle stem cells. Development [Internet]. 2002 Jun [cited 2016 Apr 5];129(12):2987–95. Available from: http://dev.biologists.org/content/129/12/2987.abstract

20. Verfaillie C. Pluripotent stem cells. Transfus Clin Biol J la Société Fr Transfus Sang [Internet]. 2009 May [cited 2016 Apr 5];16(2):65–9. Available from: http://www.sciencedirect.com/science/article/pii/S1246782009000718

21. Goldstein B, Kiehart DP. Moving Inward: Establishing the Mammalian Inner Cell Mass. Dev Cell [Internet]. Elsevier; 2015 Aug 24 [cited 2016 Apr 5];34(4):385–6. Available from: http://www.cell.com/article/S1534580715005213/fulltext

22. Martin GR. Isolation of a pluripotent cell line from early mouse embryos cultured in medium conditioned by teratocarcinoma stem cells. Proc Natl Acad Sci U S A [Internet]. 1981 Dec [cited 2014 Nov 10];78(12):7634–8. Available from: http://www.pubmedcentral.nih.gov/articlerender.fcgi?artid=349323&tool=pmcentrez&rendertype=abstract

23. Slack JM. Stem Cells in Epithelial Tissues. Science (80-) [Internet]. American Association for the Advancement of Science; 2000 Feb 25 [cited 2016 Apr 5];287(5457):1431–3. Available from: http://science.sciencemag.org/content/287/5457/1431.abstract

24. Gage FH. Mammalian Neural Stem Cells. Science (80-) [Internet]. American Association for the Advancement of Science; 2000 Feb 25 [cited 2014 Jul 10];287(5457):1433–8. Available

from: http://science.sciencemag.org/content/287/5457/1433.abstract

25. Sanai N, Tramontin AD, Quiñones-Hinojosa A, Barbaro NM, Gupta N, Kunwar S, et al. Unique astrocyte ribbon in adult human brain contains neural stem cells but lacks chain migration. Nature [Internet]. Macmillian Magazines Ltd.; 2004 Feb 19 [cited 2016 Feb 8];427(6976):740–4. Available from: http://dx.doi.org/10.1038/nature02301

26. Doetsch F, Caillé I, Lim DA, García-Verdugo JM, Alvarez-Buylla A. Subventricular Zone Astrocytes Are Neural Stem Cells in the Adult Mammalian Brain. Cell [Internet]. Elsevier; 1999 Jun 11 [cited 2015 Feb 2];97(6):703–16. Available from: http://www.cell.com/article/S0092867400807837/fulltext

27. Kassar-Duchossoy L, Giacone E, Gayraud-Morel B, Jory A, Gomès D, Tajbakhsh S. Pax3/Pax7 mark a novel population of primitive myogenic cells during development. Genes Dev [Internet]. 2005 Jun 15 [cited 2016 Apr 19];19(12):1426–31. Available from: http://www.pubmedcentral.nih.gov/articlerender.fcgi?artid=1151658&tool=pmcentrez&rendertype=abstract

28. Kanisicak O, Mendez JJ, Yamamoto S, Yamamoto M, Goldhamer DJ. Progenitors of skeletal muscle satellite cells express the muscle determination gene, MyoD. Dev Biol. 2009;332(1):131–41.

29. Takahashi K, Yamanaka S. Induction of pluripotent stem cells from mouse embryonic and adult fibroblast cultures by defined factors. Cell [Internet]. Elsevier; 2006 Aug 25 [cited 2014 Jul 9];126(4):663–76. Available from: http://www.cell.com/article/S0092867406009767/fulltext

30. Bhagavati S, Xu W. Generation of skeletal muscle from transplanted embryonic stem cells in dystrophic mice. Biochem Biophys Res Commun [Internet]. 2005 Jul 29 [cited 2016 Feb 5];333(2):644–9. Available from: http://www.sciencedirect.com/science/article/pii/S0006291X05011186

31. Yamanaka S. Induced pluripotent stem cells: past, present, and future. Cell Stem Cell [Internet]. 2012 Jun 14 [cited 2014 Jul 9];10(6):678–84. Available from: http://www.sciencedirect.com/science/article/pii/S1934590912002378

32. Malik N, Rao MS. A review of the methods for human iPSC derivation. Methods Mol Biol [Internet]. 2013 Jan [cited 2015 Nov 13];997:23–33. Available from: http://www.pubmedcentral.nih.gov/articlerender.fcgi?artid=4176696&tool=pmcentrez&rendertype=abstract

33. Noggle S, Fung H-L, Gore A, Martinez H, Satriani KC, Prosser R, et al. Human oocytes reprogram somatic cells to a pluripotent state. Nature [Internet]. Nature Publishing Group, a division of Macmillan Publishers Limited. All Rights Reserved.; 2011 Oct 6 [cited 2016 Feb 10];478(7367):70–5. Available from: http://dx.doi.org/10.1038/nature10397

34. Okita K, Matsumura Y, Sato Y, Okada A, Morizane A, Okamoto S, et al. A more efficient method to generate integration-free human iPS cells. Nat Methods [Internet]. Nature Publishing Group, a division of Macmillan Publishers Limited. All Rights Reserved.; 2011 May [cited 2015 Sep 30];8(5):409–12. Available from: http://dx.doi.org/10.1038/nmeth.1591

35. Sebban S, Buganim Y. Nuclear Reprogramming by Defined Factors: Quantity Versus Quality. Trends Cell Biol [Internet]. 2015 Sep 20 [cited 2015 Nov 10];26(1):65–75. Available from: http://www.sciencedirect.com/science/article/pii/S0962892415001579

36. Yu J, Vodyanik MA, Smuga-Otto K, Antosiewicz-Bourget J, Frane JL, Tian S, et al. Induced pluripotent stem cell lines derived from human somatic cells. Science [Internet]. American Association for the Advancement of Science; 2007 Dec 21 [cited 2014 Jul

9];318(5858):1917–20. Available from: http://science.sciencemag.org/content/318/5858/1917.abstract

37. Gilbert PM, Havenstrite KL, Magnusson KEG, Sacco A, Leonardi NA, Kraft P, et al. Substrate elasticity regulates skeletal muscle stem cell self-renewal in culture. Science [Internet]. American Association for the Advancement of Science; 2010 Aug 27 [cited 2015 Feb 21];329(5995):1078–81. Available from: http://www.pubmedcentral.nih.gov/articlerender.fcgi?artid=2929271&tool=pmcentrez&rendertype=abstract

38. Fang T-C, Alison MR, Wright NA, Poulsom R. Adult stem cell plasticity: will engineered tissues be rejected? Int J Exp Pathol [Internet]. 2004 Jun [cited 2016 Feb 10];85(3):115–24. Available from: http://www.pubmedcentral.nih.gov/articlerender.fcgi?artid=2517466&tool=pmcentrez&rendertype=abstract

39. Wen Z, Zheng S, Zhou C, Wang J, Wang T. Repair mechanisms of bone marrow mesenchymal stem cells in myocardial infarction. J Cell Mol Med [Internet]. 2011 May [cited 2016 Feb 10];15(5):1032–43. Available from: http://www.pubmedcentral.nih.gov/articlerender.fcgi?artid=3822616&tool=pmcentrez&rendertype=abstract

40. Haider HK, Ashraf M. Bone marrow stem cell transplantation for cardiac repair. Am J Physiol Heart Circ Physiol [Internet]. 2005 Jun [cited 2016 Feb 10];288(6):H2557-67. Available from: http://www.ncbi.nlm.nih.gov/pubmed/15897328

41. Raisman G. Olfactory ensheathing cells - another miracle cure for spinal cord injury? Nat Rev Neurosci [Internet]. 2001 May [cited 2016 Feb 10];2(5):369–75. Available from: http://dx.doi.org/10.1038/35072576

42. Partridge TA, Morgan JE, Coulton GR, Hoffman EP, Kunkel LM. Conversion of mdx myofibres from dystrophin-negative to -positive by injection of normal myoblasts. Nature [Internet]. 1989 Jan 12 [cited 2016 Jan 19];337(6203):176–9. Available from: http://www.ncbi.nlm.nih.gov/pubmed/2643055

43. Wang B, Li J, Xiao X. Adeno-associated virus vector carrying human minidystrophin genes effectively ameliorates muscular dystrophy in mdx mouse model. Proc Natl Acad Sci U S A [Internet]. National Academy of Sciences; 2000 Dec 5 [cited 2016 Oct 26];97(25):13714–9. Available from: http://www.ncbi.nlm.nih.gov/pubmed/11095710

44. Mendell JR, Clark KR. Challenges for gene therapy for muscular dystrophy. Curr Neurol Neurosci Rep [Internet]. 2006 Jan [cited 2016 Feb 10];6(1):47–56. Available from: http://www.ncbi.nlm.nih.gov/pubmed/16469271

45. van Deutekom JC, Bremmer-Bout M, Janson AA, Ginjaar IB, Baas F, den Dunnen JT, et al. Antisense-induced exon skipping restores dystrophin expression in DMD patient derived muscle cells. Hum Mol Genet [Internet]. Oxford University Press; 2001 Jul 15 [cited 2016 Oct 26];10(15):1547–54. Available from: http://www.ncbi.nlm.nih.gov/pubmed/11468272

46. Goyenvalle A, Vulin A, Fougerousse F, Leturcq F, Kaplan J-C, Garcia L, et al. Rescue of dystrophic muscle through U7 snRNA-mediated exon skipping. Science [Internet]. 2004 Dec 3 [cited 2016 Oct 26];306(5702):1796–9. Available from: http://www.ncbi.nlm.nih.gov/pubmed/15528407

47. Jones SW, Hill RJ, Krasney PA, O'Conner B, Peirce N, Greenhaff PL. Disuse atrophy and exercise rehabilitation in humans profoundly affects the expression of genes associated with the regulation of skeletal muscle mass. FASEB J [Internet]. 2004 Jun 1 [cited 2016 Jan 18];18(9):1025–7. Available from: http://www.fasebj.org/content/18/9/1025.full

48. Appell HJ. Muscular atrophy following immobilisation. A review. Sports Med [Internet]. 1990 Jul [cited 2016 Feb 10];10(1):42–58. Available from: http://www.ncbi.nlm.nih.gov/pubmed/2197699

49. Zinna EM, Yarasheski KE. Exercise treatment to counteract protein wasting of chronic diseases. Curr Opin Clin Nutr Metab Care [Internet]. 2003 Jan [cited 2016 Feb 10];6(1):87–93. Available from: http://www.ncbi.nlm.nih.gov/pubmed/12496685

50. Doherty TJ. Invited review: Aging and sarcopenia. J Appl Physiol [Internet]. 2003 Oct 1 [cited 2015 Oct 31];95(4):1717–27. Available from: http://jap.physiology.org/content/95/4/1717.long

51. Cruz-Jentoft AJ, Landi F, Schneider SM, Zúñiga C, Arai H, Boirie Y, et al. Prevalence of and interventions for sarcopenia in ageing adults: a systematic review. Report of the International Sarcopenia Initiative (EWGSOP and IWGS). Age Ageing [Internet]. 2014 Nov 21 [cited 2015 Dec 19];43(6):748–59. Available from: http://ageing.oxfordjournals.org/content/early/2014/09/19/ageing.afu115.full

52. Tedesco FS, Dellavalle A, Diaz-Manera J, Messina G, Cossu G. Repairing skeletal muscle: regenerative potential of skeletal muscle stem cells. J Clin Invest [Internet]. American Society for Clinical Investigation; 2010 Jan 4 [cited 2016 Feb 10];120(1):11–9. Available from: http://www.pubmedcentral.nih.gov/articlerender.fcgi?artid=2798695&tool=pmcentrez&rendertype=abstract

53. Glimm H, Oh IH, Eaves CJ. Human hematopoietic stem cells stimulated to proliferate in vitro lose engraftment potential during their S/G(2)/M transit and do not reenter G(0). Blood [Internet]. 2000 Dec 15 [cited 2016 Feb 11];96(13):4185–93. Available from: http://www.ncbi.nlm.nih.gov/pubmed/11110690

54. Galderisi U, Helmbold H, Squillaro T, Alessio N, Komm N, Khadang B, et al. In vitro senescence of rat mesenchymal stem cells is accompanied by downregulation of stemness-related and DNA damage repair genes. Stem Cells Dev [Internet]. Mary Ann Liebert, Inc. publishers140 Huguenot Street, 3rd FloorNew Rochelle, NY 10801-5215USA; 2009 Sep 10 [cited 2016 Feb 11];18(7):1033–42. Available from: http://online.liebertpub.com/doi/abs/10.1089/scd.2008.0324

55. Le Grand F, Rudnicki MA. Skeletal muscle satellite cells and adult myogenesis. Curr Opin Cell Biol [Internet]. 2007 Dec [cited 2015 Oct 24];19(6):628–33. Available from: http://www.pubmedcentral.nih.gov/articlerender.fcgi?artid=2215059&tool=pmcentrez&rendertype=abstract

56. Bentzinger CF, Wang YX, von Maltzahn J, Rudnicki MA. The emerging biology of muscle stem cells: implications for cell-based therapies. Bioessays [Internet]. 2013 Mar [cited 2016 Feb 11];35(3):231–41. Available from: http://www.pubmedcentral.nih.gov/articlerender.fcgi?artid=3594813&tool=pmcentrez&rendertype=abstract

57. Bentzinger CF, Wang YX, Rudnicki MA. Building muscle: molecular regulation of myogenesis. Cold Spring Harb Perspect Biol [Internet]. 2012 Feb 1 [cited 2015 Mar 20];4(2):a008342-. Available from: http://cshperspectives.cshlp.org/content/4/2/a008342.full

58. Potthoff MJ, Arnold MA, McAnally J, Richardson JA, Bassel-Duby R, Olson EN. Regulation of skeletal muscle sarcomere integrity and postnatal muscle function by Mef2c. Mol Cell Biol [Internet]. 2007 Dec 1 [cited 2016 Jan 14];27(23):8143–51. Available from: http://mcb.asm.org/content/27/23/8143.short

59. Gilbert SF. Developmental Biology [Internet]. Sinauer Associates; 2000 [cited 2016 Jan 13].

Available from: http://www.ncbi.nlm.nih.gov/books/NBK9983/

60. Martin BL, Harland RM. Hypaxial muscle migration during primary myogenesis in Xenopus laevis. Dev Biol [Internet]. 2001 Nov 15 [cited 2016 Jan 20];239(2):270–80. Available from: http://www.sciencedirect.com/science/article/pii/S0012160601904348

61. Shimizu T, Dennis JE, Masaki T, Fischman DA. Axial Arrangement of the Myosin Rod in Vertebrate Thick Filaments : Immunoelectron Microscopy with a Monoclonal Antibody to Light Meromyosin Immunofluorescent Labeling of Myofibrils. 1985;101(September).

62. Cooper GM. Actin, Myosin, and Cell Movement [Internet]. Sinauer Associates; 2000 [cited 2016 Feb 11]. Available from: http://www.ncbi.nlm.nih.gov/books/NBK9961/

63. Lodish H, Berk A, Zipursky SL, Matsudaira P, Baltimore D, Darnell J. Myosin: The Actin Motor Protein [Internet]. W. H. Freeman; 2000 [cited 2016 Feb 11]. Available from: http://www.ncbi.nlm.nih.gov/books/NBK21724/

64. Buss F, Spudich G, Kendrick-Jones J. MYOSIN VI: Cellular Functions and Motor Properties. Annual Reviews; 2004 Oct 8 [cited 2016 Feb 11]; Available from: http://www.annualreviews.org/doi/abs/10.1146/annurev.cellbio.20.012103.094243

65. Cooper GM. Structure and Organization of Actin Filaments [Internet]. Sinauer Associates; 2000 [cited 2016 Feb 11]. Available from: http://www.ncbi.nlm.nih.gov/books/NBK9908/

66. Buckingham M, Bajard L, Chang T, Daubas P, Hadchouel J, Meilhac S, et al. The formation of skeletal muscle: from somite to limb. J Anat. 2003;202(1):59–68.

67. Tajbakhsh S. Skeletal muscle stem cells in developmental versus regenerative myogenesis. J Intern Med [Internet]. 2009 Oct [cited 2016 Jan 19];266(4):372–89. Available from: http://www.ncbi.nlm.nih.gov/pubmed/19765181

68. MAURO A. Satellite cell of skeletal muscle fibers. J Biophys Biochem Cytol [Internet]. 1961 Feb [cited 2015 Mar 8];9:493–5. Available from: http://www.pubmedcentral.nih.gov/articlerender.fcgi?artid=2225012&tool=pmcentrez&rendertype=abstract

69. Bischoff R. Regeneration of single skeletal muscle fibers in vitro. Anat Rec [Internet]. 1975 Jun [cited 2016 Feb 12];182(2):215–35. Available from: http://www.ncbi.nlm.nih.gov/pubmed/168794

70. Konigsberg UR, Lipton BH, Konigsberg IR. The regenerative response of single mature muscle fibers isolated in vitro. Dev Biol [Internet]. 1975 Aug [cited 2016 Feb 12];45(2):260–75. Available from: http://www.ncbi.nlm.nih.gov/pubmed/1193298

71. Holterman CE, Rudnicki MA. Molecular regulation of satellite cell function. Semin Cell Dev Biol [Internet]. 2005 Jan [cited 2016 Feb 11];16(4–5):575–84. Available from: http://www.sciencedirect.com/science/article/pii/S1084952105000856

72. Relaix F, Montarras D, Zaffran S, Gayraud-Morel B, Rocancourt D, Tajbakhsh S, et al. Pax3 and Pax7 have distinct and overlapping functions in adult muscle progenitor cells. J Cell Biol [Internet]. 2006 Jan 2 [cited 2014 May 1];172(1):91–102. Available from: http://www.pubmedcentral.nih.gov/articlerender.fcgi?artid=2063537&tool=pmcentrez&rendertype=abstract

73. Troy A, Cadwallader AB, Fedorov Y, Tyner K, Tanaka KK, Olwin BB. Coordination of satellite cell activation and self-renewal by par-complex-dependent asymmetric activation of p38??/?? MAPK. Cell Stem Cell [Internet]. Elsevier Inc.; 2012 Oct 5 [cited 2014 May 8];11(4):541–53. Available from: http://www.pubmedcentral.nih.gov/articlerender.fcgi?artid=4077199&tool=pmcentrez&rendertype=abstract

74. Zammit PS. Pax7 and myogenic progression in skeletal muscle satellite cells. J Cell Sci [Internet]. 2006 May 1 [cited 2015 Oct 12];119(9):1824–32. Available from: http://jcs.biologists.org/content/119/9/1824

75. Collins CA, Zammit PS, Ruiz AP, Morgan JE, Partridge TA. A population of myogenic stem cells that survives skeletal muscle aging. Stem Cells [Internet]. 2007 Apr [cited 2016 Feb 11];25(4):885–94. Available from: http://www.ncbi.nlm.nih.gov/pubmed/17218401

76. Hutcheson DA, Zhao J, Merrell A, Haldar M, Kardon G. Embryonic and fetal limb myogenic cells are derived from developmentally distinct progenitors and have different requirements for beta-catenin. Genes Dev [Internet]. 2009 Apr 15 [cited 2016 Feb 4];23(8):997–1013. Available from: http://genesdev.cshlp.org/content/23/8/997.short

77. Wang YX, Rudnicki MA. Satellite cells, the engines of muscle repair. Nat Rev Mol Cell Biol [Internet]. Nature Publishing Group, a division of Macmillan Publishers Limited. All Rights Reserved.; 2012 Feb [cited 2016 Jan 29];13(2):127–33. Available from: http://dx.doi.org/10.1038/nrm3265

78. Sacco A, Doyonnas R, Kraft P, Vitorovic S, Blau HM. Self-renewal and expansion of single transplanted muscle stem cells. Nature [Internet]. Macmillan Publishers Limited. All rights reserved; 2008 Nov 27 [cited 2016 Jan 18];456(7221):502–6. Available from: http://dx.doi.org/10.1038/nature07384

79. Troy A, Cadwallader AB, Fedorov Y, Tyner K, Tanaka KK, Olwin BB. Coordination of satellite cell activation and self-renewal by Par-complex-dependent asymmetric activation of p38α/β MAPK. Cell Stem Cell [Internet]. 2012 Oct 5 [cited 2016 Feb 10];11(4):541–53. Available from: http://www.pubmedcentral.nih.gov/articlerender.fcgi?artid=4077199&tool=pmcentrez&rendertype=abstract

80. Jones NC, Tyner KJ, Nibarger L, Stanley HM, Cornelison DDW, Fedorov Y V, et al. The p38alpha/beta MAPK functions as a molecular switch to activate the quiescent satellite cell. J Cell Biol [Internet]. 2005 Apr 11 [cited 2016 Feb 12];169(1):105–16. Available from: http://jcb.rupress.org/content/169/1/105

81. Zhang K, Sha J, Harter ML. Activation of Cdc6 by MyoD is associated with the expansion of quiescent myogenic satellite cells. J Cell Biol [Internet]. 2010 Jan 11 [cited 2016 Feb 12];188(1):39–48. Available from: http://jcb.rupress.org/content/188/1/39.short

82. Walsh K, Perlman H. Cell cycle exit upon myogenic differentiation. Curr Opin Genet Dev [Internet]. 1997 Oct [cited 2016 Jan 18];7(5):597–602. Available from: http://www.sciencedirect.com/science/article/pii/S0959437X97800056

83. Berti F, Nogueira JM, Wöhrle S, Sobreira DR, Hawrot K, Dietrich S, et al. Time course and side-by-side analysis of mesodermal, pre-myogenic, myogenic and differentiated cell markers in the chicken model for skeletal muscle formation. J Anat [Internet]. 2015;227(3):361–82. Available from: http://doi.wiley.com/10.1111/joa.12353

84. Sabillo A, Ramirez J, Domingo CR. Making muscle: Morphogenetic movements and molecular mechanisms of myogenesis in Xenopus laevis. Semin Cell Dev Biol [Internet]. 2016 Feb 4 [cited 2016 Feb 9]; Available from: http://www.sciencedirect.com/science/article/pii/S1084952116300441

85. Rocheteau P, Gayraud-Morel B, Siegl-Cachedenier I, Blasco MA, Tajbakhsh S. A subpopulation of adult skeletal muscle stem cells retains all template DNA strands after cell division. Cell [Internet]. 2012 Jan 20 [cited 2016 Jan 22];148(1–2):112–25. Available from: http://www.sciencedirect.com/science/article/pii/S0092867411014437

86. Tanaka KK, Hall JK, Troy AA, Cornelison DDW, Majka SM, Olwin BB. Syndecan-4-expressing

muscle progenitor cells in the SP engraft as satellite cells during muscle regeneration. Cell Stem Cell [Internet]. 2009 Mar 6 [cited 2016 Jan 19];4(3):217–25. Available from: http://www.pubmedcentral.nih.gov/articlerender.fcgi?artid=3142572&tool=pmcentrez&rendertype=abstract

87. Dumont NA, Wang YX, Rudnicki MA. Intrinsic and extrinsic mechanisms regulating satellite cell function. Development [Internet]. 2015 May 1 [cited 2015 Apr 30];142(9):1572–81. Available from: http://dev.biologists.org/content/142/9/1572.short

88. von Maltzahn J, Jones AE, Parks RJ, Rudnicki MA. Pax7 is critical for the normal function of satellite cells in adult skeletal muscle. Proc Natl Acad Sci U S A [Internet]. 2013 Oct 8 [cited 2016 Feb 15];110(41):16474–9. Available from: http://www.pubmedcentral.nih.gov/articlerender.fcgi?artid=3799311&tool=pmcentrez&rendertype=abstract

89. Buckingham M, Relaix F. The role of Pax genes in the development of tissues and organs: Pax3 and Pax7 regulate muscle progenitor cell functions. Annu Rev Cell Dev Biol [Internet]. 2007 Jan [cited 2016 Feb 15];23:645–73. Available from: http://www.ncbi.nlm.nih.gov/pubmed/17506689

90. Galli LM, Knight SR, Barnes TL, Doak AK, Kadzik RS, Burrus LW. Identification and characterization of subpopulations of Pax3 and Pax7 expressing cells in developing chick somites and limb buds. Dev Dyn [Internet]. 2008 Jul [cited 2016 Feb 17];237(7):1862–74. Available from: http://www.pubmedcentral.nih.gov/articlerender.fcgi?artid=2854025&tool=pmcentrez&rendertype=abstract

91. Buckingham M. Myogenic progenitor cells and skeletal myogenesis in vertebrates. Curr Opin Genet Dev [Internet]. 2006 Oct [cited 2014 May 23];16(5):525–32. Available from: http://www.ncbi.nlm.nih.gov/pubmed/16930987

92. Soleimani VD, Punch VG, Kawabe Y, Jones AE, Palidwor GA, Porter CJ, et al. Transcriptional dominance of Pax7 in adult myogenesis is due to high-affinity recognition of homeodomain motifs. Dev Cell [Internet]. 2012 Jun 12 [cited 2016 Feb 15];22(6):1208–20. Available from: http://www.pubmedcentral.nih.gov/articlerender.fcgi?artid=3376216&tool=pmcentrez&rendertype=abstract

93. Günther S, Kim J, Kostin S, Lepper C, Fan C-M, Braun T. Myf5-Positive Satellite Cells Contribute to Pax7-Dependent Long-Term Maintenance of Adult Muscle Stem Cells. Cell Stem Cell [Internet]. 2013 Nov 7 [cited 2015 Oct 19];13(5):590–601. Available from: http://www.pubmedcentral.nih.gov/articlerender.fcgi?artid=4082715&tool=pmcentrez&rendertype=abstract

94. Crist CG, Montarras D, Buckingham M. Muscle satellite cells are primed for myogenesis but maintain quiescence with sequestration of Myf5 mRNA targeted by microRNA-31 in mRNP granules. Cell Stem Cell [Internet]. 2012 Jul 6 [cited 2016 Feb 9];11(1):118–26. Available from: http://www.ncbi.nlm.nih.gov/pubmed/22770245

95. Olguin HC, Olwin BB. Pax-7 up-regulation inhibits myogenesis and cell cycle progression in satellite cells: a potential mechanism for self-renewal. Dev Biol [Internet]. 2004 Nov 15 [cited 2014 Jun 3];275(2):375–88. Available from: http://www.pubmedcentral.nih.gov/articlerender.fcgi?artid=3322464&tool=pmcentrez&rendertype=abstract

96. Conboy IM, Rando TA. The Regulation of Notch Signaling Controls Satellite Cell Activation and Cell Fate Determination in Postnatal Myogenesis. Dev Cell [Internet]. 2002 Sep [cited 2015 Jun 1];3(3):397–409. Available from: http://www.ncbi.nlm.nih.gov/pubmed/12361602

97. Kumar D, Shadrach JL, Wagers AJ, Lassar AB. Id3 is a direct transcriptional target of Pax7 in quiescent satellite cells. Mol Biol Cell [Internet]. 2009 Jul [cited 2016 Feb 15];20(14):3170–7. Available from: http://www.pubmedcentral.nih.gov/articlerender.fcgi?artid=2710837&tool=pmcentrez&rendertype=abstract

98. Poss KD. Advances in understanding tissue regenerative capacity and mechanisms in animals. Nat Rev Genet [Internet]. Nature Publishing Group, a division of Macmillan Publishers Limited. All Rights Reserved.; 2010 Oct [cited 2015 Nov 27];11(10):710–22. Available from: http://dx.doi.org/10.1038/nrg2879

99. Chuai M, Zeng W, Yang X, Boychenko V, Glazier JA, Weijer CJ. Cell movement during chick primitive streak formation. Dev Biol [Internet]. 2006 Aug 1 [cited 2016 Jan 13];296(1):137–49. Available from: http://www.sciencedirect.com/science/article/pii/S0012160606007299

100. Handrigan GR. Concordia discors: duality in the origin of the vertebrate tail. J Anat [Internet]. 2003 Mar [cited 2016 Apr 6];202(Pt 3):255–67. Available from: http://www.pubmedcentral.nih.gov/articlerender.fcgi?artid=1571085&tool=pmcentrez&rendertype=abstract

101. Pourquié O. The segmentation clock: converting embryonic time into spatial pattern. Science [Internet]. 2003 Jul 18 [cited 2016 Feb 18];301(5631):328–30. Available from: http://www.ncbi.nlm.nih.gov/pubmed/12869750

102. Gossler A, Hrabě de Angelis M. Somitogenesis. Curr Top Dev Biol [Internet]. 1998 Jan [cited 2016 Apr 6];38:225–87. Available from: http://www.ncbi.nlm.nih.gov/pubmed/9399080

103. Goulding MD, Lumsden A, Gruss P. Signals from the notochord and floor plate regulate the region-specific expression of two Pax genes in the developing spinal cord. Development [Internet]. 1993 Mar [cited 2016 Apr 6];117(3):1001–16. Available from: http://www.ncbi.nlm.nih.gov/pubmed/8100762

104. Burgess R, Rawls A, Brown D, Bradley A, Olson EN. Requirement of the paraxis gene for somite formation and musculoskeletal patterning. Nature [Internet]. 1996 Dec 12 [cited 2016 Feb 16];384(6609):570–3. Available from: http://www.ncbi.nlm.nih.gov/pubmed/8955271

105. Šošić D, Brand-Saberi B, Schmidt C, Christ B, Olson EN. Regulation of paraxis expression and somite formation by ectoderm- and neural tube-derived signals. Dev Biol [Internet]. 1997 May 15 [cited 2016 Feb 17];185(2):229–43. Available from: http://www.ncbi.nlm.nih.gov/pubmed/9187085

106. Sambasivan R, Tajbakhsh S. Skeletal muscle stem cell birth and properties. Semin Cell Dev Biol [Internet]. 2007 Dec [cited 2016 Apr 9];18(6):870–82. Available from: http://www.sciencedirect.com/science/article/pii/S1084952107001553

107. Chapman DL, Papaioannou VE. Three neural tubes in mouse embryos with mutations in the T-box gene Tbx6. Nature [Internet]. 1998 Feb 12 [cited 2016 Feb 17];391(6668):695–7. Available from: http://www.ncbi.nlm.nih.gov/pubmed/9490412

108. Chapman DL, Cooper-Morgan A, Harrelson Z, Papaioannou VE. Critical role for Tbx6 in mesoderm specification in the mouse embryo. Mech Dev [Internet]. 2003 Jul [cited 2016 Feb 17];120(7):837–47. Available from: http://www.sciencedirect.com/science/article/pii/S0925477303000662

109. Windner SE, Bird NC, Patterson SE, Doris RA, Devoto SH. Fss/Tbx6 is required for central dermomyotome cell fate in zebrafish. Biol Open [Internet]. 2012 Aug 15 [cited 2016 Feb 17];1(8):806–14. Available from: http://bio.biologists.org/content/early/2012/06/26/bio.20121958.abstract

110. White PH. Defective somite patterning in mouse embryos with reduced levels of Tbx6. Development [Internet]. 2003 Apr 15 [cited 2016 Feb 17];130(8):1681–90. Available from: http://dev.biologists.org/content/130/8/1681.short

111. Watabe-Rudolph M, Schlautmann N, Papaioannou VE, Gossler A. The mouse rib-vertebrae mutation is a hypomorphic Tbx6 allele. Mech Dev [Internet]. 2002 Dec [cited 2016 Feb 17];119(2):251–6. Available from: http://www.sciencedirect.com/science/article/pii/S0925477302003945

112. Beckers J, Caron A, Hrabé de Angelis M, Hans S, Campos-Ortega JA, Gossler A. Distinct regulatory elements direct Delta1 expression in the nervous system and paraxial mesoderm of transgenic mice. Mech Dev [Internet]. 2000 Jul [cited 2016 Feb 17];95(1–2):23–34. Available from: http://www.sciencedirect.com/science/article/pii/S0925477300003221

113. Marics I, Padilla F, Guillemot J-F, Scaal M, Marcelle C. FGFR4 signaling is a necessary step in limb muscle differentiation. Development [Internet]. 2002 Oct 1 [cited 2016 Feb 3];129(19):4559–69. Available from: http://dev.biologists.org/content/129/19/4559.abstract?ijkey=3fa246a8e0657acecff9cf15da53c6acb9078970&keytype2=tf_ipsecsha

114. Cauthen CA, Berdougo E, Sandler J, Burrus LW. Comparative analysis of the expression patterns of Wnts and Frizzleds during early myogenesis in chick embryos. Mech Dev [Internet]. 2001 Jun [cited 2016 Feb 18];104(1–2):133–8. Available from: http://www.ncbi.nlm.nih.gov/pubmed/11404091

115. Schubert FR, Mootoosamy RC, Walters EH, Graham A, Tumiotto L, Münsterberg AE, et al. Wnt6 marks sites of epithelial transformations in the chick embryo. Mech Dev [Internet]. 2002 Jun [cited 2016 Feb 18];114(1–2):143–8. Available from: http://www.ncbi.nlm.nih.gov/pubmed/12175501

116. Rodríguez-Niedenführ M, Dathe V, Jacob HJ, Pröls F, Christ B. Spatial and temporal pattern of Wnt-6 expression during chick development. Anat Embryol (Berl) [Internet]. 2003 May [cited 2016 Feb 18];206(6):447–51. Available from: http://www.ncbi.nlm.nih.gov/pubmed/12695910

117. Schmidt C, Stoeckelhuber M, McKinnell I, Putz R, Christ B, Patel K. Wnt 6 regulates the epithelialisation process of the segmental plate mesoderm leading to somite formation. Dev Biol [Internet]. 2004 Jul 1 [cited 2016 Feb 18];271(1):198–209. Available from: http://www.sciencedirect.com/science/article/pii/S0012160604002040

118. Linker C, Lesbros C, Gros J, Burrus LW, Rawls A, Marcelle C. beta-Catenin-dependent Wnt signalling controls the epithelial organisation of somites through the activation of paraxis. Development [Internet]. 2005;132(17):3895–905. Available from: http://www.ncbi.nlm.nih.gov/entrez/query.fcgi?cmd=Retrieve&db=PubMed&dopt=Citation&list_uids=16100089

119. Delfini MC, Hirsinger E, Pourquié O, Duprez D. Delta 1-activated notch inhibits muscle differentiation without affecting Myf5 and Pax3 expression in chick limb myogenesis. Development [Internet]. 2000 Dec;127(23):5213–24. Available from: http://www.ncbi.nlm.nih.gov/pubmed/11060246

120. Montarras D, L'honoré A, Buckingham M. Lying low but ready for action: the quiescent muscle satellite cell. FEBS J [Internet]. 2013 Sep [cited 2016 Feb 9];280(17):4036–50. Available from: http://www.ncbi.nlm.nih.gov/pubmed/23735050

121. McKinnell IW, Ishibashi J, Le Grand F, Punch VGJ, Addicks GC, Greenblatt JF, et al. Pax7 activates myogenic genes by recruitment of a histone methyltransferase complex. Nat Cell Biol [Internet]. Nature Publishing Group; 2008 Jan [cited 2016 Jan 22];10(1):77–84.

Available from: http://dx.doi.org/10.1038/ncb1671

122. Bulut-Karslioglu A, Perrera V, Scaranaro M, de la Rosa-Velazquez IA, van de Nobelen S, Shukeir N, et al. A transcription factor-based mechanism for mouse heterochromatin formation. Nat Struct Mol Biol [Internet]. Nature Publishing Group, a division of Macmillan Publishers Limited. All Rights Reserved.; 2012 Oct [cited 2016 Feb 18];19(10):1023–30. Available from: http://dx.doi.org/10.1038/nsmb.2382

123. Selleck MA, Stern CD. Fate mapping and cell lineage analysis of Hensen's node in the chick embryo. Development [Internet]. 1991;112(2):615–26. Available from: http://www.ncbi.nlm.nih.gov/pubmed/1794328

124. Fan CM, Tessier-Lavigne M. Patterning of mammalian somites by surface ectoderm and notochord: evidence for sclerotome induction by a hedgehog homolog. Cell [Internet]. 1994 Dec 30 [cited 2016 Feb 16];79(7):1175–86. Available from: http://www.ncbi.nlm.nih.gov/pubmed/8001153

125. Christ B, Huang R, Scaal M. Formation and differentiation of the avian sclerotome. Anat Embryol (Berl) [Internet]. 2004 Aug [cited 2016 Apr 6];208(5):333–50. Available from: http://www.ncbi.nlm.nih.gov/pubmed/15309628

126. Scaal M, Christ B. Formation and differentiation of the avian dermomyotome. Anat Embryol (Berl) [Internet]. 2004 Sep [cited 2016 Feb 17];208(6):411–24. Available from: http://www.ncbi.nlm.nih.gov/pubmed/15338303

127. Cheng L, Alvares LE, Ahmed MU, El-Hanfy AS, Dietrich S. The epaxial-hypaxial subdivision of the avian somite. Dev Biol [Internet]. 2004 Oct 15 [cited 2016 Feb 15];274(2):348–69. Available from: http://www.ncbi.nlm.nih.gov/pubmed/15385164

128. Christ B, Ordahl CP. Early stages of chick somite development. Anat Embryol (Berl) [Internet]. 1995 May [cited 2016 Apr 3];191(5):381–96. Available from: http://link.springer.com/10.1007/BF00304424

129. Münsterberg AE, Kitajewski J, Bumcrot DA, McMahon AP, Lassar AB. Combinatorial signaling by Sonic hedgehog and Wnt family members induces myogenic bHLH gene expression in the somite. Genes Dev [Internet]. 1995 Dec 1 [cited 2016 Feb 16];9(23):2911–22. Available from: http://www.ncbi.nlm.nih.gov/pubmed/7498788

130. Ikeya M, Takada S. Wnt signaling from the dorsal neural tube is required for the formation of the medial dermomyotome. Development [Internet]. 1998 Dec [cited 2016 Feb 16];125(24):4969–76. Available from: http://www.ncbi.nlm.nih.gov/pubmed/9811581

131. Ordahl CP, Le Douarin NM. Two myogenic lineages within the developing somite. Development [Internet]. 1992 Feb 1 [cited 2015 Dec 2];114(2):339–53. Available from: http://www.ncbi.nlm.nih.gov/pubmed/1591996

132. Vasyutina E, Birchmeier C. The development of migrating muscle precursor cells. Anat Embryol (Berl) [Internet]. 2006 Dec [cited 2016 Jan 28];211 Suppl:37–41. Available from: http://www.ncbi.nlm.nih.gov/pubmed/16977478

133. Kalcheim C, Cinnamon Y, Kahane N. Myotome formation: a multistage process. Cell Tissue Res [Internet]. 1999 Mar 29 [cited 2016 Apr 7];296(1):161–73. Available from: http://link.springer.com/10.1007/s004410051277

134. Kahane N, Cinnamon Y, Kalcheim C. The roles of cell migration and myofiber intercalation in patterning formation of the postmitotic myotome. Development [Internet]. 2002 Jun [cited 2016 Apr 7];129(11):2675–87. Available from: http://www.ncbi.nlm.nih.gov/pubmed/12015295

135. Kahane N, Cinnamon Y, Kalcheim C. The cellular mechanism by which the dermomyotome

contributes to the second wave of myotome development. Development [Internet]. 1998 Nov 1 [cited 2016 Apr 7];125(21):4259–71. Available from: http://www.ncbi.nlm.nih.gov/pubmed/9753680

136. Cinnamon Y, Kahane N, Bachelet I, Kalcheim C. The sub-lip domain--a distinct pathway for myotome precursors that demonstrate rostral-caudal migration. Development [Internet]. 2001 Feb 1 [cited 2016 Apr 7];128(3):341–51. Available from: http://dev.biologists.org/content/128/3/341

137. Cinnamon Y, Kahane N, Kalcheim C. Characterization of the early development of specific hypaxial muscles from the ventrolateral myotome. Development [Internet]. 1999 Oct [cited 2016 Apr 7];126(19):4305–15. Available from: http://www.ncbi.nlm.nih.gov/pubmed/10477298

138. Gros J, Scaal M, Marcelle C. A two-step mechanism for myotome formation in chick. Dev Cell [Internet]. 2004 Jun [cited 2015 Dec 2];6(6):875–82. Available from: http://www.sciencedirect.com/science/article/pii/S1534580704001674

139. Kahane N, Cinnamon Y, Bachelet I, Kalcheim C. The third wave of myotome colonization by mitotically competent progenitors: regulating the balance between differentiation and proliferation during muscle development. Development [Internet]. 2001 Jun [cited 2016 Apr 7];128(12):2187–98. Available from: http://www.ncbi.nlm.nih.gov/pubmed/11493539

140. Olivera-Martinez I, Missier S, Fraboulet S, Thélu J, Dhouailly D. Differential regulation of the chick dorsal thoracic dermal progenitors from the medial dermomyotome. Development [Internet]. 2002 Oct [cited 2016 Apr 7];129(20):4763–72. Available from: http://www.ncbi.nlm.nih.gov/pubmed/12361968

141. Ben-Yair R, Kalcheim C. Lineage analysis of the avian dermomyotome sheet reveals the existence of single cells with both dermal and muscle progenitor fates. Development [Internet]. 2005 Jan 27;132(4):689–701. Available from: http://dev.biologists.org/content/132/4/689.abstract

142. Gros J, Manceau M, Thomé V, Marcelle C. A common somitic origin for embryonic muscle progenitors and satellite cells. Nature [Internet]. 2005 Jun 16 [cited 2016 Feb 16];435(7044):954–8. Available from: http://dx.doi.org/10.1038/nature03572

143. Krneta-Stankic V, Sabillo A, Domingo CR. Temporal and spatial patterning of axial myotome fibers in Xenopus laevis. Dev Dyn [Internet]. 2010 Apr [cited 2016 Feb 16];239(4):1162–77. Available from: http://www.pubmedcentral.nih.gov/articlerender.fcgi?artid=3086394&tool=pmcentrez&rendertype=abstract

144. Grimaldi A, Tettamanti G, Martin BL, Gaffield W, Pownall ME, Hughes SM. Hedgehog regulation of superficial slow muscle fibres in Xenopus and the evolution of tetrapod trunk myogenesis. Development [Internet]. 2004 Jul 15 [cited 2016 Feb 16];131(14):3249–62. Available from: http://dev.biologists.org/content/131/14/3249.short

145. Della Gaspera B, Armand AS, Sequeira I, Chesneau A, Mazabraud A, Lécolle S, et al. Myogenic waves and myogenic programs during Xenopus embryonic myogenesis. Dev Dyn. 2012;241(5):995–1007.

146. Edmondson D, Lyons G, Martin J, Olson E. Mef2 gene expression marks the cardiac and skeletal muscle lineages during mouse embryogenesis. Development [Internet]. 1994 May 1 [cited 2016 Feb 16];120(5):1251–63. Available from: http://dev.biologists.org/content/120/5/1251.short

147. della Gaspera B, Armand A-S, Sequeira I, Lecolle S, Gallien CL, Charbonnier F, et al. The Xenopus MEF2 gene family: evidence of a role for XMEF2C in larval tendon development.

Dev Biol [Internet]. 2009 Apr 15 [cited 2016 Feb 16];328(2):392–402. Available from: http://www.ncbi.nlm.nih.gov/pubmed/19389348

148. Montarras D, Morgan J, Collins C, Relaix F, Zaffran S, Cumano A, et al. Direct isolation of satellite cells for skeletal muscle regeneration. Science [Internet]. 2005 Sep 23 [cited 2016 Jan 19];309(5743):2064–7. Available from: http://www.ncbi.nlm.nih.gov/pubmed/16141372

149. Chen J-F, Mandel EM, Thomson JM, Wu Q, Callis TE, Hammond SM, et al. The role of microRNA-1 and microRNA-133 in skeletal muscle proliferation and differentiation. Nat Genet [Internet]. 2006 Feb [cited 2016 Apr 29];38(2):228–33. Available from: http://dx.doi.org/10.1038/ng1725

150. Kiełbówna L, Daczewska M. The origin of syncytial muscle fibres in the myotomes of Xenopus laevis - A revision. Folia Biol (Praha). 2005;53(1–2):39–44.

151. Pownall ME, Gustafsson MK, Emerson CP. Myogenic regulatory factors and the specification of muscle progenitors in vertebrate embryos. Annu Rev Cell Dev Biol [Internet]. 2002 Jan [cited 2016 Apr 7];18:747–83. Available from: http://www.ncbi.nlm.nih.gov/pubmed/12142270

152. Buckingham M. Making muscle in mammals. Trends Genet [Internet]. 1992 Apr [cited 2016 Feb 13];8(4):144–8. Available from: http://www.ncbi.nlm.nih.gov/pubmed/1321521

153. Braun T, Rudnicki MA, Arnold HH, Jaenisch R. Targeted inactivation of the muscle regulatory gene Myf-5 results in abnormal rib development and perinatal death. Cell [Internet]. 1992 Oct 30 [cited 2016 Mar 21];71(3):369–82. Available from: http://www.ncbi.nlm.nih.gov/pubmed/1423602

154. Rudnicki MA, Schnegelsberg PN, Stead RH, Braun T, Arnold HH, Jaenisch R. MyoD or Myf-5 is required for the formation of skeletal muscle. Cell [Internet]. 1993 Dec 31 [cited 2016 Feb 16];75(7):1351–9. Available from: http://www.ncbi.nlm.nih.gov/pubmed/8269513

155. Berkes C a, Tapscott SJ. MyoD and the transcriptional control of myogenesis. Semin Cell Dev Biol [Internet]. 2005 Jan [cited 2014 May 28];16(4–5):585–95. Available from: http://www.sciencedirect.com/science/article/pii/S108495210500087X

156. Gerber AN, Klesert TR, Bergstrom DA, Tapscott SJ. Two domains of MyoD mediate transcriptional activation of genes in repressive chromatin: a mechanism for lineage determination in myogenesis. Genes Dev [Internet]. 1997 Feb 15 [cited 2014 May 2];11(4):436–50. Available from: http://www.ncbi.nlm.nih.gov/pubmed/9042858

157. Bergstrom DA, Tapscott SJ. Molecular distinction between specification and differentiation in the myogenic basic helix-loop-helix transcription factor family. Mol Cell Biol [Internet]. 2001 Apr [cited 2016 Feb 9];21(7):2404–12. Available from: http://www.pubmedcentral.nih.gov/articlerender.fcgi?artid=86873&tool=pmcentrez&rendertype=abstract

158. Jones S, Massari M, Murre C, Ledent V, Vervoort M, Robinson K, et al. An overview of the basic helix-loop-helix proteins. Genome Biol [Internet]. BioMed Central; 2004 [cited 2016 Oct 26];5(6):226. Available from: http://genomebiology.biomedcentral.com/articles/10.1186/gb-2004-5-6-226

159. Massari ME, Murre C. Helix-loop-helix proteins: regulators of transcription in eucaryotic organisms. Mol Cell Biol [Internet]. 2000 Jan [cited 2016 Oct 24];20(2):429–40. Available from: http://www.ncbi.nlm.nih.gov/pubmed/10611221

160. Yang Z, MacQuarrie KL, Analau E, Tyler AE, Dilworth FJ, Cao Y, et al. MyoD and E-protein heterodimers switch rhabdomyosarcoma cells from an arrested myoblast phase to a differentiated state. Genes Dev [Internet]. 2009 Mar 15 [cited 2016 Oct 24];23(6):694–707.

Available from: http://www.ncbi.nlm.nih.gov/pubmed/19299559

161. Kumar JP. The sine oculis homeobox (SIX) family of transcription factors as regulators of development and disease. Cell Mol Life Sci [Internet]. 2009 Feb [cited 2016 Feb 24];66(4):565–83. Available from: http://www.pubmedcentral.nih.gov/articlerender.fcgi?artid=2716997&tool=pmcentrez&rendertype=abstract

162. Liu Y, Han N, Zhou S, Zhou R, Yuan X, Xu H, et al. The DACH/EYA/SIX gene network and its role in tumor initiation and progression. Int J Cancer [Internet]. 2016 Mar 1 [cited 2016 Jan 25];138(5):1067–75. Available from: http://www.ncbi.nlm.nih.gov/pubmed/26096807

163. Esteve P, Bovolenta P. cSix4, a member of the six gene family of transcription factors, is expressed during placode and somite development. Mech Dev [Internet]. 1999 Jul [cited 2016 Feb 24];85(1–2):161–5. Available from: http://www.ncbi.nlm.nih.gov/pubmed/10415356

164. Grifone R, Demignon J, Houbron C, Souil E, Niro C, Seller MJ, et al. Six1 and Six4 homeoproteins are required for Pax3 and Mrf expression during myogenesis in the mouse embryo. Development [Internet]. 2005 May 1 [cited 2014 Jun 3];132(9):2235–49. Available from: http://www.ncbi.nlm.nih.gov/pubmed/15788460

165. Heanue TA, Reshef R, Davis RJ, Mardon G, Oliver G, Tomarev S, et al. Synergistic regulation of vertebrate muscle development by Dach2, Eya2, and Six1, homologs of genes required for Drosophila eye formation. Genes Dev [Internet]. 1999 Dec 15 [cited 2016 Feb 10];13(24):3231–43. Available from: http://www.pubmedcentral.nih.gov/articlerender.fcgi?artid=317207&tool=pmcentrez&rendertype=abstract

166. Sartorelli V, Puri PL, Hamamori Y, Ogryzko V, Chung G, Nakatani Y, et al. Acetylation of MyoD Directed by PCAF Is Necessary for the Execution of the Muscle Program. Mol Cell [Internet]. 1999 Nov [cited 2016 Feb 19];4(5):725–34. Available from: http://www.sciencedirect.com/science/article/pii/S1097276500803834

167. Oliver G, Wehr R, Jenkins NA, Copeland NG, Cheyette BN, Hartenstein V, et al. Homeobox genes and connective tissue patterning. Development [Internet]. 1995 Mar [cited 2016 Feb 24];121(3):693–705. Available from: http://www.ncbi.nlm.nih.gov/pubmed/7720577

168. Schubert FR, Lumsden A. Transcriptional control of early tract formation in the embryonic chick midbrain. Development [Internet]. 2005 Apr 15 [cited 2016 Jan 29];132(8):1785–93. Available from: http://dev.biologists.org/content/132/8/1785

169. Wu W, Huang R, Wu Q, Li P, Chen J, Li B, et al. The role of Six1 in the genesis of muscle cell and skeletal muscle development. Int J Biol Sci [Internet]. 2014 Jan [cited 2016 Jan 14];10(9):983–9. Available from: http://www.pubmedcentral.nih.gov/articlerender.fcgi?artid=4159689&tool=pmcentrez&rendertype=abstract

170. Li X, Oghi KA, Zhang J, Krones A, Bush KT, Glass CK, et al. Eya protein phosphatase activity regulates Six1-Dach-Eya transcriptional effects in mammalian organogenesis. Nature [Internet]. 2003 Nov 20 [cited 2016 Jan 29];426(6964):247–54. Available from: http://www.ncbi.nlm.nih.gov/pubmed/14628042

171. Tootle TL, Silver SJ, Davies EL, Newman V, Latek RR, Mills IA, et al. The transcription factor Eyes absent is a protein tyrosine phosphatase. Nature [Internet]. 2003 Nov 20 [cited 2016 Jan 29];426(6964):299–302. Available from: http://dx.doi.org/10.1038/nature02097

172. Tadjuidje E, Hegde RS. The Eyes Absent proteins in development and disease. Cell Mol Life Sci [Internet]. 2013 Jun [cited 2016 Feb 24];70(11):1897–913. Available from:

http://www.pubmedcentral.nih.gov/articlerender.fcgi?artid=3568240&tool=pmcentrez&rendertype=abstract

173. Fougerousse F, Durand M, Lopez S, Suel L, Demignon J, Thornton C, et al. Six and Eya expression during human somitogenesis and MyoD gene family activation. J Muscle Res Cell Motil [Internet]. 2002 Jan [cited 2016 Feb 24];23(3):255–64. Available from: http://www.ncbi.nlm.nih.gov/pubmed/12500905

174. Grifone R, Demignon J, Giordani J, Niro C, Souil E, Bertin F, et al. Eya1 and Eya2 proteins are required for hypaxial somitic myogenesis in the mouse embryo. Dev Biol [Internet]. 2007 Feb 15 [cited 2016 Feb 24];302(2):602–16. Available from: http://www.ncbi.nlm.nih.gov/pubmed/17098221

175. Bessarab DA, Chong S-W, Korzh V. Expression of zebrafish six1 during sensory organ development and myogenesis. Dev Dyn [Internet]. 2004 Aug [cited 2016 Jan 27];230(4):781–6. Available from: http://www.ncbi.nlm.nih.gov/pubmed/15254912

176. Xu PX, Cheng J, Epstein JA, Maas RL. Mouse Eya genes are expressed during limb tendon development and encode a transcriptional activation function. Proc Natl Acad Sci U S A [Internet]. 1997 Oct 28 [cited 2016 Feb 24];94(22):11974–9. Available from: http://www.ncbi.nlm.nih.gov/pubmed/9342347

177. Borsani G. EYA4, a novel vertebrate gene related to Drosophila eyes absent. Hum Mol Genet [Internet]. 1999 Jan 1 [cited 2016 Feb 24];8(1):11–23. Available from: http://hmg.oxfordjournals.org/content/8/1/11.short

178. Laclef C, Hamard G, Demignon J, Souil E, Houbron C, Maire P. Altered myogenesis in Six1-deficient mice. Development [Internet]. 2003 May [cited 2016 Feb 24];130(10):2239–52. Available from: http://www.ncbi.nlm.nih.gov/pubmed/12668636

179. Giordani J, Bajard L, Demignon J, Daubas P, Buckingham M, Maire P. Six proteins regulate the activation of Myf5 expression in embryonic mouse limbs. Proc Natl Acad Sci [Internet]. 2007 Jun 25 [cited 2016 Jan 8];104(27):11310–5. Available from: http://www.pubmedcentral.nih.gov/articlerender.fcgi?artid=2040895&tool=pmcentrez&rendertype=abstract

180. Relaix F, Demignon J, Laclef C, Pujol J, Santolini M, Niro C, et al. Six homeoproteins directly activate Myod expression in the gene regulatory networks that control early myogenesis. PLoS Genet [Internet]. Public Library of Science; 2013 Apr 25 [cited 2016 Feb 24];9(4):e1003425. Available from: http://journals.plos.org/plosgenetics/article?id=10.1371/journal.pgen.1003425

181. Spitz F, Demignon J, Porteu A, Kahn A, Concordet JP, Daegelen D, et al. Expression of myogenin during embryogenesis is controlled by Six/sine oculis homeoproteins through a conserved MEF3 binding site. Proc Natl Acad Sci U S A [Internet]. 1998 Nov 24 [cited 2016 Feb 19];95(24):14220–5. Available from: http://www.pubmedcentral.nih.gov/articlerender.fcgi?artid=24354&tool=pmcentrez&rendertype=abstract

182. Grifone R, Laclef C, Spitz F, Lopez S, Demignon J, Guidotti J-E, et al. Six1 and Eya1 expression can reprogram adult muscle from the slow-twitch phenotype into the fast-twitch phenotype. Mol Cell Biol [Internet]. 2004 Jul 15 [cited 2016 Jan 14];24(14):6253–67. Available from: http://mcb.asm.org/content/24/14/6253.full

183. Le Grand F, Grifone R, Mourikis P, Houbron C, Gigaud C, Pujol J, et al. Six1 regulates stem cell repair potential and self-renewal during skeletal muscle regeneration. J Cell Biol [Internet]. 2012 Sep 3 [cited 2016 Feb 20];198(5):815–32. Available from: http://www.pubmedcentral.nih.gov/articlerender.fcgi?artid=3432771&tool=pmcentrez&rendertype=abstract

184. Black BL, Olson EN. Transcriptional control of muscle development by myocyte enhancer factor-2 (MEF2) proteins. Annu Rev Cell Dev Biol [Internet]. 1998 Jan [cited 2016 Feb 18];14:167–96. Available from: http://www.ncbi.nlm.nih.gov/pubmed/9891782

185. Gossett LA, Kelvin DJ, Sternberg EA, Olson EN. A new myocyte-specific enhancer-binding factor that recognizes a conserved element associated with multiple muscle-specific genes. Mol Cell Biol [Internet]. 1989 Nov [cited 2016 Feb 18];9(11):5022–33. Available from: http://www.pubmedcentral.nih.gov/articlerender.fcgi?artid=363654&tool=pmcentrez&rendertype=abstract

186. Sumariwalla VM, Klein WH. Similar myogenic functions for myogenin and MRF4 but not MyoD in differentiated murine embryonic stem cells. Genesis [Internet]. 2001 Aug [cited 2016 Feb 18];30(4):239–49. Available from: http://www.ncbi.nlm.nih.gov/pubmed/11536430

187. Wasserman WW, Fickett JW. Identification of regulatory regions which confer muscle-specific gene expression. J Mol Biol [Internet]. 1998 Apr 24 [cited 2016 Feb 18];278(1):167–81. Available from: http://www.ncbi.nlm.nih.gov/pubmed/9571041

188. Molkentin JD, Black BL, Martin JF, Olson EN. Cooperative activation of muscle gene expression by MEF2 and myogenic bHLH proteins. Cell [Internet]. 1995 Dec 29 [cited 2015 Dec 14];83(7):1125–36. Available from: http://www.ncbi.nlm.nih.gov/pubmed/8548800

189. Molkentin JD, Black BL, Martin JF, Olson EN. Mutational analysis of the DNA binding, dimerization, and transcriptional activation domains of MEF2C. Mol Cell Biol [Internet]. 1996 Jun [cited 2015 Dec 2];16(6):2627–36. Available from: http://www.pubmedcentral.nih.gov/articlerender.fcgi?artid=231253&tool=pmcentrez&rendertype=abstract

190. Molkentin JD, Olson EN. Combinatorial control of muscle development by basic helix-loop-helix and MADS-box transcription factors. Proc Natl Acad Sci U S A [Internet]. 1996 Sep 3 [cited 2016 Feb 18];93(18):9366–73. Available from: http://www.pubmedcentral.nih.gov/articlerender.fcgi?artid=38433&tool=pmcentrez&rendertype=abstract

191. Lin Q, Schwarz J, Bucana C, Olson EN. Control of mouse cardiac morphogenesis and myogenesis by transcription factor MEF2C. Science [Internet]. 1997 May 30 [cited 2016 Feb 18];276(5317):1404–7. Available from: http://www.pubmedcentral.nih.gov/articlerender.fcgi?artid=4437729&tool=pmcentrez&rendertype=abstract

192. Penn BH, Bergstrom DA, Dilworth FJ, Bengal E, Tapscott SJ. A MyoD-generated feed-forward circuit temporally patterns gene expression during skeletal muscle differentiation. Genes Dev [Internet]. 2004 Oct 1 [cited 2016 Feb 13];18(19):2348–53. Available from: http://www.pubmedcentral.nih.gov/articlerender.fcgi?artid=522984&tool=pmcentrez&rendertype=abstract

193. Aziz A, Liu Q-C, Dilworth FJ. Regulating a master regulator: establishing tissue-specific gene expression in skeletal muscle. Epigenetics [Internet]. 2010 [cited 2014 Jun 3];5(8):691–5. Available from: http://www.pubmedcentral.nih.gov/articlerender.fcgi?artid=3052885&tool=pmcentrez&rendertype=abstract

194. Seenundun S, Rampalli S, Liu Q-C, Aziz A, Palii C, Hong S, et al. UTX mediates demethylation of H3K27me3 at muscle-specific genes during myogenesis. EMBO J [Internet]. 2010 Apr 21 [cited 2016 Feb 9];29(8):1401–11. Available from: http://www.pubmedcentral.nih.gov/articlerender.fcgi?artid=2868576&tool=pmcentrez&rendertype=abstract

195. Niro C, Demignon J, Vincent S, Liu Y, Giordani J, Sgarioto N, et al. Six1 and Six4 gene expression is necessary to activate the fast-type muscle gene program in the mouse primary myotome. Dev Biol [Internet]. 2010 Feb 15 [cited 2016 Jan 22];338(2):168–82. Available from: http://www.sciencedirect.com/science/article/pii/S0012160609013864

196. Liu Y, Chu A, Chakroun I, Islam U, Blais A. Cooperation between myogenic regulatory factors and SIX family transcription factors is important for myoblast differentiation. Nucleic Acids Res [Internet]. 2010 Jul 2 [cited 2016 Feb 1];38(20):6857–71. Available from: http://nar.oxfordjournals.org/content/38/20/6857.abstract

197. de la Serna IL, Ohkawa Y, Berkes CA, Bergstrom DA, Dacwag CS, Tapscott SJ, et al. MyoD targets chromatin remodeling complexes to the myogenin locus prior to forming a stable DNA-bound complex. Mol Cell Biol [Internet]. 2005 May [cited 2016 Feb 18];25(10):3997–4009. Available from: http://www.pubmedcentral.nih.gov/articlerender.fcgi?artid=1087700&tool=pmcentrez&rendertype=abstract

198. Perdiguero E, Sousa-Victor P, Ballestar E, Muñoz-Cánoves P, Mu??oz-C??noves P. Epigenetic regulation of myogenesis. Epigenetics [Internet]. Taylor & Francis; 2009 Oct 27 [cited 2016 Feb 19];4(8):541–50. Available from: http://www.tandfonline.com/doi/abs/10.4161/epi.4.8.10258

199. Ustanina S, Carvajal J, Rigby P, Braun T. The myogenic factor Myf5 supports efficient skeletal muscle regeneration by enabling transient myoblast amplification. Stem Cells [Internet]. 2007 Aug [cited 2016 Feb 19];25(8):2006–16. Available from: http://www.ncbi.nlm.nih.gov/pubmed/17495111

200. Liu Q-C, Zha X-H, Faralli H, Yin H, Louis-Jeune C, Perdiguero E, et al. Comparative expression profiling identifies differential roles for Myogenin and p38α MAPK signaling in myogenesis. J Mol Cell Biol [Internet]. 2012 Dec [cited 2016 Jan 22];4(6):386–97. Available from: http://www.pubmedcentral.nih.gov/articlerender.fcgi?artid=4580549&tool=pmcentrez&rendertype=abstract

201. Lazaro J, Kitzmann M, Poul M, Vandromme M, Lamb N, Fernandez A. Cyclin dependent kinase 5, cdk5, is a positive regulator of myogenesis in mouse C2 cells. J Cell Sci [Internet]. 1997 May 1 [cited 2015 Dec 17];110(10):1251–60. Available from: http://jcs.biologists.org/content/110/10/1251.long

202. Venkat A, Jauch E, Russell WS, Crist CR, Farrell R. Care of the patient with an autism spectrum disorder by the general physician. Postgrad Med J [Internet]. 2012 Aug [cited 2016 Feb 19];88(1042):472–81. Available from: http://www.ncbi.nlm.nih.gov/pubmed/22427366

203. Rodgers JT, King KY, Brett JO, Cromie MJ, Charville GW, Maguire KK, et al. mTORC1 controls the adaptive transition of quiescent stem cells from G0 to G(Alert). Nature [Internet]. Nature Publishing Group, a division of Macmillan Publishers Limited. All Rights Reserved.; 2014 Jun 19 [cited 2016 Feb 10];510(7505):393–6. Available from: http://dx.doi.org/10.1038/nature13255

204. Lindon C, Montarras D, Pinset C. Cell cycle-regulated expression of the muscle determination factor Myf5 in proliferating myoblasts. J Cell Biol [Internet]. 1998 Jan 12 [cited 2016 Feb 19];140(1):111–8. Available from: http://www.pubmedcentral.nih.gov/articlerender.fcgi?artid=2132595&tool=pmcentrez&rendertype=abstract

205. Doucet C, Gutierrez GJ, Lindon C, Lorca T, Lledo G, Pinset C, et al. Multiple phosphorylation events control mitotic degradation of the muscle transcription factor Myf5. BMC Biochem

[Internet]. 2005 Jan [cited 2016 Feb 19];6:27. Available from: http://www.pubmedcentral.nih.gov/articlerender.fcgi?artid=1322219&tool=pmcentrez&rendertype=abstract

206. Song A, Wang Q, Goebl MG, Harrington MA. Phosphorylation of Nuclear MyoD Is Required for Its Rapid Degradation. Mol Cell Biol [Internet]. 1998 Sep 1 [cited 2016 Feb 19];18(9):4994–9. Available from: http://www.pubmedcentral.nih.gov/articlerender.fcgi?artid=109084&tool=pmcentrez&rendertype=abstract

207. Tintignac LA, Leibovitch MP, Kitzmann M, Fernandez A, Ducommun B, Meijer L, et al. Cyclin E-cdk2 phosphorylation promotes late G1-phase degradation of MyoD in muscle cells. Exp Cell Res [Internet]. 2000 Aug 25 [cited 2016 Feb 19];259(1):300–7. Available from: http://www.ncbi.nlm.nih.gov/pubmed/10942602

208. Batonnet-Pichon S, Tintignac LJ, Castro A, Sirri V, Leibovitch MP, Lorca T, et al. MyoD undergoes a distinct G2/M-specific regulation in muscle cells. Exp Cell Res [Internet]. 2006 Dec 10 [cited 2016 Feb 19];312(20):3999–4010. Available from: http://www.ncbi.nlm.nih.gov/pubmed/17014844

209. Cao Y, Yao Z, Sarkar D, Lawrence M, Sanchez GJ, Parker MH, et al. Genome-wide MyoD binding in skeletal muscle cells: a potential for broad cellular reprogramming. Dev Cell [Internet]. 2010 Apr 20 [cited 2016 Jan 22];18(4):662–74. Available from: http://www.pubmedcentral.nih.gov/articlerender.fcgi?artid=2910615&tool=pmcentrez&rendertype=abstract

210. Cao Y, Kumar RM, Penn BH, Berkes C a, Kooperberg C, Boyer L a, et al. Global and gene-specific analyses show distinct roles for Myod and Myog at a common set of promoters. EMBO J [Internet]. 2006 Feb 8 [cited 2014 May 8];25(3):502–11. Available from: http://www.pubmedcentral.nih.gov/articlerender.fcgi?artid=1383539&tool=pmcentrez&rendertype=abstract

211. Blais A, Tsikitis M, Acosta-Alvear D, Sharan R, Kluger Y, Dynlacht BD. An initial blueprint for myogenic differentiation. Genes Dev [Internet]. 2005 Mar 1 [cited 2016 Feb 19];19(5):553–69. Available from: http://www.pubmedcentral.nih.gov/articlerender.fcgi?artid=551576&tool=pmcentrez&rendertype=abstract

212. De Falco G, Comes F, Simone C. pRb: master of differentiation. Coupling irreversible cell cycle withdrawal with induction of muscle-specific transcription. Oncogene [Internet]. 2006 Aug 28 [cited 2016 Jan 22];25(38):5244–9. Available from: http://dx.doi.org/10.1038/sj.onc.1209623

213. O'Donnell KA, Wentzel EA, Zeller KI, Dang C V., Mendell JT. c-Myc-regulated microRNAs modulate E2F1 expression. Nature [Internet]. 2005 Jun 9 [cited 2016 Jan 12];435(7043):839–43. Available from: http://www.ncbi.nlm.nih.gov/pubmed/15944709

214. Nagel S, Venturini L, Przybylski GK, Grabarczyk P, Schmidt CA, Meyer C, et al. Activation of miR-17-92 by NK-like homeodomain proteins suppresses apoptosis via reduction of E2F1 in T-cell acute lymphoblastic leukemia. Leuk Lymphoma [Internet]. 2009 Jan [cited 2016 Feb 7];50(1):101–8. Available from: http://www.ncbi.nlm.nih.gov/pubmed/19148830

215. Wang XH. MicroRNA in myogenesis and muscle atrophy. Curr Opin Clin Nutr Metab Care [Internet]. 2013 May [cited 2016 Apr 8];16(3):258–66. Available from: http://www.pubmedcentral.nih.gov/articlerender.fcgi?artid=3967234&tool=pmcentrez&rendertype=abstract

216. Singh K, Dilworth FJ. Differential modulation of cell cycle progression distinguishes members of the myogenic regulatory factor family of transcription factors. FEBS J

[Internet]. 2013 Sep [cited 2016 Jan 21];280(17):3991–4003. Available from: http://www.ncbi.nlm.nih.gov/pubmed/23419170

217. Ying S-Y, Chang DC, Lin S-L. The microRNA (miRNA): overview of the RNA genes that modulate gene function. Mol Biotechnol [Internet]. 2008 Mar [cited 2016 Feb 19];38(3):257–68. Available from: http://www.ncbi.nlm.nih.gov/pubmed/17999201

218. Bushati N, Cohen SM. microRNA functions. Annu Rev Cell Dev Biol [Internet]. 2007 Jan [cited 2014 Jul 15];23:175–205. Available from: http://www.ncbi.nlm.nih.gov/pubmed/17506695

219. Ge Y, Chen J. MicroRNAs in skeletal myogenesis. Cell Cycle [Internet]. 2011 Feb 1 [cited 2016 Jan 8];10(3):441–8. Available from: http://www.pubmedcentral.nih.gov/articlerender.fcgi?artid=3115018&tool=pmcentrez&rendertype=abstract

220. Chen J-F, Mandel EM, Thomson JM, Wu Q, Callis TE, Hammond SM, et al. The role of microRNA-1 and microRNA-133 in skeletal muscle proliferation and differentiation. Nat Genet [Internet]. 2006 Feb [cited 2016 Jan 8];38(2):228–33. Available from: http://www.pubmedcentral.nih.gov/articlerender.fcgi?artid=2538576&tool=pmcentrez&rendertype=abstract

221. Zhao Y, Samal E, Srivastava D. Serum response factor regulates a muscle-specific microRNA that targets Hand2 during cardiogenesis. Nature [Internet]. 2005 Jul 14 [cited 2016 Feb 19];436(7048):214–20. Available from: http://www.ncbi.nlm.nih.gov/pubmed/15951802

222. Rao PK, Kumar RM, Farkhondeh M, Baskerville S, Lodish HF. Myogenic factors that regulate expression of muscle-specific microRNAs. Proc Natl Acad Sci U S A [Internet]. 2006 Jun 6 [cited 2016 Jan 21];103(23):8721–6. Available from: http://www.pubmedcentral.nih.gov/articlerender.fcgi?artid=1482645&tool=pmcentrez&rendertype=abstract

223. Liu N, Williams AH, Kim Y, McAnally J, Bezprozvannaya S, Sutherland LB, et al. An intragenic MEF2-dependent enhancer directs muscle-specific expression of microRNAs 1 and 133. Proc Natl Acad Sci U S A [Internet]. 2007 Dec 26 [cited 2016 Feb 19];104(52):20844–9. Available from: http://www.pubmedcentral.nih.gov/articlerender.fcgi?artid=2409229&tool=pmcentrez&rendertype=abstract

224. Sweetman D, Goljanek K, Rathjen T, Oustanina S, Braun T, Dalmay T, et al. Specific requirements of MRFs for the expression of muscle specific microRNAs, miR-1, miR-206 and miR-133. Dev Biol [Internet]. 2008 Sep 15 [cited 2014 Jun 3];321(2):491–9. Available from: http://www.ncbi.nlm.nih.gov/pubmed/18619954

225. van Rooij E, Sutherland LB, Qi X, Richardson JA, Hill J, Olson EN. Control of stress-dependent cardiac growth and gene expression by a microRNA. Science [Internet]. 2007 Apr 27 [cited 2016 Jan 5];316(5824):575–9. Available from: http://www.ncbi.nlm.nih.gov/pubmed/17379774

226. Boutz PL, Chawla G, Stoilov P, Black DL. MicroRNAs regulate the expression of the alternative splicing factor nPTB during muscle development. Genes Dev [Internet]. 2007 Jan 1 [cited 2016 Feb 19];21(1):71–84. Available from: http://www.pubmedcentral.nih.gov/articlerender.fcgi?artid=1759902&tool=pmcentrez&rendertype=abstract

227. Hirai H, Verma M, Watanabe S, Tastad C, Asakura Y, Asakura A. MyoD regulates apoptosis of myoblasts through microRNA-mediated down-regulation of Pax3. J Cell Biol [Internet]. 2010 Oct 18 [cited 2016 Feb 19];191(2):347–65. Available from: http://www.pubmedcentral.nih.gov/articlerender.fcgi?artid=2958479&tool=pmcentrez&r

endertype=abstract

228. Crist CG, Montarras D, Pallafacchina G, Rocancourt D, Cumano A, Conway SJ, et al. Muscle stem cell behavior is modified by microRNA-27 regulation of Pax3 expression. Proc Natl Acad Sci U S A [Internet]. 2009 Aug 11 [cited 2016 Feb 19];106(32):13383–7. Available from: http://www.pnas.org/content/106/32/13383.short

229. Chen J-F, Tao Y, Li J, Deng Z, Yan Z, Xiao X, et al. microRNA-1 and microRNA-206 regulate skeletal muscle satellite cell proliferation and differentiation by repressing Pax7. J Cell Biol [Internet]. 2010 Sep 6 [cited 2016 Feb 19];190(5):867–79. Available from: http://jcb.rupress.org/content/190/5/867?ijkey=c614574fa3a717dd90ea28ab321b75cfbfa6d095&keytype2=tf_ipsecsha

230. Dey BK, Gagan J, Dutta A. miR-206 and -486 induce myoblast differentiation by downregulating Pax7. Mol Cell Biol [Internet]. 2011 Jan 1 [cited 2015 Nov 30];31(1):203–14. Available from: http://mcb.asm.org/content/31/1/203.abstract

231. Kleinman ME, Yamada K, Takeda A, Chandrasekaran V, Nozaki M, Baffi JZ, et al. Sequence- and target-independent angiogenesis suppression by siRNA via TLR3. Nature [Internet]. 2008 Apr 3 [cited 2016 Feb 19];452(7187):591–7. Available from: http://www.pubmedcentral.nih.gov/articlerender.fcgi?artid=2642938&tool=pmcentrez&rendertype=abstract

232. Brack AS, Rando TA. Intrinsic Changes and Extrinsic Influences of Myogenic Stem Cell Function During Aging. Stem Cell Rev [Internet]. 2007 Sep 15 [cited 2016 Apr 8];3(3):226–37. Available from: http://link.springer.com/10.1007/s12015-007-9000-2

233. Berger MJ, Doherty TJ. Sarcopenia: prevalence, mechanisms, and functional consequences. Interdiscip Top Gerontol [Internet]. 2010 Jan [cited 2016 Feb 20];37:94–114. Available from: http://www.ncbi.nlm.nih.gov/pubmed/20703058

234. Conboy IM, Rando TA. Heterochronic parabiosis for the study of the effects of aging on stem cells and their niches. Cell Cycle [Internet]. 2012 Jun 15 [cited 2016 Jan 30];11(12):2260–7. Available from: http://www.pubmedcentral.nih.gov/articlerender.fcgi?artid=3383588&tool=pmcentrez&rendertype=abstract

235. Brack AS, Conboy MJ, Roy S, Lee M, Kuo CJ, Keller C, et al. Increased Wnt signaling during aging alters muscle stem cell fate and increases fibrosis. Science [Internet]. 2007 Aug 10 [cited 2015 Nov 12];317(5839):807–10. Available from: http://www.ncbi.nlm.nih.gov/pubmed/17690295

236. Carlson ME, Silva HS, Conboy IM. Aging of signal transduction pathways, and pathology. Exp Cell Res [Internet]. 2008 Jun 10 [cited 2016 Feb 20];314(9):1951–61. Available from: http://www.pubmedcentral.nih.gov/articlerender.fcgi?artid=2572856&tool=pmcentrez&rendertype=abstract

237. Villeda SA, Luo J, Mosher KI, Zou B, Britschgi M, Bieri G, et al. The ageing systemic milieu negatively regulates neurogenesis and cognitive function. Nature [Internet]. Nature Publishing Group, a division of Macmillan Publishers Limited. All Rights Reserved.; 2011 Sep 1 [cited 2015 Jul 27];477(7362):90–4. Available from: http://dx.doi.org/10.1038/nature10357

238. Lee H-J, Macbeth AH, Pagani JH, Young WS. Oxytocin: the great facilitator of life. Prog Neurobiol [Internet]. 2009 Jun [cited 2016 Feb 20];88(2):127–51. Available from: http://www.pubmedcentral.nih.gov/articlerender.fcgi?artid=2689929&tool=pmcentrez&rendertype=abstract

239. Gimpl G, Fahrenholz F. The oxytocin receptor system: structure, function, and regulation.

Physiol Rev [Internet]. 2001 Apr [cited 2015 Oct 2];81(2):629–83. Available from: http://www.ncbi.nlm.nih.gov/pubmed/11274341

240. Elabd C, Cousin W, Upadhyayula P, Chen RY, Chooljian MS, Li J, et al. Oxytocin is an age-specific circulating hormone that is necessary for muscle maintenance and regeneration. Nat Commun [Internet]. Nature Publishing Group; 2014 Jan 10 [cited 2016 Feb 20];5:4082. Available from: http://www.nature.com/ncomms/2014/140610/ncomms5082/full/ncomms5082.html

241. Furie K, Inzucchi SE. Diabetes mellitus, insulin resistance, hyperglycemia, and stroke. Curr Neurol Neurosci Rep [Internet]. 2008 Jan [cited 2016 Feb 20];8(1):12–9. Available from: http://www.ncbi.nlm.nih.gov/pubmed/18367034

242. Venn BJ, Green TJ. Glycemic index and glycemic load: measurement issues and their effect on diet-disease relationships. Eur J Clin Nutr [Internet]. 2007 Dec [cited 2016 Feb 9];61 Suppl 1:S122-31. Available from: http://www.ncbi.nlm.nih.gov/pubmed/17992183

243. Förster O, Rudas B. Ketosis in rats with streptozotocin-induced diabetes. Lancet (London, England) [Internet]. 1969 Jun 28 [cited 2016 Feb 20];1(7609):1321–2. Available from: http://www.ncbi.nlm.nih.gov/pubmed/4182216

244. Vignaud A, Ramond F, Hourdé C, Keller A, Butler-Browne G, Ferry A. Diabetes provides an unfavorable environment for muscle mass and function after muscle injury in mice. Pathobiology [Internet]. 2007 Jan [cited 2016 Feb 8];74(5):291–300. Available from: http://www.ncbi.nlm.nih.gov/pubmed/17890896

245. Van Hateren N, Belsham A, Randall V, Borycki A-G. Expression of avian Groucho-related genes (Grgs) during embryonic development. Gene Expr Patterns [Internet]. 2005 Aug [cited 2016 Feb 24];5(6):817–23. Available from: http://www.ncbi.nlm.nih.gov/pubmed/15923151

246. Mourikis P, Tajbakhsh S. Distinct contextual roles for Notch signalling in skeletal muscle stem cells. BMC Dev Biol [Internet]. BioMed Central; 2014 Jan 24 [cited 2016 Feb 13];14(1):2. Available from: http://bmcdevbiol.biomedcentral.com/articles/10.1186/1471-213X-14-2

247. Kopan R, Nye JS, Weintraub H. The intracellular domain of mouse Notch: a constitutively activated repressor of myogenesis directed at the basic helix-loop-helix region of MyoD. Development [Internet]. 1994 Sep [cited 2016 Jan 8];120(9):2385–96. Available from: http://www.ncbi.nlm.nih.gov/pubmed/7956819

248. Jory A, Le Roux I, Gayraud-Morel B, Rocheteau P, Cohen-Tannoudji M, Cumano A, et al. Numb promotes an increase in skeletal muscle progenitor cells in the embryonic somite. Stem Cells [Internet]. 2009 Nov [cited 2016 Feb 22];27(11):2769–80. Available from: http://www.ncbi.nlm.nih.gov/pubmed/19785007

249. Lewis J, Hanisch A, Holder M. Notch signaling, the segmentation clock, and the patterning of vertebrate somites. J Biol [Internet]. BioMed Central; 2009 Jan 22 [cited 2016 Jan 4];8(4):44. Available from: http://jbiol.biomedcentral.com/articles/10.1186/jbiol145

250. Rowton M, Ramos P, Anderson DM, Rhee JM, Cunliffe HE, Rawls A. Regulation of mesenchymal-to-epithelial transition by PARAXIS during somitogenesis. Dev Dyn [Internet]. 2013 Nov [cited 2016 Feb 18];242(11):1332–44. Available from: http://www.ncbi.nlm.nih.gov/pubmed/24038871

251. Schuster-Gossler K, Cordes R, Gossler A. Premature myogenic differentiation and depletion of progenitor cells cause severe muscle hypotrophy in Delta1 mutants. Proc Natl Acad Sci U S A [Internet]. 2007 Jan 9 [cited 2016 Jan 21];104(2):537–42. Available from: http://www.pubmedcentral.nih.gov/articlerender.fcgi?artid=1766420&tool=pmcentrez&r

endertype=abstract

252. Vasyutina E, Lenhard DC, Wende H, Erdmann B, Epstein JA, Birchmeier C. RBP-J (Rbpsuh) is essential to maintain muscle progenitor cells and to generate satellite cells. Proc Natl Acad Sci U S A [Internet]. 2007 Mar 13 [cited 2016 Feb 22];104(11):4443–8. Available from: http://www.pubmedcentral.nih.gov/articlerender.fcgi?artid=1815471&tool=pmcentrez&rendertype=abstract

253. McPherron AC, Lawler AM, Lee S-J. Regulation of skeletal muscle mass in mice by a new TGF-p superfamily member. Nature [Internet]. 1997 May 1 [cited 2015 Oct 15];387(6628):83–90. Available from: http://www.ncbi.nlm.nih.gov/pubmed/9139826

254. Manceau M, Gros J, Savage K, Thomé V, McPherron A, Paterson B, et al. Myostatin promotes the terminal differentiation of embryonic muscle progenitors. Genes Dev [Internet]. 2008 Mar 1 [cited 2016 Feb 15];22(5):668–81. Available from: http://www.pubmedcentral.nih.gov/articlerender.fcgi?artid=2259035&tool=pmcentrez&rendertype=abstract

255. Zimmers TA, Davies M V, Koniaris LG, Haynes P, Esquela AF, Tomkinson KN, et al. Induction of cachexia in mice by systemically administered myostatin. Science [Internet]. 2002 May 24 [cited 2016 Feb 14];296(5572):1486–8. Available from: http://www.ncbi.nlm.nih.gov/pubmed/12029139

256. Elkina Y, von Haehling S, Anker SD, Springer J. The role of myostatin in muscle wasting: an overview. J Cachexia Sarcopenia Muscle [Internet]. 2011 Sep [cited 2016 Feb 24];2(3):143–51. Available from: http://www.pubmedcentral.nih.gov/articlerender.fcgi?artid=3177043&tool=pmcentrez&rendertype=abstract

257. Cassar-Malek I, Passelaigue F, Bernard C, Léger J, Hocquette J-F. Target genes of myostatin loss-of-function in muscles of late bovine fetuses. BMC Genomics [Internet]. BioMed Central; 2007 Jan [cited 2016 Feb 24];8:63. Available from: /pmc/articles/PMC1831773/?report=abstract

258. Thomas M, Langley B, Berry C, Sharma M, Kirk S, Bass J, et al. Myostatin, a negative regulator of muscle growth, functions by inhibiting myoblast proliferation. J Biol Chem [Internet]. 2000 Dec 22 [cited 2016 Feb 22];275(51):40235–43. Available from: http://www.ncbi.nlm.nih.gov/pubmed/10976104

259. Joulia D, Bernardi H, Garandel V, Rabenoelina F, Vernus B, Cabello G. Mechanisms involved in the inhibition of myoblast proliferation and differentiation by myostatin. Exp Cell Res [Internet]. 2003 Jun [cited 2016 Feb 22];286(2):263–75. Available from: http://www.sciencedirect.com/science/article/pii/S0014482703000740

260. McCroskery S, Thomas M, Maxwell L, Sharma M, Kambadur R. Myostatin negatively regulates satellite cell activation and self-renewal. J Cell Biol [Internet]. 2003 Sep 15 [cited 2016 Feb 10];162(6):1135–47. Available from: http://www.pubmedcentral.nih.gov/articlerender.fcgi?artid=2172861&tool=pmcentrez&rendertype=abstract

261. Amthor H, Nicholas G, McKinnell I, Kemp CF, Sharma M, Kambadur R, et al. Follistatin complexes Myostatin and antagonises Myostatin-mediated inhibition of myogenesis. Dev Biol [Internet]. 2004 Jun 1 [cited 2016 Jan 18];270(1):19–30. Available from: http://www.ncbi.nlm.nih.gov/pubmed/15136138

262. Amthor H, Otto A, Macharia R, McKinnell I, Patel K. Myostatin imposes reversible quiescence on embryonic muscle precursors. Dev Dyn [Internet]. 2006 Mar [cited 2016 Feb 22];235(3):672–80. Available from: http://www.ncbi.nlm.nih.gov/pubmed/16425219

263. Malam Z, Cohn RD. Stem cells on alert: priming quiescent stem cells after remote injury. Cell Stem Cell [Internet]. 2014 Jul 3 [cited 2016 Feb 12];15(1):7–8. Available from: http://www.sciencedirect.com/science/article/pii/S1934590914002604

264. Johnson RL, Laufer E, Riddle RD, Tabin C. Ectopic expression of Sonic hedgehog alters dorsal-ventral patterning of somites. Cell [Internet]. 1994 Dec 30 [cited 2016 Feb 16];79(7):1165–73. Available from: http://www.ncbi.nlm.nih.gov/pubmed/8001152

265. Abou-Khalil R, Le Grand F, Pallafacchina G, Valable S, Authier F-J, Rudnicki MA, et al. Autocrine and paracrine angiopoietin 1/Tie-2 signaling promotes muscle satellite cell self-renewal. Cell Stem Cell [Internet]. 2009 Sep 4 [cited 2016 Feb 20];5(3):298–309. Available from: http://www.pubmedcentral.nih.gov/articlerender.fcgi?artid=4592285&tool=pmcentrez&rendertype=abstract

266. Yablonka-Reuveni Z, Seger R, Rivera AJ. Fibroblast Growth Factor Promotes Recruitment of Skeletal Muscle Satellite Cells in Young and Old Rats. J Histochem Cytochem [Internet]. 1999 Jan 1 [cited 2016 Jan 19];47(1):23–42. Available from: http://jhc.sagepub.com/content/47/1/23.short

267. Chakkalakal J V, Jones KM, Basson MA, Brack AS. The aged niche disrupts muscle stem cell quiescence. Nature [Internet]. Nature Publishing Group, a division of Macmillan Publishers Limited. All Rights Reserved.; 2012 Oct 18 [cited 2016 Feb 20];490(7420):355–60. Available from: http://dx.doi.org/10.1038/nature11438

268. Beauchamp JR, Heslop L, Yu DS, Tajbakhsh S, Kelly RG, Wernig A, et al. Expression of CD34 and Myf5 defines the majority of quiescent adult skeletal muscle satellite cells. J Cell Biol [Internet]. 2000 Dec 11 [cited 2016 Feb 22];151(6):1221–34. Available from: http://www.pubmedcentral.nih.gov/articlerender.fcgi?artid=2190588&tool=pmcentrez&rendertype=abstract

269. Irintchev A, Zeschnigk M, Starzinski-Powitz A, Wernig A. Expression pattern of M-cadherin in normal, denervated, and regenerating mouse muscles. Dev Dyn [Internet]. 1994 Apr [cited 2016 Feb 22];199(4):326–37. Available from: http://www.ncbi.nlm.nih.gov/pubmed/8075434

270. Fukada S, Uezumi A, Ikemoto M, Masuda S, Segawa M, Tanimura N, et al. Molecular signature of quiescent satellite cells in adult skeletal muscle. Stem Cells [Internet]. 2007 Oct [cited 2016 Feb 12];25(10):2448–59. Available from: http://www.ncbi.nlm.nih.gov/pubmed/17600112

271. Carnac G, Fajas L, L'honoré A, Sardet C, Lamb NJC, Fernandez A. The retinoblastoma-like protein p130 is involved in the determination of reserve cells in differentiating myoblasts. Curr Biol [Internet]. 2000 May [cited 2016 Feb 22];10(9):543–6. Available from: http://www.sciencedirect.com/science/article/pii/S0960982200004711

272. Christov C, Chrétien F, Abou-Khalil R, Bassez G, Vallet G, Authier F-J, et al. Muscle satellite cells and endothelial cells: close neighbors and privileged partners. Mol Biol Cell [Internet]. 2007 Apr [cited 2016 Feb 19];18(4):1397–409. Available from: http://www.pubmedcentral.nih.gov/articlerender.fcgi?artid=1838982&tool=pmcentrez&rendertype=abstract

273. Saharinen P, Eklund L, Miettinen J, Wirkkala R, Anisimov A, Winderlich M, et al. Angiopoietins assemble distinct Tie2 signalling complexes in endothelial cell-cell and cell-matrix contacts. Nat Cell Biol [Internet]. 2008 May [cited 2016 Feb 22];10(5):527–37. Available from: http://www.ncbi.nlm.nih.gov/pubmed/18425119

274. Tajbakhsh S, Spörle R. Somite Development: Constructing the Vertebrate Body. Cell [Internet]. 1998 Jan 9 [cited 2016 Feb 15];92(1):9–16. Available from:

http://www.ncbi.nlm.nih.gov/pubmed/9489695

275. Clevers H. Wnt/beta-catenin signaling in development and disease. Cell [Internet]. 2006 Nov 3 [cited 2014 Jul 11];127(3):469–80. Available from: http://www.ncbi.nlm.nih.gov/pubmed/17081971

276. Gros J, Serralbo O, Marcelle C. WNT11 acts as a directional cue to organize the elongation of early muscle fibres. Nature [Internet]. 2009 Jan 29 [cited 2016 Feb 1];457(7229):589–93. Available from: http://www.ncbi.nlm.nih.gov/pubmed/18987628

277. Polesskaya A, Seale P, Rudnicki MA. Wnt Signaling Induces the Myogenic Specification of Resident CD45+ Adult Stem Cells during Muscle Regeneration. Cell [Internet]. 2003 Jun [cited 2016 Feb 19];113(7):841–52. Available from: http://www.sciencedirect.com/science/article/pii/S0092867403004379

278. Rochat A, Fernandez A, Vandromme M, Molès J-P, Bouschet T, Carnac G, et al. Insulin and wnt1 pathways cooperate to induce reserve cell activation in differentiation and myotube hypertrophy. Mol Biol Cell [Internet]. 2004 Oct [cited 2016 Feb 23];15(10):4544–55. Available from: http://www.pubmedcentral.nih.gov/articlerender.fcgi?artid=519148&tool=pmcentrez&rendertype=abstract

279. Brack AS, Conboy IM, Conboy MJ, Shen J, Rando TA. A temporal switch from notch to Wnt signaling in muscle stem cells is necessary for normal adult myogenesis. Cell Stem Cell [Internet]. 2008 Jan 10 [cited 2016 Feb 23];2(1):50–9. Available from: http://www.ncbi.nlm.nih.gov/pubmed/18371421

280. Le Grand F, Jones AE, Seale V, Scimè A, Rudnicki MA. Wnt7a activates the planar cell polarity pathway to drive the symmetric expansion of satellite stem cells. Cell Stem Cell [Internet]. 2009 Jun 5 [cited 2016 Feb 20];4(6):535–47. Available from: http://www.pubmedcentral.nih.gov/articlerender.fcgi?artid=2743383&tool=pmcentrez&rendertype=abstract

281. Bentzinger CF, Wang YX, von Maltzahn J, Soleimani VD, Yin H, Rudnicki MA. Fibronectin regulates Wnt7a signaling and satellite cell expansion. Cell Stem Cell [Internet]. 2013 Jan 3 [cited 2016 Feb 20];12(1):75–87. Available from: http://www.pubmedcentral.nih.gov/articlerender.fcgi?artid=3539137&tool=pmcentrez&rendertype=abstract

282. von Maltzahn J, Bentzinger CF, Rudnicki MA. Wnt7a-Fzd7 signalling directly activates the Akt/mTOR anabolic growth pathway in skeletal muscle. Nat Cell Biol [Internet]. Nature Publishing Group, a division of Macmillan Publishers Limited. All Rights Reserved.; 2012 Feb [cited 2016 Jan 22];14(2):186–91. Available from: http://www.pubmedcentral.nih.gov/articlerender.fcgi?artid=3271181&tool=pmcentrez&rendertype=abstract

283. Price FD, von Maltzahn J, Bentzinger CF, Dumont NA, Yin H, Chang NC, et al. Inhibition of JAK-STAT signaling stimulates adult satellite cell function. Nat Med [Internet]. 2014 Oct [cited 2016 Jan 27];20(10):1174–81. Available from: http://www.pubmedcentral.nih.gov/articlerender.fcgi?artid=4191983&tool=pmcentrez&rendertype=abstract

284. Wang K, Wang C, Xiao F, Wang H, Wu Z. JAK2/STAT2/STAT3 are required for myogenic differentiation. J Biol Chem [Internet]. 2008 Dec 5 [cited 2016 Feb 3];283(49):34029–36. Available from: http://www.pubmedcentral.nih.gov/articlerender.fcgi?artid=2662224&tool=pmcentrez&rendertype=abstract

285. Jang Y-N, Baik EJ. JAK-STAT pathway and myogenic differentiation. JAK-STAT [Internet].

2013 Apr 1 [cited 2016 Feb 23];2(2):e23282. Available from: http://www.pubmedcentral.nih.gov/articlerender.fcgi?artid=3710318&tool=pmcentrez&rendertype=abstract

286. Pourquié O. Somitogenesis Part 1 [Internet]. Current Topics in Developmental Biology. Elsevier; 1999 [cited 2016 Apr 3]. 81-105 p. (Current Topics in Developmental Biology; vol. 47). Available from: http://www.sciencedirect.com/science/article/pii/S007021530860722X

287. Hamburger V, Hamilton HL. A series of normal stages in the development of the chick embryo. J Morphol [Internet]. 1951 Jan [cited 2016 Jan 19];88(1):49–92. Available from: http://doi.wiley.com/10.1002/jmor.1050880104

288. Guille M. Microinjection into Xenopus oocytes and embryos. Methods Mol Biol [Internet]. 1999 Jan [cited 2016 Apr 4];127:111–23. Available from: http://www.ncbi.nlm.nih.gov/pubmed/10503229

289. Nieuwkoop PD FJ. Normal Table of Xenopus laevis (Daudin) Elsevier/North-Holland; New. 1956;

290. Jennings CG. Expression of the myogenic gene MRF4 during Xenopus development. Dev Biol [Internet]. 1992 May [cited 2016 Jan 21];151(1):319–32. Available from: http://www.ncbi.nlm.nih.gov/pubmed/1374354

291. Yee SP, Rigby PW. The regulation of myogenin gene expression during the embryonic development of the mouse. Genes Dev [Internet]. 1993 Jul [cited 2016 Mar 4];7(7A):1277–89. Available from: http://www.ncbi.nlm.nih.gov/pubmed/8391506

292. Brand-Saberi B, Wilting J, Ebensperger C, Christ B. The formation of somite compartments in the avian embryo. Int J Dev Biol [Internet]. 1996 Feb [cited 2016 Feb 16];40(1):411–20. Available from: http://www.ncbi.nlm.nih.gov/pubmed/8735956

293. Nogueira JM, Hawrot K, Sharpe C, Noble A, Wood WM, Jorge EC, et al. The emergence of Pax7-expressing muscle stem cells during vertebrate head muscle development. Front Aging Neurosci [Internet]. Frontiers; 2015 May 19;7:62. Available from: http://journal.frontiersin.org/article/10.3389/fnagi.2015.00062/abstract

294. Cusella-De Angelis MG. MyoD, myogenin independent differentiation of primordial myoblasts in mouse somites. J Cell Biol [Internet]. 1992 Mar 1 [cited 2016 Apr 10];116(5):1243–55. Available from: http://jcb.rupress.org/content/116/5/1243.abstract

295. White J, Barro M V, Makarenkova HP, Sanger JW, Sanger JM. Localization of sarcomeric proteins during myofibril assembly in cultured mouse primary skeletal myotubes. Anat Rec (Hoboken) [Internet]. 2014 Sep [cited 2016 Jan 28];297(9):1571–84. Available from: http://www.pubmedcentral.nih.gov/articlerender.fcgi?artid=4145531&tool=pmcentrez&rendertype=abstract

296. Sweetman D, Wagstaff L, Cooper O, Weijer C, Münsterberg A. The migration of paraxial and lateral plate mesoderm cells emerging from the late primitive streak is controlled by different Wnt signals. BMC Dev Biol [Internet]. BioMed Central; 2008 Jan 9 [cited 2014 May 31];8(1):63. Available from: http://bmcdevbiol.biomedcentral.com/articles/10.1186/1471-213X-8-63

297. Relaix F, Rocancourt D, Mansouri A, Buckingham M. A Pax3/Pax7-dependent population of skeletal muscle progenitor cells. Nature [Internet]. 2005 Jun 16 [cited 2016 Jan 28];435(7044):948–53. Available from: http://dx.doi.org/10.1038/nature03594

298. Duband JL, Dufour S, Hatta K, Takeichi M, Edelman GM, Thiery JP. Adhesion molecules during somitogenesis in the avian embryo. J Cell Biol. 1987;104(5):1361–74.

299. Naya FJ, Olson E. MEF2: a transcriptional target for signaling pathways controlling skeletal muscle growth and differentiation. Curr Opin Cell Biol [Internet]. 1999 Dec [cited 2016 Feb 18];11(6):683–8. Available from: http://www.ncbi.nlm.nih.gov/pubmed/10600704

300. Hinits Y, Osborn DPS, Hughes SM. Differential requirements for myogenic regulatory factors distinguish medial and lateral somitic, cranial and fin muscle fibre populations. Development [Internet]. 2009 Feb [cited 2016 Feb 16];136(3):403–14. Available from: http://www.pubmedcentral.nih.gov/articlerender.fcgi?artid=2687589&tool=pmcentrez&rendertype=abstract

301. Mok GF, Mohammed RH, Sweetman D. Expression of myogenic regulatory factors in chicken embryos during somite and limb development. J Anat [Internet]. 2015 Sep 16 [cited 2016 Jan 12];227(3):352–60. Available from: http://doi.wiley.com/10.1111/joa.12340

302. Jouve C, Iimura T, Pourquie O. Onset of the segmentation clock in the chick embryo: evidence for oscillations in the somite precursors in the primitive streak. Development [Internet]. 2002 Mar 1 [cited 2015 Dec 2];129(5):1107–17. Available from: http://dev.biologists.org/content/129/5/1107

303. Zhang H, Stavnezer E. Ski regulates muscle terminal differentiation by transcriptional activation of Myog in a complex with Six1 and Eya3. J Biol Chem [Internet]. 2009 Jan 30 [cited 2016 Feb 3];284(5):2867–79. Available from: http://www.pubmedcentral.nih.gov/articlerender.fcgi?artid=2631951&tool=pmcentrez&rendertype=abstract

304. Denetclaw W, Ordahl C. The growth of the dermomyotome and formation of early myotome lineages in thoracolumbar somites of chicken embryos. Development [Internet]. 2000 Feb 15 [cited 2015 Dec 2];127(4):893–905. Available from: http://dev.biologists.org/content/127/4/893.long

305. Kahane N, Ben-Yair R, Kalcheim C. Medial pioneer fibers pattern the morphogenesis of early myoblasts derived from the lateral somite. Dev Biol [Internet]. 2007 May 15 [cited 2016 Apr 22];305(2):439–50. Available from: http://www.sciencedirect.com/science/article/pii/S0012160607001455

306. Kahane N, Cinnamon Y, Kalcheim C. The origin and fate of pioneer myotomal cells in the avian embryo. Mech Dev [Internet]. 1998 Jun [cited 2016 Apr 22];74(1–2):59–73. Available from: http://www.sciencedirect.com/science/article/pii/S0925477398000665

307. Wu W, de Folter S, Shen X, Zhang W, Tao S. Vertebrate paralogous MEF2 genes: origin, conservation, and evolution. PLoS One [Internet]. Public Library of Science; 2011 Jan 4 [cited 2016 Feb 18];6(3):e17334. Available from: http://journals.plos.org/plosone/article?id=10.1371%252Fjournal.pone.0017334

308. Inuzuka H, Redies C, Takeichi M. Differential expression of R- and N-cadherin in neural and mesodermal tissues during early chicken development. Development. 1991;113(3).

309. Rosenberg P, Esni F, Sjö A, Larue L, Carlsson L, Gullberg D, et al. A Potential Role of R-cadherin in Striated Muscle Formation. Dev Biol. 1997;187:55–70.

310. Oana S, Machida S, Hiratsuka E, Furutani Y, Momma K, Takao A, et al. The complete sequence and expression patterns of the atrial myosin heavy chain in the developing chick*. Biol Cell [Internet]. Blackwell Publishing Ltd; 1998 Dec [cited 2016 Oct 27];90(9):605–13. Available from: http://doi.wiley.com/10.1111/j.1768-322X.1998.tb01069.x

311. Bader D, Masaki T, Fischman DA. Immunochemical analysis of myosin heavy chain during avian myogenesis in vivo and in vitro. J Cell Biol [Internet]. 1982 Dec [cited 2016 Apr

28];95(3):763–70. Available from: http://www.pubmedcentral.nih.gov/articlerender.fcgi?artid=2112936&tool=pmcentrez&rendertype=abstract

312. Jorge EC, Melo CMR, Rosário MF, Rossi JRS, Ledur MC, Moura ASAMT, et al. Chicken skeletal muscle-associated macroarray for gene discovery. funpecrp.com.br Genet Mol Res Genet Mol Res. 2010;9(91):188–207.

313. Yao Z, Fong AP, Cao Y, Ruzzo WL, Gentleman RC, Tapscott SJ. Comparison of endogenous and overexpressed MyoD shows enhanced binding of physiologically bound sites. Skelet Muscle [Internet]. 2013;3(1):8. Available from: http://www.pubmedcentral.nih.gov/articlerender.fcgi?artid=3666993&tool=pmcentrez&rendertype=abstract

314. Burgess R, Cserjesi P, Ligon KL, Olson EN. Paraxis: a basic helix-loop-helix protein expressed in paraxial mesoderm and developing somites. Dev Biol [Internet]. 1995 Apr [cited 2016 Feb 16];168(2):296–306. Available from: http://www.sciencedirect.com/science/article/pii/S0012160685710810

315. Kahane N, Ribes V, Kicheva A, Briscoe J, Kalcheim C. The transition from differentiation to growth during dermomyotome-derived myogenesis depends on temporally restricted hedgehog signaling. Development [Internet]. 2013 Apr 15 [cited 2016 Apr 22];140(8):1740–50. Available from: http://dev.biologists.org/content/140/8/1740

316. Wood WM, Etemad S, Yamamoto M, Goldhamer DJ. MyoD-expressing progenitors are essential for skeletal myogenesis and satellite cell development. Dev Biol [Internet]. 2013 Dec 1 [cited 2016 Apr 10];384(1):114–27. Available from: http://www.sciencedirect.com/science/article/pii/S0012160613004867

317. Zammit PS, Relaix F, Nagata Y, Ruiz AP, Collins C a, Partridge T a, et al. Pax7 and myogenic progression in skeletal muscle satellite cells. J Cell Sci [Internet]. 2006 May 1 [cited 2014 May 27];119(9):1824–32. Available from: http://jcs.biologists.org/content/119/9/1824

318. Collins CA, Gnocchi VF, White RB, Boldrin L, Perez-Ruiz A, Relaix F, et al. Integrated functions of Pax3 and Pax7 in the regulation of proliferation, cell size and myogenic differentiation. PLoS One [Internet]. 2009 Jan [cited 2016 Feb 15];4(2):e4475. Available from: http://www.pubmedcentral.nih.gov/articlerender.fcgi?artid=2637421&tool=pmcentrez&rendertype=abstract

319. Olguin HC, Yang Z, Tapscott SJ, Olwin BB. Reciprocal inhibition between Pax7 and muscle regulatory factors modulates myogenic cell fate determination. J Cell Biol [Internet]. 2007 Jun 4 [cited 2016 Feb 15];177(5):769–79. Available from: http://www.pubmedcentral.nih.gov/articlerender.fcgi?artid=2064278&tool=pmcentrez&rendertype=abstract

320. Bergstrom DA, Penn BH, Strand A, Perry RLS, Rudnicki MA, Tapscott SJ. Promoter-Specific Regulation of MyoD Binding and Signal Transduction Cooperate to Pattern Gene Expression. Mol Cell [Internet]. 2002 Mar [cited 2016 Apr 10];9(3):587–600. Available from: http://www.sciencedirect.com/science/article/pii/S1097276502004811

321. Rashid DJ, Chapman SC, Larsson HC, Organ CL, Bebin A-G, Merzdorf CS, et al. From dinosaurs to birds: a tail of evolution. Evodevo [Internet]. BioMed Central; 2014 [cited 2016 Oct 27];5(1):25. Available from: http://evodevojournal.biomedcentral.com/articles/10.1186/2041-9139-5-25

322. Tenin G, Wright D, Ferjentsik Z, Bone R, McGrew MJ, Maroto M, et al. The chick somitogenesis oscillator is arrested before all paraxial mesoderm is segmented into somites. BMC Dev Biol [Internet]. BioMed Central; 2010 [cited 2016 Oct 27];10(1):24.

Available from: http://bmcdevbiol.biomedcentral.com/articles/10.1186/1471-213X-10-24

323. Pu Q, Abduelmula A, Masyuk M, Theiss C, Schwandulla D, Hans M, et al. The dermomyotome ventrolateral lip is essential for the hypaxial myotome formation. BMC Dev Biol [Internet]. BioMed Central; 2013 Jan 18 [cited 2016 Feb 1];13(1):37. Available from: http://bmcdevbiol.biomedcentral.com/articles/10.1186/1471-213X-13-37

324. CHAFFEY N. Alberts, B., Johnson, A., Lewis, J., Raff, M., Roberts, K. and Walter, P. Molecular biology of the cell. 4th edn. Ann Bot [Internet]. Oxford University Press; 2003 Feb 1 [cited 2016 Oct 27];91(3):401–401. Available from: http://aob.oupjournals.org/cgi/doi/10.1093/aob/mcg023

325. Delfini M-C, De La Celle M, Gros J, Serralbo O, Marics I, Seux M, et al. The timing of emergence of muscle progenitors is controlled by an FGF/ERK/SNAIL1 pathway. Dev Biol. 2009;333(2):229–37.

326. Karabagli H, Karabagli P, Ladher RK, Schoenwolf GC. Survey of fibroblast growth factor expression during chick organogenesis. Anat Rec [Internet]. 2002 Sep 1 [cited 2016 Oct 27];268(1):1–6. Available from: http://www.ncbi.nlm.nih.gov/pubmed/12209559

327. Latil M, Rocheteau P, Châtre L, Sanulli S, Mémet S, Ricchetti M, et al. Skeletal muscle stem cells adopt a dormant cell state post mortem and retain regenerative capacity. Nat Commun [Internet]. Nature Publishing Group, a division of Macmillan Publishers Limited. All Rights Reserved.; 2012 Jan 12 [cited 2016 Mar 17];3:903. Available from: http://dx.doi.org/10.1038/ncomms1890

328. Buckingham M, Vincent SD. Distinct and dynamic myogenic populations in the vertebrate embryo. Curr Opin Genet Dev [Internet]. 2009 Oct [cited 2016 Feb 27];19(5):444–53. Available from: http://www.ncbi.nlm.nih.gov/pubmed/19762225

329. Bryson-Richardson RJ, Currie PD. The genetics of vertebrate myogenesis. Nat Rev Genet [Internet]. Nature Publishing Group; 2008 Aug [cited 2015 Nov 20];9(8):632–46. Available from: http://www.ncbi.nlm.nih.gov/pubmed/18636072

330. Saccone V, Puri PL. Epigenetic regulation of skeletal myogenesis. Organogenesis [Internet]. Jan [cited 2016 Apr 10];6(1):48–53. Available from: http://www.pubmedcentral.nih.gov/articlerender.fcgi?artid=2861743&tool=pmcentrez&rendertype=abstract

331. Kusakabe R, Kuraku S, Kuratani S. Expression and interaction of muscle-related genes in the lamprey imply the evolutionary scenario for vertebrate skeletal muscle, in association with the acquisition of the neck and fins. Dev Biol [Internet]. 2011 Feb 1 [cited 2016 Feb 11];350(1):217–27. Available from: http://www.ncbi.nlm.nih.gov/pubmed/21035440

332. Weintraub H, Tapscott SJ, Davis RL, Thayer MJ, Adam MA, Lassar AB, et al. Activation of muscle-specific genes in pigment, nerve, fat, liver, and fibroblast cell lines by forced expression of MyoD. Proc Natl Acad Sci U S A [Internet]. 1989 Jul [cited 2016 Feb 9];86(14):5434–8. Available from: http://www.pubmedcentral.nih.gov/articlerender.fcgi?artid=297637&tool=pmcentrez&rendertype=abstract

333. Kitzmann M, Carnac G, Vandromme M, Primig M, Lamb NJ, Fernandez A. The muscle regulatory factors MyoD and myf-5 undergo distinct cell cycle-specific expression in muscle cells. J Cell Biol [Internet]. 1998 Sep 21 [cited 2016 Apr 10];142(6):1447–59. Available from: http://www.pubmedcentral.nih.gov/articlerender.fcgi?artid=2141770&tool=pmcentrez&rendertype=abstract

334. Ludolph DC, Neff AW, Mescher AL, Malacinski GM, Parker MA, Smith RC. Overexpression of XMyoD or XMyf5 in Xenopus embryos induces the formation of enlarged myotomes

through recruitment of cells of nonsomitic lineage. Dev Biol [Internet]. 1994 Nov [cited 2016 Jan 22];166(1):18–33. Available from: http://www.sciencedirect.com/science/article/pii/S0012160684712942

335. Hopwood ND, Pluck A, Gurdon JB. Xenopus Myf-5 marks early muscle cells and can activate muscle genes ectopically in early embryos. Development [Internet]. 1991 Feb [cited 2016 Apr 10];111(2):551–60. Available from: http://www.ncbi.nlm.nih.gov/pubmed/1716555

336. Hopwood ND, Gurdon JB. Activation of muscle genes without myogenesis by ectopic expression of MyoD in frog embryo cells. Nature [Internet]. 1990 Sep 13 [cited 2016 Apr 10];347(6289):197–200. Available from: http://www.ncbi.nlm.nih.gov/pubmed/1697650

337. Delfini M-C, Duprez D. Ectopic Myf5 or MyoD prevents the neuronal differentiation program in addition to inducing skeletal muscle differentiation, in the chick neural tube. Development [Internet]. 2004 Feb [cited 2014 May 8];131(4):713–23. Available from: http://www.ncbi.nlm.nih.gov/pubmed/14724123

338. Scaal M, Gros J, Lesbros C, Marcelle C. In ovo electroporation of avian somites. Dev Dyn [Internet]. 2004 Mar [cited 2016 Jan 22];229(3):643–50. Available from: http://www.ncbi.nlm.nih.gov/pubmed/14991719

339. Momose T, Tonegawa A, Takeuchi J, Ogawa H, Umesono K, Yasuda K, et al. Efficient targeting of gene expression in chick embryos by microelectroporation. Dev Growth Differ [Internet]. 1999 Jun [cited 2016 Jan 27];41(3):335–44. Available from: http://doi.wiley.com/10.1046/j.1440-169X.1999.413437.x

340. Chapman SC, Collignon J, Schoenwolf GC, Lumsden A. Improved method for chick whole-embryo culture using a filter paper carrier. Dev Dyn [Internet]. 2001 Mar [cited 2016 Apr 3];220(3):284–9. Available from: http://www.ncbi.nlm.nih.gov/pubmed/11241836

341. Clapier CR, Cairns BR. The biology of chromatin remodeling complexes. Annu Rev Biochem [Internet]. Annual Reviews; 2009 Jan 2 [cited 2014 Jul 12];78:273–304. Available from: http://www.annualreviews.org/doi/abs/10.1146/annurev.biochem.77.062706.153223

342. Yutzey KE, Rhodes SJ, Konieczny SF. Differential trans activation associated with the muscle regulatory factors MyoD1, myogenin, and MRF4. Mol Cell Biol [Internet]. 1990 Aug 1 [cited 2016 Feb 18];10(8):3934–44. Available from: http://mcb.asm.org/content/10/8/3934.abstract

343. Fujisawa-Sehara A, Nabeshima Y, Komiya T, Uetsuki T, Asakura A. Differential trans-activation of muscle-specific regulatory elements including the mysosin light chain box by chicken MyoD, myogenin, and MRF4. J Biol Chem [Internet]. 1992 May 15 [cited 2016 Feb 18];267(14):10031–8. Available from: http://www.jbc.org/content/267/14/10031.short

344. Wei Q, Paterson BM. Regulation of MyoD function in the dividing myoblast. FEBS Lett [Internet]. 2001 Feb 16 [cited 2015 Feb 18];490(3):171–8. Available from: http://www.ncbi.nlm.nih.gov/pubmed/11223032

345. Kozak M. Point mutations define a sequence flanking the AUG initiator codon that modulates translation by eukaryotic ribosomes. Cell [Internet]. Elsevier; 1986 Jan 31 [cited 2015 Nov 20];44(2):283–92. Available from: http://www.cell.com/article/0092867486907622/fulltext

346. Kozak M. An analysis of 5'-noncoding sequences from 699 vertebrate messenger RNAs. Nucleic Acids Res [Internet]. 1987 Oct 26 [cited 2016 Feb 26];15(20):8125–48. Available from: http://www.pubmedcentral.nih.gov/articlerender.fcgi?artid=306349&tool=pmcentrez&rendertype=abstract

347. Akef A, Lee ES, Palazzo AF. Splicing promotes the nuclear export of β-globin mRNA by overcoming nuclear retention elements. RNA [Internet]. 2015 Nov [cited 2016 Oct 24];21(11):1908–20. Available from: http://www.ncbi.nlm.nih.gov/pubmed/26362019

348. Gorochowski TE, Ignatova Z, Bovenberg RAL, Roubos JA. Trade-offs between tRNA abundance and mRNA secondary structure support smoothing of translation elongation rate. Nucleic Acids Res [Internet]. Oxford University Press; 2015 Mar 31 [cited 2016 Oct 24];43(6):3022–32. Available from: http://www.ncbi.nlm.nih.gov/pubmed/25765653

349. Khan F, Legler PM, Mease RM, Duncan EH, Bergmann-Leitner ES, Angov E. Histidine affinity tags affect MSP1(42) structural stability and immunodominance in mice. Biotechnol J [Internet]. 2012 Jan [cited 2016 Feb 26];7(1):133–47. Available from: http://www.ncbi.nlm.nih.gov/pubmed/22076863

350. Shevtsova Z, Malik JMI, Michel U, Schöll U, Bähr M, Kügler S. Evaluation of epitope tags for protein detection after in vivo CNS gene transfer. Eur J Neurosci [Internet]. 2006 May [cited 2016 Jan 31];23(8):1961–9. Available from: http://www.ncbi.nlm.nih.gov/pubmed/16630044

351. Tapscott SJ, Davis RL, Thayer MJ, Cheng PF, Weintraub H, Lassar AB. MyoD1: a nuclear phosphoprotein requiring a Myc homology region to convert fibroblasts to myoblasts. Science [Internet]. 1988 Oct 21 [cited 2016 Feb 27];242(4877):405–11. Available from: http://www.ncbi.nlm.nih.gov/pubmed/3175662

352. Taylor M V. Comparison of Muscle Development in Drosophila and Vertebrates [Internet]. Landes Bioscience; 2013 [cited 2016 Apr 11]. Available from: http://www.ncbi.nlm.nih.gov/books/NBK6226/

353. Guindon S, Dufayard J-F, Lefort V, Anisimova M, Hordijk W, Gascuel O. New algorithms and methods to estimate maximum-likelihood phylogenies: assessing the performance of PhyML 3.0. Syst Biol [Internet]. 2010 May [cited 2014 Jul 9];59(3):307–21. Available from: http://www.ncbi.nlm.nih.gov/pubmed/20525638

354. Schubert FR, Sobreira DR, Janousek RG, Alvares LE, Dietrich S. Dact genes are chordate specific regulators at the intersection of Wnt and Tgf-β signaling pathways. BMC Evol Biol [Internet]. BioMed Central; 2014 Jan 6 [cited 2016 Apr 11];14(1):157. Available from: http://bmcevolbiol.biomedcentral.com/articles/10.1186/1471-2148-14-157

355. Zhao X, Yu Q, Huang L, Liu Q-X. Patterns of positive selection of the myogenic regulatory factor gene family in vertebrates. PLoS One [Internet]. Public Library of Science; 2014 Jan 20 [cited 2016 Feb 27];9(3):e92873. Available from: http://journals.plos.org/plosone/article?id=10.1371/journal.pone.0092873

356. Taylor JS, Van de Peer Y, Braasch I, Meyer A. Comparative genomics provides evidence for an ancient genome duplication event in fish. Philos Trans R Soc Lond B Biol Sci [Internet]. 2001 Oct 29 [cited 2016 Mar 10];356(1414):1661–79. Available from: http://www.pubmedcentral.nih.gov/articlerender.fcgi?artid=1088543&tool=pmcentrez&rendertype=abstract

357. Jaillon O, Aury J-M, Brunet F, Petit J-L, Stange-Thomann N, Mauceli E, et al. Genome duplication in the teleost fish Tetraodon nigroviridis reveals the early vertebrate proto-karyotype. Nature [Internet]. 2004 Oct 21 [cited 2016 Apr 11];431(7011):946–57. Available from: http://www.ncbi.nlm.nih.gov/pubmed/15496914

358. Dehal P, Boore JL. Two rounds of whole genome duplication in the ancestral vertebrate. PLoS Biol [Internet]. Public Library of Science; 2005 Oct 6 [cited 2016 Feb 11];3(10):e314. Available from: http://journals.plos.org/plosbiology/article?id=10.1371/journal.pbio.0030314

359. Li SC, Goto NK, Williams K a, Deber CM. Alpha-helical, but not beta-sheet, propensity of proline is determined by peptide environment. Proc Natl Acad Sci U S A. 1996;93(June):6676–81.

360. Salichs E, Ledda A, Mularoni L, Albà MM, de la Luna S. Genome-wide analysis of histidine repeats reveals their role in the localization of human proteins to the nuclear speckles compartment. PLoS Genet [Internet]. 2009 Mar [cited 2016 Apr 5];5(3):e1000397. Available from: http://www.pubmedcentral.nih.gov/articlerender.fcgi?artid=2644819&tool=pmcentrez&rendertype=abstract

361. Prigent C, Dimitrov S. Phosphorylation of serine 10 in histone H3, what for? J Cell Sci [Internet]. 2003 Sep 15 [cited 2016 Mar 8];116(Pt 18):3677–85. Available from: http://jcs.biologists.org/content/116/18/3677

362. Kato K, Gurdon JB. An inhibitory effect of Xenopus gastrula ectoderm on muscle cell differentiation and its role for dorsoventral patterning of mesoderm. Dev Biol [Internet]. 1994 May [cited 2016 Apr 11];163(1):222–9. Available from: http://www.ncbi.nlm.nih.gov/pubmed/8174778

363. Lours-Calet C, Alvares LE, El-Hanfy AS, Gandesha S, Walters EH, Sobreira DR, et al. Evolutionarily conserved morphogenetic movements at the vertebrate head-trunk interface coordinate the transport and assembly of hypopharyngeal structures. Dev Biol [Internet]. 2014 Jun 15 [cited 2016 Jan 25];390(2):231–46. Available from: http://www.pubmedcentral.nih.gov/articlerender.fcgi?artid=4010675&tool=pmcentrez&rendertype=abstract

364. MA P. Crystal structure of MyoD bHLH domain-DNA complex: Perspectives on DNA recognition and implications for transcriptional activation. Cell [Internet]. 1994 May [cited 2016 Apr 11];77(3):451–9. Available from: http://www.sciencedirect.com/science/article/pii/0092867494901597

365. Jorge EC, Melo CMR, Rosário MF, Rossi JRS, Ledur MC, Moura ASAMT, et al. Chicken skeletal muscle-associated macroarray for gene discovery. Genet Mol Res [Internet]. Funpec-editora; 2010 Jan 1 [cited 2016 Apr 11];9(1):188–207. Available from: http://repositorio.unesp.br/handle/11449/14420

366. Mak KL, To RQ, Kong Y, Konieczny SF. The MRF4 activation domain is required to induce muscle-specific gene expression. Mol Cell Biol [Internet]. 1992 Oct 1 [cited 2016 Apr 12];12(10):4334–46. Available from: http://mcb.asm.org/content/12/10/4334.short

367. Knoepfler PS, Bergstrom DA, Uetsuki T, Dac-Korytko I, Sun YH, Wright WE, et al. A conserved motif N-terminal to the DNA-binding domains of myogenic bHLH transcription factors mediates cooperative DNA binding with pbx-Meis1/Prep1. Nucleic Acids Res [Internet]. 1999 Sep 15 [cited 2016 Feb 27];27(18):3752–61. Available from: http://www.pubmedcentral.nih.gov/articlerender.fcgi?artid=148632&tool=pmcentrez&rendertype=abstract

368. Rogerson PJ, Jamali M, Skerjanc IS. The C-terminus of myogenin, but not MyoD, targets upregulation of MEF2C expression. FEBS Lett [Internet]. 2002 Jul 31 [cited 2016 Feb 26];524(1–3):134–8. Available from: http://www.sciencedirect.com/science/article/pii/S0014579302030247

369. Kablar B, Krastel K, Tajbakhsh S, Rudnicki MA. Myf5 and MyoD activation define independent myogenic compartments during embryonic development. Dev Biol [Internet]. 2003 Jun [cited 2016 Jan 21];258(2):307–18. Available from: http://www.sciencedirect.com/science/article/pii/S0012160603001398

370. Kassar-Duchossoy L, Gayraud-Morel B, Gomès D, Rocancourt D, Buckingham M, Shinin V,

et al. Mrf4 determines skeletal muscle identity in Myf5:Myod double-mutant mice. Nature [Internet]. 2004 Sep 23 [cited 2016 Feb 18];431(7007):466–71. Available from: http://www.ncbi.nlm.nih.gov/pubmed/15386014

371. Tapscott SJ. The circuitry of a master switch: Myod and the regulation of skeletal muscle gene transcription. Development [Internet]. 2005 Jun 15 [cited 2016 Jan 11];132(12):2685–95. Available from: http://dev.biologists.org/content/132/12/2685.short

372. Serralbo O, Marcelle C. Migrating cells mediate long-range WNT signaling. Development [Internet]. 2014 May 15 [cited 2016 Apr 12];141(10):2057–63. Available from: http://dev.biologists.org/content/141/10/2057

373. Linker C. Intrinsic signals regulate the initial steps of myogenesis in vertebrates. Development [Internet]. 2003 Oct 15 [cited 2016 Jan 12];130(20):4797–807. Available from: http://dev.biologists.org/content/130/20/4797

374. Maroto M, Bone RA, Dale JK. Somitogenesis. Development [Internet]. 2012 Jul 15 [cited 2015 Nov 28];139(14):2453–6. Available from: http://dev.biologists.org/content/139/14/2453

375. Mauch TJ, Yang G, Wright M, Smith D, Schoenwolf GC. Signals from trunk paraxial mesoderm induce pronephros formation in chick intermediate mesoderm. Dev Biol [Internet]. 2000 Apr 1 [cited 2016 Jan 19];220(1):62–75. Available from: http://www.sciencedirect.com/science/article/pii/S0012160600996234

376. Psychoyos D, Stern CD. Fates and migratory routes of primitive streak cells in the chick embryo. Development [Internet]. 1996 May [cited 2015 Dec 3];122(5):1523–34. Available from: http://www.ncbi.nlm.nih.gov/pubmed/8625839

377. Hansis C, Barreto G, Maltry N, Niehrs C. Nuclear reprogramming of human somatic cells by xenopus egg extract requires BRG1. Curr Biol [Internet]. 2004 Aug 24 [cited 2016 Apr 13];14(16):1475–80. Available from: http://www.sciencedirect.com/science/article/pii/S0960982204006086

378. Chanoine C, Hardy S. Xenopus muscle development: from primary to secondary myogenesis. Dev Dyn [Internet]. 2003 Jan [cited 2016 Jan 27];226(1):12–23. Available from: http://www.ncbi.nlm.nih.gov/pubmed/12508220

379. Sillar KT, Wedderburn JF, Simmers AJ. The development of swimming rhythmicity in post-embryonic Xenopus laevis. Proc Biol Sci [Internet]. 1991 Nov 22 [cited 2016 Jan 28];246(1316):147–53. Available from: http://rspb.royalsocietypublishing.org/content/246/1316/147.short

380. Muntz L. Myogenesis in the trunk and leg during development of the tadpole of Xenopus laevis (Daudin 1802). J Embryol Exp Morphol [Internet]. 1975 Jun 1 [cited 2016 Jan 28];33(3):757–74. Available from: http://dev.biologists.org/content/33/3/757.short

381. Berti F, Nogueira JM, Wöhrle S, Sobreira DR, Hawrot K, Dietrich S. Time course and side-by-side analysis of mesodermal, pre-myogenic, myogenic and differentiated cell markers in the chicken model for skeletal muscle formation. J Anat [Internet]. 2015;227(3):361–82. Available from: http://doi.wiley.com/10.1111/joa.12353

382. Wohlgemuth SL, Crawford BD, Pilgrim DB. The myosin co-chaperone UNC-45 is required for skeletal and cardiac muscle function in zebrafish. Dev Biol [Internet]. 2007 Mar 15 [cited 2016 Jan 28];303(2):483–92. Available from: http://www.ncbi.nlm.nih.gov/pubmed/17189627

383. Gianakopoulos PJ, Mehta V, Voronova A, Cao Y, Yao Z, Coutu J, et al. MyoD directly up-regulates premyogenic mesoderm factors during induction of skeletal myogenesis in stem cells. J Biol Chem [Internet]. 2011 Jan 28 [cited 2016 Feb 3];286(4):2517–25. Available

from:
http://www.pubmedcentral.nih.gov/articlerender.fcgi?artid=3024746&tool=pmcentrez&rendertype=abstract

384. Liu N, Nelson BR, Bezprozvannaya S, Shelton JM, Richardson JA, Bassel-Duby R, et al. Requirement of MEF2A, C, and D for skeletal muscle regeneration. Proc Natl Acad Sci U S A [Internet]. 2014 Mar 18 [cited 2015 Dec 16];111(11):4109–14. Available from: http://www.pnas.org/content/111/11/4109.abstract

385. Lu J, Mckinsey TA, Zhang C, Olson EN. Regulation of Skeletal Myogenesis by Association of the MEF2 Transcription Factor with Class II Histone Deacetylases Southwestern Medical Center at Dallas. 2000;6:233–44.

386. Bonnet A, Dai F, Brand-Saberi B, Duprez D. Vestigial-like 2 acts downstream of MyoD activation and is associated with skeletal muscle differentiation in chick myogenesis. Mech Dev [Internet]. 2010 Jan [cited 2016 Feb 28];127(1–2):120–36. Available from: http://www.sciencedirect.com/science/article/pii/S0925477309014713

387. Puri PL, Sartorelli V. Regulation of muscle regulatory factors by DNA-binding, interacting proteins, and post-transcriptional modifications. J Cell Physiol [Internet]. 2000 Nov [cited 2016 Jan 11];185(2):155–73. Available from: http://www.ncbi.nlm.nih.gov/pubmed/11025438

388. Wang DZ, Valdez MR, McAnally J, Richardson J, Olson EN. The Mef2c gene is a direct transcriptional target of myogenic bHLH and MEF2 proteins during skeletal muscle development. Development [Internet]. 2001 Nov [cited 2016 Apr 27];128(22):4623–33. Available from: http://www.ncbi.nlm.nih.gov/pubmed/11714687

389. Sweetman D, Rathjen T, Jefferson M, Wheeler G, Smith TG, Wheeler GN, et al. FGF-4 signaling is involved in mir-206 expression in developing somites of chicken embryos. Dev Dyn [Internet]. 2006 Aug [cited 2016 Jan 31];235(8):2185–91. Available from: http://www.ncbi.nlm.nih.gov/pubmed/16804893

390. Lluís F, Ballestar E, Suelves M, Esteller M, Muñoz-Cánoves P. E47 phosphorylation by p38 MAPK promotes MyoD/E47 association and muscle-specific gene transcription. EMBO J [Internet]. EMBO Press; 2005 Mar 9 [cited 2016 Jan 31];24(5):974–84. Available from: http://emboj.embopress.org/content/24/5/974.abstract

391. Ludolph DC, Konieczny SF. Transcription factor families: muscling in on the myogenic program. Faseb J [Internet]. 1995;9(15):1595–604. Available from: internal-pdf://ludolph1995-2896385551/ludolph1995.pdf%5Cnhttp://www.ncbi.nlm.nih.gov/entrez/query.fcgi?cmd=Retrieve&db=PubMed&dopt=Citation&list_uids=8529839

392. Hinterberger TJ, Sassoon DA, Rhodes SJ, Konieczny SF. Expression of the muscle regulatory factor MRF4 during somite and skeletal myofiber development. Dev Biol [Internet]. 1991 Sep [cited 2016 Apr 21];147(1):144–56. Available from: http://www.sciencedirect.com/science/article/pii/S0012160605800144

393. Macqueen DJ, Johnston IA. An update on MyoD evolution in teleosts and a proposed consensus nomenclature to accommodate the tetraploidization of different vertebrate genomes. PLoS One [Internet]. Public Library of Science; 2008 Jan 6 [cited 2016 Apr 21];3(2):e1567. Available from: http://journals.plos.org/plosone/article?id=10.1371/journal.pone.0001567

394. Shklover J, Etzioni S, Weisman-Shomer P, Yafe A, Bengal E, Fry M. MyoD uses overlapping but distinct elements to bind E-box and tetraplex structures of regulatory sequences of muscle-specific genes. Nucleic Acids Res [Internet]. 2007 Jan 18 [cited 2016 Apr 21];35(21):7087–95. Available from:

http://nar.oxfordjournals.org/content/35/21/7087.full

395. Tapscott SJ. The circuitry of a master switch: Myod and the regulation of skeletal muscle gene transcription. Development [Internet]. 2005 Jun 15 [cited 2014 May 2];132(12):2685–95. Available from: http://dev.biologists.org/content/132/12/2685.short

396. Braun T, Buschhausen-Denker G, Bober E, Tannich E, Arnold HH. A novel human muscle factor related to but distinct from MyoD1 induces myogenic conversion in 10T1/2 fibroblasts. EMBO J [Internet]. 1989 Mar [cited 2016 Feb 9];8(3):701–9. Available from: http://www.pubmedcentral.nih.gov/articlerender.fcgi?artid=400865&tool=pmcentrez&rendertype=abstract

397. Nitzan E, Avraham O, Kahane N, Ofek S, Kumar D, Kalcheim C. Dynamics of BMP and Hes1/Hairy1 signaling in the dorsal neural tube underlies the transition from neural crest to definitive roof plate. BMC Biol [Internet]. BioMed Central; 2016 Jan 24 [cited 2016 Apr 22];14(1):23. Available from: http://bmcbiol.biomedcentral.com/articles/10.1186/s12915-016-0245-6

398. Ordahl CP, Berdougo E, Venters SJ, Denetclaw WF. The dermomyotome dorsomedial lip drives growth and morphogenesis of both the primary myotome and dermomyotome epithelium. Development [Internet]. 2001 May [cited 2016 Feb 1];128(10):1731–44. Available from: http://www.ncbi.nlm.nih.gov/pubmed/11311155

399. Mok GF, Sweetman D. Many routes to the same destination: Lessons from skeletal muscle development. Reproduction [Internet]. 2011 Mar 1 [cited 2016 Jan 12];141(3):301–12. Available from: http://www.reproduction-online.org/content/141/3/301.figures-only

400. Cserjesi P, Olson EN. Myogenin induces the myocyte-specific enhancer binding factor MEF-2 independently of other muscle-specific gene products. Mol Cell Biol [Internet]. 1991 Oct [cited 2016 Mar 4];11(10):4854–62. Available from: http://www.pubmedcentral.nih.gov/articlerender.fcgi?artid=361454&tool=pmcentrez&rendertype=abstract

401. Lassar AB, Davis RL, Wright WE, Kadesch T, Murre C, Voronova A, et al. Functional activity of myogenic HLH proteins requires hetero-oligomerization with E12/E47-like proteins in vivo. Cell [Internet]. 1991 Jul 26 [cited 2016 Mar 4];66(2):305–15. Available from: http://www.ncbi.nlm.nih.gov/pubmed/1649701

402. Edmondson DG, Cheng TC, Cserjesi P, Chakraborty T. Analysis of the myogenin promoter reveals an indirect pathway for positive autoregulation mediated by the muscle-specific enhancer Analysis of the Myogenin Promoter Reveals an Indirect Pathway for Positive Autoregulation Mediated by the Muscle-Specific En. 1992;

403. Estrella NL, Desjardins CA, Nocco SE, Clark AL, Maksimenko Y, Naya FJ. MEF2 transcription factors regulate distinct gene programs in mammalian skeletal muscle differentiation. J Biol Chem. 2015;290(2):1256–68.

404. Lilly B, Zhao B, Ranganayakulu G, Paterson BM, Schulz RA, Olson EN. Requirement of MADS domain transcription factor D-MEF2 for muscle formation in Drosophila. Science [Internet]. 1995 Feb 3 [cited 2016 Feb 18];267(5198):688–93. Available from: http://www.ncbi.nlm.nih.gov/pubmed/7839146

405. Olson EN, Perry M, Schulz R a. Regulation of muscle differentiation by the MEF2 family of MADS box transcription factors. Dev Biol. 1995;172(1):2–14.

406. Dodou E, Xu S-M, Black BL. mef2c is activated directly by myogenic basic helix-loop-helix proteins during skeletal muscle development in vivo. Mech Dev [Internet]. 2003 Sep [cited 2016 Feb 18];120(9):1021–32. Available from: http://www.sciencedirect.com/science/article/pii/S0925477303001783

407. Luo D, Renault VM, Rando TA. The regulation of Notch signaling in muscle stem cell activation and postnatal myogenesis. Semin Cell Dev Biol [Internet]. 2005 Jan [cited 2016 Mar 31];16(4–5):612–22. Available from: http://www.sciencedirect.com/science/article/pii/S1084952105000832

408. Fickett JW. Coordinate positioning of MEF2 and myogenin binding sites. Gene [Internet]. 1996 Jun 12 [cited 2016 Apr 27];172(1):GC19-32. Available from: http://www.ncbi.nlm.nih.gov/pubmed/8654964

409. Grifone R, Laclef C, Spitz F, Lopez S, Demignon J, Guidotti J-E, et al. Six1 and Eya1 expression can reprogram adult muscle from the slow-twitch phenotype into the fast-twitch phenotype. Mol Cell Biol [Internet]. 2004 Jul [cited 2016 Apr 26];24(14):6253–67. Available from: http://www.pubmedcentral.nih.gov/articlerender.fcgi?artid=434262&tool=pmcentrez&rendertype=abstract

410. Hall DB, Struhl K. The VP16 activation domain interacts with multiple transcriptional components as determined by protein-protein cross-linking in vivo. J Biol Chem [Internet]. 2002 Nov 29 [cited 2016 Apr 29];277(48):46043–50. Available from: http://www.jbc.org/content/277/48/46043.full

411. Lu R, Yang P, Padmakumar S, Misra V. The herpesvirus transactivator VP16 mimics a human basic domain leucine zipper protein, luman, in its interaction with HCF. J Virol [Internet]. 1998 Aug [cited 2016 Oct 24];72(8):6291–7. Available from: http://www.ncbi.nlm.nih.gov/pubmed/9658067

412. Liu Y, Gong W, Huang CC, Herr W, Cheng X. Crystal structure of the conserved core of the herpes simplex virus transcriptional regulatory protein VP16. Genes Dev [Internet]. Cold Spring Harbor Laboratory Press; 1999 Jul 1 [cited 2016 Oct 24];13(13):1692–703. Available from: http://www.ncbi.nlm.nih.gov/pubmed/10398682

413. Hink MA, Griep RA, Borst JW, van Hoek A, Eppink MH, Schots A, et al. Structural dynamics of green fluorescent protein alone and fused with a single chain Fv protein. J Biol Chem [Internet]. American Society for Biochemistry and Molecular Biology; 2000 Jun 9 [cited 2016 Oct 24];275(23):17556–60. Available from: http://www.ncbi.nlm.nih.gov/pubmed/10748019

414. Kobayashi M, Nishikawa K, Suzuki T, Yamamoto M. The homeobox protein Six3 interacts with the Groucho corepressor and acts as a transcriptional repressor in eye and forebrain formation. Dev Biol [Internet]. 2001 Apr 15 [cited 2016 Feb 24];232(2):315–26. Available from: http://www.ncbi.nlm.nih.gov/pubmed/11401394

415. Barrow KM, Perez-Campo FM, Ward CM. Use of the cytomegalovirus promoter for transient and stable transgene expression in mouse embryonic stem cells. Methods Mol Biol [Internet]. 2006 Jan [cited 2016 Apr 29];329:283–94. Available from: http://www.ncbi.nlm.nih.gov/pubmed/16845998

416. Ryu CJ, Whitehurst CE, Chen J. Expression of Gal4-VP16 and Gal4-DNA binding domain under the control of the T lymphocyte-specific lck proximal promoter in transgenic mice. BMB Rep [Internet]. 2008;41(8):575–80. Available from: http://www.ncbi.nlm.nih.gov/pubmed/18755072

417. Neilson KM, Pignoni F, Yan B, Moody SA. Developmental expression patterns of candidate cofactors for vertebrate six family transcription factors. Dev Dyn [Internet]. 2010 Dec [cited 2016 Apr 29];239(12):3446–66. Available from: http://www.pubmedcentral.nih.gov/articlerender.fcgi?artid=3059517&tool=pmcentrez&rendertype=abstract

418. Cann GM, Lee JW, Stockdale FE. Sonic hedgehog enhances somite cell viability and

formation of primary slow muscle fibers in avian segmented mesoderm. Anat Embryol (Berl) [Internet]. 1999 Sep [cited 2016 Apr 29];200(3):239–52. Available from: http://www.ncbi.nlm.nih.gov/pubmed/10463340

419. Francetic T, Li Q. Skeletal myogenesis and Myf5 activation. Transcription [Internet]. 2011 Jan [cited 2016 Apr 22];2(3):109–14. Available from: http://www.pubmedcentral.nih.gov/articlerender.fcgi?artid=3173648&tool=pmcentrez&rendertype=abstract

420. Bajard L, Relaix F, Lagha M, Rocancourt D, Daubas P, Buckingham ME. A novel genetic hierarchy functions during hypaxial myogenesis: Pax3 directly activates Myf5 in muscle progenitor cells in the limb. Genes Dev [Internet]. 2006 Sep 1 [cited 2016 Apr 29];20(17):2450–64. Available from: http://www.pubmedcentral.nih.gov/articlerender.fcgi?artid=1560418&tool=pmcentrez&rendertype=abstract

421. Relaix F, Rocancourt D, Mansouri A, Buckingham M. Divergent functions of murine Pax3 and Pax7 in limb muscle development. Genes Dev [Internet]. 2004 May 1 [cited 2016 Feb 12];18(9):1088–105. Available from: http://genesdev.cshlp.org/content/18/9/1088

422. Chen C-H, Kuo S-C, Huang L-J, Hsu M-H, Lung F-DT. Affinity of synthetic peptide fragments of MyoD for Id1 protein and their biological effects in several cancer cells. J Pept Sci [Internet]. 2010 May [cited 2016 Feb 3];16(5):231–41. Available from: http://www.ncbi.nlm.nih.gov/pubmed/20235117

423. Czerwinska AM, Grabowska I, Archacka K, Bem J, Swierczek B, Helinska A, et al. Myogenic Differentiation of Mouse Embryonic Stem Cells That Lack a Functional Pax7 Gene. Stem Cells Dev [Internet]. 2016 Feb 15 [cited 2016 Apr 29];25(4):285–300. Available from: http://www.pubmedcentral.nih.gov/articlerender.fcgi?artid=4761802&tool=pmcentrez&rendertype=abstract

424. Kim HK, Lee YS, Sivaprasad U, Malhotra A, Dutta A. Muscle-specific microRNA miR-206 promotes muscle differentiation. J Cell Biol [Internet]. 2006 Aug 28 [cited 2016 Jan 25];174(5):677–87. Available from: http://www.pubmedcentral.nih.gov/articlerender.fcgi?artid=2064311&tool=pmcentrez&rendertype=abstract

425. Goljanek-Whysall K, Pais H, Rathjen T, Sweetman D, Dalmay T, Münsterberg A. Regulation of multiple target genes by miR-1 and miR-206 is pivotal for C2C12 myoblast differentiation. J Cell Sci [Internet]. 2012 Aug 1 [cited 2016 Apr 28];125(Pt 15):3590–600. Available from: http://jcs.biologists.org/content/125/15/3590

426. Rao SS, Chu C, Kohtz DS. Ectopic expression of cyclin D1 prevents activation of gene transcription by myogenic basic helix-loop-helix regulators. Mol Cell Biol [Internet]. 1994 Aug [cited 2016 Apr 30];14(8):5259–67. Available from: http://www.pubmedcentral.nih.gov/articlerender.fcgi?artid=359045&tool=pmcentrez&rendertype=abstract

427. Halevy O, Novitch B, Spicer D, Skapek S, Rhee J, Hannon G, et al. Correlation of terminal cell cycle arrest of skeletal muscle with induction of p21 by MyoD. Science (80-) [Internet]. American Association for the Advancement of Science; 1995 Feb 17 [cited 2016 Jan 18];267(5200):1018–21. Available from: http://science.sciencemag.org/content/267/5200/1018.abstract

428. Wang Y, Jaenisch R. Myogenin can substitute for Myf5 in promoting myogenesis but less efficiently. Development [Internet]. 1997 Jul 1 [cited 2016 Jan 22];124(13):2507–13. Available from: http://dev.biologists.org/content/124/13/2507.long

429. Skapek SX, Rhee J, Spicer DB, Lassar AB. Inhibition of myogenic differentiation in

proliferating myoblasts by cyclin D1-dependent kinase. Science [Internet]. 1995 Mar 17 [cited 2016 Apr 30];267(5200):1022–4. Available from: http://www.ncbi.nlm.nih.gov/pubmed/7863328

430. Patapoutian A, Yoon JK, Miner JH, Wang S, Stark K, Wold B. Disruption of the mouse MRF4 gene identifies multiple waves of myogenesis in the myotome. Development [Internet]. 1995 Oct 1 [cited 2016 Mar 21];121(10):3347–58. Available from: http://www.ncbi.nlm.nih.gov/pubmed/7588068

431. Pajcini K V, Corbel SY, Sage J, Pomerantz JH, Blau HM. Transient inactivation of Rb and ARF yields regenerative cells from postmitotic mammalian muscle. Cell Stem Cell [Internet]. 2010 Aug 6 [cited 2015 Nov 27];7(2):198–213. Available from: http://www.pubmedcentral.nih.gov/articlerender.fcgi?artid=2919350&tool=pmcentrez&rendertype=abstract

432. Kaushal S, Schneider JW, Nadal-Ginard B, Mahdavi V. Activation of the myogenic lineage by MEF2A, a factor that induces and cooperates with MyoD. Science [Internet]. 1994 Nov 18 [cited 2016 Feb 18];266(5188):1236–40. Available from: http://www.ncbi.nlm.nih.gov/pubmed/7973707

433. Kragl M, Knapp D, Nacu E, Khattak S, Maden M, Epperlein HH, et al. Cells keep a memory of their tissue origin during axolotl limb regeneration. Nature [Internet]. Nature Publishing Group; 2009 Jul 2 [cited 2016 Oct 27];460(7251):60–5. Available from: http://www.nature.com/doifinder/10.1038/nature08152

434. Kim S-H, Mitchell M, Fujii H, Llanos S, Peters G. Absence of p16INK4a and truncation of ARF tumor suppressors in chickens. Proc Natl Acad Sci U S A [Internet]. 2003 Jan 7 [cited 2016 Oct 27];100(1):211–6. Available from: http://www.ncbi.nlm.nih.gov/pubmed/12506196

435. Osborn DPSS, Li K, Hinits Y, Hughes SM. Cdkn1c drives muscle differentiation through a positive feedback loop with Myod. Dev Biol [Internet]. 2011 Feb 15 [cited 2016 Feb 1];350(2):464–75. Available from: http://www.pubmedcentral.nih.gov/articlerender.fcgi?artid=3044464&tool=pmcentrez&rendertype=abstract

436. Glasauer SMK, Neuhauss SCF. Whole-genome duplication in teleost fishes and its evolutionary consequences. Mol Genet Genomics [Internet]. 2014 Dec [cited 2016 Jan 17];289(6):1045–60. Available from: http://www.ncbi.nlm.nih.gov/pubmed/25092473

437. Dünzinger U, Haaf T, Zechner U. Conserved synteny of mammalian imprinted genes in chicken, frog, and fish genomes. Cytogenet Genome Res [Internet]. Karger Publishers; 2007 Jan 2 [cited 2016 May 1];117(1–4):78–85. Available from: http://www.karger.com/Article/FullText/103167

438. Chakkalakal J V, Christensen J, Xiang W, Tierney MT, Boscolo FS, Sacco A, et al. Early forming label-retaining muscle stem cells require p27kip1 for maintenance of the primitive state. Development [Internet]. 2014 Apr 15 [cited 2016 Feb 12];141(8):1649–59. Available from: http://dev.biologists.org/content/141/8/1649

439. Tsao H, Benoit E, Sober AJ, Thiele C, Haluska FG. Novel Mutations in the p16/CDKN2A Binding Region of the Cyclin-dependent Kinase-4 Gene. Cancer Res [Internet]. 1998 Jan 1 [cited 2016 May 1];58(1):109–13. Available from: http://cancerres.aacrjournals.org/content/58/1/109.short

440. Gurung R, Parnaik VK. Cyclin D3 promotes myogenic differentiation and Pax7 transcription. J Cell Biochem [Internet]. Wiley Subscription Services, Inc., A Wiley Company; 2012 Jan 1;113(1):209–19. Available from: http://dx.doi.org/10.1002/jcb.23346

441. Parker SB, Eichele G, Zhang P, Rawls A, Sands AT, Bradley A, et al. p53-independent

expression of p21Cip1 in muscle and other terminally differentiating cells. Science [Internet]. 1995 Feb 17 [cited 2016 Mar 15];267(5200):1024–7. Available from: http://www.ncbi.nlm.nih.gov/pubmed/7863329

442. Hans F, Dimitrov S. Histone H3 phosphorylation and cell division. Oncogene [Internet]. Nature Publishing Group; 2001 May 28 [cited 2016 Oct 27];20(24):3021–7. Available from: http://www.nature.com/doifinder/10.1038/sj.onc.1204326

443. Kitzmann M, Vandromme M, Schaeffer V, Carnac G, Labbé JC, Lamb N, et al. cdk1- and cdk2-mediated phosphorylation of MyoD Ser200 in growing C2 myoblasts: role in modulating MyoD half-life and myogenic activity. Mol Cell Biol [Internet]. 1999 Apr [cited 2016 Mar 10];19(4):3167–76. Available from: http://www.pubmedcentral.nih.gov/articlerender.fcgi?artid=84110&tool=pmcentrez&rendertype=abstract

444. Song A, Wang Q, Goebl MG, Harrington MA. Phosphorylation of nuclear MyoD is required for its rapid degradation. Mol Cell Biol [Internet]. 1998 Sep [cited 2016 May 1];18(9):4994–9. Available from: http://www.pubmedcentral.nih.gov/articlerender.fcgi?artid=109084&tool=pmcentrez&rendertype=abstract

445. Kitzmann M, Fernandez A. Crosstalk between cell cycle regulators and the myogenic factor MyoD in skeletal myoblasts. Cell Mol Life Sci [Internet]. 2001 Apr [cited 2016 Jan 5];58(4):571–9. Available from: http://link.springer.com/10.1007/PL00000882

446. Mal A, Harter ML. MyoD is functionally linked to the silencing of a muscle-specific regulatory gene prior to skeletal myogenesis. Proc Natl Acad Sci U S A [Internet]. 2003 Feb 18 [cited 2016 Feb 19];100(4):1735–9. Available from: http://www.pubmedcentral.nih.gov/articlerender.fcgi?artid=149902&tool=pmcentrez&rendertype=abstract

447. Chandra S, Baribault C, Lacey M, Ehrlich M. Myogenic differential methylation: diverse associations with chromatin structure. Biology (Basel) [Internet]. Multidisciplinary Digital Publishing Institute; 2014 Jan 19 [cited 2016 Feb 1];3(2):426–51. Available from: http://www.mdpi.com/2079-7737/3/2/426/htm

448. Buckingham M, Rigby PWJ. Gene regulatory networks and transcriptional mechanisms that control myogenesis. Dev Cell [Internet]. 2014 Feb 10 [cited 2015 Dec 2];28(3):225–38. Available from: http://www.sciencedirect.com/science/article/pii/S1534580713007673

449. Soleimani VD, Yin H, Jahani-Asl A, Ming H, Kockx CEM, van Ijcken WFJ, et al. Snail regulates MyoD binding-site occupancy to direct enhancer switching and differentiation-specific transcription in myogenesis. Mol Cell [Internet]. 2012 Aug 10 [cited 2016 Jan 22];47(3):457–68. Available from: http://www.pubmedcentral.nih.gov/articlerender.fcgi?artid=4580277&tool=pmcentrez&rendertype=abstract

450. Choi J, Costa ML, Mermelstein CS, Chagas C, Holtzer S, Holtzer H. MyoD converts primary dermal fibroblasts, chondroblasts, smooth muscle, and retinal pigmented epithelial cells into striated mononucleated myoblasts and multinucleated myotubes. Proc Natl Acad Sci U S A [Internet]. 1990 Oct [cited 2016 Feb 18];87(20):7988–92. Available from: http://www.pubmedcentral.nih.gov/articlerender.fcgi?artid=54877&tool=pmcentrez&rendertype=abstract

451. Kassar-Duchossoy L, Giacone E, Gayraud-Morel B, Jory A, Gomès D, Tajbakhsh S. Pax3/Pax7 mark a novel population of primitive myogenic cells during development. Genes Dev [Internet]. 2005 Jun 15 [cited 2016 Feb 12];19(12):1426–31. Available from: http://genesdev.cshlp.org/content/19/12/1426

452. Chen J-F, Tao Y, Li J, Deng Z, Yan Z, Xiao X, et al. microRNA-1 and microRNA-206 regulate skeletal muscle satellite cell proliferation and differentiation by repressing Pax7. J Cell Biol [Internet]. 2010 Sep 6 [cited 2016 Apr 28];190(5):867–79. Available from: http://jcb.rupress.org/content/190/5/867.long

453. Zhang P, Wong C, Liu D, Finegold M, Harper JW, Elledge SJ. p21CIP1 and p57KIP2 control muscle differentiation at the myogenin step. Genes Dev [Internet]. 1999 Jan 15 [cited 2016 Mar 11];13(2):213–24. Available from: http://genesdev.cshlp.org/content/13/2/213.short

454. Reynaud EG, Leibovitch MP, Tintignac L a, Pelpel K, Guillier M, Leibovitch S a. Stabilization of MyoD by direct binding to p57(Kip2). J Biol Chem [Internet]. 2000 Jun 23 [cited 2014 May 8];275(25):18767–76. Available from: http://www.ncbi.nlm.nih.gov/pubmed/10764802

455. Andrés V, Walsh K. Myogenin expression, cell cycle withdrawal, and phenotypic differentiation are temporally separable events that precede cell fusion upon myogenesis. J Cell Biol [Internet]. 1996 Feb [cited 2016 Feb 19];132(4):657–66. Available from: http://www.pubmedcentral.nih.gov/articlerender.fcgi?artid=2199863&tool=pmcentrez&rendertype=abstract

456. Knight JD, Kothary R. The myogenic kinome: protein kinases critical to mammalian skeletal myogenesis. Skelet Muscle [Internet]. BioMed Central; 2011 Jan 8 [cited 2016 Mar 14];1(1):29. Available from: http://skeletalmusclejournal.biomedcentral.com/articles/10.1186/2044-5040-1-29

457. Zhang JM, Zhao X, Wei Q, Paterson BM. Direct inhibition of G(1) cdk kinase activity by MyoD promotes myoblast cell cycle withdrawal and terminal differentiation. EMBO J. 1999;18(24):6983–93.

458. Kastner S, Elias MC, Rivera AJ, Yablonka-Reuveni Z. Gene Expression Patterns of the Fibroblast Growth Factors and Their Receptors During Myogenesis of Rat Satellite Cells. J Histochem Cytochem [Internet]. 2000 Aug 1 [cited 2016 Jan 19];48(8):1079–96. Available from: http://jhc.sagepub.com/content/48/8/1079.short

459. Chen AE, Ginty DD, Fan C-M. Protein kinase A signalling via CREB controls myogenesis induced by Wnt proteins. Nature [Internet]. Macmillian Magazines Ltd.; 2005 Jan 20 [cited 2016 Mar 31];433(7023):317–22. Available from: http://dx.doi.org/10.1038/nature03126

460. Knight JD, Kothary R. The myogenic kinome: protein kinases critical to mammalian skeletal myogenesis. Skelet Muscle [Internet]. 2011;1(1):29. Available from: http://www.pubmedcentral.nih.gov/articlerender.fcgi?artid=3180440&tool=pmcentrez&rendertype=abstract

461. Simone C, Forcales SV, Hill DA, Imbalzano AN, Latella L, Puri PL. p38 pathway targets SWI-SNF chromatin-remodeling complex to muscle-specific loci. Nat Genet [Internet]. 2004 Jul [cited 2016 Feb 19];36(7):738–43. Available from: http://www.ncbi.nlm.nih.gov/pubmed/15208625

462. Dephoure N, Gould KL, Gygi SP, Kellogg DR. Mapping and analysis of phosphorylation sites: a quick guide for cell biologists. Mol Biol Cell [Internet]. 2013 Mar [cited 2014 Jul 9];24(5):535–42. Available from: http://www.pubmedcentral.nih.gov/articlerender.fcgi?artid=3583658&tool=pmcentrez&rendertype=abstract

463. de la Serna IL, Ohkawa Y, Berkes CA, Bergstrom DA, Dacwag CS, Tapscott SJ, et al. MyoD targets chromatin remodeling complexes to the myogenin locus prior to forming a stable DNA-bound complex. Mol Cell Biol [Internet]. 2005 May [cited 2016 Feb 18];25(10):3997–4009. Available from: http://www.pubmedcentral.nih.gov/articlerender.fcgi?artid=1087700&tool=pmcentrez&r

endertype=abstract

464. Ruiz-Bonilla V, Perdiguero E, Gresh L, Serrano AL, Zamora M, Sousa-Victor P, et al. Efficient adult skeletal muscle regeneration in mice deficient in p38beta, p38gamma and p38delta MAP kinases. Cell Cycle [Internet]. 2008 Jul 15 [cited 2016 Apr 1];7(14):2208–14. Available from: http://www.ncbi.nlm.nih.gov/pubmed/18641461

465. Lluís F, Perdiguero E, Nebreda AR, Muñoz-Cánoves P. Regulation of skeletal muscle gene expression by p38 MAP kinases. Trends Cell Biol [Internet]. 2006 Jan [cited 2016 Apr 1];16(1):36–44. Available from: http://www.ncbi.nlm.nih.gov/pubmed/16325404

466. Guasconi V, Puri PL. Chromatin: the interface between extrinsic cues and the epigenetic regulation of muscle regeneration. Trends Cell Biol [Internet]. 2009 Jun [cited 2016 Feb 18];19(6):286–94. Available from: http://www.sciencedirect.com/science/article/pii/S0962892409000774

467. Dilworth FJ, Blais A. Epigenetic regulation of satellite cell activation during muscle regeneration. 2011;6:1–8.

468. Brancaccio A, Palacios D. Chromatin signaling in muscle stem cells: interpreting the regenerative microenvironment. Front Aging Neurosci [Internet]. Frontiers; 2015 Jan 7 [cited 2016 Jan 19];7:36. Available from: http://journal.frontiersin.org/article/10.3389/fnagi.2015.00036/abstract

469. Keren A, Tamir Y, Bengal E. The p38 MAPK signaling pathway: a major regulator of skeletal muscle development. Mol Cell Endocrinol [Internet]. 2006 Jul 27 [cited 2016 Mar 31];252(1–2):224–30. Available from: http://www.sciencedirect.com/science/article/pii/S030372070600133X

470. Simone C, Forcales SV, Hill DA, Imbalzano AN, Latella L, Puri PL. p38 pathway targets SWI-SNF chromatin-remodeling complex to muscle-specific loci. Nat Genet [Internet]. Nature Publishing Group; 2004 Jul 20 [cited 2016 Oct 25];36(7):738–43. Available from: http://www.nature.com/doifinder/10.1038/ng1378

471. Singh AP, Archer TK. Analysis of the SWI/SNF chromatin-remodeling complex during early heart development and BAF250a repression cardiac gene transcription during P19 cell differentiation. Nucleic Acids Res [Internet]. Oxford University Press; 2014 Mar [cited 2016 Oct 25];42(5):2958–75. Available from: http://www.ncbi.nlm.nih.gov/pubmed/24335282

472. Segalés J, Perdiguero E, Muñoz-Cánoves P. Regulation of Muscle Stem Cell Functions: A Focus on the p38 MAPK Signaling Pathway. Front cell Dev Biol [Internet]. Frontiers Media SA; 2016 [cited 2016 Oct 25];4:91. Available from: http://www.ncbi.nlm.nih.gov/pubmed/27626031

473. Ho L, Ronan JL, Wu J, Staahl BT, Chen L, Kuo A, et al. An embryonic stem cell chromatin remodeling complex, esBAF, is essential for embryonic stem cell self-renewal and pluripotency. Proc Natl Acad Sci U S A [Internet]. National Academy of Sciences; 2009 Mar 31 [cited 2016 Oct 25];106(13):5181–6. Available from: http://www.ncbi.nlm.nih.gov/pubmed/19279220

474. Lee CMY, Iorno N, Sierro F, Christ D. Selection of human antibody fragments by phage display. Nat Protoc [Internet]. 2007 Jan [cited 2016 Mar 18];2(11):3001–8. Available from: http://www.ncbi.nlm.nih.gov/pubmed/18007636

475. Ahirwar R, Vellarikkal SK, Sett A, Sivasubbu S, Scaria V, Bora U, et al. Aptamer-Assisted Detection of the Altered Expression of Estrogen Receptor Alpha in Human Breast Cancer. PLoS One [Internet]. Public Library of Science; 2016 Jan 4 [cited 2016 Apr 6];11(4):e0153001. Available from: http://journals.plos.org/plosone/article?id=10.1371%252Fjournal.pone.0153001

476. Nofziger D, Miyamoto A, Lyons K, Weinmaster G. Notch signaling imposes two distinct blocks in the differentiation of C2C12 myoblasts. Development [Internet]. 1999 Apr 15 [cited 2016 Apr 1];126(8):1689–702. Available from: http://dev.biologists.org/content/126/8/1689.short

477. Sauka-Spengler T, Barembaum M. Gain- and loss-of-function approaches in the chick embryo. Methods Cell Biol [Internet]. 2008 Jan [cited 2016 Apr 6];87:237–56. Available from: http://www.ncbi.nlm.nih.gov/pubmed/18485300

Appendices

12 Appendix 1. A-E Chordate Mrf protein alignments.

(A-D) Protein alignments of gnathostome Mrf proteins and (E) alignment of selected gnathostome proteins together with further deuterostome Mrf proteins, proteins are displayed in one letter code. The basic domain is shaded blue, the helix-loop-helix domain green and, where a Myf5 domain is present, this is shaded in pink. The position of exon boundaries are indicated by arrowheads on top of the set of sequences. Conserved amino acids at the N-terminus are indicated by brackets, conservation of the C-terminus is indicated by arrows.

Sequence names are capped after 30 characters, for full names and taxonomic classification of animals, see **Table 4.1**.

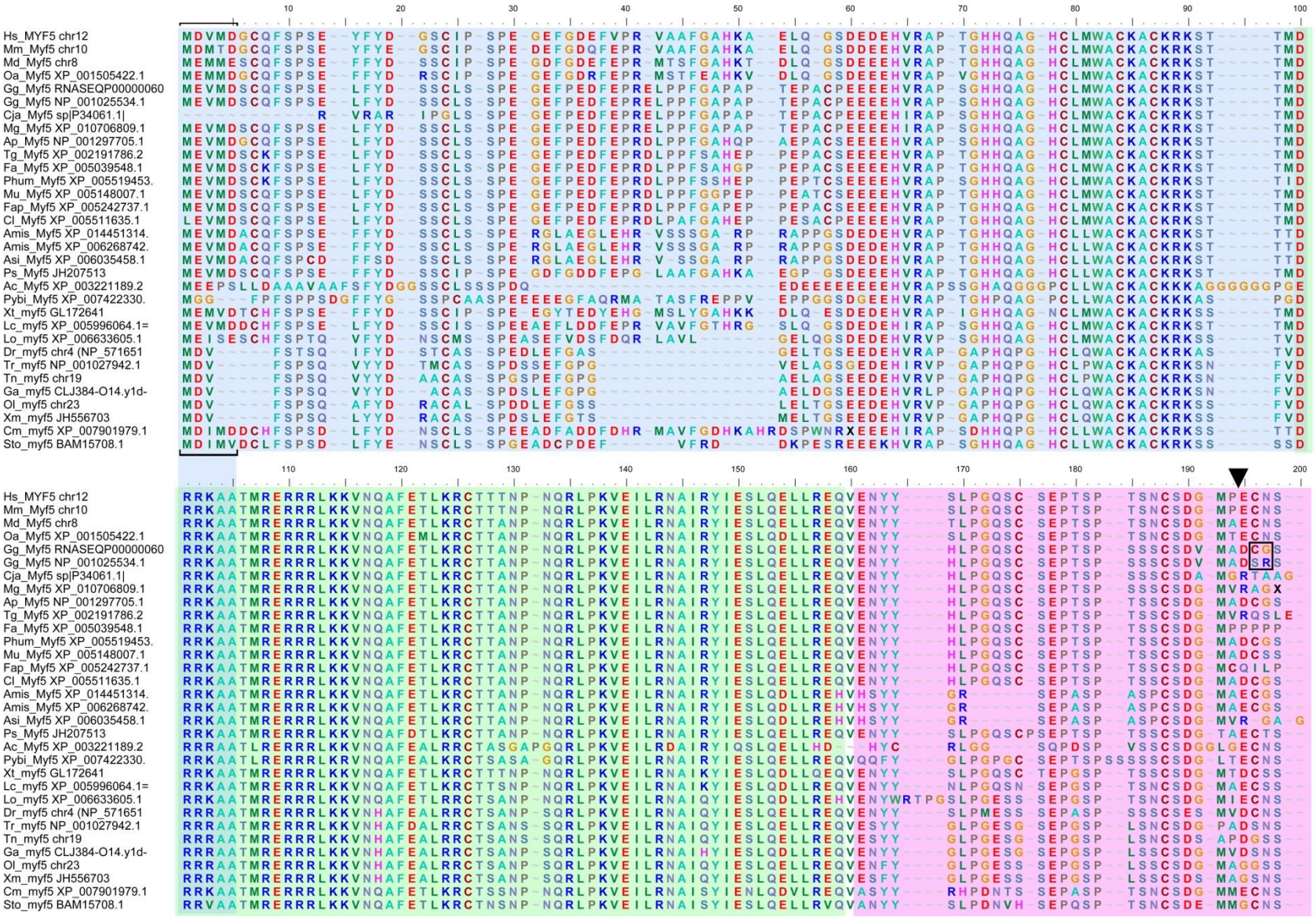
Hs_MYF5 chr12
Mm_Myf5 chr10
Md_Myf5 chr8
Oa_Myf5 XP_001505422.1
Gg_Myf5 RNASEQP00000060
Gg_Myf5 NP_001025534.1
Cja_Myf5 sp|P34061.1|
Mg_Myf5 XP_010706809.1
Ap_Myf5 NP_001297705.1
Tg_Myf5 XP_002191786.2
Fa_Myf5 XP_005039548.1
Phum_Myf5 XP_005519453.
Mu_Myf5 XP_005148007.1
Fap_Myf5 XP_005242737.1
Cl_Myf5 XP_005511635.1
Amis_Myf5 XP_014451314.
Amis_Myf5 XP_006268742.
Asi_Myf5 XP_006035458.1
Ps_Myf5 JH207513
Ac_Myf5 XP_003221189.2
Pybi_Myf5 XP_007422330.
Xt_myf5 GL172641
Lc_myf5 XP_005996064.1=
Lo_myf5 XP_006633605.1
Dr_myf5 chr4 (NP_571651
Tr_myf5 NP_001027942.1
Tn_myf5 chr19
Ga_myf5 CLJ384-O14.y1d-
Ol_myf5 chr23
Xm_myf5 JH556703
Cm_myf5 XP_007901979.1
Sto_myf5 BAM15708.1


Hs_MYF5 chr12
Mm_Myf5 chr10
Md_Myf5 chr8
Oa_Myf5 XP_001505422.1
Gg_Myf5 RNASEQP00000060
Gg_Myf5 NP_001025534.1
Cja_Myf5 sp|P34061.1|
Mg_Myf5 XP_010706809.1
Ap_Myf5 NP_001297705.1
Tg_Myf5 XP_002191786.2
Fa_Myf5 XP_005039548.1
Phum_Myf5 XP_005519453.
Mu_Myf5 XP_005148007.1
Fap_Myf5 XP_005242737.1
Cl_Myf5 XP_005511635.1
Amis_Myf5 XP_014451314.
Amis_Myf5 XP_006268742.
Asi_Myf5 XP_006035458.1
Ps_Myf5 JH207513
Ac_Myf5 XP_003221189.2
Pybi_Myf5 XP_007422330.
Xt_myf5 GL172641
Lc_myf5 XP_005996064.1=
Lo_myf5 XP_006633605.1
Dr_myf5 chr4 (NP_571651
Tr_myf5 NP_001027942.1
Tn_myf5 chr19
Ga_myf5 CLJ384-O14.y1d-
Ol_myf5 chr23
Xm_myf5 JH556703
Cm_myf5 XP_007901979.1
Sto_myf5 BAM15708.1

Appendix 1. A Gnathostome Myf5 proteins.

Protein alignment of gnathgostome Myf5 proteins. Note that for chicken Myf5, the RNAseq-derived and genomic sequences differ from the curated protein sequence at 2 positions (black boxes), with the RNAseq-derived and genomic sequences matching the sequences of other amniotes. Thus, the curated sequence was deemed unreliable, and the RNAseq-derived/ genomic sequences were used for construct design.

Also note the conserved N-terminus that yields the start of the basic domain and the conserved C-terminus (arrows). To not interfere with the function of these sequences, we designed an untagged chicken Myf5 expression construct.

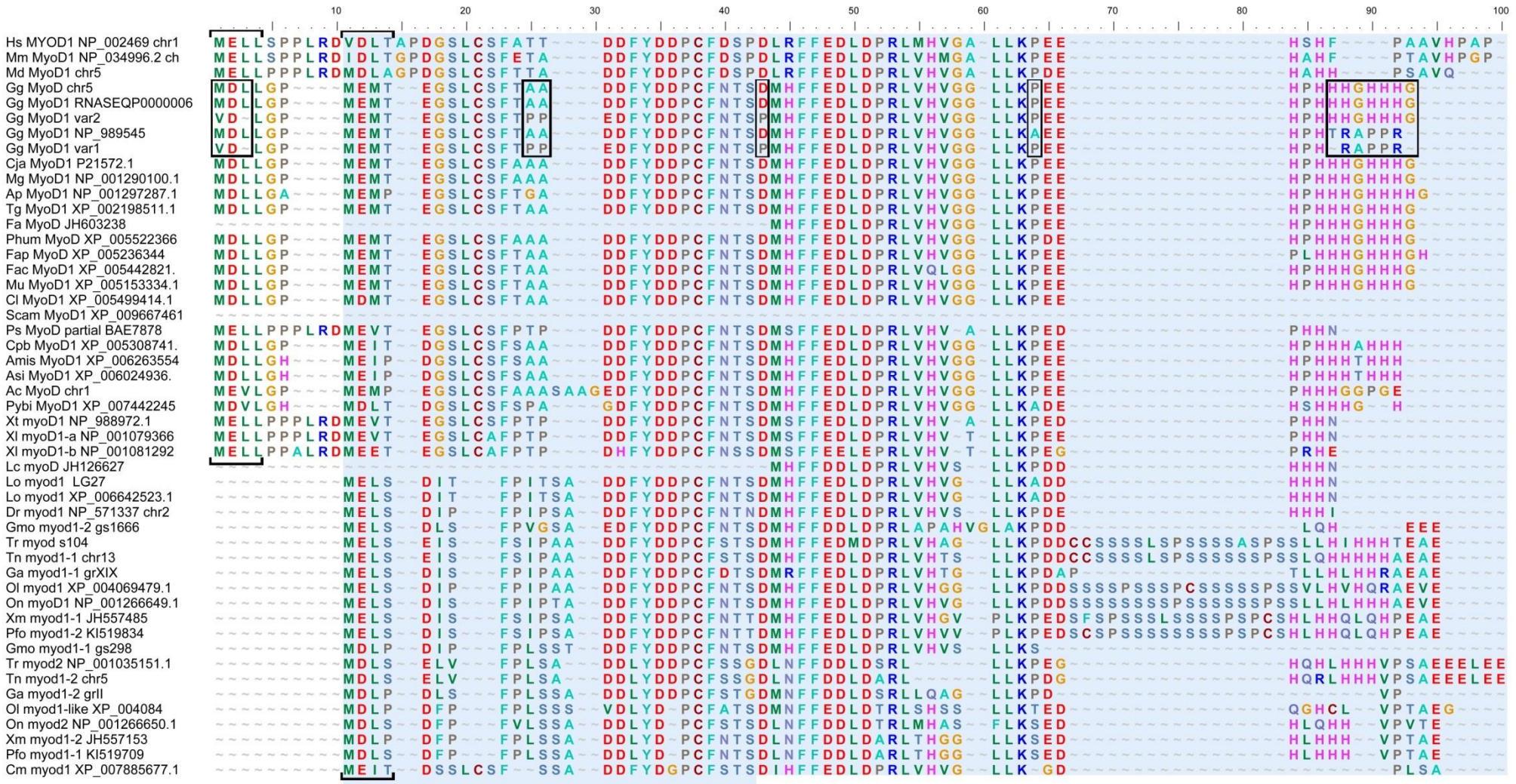
10
20
30
40
50
60
70
80
90
100
Hs MYOD1 NP_002469 chr1
Mm MyoD1 NP_034996.2 ch
Md MyoD1 chr5
Gg MyoD chr5
Gg MyoD1 RNASEQP0000006
Gg MyoD1 var2
Gg MyoD1 NP_989545
Gg MyoD1 var1
Cja MyoD1 P21572.1
Mg MyoD1 NP_001290100.1
Ap MyoD1 NP_001297287.1
Tg MyoD1 XP_002198511.1
Fa MyoD JH603238
Phum MyoD XP_005522366
Fap MyoD XP_005236344
Fac MyoD1 XP_005442821.
Mu MyoD1 XP_005153334.1
Cl MyoD1 XP_005499414.1
Scam MyoD1 XP_009667461
Ps MyoD partial BAE7878
Cpb MyoD1 XP_005308741.
Amis MyoD1 XP_006263554
Asi MyoD1 XP_006024936.
Ac MyoD chr1
Pybi MyoD1 XP_007442245
Xt myoD1 NP_988972.1
Xl myoD1-a NP_001079366
Xl myoD1-b NP_001081292
Lc myoD JH126627
Lo myod1 LG27
Lo myod1 XP_006642523.1
Dr myod1 NP_571337 chr2
Gmo myod1-2 gs1666
Tr myod s104
Tn myod1-1 chr13
Ga myod1-1 grXIX
Ol myod1 XP_004069479.1
On myoD1 NP_001266649.1
Xm myod1-1 JH557485
Pfo myod1-2 KI519834
Gmo myod1-1 gs298
Tr myod2 NP_001035151.1
Tn myod1-2 chr5
Ga myod1-2 grII
Ol myod1-like XP_004084
On myod2 NP_001266650.1
Xm myod1-2 JH557153
Pfo myod1-1 KI519709
Cm myod1 XP_007885677.1

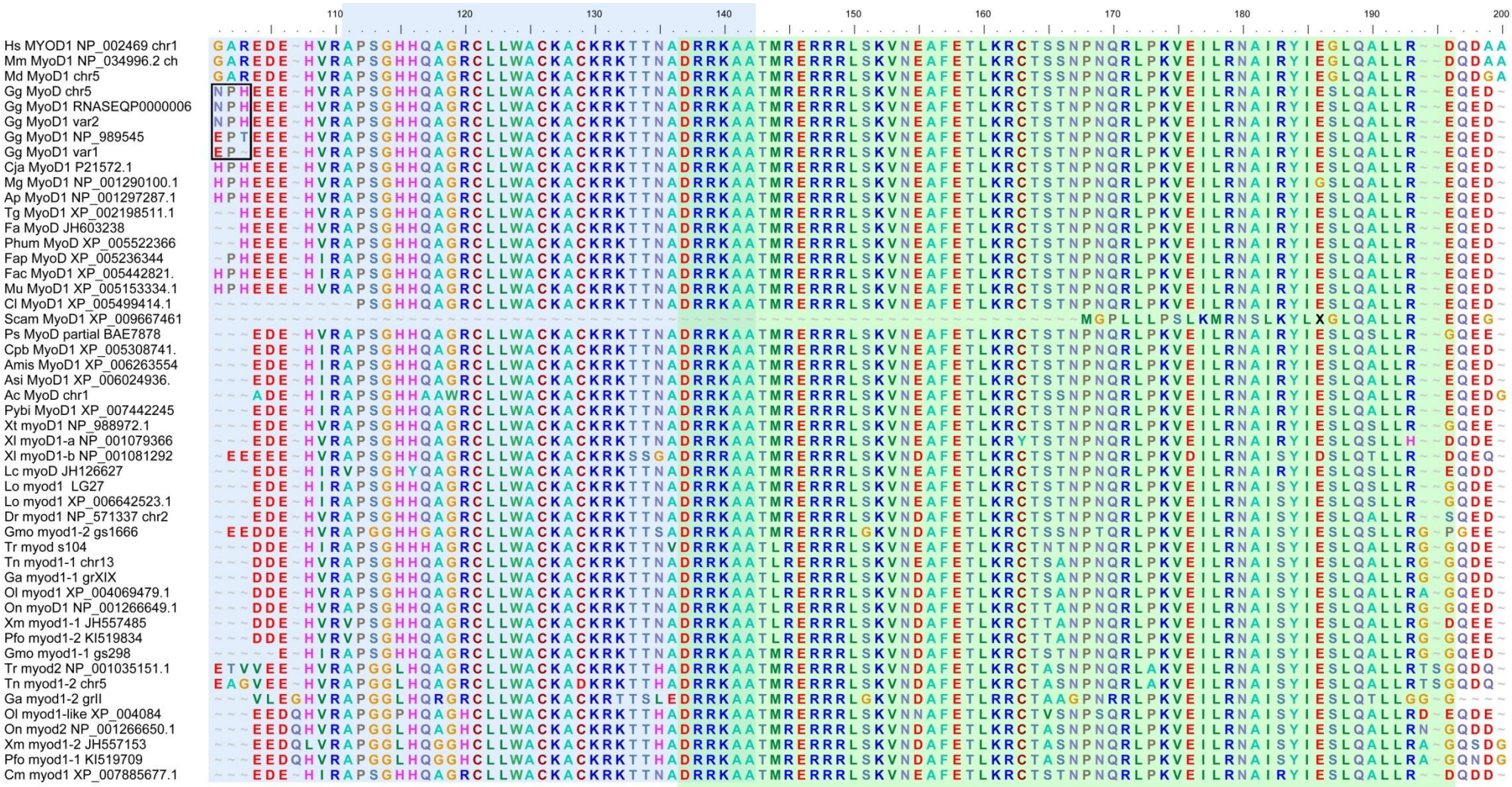
110
120
130
140
150
160
170
180
190
200
Hs MYOD1 NP_002469 chr1
Mm MyoD1 NP_034996.2 ch
Md MyoD1 chr5
Gg MyoD chr5
Gg MyoD1 RNASEQP0000006
Gg MyoD1 var2
Gg MyoD1 NP_989545
Gg MyoD1 var1
Cja MyoD1 P21572.1
Mg MyoD1 NP_001290100.1
Ap MyoD1 NP_001297287.1
Tg MyoD1 XP_002198511.1
Fa MyoD JH603238
Phum MyoD XP_005522366
Fap MyoD XP_005236344
Fac MyoD1 XP_005442821.
Mu MyoD1 XP_005153334.1
Cl MyoD1 XP_005499414.1
Scam MyoD1 XP_009667461
Ps MyoD partial BAE7878
Cpb MyoD1 XP_005308741.
Amis MyoD1 XP_006263554
Asi MyoD1 XP_006024936.
Ac MyoD chr1
Pybi MyoD1 XP_007442245
Xt myoD1 NP_988972.1
Xl myoD1-a NP_001079366
Xl myoD1-b NP_001081292
Lc myoD JH126627
Lo myod1 LG27
Lo myod1 XP_006642523.1
Dr myod1 NP_571337 chr2
Gmo myod1-2 gs1666
Tr myod s104
Tn myod1-1 chr13
Ga myod1-1 grXIX
Ol myod1 XP_004069479.1
On myoD1 NP_001266649.1
Xm myod1-1 JH557485
Pfo myod1-2 KI519834
Gmo myod1-1 gs298
Tr myod2 NP_001035151.1
Tn myod1-2 chr5
Ga myod1-2 grII
Ol myod1-like XP_004084
On myod2 NP_001266650.1
Xm myod1-2 JH557153
Pfo myod1-1 KI519709
Cm myod1 XP_007885677.1

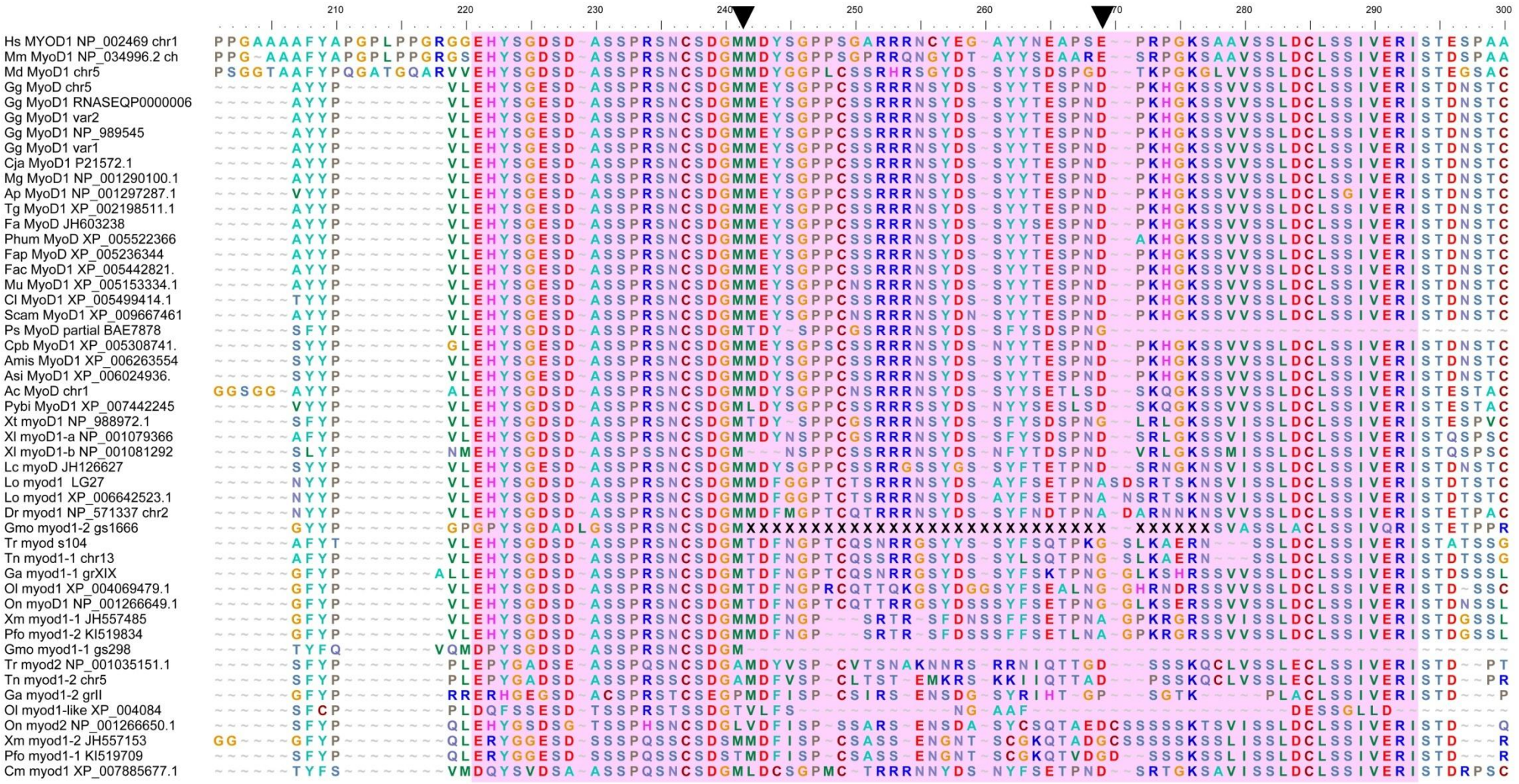
210
220
230
240
250
260
270
280
290
300
Hs MYOD1 NP_002469 chr1
Mm MyoD1 NP_034996.2 ch
Md MyoD1 chr5
Gg MyoD chr5
Gg MyoD1 RNASEQP0000006
Gg MyoD1 var2
Gg MyoD1 NP_989545
Gg MyoD1 var1
Cja MyoD1 P21572.1
Mg MyoD1 NP_001290100.1
Ap MyoD1 NP_001297287.1
Tg MyoD1 XP_002198511.1
Fa MyoD JH603238
Phum MyoD XP_005522366
Fap MyoD XP_005236344
Fac MyoD1 XP_005442821.
Mu MyoD1 XP_005153334.1
Cl MyoD1 XP_005499414.1
Scam MyoD1 XP_009667461
Ps MyoD partial BAE7878
Cpb MyoD1 XP_005308741.
Amis MyoD1 XP_006263554
Asi MyoD1 XP_006024936.
Ac MyoD chr1
Pybi MyoD1 XP_007442245
Xt myoD1 NP_988972.1
Xl myoD1-a NP_001079366
Xl myoD1-b NP_001081292
Lc myoD JH126627
Lo myod1 LG27
Lo myod1 XP_006642523.1
Dr myod1 NP_571337 chr2
Gmo myod1-2 gs1666
Tr myod s104
Tn myod1-1 chr13
Ga myod1-1 grXIX
Ol myod1 XP_004069479.1
On myoD1 NP_001266649.1
Xm myod1-1 JH557485
Pfo myod1-2 KI519834
Gmo myod1-1 gs298
Tr myod2 NP_001035151.1
Tn myod1-2 chr5
Ga myod1-2 grII
Ol myod1-like XP_004084
On myod2 NP_001266650.1
Xm myod1-2 JH557153
Pfo myod1-1 KI519709
Cm myod1 XP_007885677.1

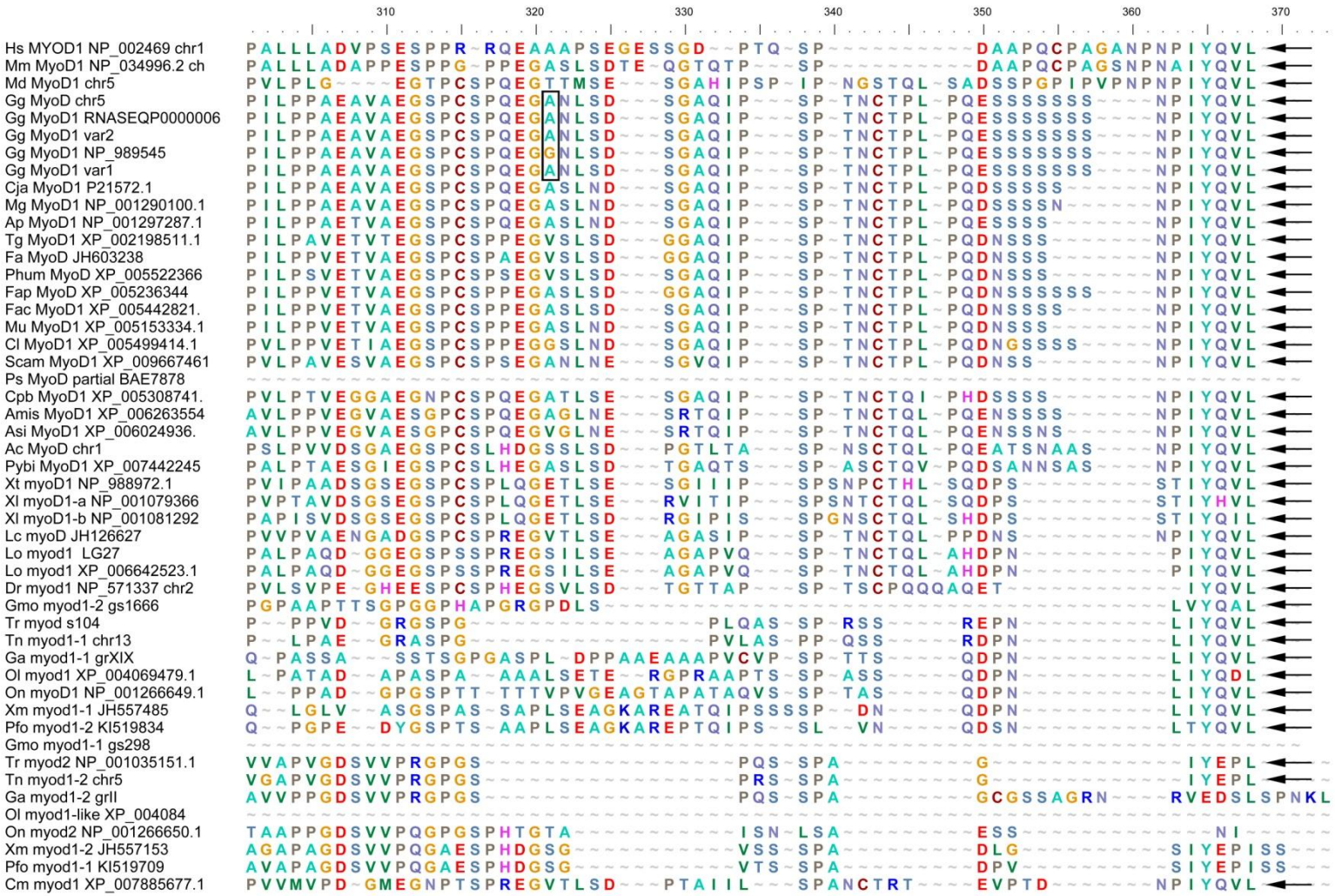
310
320
330
340
350
360
370
Hs MYOD1 NP_002469 chr1
Mm MyoD1 NP_034996.2 ch
Md MyoD1 chr5
Gg MyoD chr5
Gg MyoD1 RNASEQP0000006
Gg MyoD1 var2
Gg MyoD1 NP_989545
Gg MyoD1 var1
Cja MyoD1 P21572.1
Mg MyoD1 NP_001290100.1
Ap MyoD1 NP_001297287.1
Tg MyoD1 XP_002198511.1
Fa MyoD JH603238
Phum MyoD XP_005522366
Fap MyoD XP_005236344
Fac MyoD1 XP_005442821.
Mu MyoD1 XP_005153334.1
Cl MyoD1 XP_005499414.1
Scam MyoD1 XP_009667461
Ps MyoD partial BAE7878
Cpb MyoD1 XP_005308741.
Amis MyoD1 XP_006263554
Asi MyoD1 XP_006024936.
Ac MyoD chr1
Pybi MyoD1 XP_007442245
Xt myoD1 NP_988972.1
Xl myoD1-a NP_001079366
Xl myoD1-b NP_001081292
Lc myoD JH126627
Lo myod1 LG27
Lo myod1 XP_006642523.1
Dr myod1 NP_571337 chr2
Gmo myod1-2 gs1666
Tr myod s104
Tn myod1-1 chr13
Ga myod1-1 grXIX
Ol myod1 XP_004069479.1
On myoD1 NP_001266649.1
Xm myod1-1 JH557485
Pfo myod1-2 KI519834
Gmo myod1-1 gs298
Tr myod2 NP_001035151.1
Tn myod1-2 chr5
Ga myod1-2 grII
Ol myod1-like XP_004084
On myod2 NP_001266650.1
Xm myod1-2 JH557153
Pfo myod1-1 KI519709
Cm myod1 XP_007885677.1

Appendix 1. B Gnathostome MyoD proteins.

Protein alignment of gnathostome MyoD proteins. Note that the teleost MyoD sequences fall into two groups, which are consistent with their location at either the first or second MyoD locus. The currently available chicken MyoD sequences differ at 7 positions (black boxes); most notably the conserved proline and the histidine-stretch in the centre of the basic domain is represented in the RNAseq and genome- derived, but not the curated MyoD sequence. The protein termini are conserved (N-terminus: bracket; C-terminus: arrows). We thus decided to generate an untagged MyoD construct based on the sequence of the chicken genomic/ RNAseq sequences.

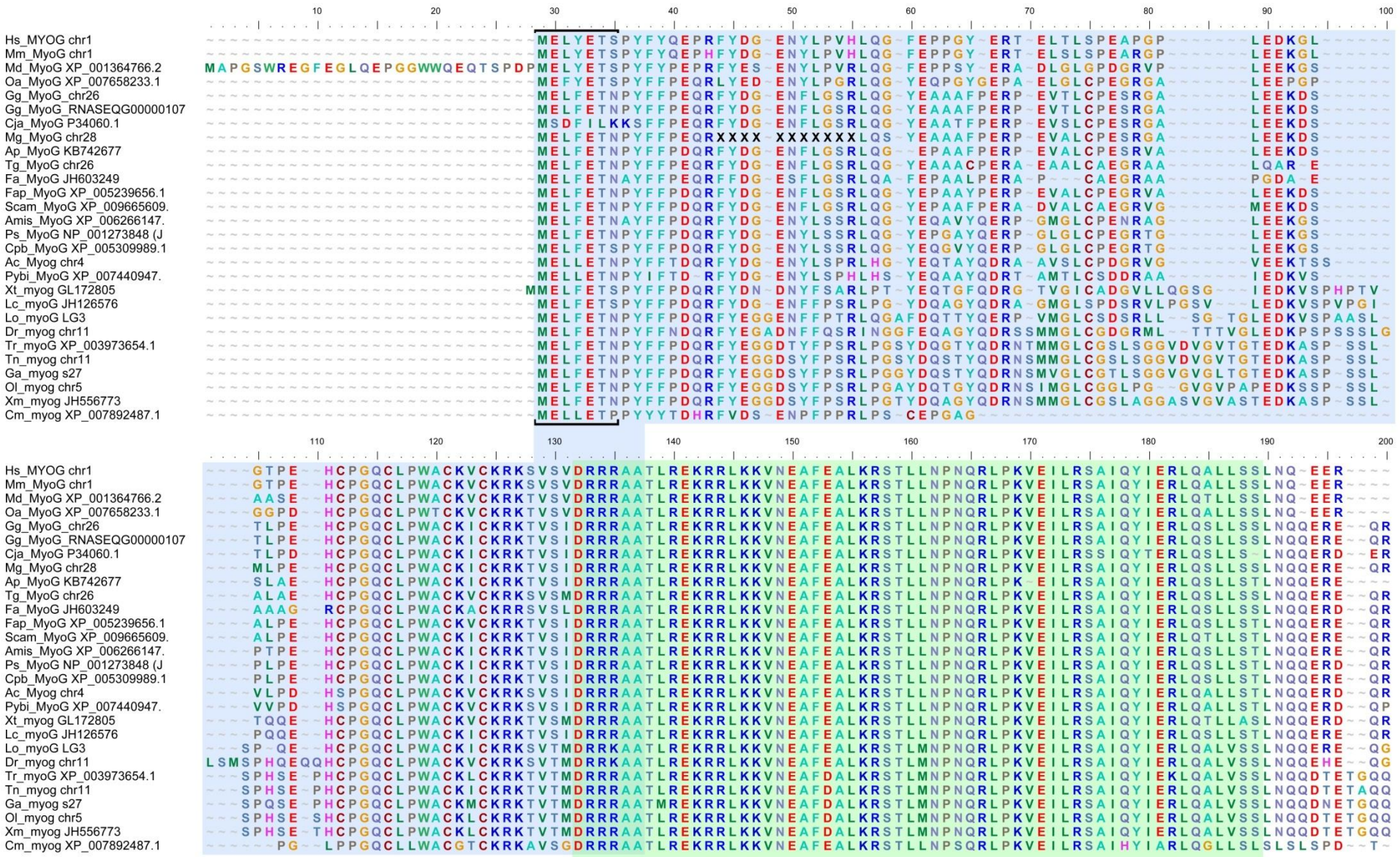
Hs_MYOG chr1
Mm_MyoG chr1
Md_MyoG XP_001364766.2
Oa_MyoG XP_007658233.1
Gg_MyoG_chr26
Gg_MyoG_RNASEQG00000107
Cja_MyoG P34060.1
Mg_MyoG chr28
Ap_MyoG KB742677
Tg_MyoG chr26
Fa_MyoG JH603249
Fap_MyoG XP_005239656.1
Scam_MyoG XP_009665609.
Amis_MyoG XP_006266147.
Ps_MyoG NP_001273848 (J
Cpb_MyoG XP_005309989.1
Ac_Myog chr4
Pybi_MyoG XP_007440947.
Xt_myog GL172805
Lc_myoG JH126576
Lo_myoG LG3
Dr_myog chr11
Tr_myoG XP_003973654.1
Tn_myog chr11
Ga_myog s27
Ol_myog chr5
Xm_myog JH556773
Cm_myog XP_007892487.1


210
220
230
240
250
260
270
280
290
Hs_MYOG chr1
Mm_MyoG chr1
Md_MyoG XP_001364766.2
Oa_MyoG XP_007658233.1
Gg_MyoG_chr26
Gg_MyoG_RNASEQG00000107
Cja_MyoG P34060.1
Mg_MyoG chr28
Ap_MyoG KB742677
Tg_MyoG chr26
Fa_MyoG JH603249
Fap_MyoG XP_005239656.1
Scam_MyoG XP_009665609.
Amis_MyoG XP_006266147.
Ps_MyoG NP_001273848 (J
Cpb_MyoG XP_005309989.1
Ac_Myog chr4
Pybi_MyoG XP_007440947.
Xt_myog GL172805
Lc_myoG JH126576
Lo_myoG LG3
Dr_myog chr11
Tr_myoG XP_003973654.1
Tn_myog chr11
Ga_myog s27
Ol_myog chr5
Xm_myog JH556773
Cm_myog XP_007892487.1

Appendix 1. C Gnathostome MyoG proteins.

Protein alignment of gnathostome MyoG proteins. Note the proteins do not have a Myf5 domain. The C-termini differ from those of Myf5 and MyoD, but are nevertheless highly conserved in diapsid (saurian) amniotes. The N-termini are also conserved. The chicken MyoG sequences we found were identical and matched the related amniote sequences. Thus, these sequences were utilised to design an untagged MyoG expression construct.

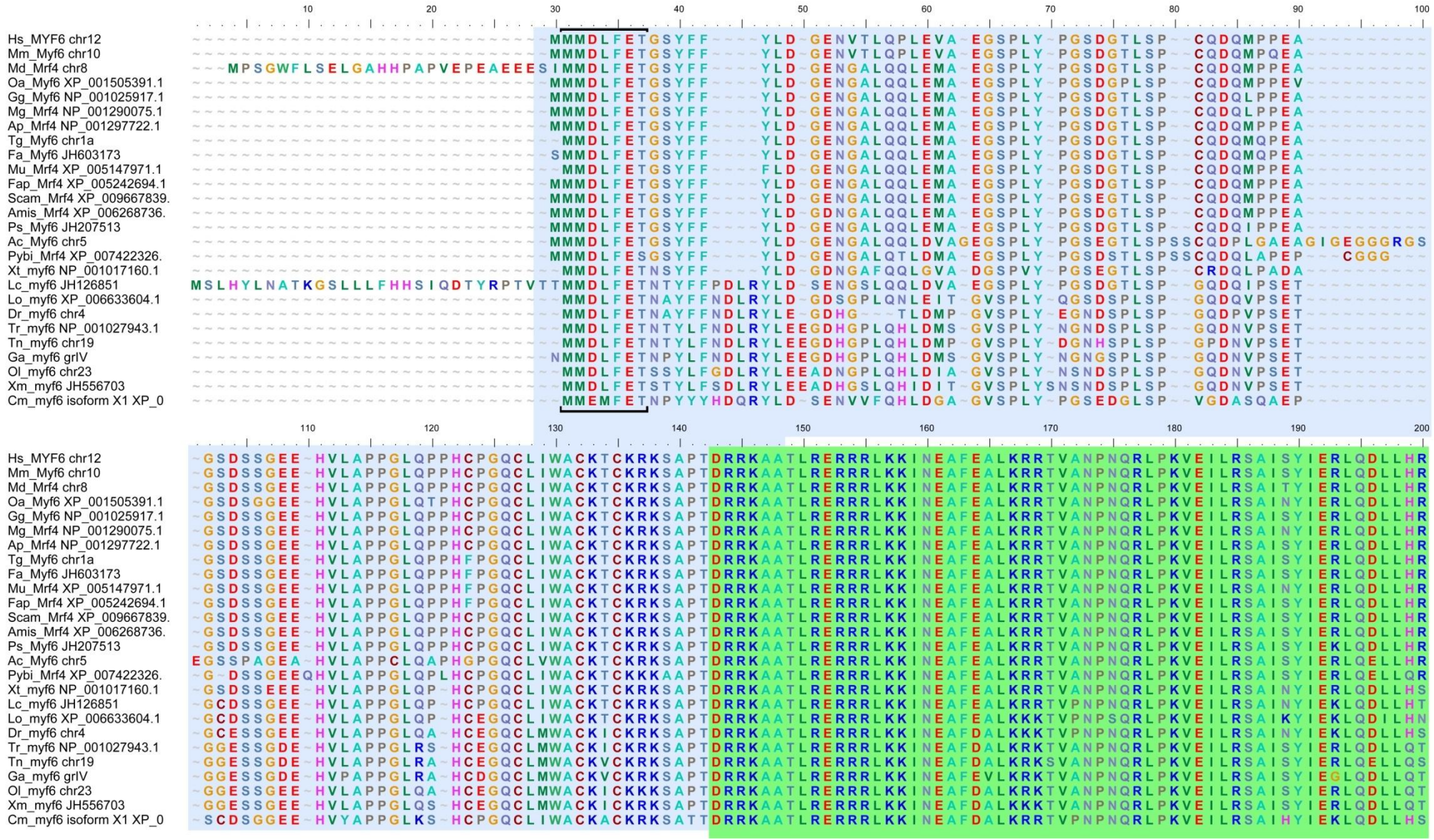
Hs_MYF6 chr12
Mm_Myf6 chr10
Md_Mrf4 chr8
Oa_Myf6 XP_001505391.1
Gg_Myf6 NP_001025917.1
Mg_Mrf4 NP_001290075.1
Ap_Mrf4 NP_001297722.1
Tg_Myf6 chr1a
Fa_Myf6 JH603173
Mu_Mrf4 XP_005147971.1
Fap_Mrf4 XP_005242694.1
Scam_Mrf4 XP_009667839.
Amis_Mrf4 XP_006268736.
Ps_Myf6 JH207513
Ac_Myf6 chr5
Pybi_Mrf4 XP_007422326.
Xt_myf6 NP_001017160.1
Lc_myf6 JH126851
Lo_myf6 XP_006633604.1
Dr_myf6 chr4
Tr_myf6 NP_001027943.1
Tn_myf6 chr19
Ga_myf6 grlV
Ol_myf6 chr23
Xm_myf6 JH556703
Cm_myf6 isoform X1 XP_0
10
20
30
40
50
60
70
80
90
100
110
120
130
140
150
160
170
180
190
200

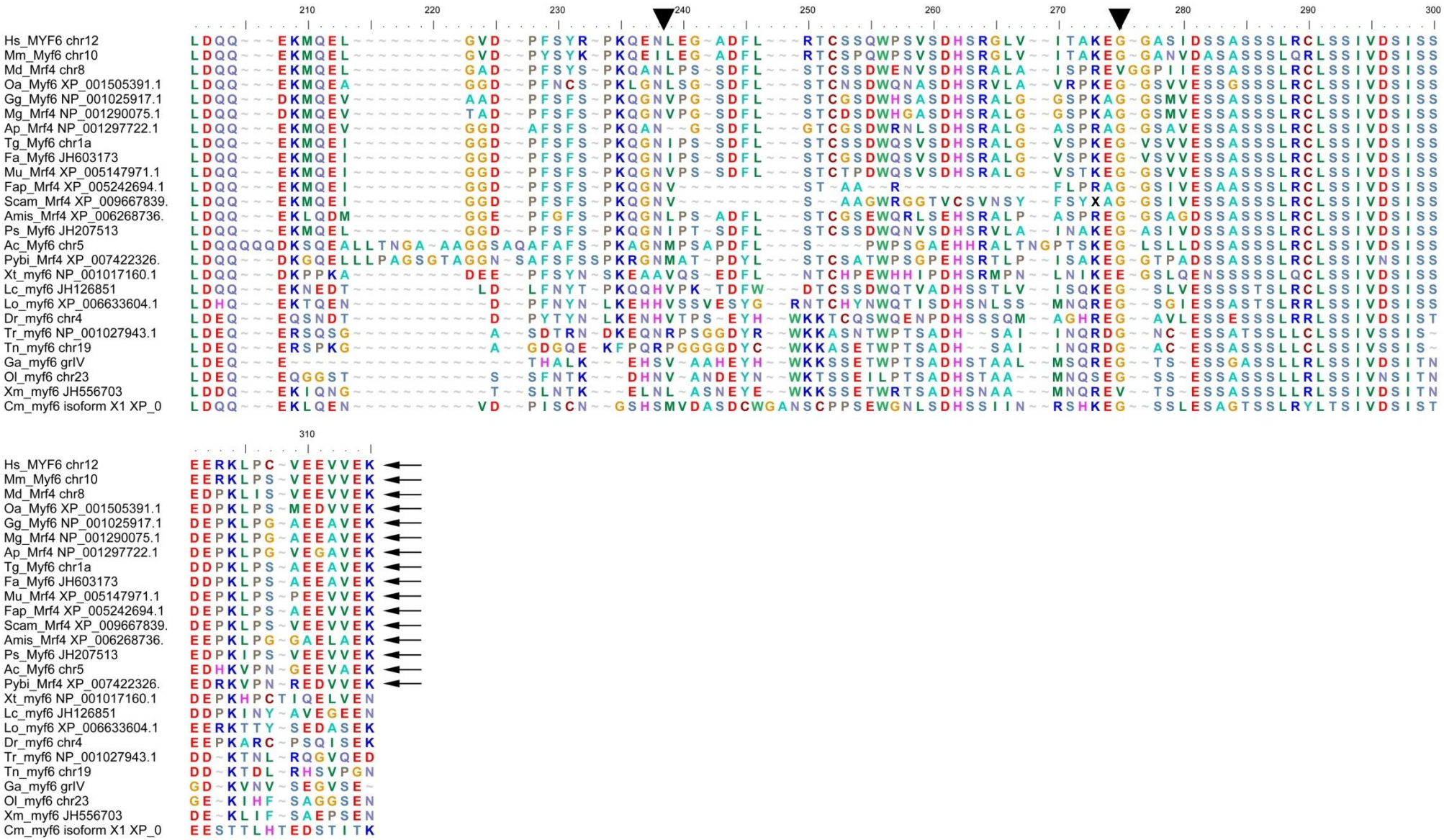
210
220
230
240
250
260
270
280
290
300
Hs_MYF6 chr12
Mm_Myf6 chr10
Md_Mrf4 chr8
Oa_Myf6 XP_001505391.1
Gg_Myf6 NP_001025917.1
Mg_Mrf4 NP_001290075.1
Ap_Mrf4 NP_001297722.1
Tg_Myf6 chr1a
Fa_Myf6 JH603173
Mu_Mrf4 XP_005147971.1
Fap_Mrf4 XP_005242694.1
Scam_Mrf4 XP_009667839.
Amis_Mrf4 XP_006268736.
Ps_Myf6 JH207513
Ac_Myf6 chr5
Pybi_Mrf4 XP_007422326.
Xt_myf6 NP_001017160.1
Lc_myf6 JH126851
Lo_myf6 XP_006633604.1
Dr_myf6 chr4
Tr_myf6 NP_001027943.1
Tn_myf6 chr19
Ga_myf6 grIV
Ol_myf6 chr23
Xm_myf6 JH556703
Cm_myf6 isoform X1 XP_0
310
Hs_MYF6 chr12
Mm_Myf6 chr10
Md_Mrf4 chr8
Oa_Myf6 XP_001505391.1
Gg_Myf6 NP_001025917.1
Mg_Mrf4 NP_001290075.1
Ap_Mrf4 NP_001297722.1
Tg_Myf6 chr1a
Fa_Myf6 JH603173
Mu_Mrf4 XP_005147971.1
Fap_Mrf4 XP_005242694.1
Scam_Mrf4 XP_009667839.
Amis_Mrf4 XP_006268736.
Ps_Myf6 JH207513
Ac_Myf6 chr5
Pybi_Mrf4 XP_007422326.
Xt_myf6 NP_001017160.1
Lc_myf6 JH126851
Lo_myf6 XP_006633604.1
Dr_myf6 chr4
Tr_myf6 NP_001027943.1
Tn_myf6 chr19
Ga_myf6 grIV
Ol_myf6 chr23
Xm_myf6 JH556703
Cm_myf6 isoform X1 XP_0

Appendix 1. D Gnathostome Mrf4 proteins.

Protein alignment of gnathostome Mrf4=Myf6 proteins. Note also these proteins do not have a Myf5 domain, but their N-termini (bracket) and in amniotes also their C-termini (arrows) are highly conserved. The chicken Mrf4 sequences we found were identical and matched the related amniote sequences. Thus, these sequences were utilised to design an untagged Mrf4 expression construct.

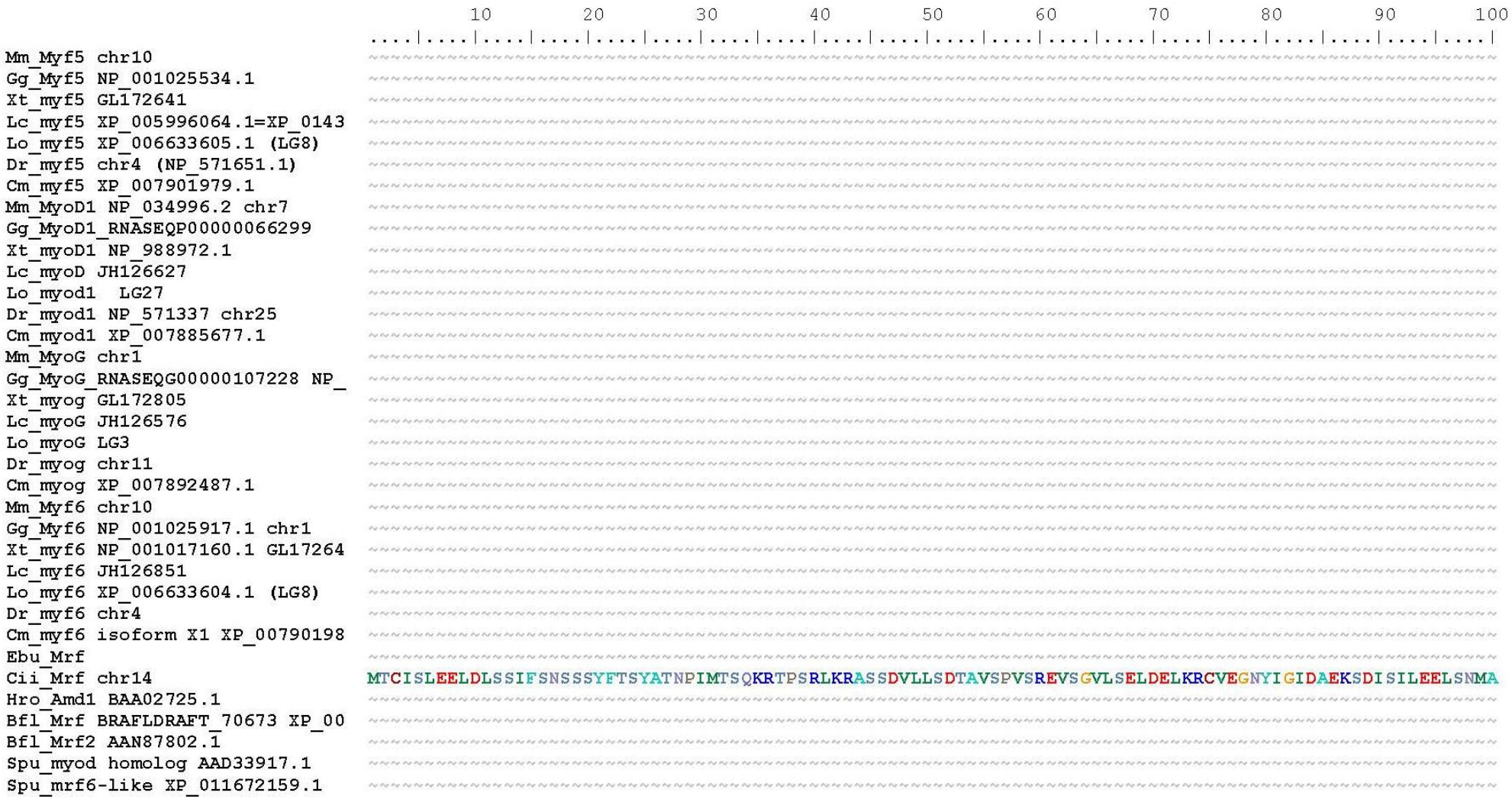
10 20 30 40 50 60 70 80 90 100
Mm_Myf5 chr10
Gg_Myf5 NP_001025534.1
Xt_myf5 GL172641
Lc_myf5 XP_005996064.1=XP_0143
Lo_myf5 XP_006633605.1 (LG8)
Dr_myf5 chr4 (NP_571651.1)
Cm_myf5 XP_007901979.1
Mm_MyoD1 NP_034996.2 chr7
Gg_MyoD1_RNASEQP00000066299
Xt_myoD1 NP_988972.1
Lc_myoD JH126627
Lo_myod1 LG27
Dr_myod1 NP_571337 chr25
Cm_myod1 XP_007885677.1
Mm_MyoG chr1
Gg_MyoG_RNASEQG00000107228 NP_
Xt_myog GL172805
Lc_myoG JH126576
Lo_myoG LG3
Dr_myog chr11
Cm_myog XP_007892487.1
Mm_Myf6 chr10
Gg_Myf6 NP_001025917.1 chr1
Xt_myf6 NP_001017160.1 GL17264
Lc_myf6 JH126851
Lo_myf6 XP_006633604.1 (LG8)
Dr_myf6 chr4
Cm_myf6 isoform X1 XP_00790198
Ebu_Mrf
Cii_Mrf chr14
MTCISLEELDLSSIFSNSSSYFTSYATNPIMTSQKRTPSRLKRASSDVLLSDTAVSPVSREVSGVLSELDELKRCVEGNYIGIDAEKSDISILEELSNMA
Hro_Amd1 BAA02725.1
Bfl_Mrf BRAFLDRAFT_70673 XP_00
Bfl_Mrf2 AAN87802.1
Spu_myod homolog AAD33917.1
Spu_mrf6-like XP_011672159.1

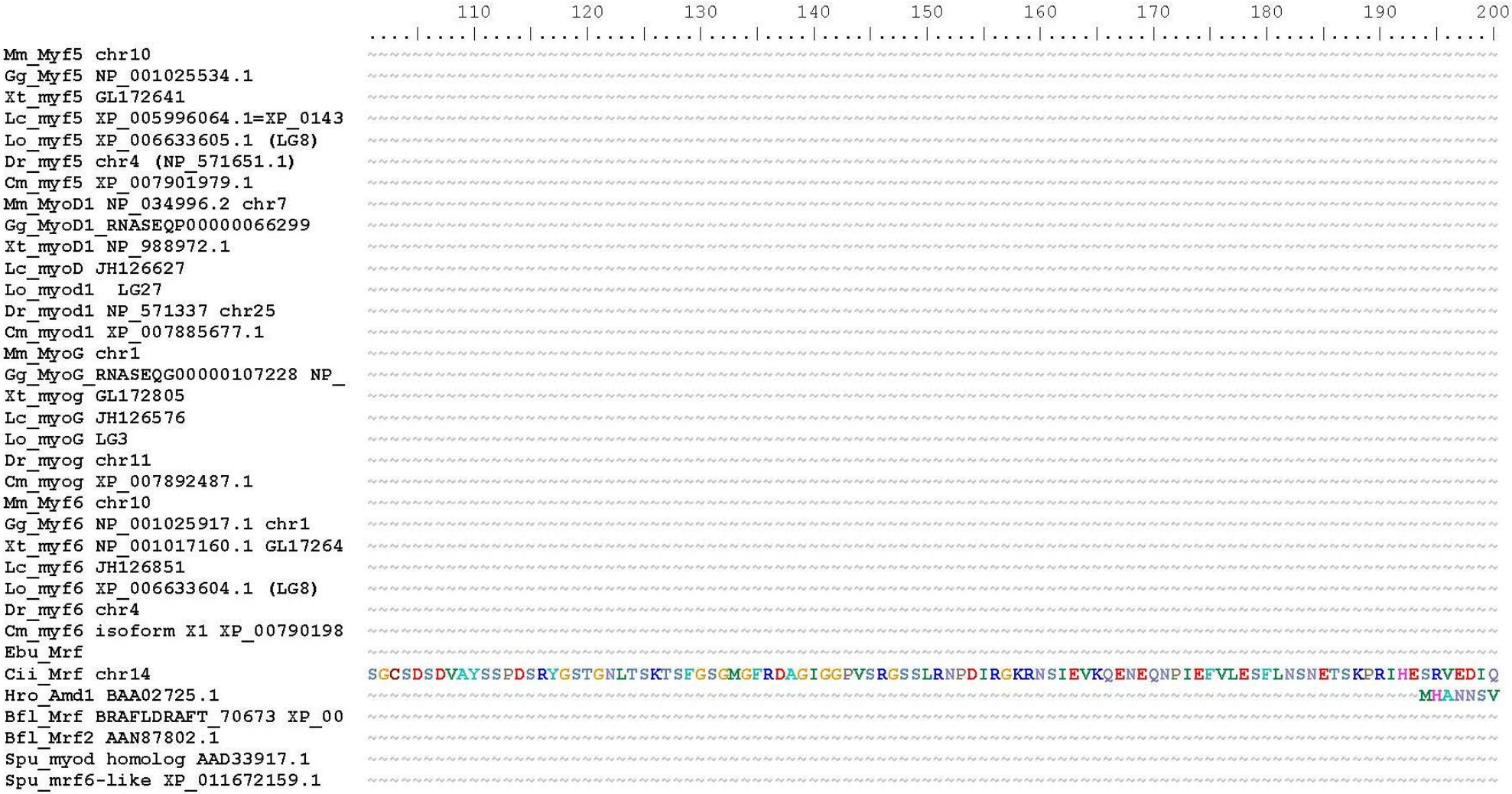
110 120 130 140 150 160 170 180 190 200
Mm_Myf5 chr10
Gg_Myf5 NP_001025534.1
Xt_myf5 GL172641
Lc_myf5 XP_005996064.1=XP_0143
Lo_myf5 XP_006633605.1 (LG8)
Dr_myf5 chr4 (NP_571651.1)
Cm_myf5 XP_007901979.1
Mm_MyoD1 NP_034996.2 chr7
Gg_MyoD1_RNASEQP00000066299
Xt_myoD1 NP_988972.1
Lc_myoD JH126627
Lo_myod1 LG27
Dr_myod1 NP_571337 chr25
Cm_myod1 XP_007885677.1
Mm_MyoG chr1
Gg_MyoG_RNASEQG00000107228 NP_
Xt_myog GL172805
Lc_myoG JH126576
Lo_myoG LG3
Dr_myog chr11
Cm_myog XP_007892487.1
Mm_Myf6 chr10
Gg_Myf6 NP_001025917.1 chr1
Xt_myf6 NP_001017160.1 GL17264
Lc_myf6 JH126851
Lo_myf6 XP_006633604.1 (LG8)
Dr_myf6 chr4
Cm_myf6 isoform X1 XP_00790198
Ebu_Mrf
Cii_Mrf chr14
SGCSDSDVAYSSPDSRYGSTGNLTSKTSFGSGMGFRDAGIGGPVSRGSSLRNPDIRGKRNSIEVKQENEQNPIEFVLESFLNSNETSKPRIHESRVEDIQ
Hro_Amd1 BAA02725.1
MHANNSV
Bfl_Mrf BRAFLDRAFT_70673 XP_00
Bfl_Mrf2 AAN87802.1
Spu_myod homolog AAD33917.1
Spu_mrf6-like XP_011672159.1

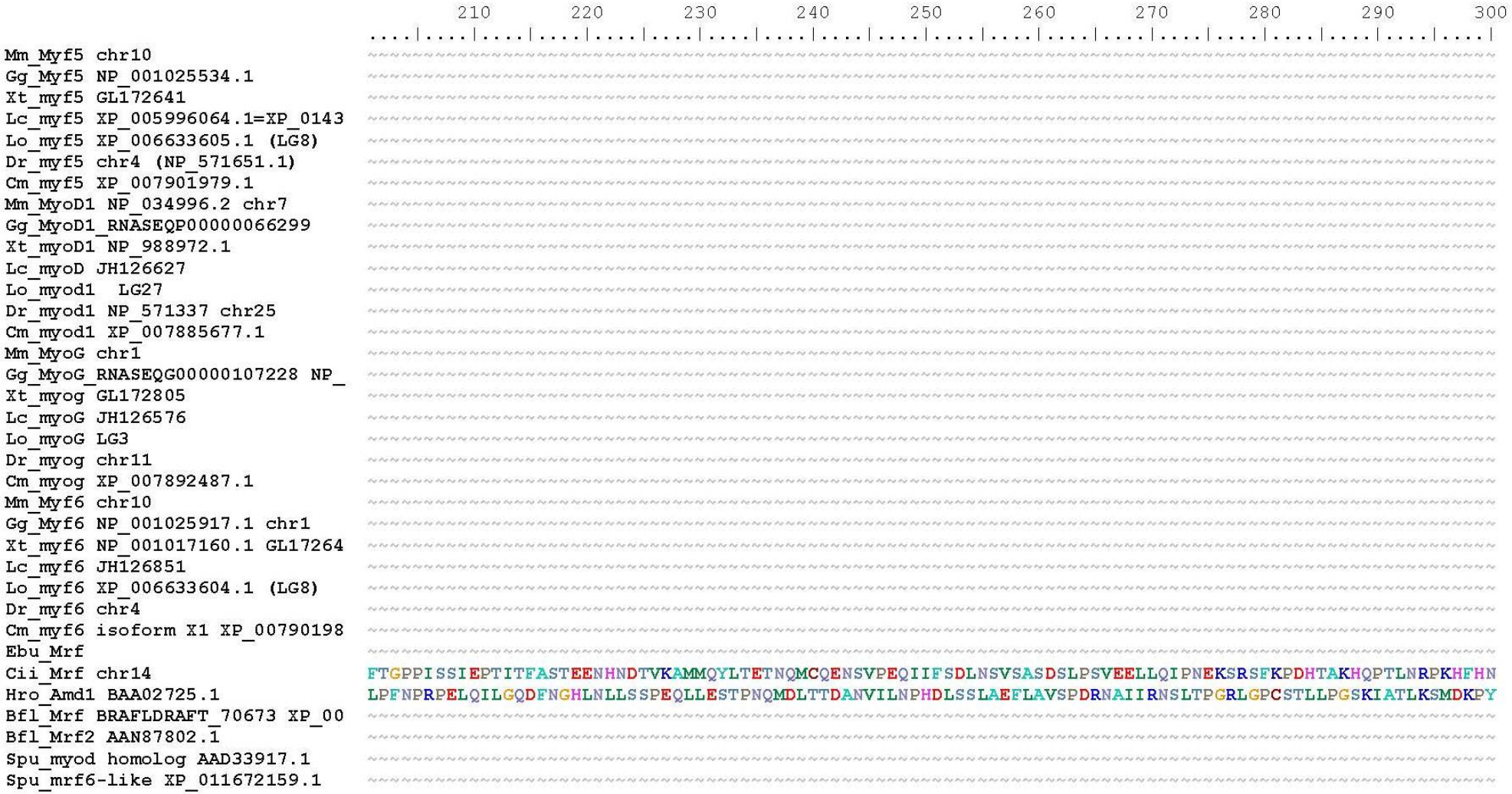
210 220 230 240 250 260 270 280 290 300
Mm_Myf5 chr10
Gg_Myf5 NP_001025534.1
Xt_myf5 GL172641
Lc_myf5 XP_005996064.1=XP_0143
Lo_myf5 XP_006633605.1 (LG8)
Dr_myf5 chr4 (NP_571651.1)
Cm_myf5 XP_007901979.1
Mm_MyoD1 NP_034996.2 chr7
Gg_MyoD1_RNASEQP00000066299
Xt_myoD1 NP_988972.1
Lc_myoD JH126627
Lo_myod1 LG27
Dr_myod1 NP_571337 chr25
Cm_myod1 XP_007885677.1
Mm_MyoG chr1
Gg_MyoG_RNASEQG00000107228 NP_
Xt_myog GL172805
Lc_myoG JH126576
Lo_myoG LG3
Dr_myog chr11
Cm_myog XP_007892487.1
Mm_Myf6 chr10
Gg_Myf6 NP_001025917.1 chr1
Xt_myf6 NP_001017160.1 GL17264
Lc_myf6 JH126851
Lo_myf6 XP_006633604.1 (LG8)
Dr_myf6 chr4
Cm_myf6 isoform X1 XP_00790198
Ebu_Mrf
Cii_Mrf chr14
Hro_Amd1 BAA02725.1
Bfl_Mrf BRAFLDRAFT_70673 XP_00
Bfl_Mrf2 AAN87802.1
Spu_myod homolog AAD33917.1
Spu_mrf6-like XP_011672159.1

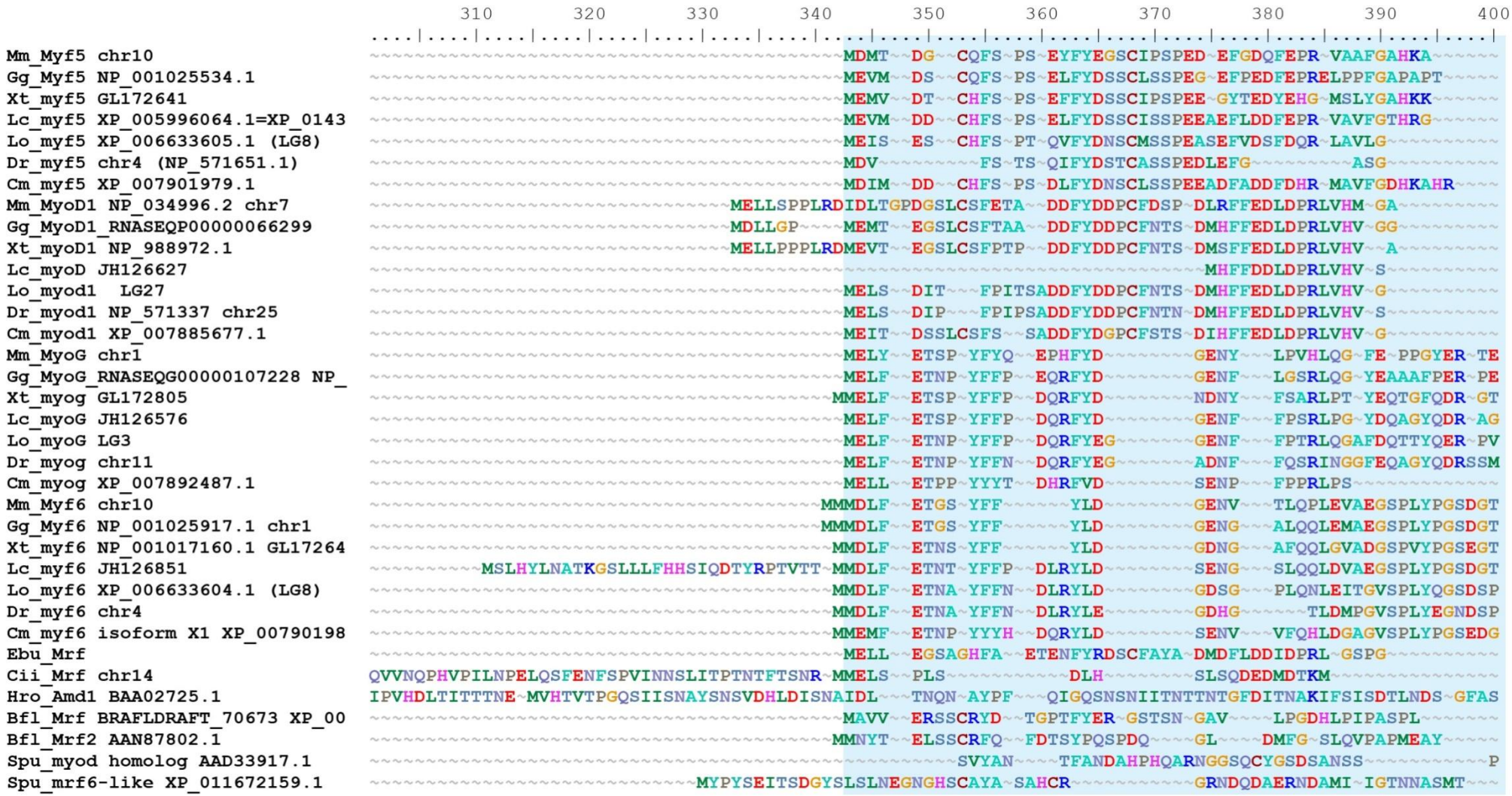
310
320
330
340
350
360
370
380
390
400
Mm_Myf5 chr10
Gg_Myf5 NP_001025534.1
Xt_myf5 GL172641
Lc_myf5 XP_005996064.1=XP_0143
Lo_myf5 XP_006633605.1 (LG8)
Dr_myf5 chr4 (NP_571651.1)
Cm_myf5 XP_007901979.1
Mm_MyoD1 NP_034996.2 chr7
Gg_MyoD1_RNASEQP00000066299
Xt_myoD1 NP_988972.1
Lc_myoD JH126627
Lo_myod1 LG27
Dr_myod1 NP_571337 chr25
Cm_myod1 XP_007885677.1
Mm_MyoG chr1
Gg_MyoG_RNASEQG00000107228 NP_
Xt_myog GL172805
Lc_myoG JH126576
Lo_myoG LG3
Dr_myog chr11
Cm_myog XP_007892487.1
Mm_Myf6 chr10
Gg_Myf6 NP_001025917.1 chr1
Xt_myf6 NP_001017160.1 GL17264
Lc_myf6 JH126851
Lo_myf6 XP_006633604.1 (LG8)
Dr_myf6 chr4
Cm_myf6 isoform X1 XP_00790198
Ebu_Mrf
Cii_Mrf chr14
Hro_Amd1 BAA02725.1
Bfl_Mrf BRAFLDRAFT_70673 XP_00
Bfl_Mrf2 AAN87802.1
Spu_myod homolog AAD33917.1
Spu_mrf6-like XP_011672159.1


410
420
430
440
450
460
470
480
490
500
Mm_Myf5 chr10
Gg_Myf5 NP_001025534.1
Xt_myf5 GL172641
Lc_myf5 XP_005996064.1=XP_0143
Lo_myf5 XP_006633605.1 (LG8)
Dr_myf5 chr4 (NP_571651.1)
Cm_myf5 XP_007901979.1
Mm_MyoD1 NP_034996.2 chr7
Gg_MyoD1_RNASEQP00000066299
Xt_myoD1 NP_988972.1
Lc_myoD JH126627
Lo_myod1 LG27
Dr_myod1 NP_571337 chr25
Cm_myod1 XP_007885677.1
Mm_MyoG chr1
Gg_MyoG_RNASEQG00000107228 NP_
Xt_myog GL172805
Lc_myoG JH126576
Lo_myoG LG3
Dr_myog chr11
Cm_myog XP_007892487.1
Mm_Myf6 chr10
Gg_Myf6 NP_001025917.1 chr1
Xt_myf6 NP_001017160.1 GL17264
Lc_myf6 JH126851
Lo_myf6 XP_006633604.1 (LG8)
Dr_myf6 chr4
Cm_myf6 isoform X1 XP_00790198
Ebu_Mrf
Cii_Mrf chr14
Hro_Amd1 BAA02725.1
Bfl_Mrf BRAFLDRAFT_70673 XP_00
Bfl_Mrf2 AAN87802.1
Spu_myod homolog AAD33917.1
Spu_mrf6-like XP_011672159.1


510
520
530
540
550
560
570
580
590
600
Mm_Myf5 chr10
Gg_Myf5 NP_001025534.1
Xt_myf5 GL172641
Lc_myf5 XP_005996064.1=XP_0143
Lo_myf5 XP_006633605.1 (LG8)
Dr_myf5 chr4 (NP_571651.1)
Cm_myf5 XP_007901979.1
Mm_MyoD1 NP_034996.2 chr7
Gg_MyoD1_RNASEQP00000066299
Xt_myoD1 NP_988972.1
Lc_myoD JH126627
Lo_myod1 LG27
Dr_myod1 NP_571337 chr25
Cm_myod1 XP_007885677.1
Mm_MyoG chr1
Gg_MyoG_RNASEQG00000107228 NP_
Xt_myog GL172805
Lc_myoG JH126576
Lo_myoG LG3
Dr_myog chr11
Cm_myog XP_007892487.1
Mm_Myf6 chr10
Gg_Myf6 NP_001025917.1 chr1
Xt_myf6 NP_001017160.1 GL17264
Lc_myf6 JH126851
Lo_myf6 XP_006633604.1 (LG8)
Dr_myf6 chr4
Cm_myf6 isoform X1 XP_00790198
Ebu_Mrf
Cii_Mrf chr14
Hro_Amd1 BAA02725.1
Bfl_Mrf BRAFLDRAFT_70673 XP_00
Bfl_Mrf2 AAN87802.1
Spu_myod homolog AAD33917.1
Spu_mrf6-like XP_011672159.1

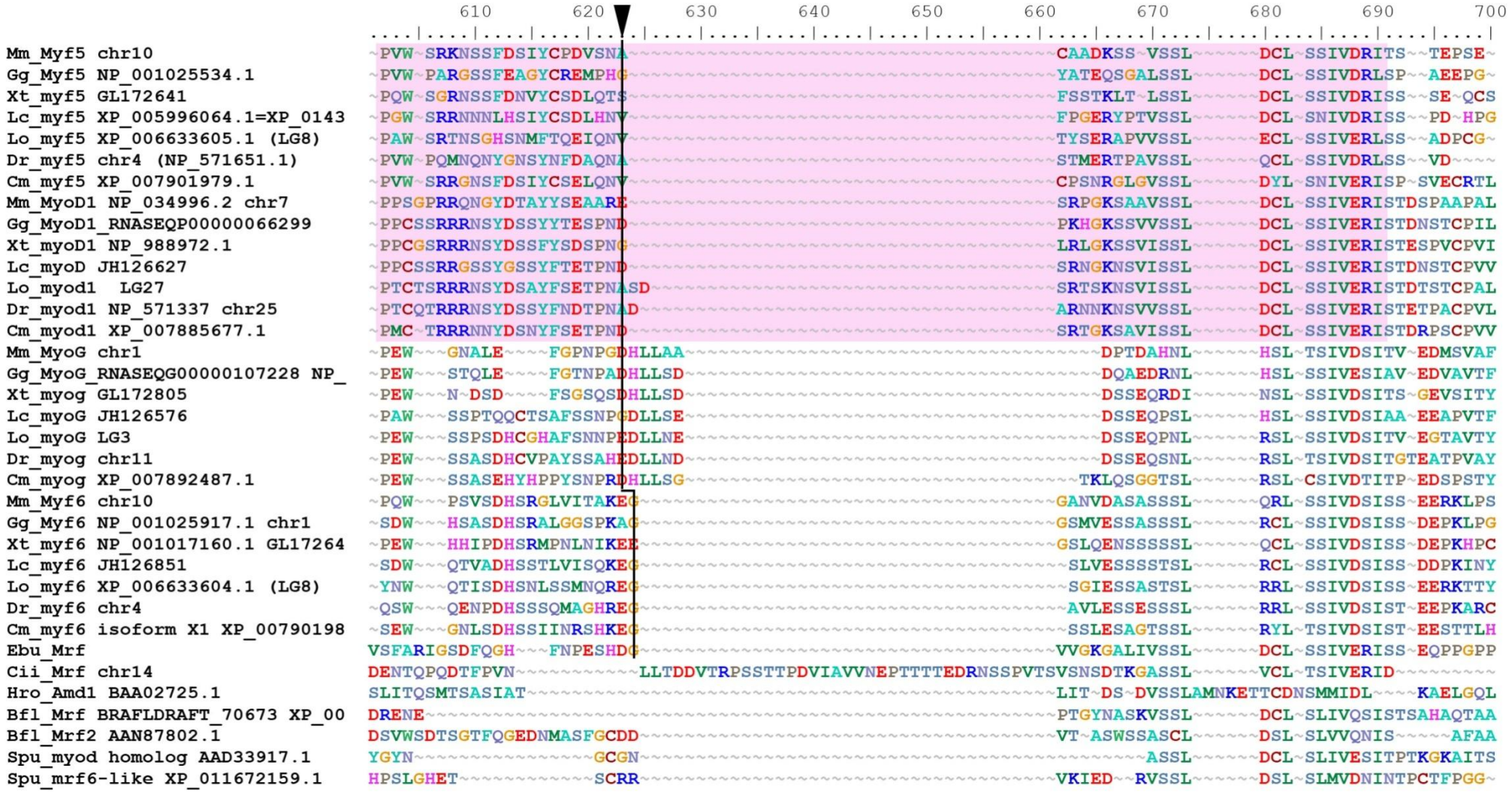
610
620
630
640
650
660
670
680
690
700
Mm_Myf5 chr10
Gg_Myf5 NP_001025534.1
Xt_myf5 GL172641
Lc_myf5 XP_005996064.1=XP_0143
Lo_myf5 XP_006633605.1 (LG8)
Dr_myf5 chr4 (NP_571651.1)
Cm_myf5 XP_007901979.1
Mm_MyoD1 NP_034996.2 chr7
Gg_MyoD1_RNASEQP00000066299
Xt_myoD1 NP_988972.1
Lc_myoD JH126627
Lo_myod1 LG27
Dr_myod1 NP_571337 chr25
Cm_myod1 XP_007885677.1
Mm_MyoG chr1
Gg_MyoG_RNASEQG00000107228 NP_
Xt_myog GL172805
Lc_myoG JH126576
Lo_myoG LG3
Dr_myog chr11
Cm_myog XP_007892487.1
Mm_Myf6 chr10
Gg_Myf6 NP_001025917.1 chr1
Xt_myf6 NP_001017160.1 GL17264
Lc_myf6 JH126851
Lo_myf6 XP_006633604.1 (LG8)
Dr_myf6 chr4
Cm_myf6 isoform X1 XP_00790198
Ebu_Mrf
Cii_Mrf chr14
Hro_Amd1 BAA02725.1
Bfl_Mrf BRAFLDRAFT_70673 XP_00
Bfl_Mrf2 AAN87802.1
Spu_myod homolog AAD33917.1
Spu_mrf6-like XP_011672159.1

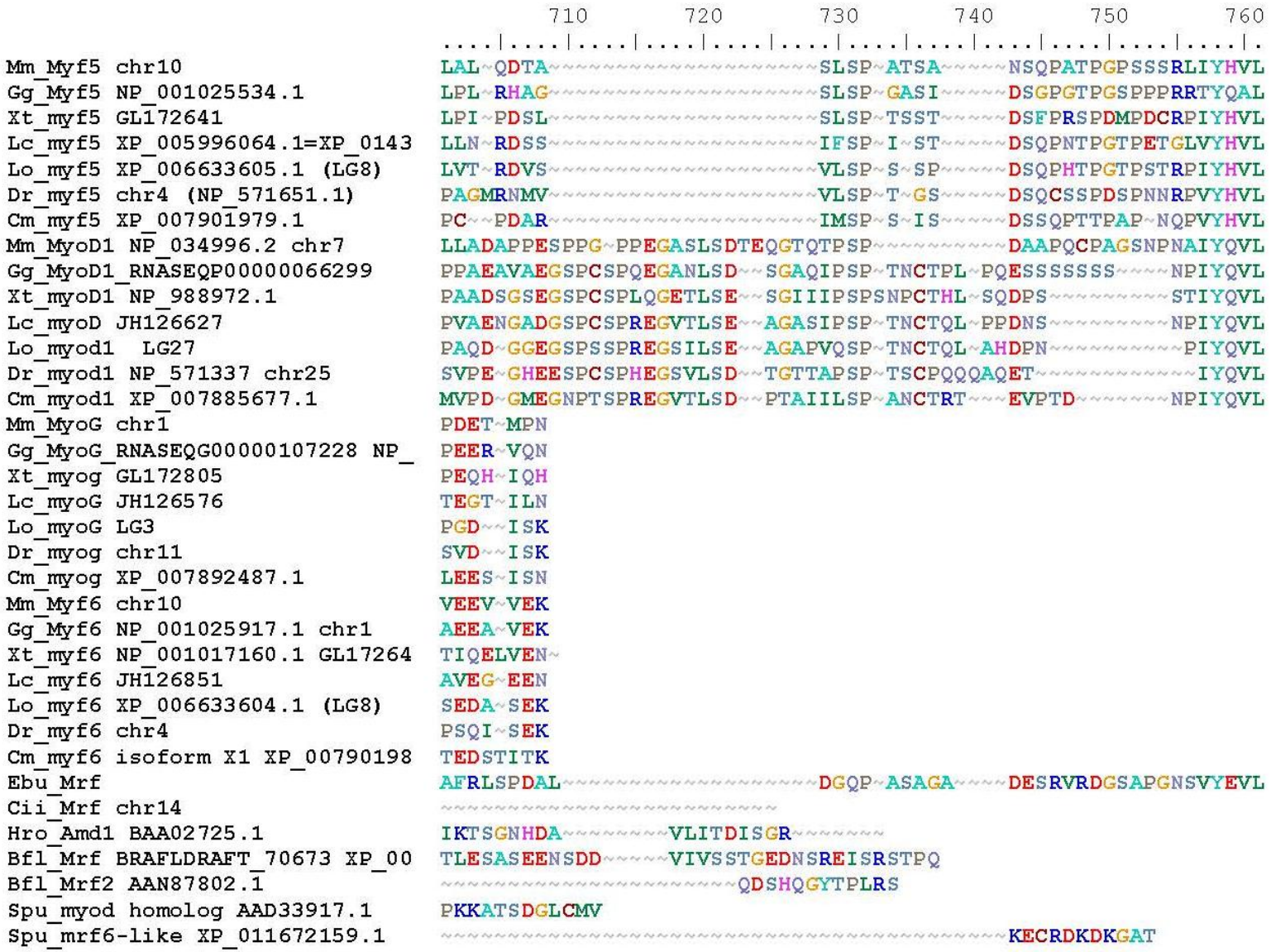
710 720 730 740 750 760
Mm_Myf5 chr10
Gg_Myf5 NP_001025534.1
Xt_myf5 GL172641
Lc_myf5 XP_005996064.1=XP_0143
Lo_myf5 XP_006633605.1 (LG8)
Dr_myf5 chr4 (NP_571651.1)
Cm_myf5 XP_007901979.1
Mm_MyoD1 NP_034996.2 chr7
Gg_MyoD1_RNASEQP00000066299
Xt_myoD1 NP_988972.1
Lc_myoD JH126627
Lo_myod1 LG27
Dr_myod1 NP_571337 chr25
Cm_myod1 XP_007885677.1
Mm_MyoG chr1
Gg_MyoG_RNASEQG00000107228 NP_
Xt_myog GL172805
Lc_myoG JH126576
Lo_myoG LG3
Dr_myog chr11
Cm_myog XP_007892487.1
Mm_Myf6 chr10
Gg_Myf6 NP_001025917.1 chr1
Xt_myf6 NP_001017160.1 GL17264
Lc_myf6 JH126851
Lo_myf6 XP_006633604.1 (LG8)
Dr_myf6 chr4
Cm_myf6 isoform X1 XP_00790198
Ebu_Mrf
Cii_Mrf chr14
Hro_Amd1 BAA02725.1
Bfl_Mrf BRAFLDRAFT_70673 XP_00
Bfl_Mrf2 AAN87802.1
Spu_myod homolog AAD33917.1
Spu_mrf6-like XP_011672159.1

Appendix 1. E Select gnathostome, agnathan and deuterostome invertebrate Mrf proteins.

Note the high degree of conservation of the basic and helix-loop-helix domains. A Myf5 domain is only present in Myf5 and MyoD proteins. However, the C-terminus of this domain is also recognisable in gnathostome MyoG and Mrf4, in agnathan Mrf and the Mrf of the deuterostome invertebrates shown here. The typical gnathostome Mrf N-terminus is present in the hagfish Mrf sequences and possibly in the Ciona sequence (depending on the actual translational start site; the predicted start site is further upstream). A variation of the C-terminal sequence typical for gnathostome Myf5/MyoD is present in the hagfish Mrf protein, suggesting that this sequence was secondarily lost in gnathostome MyoG and Mrf4. Interestingly, the first splice site shifted significantly in Myf5/MyoD compared to MyoG/Mrf4, possibly contributing to the subfunctionalisation of the proteins.

13 Appendix 2

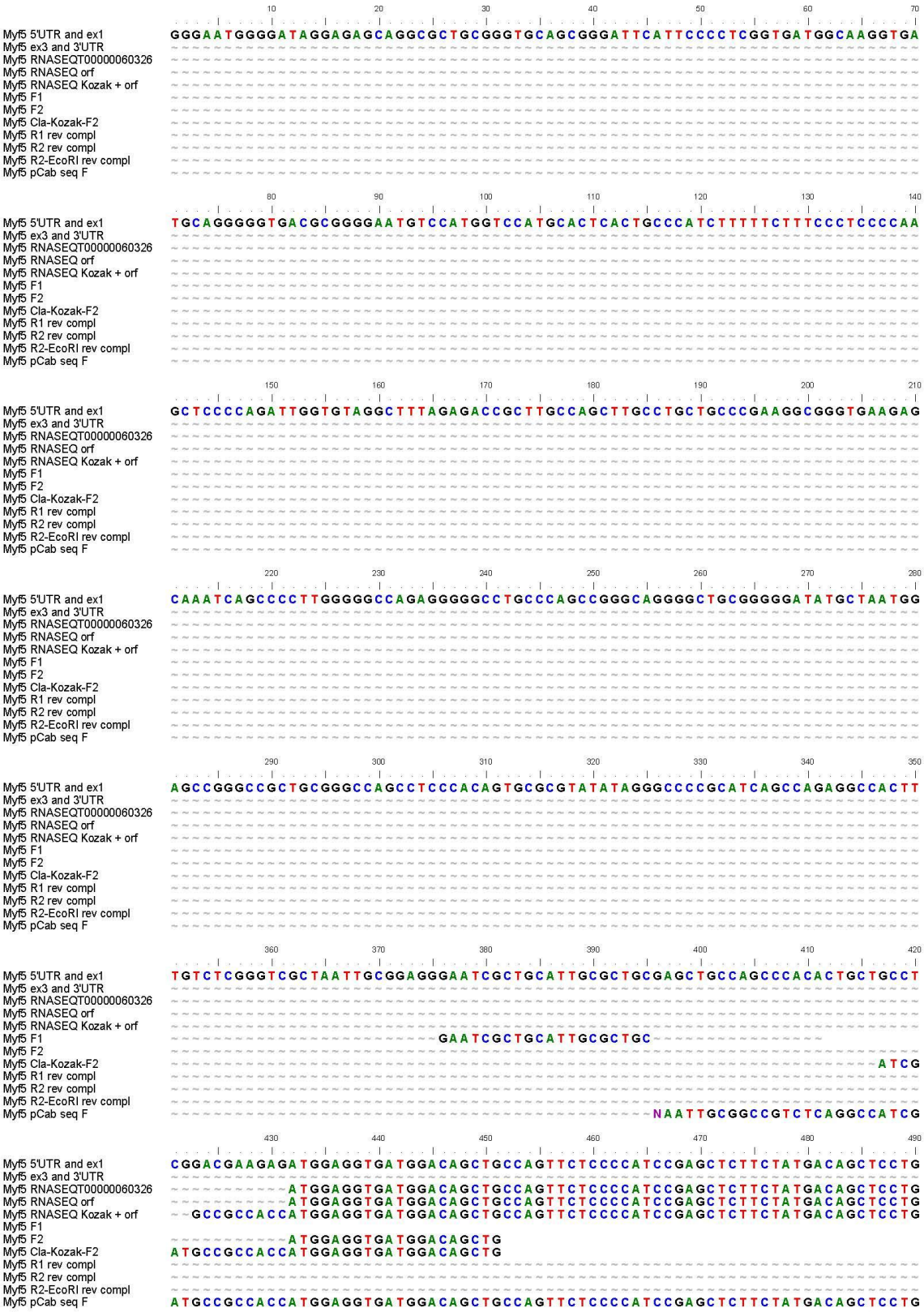

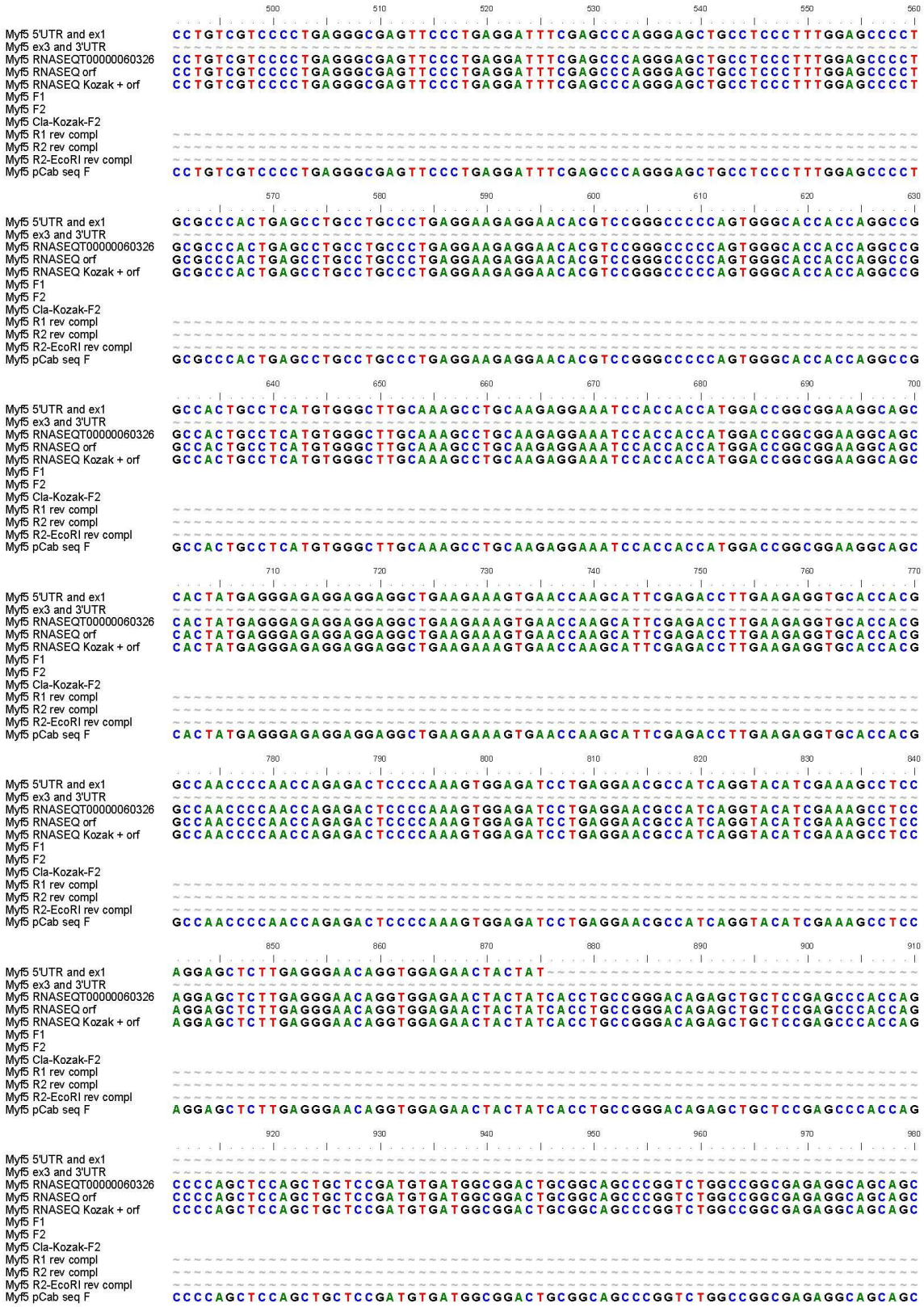
500 510 520 530 540 550 560
Myf5 5'UTR and ex1 CCTGTCGTCCCCTGAGGGCGAGTTCCCTGAGGATTTCGAGCCCAGGGAGCTGCCTCCCTTTGGAGCCCCT
Myf5 ex3 and 3'UTR
Myf5 RNASEQT00000060326 CCTGTCGTCCCCTGAGGGCGAGTTCCCTGAGGATTTCGAGCCCAGGGAGCTGCCTCCCTTTGGAGCCCCT
Myf5 RNASEQ orf CCTGTCGTCCCCTGAGGGCGAGTTCCCTGAGGATTTCGAGCCCAGGGAGCTGCCTCCCTTTGGAGCCCCT
Myf5 RNASEQ Kozak + orf CCTGTCGTCCCCTGAGGGCGAGTTCCCTGAGGATTTCGAGCCCAGGGAGCTGCCTCCCTTTGGAGCCCCT
Myf5 F1
Myf5 F2
Myf5 Cla-Kozak-F2
Myf5 R1 rev compl
Myf5 R2 rev compl
Myf5 R2-EcoRI rev compl
Myf5 pCab seq F CCTGTCGTCCCCTGAGGGCGAGTTCCCTGAGGATTTCGAGCCCAGGGAGCTGCCTCCCTTTGGAGCCCCT
570 580 590 600 610 620 630
Myf5 5'UTR and ex1 GCGCCCACTGAGCCTGCCTGCCCTGAGGAAGAGGAACACGTCCGGGCCCCCAGTGGGCACCACCAGGCCG
Myf5 ex3 and 3'UTR
Myf5 RNASEQT00000060326 GCGCCCACTGAGCCTGCCTGCCCTGAGGAAGAGGAACACGTCCGGGCCCCCAGTGGGCACCACCAGGCCG
Myf5 RNASEQ orf GCGCCCACTGAGCCTGCCTGCCCTGAGGAAGAGGAACACGTCCGGGCCCCCAGTGGGCACCACCAGGCCG
Myf5 RNASEQ Kozak + orf GCGCCCACTGAGCCTGCCTGCCCTGAGGAAGAGGAACACGTCCGGGCCCCCAGTGGGCACCACCAGGCCG
Myf5 F1
Myf5 F2
Myf5 Cla-Kozak-F2
Myf5 R1 rev compl
Myf5 R2 rev compl
Myf5 R2-EcoRI rev compl
Myf5 pCab seq F GCGCCCACTGAGCCTGCCTGCCCTGAGGAAGAGGAACACGTCCGGGCCCCCAGTGGGCACCACCAGGCCG
640 650 660 670 680 690 700
Myf5 5'UTR and ex1 GCCACTGCCTCATGTGGGCTTGCAAAGCCTGCAAGAGGAAATCCACCACCATGGACCGGCGGAAGGCAGC
Myf5 ex3 and 3'UTR
Myf5 RNASEQT00000060326 GCCACTGCCTCATGTGGGCTTGCAAAGCCTGCAAGAGGAAATCCACCACCATGGACCGGCGGAAGGCAGC
Myf5 RNASEQ orf GCCACTGCCTCATGTGGGCTTGCAAAGCCTGCAAGAGGAAATCCACCACCATGGACCGGCGGAAGGCAGC
Myf5 RNASEQ Kozak + orf GCCACTGCCTCATGTGGGCTTGCAAAGCCTGCAAGAGGAAATCCACCACCATGGACCGGCGGAAGGCAGC
Myf5 F1
Myf5 F2
Myf5 Cla-Kozak-F2
Myf5 R1 rev compl
Myf5 R2 rev compl
Myf5 R2-EcoRI rev compl
Myf5 pCab seq F GCCACTGCCTCATGTGGGCTTGCAAAGCCTGCAAGAGGAAATCCACCACCATGGACCGGCGGAAGGCAGC
710 720 730 740 750 760 770
Myf5 5'UTR and ex1 CACTATGAGGGAGAGGAGGAGGCTGAAGAAAGTGAACCAAGCATTCGAGACCTTGAAGAGGTGCACCACG
Myf5 ex3 and 3'UTR
Myf5 RNASEQT00000060326 CACTATGAGGGAGAGGAGGAGGCTGAAGAAAGTGAACCAAGCATTCGAGACCTTGAAGAGGTGCACCACG
Myf5 RNASEQ orf CACTATGAGGGAGAGGAGGAGGCTGAAGAAAGTGAACCAAGCATTCGAGACCTTGAAGAGGTGCACCACG
Myf5 RNASEQ Kozak + orf CACTATGAGGGAGAGGAGGAGGCTGAAGAAAGTGAACCAAGCATTCGAGACCTTGAAGAGGTGCACCACG
Myf5 F1
Myf5 F2
Myf5 Cla-Kozak-F2
Myf5 R1 rev compl
Myf5 R2 rev compl
Myf5 R2-EcoRI rev compl
Myf5 pCab seq F CACTATGAGGGAGAGGAGGAGGCTGAAGAAAGTGAACCAAGCATTCGAGACCTTGAAGAGGTGCACCACG
780 790 800 810 820 830 840
Myf5 5'UTR and ex1 GCCAACCCCAACCAGAGACTCCCCAAAGTGGAGATCCTGAGGAACGCCATCAGGTACATCGAAAGCCTCC
Myf5 ex3 and 3'UTR
Myf5 RNASEQT00000060326 GCCAACCCCAACCAGAGACTCCCCAAAGTGGAGATCCTGAGGAACGCCATCAGGTACATCGAAAGCCTCC
Myf5 RNASEQ orf GCCAACCCCAACCAGAGACTCCCCAAAGTGGAGATCCTGAGGAACGCCATCAGGTACATCGAAAGCCTCC
Myf5 RNASEQ Kozak + orf GCCAACCCCAACCAGAGACTCCCCAAAGTGGAGATCCTGAGGAACGCCATCAGGTACATCGAAAGCCTCC
Myf5 F1
Myf5 F2
Myf5 Cla-Kozak-F2
Myf5 R1 rev compl
Myf5 R2 rev compl
Myf5 R2-EcoRI rev compl
Myf5 pCab seq F GCCAACCCCAACCAGAGACTCCCCAAAGTGGAGATCCTGAGGAACGCCATCAGGTACATCGAAAGCCTCC
850 860 870 880 890 900 910
Myf5 5'UTR and ex1 AGGAGCTCTTGAGGGAACAGGTGGAGAACTACTAT
Myf5 ex3 and 3'UTR
Myf5 RNASEQT00000060326 AGGAGCTCTTGAGGGAACAGGTGGAGAACTACTATCACCTGCCGGGACAGAGCTGCTCCGAGCCCACCAG
Myf5 RNASEQ orf AGGAGCTCTTGAGGGAACAGGTGGAGAACTACTATCACCTGCCGGGACAGAGCTGCTCCGAGCCCACCAG
Myf5 RNASEQ Kozak + orf AGGAGCTCTTGAGGGAACAGGTGGAGAACTACTATCACCTGCCGGGACAGAGCTGCTCCGAGCCCACCAG
Myf5 F1
Myf5 F2
Myf5 Cla-Kozak-F2
Myf5 R1 rev compl
Myf5 R2 rev compl
Myf5 R2-EcoRI rev compl
Myf5 pCab seq F AGGAGCTCTTGAGGGAACAGGTGGAGAACTACTATCACCTGCCGGGACAGAGCTGCTCCGAGCCCACCAG
920 930 940 950 960 970 980
Myf5 5'UTR and ex1
Myf5 ex3 and 3'UTR
Myf5 RNASEQT00000060326 CCCCAGCTCCAGCTGCTCCGATGTGATGGCGGACTGCGGCAGCCCGGTCTGGCCGGCGAGAGGCAGCAGC
Myf5 RNASEQ orf CCCCAGCTCCAGCTGCTCCGATGTGATGGCGGACTGCGGCAGCCCGGTCTGGCCGGCGAGAGGCAGCAGC
Myf5 RNASEQ Kozak + orf CCCCAGCTCCAGCTGCTCCGATGTGATGGCGGACTGCGGCAGCCCGGTCTGGCCGGCGAGAGGCAGCAGC
Myf5 F1
Myf5 F2
Myf5 Cla-Kozak-F2
Myf5 R1 rev compl
Myf5 R2 rev compl
Myf5 R2-EcoRI rev compl
Myf5 pCab seq F CCCCAGCTCCAGCTGCTCCGATGTGATGGCGGACTGCGGCAGCCCGGTCTGGCCGGCGAGAGGCAGCAGC

```
                                       990       1000      1010      1020      1030      1040      1050
Myf5 5'UTR and ex1            ~~~~~~~~~~~~~~~~~~~~~~~~~~~~~~~~~~~~~~~~~~~~~~~~~~~~~~~~~~~~~~~~~~~~~~~
Myf5 ex3 and 3'UTR            ~~~~~~~~~~~~~~~~~~~~~~~~~~~~~~~~~~GCTACGCGACGGAGCAGAGTGGCGCGCTGTCCAGCC
Myf5 RNASEQT00000060326       TTCGAGGCGGGCTACTGCCCCGAGATGCCCCACGGCTACGCGACGGAGCAGAGTGGCGCGCTGTCCAGCC
Myf5 RNASEQ orf               TTCGAGGCGGGCTACTGCCCCGAGATGCCCCACGGCTACGCGACGGAGCAGAGTGGCGCGCTGTCCAGCC
Myf5 RNASEQ Kozak + orf       TTCGAGGCGGGCTACTGCCCCGAGATGCCCCACGGCTACGCGACGGAGCAGAGTGGCGCGCTGTCCAGCC
Myf5 F1
Myf5 F2
Myf5 Cla-Kozak-F2
Myf5 R1 rev compl             ~~~~~~~~~~~~~~~~~~~~~~~~~~~~~~~~~~~~~~~~~~~~~~~~~~~~~~~~~~~~~~~~~~~~~~
Myf5 R2 rev compl             ~~~~~~~~~~~~~~~~~~~~~~~~~~~~~~~~~~~~~~~~~~~~~~~~~~~~~~~~~~~~~~~~~~~~~~
Myf5 R2-EcoRI rev compl       ~~~~~~~~~~~~~~~~~~~~~~~~~~~~~~~~~~~~~~~~~~~~~~~~~~~~~~~~~~~~~~~~~~~~~~
Myf5 pCab seq F               TTCGAGGCGGGCTACTGCCCCGAGATGCCCCACGGCTACGCGACGGAGCAGAGTGGCGCGCTGTCCAGCC

                                       1060      1070      1080      1090      1100      1110      1120
Myf5 5'UTR and ex1            ~~~~~~~~~~~~~~~~~~~~~~~~~~~~~~~~~~~~~~~~~~~~~~~~~~~~~~~~~~~~~~~~~~~~~~
Myf5 ex3 and 3'UTR            TGGACTGCCTCTCCAGCATCGTGGACCGCCTCTCTCCGGCGGAGGAGCCGGGGCTGCCCCTCCGTCACGC
Myf5 RNASEQT00000060326       TGGACTGCCTCTCCAGCATCGTGGACCGCCTCTCTCCGGCGGAGGAGCCGGGGCTGCCCCTCCGTCACGC
Myf5 RNASEQ orf               TGGACTGCCTCTCCAGCATCGTGGACCGCCTCTCTCCGGCGGAGGAGCCGGGGCTGCCCCTCCGTCACGC
Myf5 RNASEQ Kozak + orf       TGGACTGCCTCTCCAGCATCGTGGACCGCCTCTCTCCGGCGGAGGAGCCGGGGCTGCCCCTCCGTCACGC
Myf5 F1
Myf5 F2
Myf5 Cla-Kozak-F2
Myf5 R1 rev compl             ~~~~~~~~~~~~~~~~~~~~~~~~~~~~~~~~~~~~~~~~~~~~~~~~~~~~~~~~~~~~~~~~~~~~~~
Myf5 R2 rev compl             ~~~~~~~~~~~~~~~~~~~~~~~~~~~~~~~~~~~~~~~~~~~~~~~~~~~~~~~~~~~~~~~~~~~~~~
Myf5 R2-EcoRI rev compl       ~~~~~~~~~~~~~~~~~~~~~~~~~~~~~~~~~~~~~~~~~~~~~~~~~~~~~~~~~~~~~~~~~~~~~~
Myf5 pCab seq F               TGGACTGCCTCTCCAGCATCGTGGACCGCCTCTCTCCGGCGGAGGAGCCGGGGCTGCCCCTCCGTCACGC

                                       1130      1140      1150      1160      1170      1180      1190
Myf5 5'UTR and ex1            ~~~~~~~~~~~~~~~~~~~~~~~~~~~~~~~~~~~~~~~~~~~~~~~~~~~~~~~~~~~~~~~~
Myf5 ex3 and 3'UTR            CGGCTCCCTCTCGCCAGGCGCCAGCATCGACTCGGGGCCCGGGACGCCCGGCTCGCCGCCGCCCCGACGG
Myf5 RNASEQT00000060326       CGGCTCCCTCTCGCCAGGCGCCAGCATCGACTCGGGGCCCGGGACGCCCGGCTCGCCGCCGCCCCGACGG
Myf5 RNASEQ orf               CGGCTCCCTCTCGCCAGGCGCCAGCATCGACTCGGGGCCCGGGACGCCCGGCTCGCCGCCGCCCCGACGG
Myf5 RNASEQ Kozak + orf       CGGCTCCCTCTCGCCAGGCGCCAGCATCGACTCGGGGCCCGGGACGCCCGGCTCGCCGCCGCCCCGACGG
Myf5 F1
Myf5 F2
Myf5 Cla-Kozak-F2
Myf5 R1 rev compl             ~~~~~~~~~~~~~~~~~~~~~~~~~~~~~~~~~~~~~~~~~~~~~~~~~~~~~~~~~~~~~~~~~~~~~~
Myf5 R2 rev compl             ~~~~~~~~~~~~~~~~~~~~~~~~~~~~~~~~~~~~~~~~~~~~~~~~~~~~~~~~~~~~~~~~~~~~GG
Myf5 R2-EcoRI rev compl       ~~~~~~~~~~~~~~~~~~~~~~~~~~~~~~~~~~~~~~~~~~~~~~~~~~~~~~~~~~~~~~~~~~~~GG
Myf5 pCab seq F               CGGCTCCCTCTCGCCAGGCGCCAGCATCGACTCGGGGCCCGGGACGCCCGGCTCGCCGCCGCCCCGACGG

                                       1200      1210      1220      1230      1240      1250      1260
Myf5 5'UTR and ex1
Myf5 ex3 and 3'UTR            ACCTACCAGGCGCTATGAGGGGCCGGGGCCACCGCCGGTTCCGGGGCTGACCCCGGCTGCCTCTCGTCCC
Myf5 RNASEQT00000060326       ACCTACCAGGCGCTATGAGGGGCCGGGGCCACCGCCGGTTCCGGGGCTGACCCCGGCTGCCTCTCGTCCC
Myf5 RNASEQ orf               ACCTACCAGGCGCTATGA
Myf5 RNASEQ Kozak + orf       ACCTACCAGGCGCTATGA
Myf5 F1
Myf5 F2
Myf5 Cla-Kozak-F2
Myf5 R1 rev compl             ~~~~~~~~~~~~~~~~~~~~~~~~~~~~~~~~~~~~~~~~~~~~~~~~~~~~~~~~~~~~~~~~~~~~~~
Myf5 R2 rev compl             ACCTACCAGGCGCTATGA
Myf5 R2-EcoRI rev compl       ACCTACCAGGCGCTATGAATTC~~~~~~~~~~~~~~
Myf5 pCab seq F               ACCTACCAGGCGCTATGAGAATTCCGCCCCCCCCTCTCCCTCCCCCCCCCCTAACGTTACTGGCCGAAG

                                       1270      1280      1290      1300      1310      1320      1330
Myf5 5'UTR and ex1
Myf5 ex3 and 3'UTR            GCCGCCCCGCAAAACCTCTCGGGCGGGAGGGGCGGCCCCGGCTCCGCTGCCGTCGGGGTTGGAGGCGACG
Myf5 RNASEQT00000060326       GCCGCCCCGCAAAACCTCTCGGGCGGGAGGGGCGGCCCCGGCTCCGCTGCCGTCGGGGTTGGAGGCGACG
Myf5 RNASEQ orf
Myf5 RNASEQ Kozak + orf
Myf5 F1
Myf5 F2
Myf5 Cla-Kozak-F2
Myf5 R1 rev compl             ~~~~~~~~~~~~~~~~~~~~~~~~~~~~~~~~~~~~~~~~~~~~~~~~~~~~~~~~~~~~~~~~~~~~~~
Myf5 R2 rev compl
Myf5 R2-EcoRI rev compl
Myf5 pCab seq F               CCGCTNGGNATNNNNCCGGTGTGCGTTTGTCTATATGTTATTTTCCACCATATTGCCGTCTT

                                       1340      1350      1360      1370      1380      1390      1400
Myf5 5'UTR and ex1
Myf5 ex3 and 3'UTR            CCGCCGCCCGGAGCAGCCCCCGGGGCTCGGGACGCGTGTGCTGCCCTGGAAACCCCGCTGCAAATAAAGC
Myf5 RNASEQT00000060326       CCGCCGCCCGGAGCAGCCCCCGGGGCTCGGGACGCGTGTGCTGCCCTGGAAACCCCGCTGCAAATAAAGC
Myf5 RNASEQ orf
Myf5 RNASEQ Kozak + orf
Myf5 F1
Myf5 F2
Myf5 Cla-Kozak-F2
Myf5 R1 rev compl             ~~~~~~~~~~~~~~~~~~~~~CGTGTGCTGCCCTGGAAAC~~~~~~
Myf5 R2 rev compl
Myf5 R2-EcoRI rev compl
Myf5 pCab seq F

                                       1410      1420      1430      1440      1450      1460      1470
Myf5 5'UTR and ex1
Myf5 ex3 and 3'UTR            GTGCTACCACACAGCCGGCTCGCCTGGTGCTTCTTTAACCTCATCCCCGGGTGCTCGCGGGGGCCCGGCT
Myf5 RNASEQT00000060326       GTGCTACCACACAGCCGGCTCGCCTGGTGCTTCTTTAACCTCATCCCCGGGTGCTCGCGGGGGCCCGGCT
Myf5 RNASEQ orf
Myf5 RNASEQ Kozak + orf
Myf5 F1
Myf5 F2
Myf5 Cla-Kozak-F2
Myf5 R1 rev compl
Myf5 R2 rev compl
Myf5 R2-EcoRI rev compl
Myf5 pCab seq F
```

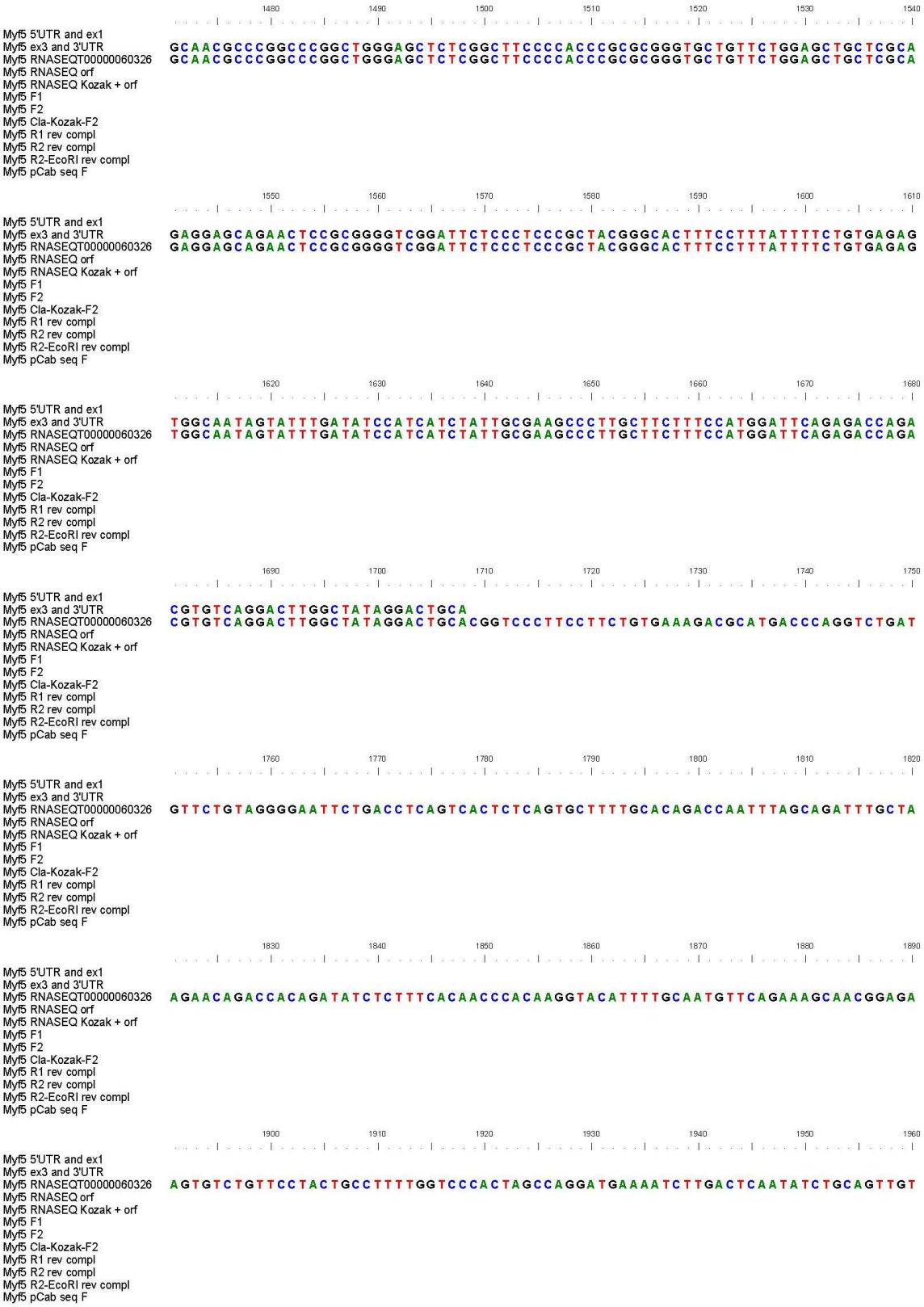
1480 1490 1500 1510 1520 1530 1540
Myf5 5'UTR and ex1
Myf5 ex3 and 3'UTR
Myf5 RNASEQT00000060326
Myf5 RNASEQ orf
Myf5 RNASEQ Kozak + orf
Myf5 F1
Myf5 F2
Myf5 Cla-Kozak-F2
Myf5 R1 rev compl
Myf5 R2 rev compl
Myf5 R2-EcoRI rev compl
Myf5 pCab seq F
GCAACGCCCGGCCCGGCTGGGAGCTCTCGGCTTCCCCACCCGCGCGGGTGCTGTTCTGGAGCTGCTCGCA
GCAACGCCCGGCCCGGCTGGGAGCTCTCGGCTTCCCCACCCGCGCGGGTGCTGTTCTGGAGCTGCTCGCA
1550 1560 1570 1580 1590 1600 1610
Myf5 5'UTR and ex1
Myf5 ex3 and 3'UTR
Myf5 RNASEQT00000060326
Myf5 RNASEQ orf
Myf5 RNASEQ Kozak + orf
Myf5 F1
Myf5 F2
Myf5 Cla-Kozak-F2
Myf5 R1 rev compl
Myf5 R2 rev compl
Myf5 R2-EcoRI rev compl
Myf5 pCab seq F
GAGGAGCAGAACTCCGCGGGGTCGGATTCTCCCTCCCGCTACGGGCACTTTCCTTTATTTTCTGTGAGAG
GAGGAGCAGAACTCCGCGGGGTCGGATTCTCCCTCCCGCTACGGGCACTTTCCTTTATTTTCTGTGAGAG
1620 1630 1640 1650 1660 1670 1680
Myf5 5'UTR and ex1
Myf5 ex3 and 3'UTR
Myf5 RNASEQT00000060326
Myf5 RNASEQ orf
Myf5 RNASEQ Kozak + orf
Myf5 F1
Myf5 F2
Myf5 Cla-Kozak-F2
Myf5 R1 rev compl
Myf5 R2 rev compl
Myf5 R2-EcoRI rev compl
Myf5 pCab seq F
TGGCAATAGTATTTGATATCCATCATCTATTGCGAAGCCCTTGCTTCTTTCCATGGATTCAGAGACCAGA
TGGCAATAGTATTTGATATCCATCATCTATTGCGAAGCCCTTGCTTCTTTCCATGGATTCAGAGACCAGA
1690 1700 1710 1720 1730 1740 1750
Myf5 5'UTR and ex1
Myf5 ex3 and 3'UTR
Myf5 RNASEQT00000060326
Myf5 RNASEQ orf
Myf5 RNASEQ Kozak + orf
Myf5 F1
Myf5 F2
Myf5 Cla-Kozak-F2
Myf5 R1 rev compl
Myf5 R2 rev compl
Myf5 R2-EcoRI rev compl
Myf5 pCab seq F
CGTGTCAGGACTTGGCTATAGGACTGCA
CGTGTCAGGACTTGGCTATAGGACTGCACGGTCCCTTCCTTCTGTGAAAGACGCATGACCCAGGTCTGAT
1760 1770 1780 1790 1800 1810 1820
Myf5 5'UTR and ex1
Myf5 ex3 and 3'UTR
Myf5 RNASEQT00000060326
Myf5 RNASEQ orf
Myf5 RNASEQ Kozak + orf
Myf5 F1
Myf5 F2
Myf5 Cla-Kozak-F2
Myf5 R1 rev compl
Myf5 R2 rev compl
Myf5 R2-EcoRI rev compl
Myf5 pCab seq F
GTTCTGTAGGGGAATTCTGACCTCAGTCACTCTCAGTGCTTTTGCACAGACCAATTTAGCAGATTTGCTA
1830 1840 1850 1860 1870 1880 1890
Myf5 5'UTR and ex1
Myf5 ex3 and 3'UTR
Myf5 RNASEQT00000060326
Myf5 RNASEQ orf
Myf5 RNASEQ Kozak + orf
Myf5 F1
Myf5 F2
Myf5 Cla-Kozak-F2
Myf5 R1 rev compl
Myf5 R2 rev compl
Myf5 R2-EcoRI rev compl
Myf5 pCab seq F
AGAACAGACCACAGATATCTCTTTCACAACCCACAAGGTACATTTTGCAATGTTCAGAAAGCAACGGAGA
1900 1910 1920 1930 1940 1950 1960
Myf5 5'UTR and ex1
Myf5 ex3 and 3'UTR
Myf5 RNASEQT00000060326
Myf5 RNASEQ orf
Myf5 RNASEQ Kozak + orf
Myf5 F1
Myf5 F2
Myf5 Cla-Kozak-F2
Myf5 R1 rev compl
Myf5 R2 rev compl
Myf5 R2-EcoRI rev compl
Myf5 pCab seq F
AGTGTCTGTTCCTACTGCCTTTTGGTCCCACTAGCCAGGATGAAAATCTTGACTCAATATCTGCAGTTGT

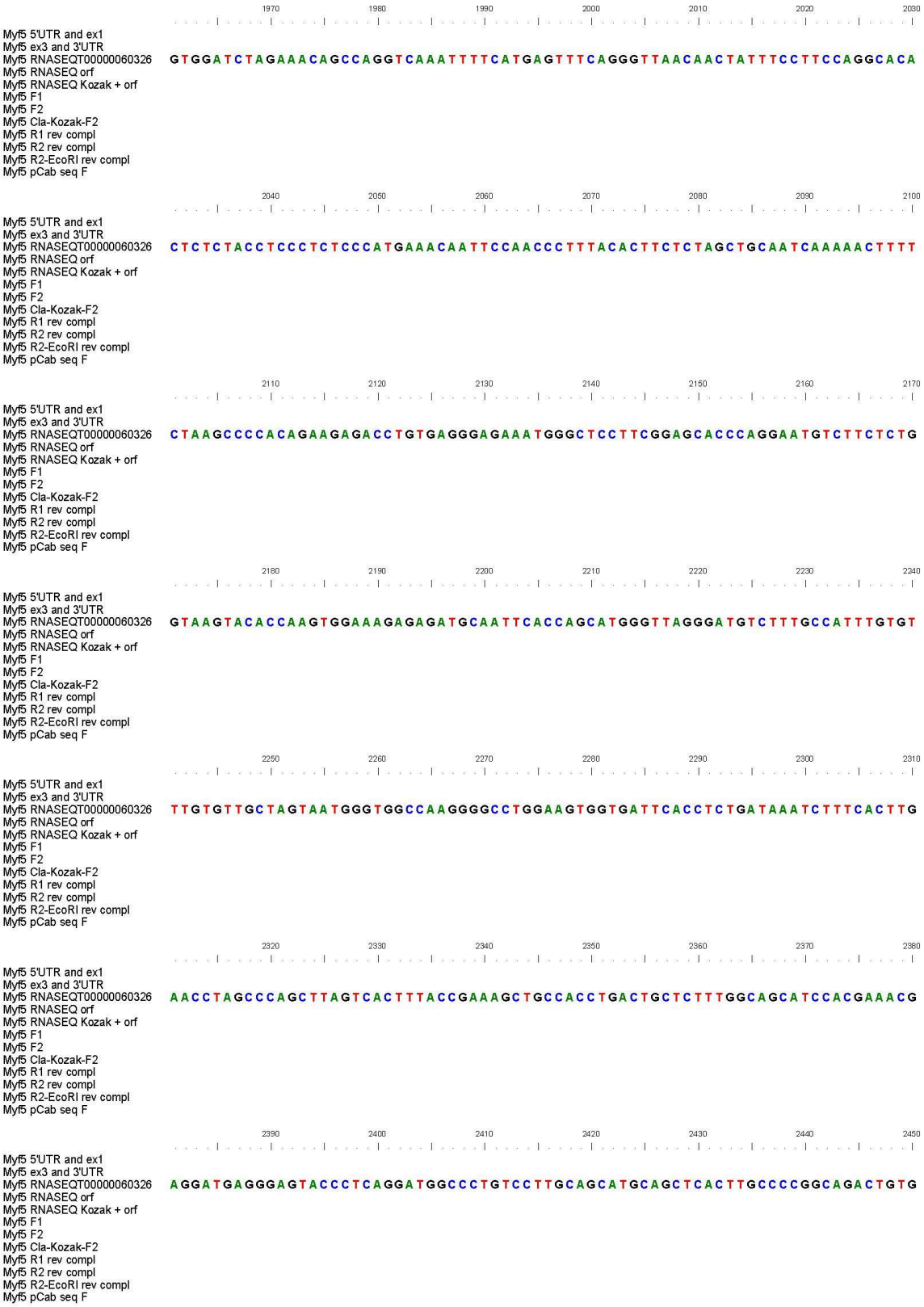
1970 1980 1990 2000 2010 2020 2030
Myf5 5'UTR and ex1
Myf5 ex3 and 3'UTR
Myf5 RNASEQT00000060326
Myf5 RNASEQ orf
Myf5 RNASEQ Kozak + orf
Myf5 F1
Myf5 F2
Myf5 Cla-Kozak-F2
Myf5 R1 rev compl
Myf5 R2 rev compl
Myf5 R2-EcoRI rev compl
Myf5 pCab seq F
GTGGATCTAGAAACAGCCAGGTCAAATTTTCATGAGTTTCAGGGTTAACAACTATTTCCTTCCAGGCACA
2040 2050 2060 2070 2080 2090 2100
Myf5 5'UTR and ex1
Myf5 ex3 and 3'UTR
Myf5 RNASEQT00000060326
Myf5 RNASEQ orf
Myf5 RNASEQ Kozak + orf
Myf5 F1
Myf5 F2
Myf5 Cla-Kozak-F2
Myf5 R1 rev compl
Myf5 R2 rev compl
Myf5 R2-EcoRI rev compl
Myf5 pCab seq F
CTCTCTACCTCCCTCTCCCATGAAACAATTCCAACCCTTTACACTTCTCTAGCTGCAATCAAAAACTTTT
2110 2120 2130 2140 2150 2160 2170
Myf5 5'UTR and ex1
Myf5 ex3 and 3'UTR
Myf5 RNASEQT00000060326
Myf5 RNASEQ orf
Myf5 RNASEQ Kozak + orf
Myf5 F1
Myf5 F2
Myf5 Cla-Kozak-F2
Myf5 R1 rev compl
Myf5 R2 rev compl
Myf5 R2-EcoRI rev compl
Myf5 pCab seq F
CTAAGCCCCACAGAAGAGACCTGTGAGGGAGAAATGGGCTCCTTCGGAGCACCCAGGAATGTCTTCTCTG
2180 2190 2200 2210 2220 2230 2240
Myf5 5'UTR and ex1
Myf5 ex3 and 3'UTR
Myf5 RNASEQT00000060326
Myf5 RNASEQ orf
Myf5 RNASEQ Kozak + orf
Myf5 F1
Myf5 F2
Myf5 Cla-Kozak-F2
Myf5 R1 rev compl
Myf5 R2 rev compl
Myf5 R2-EcoRI rev compl
Myf5 pCab seq F
GTAAGTACACCAAGTGGAAAGAGAGATGCAATTCACCAGCATGGGTTAGGGATGTCTTTGCCATTTGTGT
2250 2260 2270 2280 2290 2300 2310
Myf5 5'UTR and ex1
Myf5 ex3 and 3'UTR
Myf5 RNASEQT00000060326
Myf5 RNASEQ orf
Myf5 RNASEQ Kozak + orf
Myf5 F1
Myf5 F2
Myf5 Cla-Kozak-F2
Myf5 R1 rev compl
Myf5 R2 rev compl
Myf5 R2-EcoRI rev compl
Myf5 pCab seq F
TTGTGTTGCTAGTAATGGGTGGCCAAGGGGCCTGGAAGTGGTGATTCACCTCTGATAAATCTTTCACTTG
2320 2330 2340 2350 2360 2370 2380
Myf5 5'UTR and ex1
Myf5 ex3 and 3'UTR
Myf5 RNASEQT00000060326
Myf5 RNASEQ orf
Myf5 RNASEQ Kozak + orf
Myf5 F1
Myf5 F2
Myf5 Cla-Kozak-F2
Myf5 R1 rev compl
Myf5 R2 rev compl
Myf5 R2-EcoRI rev compl
Myf5 pCab seq F
AACCTAGCCCAGCTTAGTCACTTTACCGAAAGCTGCCACCTGACTGCTCTTTGGCAGCATCCACGAAACG
2390 2400 2410 2420 2430 2440 2450
Myf5 5'UTR and ex1
Myf5 ex3 and 3'UTR
Myf5 RNASEQT00000060326
Myf5 RNASEQ orf
Myf5 RNASEQ Kozak + orf
Myf5 F1
Myf5 F2
Myf5 Cla-Kozak-F2
Myf5 R1 rev compl
Myf5 R2 rev compl
Myf5 R2-EcoRI rev compl
Myf5 pCab seq F
AGGATGAGGGAGTACCCTCAGGATGGCCCTGTCCTTGCAGCATGCAGCTCACTTGCCCCGGCAGACTGTG

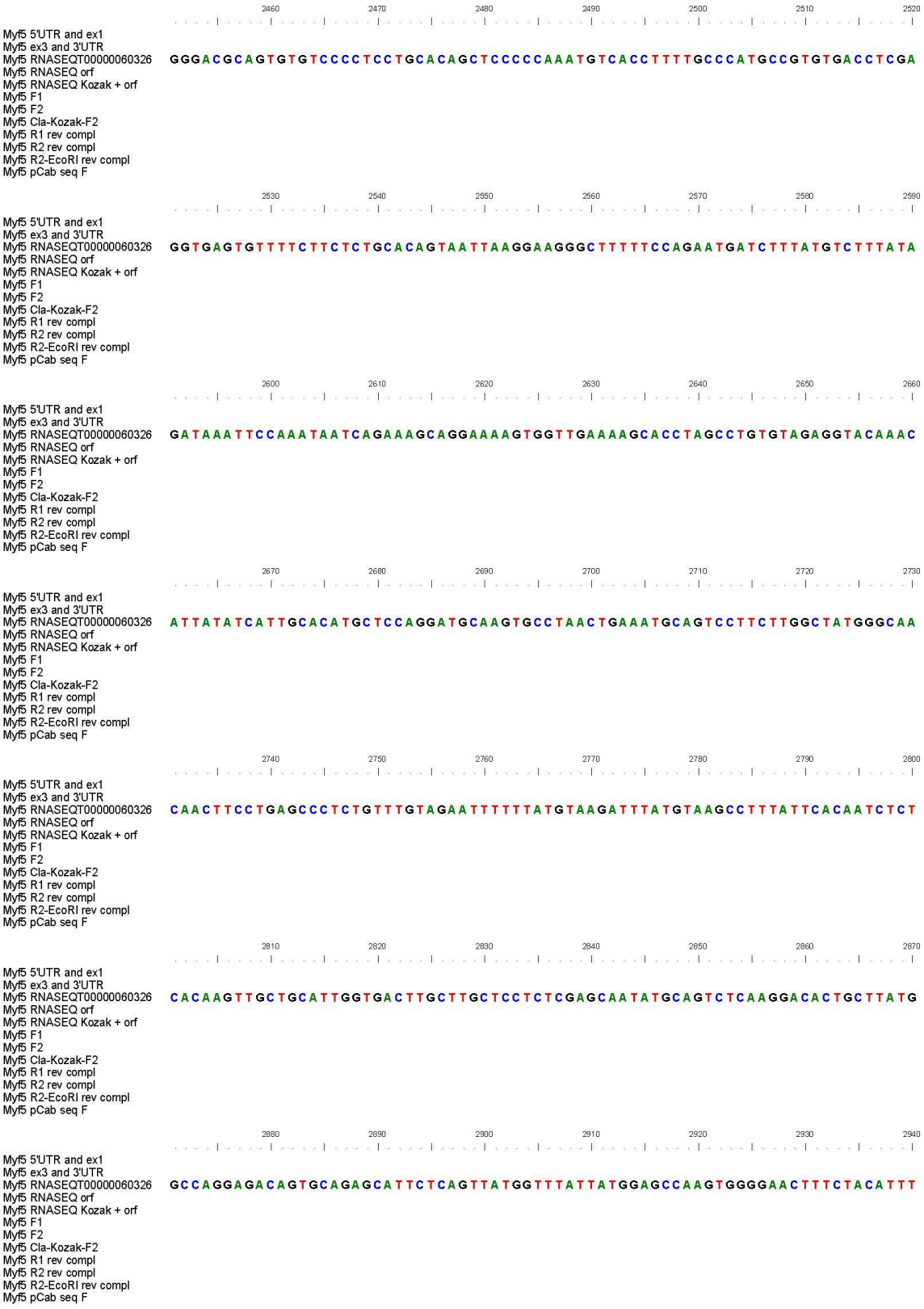
2460 2470 2480 2490 2500 2510 2520
Myf5 5'UTR and ex1
Myf5 ex3 and 3'UTR
Myf5 RNASEQT00000060326
Myf5 RNASEQ orf
Myf5 RNASEQ Kozak + orf
Myf5 F1
Myf5 F2
Myf5 Cla-Kozak-F2
Myf5 R1 rev compl
Myf5 R2 rev compl
Myf5 R2-EcoRI rev compl
Myf5 pCab seq F
GGGACGCAGTGTGTCCCCTCCTGCACAGCTCCCCCAAATGTCACCTTTTGCCCATGCCGTGTGACCTCGA
2530 2540 2550 2560 2570 2580 2590
Myf5 5'UTR and ex1
Myf5 ex3 and 3'UTR
Myf5 RNASEQT00000060326
Myf5 RNASEQ orf
Myf5 RNASEQ Kozak + orf
Myf5 F1
Myf5 F2
Myf5 Cla-Kozak-F2
Myf5 R1 rev compl
Myf5 R2 rev compl
Myf5 R2-EcoRI rev compl
Myf5 pCab seq F
GGTGAGTGTTTTCTTCTCTGCACAGTAATTAAGGAAGGGCTTTTTCCAGAATGATCTTTATGTCTTTATA
2600 2610 2620 2630 2640 2650 2660
Myf5 5'UTR and ex1
Myf5 ex3 and 3'UTR
Myf5 RNASEQT00000060326
Myf5 RNASEQ orf
Myf5 RNASEQ Kozak + orf
Myf5 F1
Myf5 F2
Myf5 Cla-Kozak-F2
Myf5 R1 rev compl
Myf5 R2 rev compl
Myf5 R2-EcoRI rev compl
Myf5 pCab seq F
GATAAATTCCAAATAATCAGAAAGCAGGAAAAGTGGTTGAAAAGCACCTAGCCTGTGTAGAGGTACAAAC
2670 2680 2690 2700 2710 2720 2730
Myf5 5'UTR and ex1
Myf5 ex3 and 3'UTR
Myf5 RNASEQT00000060326
Myf5 RNASEQ orf
Myf5 RNASEQ Kozak + orf
Myf5 F1
Myf5 F2
Myf5 Cla-Kozak-F2
Myf5 R1 rev compl
Myf5 R2 rev compl
Myf5 R2-EcoRI rev compl
Myf5 pCab seq F
ATTATATCATTGCACATGCTCCAGGATGCAAGTGCCTAACTGAAATGCAGTCCTTCTTGGCTATGGGCAA
2740 2750 2760 2770 2780 2790 2800
Myf5 5'UTR and ex1
Myf5 ex3 and 3'UTR
Myf5 RNASEQT00000060326
Myf5 RNASEQ orf
Myf5 RNASEQ Kozak + orf
Myf5 F1
Myf5 F2
Myf5 Cla-Kozak-F2
Myf5 R1 rev compl
Myf5 R2 rev compl
Myf5 R2-EcoRI rev compl
Myf5 pCab seq F
CAACTTCCTGAGCCCTCTGTTTGTAGAATTTTTTATGTAAGATTTATGTAAGCCTTTATTCACAATCTCT
2810 2820 2830 2840 2850 2860 2870
Myf5 5'UTR and ex1
Myf5 ex3 and 3'UTR
Myf5 RNASEQT00000060326
Myf5 RNASEQ orf
Myf5 RNASEQ Kozak + orf
Myf5 F1
Myf5 F2
Myf5 Cla-Kozak-F2
Myf5 R1 rev compl
Myf5 R2 rev compl
Myf5 R2-EcoRI rev compl
Myf5 pCab seq F
CACAAGTTGCTGCATTGGTGACTTGCTTGCTCCTCTCGAGCAATATGCAGTCTCAAGGACACTGCTTATG
2880 2890 2900 2910 2920 2930 2940
Myf5 5'UTR and ex1
Myf5 ex3 and 3'UTR
Myf5 RNASEQT00000060326
Myf5 RNASEQ orf
Myf5 RNASEQ Kozak + orf
Myf5 F1
Myf5 F2
Myf5 Cla-Kozak-F2
Myf5 R1 rev compl
Myf5 R2 rev compl
Myf5 R2-EcoRI rev compl
Myf5 pCab seq F
GCCAGGAGACAGTGCAGAGCATTCTCAGTTATGGTTTATTATGGAGCCAAGTGGGGAACTTTCTACATTT

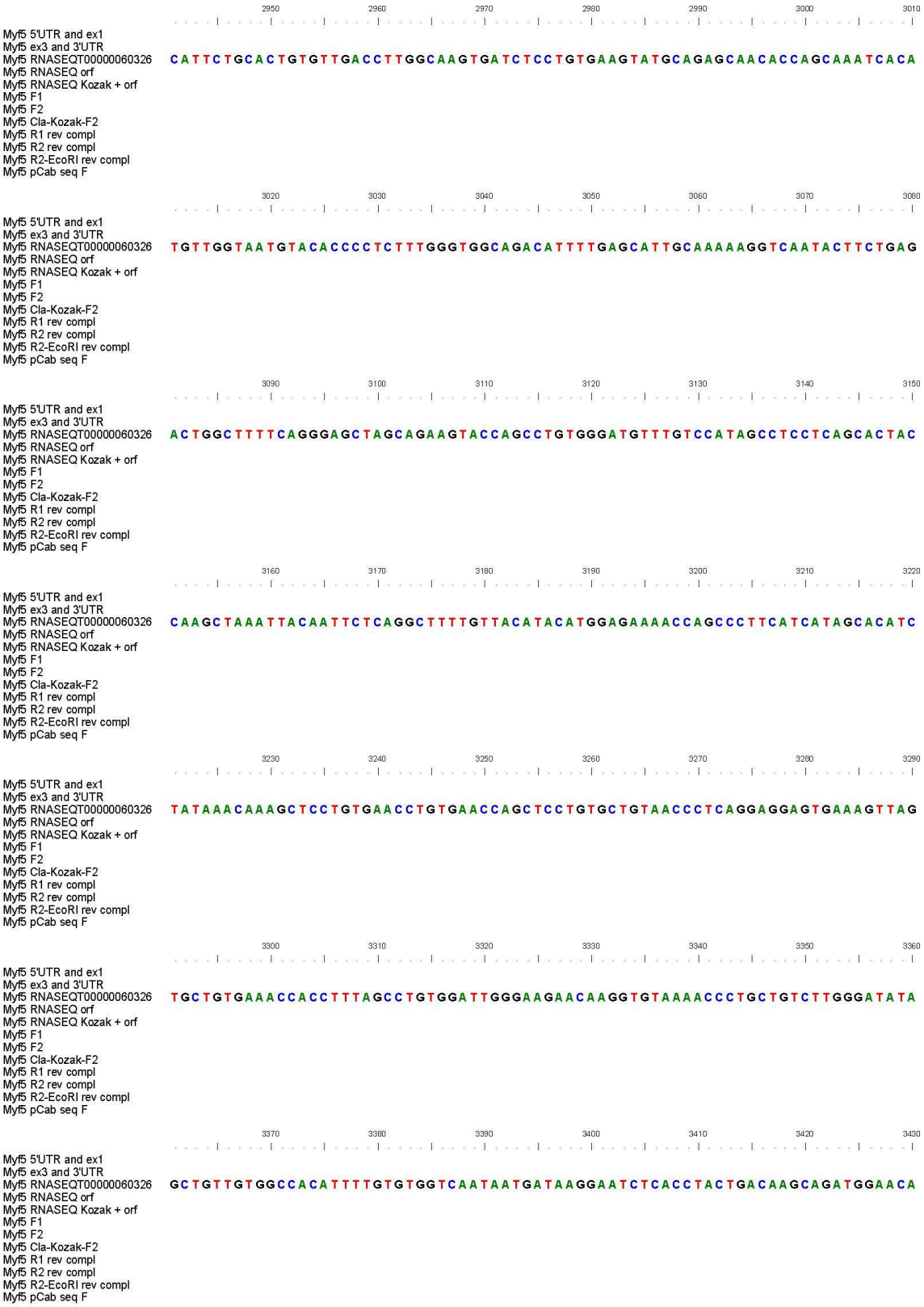
2950 2960 2970 2980 2990 3000 3010
Myf5 5'UTR and ex1
Myf5 ex3 and 3'UTR
Myf5 RNASEQT00000060326
Myf5 RNASEQ orf
Myf5 RNASEQ Kozak + orf
Myf5 F1
Myf5 F2
Myf5 Cla-Kozak-F2
Myf5 R1 rev compl
Myf5 R2 rev compl
Myf5 R2-EcoRI rev compl
Myf5 pCab seq F
CATTCTGCACTGTGTTGACCTTGGCAAGTGATCTCCTGTGAAGTATGCAGAGCAACACCAGCAAATCACA
3020 3030 3040 3050 3060 3070 3080
Myf5 5'UTR and ex1
Myf5 ex3 and 3'UTR
Myf5 RNASEQT00000060326
Myf5 RNASEQ orf
Myf5 RNASEQ Kozak + orf
Myf5 F1
Myf5 F2
Myf5 Cla-Kozak-F2
Myf5 R1 rev compl
Myf5 R2 rev compl
Myf5 R2-EcoRI rev compl
Myf5 pCab seq F
TGTTGGTAATGTACACCCCTCTTTGGGTGGCAGACATTTTGAGCATTGCAAAAAGGTCAATACTTCTGAG
3090 3100 3110 3120 3130 3140 3150
Myf5 5'UTR and ex1
Myf5 ex3 and 3'UTR
Myf5 RNASEQT00000060326
Myf5 RNASEQ orf
Myf5 RNASEQ Kozak + orf
Myf5 F1
Myf5 F2
Myf5 Cla-Kozak-F2
Myf5 R1 rev compl
Myf5 R2 rev compl
Myf5 R2-EcoRI rev compl
Myf5 pCab seq F
ACTGGCTTTTCAGGGAGCTAGCAGAAGTACCAGCCTGTGGGATGTTTGTCCATAGCCTCCTCAGCACTAC
3160 3170 3180 3190 3200 3210 3220
Myf5 5'UTR and ex1
Myf5 ex3 and 3'UTR
Myf5 RNASEQT00000060326
Myf5 RNASEQ orf
Myf5 RNASEQ Kozak + orf
Myf5 F1
Myf5 F2
Myf5 Cla-Kozak-F2
Myf5 R1 rev compl
Myf5 R2 rev compl
Myf5 R2-EcoRI rev compl
Myf5 pCab seq F
CAAGCTAAATTACAATTCTCAGGCTTTTGTTACATACATGGAGAAAACCAGCCCTTCATCATAGCACATC
3230 3240 3250 3260 3270 3280 3290
Myf5 5'UTR and ex1
Myf5 ex3 and 3'UTR
Myf5 RNASEQT00000060326
Myf5 RNASEQ orf
Myf5 RNASEQ Kozak + orf
Myf5 F1
Myf5 F2
Myf5 Cla-Kozak-F2
Myf5 R1 rev compl
Myf5 R2 rev compl
Myf5 R2-EcoRI rev compl
Myf5 pCab seq F
TATAAACAAAGCTCCTGTGAACCTGTGAACCAGCTCCTGTGCTGTAACCCTCAGGAGGAGTGAAAGTTAG
3300 3310 3320 3330 3340 3350 3360
Myf5 5'UTR and ex1
Myf5 ex3 and 3'UTR
Myf5 RNASEQT00000060326
Myf5 RNASEQ orf
Myf5 RNASEQ Kozak + orf
Myf5 F1
Myf5 F2
Myf5 Cla-Kozak-F2
Myf5 R1 rev compl
Myf5 R2 rev compl
Myf5 R2-EcoRI rev compl
Myf5 pCab seq F
TGCTGTGAAACCACCTTTAGCCTGTGGATTGGGAAGAACAAGGTGTAAAACCCTGCTGTCTTGGGATATA
3370 3380 3390 3400 3410 3420 3430
Myf5 5'UTR and ex1
Myf5 ex3 and 3'UTR
Myf5 RNASEQT00000060326
Myf5 RNASEQ orf
Myf5 RNASEQ Kozak + orf
Myf5 F1
Myf5 F2
Myf5 Cla-Kozak-F2
Myf5 R1 rev compl
Myf5 R2 rev compl
Myf5 R2-EcoRI rev compl
Myf5 pCab seq F
GCTGTTGTGGCCACATTTTGTGTGGTCAATAATGATAAGGAATCTCACCTACTGACAAGCAGATGGAACA

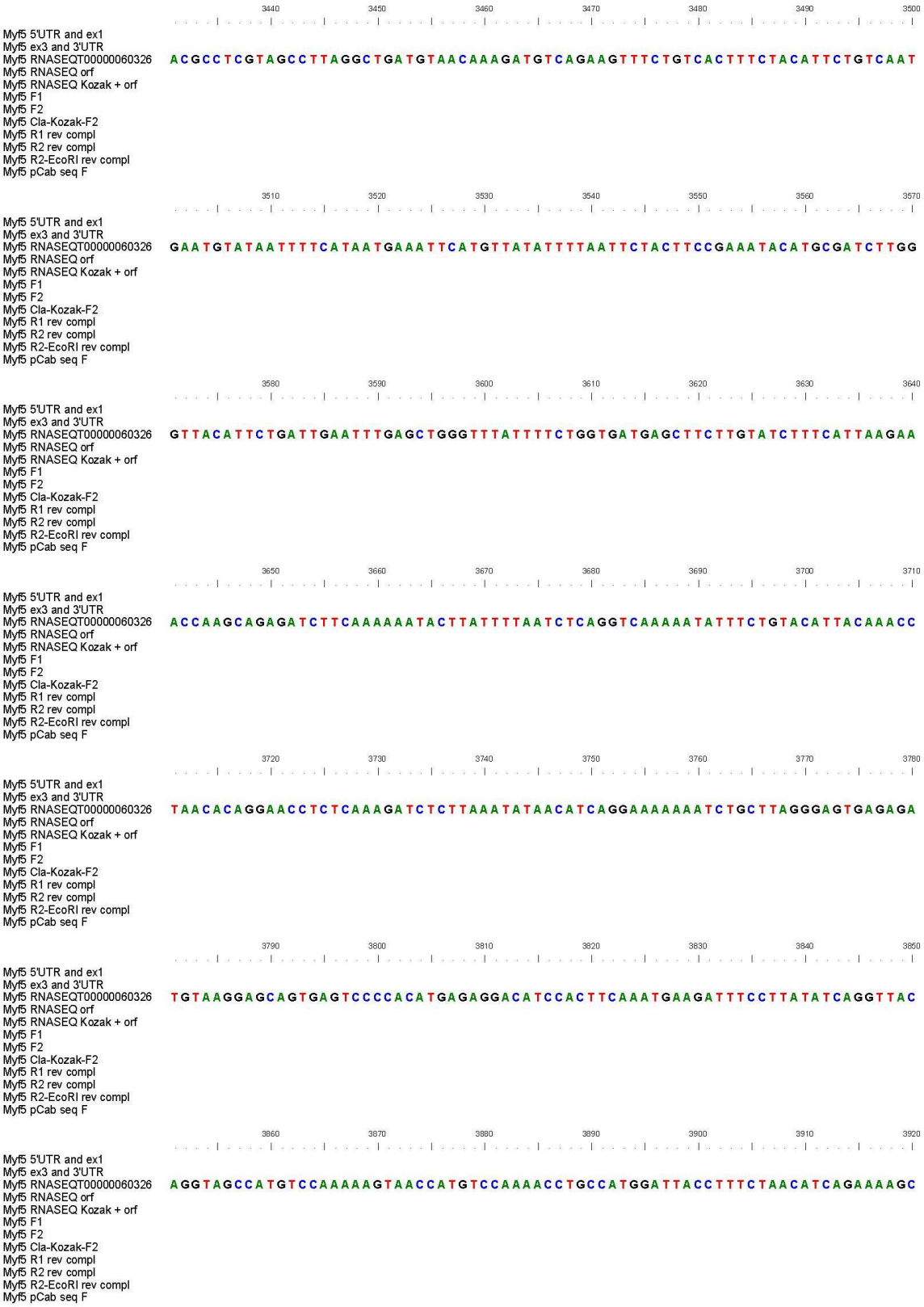
3440 3450 3460 3470 3480 3490 3500
Myf5 5'UTR and ex1
Myf5 ex3 and 3'UTR
Myf5 RNASEQT00000060326
Myf5 RNASEQ orf
Myf5 RNASEQ Kozak + orf
Myf5 F1
Myf5 F2
Myf5 Cla-Kozak-F2
Myf5 R1 rev compl
Myf5 R2 rev compl
Myf5 R2-EcoRI rev compl
Myf5 pCab seq F
ACGCCTCGTAGCCTTAGGCTGATGTAACAAAGATGTCAGAAGTTTCTGTCACTTTCTACATTCTGTCAAT
3510 3520 3530 3540 3550 3560 3570
GAATGTATAATTTTCATAATGAAATTCATGTTATATTTTAATTCTACTTCCGAAATACATGCGATCTTGG
3580 3590 3600 3610 3620 3630 3640
GTTACATTCTGATTGAATTTGAGCTGGGTTTATTTTCTGGTGATGAGCTTCTTGTATCTTTCATTAAGAA
3650 3660 3670 3680 3690 3700 3710
ACCAAGCAGAGATCTTCAAAAAATACTTATTTTAATCTCAGGTCAAAAATATTTCTGTACATTACAAACC
3720 3730 3740 3750 3760 3770 3780
TAACACAGGAACCTCTCAAAGATCTCTTAAATATAACATCAGGAAAAAAATCTGCTTAGGGAGTGAGAGA
3790 3800 3810 3820 3830 3840 3850
TGTAAGGAGCAGTGAGTCCCCACATGAGAGGACATCCACTTCAAATGAAGATTTCCTTATATCAGGTTAC
3860 3870 3880 3890 3900 3910 3920
AGGTAGCCATGTCCAAAAAGTAACCATGTCCAAAACCTGCCATGGATTACCTTTCTAACATCAGAAAAGC

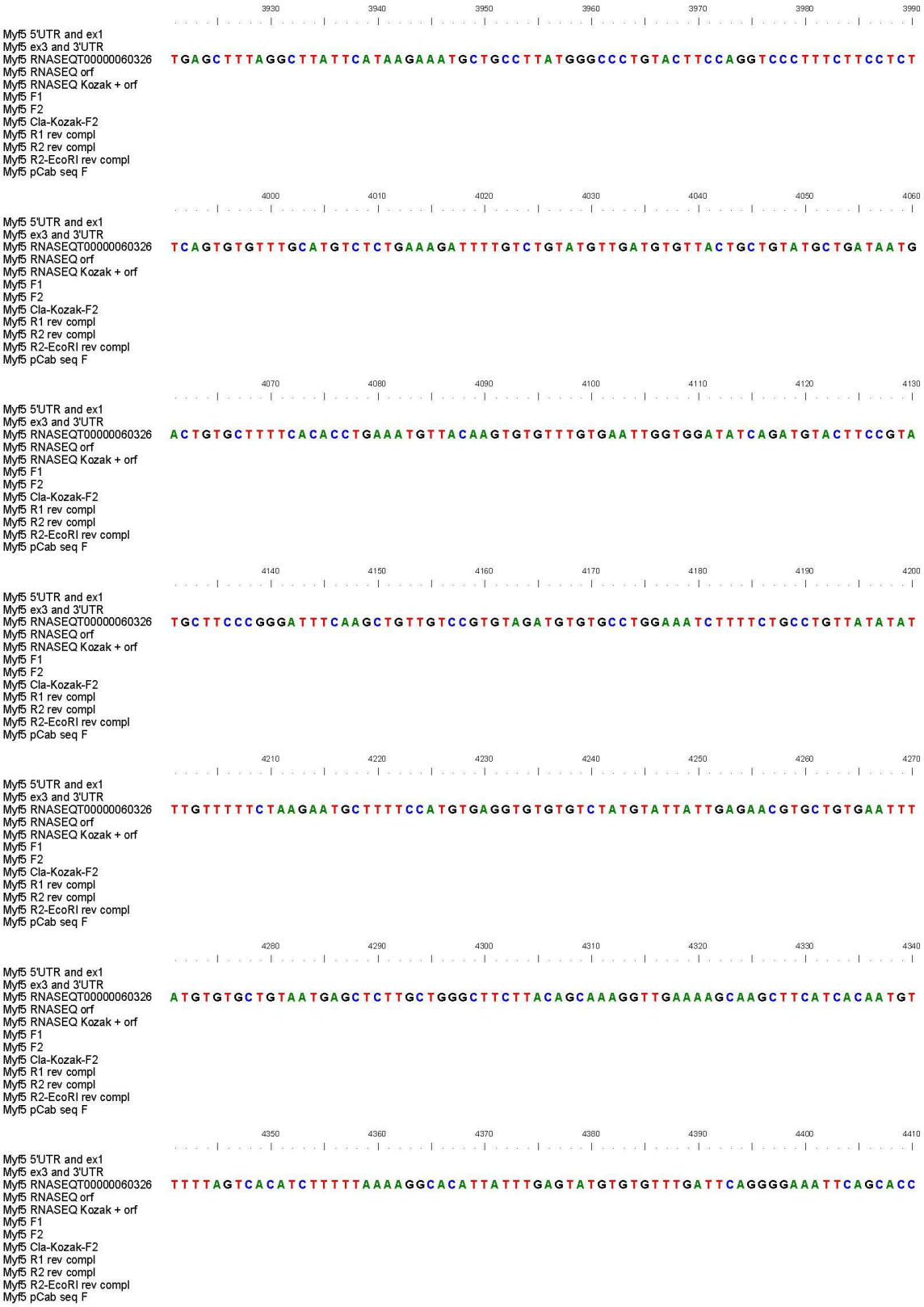
3930 3940 3950 3960 3970 3980 3990
Myf5 5'UTR and ex1
Myf5 ex3 and 3'UTR
Myf5 RNASEQT00000060326
Myf5 RNASEQ orf
Myf5 RNASEQ Kozak + orf
Myf5 F1
Myf5 F2
Myf5 Cla-Kozak-F2
Myf5 R1 rev compl
Myf5 R2 rev compl
Myf5 R2-EcoRI rev compl
Myf5 pCab seq F
TGAGCTTTAGGCTTATTCATAAGAAATGCTGCCTTATGGGCCCTGTACTTCCAGGTCCCTTTCTTCCTCT
4000 4010 4020 4030 4040 4050 4060
Myf5 5'UTR and ex1
Myf5 ex3 and 3'UTR
Myf5 RNASEQT00000060326
Myf5 RNASEQ orf
Myf5 RNASEQ Kozak + orf
Myf5 F1
Myf5 F2
Myf5 Cla-Kozak-F2
Myf5 R1 rev compl
Myf5 R2 rev compl
Myf5 R2-EcoRI rev compl
Myf5 pCab seq F
TCAGTGTGTTTGCATGTCTCTGAAAGATTTTGTCTGTATGTTGATGTGTTACTGCTGTATGCTGATAATG
4070 4080 4090 4100 4110 4120 4130
Myf5 5'UTR and ex1
Myf5 ex3 and 3'UTR
Myf5 RNASEQT00000060326
Myf5 RNASEQ orf
Myf5 RNASEQ Kozak + orf
Myf5 F1
Myf5 F2
Myf5 Cla-Kozak-F2
Myf5 R1 rev compl
Myf5 R2 rev compl
Myf5 R2-EcoRI rev compl
Myf5 pCab seq F
ACTGTGCTTTTCACACCTGAAAATGTTACAAGTGTGTTTGTGAATTGGTGGATATCAGATGTACTTCCGTA
4140 4150 4160 4170 4180 4190 4200
Myf5 5'UTR and ex1
Myf5 ex3 and 3'UTR
Myf5 RNASEQT00000060326
Myf5 RNASEQ orf
Myf5 RNASEQ Kozak + orf
Myf5 F1
Myf5 F2
Myf5 Cla-Kozak-F2
Myf5 R1 rev compl
Myf5 R2 rev compl
Myf5 R2-EcoRI rev compl
Myf5 pCab seq F
TGCTTCCCGGGATTTCAAGCTGTTGTCCGTGTAGATGTGTGCCTGGAAATCTTTTCTGCCTGTTATATAT
4210 4220 4230 4240 4250 4260 4270
Myf5 5'UTR and ex1
Myf5 ex3 and 3'UTR
Myf5 RNASEQT00000060326
Myf5 RNASEQ orf
Myf5 RNASEQ Kozak + orf
Myf5 F1
Myf5 F2
Myf5 Cla-Kozak-F2
Myf5 R1 rev compl
Myf5 R2 rev compl
Myf5 R2-EcoRI rev compl
Myf5 pCab seq F
TTGTTTTTCTAAGAATGCTTTTCCATGTGAGGTGTGTGTCTATGTATTATTGAGAACGTGCTGTGAATTT
4280 4290 4300 4310 4320 4330 4340
Myf5 5'UTR and ex1
Myf5 ex3 and 3'UTR
Myf5 RNASEQT00000060326
Myf5 RNASEQ orf
Myf5 RNASEQ Kozak + orf
Myf5 F1
Myf5 F2
Myf5 Cla-Kozak-F2
Myf5 R1 rev compl
Myf5 R2 rev compl
Myf5 R2-EcoRI rev compl
Myf5 pCab seq F
ATGTGTGCTGTAATGAGCTCTTGCTGGGCTTCTTACAGCAAAGGTTGAAAAGCAAGCTTCATCACAATGT
4350 4360 4370 4380 4390 4400 4410
Myf5 5'UTR and ex1
Myf5 ex3 and 3'UTR
Myf5 RNASEQT00000060326
Myf5 RNASEQ orf
Myf5 RNASEQ Kozak + orf
Myf5 F1
Myf5 F2
Myf5 Cla-Kozak-F2
Myf5 R1 rev compl
Myf5 R2 rev compl
Myf5 R2-EcoRI rev compl
Myf5 pCab seq F
TTTTAGTCACATCTTTTTTAAAAGGCACATTATTTGAGTATGTGTGTTTGATTCAGGGGAAATTCAGCACC

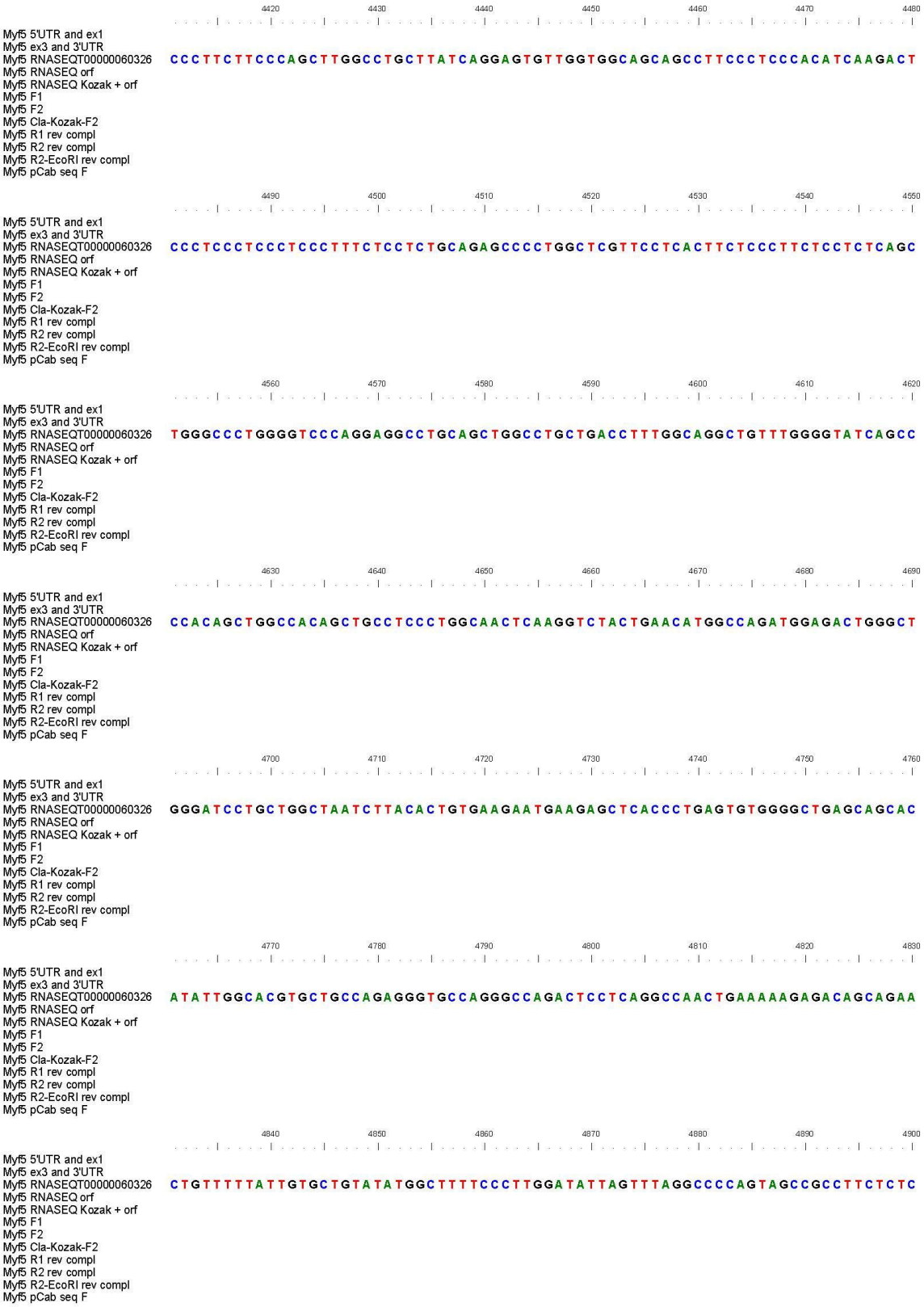
4420 4430 4440 4450 4460 4470 4480
Myf5 5'UTR and ex1
Myf5 ex3 and 3'UTR
Myf5 RNASEQT00000060326 CCCTTCTTCCCAGCTTGGCCTGCTTATCAGGAGTGTTGGTGGCAGCAGCCTTCCCTCCCACATCAAGACT
Myf5 RNASEQ orf
Myf5 RNASEQ Kozak + orf
Myf5 F1
Myf5 F2
Myf5 Cla-Kozak-F2
Myf5 R1 rev compl
Myf5 R2 rev compl
Myf5 R2-EcoRI rev compl
Myf5 pCab seq F
4490 4500 4510 4520 4530 4540 4550
Myf5 5'UTR and ex1
Myf5 ex3 and 3'UTR
Myf5 RNASEQT00000060326 CCCTCCCTCCCTCCCTTTCTCCTCTGCAGAGCCCCTGGCTCGTTCCTCACTTCTCCCTTCTCCTCTCAGC
Myf5 RNASEQ orf
Myf5 RNASEQ Kozak + orf
Myf5 F1
Myf5 F2
Myf5 Cla-Kozak-F2
Myf5 R1 rev compl
Myf5 R2 rev compl
Myf5 R2-EcoRI rev compl
Myf5 pCab seq F
4560 4570 4580 4590 4600 4610 4620
Myf5 5'UTR and ex1
Myf5 ex3 and 3'UTR
Myf5 RNASEQT00000060326 TGGGCCCTGGGGTCCCAGGAGGCCTGCAGCTGGCCTGCTGACCTTTGGCAGGCTGTTTGGGGTATCAGCC
Myf5 RNASEQ orf
Myf5 RNASEQ Kozak + orf
Myf5 F1
Myf5 F2
Myf5 Cla-Kozak-F2
Myf5 R1 rev compl
Myf5 R2 rev compl
Myf5 R2-EcoRI rev compl
Myf5 pCab seq F
4630 4640 4650 4660 4670 4680 4690
Myf5 5'UTR and ex1
Myf5 ex3 and 3'UTR
Myf5 RNASEQT00000060326 CCACAGCTGGCCACAGCTGCCTCCCTGGCAACTCAAGGTCTACTGAACATGGCCAGATGGAGACTGGGCT
Myf5 RNASEQ orf
Myf5 RNASEQ Kozak + orf
Myf5 F1
Myf5 F2
Myf5 Cla-Kozak-F2
Myf5 R1 rev compl
Myf5 R2 rev compl
Myf5 R2-EcoRI rev compl
Myf5 pCab seq F
4700 4710 4720 4730 4740 4750 4760
Myf5 5'UTR and ex1
Myf5 ex3 and 3'UTR
Myf5 RNASEQT00000060326 GGGATCCTGCTGGCTAATCTTACACTGTGAAGAATGAAGAGCTCACCCTGAGTGTGGGGCTGAGCAGCAC
Myf5 RNASEQ orf
Myf5 RNASEQ Kozak + orf
Myf5 F1
Myf5 F2
Myf5 Cla-Kozak-F2
Myf5 R1 rev compl
Myf5 R2 rev compl
Myf5 R2-EcoRI rev compl
Myf5 pCab seq F
4770 4780 4790 4800 4810 4820 4830
Myf5 5'UTR and ex1
Myf5 ex3 and 3'UTR
Myf5 RNASEQT00000060326 ATATTGGCACGTGCTGCCAGAGGGTGCCAGGGCCAGACTCCTCAGGCCAACTGAAAAAGAGACAGCAGAA
Myf5 RNASEQ orf
Myf5 RNASEQ Kozak + orf
Myf5 F1
Myf5 F2
Myf5 Cla-Kozak-F2
Myf5 R1 rev compl
Myf5 R2 rev compl
Myf5 R2-EcoRI rev compl
Myf5 pCab seq F
4840 4850 4860 4870 4880 4890 4900
Myf5 5'UTR and ex1
Myf5 ex3 and 3'UTR
Myf5 RNASEQT00000060326 CTGTTTTTATTGTGCTGTATATGGCTTTTCCCTTGGATATTAGTTTAGGCCCCAGTAGCCGCCTTCTCTC
Myf5 RNASEQ orf
Myf5 RNASEQ Kozak + orf
Myf5 F1
Myf5 F2
Myf5 Cla-Kozak-F2
Myf5 R1 rev compl
Myf5 R2 rev compl
Myf5 R2-EcoRI rev compl
Myf5 pCab seq F

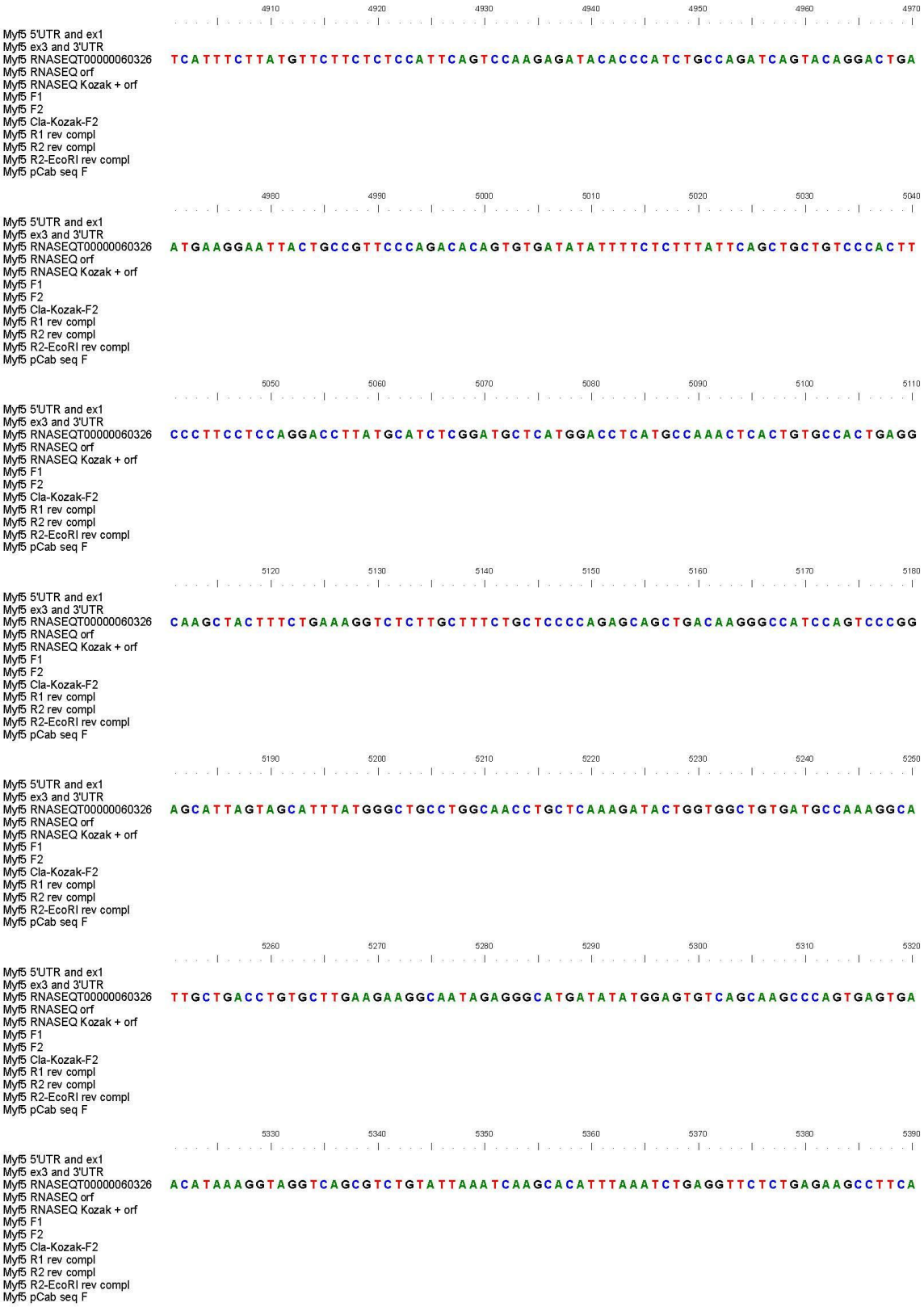
4910 4920 4930 4940 4950 4960 4970
Myf5 5'UTR and ex1
Myf5 ex3 and 3'UTR
Myf5 RNASEQT00000060326
Myf5 RNASEQ orf
Myf5 RNASEQ Kozak + orf
Myf5 F1
Myf5 F2
Myf5 Cla-Kozak-F2
Myf5 R1 rev compl
Myf5 R2 rev compl
Myf5 R2-EcoRI rev compl
Myf5 pCab seq F
TCATTTCTTATGTTCTTCTCTCCATTCAGTCCAAGAGATACACCCATCTGCCAGATCAGTACAGGACTGA
4980 4990 5000 5010 5020 5030 5040
ATGAAGGAATTACTGCCGTTCCCAGACACAGTGTGATATATTTTCTCTTTATTCAGCTGCTGTCCCACTT
5050 5060 5070 5080 5090 5100 5110
CCCTTCCTCCAGGACCTTATGCATCTCGGATGCTCATGGACCTCATGCCAAACTCACTGTGCCACTGAGG
5120 5130 5140 5150 5160 5170 5180
CAAGCTACTTTCTGAAAGGTCTCTTGCTTTCTGCTCCCCAGAGCAGCTGACAAGGGCCATCCAGTCCCGG
5190 5200 5210 5220 5230 5240 5250
AGCATTAGTAGCATTTATGGGCTGCCTGGCAACCTGCTCAAAGATACTGGTGGCTGTGATGCCAAAGGCA
5260 5270 5280 5290 5300 5310 5320
TTGCTGACCTGTGCTTGAAGAAGGCAATAGAGGGCATGATATATGGAGTGTCAGCAAGCCCAGTGAGTGA
5330 5340 5350 5360 5370 5380 5390
ACATAAAGGTAGGTCAGCGTCTGTATTAAATCAAGCACATTTAAATCTGAGGTTCTCTGAGAAGCCTTCA

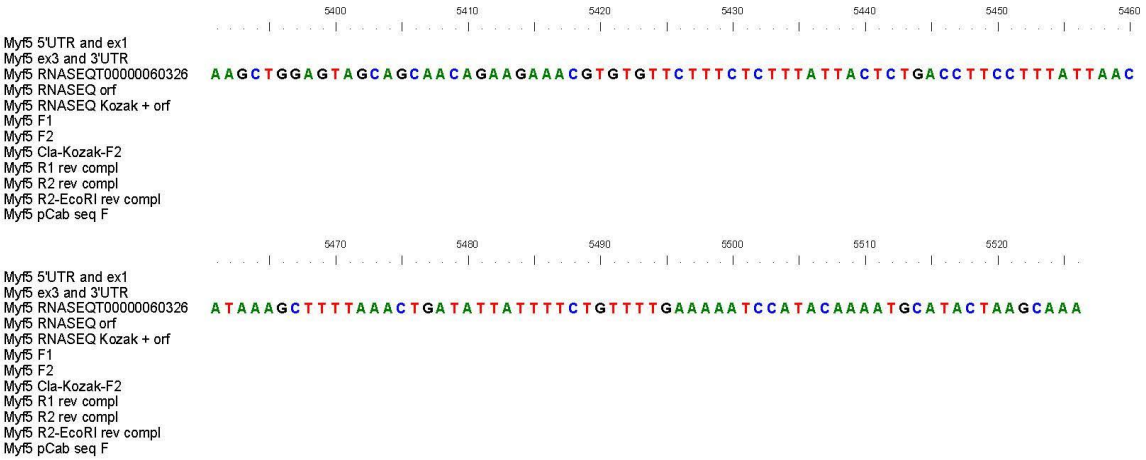

Appendix 2. A Myf5 cDNA, primers and synthesis products.

Alignment of the chicken Myf5 UTR sequences extracted from Ensembl, the RNAseq sequence on which the construct is based, the open reading frame (orf), the orf equipped with the Kozak sequence, the cloning primers and the re-sequenced Life Technology product cloned into pCab, indicating that the desired construct was obtained.

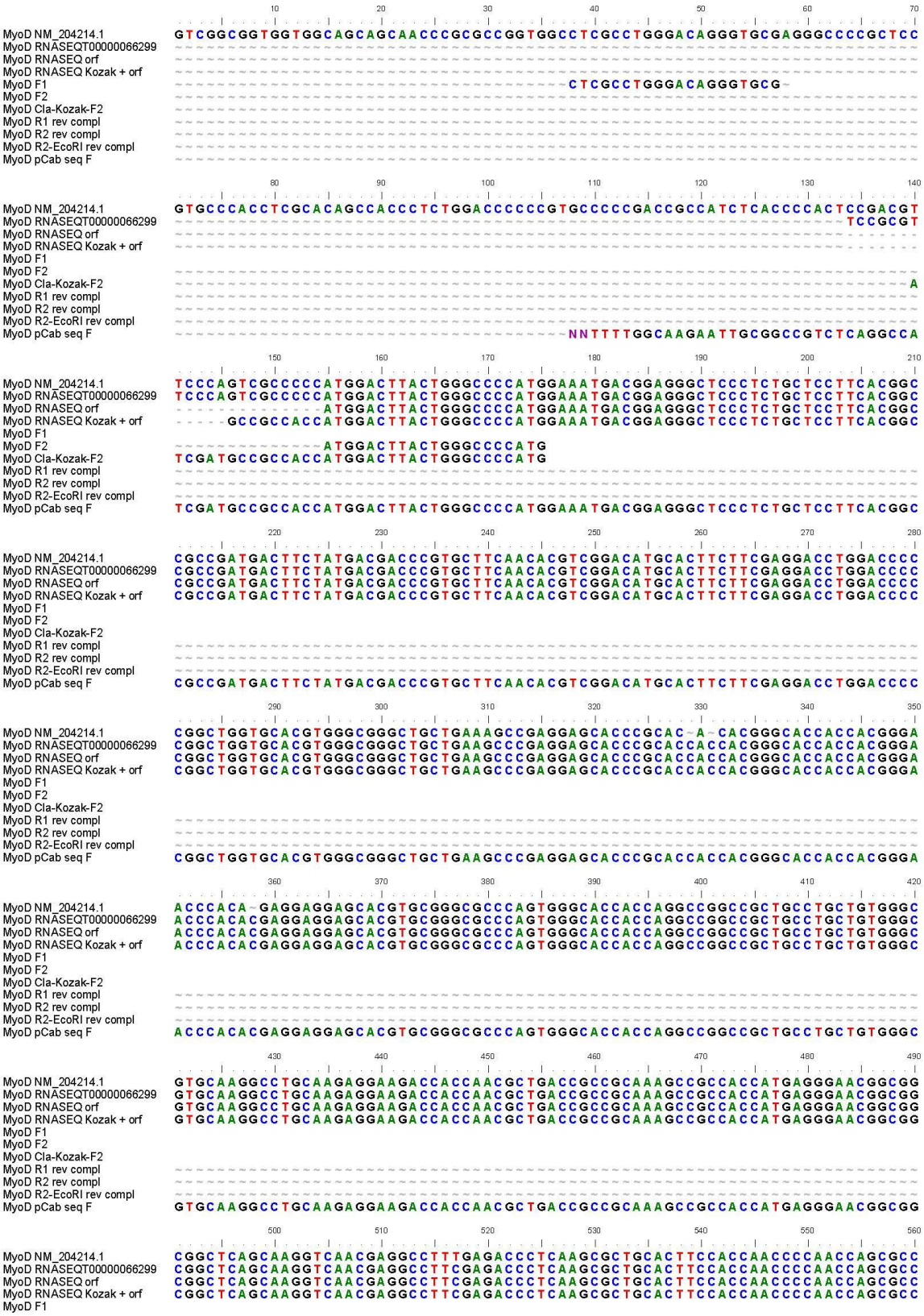
MyoD NM_204214.1
MyoD RNASEQT00000066299
MyoD RNASEQ orf
MyoD RNASEQ Kozak + orf
MyoD F1
MyoD F2
MyoD Cla-Kozak-F2
MyoD R1 rev compl
MyoD R2 rev compl
MyoD R2-EcoRI rev compl
MyoD pCab seq F

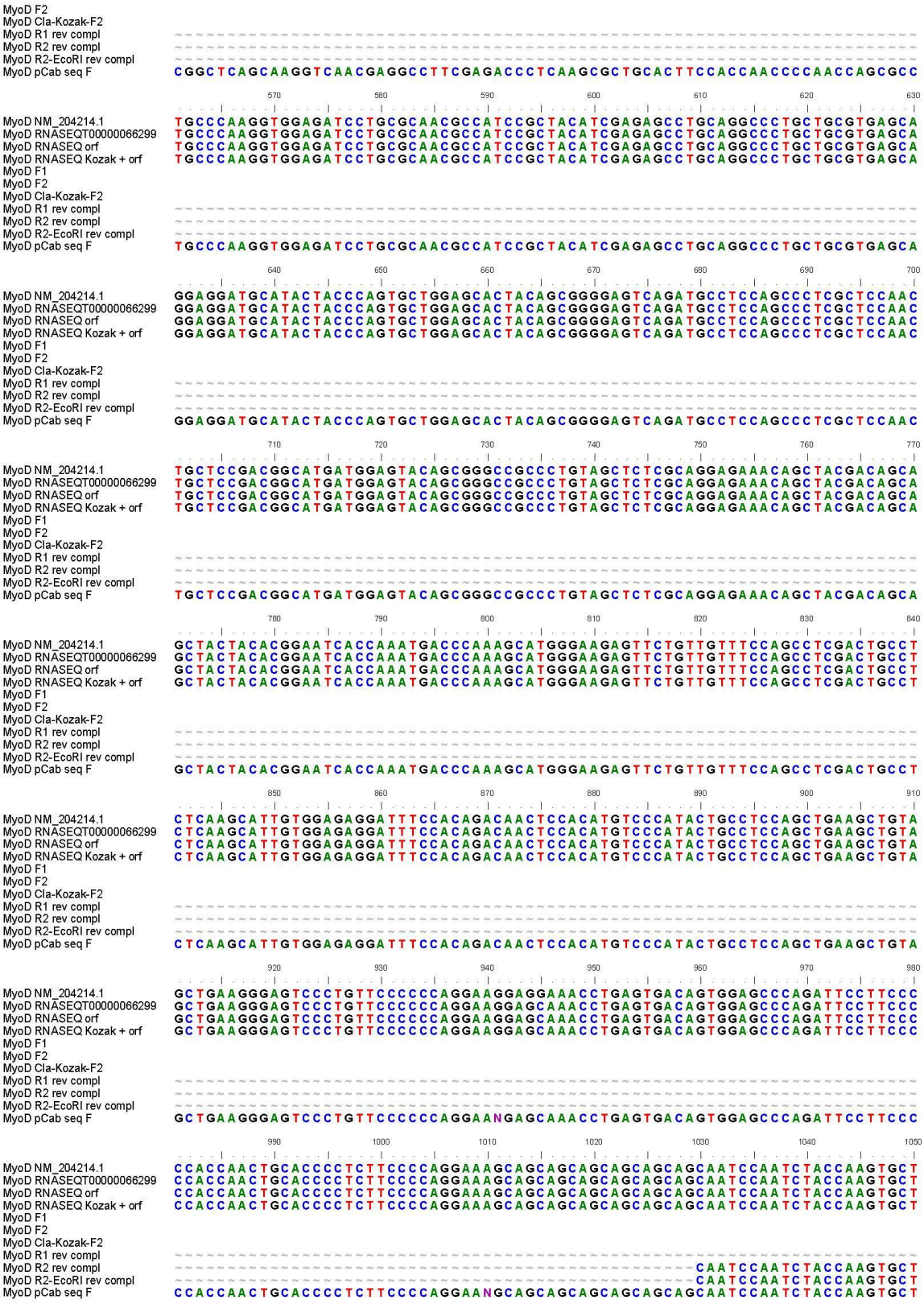
MyoD F2
MyoD Cla-Kozak-F2
MyoD R1 rev compl
MyoD R2 rev compl
MyoD R2-EcoRI rev compl
MyoD pCab seq F
CGGCTCAGCAAGGTCAACGAGGCCTTCGAGACCCTCAAGCGCTGCACTTCCACCAACCCCAACCAGCGCC
570 580 590 600 610 620 630
MyoD NM_204214.1
MyoD RNASEQT00000066299
MyoD RNASEQ orf
MyoD RNASEQ Kozak + orf
TGCCCAAGGTGGAGATCCTGCGCAACGCCATCCGCTACATCGAGAGCCTGCAGGCCCTGCTGCGTGAGCA
MyoD F1
MyoD F2
MyoD Cla-Kozak-F2
MyoD R1 rev compl
MyoD R2 rev compl
MyoD R2-EcoRI rev compl
MyoD pCab seq F
TGCCCAAGGTGGAGATCCTGCGCAACGCCATCCGCTACATCGAGAGCCTGCAGGCCCTGCTGCGTGAGCA
640 650 660 670 680 690 700
MyoD NM_204214.1
MyoD RNASEQT00000066299
MyoD RNASEQ orf
MyoD RNASEQ Kozak + orf
GGAGGATGCATACTACCCAGTGCTGGAGCACTACAGCGGGGAGTCAGATGCCTCCAGCCCTCGCTCCAAC
MyoD F1
MyoD F2
MyoD Cla-Kozak-F2
MyoD R1 rev compl
MyoD R2 rev compl
MyoD R2-EcoRI rev compl
MyoD pCab seq F
GGAGGATGCATACTACCCAGTGCTGGAGCACTACAGCGGGGAGTCAGATGCCTCCAGCCCTCGCTCCAAC
710 720 730 740 750 760 770
MyoD NM_204214.1
MyoD RNASEQT00000066299
MyoD RNASEQ orf
MyoD RNASEQ Kozak + orf
TGCTCCGACGGCATGATGGAGTACAGCGGGCCGCCCTGTAGCTCTCGCAGGAGAAACAGCTACGACAGCA
MyoD F1
MyoD F2
MyoD Cla-Kozak-F2
MyoD R1 rev compl
MyoD R2 rev compl
MyoD R2-EcoRI rev compl
MyoD pCab seq F
TGCTCCGACGGCATGATGGAGTACAGCGGGCCGCCCTGTAGCTCTCGCAGGAGAAACAGCTACGACAGCA
780 790 800 810 820 830 840
MyoD NM_204214.1
MyoD RNASEQT00000066299
MyoD RNASEQ orf
MyoD RNASEQ Kozak + orf
GCTACTACACGGAATCACCAAATGACCCAAAGCATGGGAAGAGTTCTGTTGTTTCCAGCCTCGACTGCCT
MyoD F1
MyoD F2
MyoD Cla-Kozak-F2
MyoD R1 rev compl
MyoD R2 rev compl
MyoD R2-EcoRI rev compl
MyoD pCab seq F
GCTACTACACGGAATCACCAAATGACCCAAAGCATGGGAAGAGTTCTGTTGTTTCCAGCCTCGACTGCCT
850 860 870 880 890 900 910
MyoD NM_204214.1
MyoD RNASEQT00000066299
MyoD RNASEQ orf
MyoD RNASEQ Kozak + orf
CTCAAGCATTGTGGAGAGGATTTCCACAGACAACTCCACATGTCCCATACTGCCTCCAGCTGAAGCTGTA
MyoD F1
MyoD F2
MyoD Cla-Kozak-F2
MyoD R1 rev compl
MyoD R2 rev compl
MyoD R2-EcoRI rev compl
MyoD pCab seq F
CTCAAGCATTGTGGAGAGGATTTCCACAGACAACTCCACATGTCCCATACTGCCTCCAGCTGAAGCTGTA
920 930 940 950 960 970 980
MyoD NM_204214.1
MyoD RNASEQT00000066299
MyoD RNASEQ orf
MyoD RNASEQ Kozak + orf
GCTGAAGGGAGTCCCTGTTCCCCCCAGGAAGGAGCAAACCTGAGTGACAGTGGAGCCCAGATTCCTTCCC
MyoD F1
MyoD F2
MyoD Cla-Kozak-F2
MyoD R1 rev compl
MyoD R2 rev compl
MyoD R2-EcoRI rev compl
MyoD pCab seq F
GCTGAAGGGAGTCCCTGTTCCCCCCAGGAANGAGCAAACCTGAGTGACAGTGGAGCCCAGATTCCTTCCC
990 1000 1010 1020 1030 1040 1050
MyoD NM_204214.1
MyoD RNASEQT00000066299
MyoD RNASEQ orf
MyoD RNASEQ Kozak + orf
CCACCAACTGCACCCCTCTTCCCCAGGAAAGCAGCAGCAGCAGCAGCAGCAATCCAATCTACCAAGTGCT
MyoD F1
MyoD F2
MyoD Cla-Kozak-F2
MyoD R1 rev compl
MyoD R2 rev compl
MyoD R2-EcoRI rev compl
MyoD pCab seq F
CCACCAACTGCACCCCTCTTCCCCAGGAANGCAGCAGCAGCAGCAGCAATCCAATCTACCAAGTGCT

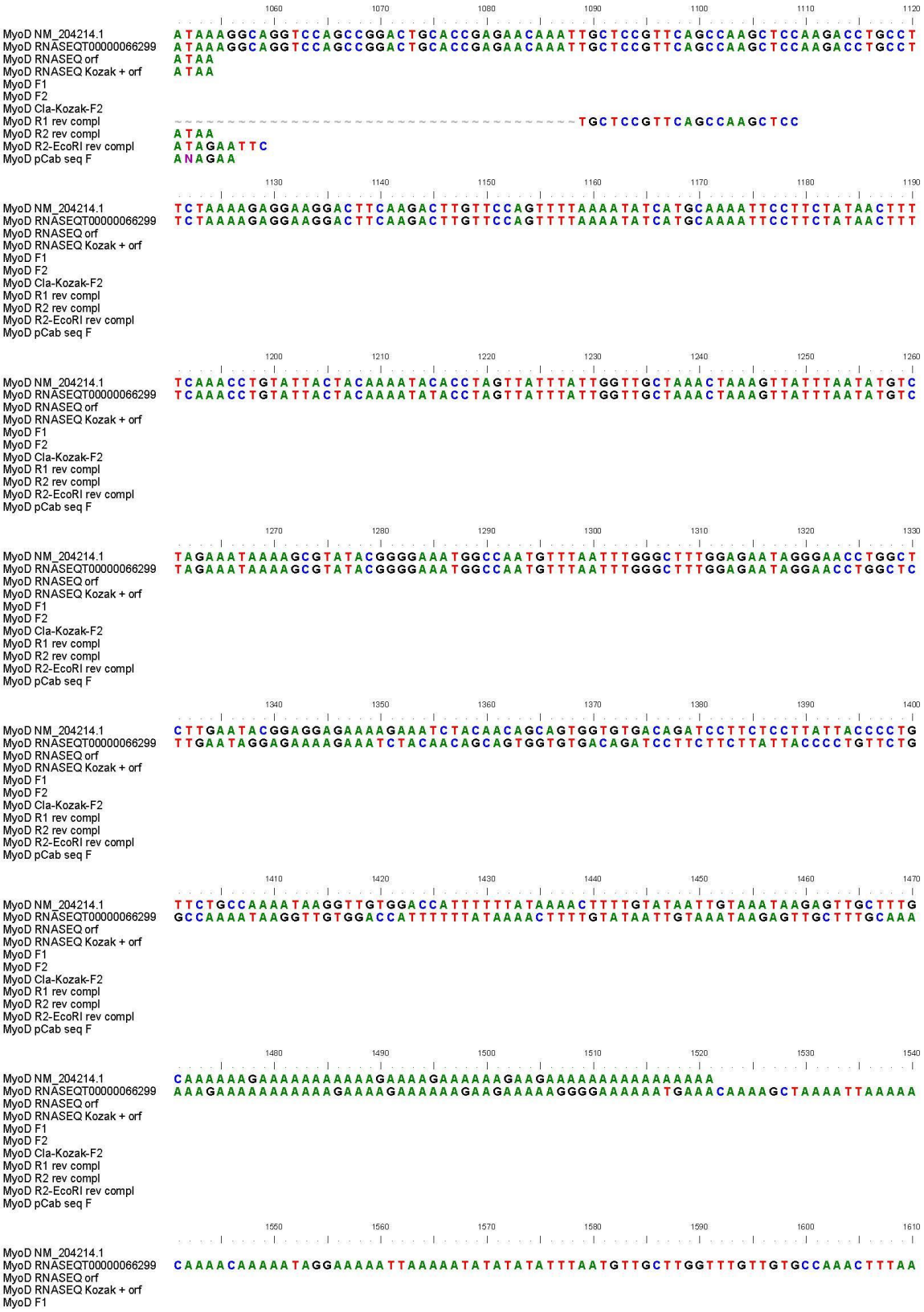
1060 1070 1080 1090 1100 1110 1120
MyoD NM_204214.1 ATAAAGGCAGGTCCAGCCGGACTGCACCGAGAACAAATTGCTCCGTTCAGCCAAGCTCCAAGACCTGCCT
MyoD RNASEQT00000066299 ATAAAGGCAGGTCCAGCCGGACTGCACCGAGAACAAATTGCTCCGTTCAGCCAAGCTCCAAGACCTGCCT
MyoD RNASEQ orf ATAA
MyoD RNASEQ Kozak + orf ATAA
MyoD F1
MyoD F2
MyoD Cla-Kozak-F2
MyoD R1 rev compl TGCTCCGTTCAGCCAAGCTCC
MyoD R2 rev compl ATAA
MyoD R2-EcoRI rev compl ATAGAATTC
MyoD pCab seq F ANAGAA
1130 1140 1150 1160 1170 1180 1190
MyoD NM_204214.1 TCTAAAAGAGGAAGGACTTCAAGACTTGTTCCAGTTTTAAAATATCATGCAAAATTCCTTCTATAACTTT
MyoD RNASEQT00000066299 TCTAAAAGAGGAAGGACTTCAAGACTTGTTCCAGTTTTAAAATATCATGCAAAATTCCTTCTATAACTTT
MyoD RNASEQ orf
MyoD RNASEQ Kozak + orf
MyoD F1
MyoD F2
MyoD Cla-Kozak-F2
MyoD R1 rev compl
MyoD R2 rev compl
MyoD R2-EcoRI rev compl
MyoD pCab seq F
1200 1210 1220 1230 1240 1250 1260
MyoD NM_204214.1 TCAAACCTGTATTACTACAAAATACACCTAGTTATTTATTGGTTGCTAAACTAAAGTTATTTAATATGTC
MyoD RNASEQT00000066299 TCAAACCTGTATTACTACAAAATATACCTAGTTATTTATTGGTTGCTAAACTAAAGTTATTTAATATGTC
MyoD RNASEQ orf
MyoD RNASEQ Kozak + orf
MyoD F1
MyoD F2
MyoD Cla-Kozak-F2
MyoD R1 rev compl
MyoD R2 rev compl
MyoD R2-EcoRI rev compl
MyoD pCab seq F
1270 1280 1290 1300 1310 1320 1330
MyoD NM_204214.1 TAGAAATAAAAGCGTATACGGGGAAATGGCCAATGTTTAATTTGGGCTTTGGAGAATAGGAACCTGGCT
MyoD RNASEQT00000066299 TAGAAATAAAAGCGTATACGGGGAAATGGCCAATGTTTAATTTGGGCTTTGGAGAATAGGAACCTGGCTC
MyoD RNASEQ orf
MyoD RNASEQ Kozak + orf
MyoD F1
MyoD F2
MyoD Cla-Kozak-F2
MyoD R1 rev compl
MyoD R2 rev compl
MyoD R2-EcoRI rev compl
MyoD pCab seq F
1340 1350 1360 1370 1380 1390 1400
MyoD NM_204214.1 CTTGAATACGGAGGAGAAAAGAAATCTACAACAGCAGTGGTGTGACAGATCCTTCTCCTTATTACCCCTG
MyoD RNASEQT00000066299 TTGAATAGGAGAAAAGAAATCTACAACAGCAGTGGTGTGACAGATCCTTCTTCTTATTACCCCTGTTCTG
MyoD RNASEQ orf
MyoD RNASEQ Kozak + orf
MyoD F1
MyoD F2
MyoD Cla-Kozak-F2
MyoD R1 rev compl
MyoD R2 rev compl
MyoD R2-EcoRI rev compl
MyoD pCab seq F
1410 1420 1430 1440 1450 1460 1470
MyoD NM_204214.1 TTCTGCCAAAATAAGGTTGTGGACCATTTTTTATAAAACTTTTGTATAATTGTAAATAAGAGTTGCTTTG
MyoD RNASEQT00000066299 GCCAAAATAAGGTTGTGGACCATTTTTTATAAAACTTTTGTATAATTGTAAATAAGAGTTGCTTTGCAAA
MyoD RNASEQ orf
MyoD RNASEQ Kozak + orf
MyoD F1
MyoD F2
MyoD Cla-Kozak-F2
MyoD R1 rev compl
MyoD R2 rev compl
MyoD R2-EcoRI rev compl
MyoD pCab seq F
1480 1490 1500 1510 1520 1530 1540
MyoD NM_204214.1 CAAAAAAGAAAAAAAAAAAGAAAAGAAAAAAGAAGAAAAAAAAAAAAAAAA
MyoD RNASEQT00000066299 AAAGAAAAAAAAAAAGAAAAGAAAAAAGAAGAAAAAGGGGAAAAAATGAAACAAAAGCTAAAATTAAAAA
MyoD RNASEQ orf
MyoD RNASEQ Kozak + orf
MyoD F1
MyoD F2
MyoD Cla-Kozak-F2
MyoD R1 rev compl
MyoD R2 rev compl
MyoD R2-EcoRI rev compl
MyoD pCab seq F
1550 1560 1570 1580 1590 1600 1610
MyoD NM_204214.1
MyoD RNASEQT00000066299 CAAAACAAAAATAGGAAAAATTAAAAATATATATATTTAATGTTGCTTGGTTTGTTGTGCCAAACTTTAA
MyoD RNASEQ orf
MyoD RNASEQ Kozak + orf
MyoD F1

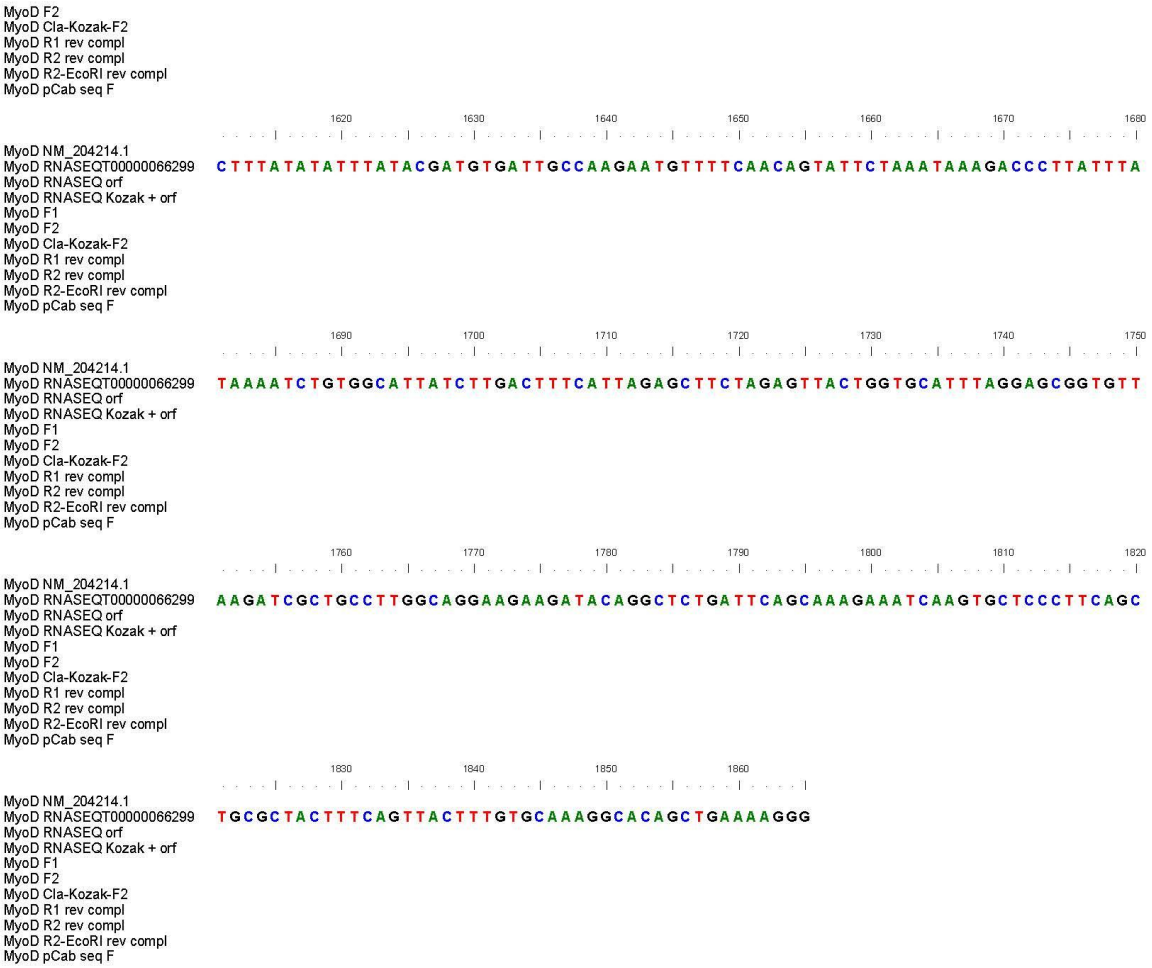

Appendix 2. B *MyoD* cDNA, primers and synthesis products.

Alignment of the curated chicken MyoD cDNA, the RNAseq sequence on which the construct is based, the open reading frame (orf), the orf equipped with the Kozak sequence, the cloning primers and the re-sequenced Life Technology product cloned into pCab. The desired construct was obtained.

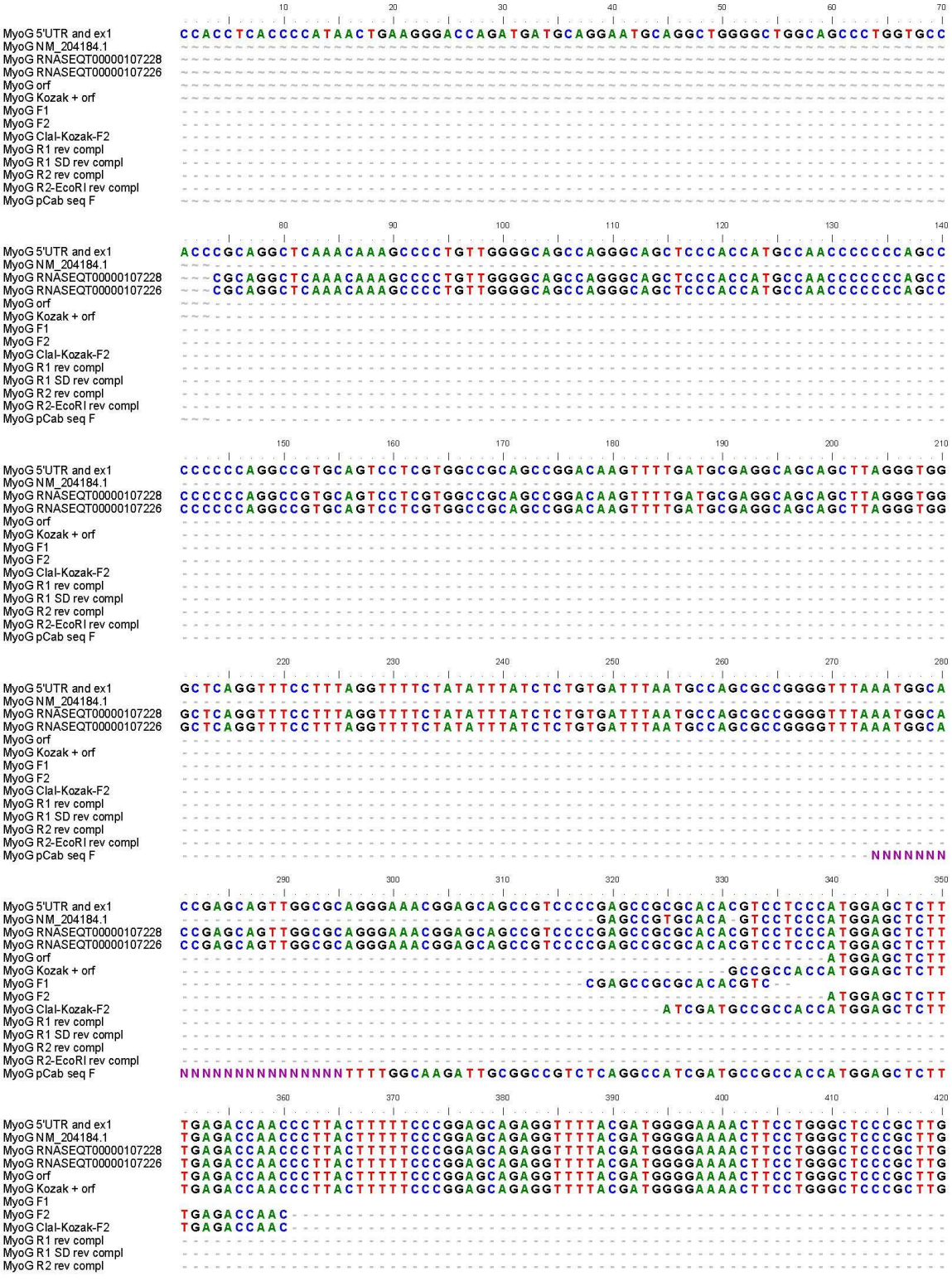
MyoG 5'UTR and ex1
MyoG NM_204184.1
MyoG RNASEQT00000107228
MyoG RNASEQT00000107226
MyoG orf
MyoG Kozak + orf
MyoG F1
MyoG F2
MyoG ClaI-Kozak-F2
MyoG R1 rev compl
MyoG R1 SD rev compl
MyoG R2 rev compl
MyoG R2-EcoRI rev compl
MyoG pCab seq F

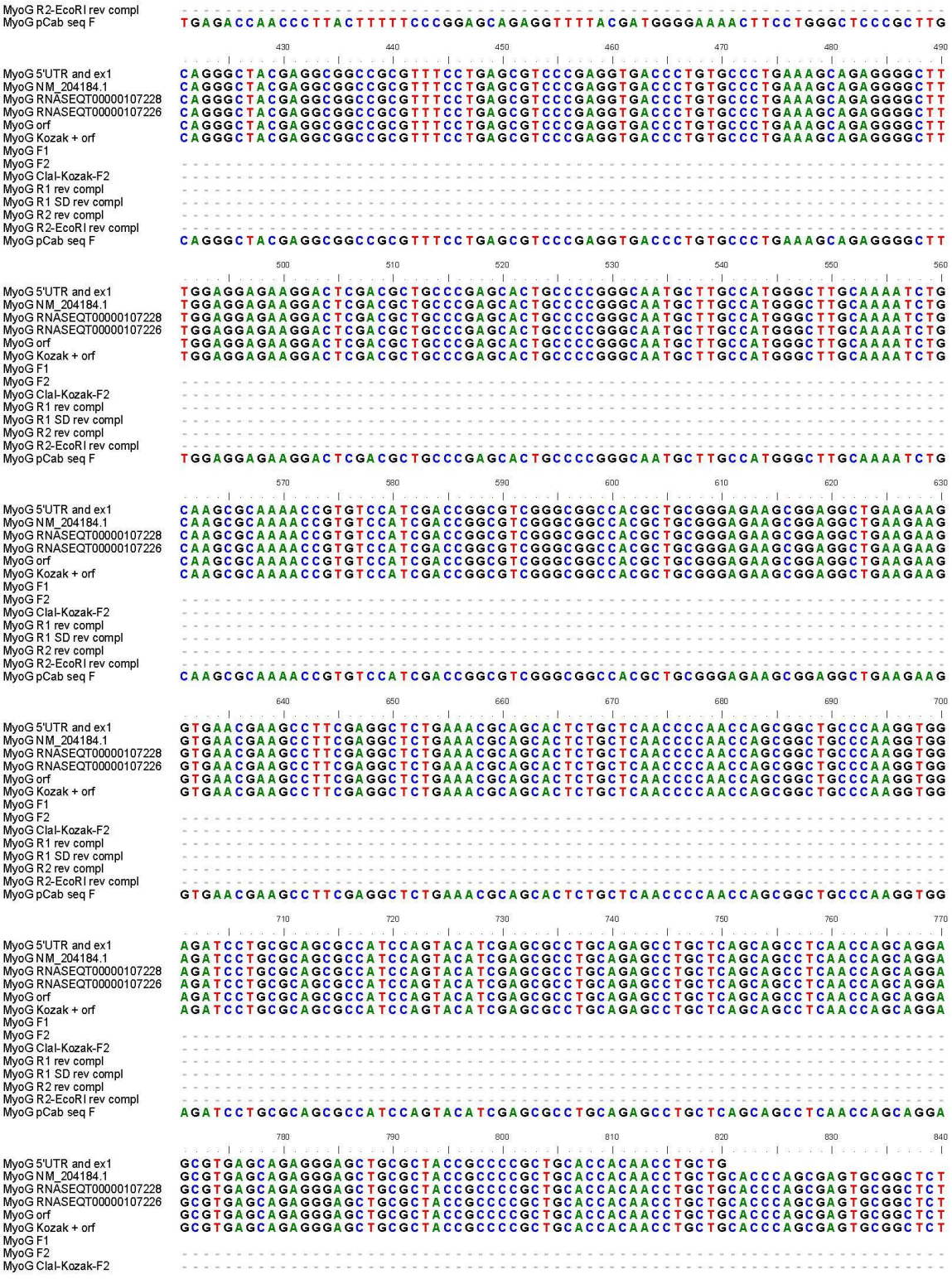
MyoG R2-EcoRI rev compl
MyoG pCab seq F
TGAGACCAACCCTTACTTTTTCCCGGAGCAGAGGTTTTACGATGGGGAAAACTTCCTGGGCTCCCGCTTG
430 440 450 460 470 480 490
MyoG 5'UTR and ex1
MyoG NM_204184.1
MyoG RNASEQT00000107228
MyoG RNASEQT00000107226
MyoG orf
MyoG Kozak + orf
MyoG F1
MyoG F2
MyoG ClaI-Kozak-F2
MyoG R1 rev compl
MyoG R1 SD rev compl
MyoG R2 rev compl
MyoG R2-EcoRI rev compl
MyoG pCab seq F
CAGGGCTACGAGGCGGCCGCGTTTCCTGAGCGTCCCGAGGTGACCCTGTGCCCTGAAAGCAGAGGGGCTT
500 510 520 530 540 550 560
MyoG 5'UTR and ex1
MyoG NM_204184.1
MyoG RNASEQT00000107228
MyoG RNASEQT00000107226
MyoG orf
MyoG Kozak + orf
MyoG F1
MyoG F2
MyoG ClaI-Kozak-F2
MyoG R1 rev compl
MyoG R1 SD rev compl
MyoG R2 rev compl
MyoG R2-EcoRI rev compl
MyoG pCab seq F
TGGAGGAGAAGGACTCGACGCTGCCCGAGCACTGCCCCGGGCAATGCTTGCCATGGGCTTGCAAAATCTG
570 580 590 600 610 620 630
MyoG 5'UTR and ex1
MyoG NM_204184.1
MyoG RNASEQT00000107228
MyoG RNASEQT00000107226
MyoG orf
MyoG Kozak + orf
MyoG F1
MyoG F2
MyoG ClaI-Kozak-F2
MyoG R1 rev compl
MyoG R1 SD rev compl
MyoG R2 rev compl
MyoG R2-EcoRI rev compl
MyoG pCab seq F
CAAGCGCAAAACCGTGTCCATCGACCGGCGTCGGGCGGCCACGCTGCGGGAGAAGCGGAGGCTGAAGAAG
640 650 660 670 680 690 700
MyoG 5'UTR and ex1
MyoG NM_204184.1
MyoG RNASEQT00000107228
MyoG RNASEQT00000107226
MyoG orf
MyoG Kozak + orf
MyoG F1
MyoG F2
MyoG ClaI-Kozak-F2
MyoG R1 rev compl
MyoG R1 SD rev compl
MyoG R2 rev compl
MyoG R2-EcoRI rev compl
MyoG pCab seq F
GTGAACGAAGCCTTCGAGGCTCTGAAACGCAGCACTCTGCTCAACCCCAACCAGCGGCTGCCCAAGGTGG
710 720 730 740 750 760 770
MyoG 5'UTR and ex1
MyoG NM_204184.1
MyoG RNASEQT00000107228
MyoG RNASEQT00000107226
MyoG orf
MyoG Kozak + orf
MyoG F1
MyoG F2
MyoG ClaI-Kozak-F2
MyoG R1 rev compl
MyoG R1 SD rev compl
MyoG R2 rev compl
MyoG R2-EcoRI rev compl
MyoG pCab seq F
AGATCCTGCGCAGCGCCATCCAGTACATCGAGCGCCTGCAGAGCCTGCTCAGCAGCCTCAACCAGCAGGA
780 790 800 810 820 830 840
MyoG 5'UTR and ex1
MyoG NM_204184.1
MyoG RNASEQT00000107228
MyoG RNASEQT00000107226
MyoG orf
MyoG Kozak + orf
MyoG F1
MyoG F2
MyoG ClaI-Kozak-F2
GCGTGAGCAGAGGGAGCTGCGCTACCGCCCCGCTGCACCACAACCTGCTG
GCGTGAGCAGAGGGAGCTGCGCTACCGCCCCGCTGCACCACAACCTGCTGCACCCAGCGAGTGCGGCTCT

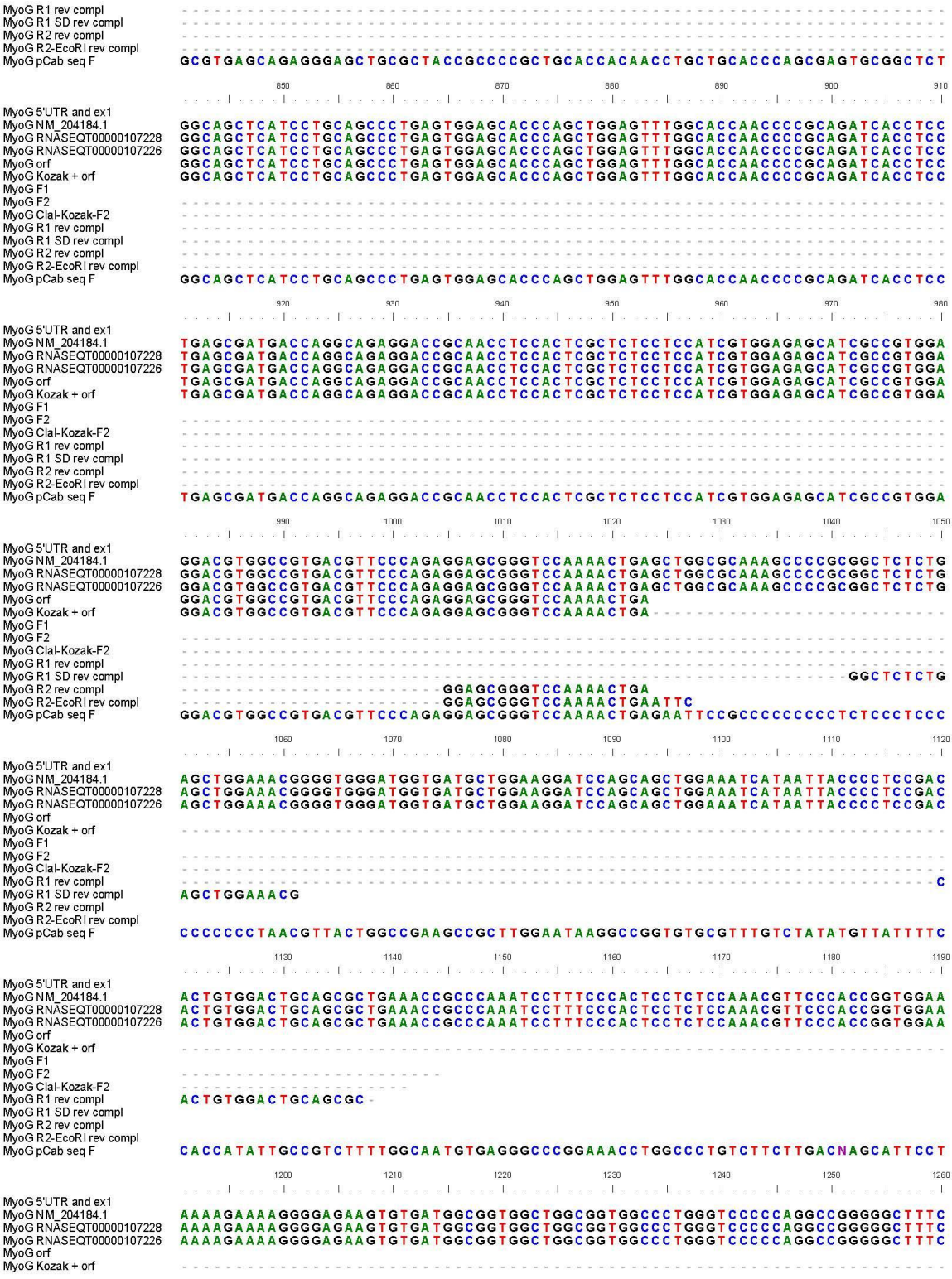
MyoG R1 rev compl
MyoG R1 SD rev compl
MyoG R2 rev compl
MyoG R2-EcoRI rev compl
MyoG pCab seq F
GCGTGAGCAGAGGGAGCTGCGCTACCGCCCCGCTGCACCACAACCTGCTGCACCCAGCGAGTGCGGCTCT
850 860 870 880 890 900 910
MyoG 5'UTR and ex1
MyoG NM_204184.1
MyoG RNASEQT00000107228
MyoG RNASEQT00000107226
MyoG orf
MyoG Kozak + orf
GGCAGCTCATCCTGCAGCCCTGAGTGGAGCACCCAGCTGGAGTTTGGCACCAACCCCGCAGATCACCTCC
MyoG F1
MyoG F2
MyoG ClaI-Kozak-F2
MyoG R1 rev compl
MyoG R1 SD rev compl
MyoG R2 rev compl
MyoG R2-EcoRI rev compl
MyoG pCab seq F
GGCAGCTCATCCTGCAGCCCTGAGTGGAGCACCCAGCTGGAGTTTGGCACCAACCCCGCAGATCACCTCC
920 930 940 950 960 970 980
MyoG 5'UTR and ex1
MyoG NM_204184.1
MyoG RNASEQT00000107228
MyoG RNASEQT00000107226
MyoG orf
MyoG Kozak + orf
TGAGCGATGACCAGGCAGAGGACCGCAACCTCCACTCGCTCTCCTCCATCGTGGAGAGCATCGCCGTGGA
MyoG F1
MyoG F2
MyoG ClaI-Kozak-F2
MyoG R1 rev compl
MyoG R1 SD rev compl
MyoG R2 rev compl
MyoG R2-EcoRI rev compl
MyoG pCab seq F
TGAGCGATGACCAGGCAGAGGACCGCAACCTCCACTCGCTCTCCTCCATCGTGGAGAGCATCGCCGTGGA
990 1000 1010 1020 1030 1040 1050
MyoG 5'UTR and ex1
MyoG NM_204184.1
MyoG RNASEQT00000107228
MyoG RNASEQT00000107226
MyoG orf
MyoG Kozak + orf
MyoG F1
MyoG F2
MyoG ClaI-Kozak-F2
MyoG R1 rev compl
MyoG R1 SD rev compl
MyoG R2 rev compl
MyoG R2-EcoRI rev compl
MyoG pCab seq F
1060 1070 1080 1090 1100 1110 1120
MyoG 5'UTR and ex1
MyoG NM_204184.1
MyoG RNASEQT00000107228
MyoG RNASEQT00000107226
MyoG orf
MyoG Kozak + orf
MyoG F1
MyoG F2
MyoG ClaI-Kozak-F2
MyoG R1 rev compl
MyoG R1 SD rev compl
MyoG R2 rev compl
MyoG R2-EcoRI rev compl
MyoG pCab seq F
AGCTGGAAACGGGGGTGGGATGGTGATGCTGGAAGGATCCAGCAGCTGGAAATCATAATTACCCCTCCGAC
AGCTGGAAACG
CCCCCCCTAACGTTACTGGCCGAAGCCGCTTGGAATAAGGCCGGTGTGCGTTTGTCTATATGTTATTTTC
1130 1140 1150 1160 1170 1180 1190
MyoG 5'UTR and ex1
MyoG NM_204184.1
MyoG RNASEQT00000107228
MyoG RNASEQT00000107226
MyoG orf
MyoG Kozak + orf
MyoG F1
MyoG F2
MyoG ClaI-Kozak-F2
MyoG R1 rev compl
MyoG R1 SD rev compl
MyoG R2 rev compl
MyoG R2-EcoRI rev compl
MyoG pCab seq F
ACTGTGGACTGCAGCGCTGAAACCGCCCAAATCCTTTCCCACTCCTCTCCAAACGTTCCCACCGGTGGAA
ACTGTGGACTGCAGCGC
CACCATATTGCCGTCTTTTGGCAATGTGAGGGCCCGGAAACCTGGCCCTGTCTTCTTGACNAGCATTCCT
1200 1210 1220 1230 1240 1250 1260
MyoG 5'UTR and ex1
MyoG NM_204184.1
MyoG RNASEQT00000107228
MyoG RNASEQT00000107226
MyoG orf
MyoG Kozak + orf
AAAAGAAAAGGGGAGAAGTGTGATGGCGGTGGCTGGCGGTGGCCCTGGGTCCCCCAGGCCGGGGGCTTTC

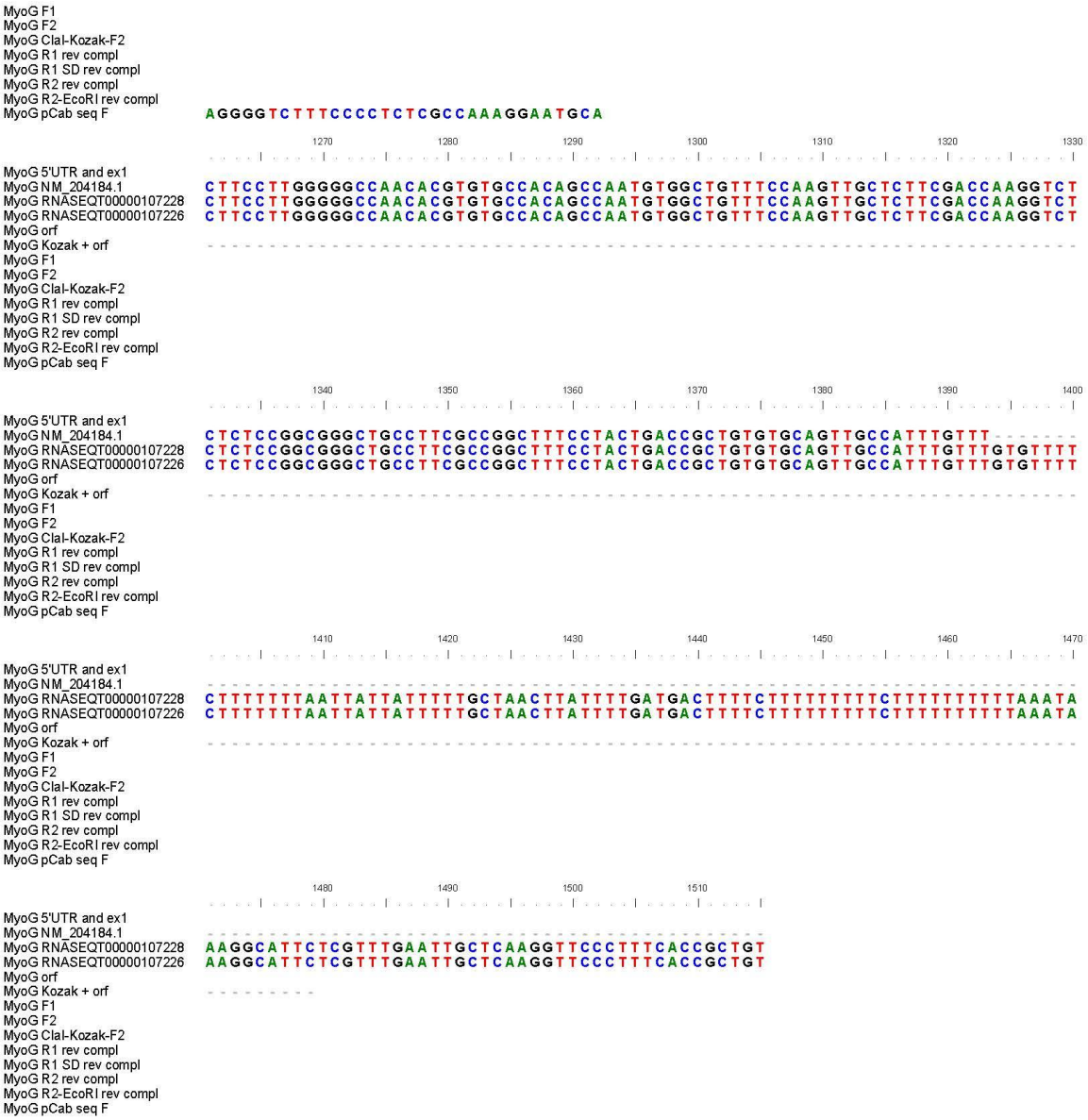

Appendix 2. C *MyoG* cDNA, primers and synthesis products.

Alignment of the chicken MyoG 5'UTR sequences extracted from Ensembl, the curated and RNAseq derived cDNAs that all produce the same open reading frame (orf), the orf alone and equipped with the Kozak sequence, the cloning primers and the re-sequenced Life Technology product cloned into pCab. The desired construct was obtained.

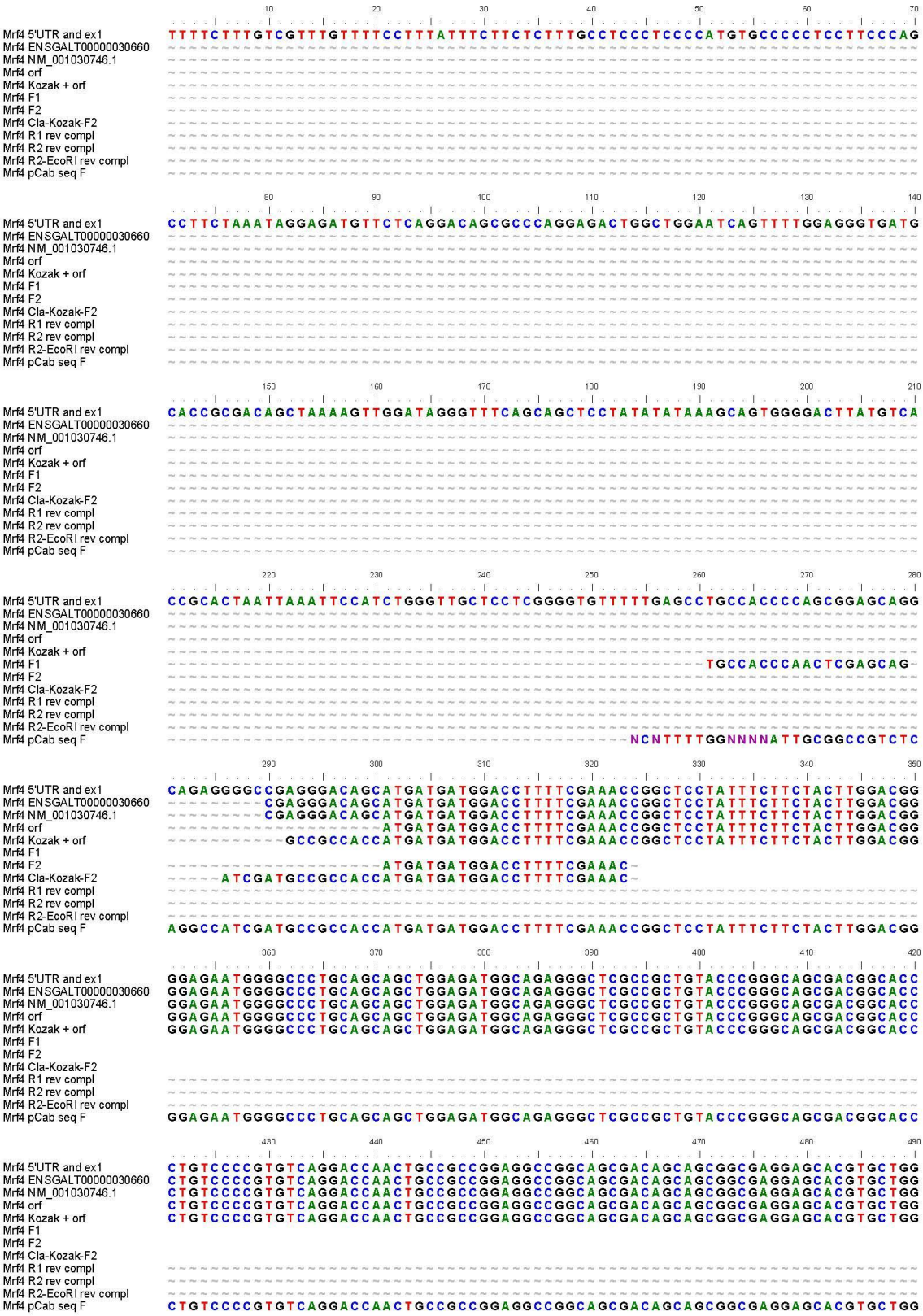
Mrf4 5'UTR and ex1
Mrf4 ENSGALT00000030660
Mrf4 NM_001030746.1
Mrf4 orf
Mrf4 Kozak + orf
Mrf4 F1
Mrf4 F2
Mrf4 Cla-Kozak-F2
Mrf4 R1 rev compl
Mrf4 R2 rev compl
Mrf4 R2-EcoRI rev compl
Mrf4 pCab seq F

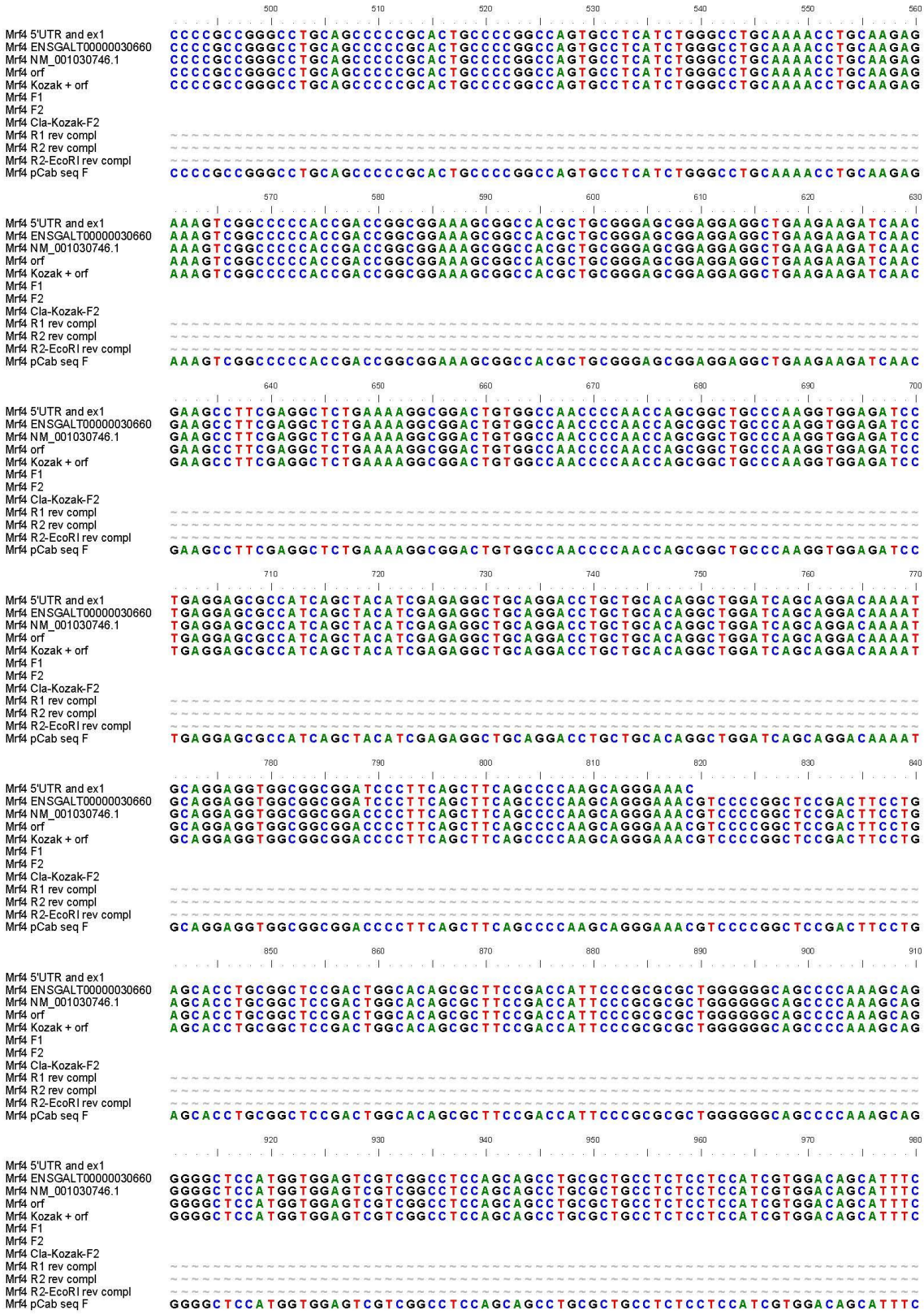
500 510 520 530 540 550 560
Mrf4 5'UTR and ex1 CCCCGCCGGGCCTGCAGCCCCCGCACTGCCCCGGCCAGTGCCTCATCTGGGCCTGCAAAACCTGCAAGAG
Mrf4 ENSGALT00000030660 CCCCGCCGGGCCTGCAGCCCCCGCACTGCCCCGGCCAGTGCCTCATCTGGGCCTGCAAAACCTGCAAGAG
Mrf4 NM_001030746.1 CCCCGCCGGGCCTGCAGCCCCCGCACTGCCCCGGCCAGTGCCTCATCTGGGCCTGCAAAACCTGCAAGAG
Mrf4 orf CCCCGCCGGGCCTGCAGCCCCCGCACTGCCCCGGCCAGTGCCTCATCTGGGCCTGCAAAACCTGCAAGAG
Mrf4 Kozak + orf CCCCGCCGGGCCTGCAGCCCCCGCACTGCCCCGGCCAGTGCCTCATCTGGGCCTGCAAAACCTGCAAGAG
Mrf4 F1
Mrf4 F2
Mrf4 Cla-Kozak-F2
Mrf4 R1 rev compl
Mrf4 R2 rev compl
Mrf4 R2-EcoRI rev compl
Mrf4 pCab seq F CCCCGCCGGGCCTGCAGCCCCCGCACTGCCCCGGCCAGTGCCTCATCTGGGCCTGCAAAACCTGCAAGAG
570 580 590 600 610 620 630
Mrf4 5'UTR and ex1 AAAGTCGGCCCCCACCGACCGGCGGAAAGCGGCCACGCTGCGGGAGCGGAGGAGGCTGAAGAAGATCAAC
Mrf4 ENSGALT00000030660 AAAGTCGGCCCCCACCGACCGGCGGAAAGCGGCCACGCTGCGGGAGCGGAGGAGGCTGAAGAAGATCAAC
Mrf4 NM_001030746.1 AAAGTCGGCCCCCACCGACCGGCGGAAAGCGGCCACGCTGCGGGAGCGGAGGAGGCTGAAGAAGATCAAC
Mrf4 orf AAAGTCGGCCCCCACCGACCGGCGGAAAGCGGCCACGCTGCGGGAGCGGAGGAGGCTGAAGAAGATCAAC
Mrf4 Kozak + orf AAAGTCGGCCCCCACCGACCGGCGGAAAGCGGCCACGCTGCGGGAGCGGAGGAGGCTGAAGAAGATCAAC
Mrf4 F1
Mrf4 F2
Mrf4 Cla-Kozak-F2
Mrf4 R1 rev compl
Mrf4 R2 rev compl
Mrf4 R2-EcoRI rev compl
Mrf4 pCab seq F AAAGTCGGCCCCCACCGACCGGCGGAAAGCGGCCACGCTGCGGGAGCGGAGGAGGCTGAAGAAGATCAAC
640 650 660 670 680 690 700
Mrf4 5'UTR and ex1 GAAGCCTTCGAGGCTCTGAAAAGGCGGACTGTGGCCAACCCCAACCAGCGGCTGCCCAAGGTGGAGATCC
Mrf4 ENSGALT00000030660 GAAGCCTTCGAGGCTCTGAAAAGGCGGACTGTGGCCAACCCCAACCAGCGGCTGCCCAAGGTGGAGATCC
Mrf4 NM_001030746.1 GAAGCCTTCGAGGCTCTGAAAAGGCGGACTGTGGCCAACCCCAACCAGCGGCTGCCCAAGGTGGAGATCC
Mrf4 orf GAAGCCTTCGAGGCTCTGAAAAGGCGGACTGTGGCCAACCCCAACCAGCGGCTGCCCAAGGTGGAGATCC
Mrf4 Kozak + orf GAAGCCTTCGAGGCTCTGAAAAGGCGGACTGTGGCCAACCCCAACCAGCGGCTGCCCAAGGTGGAGATCC
Mrf4 F1
Mrf4 F2
Mrf4 Cla-Kozak-F2
Mrf4 R1 rev compl
Mrf4 R2 rev compl
Mrf4 R2-EcoRI rev compl
Mrf4 pCab seq F GAAGCCTTCGAGGCTCTGAAAAGGCGGACTGTGGCCAACCCCAACCAGCGGCTGCCCAAGGTGGAGATCC
710 720 730 740 750 760 770
Mrf4 5'UTR and ex1 TGAGGAGCGCCATCAGCTACATCGAGAGGCTGCAGGACCTGCTGCACAGGCTGGATCAGCAGGACAAAAT
Mrf4 ENSGALT00000030660 TGAGGAGCGCCATCAGCTACATCGAGAGGCTGCAGGACCTGCTGCACAGGCTGGATCAGCAGGACAAAAT
Mrf4 NM_001030746.1 TGAGGAGCGCCATCAGCTACATCGAGAGGCTGCAGGACCTGCTGCACAGGCTGGATCAGCAGGACAAAAT
Mrf4 orf TGAGGAGCGCCATCAGCTACATCGAGAGGCTGCAGGACCTGCTGCACAGGCTGGATCAGCAGGACAAAAT
Mrf4 Kozak + orf TGAGGAGCGCCATCAGCTACATCGAGAGGCTGCAGGACCTGCTGCACAGGCTGGATCAGCAGGACAAAAT
Mrf4 F1
Mrf4 F2
Mrf4 Cla-Kozak-F2
Mrf4 R1 rev compl
Mrf4 R2 rev compl
Mrf4 R2-EcoRI rev compl
Mrf4 pCab seq F TGAGGAGCGCCATCAGCTACATCGAGAGGCTGCAGGACCTGCTGCACAGGCTGGATCAGCAGGACAAAAT
780 790 800 810 820 830 840
Mrf4 5'UTR and ex1 GCAGGAGGTGGCGGCGGATCCCTTCAGCTTCAGCCCCAAGCAGGGAAAC
Mrf4 ENSGALT00000030660 GCAGGAGGTGGCGGCGGATCCCTTCAGCTTCAGCCCCAAGCAGGGAAACGTCCCCGGCTCCGACTTCCTG
Mrf4 NM_001030746.1 GCAGGAGGTGGCGGCGGACCCCTTCAGCTTCAGCCCCAAGCAGGGAAACGTCCCCGGCTCCGACTTCCTG
Mrf4 orf GCAGGAGGTGGCGGCGGACCCCTTCAGCTTCAGCCCCAAGCAGGGAAACGTCCCCGGCTCCGACTTCCTG
Mrf4 Kozak + orf GCAGGAGGTGGCGGCGGACCCCTTCAGCTTCAGCCCCAAGCAGGGAAACGTCCCCGGCTCCGACTTCCTG
Mrf4 F1
Mrf4 F2
Mrf4 Cla-Kozak-F2
Mrf4 R1 rev compl
Mrf4 R2 rev compl
Mrf4 R2-EcoRI rev compl
Mrf4 pCab seq F GCAGGAGGTGGCGGCGGACCCCTTCAGCTTCAGCCCCAAGCAGGGAAACGTCCCCGGCTCCGACTTCCTG
850 860 870 880 890 900 910
Mrf4 5'UTR and ex1
Mrf4 ENSGALT00000030660 AGCACCTGCGGCTCCGACTGGCACAGCGCTTCCGACCATTCCCGCGCGCTGGGGGGCAGCCCCAAAGCAG
Mrf4 NM_001030746.1 AGCACCTGCGGCTCCGACTGGCACAGCGCTTCCGACCATTCCCGCGCGCTGGGGGGCAGCCCCAAAGCAG
Mrf4 orf AGCACCTGCGGCTCCGACTGGCACAGCGCTTCCGACCATTCCCGCGCGCTGGGGGGCAGCCCCAAAGCAG
Mrf4 Kozak + orf AGCACCTGCGGCTCCGACTGGCACAGCGCTTCCGACCATTCCCGCGCGCTGGGGGGCAGCCCCAAAGCAG
Mrf4 F1
Mrf4 F2
Mrf4 Cla-Kozak-F2
Mrf4 R1 rev compl
Mrf4 R2 rev compl
Mrf4 R2-EcoRI rev compl
Mrf4 pCab seq F AGCACCTGCGGCTCCGACTGGCACAGCGCTTCCGACCATTCCCGCGCGCTGGGGGGCAGCCCCAAAGCAG
920 930 940 950 960 970 980
Mrf4 5'UTR and ex1
Mrf4 ENSGALT00000030660 GGGGCTCCATGGTGGAGTCGTCGGCCTCCAGCAGCCTGCGCTGCCTCTCCTCCATCGTGGACAGCATTTC
Mrf4 NM_001030746.1 GGGGCTCCATGGTGGAGTCGTCGGCCTCCAGCAGCCTGCGCTGCCTCTCCTCCATCGTGGACAGCATTTC
Mrf4 orf GGGGCTCCATGGTGGAGTCGTCGGCCTCCAGCAGCCTGCGCTGCCTCTCCTCCATCGTGGACAGCATTTC
Mrf4 Kozak + orf GGGGCTCCATGGTGGAGTCGTCGGCCTCCAGCAGCCTGCGCTGCCTCTCCTCCATCGTGGACAGCATTTC
Mrf4 F1
Mrf4 F2
Mrf4 Cla-Kozak-F2
Mrf4 R1 rev compl
Mrf4 R2 rev compl
Mrf4 R2-EcoRI rev compl
Mrf4 pCab seq F GGGGCTCCATGGTGGAGTCGTCGGCCTCCAGCAGCCTGCGCTGCCTCTCCTCCATCGTGGACAGCATTTC

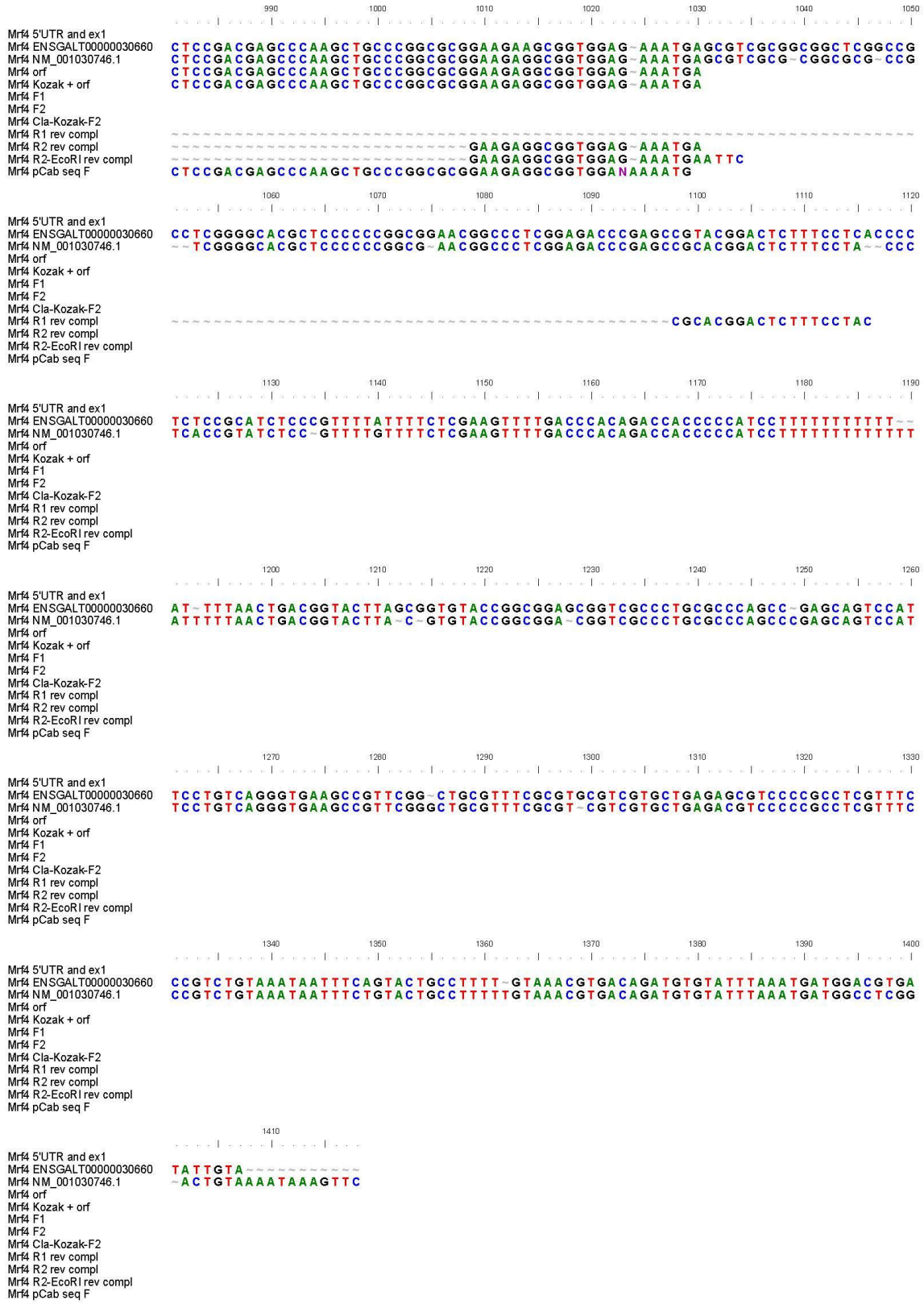

Appendix 2. D *Mrf4* cDNA, primers and synthesis products.

Alignment of the chicken Mrf4 5'UTR sequences extracted from Ensembl, the curated and RNAseq derived cDNAs that all produce the same open reading frame (orf), the orf alone and equipped with the Kozak sequence, the cloning primers and the re-sequenced Life Technology product cloned into pCab. The desired construct was obtained.

FORM UPR16

14 Research Ethics Review Checklist

14.1 Please include this completed form as an appendix to your thesis (see the Postgraduate Research Student Handbook for more information

Postgraduate Research Student (PGRS) Informat			**Student ID**	479101	
PGRS Name:	Federica Berti				
Department:	Pharmacy	**First Supervisor**	Dr. Susanne Dietrich		
Start Date: (or progression date for Prof Doc students)	**2.10.2011**				
Study Mode and Route	Part-time ☐	MPhil ☐	MD ☐		
	Full-time ☒	PhD ☒	Professional Doctorate ☐		

Title of Thesis:	Protection of the Muscle Stem Cell State from Premature differentiation
Thesis Word Count: (excluding ancillary data)	69938

If you are unsure about any of the following, please contact the local representative on your Faculty Ethics Committee for advice. Please note that it is your responsibility to follow the University's Ethics Policy and any relevant University, academic or professional guidelines in the conduct of your study

Although the Ethics Committee may have given your study a favourable opinion, the final

responsibility for the ethical conduct of this work lies with the researcher(s). 14.1.1

UKRIO Finished Research Checklist: (If you would like to know more about the checklist, please see your Faculty or Departmental Ethics Committee rep or see the online version of the full checklist at: http://www.ukrio.org/what-we-do/code-of-practice-for-research/)	
a) Have all of your research and findings been reported accurately, honestly and within a reasonable time frame?	YES ☒ NO ☐
b) Have all contributions to knowledge been acknowledged?	YES ☒ NO ☐
c) Have you complied with all agreements relating to intellectual property, publication and authorship?	YES ☒ NO ☐
d) Has your research data been retained in a secure and accessible form and will it remain so for the required duration?	YES ☒ NO ☐
e) Does your research comply with all legal, ethical, and contractual requirements?	YES ☒ NO ☐

Candidate Statement:	
I have considered the ethical dimensions of the above named research project, and have successfully obtained the necessary ethical approval(s)	
Ethical review number(s) from Faculty Ethics Committee (or from NRES/SCREC):	Awerb14005
If you have *not* submitted your work for ethical review, and/or you have answered 'No' to one or more of questions a) to e), please explain below why this is so:	

Signed *(PGRS)*:		**Date:** 3.5.16